Towards the Structural Elucidation and Total Synthesis of Hemicalide: Assignment of the C29-C46 Region

This thesis is submitted for the degree of Doctor of Philosophy

at the University of Cambridge

March 2022

Tegan Paige Stockdale

Corpus Christi College

Supervised by Professor Ian Paterson

Declaration

This thesis is the result of my own work and includes nothing that is the outcome of work done in collaboration, except as declared in the preface and specified in the text. I further state that no substantial part of my thesis has already been submitted, or, is being concurrently submitted for any such degree, diploma or other qualification at the University of Cambridge or any other University or similar institution except as declared in the Preface and specified in the text. It does not exceed the prescribed word limit for the Physics and Chemistry Degree Committee, excluding experimental data.

_____

Tegan P. Stockdale

March 2022

Abstract

Towards the Structural Elucidation and Total Synthesis of Hemicalide: Assignment of the C29-C46 Region

Tegan P. Stockdale

Marine natural products are a known source of novel bioactive compounds. However, in many cases, low isolation yields and lack of full structural information necessitate total synthesis to achieve their structural elucidation, and produce sufficient material for biological studies. This thesis outlines the synthesis and stereochemical assignment of the C29-C46 region of hemicalide (**1**), a complex, highly bioactive polyketide marine natural product. Chapter one introduces the complex polyketide hemicalide and summarises previous work on this natural product. Hemicalide displays impressive bioactivity, registering picomolar IC_{50} values against numerous cancer cell lines. Preliminary biological evaluation indicated a novel antimitotic mechanism of action, involving microtubule destabilisation. While 1D- and 2D-NMR experiments established the planar 46-carbon structure, the low isolation yield precluded full stereochemical assignment and further biological studies. Previous synthetic and computational studies have determined the relative configuration within the C1-C24 and C34-C42 stereoclusters. However, the configuration of five stereocentres and the interrelationships between isolated stereoclusters remained unassigned.

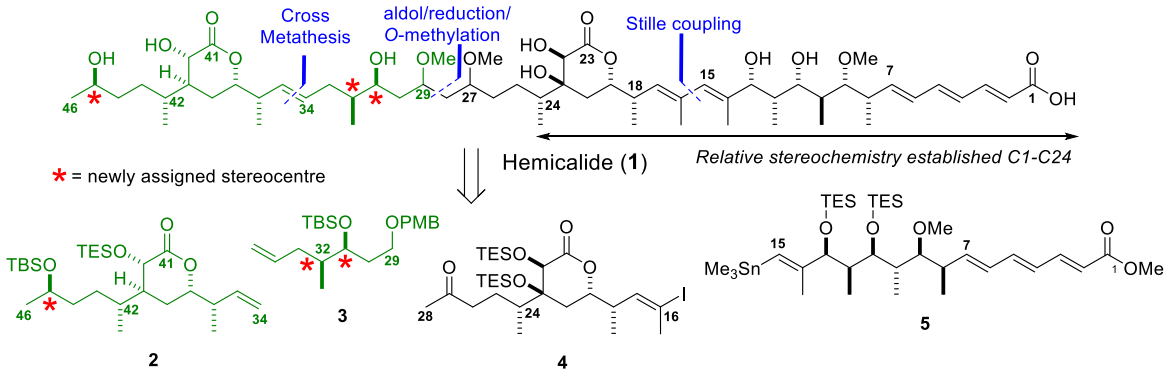

Chapter two describes the synthesis of the δ-lactone-containing C34-C46 (**2**) region of hemicalide. A highly diastereoselective route was developed, based on boron-aldol methodology, with flexible installation of (*R*)- or (*S*)-configuration at C45. This versatile approach facilitated the configurational assignment of C45, completing the assignment for the C34-C46 region of hemicalide. Chapter three describes the synthesis of the largely unexplored C29-C35 fragment (**3**) of hemicalide. Literature analysis of previous reports led to the synthesis of two *syn*-diastereomers believed to contain the most likely configuration for this region. Chapter four outlines the controlled union of the C29-C35 and C34-C46 fragments, by olefin cross metathesis, to produce three diastereomers of the fully elaborated C29-C46 region. This work allowed the relative stereochemistry of C31 and C32 to be assigned and established the relationship between the C27-C32 and C36-C45 stereoclusters. Production of a late-stage aldehyde intermediate positions the synthetic campaign four steps from the final target molecule. Chapter five draws conclusions and outlines future work on the project.

Acknowledgements

Foremost, my thanks to Professor Ian Paterson, who from my initial application has made me welcome in his lab group. Thank you for your time, consideration and countless ideas and suggestions. It has been an honour and a pleasure to get to know you and hold the place of your final PhD student and lab group member. Thank you also to Professor Jonathan Goodman, who stepped in as my temporary supervisor, upon my arrival to Cambridge.

My thanks to the members of the Paterson group and the Spring group, during their time in Lab 122. Lastly, to the Phipps group, who treated me as one of their own - there was many a time during pandemic restrictions when you all brightened my days and gave me inspiration to tackle the latest in the long line of synthetic challenges that come your way in a total synthesis. Thanks to the NMR users, Bing, Nelson and Talia for running samples for me, to help unravel the latest mystery that my reactions had thrown at me.

I also owe my thanks to other members of the chemistry department. Firstly, the first floor technicians Nic, Nick and Naomi. Especially Nic who, apart from being immensely helpful in the lab, gave me many a smile, laugh and good chat over the years. Secondly, the NMR technicians, Duncan, Andrew and Pete, who are not only skilled and helpful, but also kind.

My thanks also to my family and friends, who celebrated with me the successes and held me up in the tough times. Especially, my new college family of Corpus Christi, who have provided me friends from so many different disciplines and paths of life, whom I may otherwise not have had the opportunity to meet. You all provided me outlet, laughs, dinners and drinks when Chemistry is being challenging. Especially, my fiancé Theo, who has helped keep me sane through the hills and valleys of the hemicalide synthetic campaign and for whose quiet kindness and support I am immensely grateful.

Lastly, thank you to the Herchel Smith Research Studentship and the Cambridge Trust, without whose financial support I would not have been able to undertake a PhD at Cambridge University.

Contents

Abbreviations

Å	Ångstrom
Ac	Acetyl
ADC	Antibody-drug conjugate
aq.	Aqueous
BDP	1,2-Bis(diphenylphosphino)benzene
BINOL	1,1'-Bi-2-naphthol
Bipy	Bipyridyl
Bn	Benzyl
brsm	Based on recovered starting material
Bu or *n*Bu	*n*-Butyl
cat.	Catalytic
CBS	Corey-Bakshi-Shibata
cm^{-1}	Wavenumbers
COSY	^{1}H-^{1}H correlation spectroscopy
cod	cyclooctadiene
Cp	Cyclopentadienyl
CSA	Camphorsulfonic acid
*c*Hex	Cyclohexyl
dr	Diastereomeric ratio
d	Doublet
dd	Doublet of doublets
ddd	Doublets of doublets of doublets
dddd	Doublets of doublets of doublets of doublets
dt	Doublet of triplets
dba	Dibenzylideneacetone
DBU	1,8-Diazabicyclo[5.4.0]undec-7-ene
DCC	*N*,*N*'-Dicyclohexylcarbodiimide
DDQ	2,3-Dichloro-5,6-dicyano-1,4-benzoquinone
DEAD	Diethyl azodicarboxylate
DFT	Density Functional Theory
DIBAL	Diisobutylaluminium hydride
DIPEA	Diisopropylethylamine

diphos-4	1,4-bis(diphenylphosphino)butane
DMAP	4-Dimethylaminopyridine
DMF	*N*,*N*-Dimethylformamide
DMP	Dess-Martin Periodinane
DMSO	Dimethyl sulfoxide
e.e.	Enantiomeric excess
EDC	1-Ethyl-3-(3-dimethylaminopropyl)carbodiimide
EMA	European Medical Association
eq.	Equivalents
Et	Ethyl
ETSA	Ethyltrimethylsilyl acetate
FDA	Federal Drug Administration (America)
FTMS	Fourier-Transform Mass Spectrometry
g	Gram(s)
GC	Gas chromatography
GIAO	Gauge-independent atomic orbitals
h	Hour(s)
HMBC	Heteronuclear Multiple Bond Correlation Spectroscopy
HPLC	High Performance Liquid Chromatography
HRESITOFMS	High Resolution Electrospray Ionisation Time of Flight Mass Spectrometry
HWE	Horner-Wadsworth-Emmons
Hz	Hertz
IC_{50}	Half maximal inhibitory concentration
Imid.	Imidazole
Ipc	Isopinocamphenyl
*i*Pr	Isopropyl
IR	Infrared Spectroscopy
J	^{1}H - ^{1}H coupling constant
L	Unspecified ligand
LA	Lewis acid
LD_{50}	Median lethal dose
LDA	Lithium diisopropylamide
LLS	Longest linear sequence
M	Molar (mol/L or mol/dm^3) or Unspecified metal

MAB	Monoclonal antibody
Me	Methyl
mg	Milligram(s)
MHz	Megahertz
min.	Minute(s)
mL	Millilitre(s)
µL	Microlitre(s)
mmol	Millimole(s)
MNP	Marine natural product
µmol	Micromoles
mol	Mole(s)
MS	Molecular sieves or Mass Spectrometry
Ms	Mesyl (methanesulfonyl)
MTPA	α-Methoxy-α-(trifluoromethyl)phenylacetate
NCI	National Cancer Institute
nM	Nanomolar
NMO	*N*-Methylmorpholine *N*-oxide
NMR	Nuclear Magnetic Resonance Spectroscopy
nOe	Nuclear Overhauser Effect
NOESY	Nuclear Overhauser Effect Spectroscopy
O/N	Over night
P	Unspecified protecting group
PE 30 - 40	Petroleum Ether, bp 30 - 40 °C
PE 40 - 60	Petroleum Ether, bp 40 - 60 °C
Ph	Phenyl
pin	pinacol
PMB	*para*-Methoxybenzyl
PMBTCA	*para*-Methoxybenzyl trichloroacetimidate
PPTS	Pyridinium *para*-toluenesulfonate
py	Pyridine
q	Quartet
qn	Quintet
quant.	Quantitative
R	Unspecified substituent

RCM	Ring-closing metathesis
R_f	Retention factor
rt	Room temperature
SAR	Structure activity relationship
SCUBA	Self-Contained Underwater Breathing Apparatus
SM	Starting material
sp.	Species
t	Triplet
TBAF	Tetrabutylammonium fluoride
TBS	*tert*-butyldimethylsilyl
*t*Bu	*tert*-butyl
TC	Thiophene-2-carboxylate
TfOH	Trifluoromethanesulfonic acid
TFP	Tri(2-furyl)phosphine
TEMPO	(2,2,6,6-Tetramethylpiperidin-1-yl)oxyl
TES	Triethylsilyl
Tf	Trifluoromethanesulfonyl
THF	Tetrahydrofuran
TLC	Thin layer chromatography
TMS	Tetramethylsilane or trimethylsilyl
TMDS	Tetramethyldisiloxane
Ts	Tosyl (*para*-toluenesulfonyl)
VCD	Vibrational circular dichroism

Nomenclature

Compound numbering

The numbering system used for hemicalide and its associated fragments follows that of Carletti *et al*.[1] Substituents are defined by the skeletal carbon to which they are attached (Figure I).

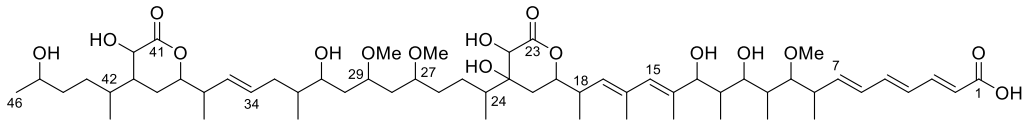

Figure I. Numbering scheme for hemicalide (1)

Metal enolate and olefin geometry

The geometry of olefins and enolates are assigned based on the accepted IUPAC convention, where the enolate oxygen is defined as having the higher priority group. Side chains R^1 and R^2 are in order of decreasing priority. (*E*)-Olefins and enolates are defined by having the higher priority groups located on opposite sides of the double bond (Figure II). (*Z*)-Olefins and enolates are defined by having the highest priority groups located on the same side.

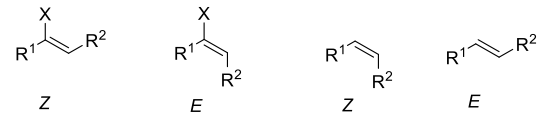

Figure II. Definition of enolate and olefin geometries

Stereochemical relationships

The relative stereochemical relationship between two substituents is defined by the convention set out by Masamune *et al*.[2] A *syn* relationship has the two substituents pointing in the same direction relative to the plane of the carbon skeleton when drawn in a linear fashion, whereas an *anti*-relationship has the two substituents pointing in the opposite direction (Figure III).

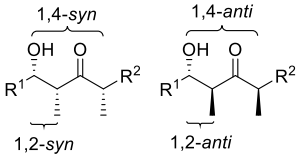

Figure III. Definition of stereochemical relationships

Figures

Schemes

Tables

1. Introduction

1.1 Natural Products as Medicines

Natural products have an exceedingly long history as human medicines. Indeed, natural pharmacopoeias have been found dating back to the third millennium BC, with oral histories thought to further predate written records.[3] Even today, natural medicines continue to be highly important, remaining the primary form of healthcare for 70-95% of people in developing nations.[4] These compounds also provide the inspiration for a significant percentage of conventional pharmaceuticals.[5,6] For example, acetylsalicylic acid (**6**), from willow and poplar bark, traditionally used for pain relief, is now the key component of the mild analgesic Aspirin (**Figure 1**).[7] Similarly, artemesinin (**7**), an active ingredient in commercial malaria treatments, was isolated from sweet wormwood, traditionally used in China to treat intermittent fevers.[8] Over the period of 1981 to 2014, 51% of approved pharmaceutical drugs were natural products, mimics, derivatives or have incorporated natural product pharmacophores.[5] Clearly, these compounds continue to play a highly significant role in drug discovery and development.

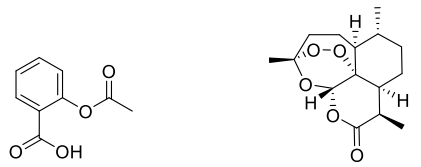

acetylsalicylic acid (**6**) artemesinin (**7**)

Figure 1. Approved natural product pharmaceutical compounds: acetylsalicylic acid (**6**) and artemesinin (**7**)

1.2 Marine Natural Products

Over 70% of the earth's surface is covered by water and, unsurprisingly, much of the earth's biodiversity is found within the oceans, with marine organisms spanning 36 distinct phyla.[9–11] With the advent of technological advances, such a SCUBA and submersibles, gaining access to this under-explored marine environment has become much more feasible. This has led to the discovery that marine invertebrates, including sponges, molluscs and their associated microbiota are vast reservoirs of potent bioactive compounds.[9,10] The cause for this phenomenon may reside in a culmination of evolutionary pressures, such as competitive growth environments, limited mobility and lack of physical defences, that have forced these creatures to rely on chemical

defence mechanisms to deter predation.[12–17] In the context of the marine environment, where dilution is a key consideration, these compounds must also be highly potent in small quantities in order to be effective. The range of different organisms has led to a remarkably broad array of marine natural product (MNP) structural motifs being discovered that are unique to the marine environment. These encompass a wide range of compound classes from nucleosides (e.g. cytarabine (**8**)), peptide derivatives (e.g. diazonamide A (**9**)), diterpenoids (e.g. eleutherobin (**10**)) and polyketides (e.g. spongistatin-1 (**11**), PM050489 (**12**) and PM060184 (**13**)) among many others (**Figure 2**).

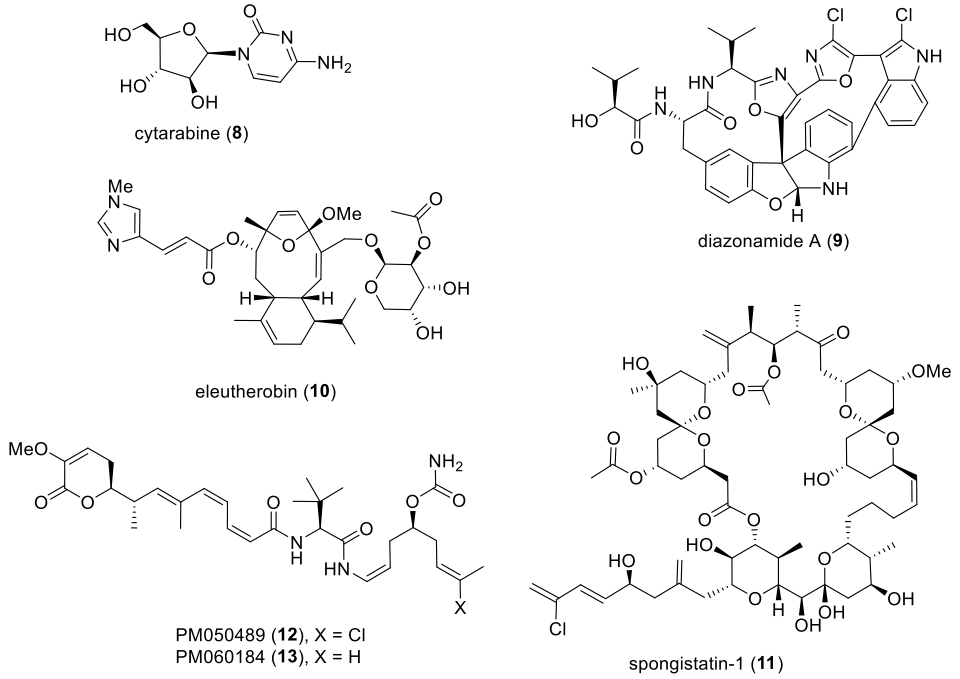

Figure 2. Examples of the structural diversity within marine natural products: cytarabine (**8**), diazonamide A (**9**), eleutherobin (**10**), spongistatin-1 (**11**) PM050489 (12) and PM060184 (**13**).

Of the over 20,000 novel MNPs reported to date, the majority of bioactive MNPs have been isolated from marine invertebrates (75%), particularly sponges (47%).[9,18–20] A feature thought to be key to the potency of these compounds is their molecular complexity, evolutionarily refined over generations to hone the properties and fit of these molecules to their equally complex biological binding sites. It has been suggested that this molecular complexity is also a reason that MNPs often display novel modes of action or differences in binding sites.[21] Novel modes of binding are valuable to more efficacious treatment of disease targets, potentially allowing these compounds to remain biologically active in cases where resistance arises for first-line treatments.

A large number of MNPs display antifungicidal, cytotoxic or antineoplastic activities, making them very attractive drugs candidates, particularly in the area of cancer research.[9,21] Interestingly, many MNPs target the cytoskeleton of eukaryotic cells, particularly microtubules, which are essential to cell integrity, growth and replication.[18] Whether this is a common feature of marine MNPs isolated from marine invertebrates, a bias imposed by the manner of bioactivity guided isolation or a combination of these and other factors is unclear.

Despite their often novel modes of action and high potency, there are hurdles to the use of MNPs as drug candidates. Often only an extremely small amount of the target compound is isolated from sizeable quantities of the host organism, making production and extraction from natural sources unsustainable.[10,22] For example, to isolate halichondrin B (**14**, **Figure 3**), 600 kg of sponge was needed to extract 12.5 mg of compound, representing a 2.1×10^{-8} % yield.[23] While initially isolated amounts may be sufficient for preliminary biological tests, they are often not sufficient for full stereochemical elucidation nor detailed mechanistic or structure-activity relationship (SAR) studies, let alone clinical evaluation. A number of solutions have been proffered to address this supply problem, including biosynthesis, through fermentation or gene isolation and expression; partial synthesis, from an advanced intermediate; and total synthesis. In fact, total synthesis may present the only viable option to address the chemical supply issue in cases where the MNP has not been fully characterised, biosynthesis is not feasible, an advanced intermediate is not available or significant modifications to the structure are sought during SAR studies.[9,10]

A series of illustrative examples have been selected here, where total synthesis of an MNP has been indispensable to the research and development of a compound for pharmaceutical purposes. An inspiring success story is that of eribulin mesylate (**15**, **Figure 3**). Marketed as Halaven® by Eisai, this drug is FDA and EMA approved to treat metastatic breast cancer. It has also, more recently, been FDA approved to treat inoperable liposarcoma.[20,24] Eribulin meslylate is a truncated and modified synthetic analogue of halichondrin B. This complex MNP was originally reported in 1986,[23] as the most potent member of a new class of polyether macrolides, isolated from the common Japanese sponge *Halichondria okadai*. Despite extremely small quantities, the hyperpotent antineoplastic properties of halichondrin B against numerous human cancer cell lines, and its promising performance at low concentrations in early animal studies, led researchers to dedicate themselves to the total synthesis of this molecule.

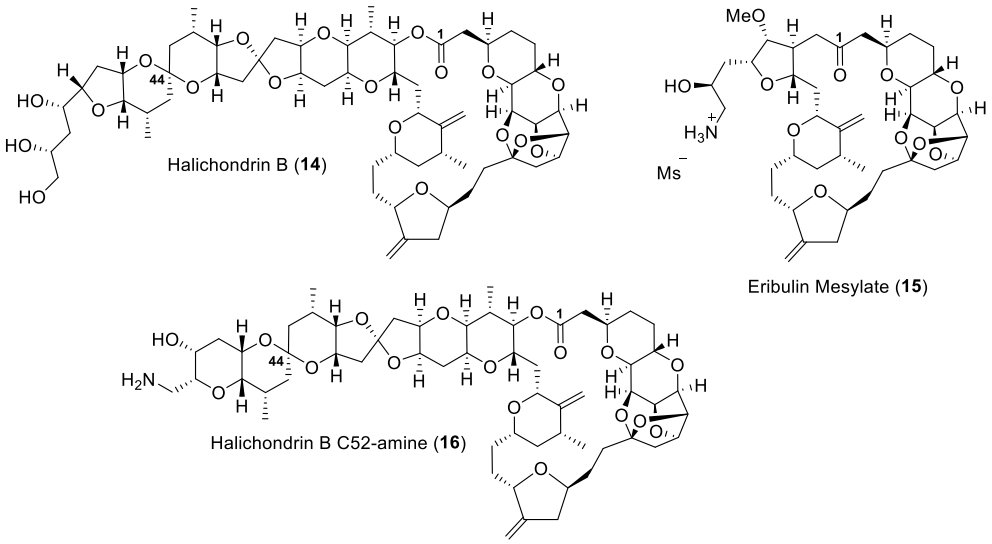

Figure 3. Halichondrin B (**14**), its synthetic truncate Eribulin mesylate (**15**) and C52-amine derivative (**16**)

This was no small endeavour for a molecule with a 54-carbon skeleton and 32 stereocentres. The first total synthesis route, reported by Kishi in 1992, proceeded *via* a highly convergent pathway, coupling four major fragments, involving over 100 total steps (47 steps LLS).[25] Further biological and mechanistic studies, enabled by this ready supply of intermediates, showed that these compounds act as antimitotic agents by occupying the *vinca* domain on β-tubulin, thereby destabilising the microtubule and preventing polymerisation.[26] Sponge cultivation was attempted. However, from over a tonne of raw material, only 300 mg of halichondrin B was obtained. SAR studies, on intermediates made available by the total synthesis, revealed that a significantly truncated intermediate retained comparable potency to the NP.[27]

Combining information from mechanistic and SAR studies along with bioassays on intermediates, this scaffold was stripped back to its functionalised macrocycle pharmacophore, in the form of eribulin mesylate (**15**). This was a significant achievement and, after considerable optimisation, the commercial synthesis of Halaven® proceeds in 30 steps (LLS) and delivers a yield of 0.16%. Although intensive, this is currently the only means of delivering Halaven® on a multi-kilogram scale, sufficient for drug purposes.[28]

In a landmark demonstration of the power of total synthesis, a more recent paper by the Kishi group reports the synthesis of a full C52-halichondrin-B amine derivative (**16**, **Figure 3**) on a 10 g scale.[29] Solving this supply problem, allowed biological studies to be pursued on amine **16**.[30] These studies showed impressive bioactivity and a novel mode of action. The promising anti-cancer properties of amine **16** in animal studies has led to the full halichondrin scaffold being pursued as

a drug in clinical trials. This work clearly shows that total synthesis can meet the challenge of limited supply of complex natural products to facilitate drug discovery and development.

Most MNP total synthesis examples arise from research projects taking place at academic institutions, which are subsequently optimised for industry production. The mixed lineage polyenes PM050489 (**12**) and PM060184 (**13**) (**Figure 2**) present a rare exception. These two compounds were reported in 2013 by PharmaMar (Spain) after being obtained by bioactivity guided isolation from the Madagascan sponge *Lithoplocamia lithistoides*.[31] Both compounds were isolated in trace quantities of 161 mg (0.002%) and 2.6 mg (0.00003%) for PM050489 and PM060184, respectively. The polyketide-derived metabolites both feature a valerolactone moiety, with the δ-position bearing an extended, functionalised polyunsaturated tail. Due to the degree of unsaturation, these compounds bear only four stereocentres. The amounts initially isolated were sufficient for preliminary biological studies, showing sub-nanomolar growth inhibition against a panel of human cancer cell lines, through an antimitotic mechanism of action.[32] The results of these tests led to PM060184 being selected as the primary clinical candidate. However, the amounts isolated were insufficient to fully elucidate all stereochemical features of the compounds, with the absolute stereochemistry of C6 and C21 of the molecules remaining unassigned.

In the original isolation paper, multigram total synthesis routes were also reported (17 steps LLS, 29 steps total). By comparing spectroscopic data of candidate diastereomers with the natural product, this allowed assignment of the C6 and C21 stereocentres. The routes involved a number of stereoretentive sp^2 cross couplings to install crucial *Z*-olefins and gave an overall yield of 5.5% for PM060184.[31] Adaptation of the synthetic route has already been undertaken to allow production of PM060184 on a commercial scale.[33] Further mechanistic studies showed that these compounds bind to the *vinca* domain of β-tubulin at the maytansine site.[34] This results in suppression of the dynamic instability of β-tubulin, increasing the time spent in pause stage (G_0 a separate phase of interphase that cells can use to pause the cell cycle), by blocking tubulin addition and thereby preventing longitudinal polymerisation.[35] Promisingly, this activity appears to be sustained even in P-glycoprotein (P-gp) efflux pump overexpressing cancer lines.[36] This is a highly desirable feature, as resistance mechanisms affecting many first-line cancer chemotherapeutics involve the drug being recognised and effluxed from cancerous cells by these P-gp pumps. The reasonable safety profile shown by PM060184 was considered to bode well for Phase II clinical trials.[37]

The third case study is on the depsipeptide compound dolastatin-10 (**17**, **Figure 4**), where 29 mg of pure compound was isolated from 1000 kg of the sea hare *Dolabella auricularia*.[38] It has also subsequently been found in cyanobacteria *Caldora penicillata* and *Symploca hydnoides*, a fact which has allowed semisynthesis of its analogues in the quantities needed for commercial purposes.[39–41] However, the amount originally isolated by the Pettit lab was insufficient for full 3D-characterisation. They determined that the most attractive solution to address both stereochemical assignment and preclinical supply issues was total synthesis.[42] This heavily modified pentapeptide was, at that time, the most potent antineoplastic compound known, displaying sub-nanomolar IC_{50} values against a number of human cell lines.[38] Samples produced by total synthesis enabled further biological and mechanistic studies, which showed that dolastatin-10 acts as an antimitotic agent, inducing microtubule instability and depolymerisation by binding to the *vinca* domain on β-tubulin.[43]

Dolastatin-10 reached Phase II clinical trials before being discontinued, due to peripheral toxicity and lack of sufficient efficacy. Yet, these studies laid the groundwork for the development of the semisynthetic analogue monomethyl auristatin E (**18**).[44] The analogue was coupled to a monoclonal antibody to give the antibody-drug conjugate (ADC) brentuximab vedotin (**19**) (Adcetris®). This increased the specificity and addressed the efficacy and toxicity issues encountered by dolastatin-10.[44] Adcetris® is FDA approved and conditionally EMA approved to treat Hodgkin's lymphoma and systematic anaplastic large cell lymphoma.[10] Two further dolastatin-10 semisynthetic analogues, soblidotin and tasidotin, reached Phase II trials as antimitotics to treated advanced tumours.[45,46] This last case study provides an example of where total synthesis enabled further development of an MNP necessary to create a compound suitable for the pharmaceutical market. It also demonstrates the utility that an immunoconjugate can play in addressing peripheral toxicity issues, common in cytotoxic MNPs,[34,47] that would otherwise have prevented pharmaceutical viability of the compound.

Together these three cases illustrate some of the bioactivity, utility and unexhausted potential of MNPs. They also highlight the indispensable use of total synthesis. These include acting as a means of constructing otherwise inaccessible compounds for full structural characterisation and providing samples to allow biological, mechanistic and SAR studies. Such studies are essential in order to properly evaluate the pharmaceutical potential of these lead compounds. MNPs have been of consistent interest and value across the years, due in part to their high bioactivity and

novel mechanisms of action.[48] This is particularly true in the area of cancer drugs, where the antimitotic activity of numerous MNPs perhaps finds its greatest utility.[49] As such, the search for bioactive MNPs and new treatments continues with vigour and the area of MNP research presents an opportunity for continuing growth.

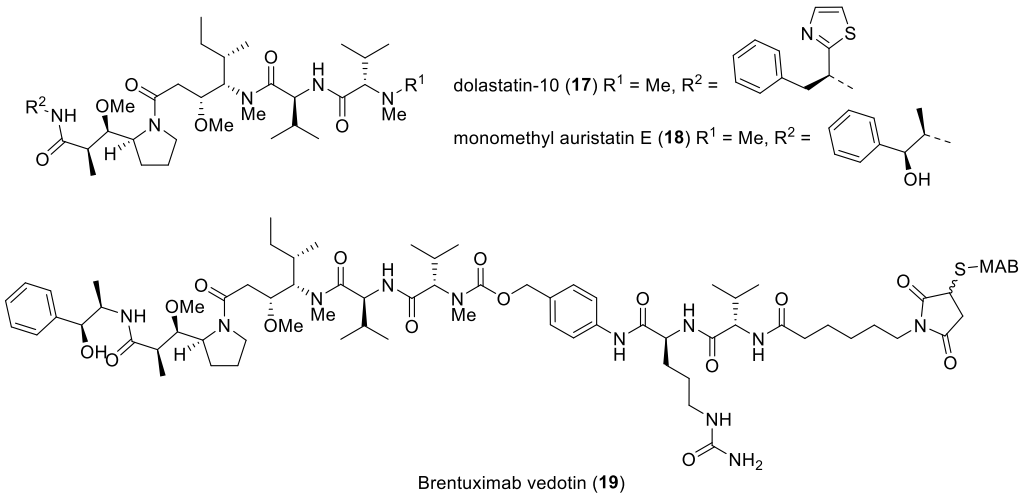

Figure 4. Dolastatin-10 (**17**), monomethylauristatin E (**18**) and the derived immunoconjugate brentuximab vedotin (**19**)

1.3 Isolation, Characterisation and Preliminary Biological Evaluation of Hemicalide

Reported in the patent literature in 2011, hemicalide (**1**) was isolated by bioactivity-guided fractionation from the *Hemimycale* sp. sponge, collected in deep water off the Vanuatu Torres Islands in the South Pacific.[1] This exploratory expedition was a collaboration between two French groups, the National Centre for Scientific Research — Pierre Fabre Laboratories and the Research Institute for Development. From 5 kg of sponge, only 0.5 mg of hemicalide was isolated (1.0×10^{-5} %); an extremely small amount, even in a MNP isolation context. Preliminary studies revealed that hemicalide was a complex polyketide secondary metabolite. HRESITOFMS identified an $[M–H]^-$ pseudomolecular ion (*m/z* 1061.6780, calculated 1061.6782) consistent with a molecular formula of $C_{59}H_{97}O_{16}$. Extensive 1D and 2D NMR experiments established the constitutional arrangement of the molecule, with a 46 carbon skeleton bearing 21 stereocentres. It displays a range of functionalities including a conjugated trienic acid (C1-C7), contiguous polypropionate stereohexad (C8-C13), conjugated diene (C14-C17), α,β-dihydroxy-δ-lactone (C19-C23), polyacetate stereotetrad (C27-C32) and an α-hydroxy-δ-lactone (C37-C41) (**Figure 5**). However, the amount isolated was insufficient to allow determination of the absolute configuration at any

of the stereocentres. Furthermore, derivatisation or degradation experiments that may have assisted in assigning relative and absolute configuration were not undertaken.

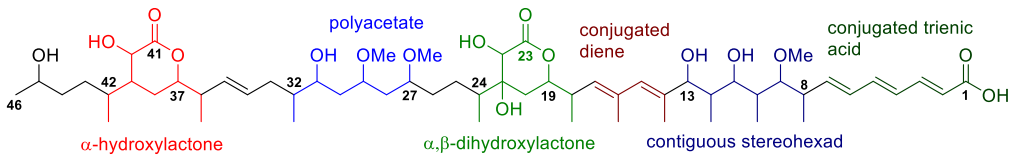

Figure 5. Structure of hemicalide, showing major stereoclusters

Preliminary bioactivity studies showed that hemicalide was highly potent, displaying subnanomolar IC_{50} values against a number of human cancer cell lines (**Table 1**).[1] Preliminary mechanistic studies were also encouraging, disclosing that hemicalide exhibited antimitotic effects through microtubule destabilisation and appeared to do so by means of a novel mode of action. Fluorescence microscopy showed HeLa tumoural cells arrested in prometaphase. This contrasts with other antimitotic compounds, such as the taxoids and other classes that bind to the *taxoid* domain. These are microtubule stabilisers and cause cell cycle arrest at the metaphase/anaphase boundary. It also contrasts with the vinca alkaloids and those ligands that bind to the *vinca* domain, which are microtubule destabilisers.[9,18,33,34,50–53] Interestingly, immunohistochemical labelling of α-tubulin revealed an absence of normal microtubules in prometaphase, as well as interphase cells. Cell cycle arrest at not one, but two phases of the cell cycle is different to the known modes of action of existing chemotherapeutics. Thus, hemicalide appears to detrimentally impact both normal cell growth and stall cell replication, by disrupting crucial tubulin cytoskeletal components, seeming to do so in a novel manner. Given that resistance to existing chemotherapeutics severely impacts on positive outcomes of first-line treatments, a novel mode of action may allow hemicalide to circumvent existing resistance mechanisms. Thus, hemicalide presents a potentially promising chemotherapeutic compound candidate.

Table 1. Antiproliferative activity of hemicalide against selected human cancer cell lines[1]

Cell Line	**Disease Model**	**IC_{50} (nM)**
A549	Non small cell lung cancer	0.82
BxPC3	Pancreatic cancer	0.47
LoVo	Colon cancer	0.081
MCF7	Breast cancer	0.011
Namalwa	Burkitt's lymphoma	1.1
SK-OV-3	Ovarian cancer	0.33

The combination of high potency, structural complexity, unassigned stereochemistry, novel mode of action and exceedingly low natural abundance renders hemicalide an attractive target for total synthesis. Indeed a total synthesis campaign presently offers the only means of stereochemical elucidation and obtaining reliable compound supplies for further studies. For these reasons, in recent years, the Ardisson, Cossy and Paterson groups have risen to the challenge of pursuing the total synthesis of hemicalide.[54–62]

The first objective towards the goal of full structural elucidation and stereochemical assignment is to establish the relative configuration of hemicalide, followed by the absolute configuration. It should be noted that, as no optical rotation ($[\boldsymbol{\alpha}]_{\mathbf{D}}^{\mathbf{20}}$) value has been reported, absolute stereochemistry will only be confirmed by bioactivity comparison of hemicalide stereoisomer candidates. Given the extremely potent nature of hemicalide, the possibility of using hemicalide as a payload in an ADC context, much like monomethylauristatin E (**18**) (*vide supra*),[44] may also be considered in future, as a way to improve selectivity and efficacy.

1.4 Synthetic Endeavours and Progress towards Establishing the Relative Stereochemistry of Hemicalide

With all 21 stereocentres unassigned, hemicalide had over 2 million possible stereoisomers. This rendered it necessary to reduce these permutations in order to facilitate elucidation of its 3D structure. The functionalities of hemicalide (*vide supra*, **Figure 5**) offered convenient points at which to break the molecule into isolated stereoclusters, thereby allowing the relative configurational assignments within these to be explored. Drawing evidence from the extensive 1D and 2D NMR data on hemicalide, comparison with characteristic features of polyketide motifs, computational NMR predictions and exploratory synthetic studies, much of the relative configuration within the various stereoclusters has been asserted and will be discussed in turn.

1.4.1 Relative Configuration of the C1-C15 Region

In 2009, the Ardisson group reported their first work on the C1-C15 trienic acid and stereohexad portion of hemicalide (**20**, **Figure 6**), before the full 2D structure of hemicalide had been disclosed.[54] This region contains six stereocentres, leading to 32 possible diastereomers. By comparison to known polyketide motifs, the unusually low ^{13}C NMR shift of Me12 (δ_C = 7.6 ppm)

was noted to be characteristic of a *syn-syn* stereotriad,[63] thus C11-C13 had a *syn-syn* relationship. However, Me10 was not similarly shifted upfield (δ_C = 13.0 ppm), thereby excluding another *syn-syn* stereotriad. This left C9-C11 possessing a *syn-anti*, *anti-syn* or *anti-anti* stereotriad. In effect, this reduced the number of possible C8-C13 diastereomers from 32 to six, as shown in **20a-20f** (**Figure 6**).

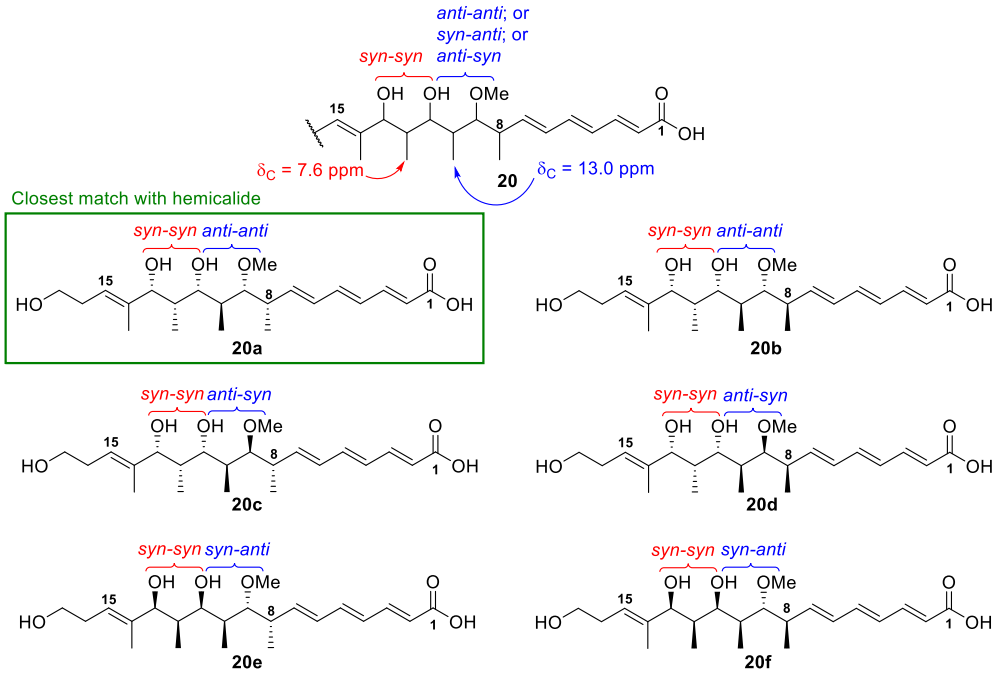

Figure 6. C1-C15 fragments **20a-f** reported by Ardisson et al.[54] permitted comparison of NMR spectroscopic data for each diastereomer with hemicalide

The Ardisson group retrosynthetic analysis of the C1-C15 model diastereomers (**20a-f**) broke the molecule into three regions: a C1-C6 trienoic acid fragment **21**, a C7-C13 polypropionate stereohexad **22** and a C14-C17 vinyl halide **23** (**Scheme 1**). Isolating the unknown stereocluster in one fragment, C7-C13 stereohexad **22**, permitted manipulation of the stereochemistry in this region, followed by a common coupling sequence to acquire the target diastereomers. This approach entailed disconnection across C6-C7, *via* a HWE olefination, to reveal phosphonate **21**; and disconnection across C13-C14, *via* a nucleophilic addition and reduction sequence, leading back to Weinreb amide **22** and vinyl halide **23**. Aldol disconnections across C11-C12 and C9-C10 allow access to the high oxygenation patterns characteristic of polyketides, disclosing chiral pool starting materials: Roche ester (*S*)-**24** or (*R*)-**25** and oxazolidinone (*S*)-**26** or (*R*)-**27**. Given the putative *syn*-C11-C12 relationship, oxazolidinones (*S*)-**26** and (*R*)-**27** were used to facilitate *syn* Evans aldol reactions in **20a-d** and **20e-f**, respectively.[64,65] However, given that all four relative configurations across C8-C10 were desired, the Paterson aldol reaction[66,67] was also employed.

This uses either lactate-derived ketone **28** or **29**, providing access to *syn* and *anti*-aldol adducts, depending on the starting ketone and enolisation conditions.[68]

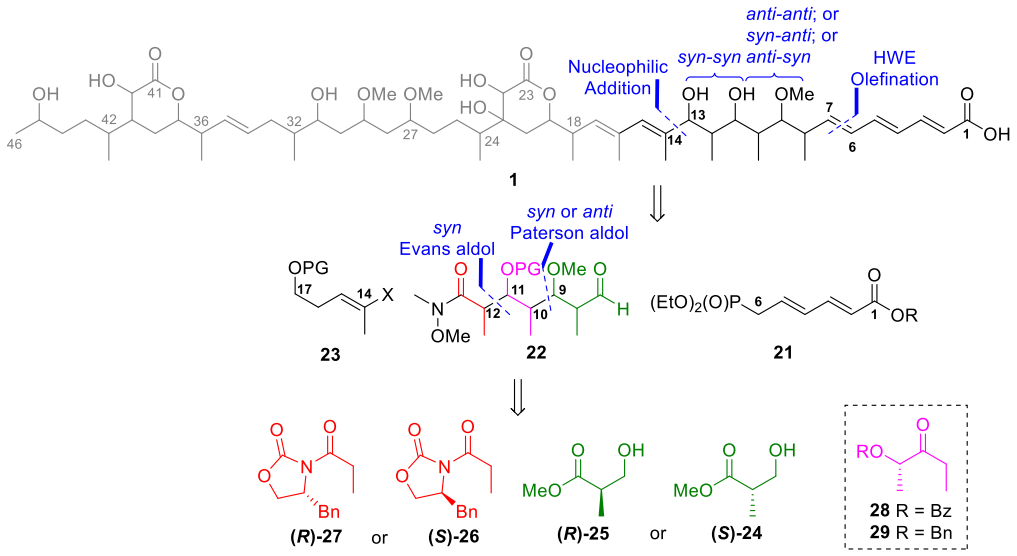

Scheme 1. Retrosynthetic analysis of C1-C15 by Ardisson et al.[54]

The synthesis of C7-11 aldehyde **30a** commenced from Roche ester (*S*)-**24**, with a silylation, reduction and Swern oxidation[69–72] sequence to give aldehyde **31** (**Scheme 2a**). A boron-mediated aldol reaction,[73–75] with lactate-derived ketone **28** *via* the *E*-enolate, delivered the 1,2-*anti* adduct,[76] which was methylated to give **32a**. Concomitant reduction of the ketone and benzoyl ester, followed by oxidative cleavage, gave aldehyde **30a**. By replacing the starting ester with (*R*)-**25** the same pathway provided C7-C11 aldehyde **30b.**

To access aldehyde **30c**, a boron-mediated aldol reaction,[77,78] between aldehyde **31** and lactate-derived ketone **29** *via* the *Z*-enolate, delivered the 1,2-*syn* adduct, which was methylated to give **32c**. After ketone reduction, hydrogenolysis cleaved the benzyl ether before oxidative cleavage to give C7-C11 aldehyde **30c**. By replacing the starting ester with (*R*)-**25** the same pathway provided C7-C11 aldehyde **30d**.

An Evans aldol reaction,[79,80] using (*S*)-oxazolidinone **26** with aldehyde **30a**, installed the desired C11-C12 stereochemistry. The auxiliary was transformed into a Weinreb amide and the hydroxyl group was TMS protected to give C7-C13 **33a**. The same process was performed with aldehydes **30b-d** to provide **33b-d** respectively. By using (*R*)-oxazolidinone **27** with aldehydes **30a-b**, the same steps provided **33e-f** respectively.

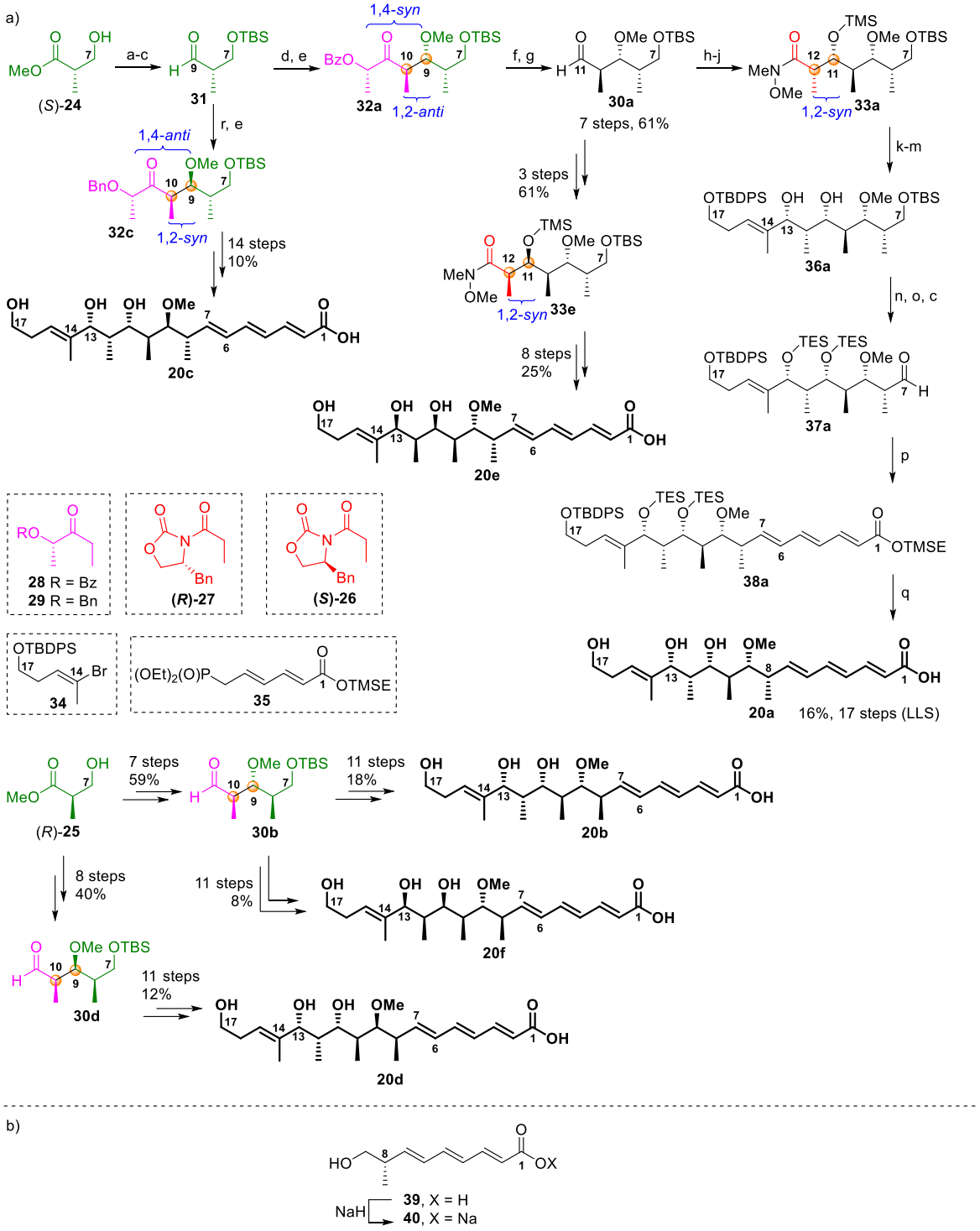

Reagents: (a) TBSCl, imidazole, DMF, rt; (b) DIBAL, CH_2Cl_2, –40°C to –20°C, 98% (two steps); (c) $(COCl)_2$, DMSO CH_2Cl_2, *then* alcohol, NEt_3, –55°C to rt, 100%; (d) *c*Hex_2BCl, Me_2NEt, Et_2O, 0°C, **28**, *then* **31**, –78°C to –25°C, 98%, *dr* >19:1; (e) MeOTf, DTBMP, CH_2Cl_2, 45°C , 76%; (f) $LiBH_4$, THF, –78°C to rt; (g) $NaIO_4$, MeOH, rt, 84% (two steps); (h) (*S*)-**26**, *n*Bu_2BOTf, Et_3N, CH_2Cl_2, 0°C, **30a**, –78°C to 0°C, 91%; (i) $MeONHMe_3$·HCl, $AlMe_3$, CH_2Cl_2, –20°C to rt, 75%; (j) TMSOTf, 2,6-lutidine, CH_2Cl_2, –30°C, 93%; (k) **34**, *t*BuLi, Et_2O, –90°C *then* **33a**, –78°C to –50°C; (l) Amberlyst-15, MeOH, rt, 85% (two steps); (m) $Zn(BH_4)_2$, Et_2O, CH_2Cl_2, –78°C to –50°C, 91%, *dr* >9:1; (n) AcOH, THF, H_2O, rt, 88%; (o) TESOTf, 2,6-lutidine, CH_2Cl_2, 0°C, 99%; (p) **35**, LDA, THF, –78°C *then* **37a**, –78°C to 0°C, 59% (2 steps); (q) TASF, DMF, 67%; (r) *c*Hex_2BCl, NEt_3, Et_2O, –78°C, **29**, *then* **31**, –78°C to –25°C, 84%, *dr* >9:1.

Scheme 2. a) Synthesis of C1-C17 diastereomers Ardisson et al,[54] with orange markers to highlight generation of new stereocentres and bolding of final model fragments; b) Model carboxylate salt **40** hypothesised to be the form in which hemicalide was isolated.

To complete the syntheses, it was necessary to couple vinyl bromide **34** and phosphonate **35** to **33a-f**. Nucleophilic addition of the lithiated species (derived from vinyl bromide **34**) into **33a**, TMS cleavage and 1,3-*syn* reduction, completed installation of the *syn-syn* stereotriad and gave diol **36a**. Terminal TBS deprotection, TES protection and selective Swern oxidation of the primary TES ether[69–72] gave aldehyde **37a**. HWE olefination completed the C1-C17 carbon chain (**38a**) and global deprotection secured C1-C17 trienic acid **20a**.[54] Repetition of the same pathway with **33b-f** gave C1-C17 trienic acids **20b-f**, respectively.

Synthesis of these diastereomers revealed significant NMR chemical shift deviations from the natural product in the C1-C7 region, leading Ardisson to hypothesise that hemicalide had been isolated as its carboxylate salt. Transformation of a model trienic acid (**39**) to the sodium salt (**40**) (**Scheme 2b**) showed shifts more consistent with the natural product and also indicated that the shift variation did not extend much further than the C1-C7 conjugated trienic acid region, allowing comparison of the model fragments with hemicalide data.[54] Four diastereomers, **20c-f**, were able to be excluded on the basis of sizeable deviations in ^{13}C NMR ($|\Delta\delta_C| > 1$ ppm). Comparison of the ^{1}H NMR data for the remaining two diastereomers, **20a-b**, showed that **20a** exhibited a better fit ($|\Delta\delta_H| < 0.1$ ppm) and it was concluded that the relative configuration within **20a** , bearing the *syn*-a*nti-anti*-configuration across C8-C11, was the best match for hemicalide.

Ab initio NMR prediction has become an increasingly powerful tool to assist in structural and stereochemical elucidation of novel NPs. DP4-GIAO methodology, developed by Smith and Goodman,[55] uses combined density functional theory (DFT) and GIAO calculations of ^{1}H and ^{13}C NMR shifts for candidate diastereomers. By comparing these predictions to experimental NMR data, the DP4 algorithm outputs the probability of each diastereomeric permutation matching the experimental data. In this way, it provides a prediction of the most likely relative stereochemistry for a molecule. Given that the physical properties, and therefore, the NMR spectra, of enantiomers are identical, DP4 can only predict the relative, rather than absolute, configuration of molecules.

Given that the computational resources scale non-linearly with the size and complexity of NPs, it can be prohibitively resource expensive to run predictions for an entire molecule. In instances in which stereoclusters are sufficiently distal that they will have minimal effect on one another, calculations can be conducted on molecular fragments (DP4f). Although a somewhat lesser degree of confidence can be assigned to DP4f calculations, this approach has precedent for successfully

assigning relative stereochemistry in NPs.[81,82] In 2010, DP4f calculations on the C1-C15 region of hemicalide, undertaken by Smith and Goodman,[55] provided additional support for the relative stereochemical arrangement proposed by Ardisson, with diastereomer **20a** producing the highest probability match with the experimental data.

In 2013, as part of the synthesis of a C1-C25 moiety, Ardisson reported a revised route to access the C1-C15 region (**Scheme 3**),[57] starting from the C7-C13 Weinreb amide (**33a**) (**Scheme 2**).[54] Due to the difference in intended chain length, the lithiated species for nucleophilic attack was derived from vinyl iodide **41**. Following 1,3-*syn* reduction, to finish installing the *syn*-*syn* stereotriad and TMS deprotection, the resulting diol was protected as the cyclic siloxane **42**. Iododesilylation, terminal TBS deprotection and DMP oxidation[83,84] then gave aldehyde **43**. This was engaged in a HWE olefination with C1-C6 phosphonate **44** to deliver C1-C15 moiety **45**.

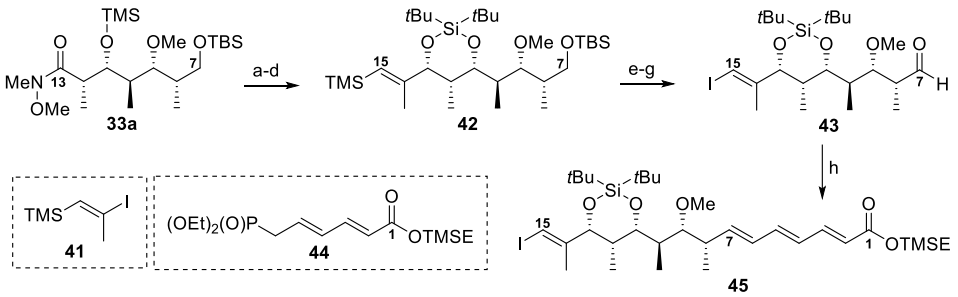

Reagents: (a) **41**, *t*BuLi, Et_2O, –78°C *then* **33a**, –78°C to –50°C, 99%; (b) Amberlyst-15, MeOH, rt, 99%; (c) $Zn(BH_4)_2$, Et_2O, CH_2Cl_2, –78°C to –50°C, 87%, *dr* 9:1; (d) $tBu_2Si(OTf)_2$, 2,6-lutidine, DMF, rt, 76%; (e), NIS, THF, 0°C, 87%; (f) CSA, MeOH, 0°C, 87%; (g), DMP, CH_2Cl_2, rt; (h) LDA, **44**, THF, –78°C *then* **43**, –78°C to 0°C, 92% (two steps).

Scheme 3. Revised synthesis of C1-C15 region by Ardisson et al.[57]

In 2018, as part of a C1-C28 region synthesis, the Paterson group reported their own synthesis of the C1-C15 portion of hemicalide. Retrosynthetically, this entailed disconnection across C7-C8, *via* a HWE olefination, and a series of diastereoselective aldol reactions to install the C8-C13 stereohexad. In contrast to the work by the Ardisson group, the Paterson approach had the goal of accessing both enantiomers of a single diastereomer. A 1,2-*syn* relationship exists between the C13 hydroxyl and Me12, signalling a *syn*-aldol type disconnection across C12-C13. In addition, the C11 hydroxyl has a 1,2-*anti* relationship with Me10, and a 1,4-*syn* relationship with Me8, indicating an asymmetric aldol type disconnection to set C9 and C11. Based on these observations, it was proposed that the desired C8-C13 stereohexad could be constructed employing a series of asymmetric boron-mediated aldol reactions (**Scheme 4**).

Aldehyde **46** was prepared from diethyl methylmalonate in four steps.[85–87] An Evans aldol reaction[88] between aldehyde **46** and oxazolidinone (*R*)-**27** installed the 12,13-*syn* relationship in adduct **47**. Protection of the C13 hydroxyl as its TES ether, reductive cleavage of the chiral auxiliary and Swern oxidation gave aldehyde **48**. Ketone **49** was prepared, in three steps, from commercially available Roche ester (*S*)-**24**.[89]

An asymmetric boron-mediated aldol reaction between aldehyde **48** and ketone **49**, *via* the (*E*)-enolate, delivered 1,2-*anti* 1,4-*syn* adduct **50** (>20:1 *dr*). The C11 hydroxyl was then protected as its TES ether and controlled reduction gave alcohol **51** (>20:1 *dr*). *O*-Methylation, DDQ deprotection of the PMB ether and DMP oxidation delivered aldehyde **52**. A HWE olefination with phosphonate **53**, coupled the C1-C6 region. The C15 vinyl iodide was then transformed to a stannane, under Wulff-Stille conditions[90] to give C1-C15 stannane **5**. The enantiomeric series was prepared analogously by utilising (*S*)-**26** and ketone *ent*-**49**.

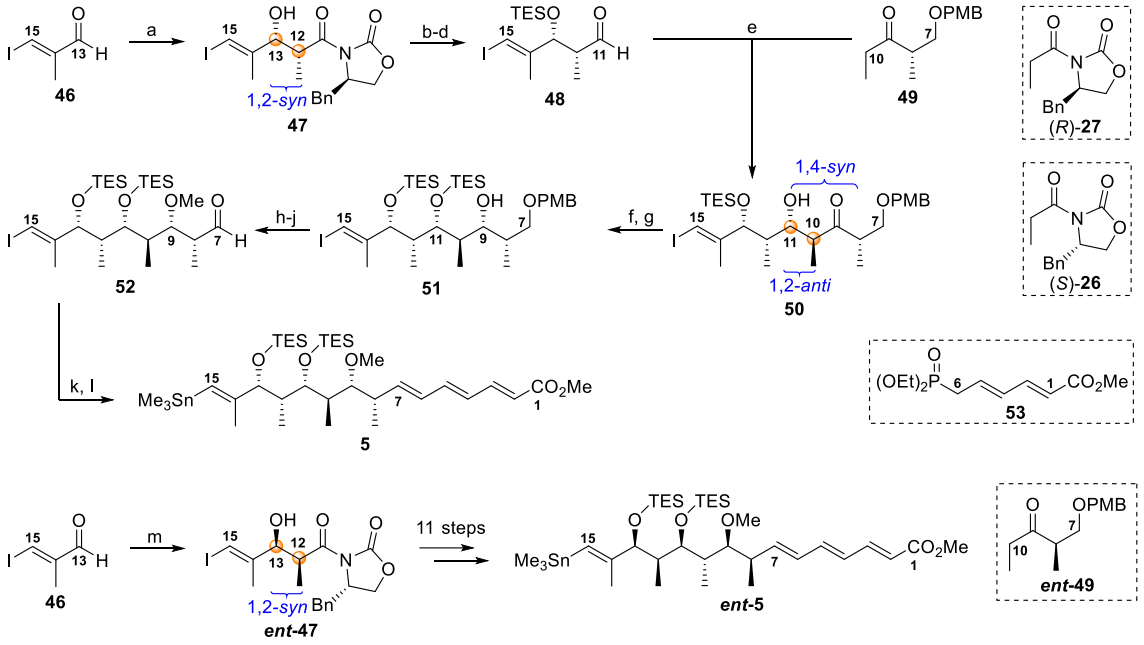

Reagents: (a) (*R*)-**27**, Bu_2BOTf, DIPEA, 0°C *then* aldehyde, –78°C to –20°C, 83%; (b) TESCl, imidazole, rt, 99%; (c) $LiBH_4$, 0°C, 65%; (d) $(COCl)_2$, DMSO, Et_3N, CH_2Cl_2, –78°C to –20°C, 99%; (e) ketone, *c*Hex_2BCl, Et_3N, Et_2O, 0°C *then* aldehyde, –78°C to –20°C, 65%, *dr* >20:1 dr; (f) TESOTf, 2,6-lutidine, CH_2Cl_2, 0°C, 70%; (g) DIBAL, –40°C, 70%; (h) $Me_3O{\cdot}BF_4$, Proton Sponges, 4Å MS, rt, 72%; (i) DDQ, CH_2Cl_2, pH 7 buffer, 0°C to rt, 99%, (j) DMP, $NaHCO_3$, CH_2Cl_2, 0°C to rt, 99%; (k) LDA, **53**,–78°C *then* aldehyde, –78°C to –20°C, 65%; (l) $(Me_3Sn)_2$, Li_2CO_3, $Pd(PPh_3)_2Cl_2$ (10 mol%), DMF, 80°C, 70%; (m) (*S*)-**26**, Bu_2BOTf, DIPEA, 0°C *then* aldehyde, –78°C to –20°C, 83%.

Scheme 4. Paterson synthesis of the C1-C15 region of hemicalide.[62]

1.4.2 Relative Configuration of the C16-C27 Region

In January 2013, the Ardisson group reported work on the C18-C24 region encompassing the α,β-dihydroxy-δ-lactone (**Figure 7a**).[56] This region includes five stereocentres, giving rise to 16 possible diastereomers. Noting that six-membered rings typically adopt well-defined conformations, the Ardisson group drew upon 1D and 2D NMR data from hemicalide, particularly NOESY correlations, to narrow the number of possible stereoisomers for this stereocluster. Given the steric bulk of the C19 and C21 alkyl chains, the ring was expected to adopt a chair conformation that places both of these groups equatorial. A large coupling constant, characteristic of a *trans* diaxial relationship, was shown between H19 and H20a ($^3J_{H19\text{-}H20a}$ = 11.5 Hz). Additionally, H22 exhibited nOe correlations with H20a, H24 and Me24. These observations are consistent with the δ-lactone adopting a chair conformation, in which the C21 hydroxyl is *cis* to both the C22 hydroxyl and the H19 oxymethine proton, but *trans* to the C19 alkyl chain. This analysis, which was supported by molecular modelling, allowed the possible diastereomers to be reduced from 16 to four (**54a-d**, **Figure 7b**).

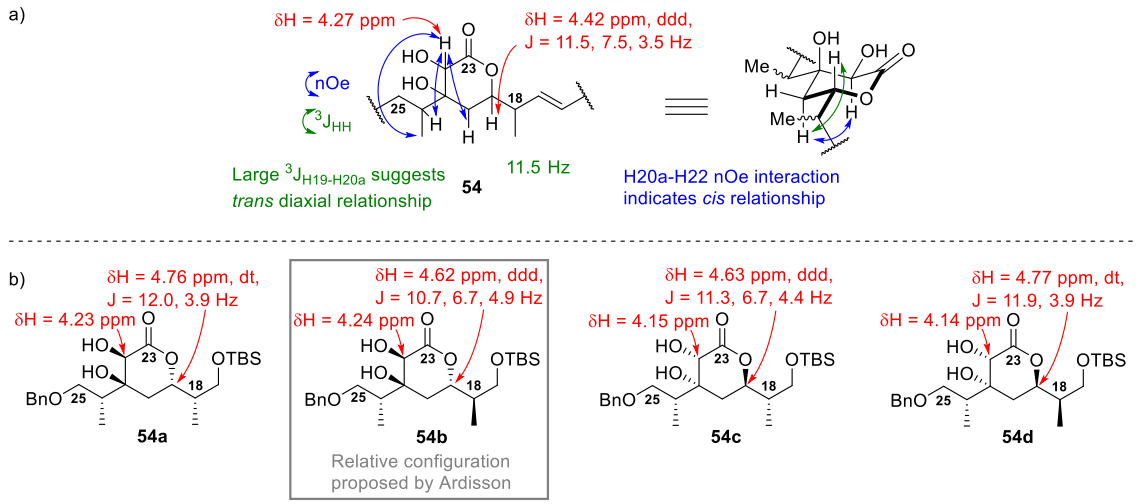

Figure 7. C17-C25 model diastereomeric fragments (**54a-d**) prepared by the Ardisson group[56]

In approaching the synthesis of these compounds, it was necessary to allow sufficient flexibility to provide controlled access to all four desired diastereomers. The C21,C22-*syn*-diol was recognised as a key structural motif prompting installation *via syn*-dihydroxylation, under substrate-control (**Scheme 5**). This revealed cyclic enoate **55**, which was proposed to arise from olefination of a suitably appended precursor of homoallylic alcohol **56**. The embedded 1,2- and 1,4-substitution in alcohol **56** signalled the potential for a substrate-controlled allylation, revealing allylsilane **57**

and aldehyde **31** or ***ent*-31**, as the required building blocks. Use of Roche ester (*R*)-**25** and (*S*)-**24** chiral pool building blocks facilitates access to all four diastereomer candidates.

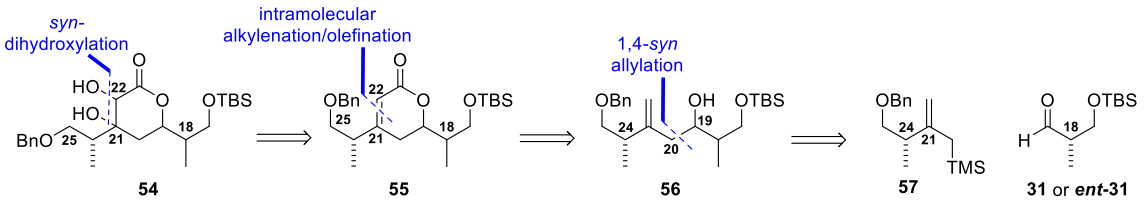

Scheme 5. Retrosynthesis of C17-C25 by Ardisson et al.[56]

Allylsilane **57** was accessed from (*R*)-**25** *via* a sequence of benzyl protection, Grignard addition to the ester carbonyl,[91] and Peterson olefination[92] (**Scheme 6**). Dias allylation[93–95] of allylsilane **57** with aldehyde **31** or ***ent*-31** gave 1,2-*syn* adduct **58a** or 1,2-*anti* adduct **58b**, respectively (*dr* <19:1), with diastereocontrol stemming from the allyl silane in a similar manner to a 1,4-*syn* aldol. Ring closing metathesis was initially attempted on acyclic enoate **59a** to secure enoate **55a**, but suffered from poor yields even under forcing conditions and with high catalyst loadings. Conversion of adduct **58a** to the phosphonate ester, under Steglich conditions,[96] and ozonolysis to C21 carbonyl **60a**, followed by intramolecular HWE olefination,[97] secured enoate **55a**. However, despite trialling a range of HWE conditions, this route was hampered by competing elimination. The key *syn*-dihydroxylation was then undertaken by OsO_4-mediated dihydroxylation to give dihydroxylactone **54a** (97%, *dr* >19:1). Dihydroxylactone **54b**, **54c** and **54d**, were accessed in a similar manner, with additional steps to allow for a Mitsunobu inversion of C19 (**61c** and **61d**) in the latter two compounds.

Upon ^{13}C NMR comparison of the model fragments with hemicalide, similar deviations were observed for all diastereomers. This did not allow any of the fragments to be excluded on the basis of ^{13}C NMR. Consequently, focus was turned to the ^{1}H NMR spectral data, particularly analysis of peak shape and multiplicity. In hemicalide, H20 and H24 were found as part of a broad 22 proton multiplet, while H18 and H25 were each present as separate broad multiplets. This limited the diagnostic value of these signals. Furthermore, the model compounds of these C17-C25 diastereomers (**54a-d**) bore C17 TBS ethers and C25 benzyl ethers. Due to the adjacent ethers in the model fragment, neither H18 nor H24 were in comparable chemical environments to their namesakes in hemicalide and were excluded from the evaluation. The H19 and H22 oxymethine protons were considered particularly crucial, as their chemical shift and peak shape were expected to noticeably change based on their relative configurations.

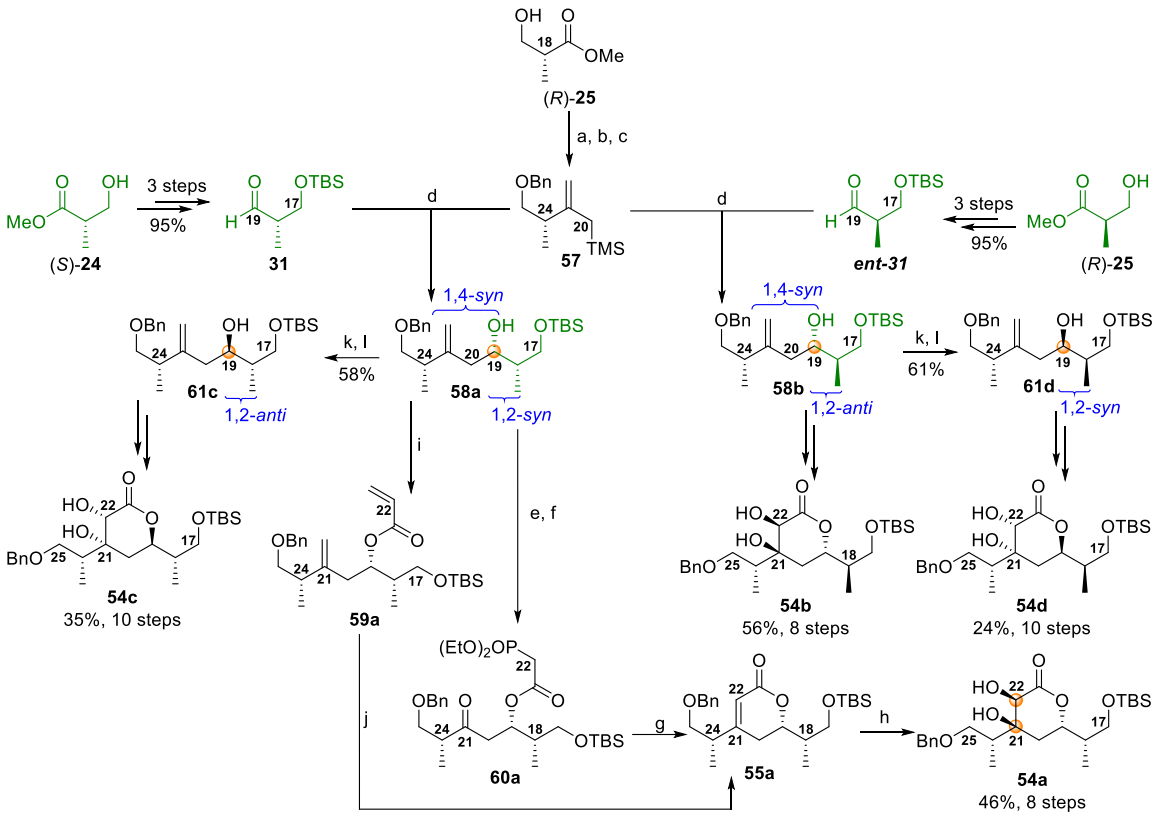

Reagents: (a) $BnOC(NH)CCl_3$, TfOH, *c*Hex/CH_2Cl_2 (2:1), rt, 85%; (b) $TMSCH_2MgCl$, CeCl3, THF, –78°C to rt, 67%; (c) Amberlyst-15, *n*Hex, rt, 90%; (d) $SnCl_4$, **57**, CH_2Cl_2, –78°C *then* **31** or ***ent*-31**, 74%-85%, *dr* <19:1; (e) DCC, DMAP, $HOOCCH_2P(O)(OEt)_2$, CH_2Cl_2, rt, quant.; (f) O_3, CH_2Cl_2, –78°C, Sudan Red, PPh_3, 91%; (g) LiO-*t*Bu 0.5M in THF (90 mol %), THF, 30-40°C, 70%; (h) $K_2SO_4{\cdot}2H_2O$ (5 mol %), NMO, acetone/H_2O, rt, 97%; (i) acryloyl chloride, Et_3N, CH_2Cl_2, rt, 99%; (j) Hoveyda-Grubbs II (30 mol %), PhMe, reflux, 15%; (k) *p*NO_2-C_6H_4-COOH, PPh_3, DIAD, THF, rt, 58-66%; (l) K_2CO_3, MeOH, rt, 93%-quant.

Scheme 6. Ardisson Synthesis of C17-C25 diastereomers **54a-d**.[56]

Diastereomers **54a** (δ_H = 4.23 ppm) and **54b** (δ_H = 4.24 ppm) with a *cis* relationship between H22 and Me24 were found to match more closely with H22 in hemicalide (δ_H = 4.21 ppm), while **54c** (δ_H = 4.15 ppm) and **54d** (δ_H = 4.14 ppm) were found to differ notably and were excluded from further consideration. Although the shift of H19 in the model diastereomeric fragments differed from hemicalide, its multiplicity was considered to be important. Both **54b** and **54d**, bearing 18,19-*anti* relationships, displayed ddd multiplicity for H19. Whereas, **54a** and **54d**, bearing 18,19-*syn* relationships, displayed dt multiplicity for H19. On this basis, Ardisson argued that the ddd multiplicity exhibited by H19 in hemicalide was consistent with an 18,19-*anti* relationship between the adjacent methyl and lactone acyloxy groups and, thus, asserted that **54b** reflected the configuration of the α,β-dihydroxy-δ-lactone stereocluster.

In March 2013, the Ardisson and Cossy groups reported a revised synthesis of the C16-C25 region of hemicalide.[57] After challenges with the previous C17 aldehyde group, particular importance was placed on installation of an appropriate coupling handle at C16. Furthermore, given the

elimination issues experienced with the previous ring closure approach, promotion of efficient, high yielding strategies and avoidance of product loss were also treated as key focusses.

In this revised route, the C16 tri-substituted vinyl bromide coupling handle was incorporated early in the synthesis (**Scheme 7**). Vinyl bromide aldehyde **62** was prepared in three steps from Roche ester (*S*)-**24** as an inseparable mixture of isomers (*E/Z* = 85:15). An initially trialled route to ketone **63**, analogous to the earlier synthesis of the C17-C25 region,[56] involved a tin-mediated Dias allylation[93–95] between allylsilane **57** and vinyl bromide aldehyde **62** to give adduct **64** (*dr* >19:1). This was followed by bromoacetyl bromide addition and ozonolysis to obtain ketone **63** (31% over three steps). However, a titanium-mediated 1,2-*anti* aldol reaction[98] (*dr* 9:1) between ketone *ent*-**65** and allylsilane **57**, followed by acylation of the C19 alcohol with bromoacetyl bromide, provided a more efficient route to ketone **63** (73% over two steps).

The α,β-unsaturated lactone **66** was obtained by a samarium diiodide-induced intramolecular Reformatsky reaction,[99] followed by dehydration, in much improved yield (79%) compared to previous pathways (15%-64%). *Syn*-dihydroxylation was carried out as before to give diol **67** (*dr* >19:1). Subsequent *bis*-TES protection and palladium-catalyzed borylation of the vinyl bromide functionality delivered target C16-C25 intermediate **68**.

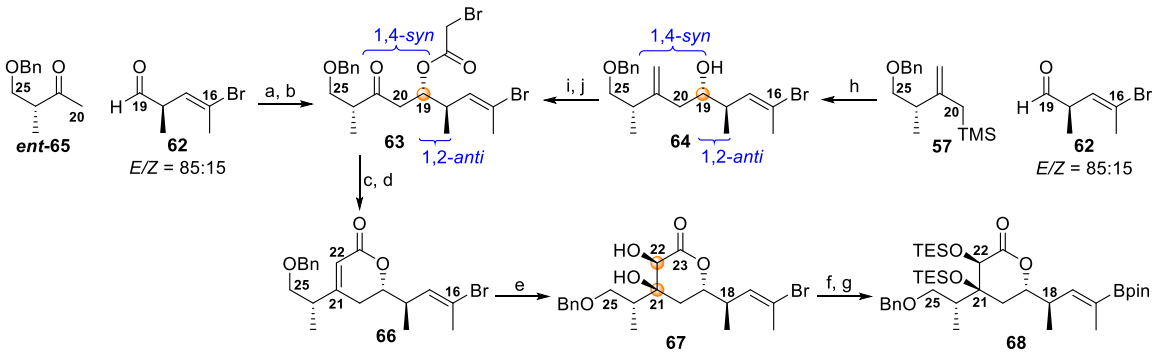

Reagents: (a) $TiCl_4$, *i*Pr_2NEt, *ent*-**65**, CH_2Cl_2, –78°C *then* **62**, 73%, *dr* 9:1; (b) $BrCH_2COBr$, Py, CH_2Cl_2, 0°C, quant.; (c) SmI_2, THF, rt; (d) $SOCl_2$, Py, CH_2Cl_2, 0°C, 79% (over two steps); (e) $K_2SO_4{\cdot}2H_2O$ (5 mol %), NMO, acetone/H_2O, rt, quant., >19:1; (f) TESOTf, 2,6-lutidine, CH_2Cl_2, rt, 77%; (g) $PdCl_2(PPh_3)_2$ (2.4 mol %), PPh_3 (4.8 mol %), PhOK, B_2pin_2, THF, 82%; (h) $SnCl_4$, CH_2Cl_2, –78°C *then* **62**, 62%; (i) $BrCH_2COBr$, Py, CH_2Cl_2, 0°C; (j) O_3, Sundan Red III, CH_2Cl_2, –78°C *then* PPh_3, 50% (over two steps).
Scheme 7. Ardisson optimised synthesis of C16-C25 protected dihydroxylactone **68**, with coupling handle, as part of the synthesis of the C1-C27 region of hemicalide.[57]

The Paterson group were sceptical about the 18,19-*anti* assignment asserted in both of the preceding Ardisson α,β-dihydroxylactone syntheses.[60] It was noted that a similar δ-lactone **69**, synthesised *en route* to rhizoxin D,[100] showed a ddd multiplicity for the relevant oxymethine

proton in a *syn* arrangement (**Figure 8a**). Furthermore, the analogous 36,37-*syn* relationship, in C36-C42 α-hydroxy-δ-lactone fragment **70** (**Figure 8b,**) reported by the Cossy group in 2014 and 2015,[59] also resulted in ddd multiplicity for the oxymethine proton. This is in contrast with the dt multiplicity of the oxymethine proton that resulted from the Ardisson group synthesis of C16-C25 intermediate **67** (**Figure 8c**). To assess these apparent discrepancies, DP4f calculations were undertaken on all 16 possible diastereomers for the C13-C27 region, incorporating the relevant substitution patterns to more closely resemble the NP (e.g. DP4f model **71**, **Figure 8d**).[60] These calculations indicated with 99% probability that, on the basis of ^{1}H and ^{13}C NMR data, diastereomer **71**, with an 18,19-*syn* relationship matching the relative configuration of **54a** (**Figure 7b**), was consistent with the relative configuration of the α,β-dihydroxy-δ-lactone in hemicalide. In contrast, the **54b** diastereomer, asserted by Ardisson, had a 1% probability. To fully evaluate this assertion, synthesis of intermediates ***ent-4*** and **72** (**Figure 8e** and **Figure 8f**) was undertaken within the Paterson group and reported in 2016.[60]

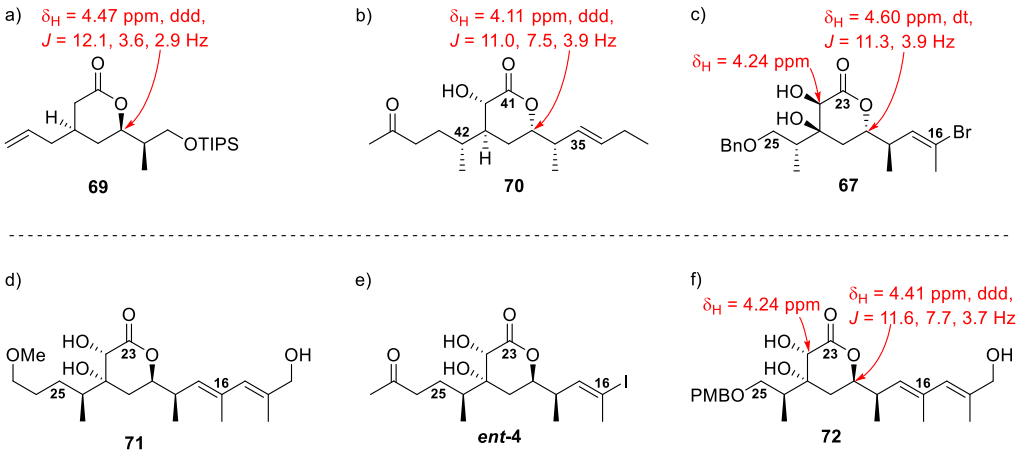

Figure 8. a) Rhizoxin D δ-lactone fragment (**69**);[100] b) C32-C46 diastereomer (**70**) synthesised by Cossy et al.[59]; c) C16-C25 intermediate (**67**) synthesised by Ardisson et al.;[57] d) Example C13-C27 model hemicalide fragment (**71**) bearing the most probably relative stereochemistry as predicted by DP4f analysis;[101] e) C16-C28 hemicalide intermediate (*ent*-**4**) synthesised by MacGregor et al.[60,101] and f) C13-C25 intermediate (**72**) synthesised by MacGregor et al.[60,101]

Noting the revised 1,4-*syn* relationship between the C19 oxygen substituent and Me24, a boron-mediated aldol reaction was envisioned between methyl ketone *ent*-**73**[102] and aldehyde **74**, both of which are accessible from Roche ester (*S*)-**24**. A Corey-Fuchs[103] reaction, followed by elimination-methylenation on aldehyde **75**, gave alkyne **76** (**Scheme 8**).[104] Regioselective hydrozirconation[105] and iodination provided the (*E*)-vinyl iodide analogue. PMB deprotection and DMP oxidation[83] then gave aldehyde **74**.

As mentioned (*vide supra*), boron-mediated aldol reactions have previously been extensively used in the Paterson group to install 1,4-*syn* relationships with high selectivity.[106–108] However, to ensure high levels of diastereoselectivity during the formation of the C19-C20 bond, chiral ligands are sometimes needed on the boron Lewis acid to enhance the inherent 1,4-*syn* diastereoselectivity. Here, an asymmetric (–)-Ipc$_2$BCl-mediated aldol reaction provided aldol adduct **77** (>20:1 *dr*). Protection of the alcohol as its TBS ether, followed by a lithium-mediated aldol reaction gave adduct **78**. Concomitant deprotection and lactonisation, under fluorous conditions, and subsequent dehydration gave unsaturated lactone **79**.

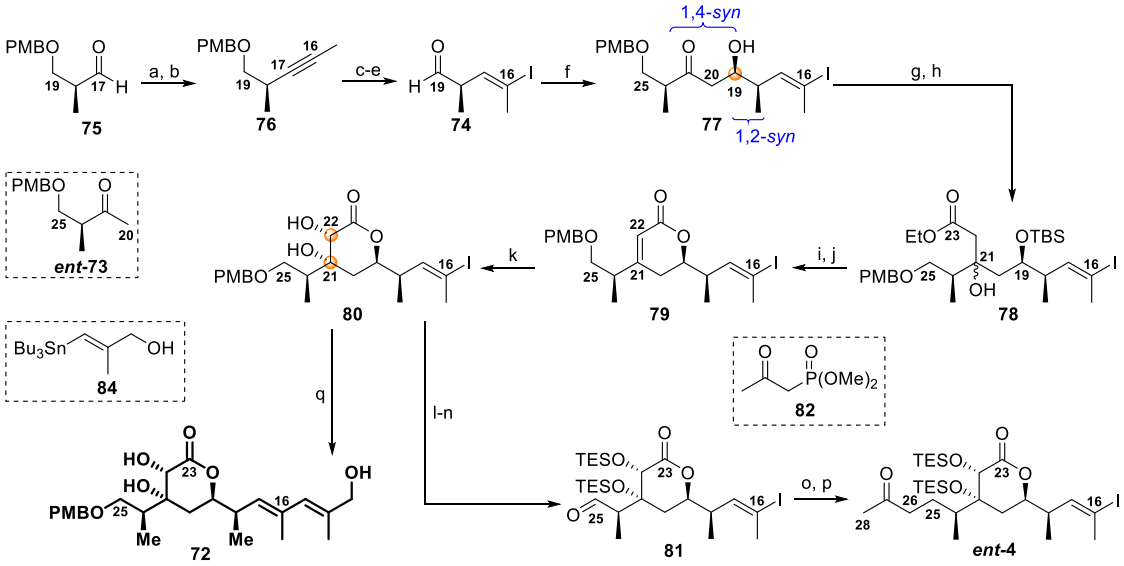

Reagents: (a) CBr_4, PPh_3, CH_2Cl_2, –78°C to 0 °C, 75%; (b) nBuLi, MeI, THF, –78°C to 0°C, 94%; (c) Cp_2ZrCl_2, DIBAL, THF, 0°C to rt *then* I_2, –78°C, 88%; (d) DDQ, CH_2Cl_2, pH 7 buffer, 0°C to rt, 90%; (e) DMP, $NaHCO_3$, CH_2Cl_2, 0°C to rt, 80%; (f) *Ent*-**73**, (–)-Ipc$_2$BCl, Et_3N, Et_2O, 0°C *then* **74**, –78°C to –20°C, 70%, *dr* >20:1; (g) TBSOTf, 2,6-lutidine, CH_2Cl_2, –78°C to 0°C, 95%; (h) EtOAc, LDA, THF, –78°C to 0°C, 97%; (i) HF·py, py, THF, 0°C to rt, 85%; (j) Ac_2O/py/PhH, DMAP, reflux, 83%; (k) $K_2OsO_4.2H_2O$ (2 mol%), NMO, citric acid, *t*BuOH/H_2O/THF, rt, 85% *brsm*; (l) TESOTf, 2,6-lutidine, CH_2Cl_2, 0°C, 88%; (m) DDQ, CH_2Cl_2, pH 7 buffer, 0°C to rt, 80%; (n) DMP, $NaHCO_3$, CH_2Cl_2, 0°C to rt; (o) $Ba(OH)_2$, **82**, THF, 0°C to rt, 64% (over 3 steps) (p) $[Ph_3PCuH]_6$, PhMe, rt, 67%; (q) $Pd(PPh_3)_4$ (20 mol%), CuTC, $[Ph_2PO_2][NBu_4]$, **84**, DMF, 0 °C, 74%.
Scheme 8. Paterson group synthesis of C16-C28 (*ent*-**4**) and C13-C25 (**72**) fragments of hemicalide.[60]

With lactone **79** in hand, a *syn*-dihydroxylation, under osmium tetroxide conditions, also utilised in the Ardisson group synthesis,[56] delivered dihydroxylactone **80** as a single diastereomer. *Bis*-TES protection of the diol, followed by C27 PMB cleavage and DMP oxidation, gave aldehyde **81**. HWE olefination[109] with phosphonate **82** and reduction of the enone[110] culminated in C16-C28 ketone ***ent*-4**. This fragment is equipped with appropriate coupling handles for connection to other hemicalide fragments and was subsequently used in the Paterson group synthesis of the two possible C1-C28 diastereomers 13,18-*syn*-**83a** and 13,18-*anti*-**83b** (*vide infra*, **Figure 10**). To aid spectroscopic comparison with hemicalide, C13-C25 diene **72** was synthesised by Stille coupling

of dihydroxylactone **80** with stannane **84**. This delivered C13-C25 diene **72**, a model compound having greater similarity with hemicalide for NMR spectroscopic comparison purposes, and with DP4f model fragment **71**, to validate the computational predictions.

Intermediate **72**, bearing an 18,19-*syn* relationship, showed much closer agreement with hemicalide than diastereomer **54b** asserted by Ardisson, which displayed an 18,19-*anti* relationship. This was true for the diagnostic H19 ($|\Delta\delta_H|$ = 0.01 ppm) and H22 signals ($|\Delta\delta_H|$ = 0.04 ppm), which exhibited much smaller ^{1}H NMR chemical shift differences. Crucially, the H19 oxymethine proton exhibited matching ddd peak multiplicity and very similar coupling constants (*J* = 11.6, 7.7, 3.7 Hz) when compared to hemicalide (*J* = 11.3, 7.5, 3.5 Hz) (**Figure 8c**). This is in contrast to the dt multiplicity for H19 displayed in Ardisson's truncated C18-C25 18,19-*syn* diastereomers, **54a** and **54d**. This change in peak shape may be caused the close proximity of the C17 TBS ether, a feature that is not present in the natural product nor in C13-C25 fragment **72** synthesised by the Paterson group. Importantly, the Paterson synthesis provided firm evidence for an 18,19-*syn* relationship, allowing a more confident assignment of the relative stereochemistry within the α,β-dihydroxy-δ-lactone stereocluster.

In 2016, based on these revised findings, the Ardisson group synthesised a C16-C27 fragment **85** bearing the 18,19-*syn* relationship, as part of a C1-C27 region diastereomer.[61] They evolved their synthetic approach, starting from (*S*)-citronellol as a chiral pool molecule to pre-set the C24 methyl stereocentre. TES protection of (*S*)-citronellol, followed by an ozonolysis, reduction sequence gave primary alcohol **86** (**Scheme 9**), which was then telescoped through a five-step sequence, without purification. This involved benzyl protection of the primary alcohol, followed by Swern oxidation[69–72] and Pihko homologation[111] to produce α,β-unsaturated aldehyde **87**. Reduction and benzoyl protection completed the process, giving allylic benzoate **88**. Palladium-mediated stannylation of allylic benzoate **88**, under Trost conditions,[112,113] gave allylstannane **89**. The C16-C19 region was then introduced *via* 1,2-*syn* selective allylation of allylstannane **89** with aldehyde **90**, under Williams conditions.[114–116] The diastereoselection in this reaction is controlled by the allyl substrate, *via* the 1,4-*syn* interaction, matching with the Felkin selectivity of aldehyde **89**, producing 18, 19-*syn* vinyl bromide **91**. Acylation with acryloyl chloride delivered intermediate **92** ready for ring closing metathesis.

Ardisson/Cossy also revised their approach to the α,β-unsaturated lactone moiety. A return to the ring closing metathesis approach initially explored[56] was facilitated by identification of a suitable

ruthenium catalyst for sterically demanding systems. This led to selection of Nolan's catalyst (10 mol %), which achieved a much improved yield of α,β-unsaturated lactone **93**. Subjection of lactone **93** to *syn*-dihydroxylation gave diol **94**, for comparison to hemicalide. Diol **94** exhibited an improved fit with the NMR data for hemicalide. This was particularly the case for the diagnostic H/C19 and H/C22 in both the ^{1}H and ^{13}C NMR spectra. Subsequent *bis*-TES protection gave target C16-C27 fragment **85**. Palladium-catalysed borylation of the vinyl bromide functionality delivered boronate **95**, ready for coupling with the C1-C15 region. Overall this synthesis acts to further validate the 18,19-*syn* relationship and corroborates the assertions of the earlier Paterson work.[60]

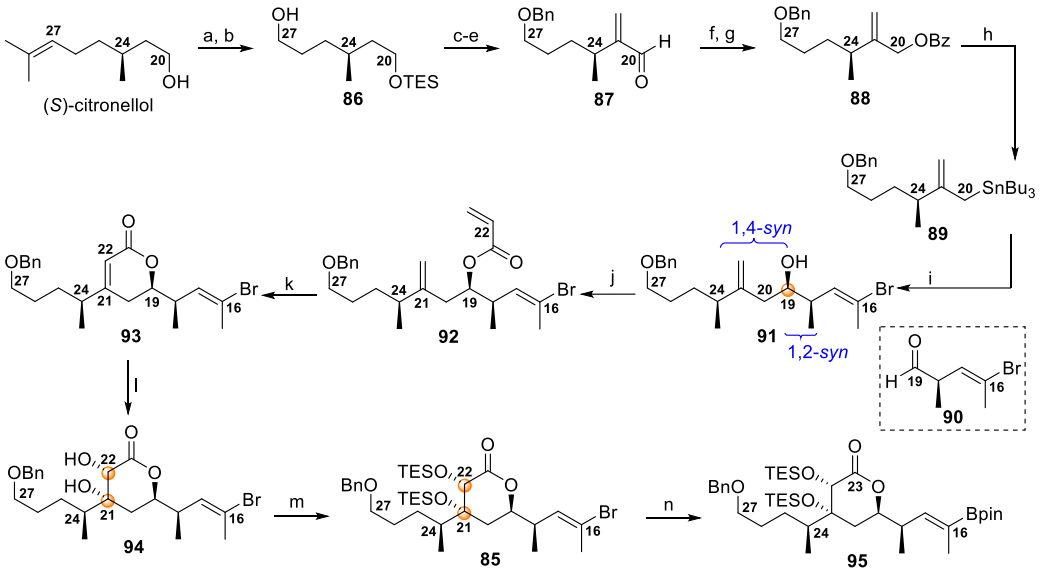

Reagents: (a) TESCl, Et_3N, CH_2Cl_2, 0°C to rt, quant.; (b) O_3, CH_2Cl_2, –78°C *then* $NaBH_4$, MeOH, rt, quant.; (c) NaH, THF, 0°C *then* BnBr, TBAI, 0°C; (d) $(COCl)_2$, DMSO, –78°C to –45°C *then* alcohol, –78°C *then* Et_3N, –78°C to rt; (e) HCHO (35 wt. % in H_2O), pyrrolidine, propionic acid, *i*PrOH, 45°C; (f) $LiAlH_4$, THF, 0°C; (g) benzoyl chloride, Et_3N, rt (64% over five steps); (h) $(nBu_3Sn)_2$, Et_2AlCl, *n*BuLi, $Pd(PPh_3)_4$, THF, –78°C to rt, quant.; (i) (*R*, *R*)-1,2-diamino-1,2-piphenylethane *bis*(sulfonamide), BBr_3, CH_2Cl_2, 0°C *then* **89**, rt *then* **90**, –78°C, 78%, *dr* 88:12, 69% of **91** isolated; (j) acryloyl chloride, *i*Pr_2EtN, CH_2Cl_2, –78°C, 91%; (k) Nolan catalyst (10 mol %), PhMe, 100°C, 83%; (l) $K_2OsO_4{\cdot}2H_2O$ (2 mol %), NMO, citric acid, THF/H_2O (8:2), rt, 70%; (m) TESOTf, 2, 6-lutidine, CH_2Cl_2, 0°C, 96%; (n) B_2pin_2, $PdCl_2(PPh_3)_2$, $PPhs_3$, KOPh, 50°C, 66%.

Scheme 9. 2016 Ardisson/Cossy synthesis of the C16-C27 region of hemicalide with reassigned stereochemistry, as part of the synthesis of the C1-C27 region of hemicalide.[61]

1.4.3 Relative configuration of the C1-C24 Region: Assessing the relationship between the C1-C15 polypropionate and C16-C27 α,β-dihydroxy-δ-lactone stereoclusters

In 2013, the Ardisson group reported the synthesis of C1-C25 moiety **96**, one of the possible stereoisomers of the C1-C25 region (**Figure 9a**).[57] This fragment bore a 13,18-*anti* relationship and preserved the previously asserted 18,19-*anti* relationship in the α,β-dihydroxy-δ-lactone

stereocluster. In the absence of clear rationale, it appears that the 13,18-*anti* diastereomer was arbitrarily chosen.

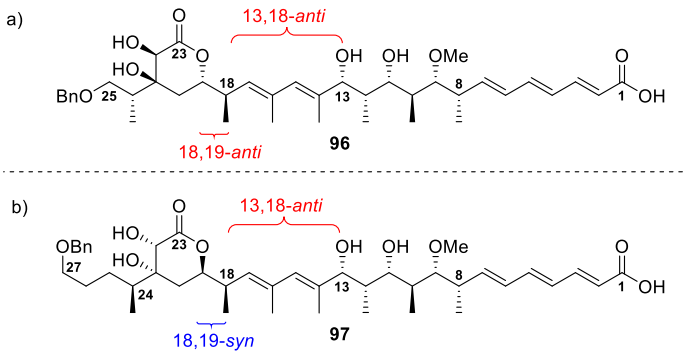

Figure 9. a) Proposed C1-C25 fragment **96** of hemicalide by the Ardisson group;[57] and b) Proposed C1-C27 fragment **97** of hemicalide by the Ardisson group.[61]

The syntheses of C1-C15 vinyl iodide **20a** and C16-C25 boronate **68** have been previously described (see sections **1.4.1** and **1.4.2**, respectively). Suzuki-Miyaura coupling of these fragments proceeded efficiently to give C1-C25 *E*, *E*-diene **98** (**Scheme 10**). Global deprotection, using TASF, followed by HF·pyridine in pyridine, proceeded with some difficulty, giving only a moderate 40% yield of C1-C25 fragment **96**.

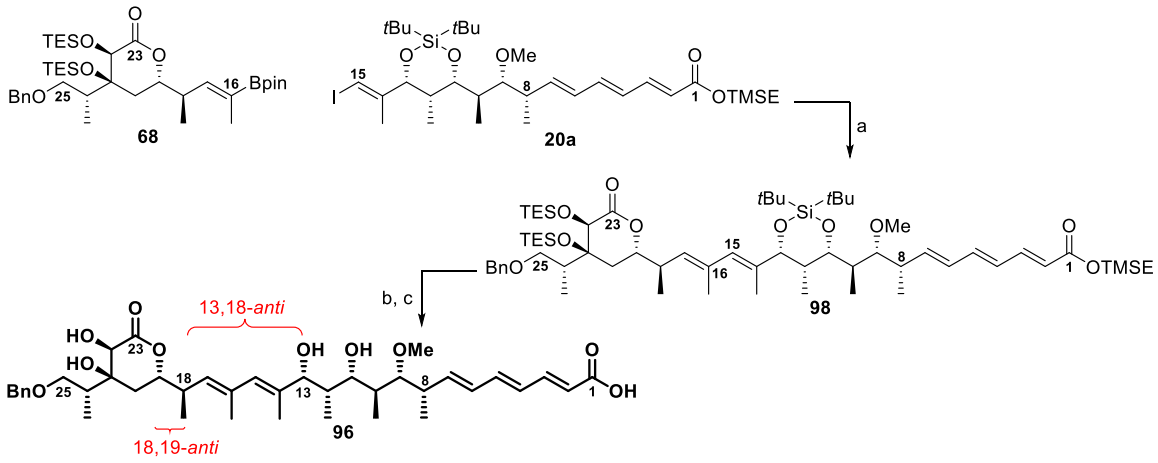

Reagents: (a) $Pd(PPh_3)_4$ (1 mol%), TlOEt, THF/H_2O (3:1), rt, 97%; (b) TASF, DMF, rt; (c) HF·py, py, THF, 0°C, 40% (over two steps).
Scheme 10. 2013 Ardisson/Cossy synthesis of the C1-C25 region of hemicalide.[57]

This fragment resulted in a generally reasonable fit for the hemicalide NMR data. The deviation seen for the conjugated trienic acid (*vide supra*) was again apparent, but the C8-C24 region showed reasonable agreement with the ^{1}H ($|\Delta\delta_H| \leq 0.12$ ppm) and ^{13}C ($|\Delta\delta_C| \leq 1.2$ ppm) NMR data. It was within the α,β-dihydroxy-δ-lactone stereocluster that the most significant deviations

were observed, particularly at the C18 and C19 centres. In the ^{13}C NMR comparison, the largest difference was at C18 compared to hemicalide ($|\Delta\delta_C|$ = 1.2 ppm). In the ^{1}H NMR, the largest differences were at the diagnostic H19 ($|\Delta\delta_H|$ = 0.12 ppm) and H22 ($|\Delta\delta_H|$ = 0.10 ppm) centres.

These discrepancies, especially in light of the Paterson assertion of an 18,19-*syn* relationship,[60] appear to have prompted Ardisson group work reported in 2016, where C1-C27 fragment **97** bears an 18,19-*syn* relationship (**Figure 9b**).[61] The route began with modified C16-C27 boronate **95** (see section **1.4.2**), bearing the 18,19-*syn* relationship, but in the context of an enantiomer that would lead to a C1-C27 diastereomer that maintained the 13,18-*anti* relationship previously reported.[57] Suzuki-Miyaura[117,118] coupling of C16-C27 boronate **95** to vinyl iodide **20a** provided C1-C27 *E*,*E*-diene **99**, subsequent global deprotection using TASF, followed by HF·pyridine in pyridine, gave 13,18-*anti* diastereomer **97** (**Scheme 11**).

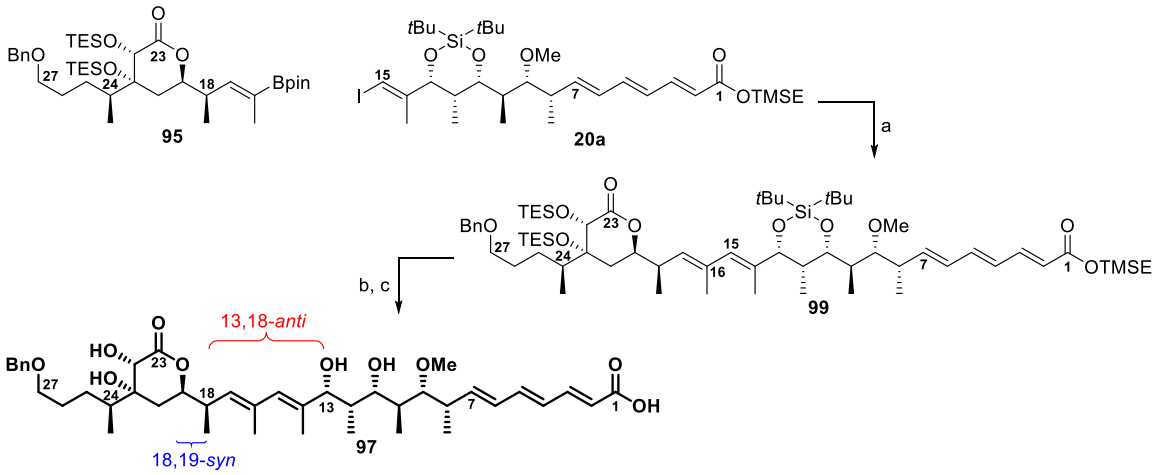

Reagents: (a) $Pd(PPh_3)_4$, TlOEt, THF, rt, 82%; (b) TASF, DMF, rt; (c) HF·py, py, THF, 0°C, 90% (over two steps).
Scheme 11. 2016 Ardisson/Cossy synthesis of the C1-C27 region of hemicalide.[61]

Seeking more definitive stereochemical proof for the relationship between the C8-C13 and C18-C24 stereoclusters and, thus, the relative configuration of the whole of the C1-C28 region, the Paterson group synthesised the two diastereomeric possibilities (13,18-*syn*-**100a** and 13,18-*anti*-**100b**, **Figure 10a**) and their corresponding sodium carboxylate salts.[62] This synthesis, conducted by Han and Lam, incorporates the asserted 18,19-*syn* relationship. Crucially, the synthesis of both diastereomers (13,18-*syn*-**100a** and 13,18-*anti*-**100b**) allowed comprehensive spectroscopic evaluation against the natural product. Although the C13 and C18 centres are in a distal 1,6-relationship, separated by an *E*,*E*-diene, previous work towards the total synthesis of leiodermatolide (**101**) noted spectroscopic deviations for diastereomers across similar systems (**Figure 10b**).[81] Deviations may not be large across in such distal relationships, but were

observable. In these cases, reference to coupling constants and multiplicity was also found to be assistive. This precedent provided some support that valuable spectroscopic differences may be observed, despite the distal relationship between the two stereoclusters.

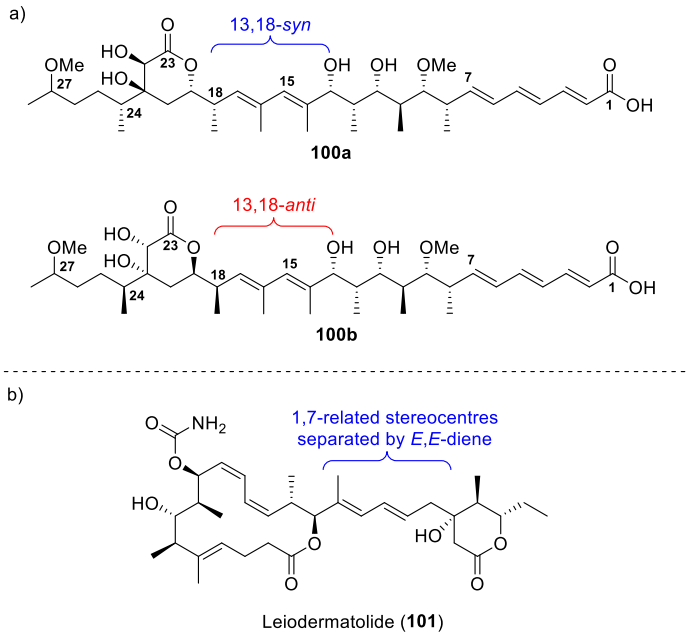

Figure 10. a) Possible diastereomers of the C1-28 region of hemicalide (**100a-b**) proposed by the Paterson group;[62] b) Leiodermatolide (**101**) acts as an example of a distal 1,7-related stereochemical relationship across which deviations were seen for different diastereomeric candidates.[81]

The Paterson group syntheses of both enantiomers of the C1-C15 and C16-C28 regions has been described (see sections **1.4.1** and **1.4.2**, respectively). The positioning of the coupling handles turned out to be an important consideration. It was necessary to install the stannane handle at C15, as experimentation revealed that reversal of the coupling handles, with the stannane affixed to C16, resulted in an unstable compound prone to rapid decomposition. In line with this, the C15 vinyl iodide was transformed to a stannane, under Wulff-Stille conditions[90] to give C1-C15 stannane **5** (**Scheme 4**). The enantiomeric series was synthesised analogously, but utilising oxazolidinone (*S*)-**26** in the original 1,2-*syn* Evans aldol reaction to give *ent*-**48,** and undergoing a 1,4-*syn* boron-mediated aldol with ketone ***ent*-49** to set the absolute stereochemistry of the C8-C13 stereohexad. Stille-Migita coupling[119] of C1-C15 stannane **5** to C16-C28 α,β-dihydroxy-δ-lactone **4**,[62] previously reported by the Paterson group in the enantiomeric series,[60] afforded C1-C28 ketone 13,18-*syn*-**83a** (**Scheme 12**). In a similar manner coupling C1-C15 stannane *ent*-**5** with C16-C28 vinyl iodide **4** afforded C1-C28 ketone 13,18-*anti*-**83b**.

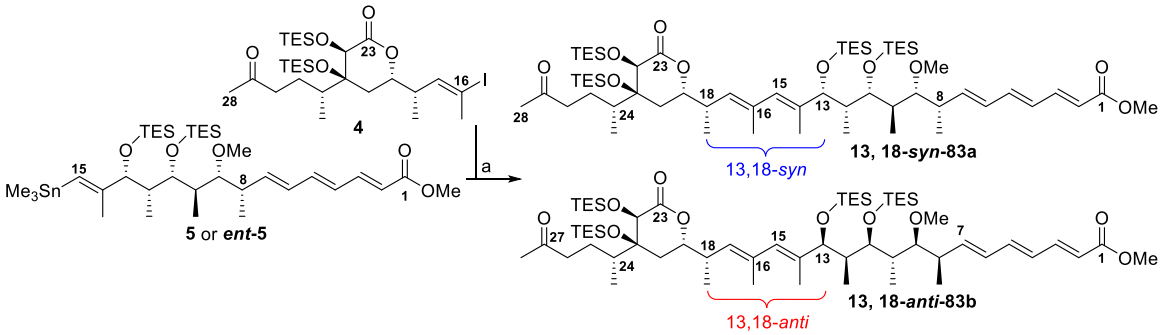

Reagents: (a) $Pd(PPh_3)_4$ (20 mol%), **4**, CuTC, DMF, 0°C, 72%.
Scheme 12. Paterson group synthesis of the C1-C28 region of hemicalide[62]

To attain greater similarity with hemicalide for NMR spectroscopic comparison purposes, the C27 ketone was converted to the methyl ether, the system deprotected and the terminal methyl ester hydrolysed to the acid (**Scheme 13a**). The step order in this process was crucial, as earlier work by MacGregor[101] had shown that global deprotection of C16-C28 ketone *ent*-**4** resulted not only in deprotection, but also undesirable spiroacetal (**102**) formation, limiting any useful structural comparison (**Scheme 13b**). However, attempts to stereoselectively reduce the C27 ketone proved unfruitful. At this point, consideration was given to the fact that the configuration of the similarly distal C45 centre has little spectroscopic effect on the C36-C42 α-hydroxy-δ-lactone stereocluster.[58,59] By analogy, it was reasoned that the configuration of the C27 centre was unlikely to have a large impact on the chemical shifts within the C18-C24 stereocluster. On this basis, reduction of the C27 ketone in 13,18-*syn*-**83a** was carried out non-selectively ($NaBH_4$) (**Scheme 13a**). The resulting alcohol was methylated to give ether **103a**. Successive treatment with TASF and HF·py/py effected global deprotection and ester hydrolysis afforded target fragment 13,18-*syn*-**100a**. Analogous manipulations on 13,18-*anti*-**83b** afforded 13,18-*anti*-**100b**.

The extended 13,18-*anti*-**100b** fragment (**Figure 10**) correlated very well with Ardisson's C1-C27 fragment **97** (**Figure 9b**), reinforcing the validity of the Paterson structure. The spectroscopic differences between 13,18-*syn*-**100a** and 13,18-*anti*-**100b** in the ^{1}H NMR and ^{13}C NMR were noticeable, but not very large ($\sum|\Delta\delta_H| = 0.43$ ppm; $\sum|\Delta\delta_C| = 3.0$ ppm; $|\Delta\delta_H| \leq 0.05$ ppm, $|\Delta\delta_C| \leq 0.5$ ppm). Importantly, both showed relevant differences between the fragments when compared to hemicalide. The global absolute and maximum errors between 13,18-*syn*-**100a** and hemicalide ($|\Delta\delta_H| \leq 0.01$ ppm, $|\Delta\delta_C| \leq 0.1$ ppm) were measurably reduced compared to 13,18-*anti*-**100b** ($|\Delta\delta_H| \leq 0.04$ ppm, $|\Delta\delta_C| \leq 0.6$ ppm), indicating that hemicalide is more likely to possess the 13,18-*syn* relationship.

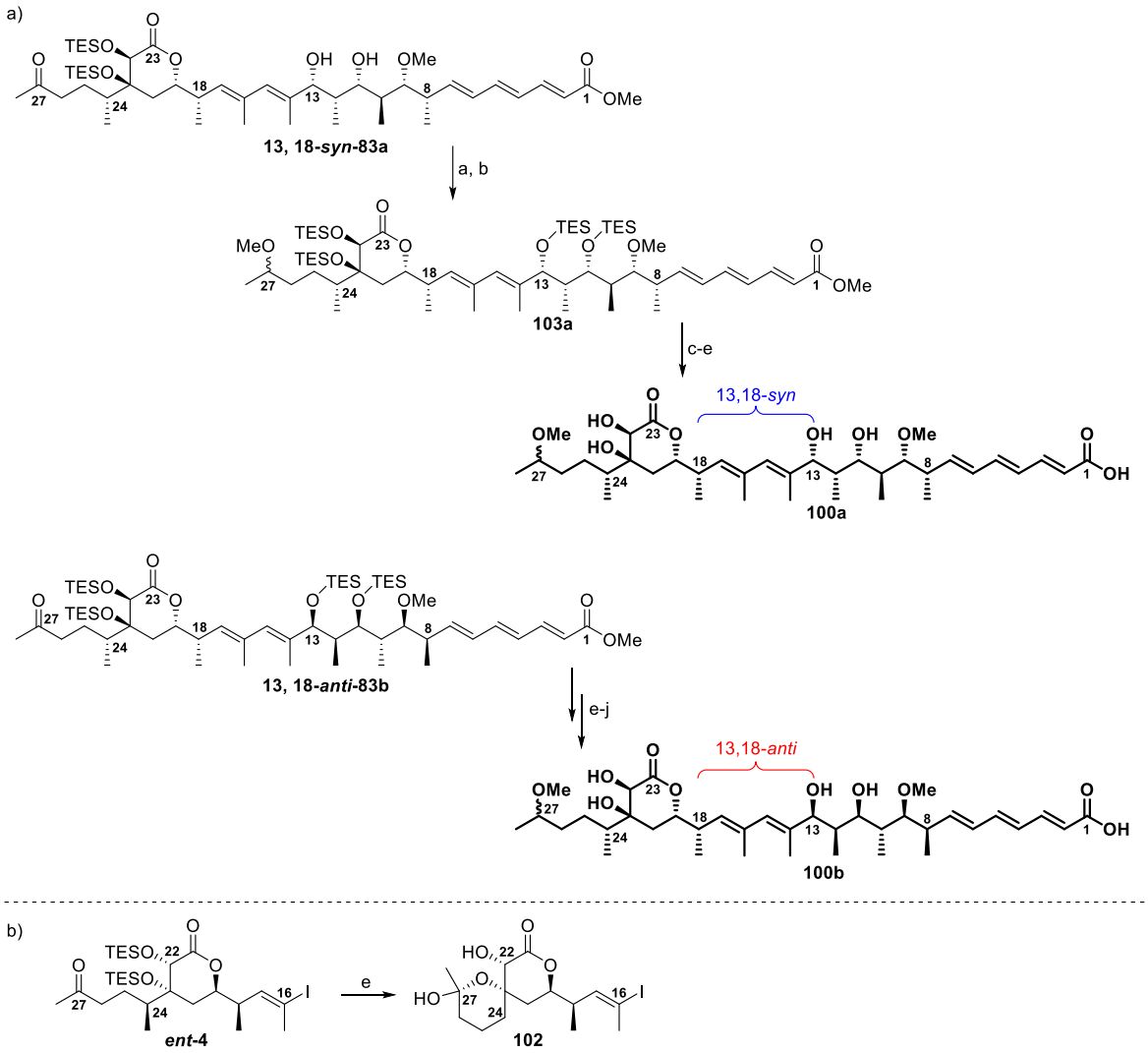

Reagents: (a) $NaBH_4$, MeOH, 95%; (b) $Me_3O{\cdot}BF_4$, Proton Sponge®, 4Å molecular sieves, CH_2Cl_2, 87%; (c) TASF, THF/DMF, 0°C; (d) HF·py/py, THF, 0°C, 95% (over 2 steps); (e) $Ba(OH)_2{\cdot}8H_2O$, MeOH, 50%; (f) $NaBH_4$, MeOH, 92%; (g) $Me_3O{\cdot}BF_4$, Proton Sponge®, 4Å molecular sieves, CH_2Cl_2, 68%; (h) TASF, THF/DMF, 0°C; (i) HF·py/py, THF, 0°C, 67% (over 2 steps); (j) $Ba(OH)_2{\cdot}8H_2O$, MeOH, 50%.

Scheme 13. a) Paterson group manipulation of C1-C28 ketones **83a** and **83b** to attain fully deprotected C1-C27 fragments **100a** and **100b** for spectral comparison purposes; b) Undesirable spiroacetalisation occurring upon deprotection of ketone *ent*-**4**.

Consistent with the Ardisson group's earlier observations (*vide supra*), it was noted that the protonation state of the acid significantly affected the shifts in the trienoic acid region. Interestingly, comparisons of both the acids and the carboxylate salts of each diastereomer showed better correlation between the acids and hemicalide, than the corresponding salts, indicating that hemicalide was likely to have been isolated as the acid. Collecting data across a range of pH values indicated that the shifts in the trienoic acid region are quite pH dependent.[62] This contrasts with Ardisson's earlier assertions (*vide supra*) that hemicalide was isolated in its carboxylate salt form.[54] Importantly, the most recent Paterson group synthetic work towards the

C1-C28 region of hemicalide achieves a comprehensive assignment of the relative configuration across this substantial region of hemicalide.

1.4.4 Relative Configuration of the C25-C34 Polyacetate Stereotetrad

Currently there have been no synthetic nor computational studies reported on the C25-C34 polyacetate moiety. A key reason for this is the fact that stereochemical assignment of this region, through spectroscopic comparison, is particularly difficult. This region bears four stereocentres, giving rise to eight possible diastereomers (**104a-h**, **Figure 11**). Over 50% of the ^{1}H NMR signals for this region (H25, H26, H28, H30, H32, H33) are obscured within a broad 22 proton multiplet, spanning the 2.02-1.22 ppm region.[1] Unfortunately, the remaining ^{1}H NMR signals (H27, H29, H31) are reported in the original patent only as broad multiplets, with no associated coupling data provided. The ^{13}C NMR data is comparably ambiguous, with the exception of C30, which exhibits an unusually low shift (δ_C = 33.0 ppm). Although 1,3,5-oxygenation patterns are common in MNP polyketides, the dimethoxy-hydroxy motif appears only to have been found in hemicalide. Thus, comparison with other literature NPs, such as those in Kishi's database,[120] has not been assistive.

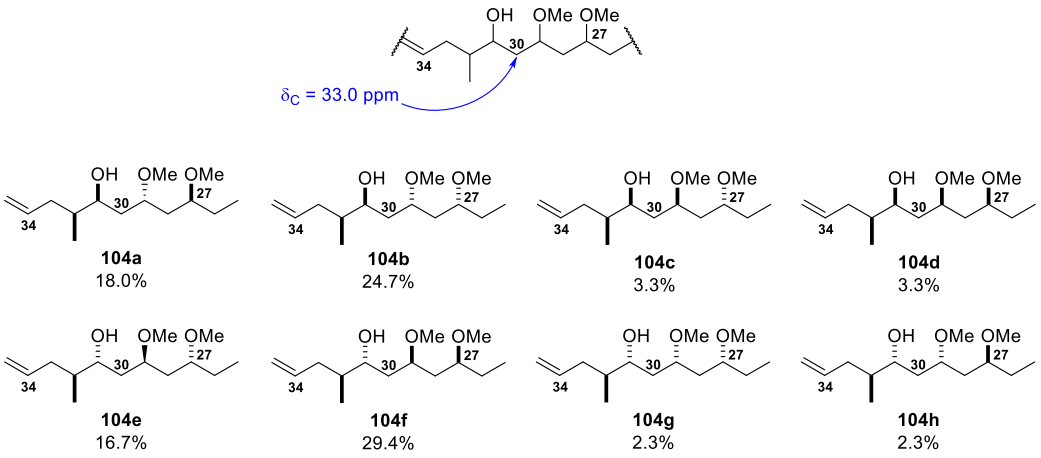

Figure 11. MacGregor's C25-C34 model diastereomers (**104a-h**) used in DP4f studies, showing the possible diastereomers for the polyacetate region.[101]

Perhaps unsurprisingly in this challenging context, attempts to apply DP4f methodology were not able to predict any single fragment with high probability (≤ 30%).[101] The multiple low energy conformations likely arise due to the high flexibility of the truncate. Given these constraints, it appears that elucidation of the relative configuration of this region presents an occasion well suited to synthetic studies. In this endeavour, the chemical shifts of the C27, C29 and C31 oxymethine protons and their respective carbons are likely to be particularly diagnostic, as may

be the olefinic protons on the C34-C35 double bond and the unusually downfield C30 ^{13}C signal. The opportunities presented by a synthesis enabled assignment of the relative stereochemistry of the polyacetate region are discussed in Chapters Three and Four.

1.4.5 Relative Configuration of the C36-C46 α-Hydroxy-δ-Lactone Region

The Ardisson group collaborated with the Cossy group to assign the relative stereochemistry of the C34-C46 region (**105**) encompassing the α-hydroxy-δ-lactone stereocluster (**Figure 12**).[58,59] This region contains six stereocentres, giving 32 possible diastereomers. Similarly to other regions, ^{1}H and ^{13}C NMR analysis was used to narrow the number of options to a more synthetically feasible number and NOESY data was particularly helpful. Key nOe correlations between H37 and H40, as well as between H37 and Me42 implied a *cis* relationship between protons H37 and H40, and a *trans* relationship between H37 and H42. The large coupling constant shown between H39 and H40 ($^{3}J_{H39\text{-}H40}$ = 11.3 Hz) was also consistent with a *trans* relationship between these groups. The remaining signals, H38, H39 and H42, were found within the broad 22 proton multiplet (2.02-1.22 ppm). These constraints narrowed the possibilities to eight diastereomers and synthesis of model fragments commenced.

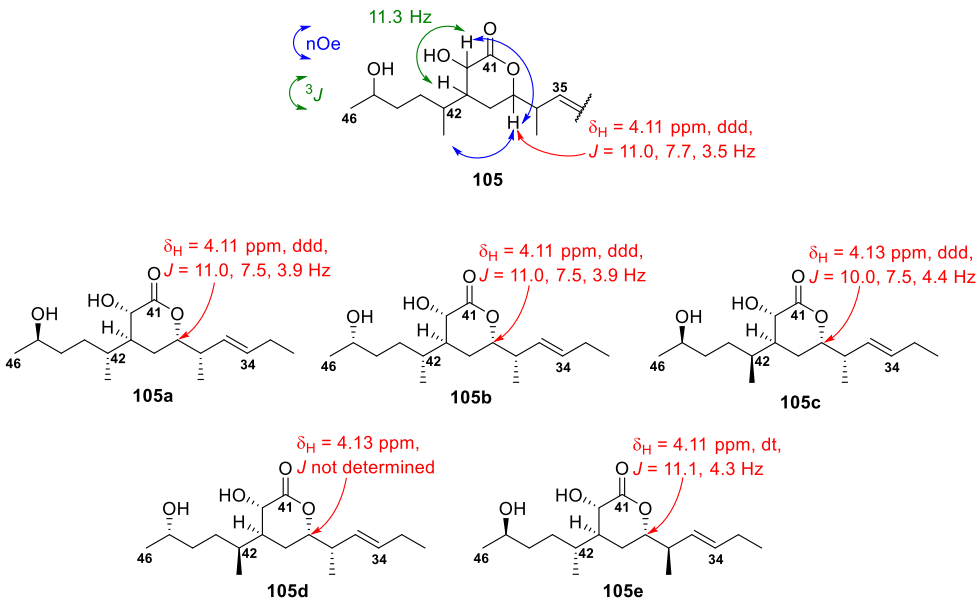

Figure 12. C32-C46 model diastereomers (**105a-e**) by the Cossy group.[58,59]

In their 2014 paper, the Cossy group reported NMR, IR and VCD spectroscopy results for selected diastereomers encompassing the the C36-C42 stereocluster for the purposes of determining the relative configuration within the stereocluster. They noted that during their synthetic campaign

two key points became apparent and effectively enabled the diastereomeric options to be further narrowed.[58] Firstly, a 36,37-*anti* relationship displayed a H37 dt splitting pattern. This is in contrast to the H37 ddd splitting displayed by both hemicalide and the 36,37-*syn* model fragments, allowing **105e** to be excluded. Secondly, the distal nature of the C45 epimers appeared to make little difference to the C36-C42 stereocluster. Arbitrarily assigning this centre allowed the diastereomeric targets to be narrowed to only two diastereomers, **105a** and **105c** (or **105b** and **105d**), epimeric at C42. Consequently, in their subsequent 2015 paper, only the synthesis and evaluation of five diastereomers, rather than the original possible eight possible diastereomers, was pursued (**105a-e**, **Figure 12**).

In the Ardisson/Cossy retrosynthetic analysis, target compound **105** was disconnected across the C34-C35 bond, *via* an oxidation, Julia-Kocienski olefination sequence (**Scheme 14**). This allowed increased structural similarity of the fragment for spectroscopic comparison purposes, subsequent to installation of stereochemistry. Hydrogenation across C42-C43 would provide access to both C42 epimers, revealing lactone **106**. α-Hydroxylation at C40 and disconnection across the C39-C42 bond, *via* 1,4 conjugate addition, disclosed C42-C46 alkenyl boronate **107** and α,β-unsaturated lactone **108**. The choice of C42-C46 alkenyl boronate **107** enantiomer used allows control of the C45 stereocentre. Acylation at the C37 alcohol and disconnection across C39-C40, *via* ring closing metathesis (RCM), reveals homoallylic alcohol **109**, which is accessible in four steps from Roche ester ((*S*)-**24** and (R)-**25**).

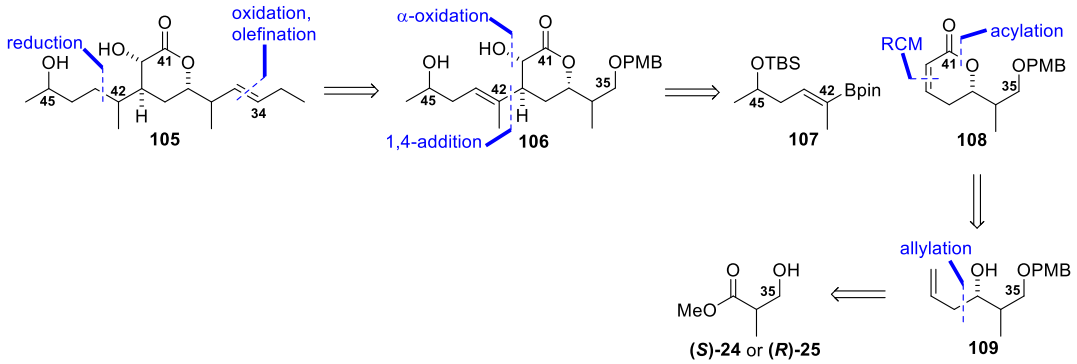

Scheme 14. Retrosynthetic analysis of the C32-C46 region of hemicalide by the Cossy group[59]

In their synthesis, the C35-C41 lactones needed to create both the 36,37-*syn* (*syn*-**108a**) and the 36,37-*anti* (*anti*-**108e**) diastereomers were obtained from the corresponding enantiomers of Roche ester ((*S*)-**24** or (*R*)-**25**) (**Scheme 15**). Reagent-controlled allylation of Weinreb amide **110a**, with Hafner-Duthaler's allyltitanium complex (*R*,*R*)-[Ti]-**I**,[121,122] delivered homoallylic alcohol *syn*-

109a (*dr* >96:4). Use of this reagent was necessary to overcome the substrate-imposed diastereoselection from the mismatched Roche ester. α,β-Unsaturated-δ-lactone *syn*-**108a** was obtained by successive acylation of alcohol *syn*-**109a**, then RCM with second-generation Grubbs catalyst (Grubbs-II). An analogous route, starting from Roche ester (*R*)-**25**, delivered the corresponding unsaturated lactone *anti*-**108e**.

Enantiomeric homoallylic alcohols, protected as their TBS ethers ((*S*)-**111** and (*R*)-**111**), were obtained from commercially available (*S*)-propylene oxide ((*S*)-**112**) and (*R*)-pent-4-en-2-ol, respectively. In the former case, this required epoxide opening with vinylmagnesium Grignard, before protection of the alcohol. Cross metathesis of (*S*)-**111** and (*R*)-**111** with isopropenyl pinacol boronate (**114**), in the presence of Grubbs-II catalyst, afforded a separable 85:15 mixture of *Z*/*E* geometric isomers, delivering alkenyl boronate species C42-C46 (*S*)-**113** and (*R*)-**113**, respectively.

Coupling of the α,β-unsaturated-δ-lactone species with the alkenyl boronate species, to give intermediate **115b** (*dr* 83:17 with C39 epimer), was achieved by 1,4-conjugate addition in the presence of $[Rh(cod)Cl]_2$ catalyst.[123–125] Diastereoselective α-hydroxylation proceeded under substrate control by treatment of the lactone enolate with Davis oxaziridine to give compound **116b** (*dr* 96:4).[126] The next step was the key hydrogenation to set the C42 centre. Hydrogenation did not occur at atmospheric pressure of hydrogen gas with palladium on carbon catalysis, but did occur under forcing conditions (Pd/C, 40 bar, 50 °C) to give a practically equimolar mixture of diastereomers (45:55, **117b**:**117d**). Switching to hydroxyl-directed reduction, in the presence of Crabtree's catalyst ([Ir]-**I**)[127], allowed exploitation of the C40 alcohol and use of atmospheric pressures of hydrogen. This afforded both C42 epimers with moderate selectivity (63:37, **117b**:**117d**), which was attributed to lack of significant conformational constraint around the C39-C42 bond. Saturated lactones **117b** and **117d** were separable by chromatography and their relative configurations characterised by VCD.[58] While this degree of diastereoselectivity was acceptable in the stereochemical exploration, it is an issue that will need to be addressed in the targeted synthesis of this stereocluster in the context of the total synthesis to hemicalide.

The final model diastereomers were each obtained in a further five steps. Protecting group manipulation was first necessary to protect the C40 alcohol as its TBS ether and deprotect the C35 PMB ether. The resulting alcohol was subjected to DMP oxidation to afford the C35 aldehyde **118b**. The key Julia-Kocienski olefination,[128–130] with sulfone **119**, produced the C34-C35 olefin (*E*/*Z* 95:5). Global deprotection, under fluorous conditions, afforded C35-C46 **105b**. The corresponding

C42 epimer **105d** was obtained *via* the same route, starting from the minor C42 epimer **117d**. C35-C46 **105a** and **105c** were obtained *via* the same route using *syn*-**108a** and enantiomeric alkenyl boronate (*R*)-**113**, diverging at the major and minor C42 epimers (**117a** and **117c**), respectively. Model fragment **105e** was analogously sourced from lactone *anti*-**108e** and alkenyl boronate (*R*)-**113**.

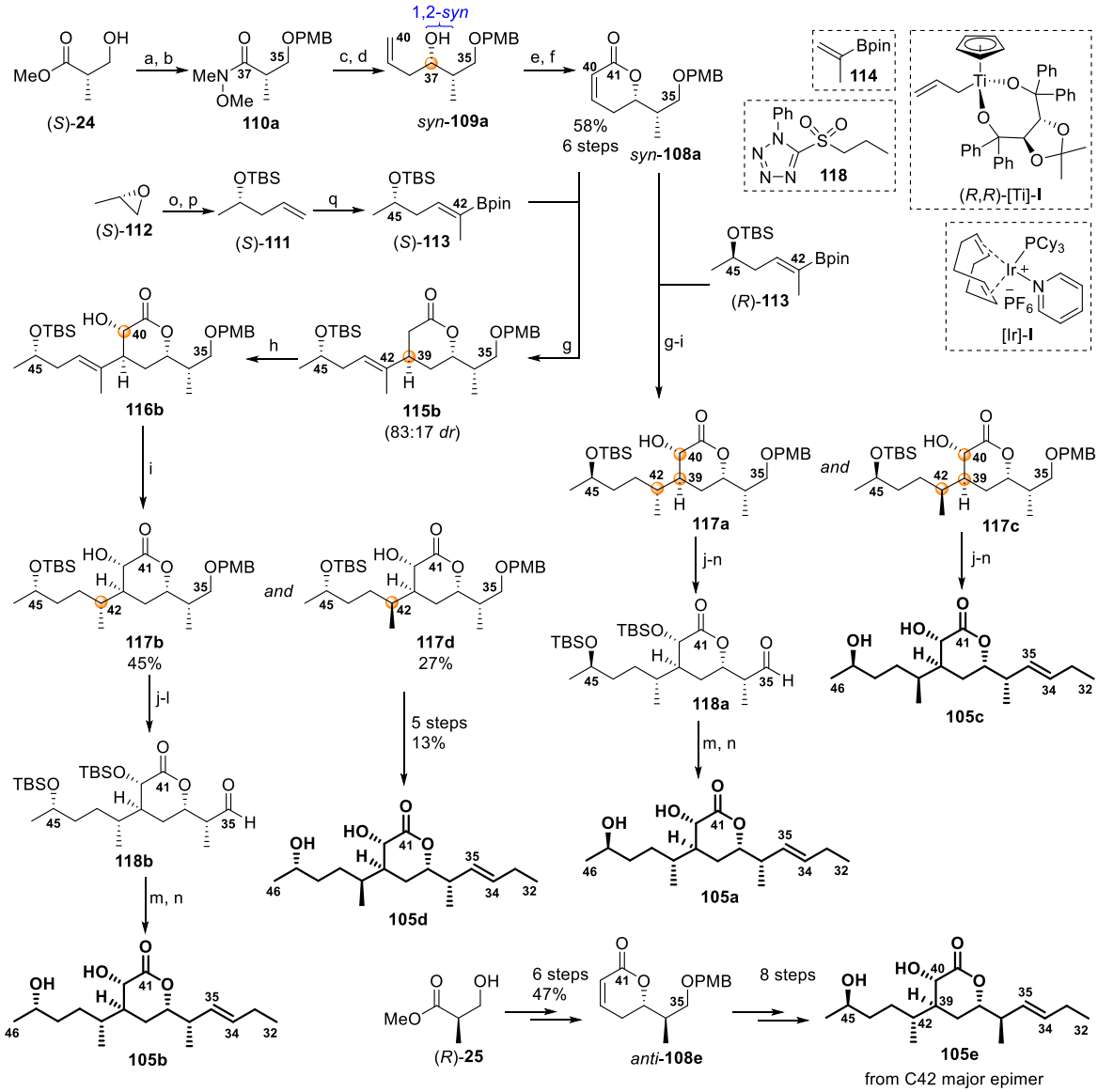

Reagents: PMBOC(=NH)CCl_3, cat. CSA, CH_2Cl_2, rt; (b) MeONHMe·HCl, *i*PrMgCl, THF, –40°C to –10°C, 87% (2 steps); (c) DIBAL-H, THF, –78°C to –40°C; (d) (*R*,*R*)-[Ti]-I, Et_2O, –78°C, 92% (2 steps); (e) H_2C=CHCOCl, *i*Pr_2NEt, CH_2Cl_2, –78°C, (f) Grubbs-II (5 mol %), CH_2Cl_2, reflux 72% (2 steps); (g) (*S*)-**113** or (*R*)-**113**, $[Rh(cod)Cl]_2$ (3 mol %), LiOH, dioxane/H_2O (10:1), 40°C, 74 %, *dr* 83:17; (h) NaHMDS, 2-(phenylsulfonyl)-3-phenyloxaziridine, THF, –78°C, 72%, *dr* >20:1; (i) [Ir]-I (8 mol %), H_2 (1 atm), CH_2Cl_2, rt, 72%, *dr* 63:37; (j) TBSOTf, 2,6-lutidine, CH_2Cl_2, 0°C; (k) DDQ, CH_2Cl_2/H_2O, rt; (l) DMP, $NaHCO_3$, CH_2Cl_2, rt, 92% (3 steps); (m) KHMDS, THF, –78°C to rt, 70%, *E*/*Z*=95:5; (n) HF·py, py, THF, rt, 95%; (o) VinylMgCl, CuI, THF, –50°C to –15°C; (p) TBSCl, imidazole, DMF, rt, 92% (2 steps); (q) Grubbs-II (4 mol %), CH_2Cl_2, reflux, 56%, *Z*/*E*=85:15.

Scheme 15. Cossy synthesis of C32-C46 α,β-unsaturated-δ-lactone diastereomers **105a-e**.[59]

By comparing the ^{13}C NMR data of diastereomers **105a** and **105c** with hemicalide it was noted that the best agreement was achieved with **105a** ($|\Delta\delta_C| \leq 0.5$ ppm), whereas significant variations were observed, particularly at C43 and Me42 ($|\Delta\delta_C| > 4$ ppm), for **105c**. This was consistent with the initial observations of nOe correlations between H37, H40 and Me42, but not with H42, which provided evidence that these groups were *cis* to one another (**Figure 12**). Thus, the relative stereochemistry of hemicalide within the C36-C42 stereocluster appears to be that present in **105a** and **105b**.

Relevantly, DP4f studies, undertaken by MacGregor in the Paterson group, on six diastereomeric C34-C46 model fragments (**120a-f**, **Figure 13**) predicted that **120a**, sharing the relative stereochemistry of **105a** and **105b** in the C36-C42 stereocluster, but exhibiting a 42,45-*anti* relationship, as in **105a**, was the best fit for the combined ^{1}H and ^{13}C NMR data, with a probability >95%.

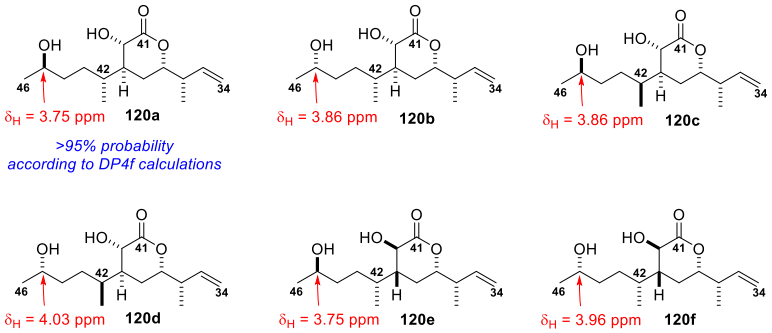

Figure 13. C34-C46 DP4f model fragments (**120a-e**) by the Paterson group.[101]

1.4.6 Cossy and Ardisson's Synthesis of a Hemicalide Backbone Stereoisomer

The Ardisson and Cossy groups have constructed candidate fragments for three of the major stereoclusters encompassing the C8-C13 stereohexad, the C18-C24 dihydroxylactone and the C36-C42 hydroxylactone regions. However, determining the relative configuration between the five remaining unassigned stereocentres, the relationship between the stereoclusters and construction of the full carbon skeleton of hemicalide had yet to be completed. In 2019, Ardisson/Cossy reported the synthesis of hemicalide stereoisomer **121** (**Scheme 16**), wherein the five unknown stereocentres were randomly assigned.[131] While this represents the first reported synthesis of a full hemicalide backbone stereoisomer, Ardisson/Cossy were unable to achieve full deprotection of the molecule, leaving a TBS ether at either C40 or C45. Nonetheless, this allowed for a representative derivative of the natural product to be made, and for detailed spectroscopic

comparisons to be undertaken. Significant chemical shift deviations present across various points of the molecule, particularly across the randomly assigned C27-C32 stereotetrad (*vide infra*), provide strong evidence that stereoisomer **121** does not bear the correct relative configuration for hemicalide.

For this synthesis, hemicalide was disconnected at C15-C16 *via* a Suzuki coupling, at C27-C28 *via* an aldol reaction, and across the C34-C35 olefin *via* a Julia-Kocienski olefination (**Scheme 16**). This reveals four major fragments: C1-C15 vinyl iodide **45**, C16-C27 aldehyde **122**, C28-C34 ketosulfone **123** and C35-C46 aldehyde **118a**. The syntheses of C1-C15 vinyl iodide **45**, C35-C46 aldehyde **118a** and the immediate precursor of C16-C27 aldehyde **122** have been described (*vide supra*). In contrast, the C28-C34 ketosulfone **123** had not previously been reported. This region has C31 and C32 planned to arise from reagent control, allowing C27 to be set in the aldol fragment coupling with C16-C27 aldehyde **122** and C29 to be set in a subsequent diastereoselective reduction.

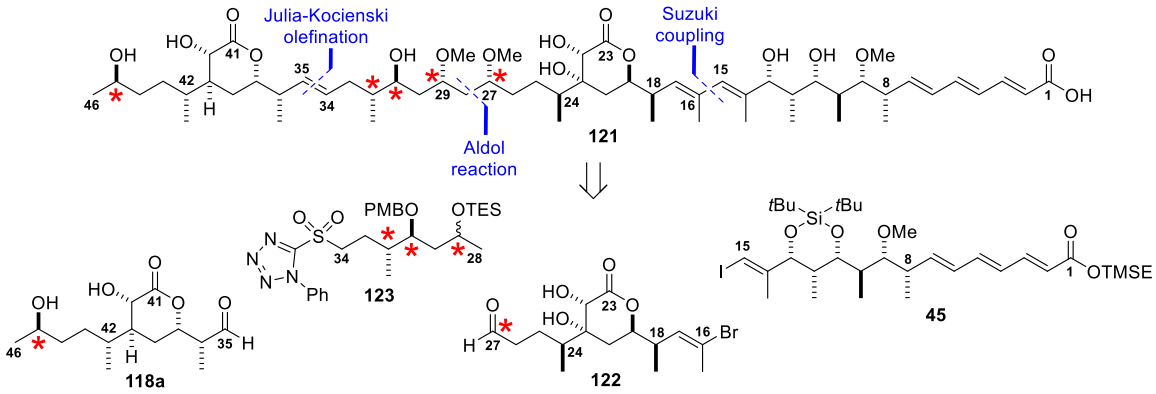

Scheme 16. Ardisson/Cossy retrosynthetic analysis of hemicalide stereoisomer **121**, with randomly assigned stereocentres marked in red.[131]

C28-C34 ketosulfone **123** was accessed in seven steps from aldehyde **124** (**Scheme 17**). An enantioselective crotylation strategy was pursued to allow potentially flexible installation of stereochemistry at C31 and C32.[121,122,132] Utilisation of (*E*)-crotyltitanium reagent (*S*,*S*)-[Ti]-**I**[121,122] provided access to C31, C32-*anti* adduct **125** (*dr* >96:4, *ee* not stated). The C29 centre, which would later be transformed, was carried through as an epimeric mixture. PMB protection, hydroboration with 9-BBN and oxidation gave access to C34-alcohol **126**. A Mitsunobu reaction with 1-phenyltetrazol-5-yl-thiol (PTSH) to provide thioether functionality, a protecting group swap from a TBS ether to a more labile TES ether at C29 and oxidation of the thioether gave C28-C34 sulfone **123**. This protecting group switch was necessary to allow later selective oxidation of C29 to the desired ketone.

Julia-Kocienski olefination[128–130] delivered C28-C46 **127** with the desired C34*E*-olefin. A deprotection, oxidation sequence at C29 gave ketone **128**. C28-C46 ketone **128** was coupled with C16-C27 aldehyde **122**, *via* a boron-mediated 1,5-*anti* aldol reaction.[133,134] The intermediate boron aldolate was taken through to a 1,3-*syn* reduction[135,136] giving the corresponding diol (C27 and C29 *dr* >95:5). Subsequent *bis*-*O*-methylation delivered C16-C46 fragment **129**.

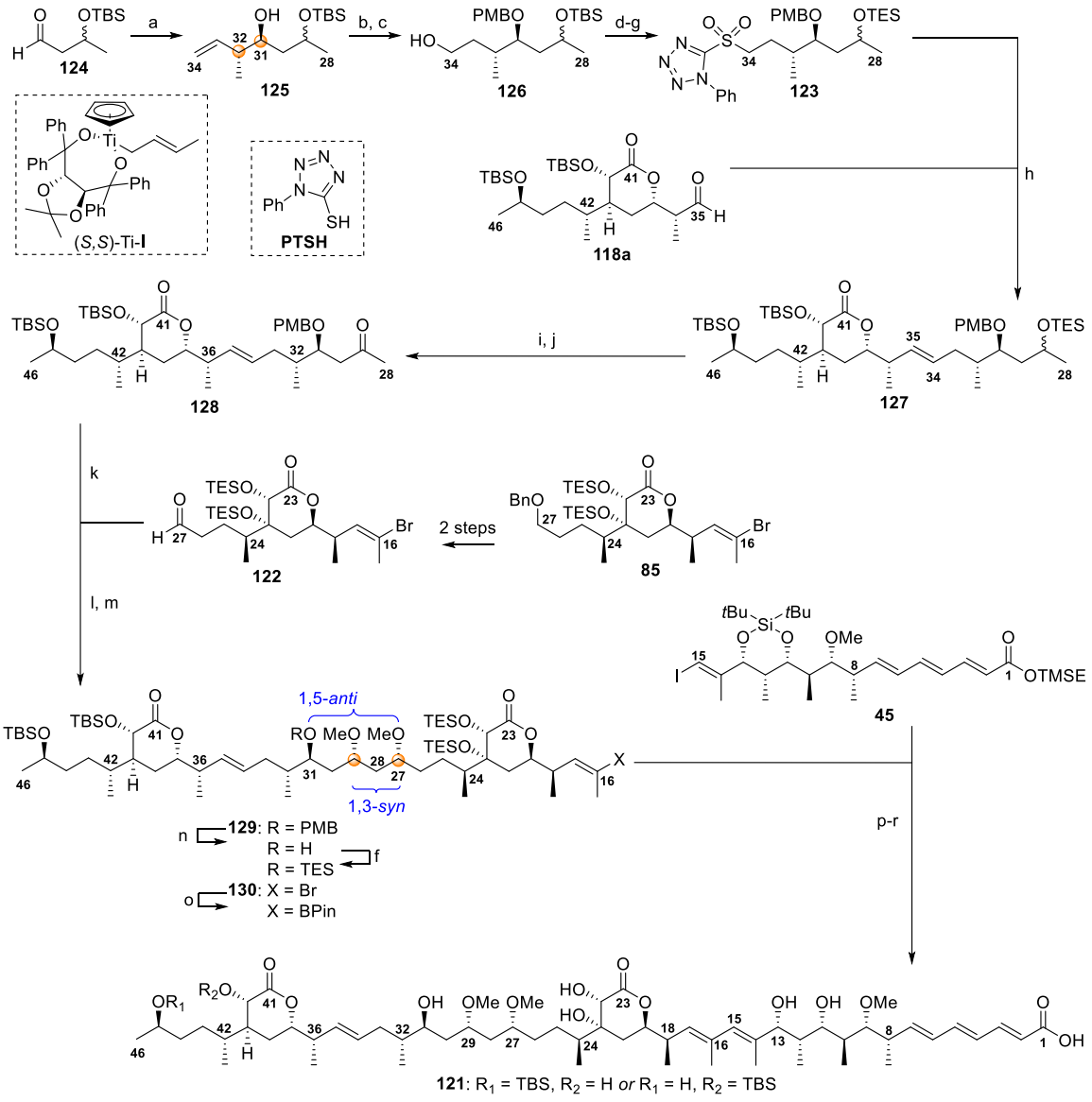

Reagents: (a) (S,S)-Ti-**I**, Et_2O/THF, –78°C, 76%, *dr* >96:4; (b) KHMDS, PMBBr, THF, 0°C; (c) 9-BBN-H, THF, reflux *then* NaOH, H_2O_2, 79% (2 steps); (d) PTSH, PPh_3, DEAD, THF, 0°C, 86%; (e) HF·py, py, THF, rt, 95%; (f) TESOTf, 2,6-lutidine, CH_2Cl_2, 0°C; (g) *m*CPBA, CH_2Cl_2, rt, 72% (2 steps); (h) KHMDS, **123**, THF *then* **118a**, –78°C to –40°C, 49-57% (2 steps from C35-C46 C35-OH), *E*/*Z* >96:4; (i) HF·Et_3N, THF, rt, 94%; (j) DMP, $NaHCO_3$, CH_2Cl_2, rt, 97%; (k) *c*Hex_2BCl, Et_3N, **128**, Et_2O, –78°C to 0°C *then* **122**, –78°C, *dr* >95:5; (l) $LiBH_4$, Et_2BOMe, THF/MeOH, –78°C to –40°C, 56% (2 steps from **122**), *dr* >95:5; (m) Me_3OBF_4, Proton Sponge®, CH_2Cl_2, rt, 71%; (n) DDQ, CH_2Cl_2/H_2O (pH 7.2), rt; (o) B_2pin_2, $PdCl_2(PPh_3)_2$ (12 mol%), PPh_3 (24 mol%), PhOK, PhMe, 50°C; (p) **45**, $Pd(PPh_3)_4$, TlOEt, THF/H_2O (3:1), rt, 12% (4 steps from **130**); (q) TASF, DMF, 0°C to rt; (r) HF·py/py (1:2), THF, 10°C to 15°C, *ca* 91% (2 steps).

Scheme 17. Synthesis of hemicalide carbon backbone stereoisomer by Ardisson/Cossy.[131]

The C31 PMB ether, which had facilitated stereocontrol in the aldol reaction, was swapped to a more labile TES ether (**130**). This was conducted to avoid potential downstream issues with isomerisation of the C2-C7 conjugated triene under deprotection conditions. The C16-C46 vinyl bromide was then exposed to palladium catalysed borylation conditions and subsequent Suzuki-Miyaura cross coupling[117] with C1-C15 vinyl iodide **45**. This cross coupling strategy was previously utilised by Ardisson/Cossy in the construction of the C1-C27 region.[61] However, here the cross coupling proceeded to give the full C1-C46 skeleton in only 13% yield (over two steps). This low yield was attributed to a combination of ineffective borylation and the necessity of telescoping the boronate into the cross coupling reaction due to degradation issues. Global deprotection was attempted *via* a two step process (TASF, HF·py). However, the resulting *ca.* 2 mg of product still bore a TBS ether at C40 or C45 (unassigned by the authors) and was contaminated by solvent impurities, including phthalates and paraffins.

Analysis of the ^{1}H and ^{13}C NMR spectroscopic data of hemicalide backbone stereoisomer **121** revealed a number of significant deviations from the natural product. One region of notable difference is within the H/C1-H/C7 region. It was previously suggested by Ardisson that these shift differences were attributable to the isolation of hemicalide as its sodium salt.[54] Previous work by Han and Lam,[62] within the Paterson group, synthesising the diastereomeric C1-C28 13,18-*syn* and 13,18-*anti* acids (**83a** and **83b**) noted the H/C1-H/C7 shift dependence on the protonation state of C1 and observed worse correlations for the corresponding sodium salts. Thus, difference in pH conditions between the originally collected sample and stereoisomer **121** likely explains the H/C1-H/C7 shift differences of up to 4.7 ppm observed. However, these were readily excluded given that the relative configuration of the C1-C24 region has been convincingly established. In addition, despite the C1-C28 13,18-*syn* acid (**83a**) ($|\Delta\delta_H| \leq 0.01$ ppm, $|\Delta\delta_C| \leq 0.1$ ppm) previously being reported[62] to be a better match for the natural product than the 13,18-*anti* acid (**83b**) ($|\Delta\delta_H| \leq 0.04$ ppm, $|\Delta\delta_C| \leq 0.6$ ppm), stereoisomer **121** bears the previously asserted 13,18-*anti* relationship. This leads to deviations of up to 0.8 ppm (C10) in the ^{13}C NMR across this region. However, again these deviations were less relevant to the evaluation of the five remaining unassigned centres, given that the relative configuration of the C1-C24 region has been established. It is across the C26-C35 region, which encompasses the randomly assigned C27-C32 stereotetrad, that the observed spectroscopic deviations are especially apparent ($\Delta\delta_C$ >1 ppm: C26, C28, Me32, C33; $\Delta\delta_H$ >0.05 ppm: H31). This provides strong evidence that stereoisomer **121** is unlikely to bear the correct relative configuration for hemicalide. Importantly, these synthetic

studies still leave five stereocentres and the relationships between stereoclusters (outside of the C1-C24 region) unassigned.

1.5 Summary of the Work on the Structural Elucidation of Hemicalide to Date

Hemicalide is a highly complex MNP displaying potent antimitotic bioactivity *via* a novel mechanism of action. It presents promising potential for development as a chemotherapeutic compound. Yet, the low isolation yield (0.5 mg) precluded the assignment of the absolute configuration of any of the 2^{21} stereocentres that it contains. At present, the Ardisson and Cossy groups have suggested the relative configuration of the C1-C27 region (**96** then **97**) and the C32-C42 stereocluster (**118a** or **118b**) of the molecule.[54,56–59,61] Through combined computational and synthetic studies, the Paterson group have revised the relative configuration of the C16-C28 region of hemicalide (**72**). In addition, the Paterson group synthesis of both possible diastereomers of the C1-C28 region (**83a** and **83b**) established a 13,18-*syn* relationship between the C8-C13 and the C18-C24 stereoclusters.[62]

To date, the relative configuration of the C27-C32 polyacetate region and the distal C45 hydroxyl group remains unassigned. The current project starts with work towards the C34-C46 α-hydroxy-δ-lactone region of hemicalide, with focus on devising a highly convergent and stereoselective synthesis, incorporating flexible handles to facilitate ready coupling of this region to the polyacetate region and, in turn, the remainder of the molecule. The present work employs synthesis-enabled structural eludication to allow a series of key assignments to be made.

2. Results and Discussion: Synthesis of C34-C46 Region and Assignment of C45

2.1 Synthetic Approach

Previous computational and experimental work in the Ardisson/Cossy and Paterson groups has established the relative stereochemistry within the C1-C24 and C36-C42 regions of hemicalide. This has allowed the possible stereoisomers to be narrowed down from over two million permutations to a much reduced 128 possibilities. A highly stereocontrolled, flexible and convergent strategy is necessary to both validate a synthetic route to hemicalide and allow assignment of the remaining stereocentres, particularly within the C27-C32 stereotetrad, as well as the relationships between the stereoclusters.

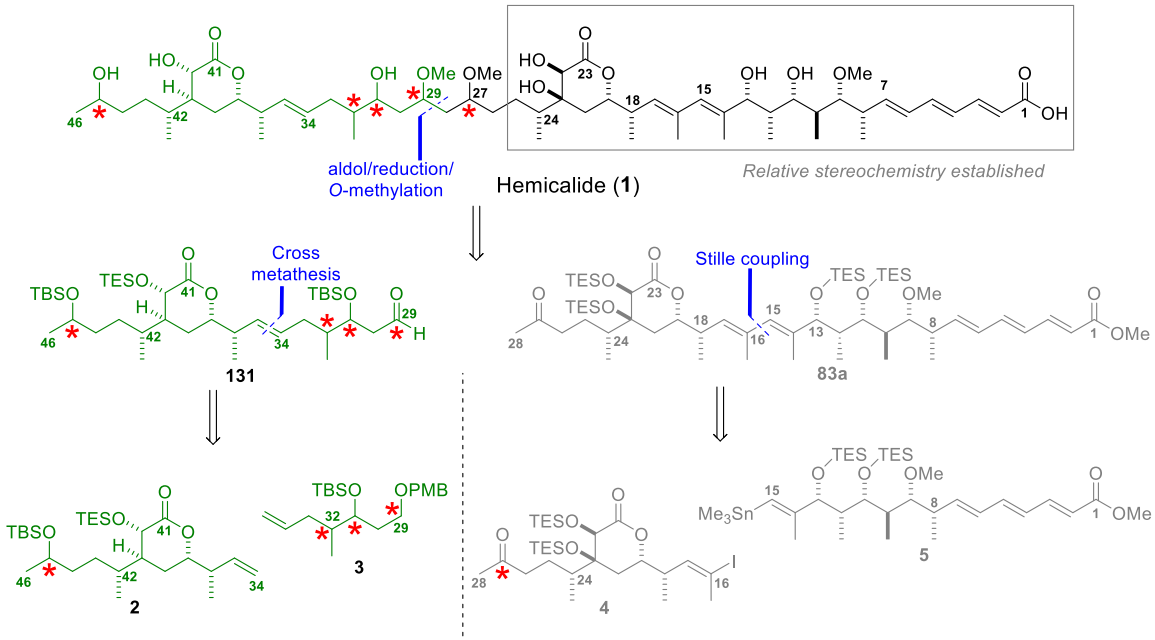

Scheme 18. Paterson hemicalide (**1**) retrosynthetic approach with unassigned stereocentres marked in red.

The Paterson approach envisages a key enantioselective aldol disconnection across C28-C29, *syn*- or *anti*-reduction and *bis*-O-methylation sequence to permit late-stage access to the four possible C27, C29 diastereomers (**Scheme 18**). This analysis reveals C1-C28 methyl ketone **83a** and C29-C46 aldehyde **131**. The versatility of the approach allows late-stage divergence and flexibility under one synthetic strategy to selectively access all desired diastereomers. Given that installation of C29 was planned to rely on reagent control, enforced by a chiral boron Lewis acid, it is necessary

to consider any 1,3-stereoelectonic effects attributable to the protecting group at C31. A silyl group in this position (in contrast to a PMB group) imparts low stereoinduction in the closed aldol transition state.[160] The C29-C46 region can be further disconnected, *via* a cross metathesis, presenting C29-C35 alkene **3**, which contains two more unassigned stereocentres, and C34-C46 alkene **2**, which contains the last remaining unassigned stereocentre. This strategy effectively isolates most of the unassigned stereocentres into a single, small fragment. A disconnection across C15-C16, *via* a Stille reaction, and the resulting C1-15 stannane **5** and C16-C28 vinyl iodide **4** have been previously discussed (Sections **1.4.1**-**1.4.3**).[60,62]

2.2 Retrosynthesis of the C34-C46 Region

The Ardisson/Cossy work on the C36-C42 region required a high degree of modularity, in order to access a range of desired diastereomers and determine the relative configuration within this stereocluster.[58,59] However, designing a route able to access numerous diastereomers was not consistent with prioritising high levels of stereocontrol. With the C36-C42 relative configuration established, the approach taken in the present work focussed on devising a streamlined and highly diastereoselective route, with plasticity only at the unassigned C45 stereocentre, to generate the two candidate diastereomers 42,45-*anti*-**2a** and 42,45-*syn*-**2b**.

The proposed alkene coupling handle in **2a** and **2b** for cross metathesis could be installed through methylenation, with further redox and functional group manipulations revealing alcohol 42, 45-*anti*-**132a** and 42, 45-*syn*-**132b** (**Scheme 19**). The only reagent-controlled reaction, the reduction of the C45 ketone, was planned to be performed on the corresponding enone in order to allow greater steric and electronic facial distinction of this prochiral carbonyl. Disconnection across C43-C44, *via* a sequence of olefination and enantioselective reduction, discloses truncated α-hydroxylactone **133**. Performing the α-oxidation on the lactone allows high diastereocontrol in the creation of C40, due to the preference for diaxial attack. A series of α-oxidation and lactonisation steps presents acyclic intermediate **134**. This acyclic intermediate should allow hydroxyl-directed reduction to be employed to install the C39 stereocentre. Disconnection across C39-C40, *via* a reduction, olefination sequence exposes β-hydroxy ketone **135**. Finally, given the 37,42-*syn* relationship, a 1,4-*syn* aldol can be utilised to forge the C37-C38 bond and set the C37 stereocentre. This disconnection reveals the two starting fragments, ketone **73** and aldehyde **136**. Here the PMB and benzyl ethers were employed to allow exploitation of the 1,3-stereoinduction in aldol transition states (*vide infra*), while still allowing orthogonal manipulation of these groups.

These can each be readily elaborated from the relevant enantiomers of commercially available Roche ester, (*S*)-**24** and (*R*)-**25**, respectively. The opposite enantiomeric series of this fragment (***ent*-2**) could be readily accessed by starting from the enantiomeric (*R*)-**25** and (*S*)-**24** Roche esters, respectively, when building the initial ketone and aldehyde intermediates.

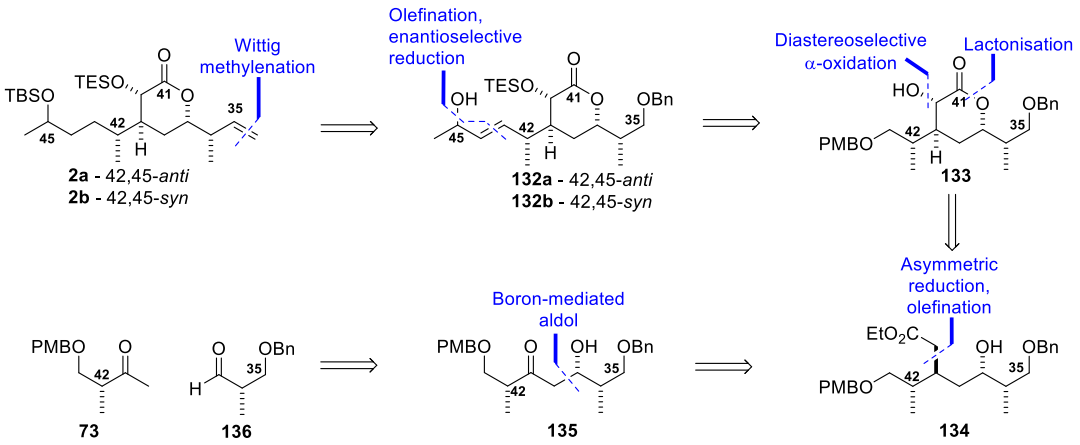

Scheme 19. Retrosynthetic analysis of the C34-C46 fragment of hemicalide

2.3 Synthesis of the C34-C46 Fragment

Methyl ketone **73**, providing the backbone for the C38-C43 region, was obtained in three steps from Roche ester (*R*)-**25**. (*R*)-**25** was first protected as the corresponding PMB ether (PMBOC(=NH)CCl_3, cat. CSA, CH_2Cl_2, rt), then reacted to form corresponding Weinreb amide **137** (Me(MeO)NH_2Cl, *i*PrMgCl, THF, –10 °C) (**Scheme 20a**). This two-step transformation,[89] well-known in the Paterson group, created a ready supply of the Weinreb amide.* Conversion to Weinreb amide **137**, before treatment with methylmagnesium bromide, circumvents issues of over-addition resulting in tertiary alcohol product that occur in Grignard addition to esters. This is due to a change in hybridisation and lack of electrophilic sites in six-membered metal chelate **138**, formed after the first addition to the Weinreb amide, which breaks down to selectively form methyl ketone **73** upon acidic workup.

Aldehyde **136**, comprising the C35-C37 region of the carbon backbone, was produced in three steps from Roche ester (*S*)-**24** (**Scheme 20b**). This hydroxyl was protected differently to that in ketone **73**, as benzyl ether **139**. This was possible through reaction of (*S*)-**24** with benzyl

* Acknowledgements to Talia Pettigrew for supplying this compound.

trichoroacetimidate. Interestingly, unlike creation of the similar PMB ether, utilised in the C1-C28 fragment, which proceeded under mildly acidic conditions, **139** will not form under such conditions, instead requiring treatment with triflic acid. This modification afforded benzyl ether **139** in excellent yield. Reduction of ester **139**, with lithium aluminium hydride, provided primary alcohol **140**, which was subjected to Swern oxidation[69–72] to give aldehyde **136**. This delicate intermediate is prone to racemisation and must be immediately used, in crude form, in the subsequent boron-mediated aldol reaction.

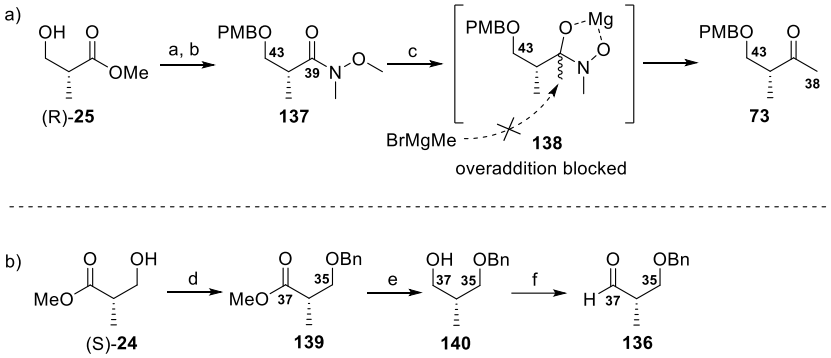

Reagents: (a) PMBOC(=NH)CCl_3, cat. CSA, CH_2Cl_2, rt, 88%; (b) Me(MeO)NH_2Cl, *i*PrMgCl, THF, –10°C; (c) MeMgBr, Et_2O, 0°C, 71%; (d) BnOC(=NH)CCl_3, cat. TfOH, CH_2Cl_2, *c*Hex, –15°C to rt, 76%; (e) $LiAlH_4$, 0°C, THF, 63%; (f) $(COCl)_2$, DMSO, CH_2Cl_2, –78°C *then* **140**, Et_3N, –78°C to –20°C.

Scheme 20. a) Synthesis of methyl ketone **73**, including mechanism for the selective monoaddition of methyl Grignard reagent into Weinreb amide **137**; b) Synthesis of aldehyde **136**.

Inspiration to use a boron-mediated aldol reaction to link the C35-C37 and C38-C46 regions in a 1,4-*syn* fashion stems from previous work in the Paterson group on other complex polyketide MNPs. For example, a 1,4-*syn* relationship was desired in the context of (–)-aurisides A and B[137] and in the synthesis of the C13-C28 region of hemicalide itself (**Scheme 21a**).[60] The predictability of the boron-mediated aldol reaction between ketone **73** and aldehyde **136**, where the outcome favours the 1,4-*syn*-product (**Scheme 21b**), stems from the diastereomeric six-membered transition states (**TS-I** and **TS-II**, **Scheme 21c**) through which this reaction proceeds.[134,138] In these transition states, the aldehyde and the ketone-derived boron enolate are thought to adopt a boat conformation, permitting a stabilising formyl-H bond to form between the electron-rich PMB protected oxygen and the activated aldehyde.[134] Two transition states can form this stabilising interaction (**TS-I** and **TS-II**). However, **TS-I** is preferred. Firstly, this is due to reduction in allylic strain between C38 and Me42 relative to that experienced in **TS-II**.[138] Secondly, in **TS-I** the enolate approaches the aldehyde in a favourable Felkin-Anh manner. Lastly, the (+)-Ipc_2BCl reagent enhances diastereoselectivity through an additional steric interaction between the Ipc Me group and the C43 methylene of the boron enolate in **TS-II**, thereby increasing the energetic difference

between these transition states.[138] This is crucial, even in this 'matched' reaction context. Notably, the diastereoselectivity is significantly reduced when the achiral Lewis acid *c*Hex$_2$BCl (*dr* 2:1) is used in place of (+)-Ipc$_2$BCl. After some degree of optimisation (**Table 2**), the reaction proceeded with both excellent yield (91%) and diastereoselectivity (*dr* >20:1) to give β-hydroxy ketone **135**. To achieve this, it was necessary to use methyl ketone **73** as the limiting reagent. This reaction scales very well and can be undertaken in >5 g batches, indicating its potential suitability for future scale-up.

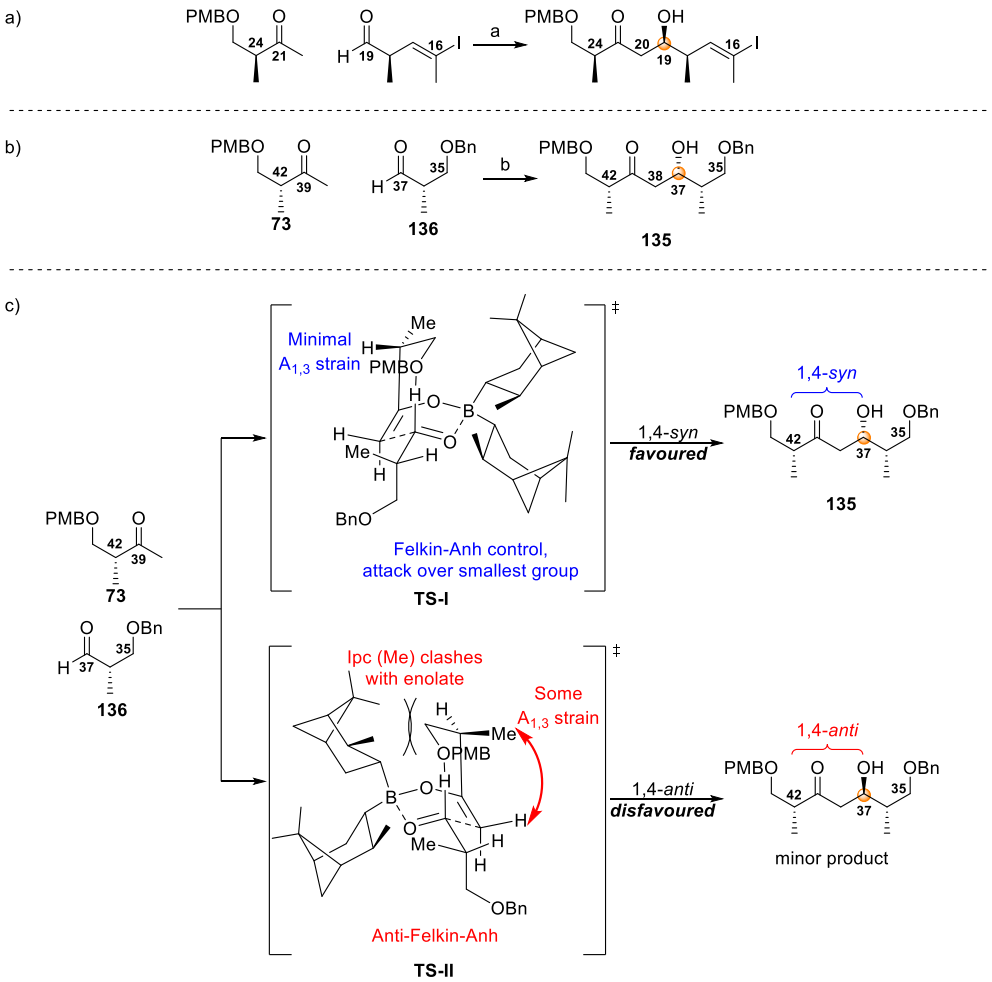

Reagents: (a) (–)-Ipc$_2$BCl, Et$_3$N, Et$_2$O, **73**, 0°C *then* **136**, –78°C to –20°C, 70%, *dr* >20:1; (b) LA, Et$_3$N, Et$_2$O, **73**, 0°C (1 h) *then* **136**, –78°C (1 h) to –20°C (16 h) *then* pH 7 buffer, MeOH, H$_2$O$_2$, –20°C to rt (LA = (+)-Ipc$_2$BCl: 91%, *dr* >20:1; LA = *c*Hex$_2$BCl: 66%, *dr* 2:1).

Scheme 21. a) (–)-Ipc$_2$BCl mediated aldol reaction employed by the Paterson group in the synthesis of the C13-C28 region of hemicalide;[60] b) Boron-mediated aldol reaction between ketone **73** and aldehyde **136**; and c) (+)-Ipc$_2$BCl boron-mediated aldol reaction transition states.

Table 2. Optimisation and scale-up of boron-mediated aldol reaction to give β-hydroxy ketone **135**

Aldehyde equivalent	Ketone equivalent	Lewis acid	Scale (g)	Yield (%)	*dr*
1	1.2	*c*Hex$_2$BCl	0.10	66	2:1
1	1.5	(+)-Ipc$_2$BCl	0.25	45	>20:1
1	1.2	(+)-Ipc$_2$BCl	1.00	54	>20:1
1	1.1	(+)-Ipc$_2$BCl	1.00	66	>20:1
1.2	1	(+)-Ipc$_2$BCl	0.60	79	>20:1
1.2	1	(+)-Ipc$_2$BCl	6.35	91	>20:1

To confirm that the reaction had generated the desired configuration at the new C37 secondary alcohol, diastereomeric Mosher esters **141** and **142** were prepared from the corresponding (*R*)- and (*S*)-Mosher acids, under Steglich conditions (**Scheme 22a**).[96] In Mosher esters of secondary alcohols, the carbinol proton, carbonyl and CF_3 groups lie in the same plane, due to the hyperconjugation arising between the carbonyl group and the electronegative trifluoromethyl group (**Scheme 22b**).[139,140] Compared to the groups lying on the same side as the methoxy group, groups lying on the same side as the phenyl group will be shielded by the π-electron density of the aromatic ring.[141] This results in an upfield shift being observed in NMR spectra of such groups. Thus, in (*R*)-esters, groups on the left hand side of the ester moiety as drawn will be shifted upfield compared to those in the (*S*)-ester, exhibiting $\Delta\delta > 0$ ($\Delta\delta = \Delta\delta_S - \Delta\delta_R$).[142] Correspondingly, groups on the right hand side of the ester as drawn should be shifted downfield compared to those in the (*S*)-ester, exhibiting $\Delta\delta < 0$.

It was found that Mosher esters **141** and **142** were prone to elimination. As such, the reaction was carefully monitored and, by shortening the reaction times, the elimination product (**143**) was able to be largely avoided. It was observed that, without exception, H38-H43 signals were shifted upfield, while H35-H37 signals were shifted downfield (**Scheme 22c**, **Table 3**). This persuasively confirmed that the product was indeed the 36,37-*syn*-36,42-*syn* adduct, possessing the expected configuration at C37.

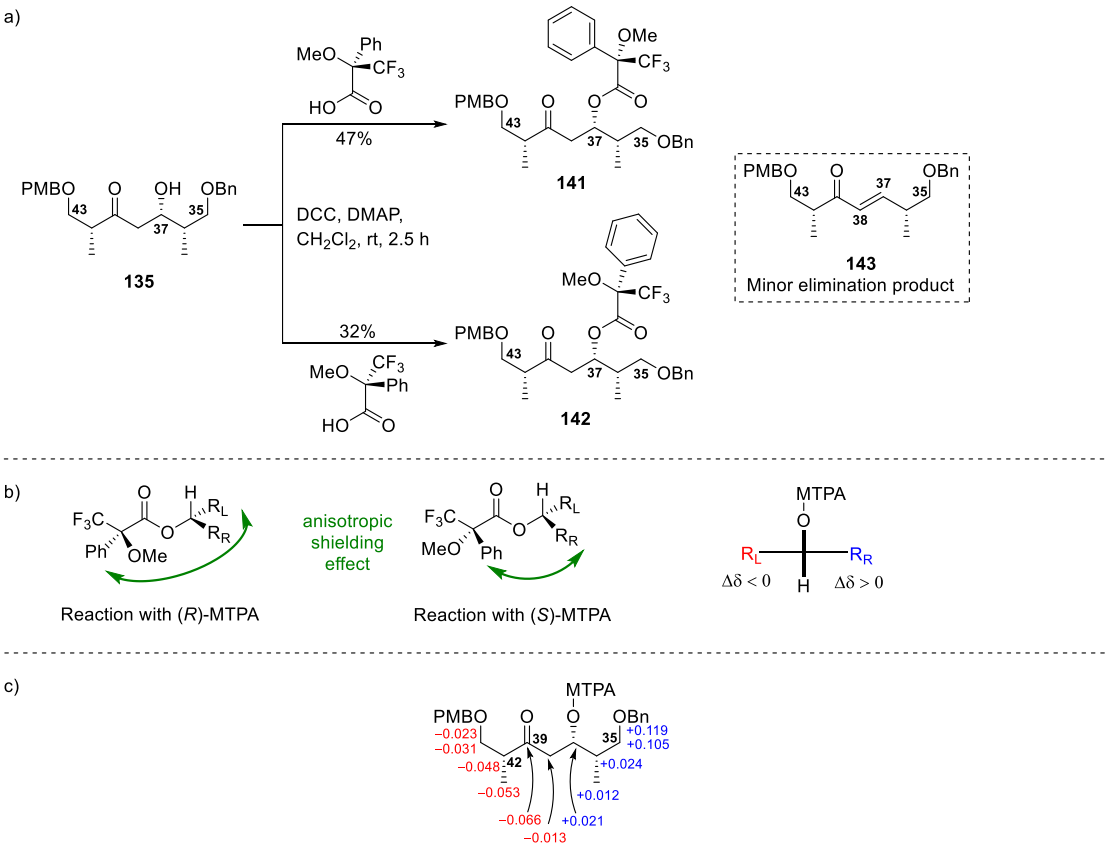

Scheme 22. a) Preparation of Mosher esters **141** and **142**; b) Preferred conformation of Mosher esters and the effect of shielding and deshielding effects in Mosher ester **141** compared to **142**; c) Δδ values for MTPA esters **141** and **142**.

Table 3. Table of ^{1}H NMR shifts for diagnostic signals in Mosher esters **141** and **142**

Proton	**δH (*S*)-ester** (ppm)	**δH (*R*)-ester** (ppm)	**$\Delta\delta_{S-R}$** (ppm)	**$\Delta\delta_{S-R}$** (Hz)
H35a	3.35	3.23	+0.119	59.7
H35b	3.29	3.18	+0.105	52.7
H36	2.17	2.14	+0.024	12.0
Me36	0.90	0.89	+0.012	5.8
H37	5.73	5.71	+0.021	10.5
H38a	2.90	2.91	–0.013	-6.3
H38b	2.72	2.79	–0.066	-32.8
H42	2.76	2.80	–0.048	-24.1
Me42	0.93	0.98	–0.053	-26.5
H43a	3.50	3.52	–0.023	-11.3
H43b	3.39	3.42	–0.031	-15.3

The next task was to construct the α-hydroxy-δ-lactone system in **133**, with the desired stereochemistry at both the C39 and C40 centres. This required configuring H39 on the face *anti* to H37 and *syn* to Me42 to give 37,39-*anti*-**144a** (**Figure 14a**). This could be done by first closing the ring in such a manner as to obtain an α,β-unsaturated δ-lactone, then diastereoselectively reducing across C39-C40 to set the C39 stereocentre. Alternatively, the C39 stereocentre could be set while the system was acyclic, before closing the ring to obtain the lactone. Initially, it was reasoned that past synthetic work on hemicalide may allow relevant approaches to be applied in analogous contexts (**Figure 14b**). In particular, the apparent structural homology between the C16-C28 α,β-dihydroxy-δ-lactone stereocluster and the C34-C46 α-hydroxy-δ-lactone stereocluster was predicted to allow for some portions of the previously established Paterson route (*vide supra* section **1.4.2**) to direct the synthesis of this fragment (**Scheme 23a**). In particular, the facial selectivity for the dihydroxylation exclusively approaches *anti* to the substituents on C18, C19 and C24, and so, perhaps, substrate-imposed diastereoselection could be leveraged to install C39. On this reasoning, initially, the planar nature and conformational constraints imposed by a lactone system were pursued (**Scheme 23b**).

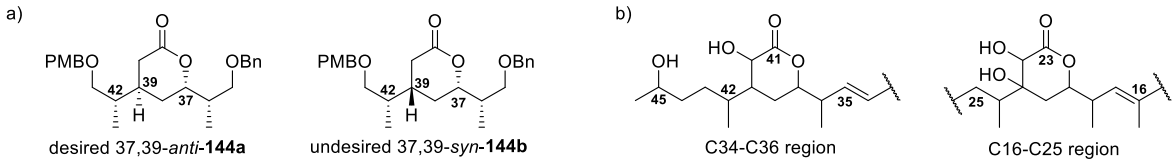

Figure 14. a) Desired and undesired lactone systems; b) Comparison of the δ-lactone regions of hemicalide shows their structural homology

To pursue a cyclic lactone strategy, analogous to the synthesis of the C16-C25 region, the C37-alcohol in β-hydroxy ketone **135** was protected as its TBS ether **145** (TBSOTf), in excellent yield (95%) (**Scheme 23b**). A lithium-mediated aldol reaction with ethyl acetate was performed on TBS ether **145** (LDA, EtOAc) to quantitatively give adduct **146** as an inconsequential mix of C39 diastereomers. Concurrent deprotection and lactonisation was undertaken, under mild acidic conditions ($TsOH{\cdot}H_2O$, MeOH), to give β-hydroxy lactone **147** in excellent yield (94%). Employing similar conditions to those utilised by Han and Lam in the synthesis of the C16-C25 α,β-dihydroxy-δ-lactone,[62] β-hydroxy lactone **147** was dehydrated in a mixture of acetic anhydride and pyridine in benzene, with DMAP catalysis. In comparison to the good yield (83%) achieved in the α,β-dihydroxy-δ-lactone system, this gave unsaturated lactone **148** in even higher yield (94%).

Test scale (2 mg) conjugate reduction of unsaturated lactone **148** with Stryker's reagent ($[PPh_3CuH]_6$),[110] afforded only a 50% conversion, despite an extended timescale and high catalyst

loading (30 mol %) (**Table 4** entry 1). This is perhaps due to the sterically demanding nature of this substrate. It may be exacerbated by the more electron rich nature of this α,β-unsaturated carbonyl system, where the ester oxygen donates into the carbonyl, reducing its electron withdrawing ability. Therefore, a more reactive BDP-Stryker's reducing agent was prepared, which replaces triphenylphosphine ligands with a 1,2-bis(diphenylphosphino)benzene (BDP) ligand.[143] This change in ligands increases the electron density on the hydride hydrogen, rendering it a better nucleophile and allowing it to more effectively attack into alkenes of α,β-unsaturated carbonyl systems.[143] Catalyst loadings of at least 10 mol% and extended reaction times were needed to push the reaction to completion, and this could be achieved only on small scales (**Scheme 23b**, (*vide infra* **Table 4** entries 2-3). On larger scales (1.2 g), even when employing this more reactive BDP-Stryker's reagent, after 4-5 days the reaction gave only a *ca* 1:1 mixture of starting material to product. Importantly, even on larger scales only a single reduction product could be detected.

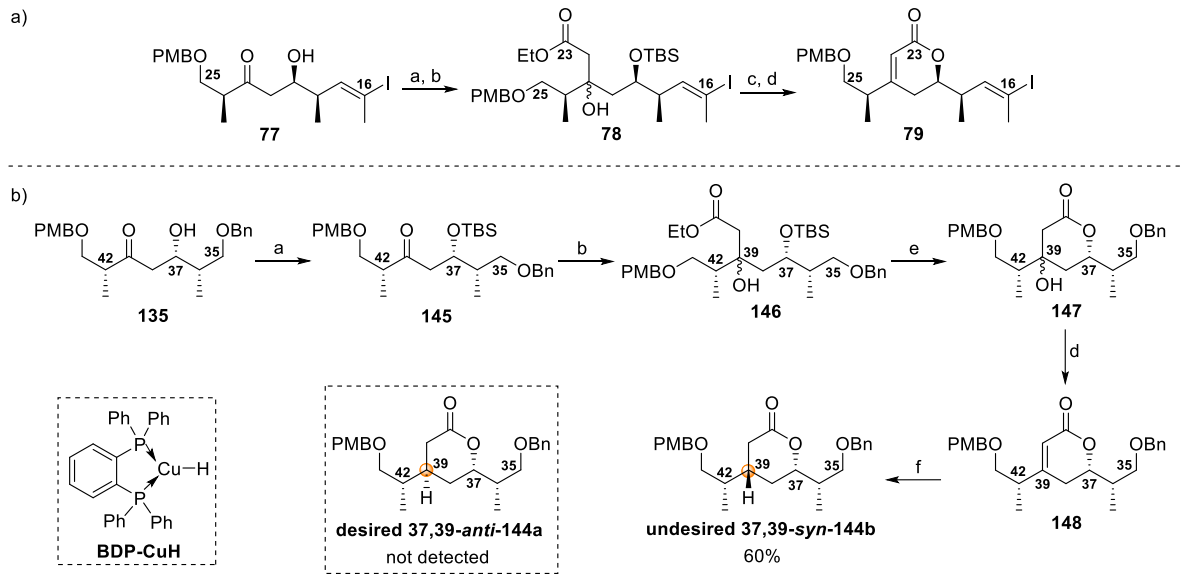

Reagents: (a) TBSOTf, 2,6-lutidine, CH_2Cl_2, –78°C to 0°C, 95%; (b) EtOAc, LDA, THF, –78°C to 0°C, 97%; (c) HF·py, py, THF, 0°C to rt, 85%; (d) Ac_2O/py/PhH (1:5:5), DMAP, reflux, 83%; (e) $TsOH·H_2O$, MeOH, rt, 94%; (f) BDP-CuH (20 mol%), PMHS, *t*BuOH, PPh_3, PhMe, 50°C, 48h, 60%.

Scheme 23. a) Previous synthesis of similar C16-C25 hemicalide lactone ring system; b) Synthesis of 37,39-syn-**144b**.

Table 4. Test scale reduction reactions on lactone **148**

Entry	Starting Material	Conditions	Catalyst & Loading	Temperature (°C)	Result
1	Lactone **148**	TMDS, PhMe, 24 h	30 mol% $[PPh_3CuH]_6$	rt	1:1 (**148**: 37,39-*syn*-**144b**)
2	Lactone **148**	PMHS, PPh_3, PhMe, 48 h	0.05 %mol BDP-CuH	rt	NR
3	Lactone **148**	PMHS, PPh_3, PhMe, 48 h	10 mol% BDP-CuH	50	60% (37,39-*syn*-**144b**)

In the case of the undesired 37,39-*syn*-diastereomer, both alkyl side chains are able to preferentially occupy equatorially positions in the chair-disposed lactone (**Figure 15a**). In this case, the $^{3}J_{H\text{-}H}$ couplings demonstrated by one of the H38 protons and one of the H40 protons would each be expected to include a large axial-axial coupling value. Indeed this is what was observed in the α,β-unsaturated-δ-lactone reduction product (**Figure 15b**); H38b exhibits a large coupling value of 11.9 Hz, while H40b exhibits a similarly large coupling of 10.8 Hz. Additionally, the newly installed H39 proton exhibits nOe correlations to the H42 and H37 methine protons. Both the large coupling constants observed with the adjacent protons and nOe correlations persuasively indicate that hydride delivery has occurred on the face *anti* to Me36 and Me42, to give undesired 37,39-*syn*-**144b** lactone as the only product.

Conformational analysis indicated that accessing the desired C37,C39-*anti*-**144a** from an α,β-unsaturated-δ-lactone substrate requires a hydride attack on the lower, more substituted face, forcing one of the C42 or C36 alkyl sidechains to unfavourably occupy an axial position in a chair conformation (**Figure 15a**). Review of the literature indicated that reduction of the unsaturated lactone system was indeed expected to preferentially proceed through a lower energy chair transition state, with axial attack of hydride, leading to the undesired 37,39-*syn*-**144b**.[110] Given the exclusive production of the undesired 37,39-*syn*-product, substrate control from the cyclic lactone was deemed too strong to be overcome by employing a chiral reagent. Given the conformational restriction imposed by cyclic structures, it was hypothesised that the reduction of an acyclic enoate might provide a tactical solution to this impasse. Consequently, focus was turned to synthesis of acyclic enoates.

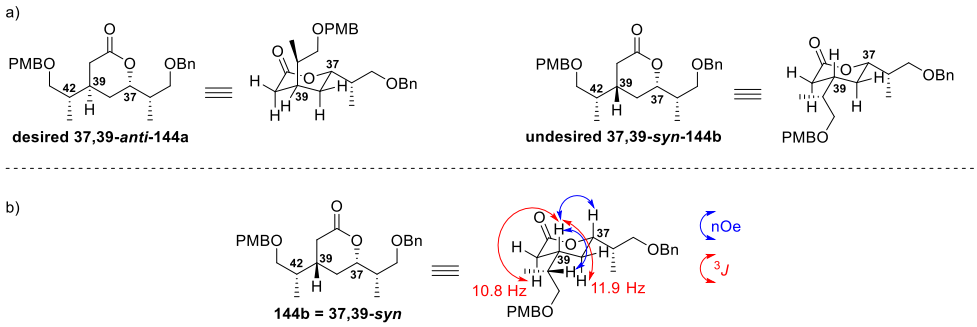

Figure 15. a) Possible chair conformations of α-hydroxy-δ-lactone system **144**; b). Structural elucidation of reduction product 37,39-*syn*-**144b**

The first hurdle was to develop a way to reliably obtain acyclic enoate **149**. To this end, a number of methodologies were trialled (**Scheme 24**, **Table 5**). The dehydration conditions that were successful with lactone **147** gave no reaction with alcohol **146** (**Table 5** entry 1), even when

temperatures were raised or acetic anhydride was used in large excess (**Table 5** entries 2 and 3). When alcohol **146** was treated with Burgess reagent, a modest yield of enoates **149a** (17%) and **149b**, in a *ca* 1:1 ratio along with other regioisomeric olefin by-products, was observed (**Table 5** entry 4). Thionyl chloride-mediated dehydration, under basic conditions, gave a modestly improved yield of the enoates (**Table 5** entry 5), still in a *ca* 1:1 ratio (35% each), with **149a** being inseparable from other olefinic by-products.

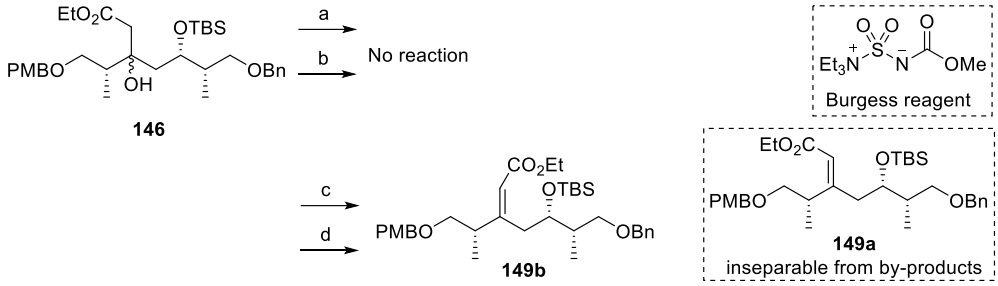

Reagents: (a) DMAP (cat.), Ac_2O:py:PhMe (1:5:5), 90°C to 125°C; (b) DMAP (cat.), Ac_2O:py:PhMe (2:1:1), 125°C; (c) methyl N-(triethylammoniumsulfonyl)carbamate (Burgess reagent), THF, rt, 17% **149b**; (d) $SOCl_2$:py (1:1), CH_2Cl_2, 0°C, 35% **149b**.

Scheme 24. Elimination conditions trialled on alcohol **146** to obtain acyclic enoate **149**

Table 5. Conditions trialled to obtain acyclic enoates

Entry	SM	Conditions	Reaction outcome	*E*:*Z*
1	Alcohol **146**	DMAP, Ac_2O:py:PhH (1:5:5), 90°C, O/N	No reaction	NA
2	Alcohol **146**	DMAP, Ac_2O:py:PhH (1:5:5), 125°C, O/N	No reaction	NA
3	Alcohol **146**	DMAP, Ac_2O:py:PhH (10:5:5), 125°C, O/N	No reaction	NA
4	Alcohol **146**	Burgess reagent, THF, rt, 20 h	17% **149b** (**149a** inseparable)	1:1
5	Alcohol **146**	$SOCl_2$:py (1:1), CH_2Cl_2, 0 °C, 4 h	35% **149b** (**149a** inseparable)	1:1

With conventional addition/dehydration strategies failing to deliver the desired results, attention was turned towards exploring methods to elaborate the ketone and thereby enable regio- and stereoselective generation of the enoate. To this end, a Peterson olefination, with ethyltrimethylsilyl acetate (ETSA), was trialled to install the required C39 olefin (**Scheme 25**). The Peterson olefination is a silicon variant of Wittig-type reactions.[92,144] The first step in the generation of both (*E*)- and (*Z*)-enoates stems from the creation of a mixture of diastereomeric β-silylcarbinols, which arises when the α-silylenolate attacks into the carbonyl. In some cases these diastereomers are sufficiently stable to be separated.[92] In these instances, treatment of each individual diastereomer with base or acid to induce *syn*- or *anti*-elimination, would then allow a

single diastereomer to be obtained. However, where the functionality adjacent to the deprotonated centre is electron withdrawing, as in the present case of ETSA, the diastereomers are insufficiently stable to be separated. In these cases, the *E*/Z isomer ratios reflect those of the β-silylcarbinol diastereomeric mixture.[145]

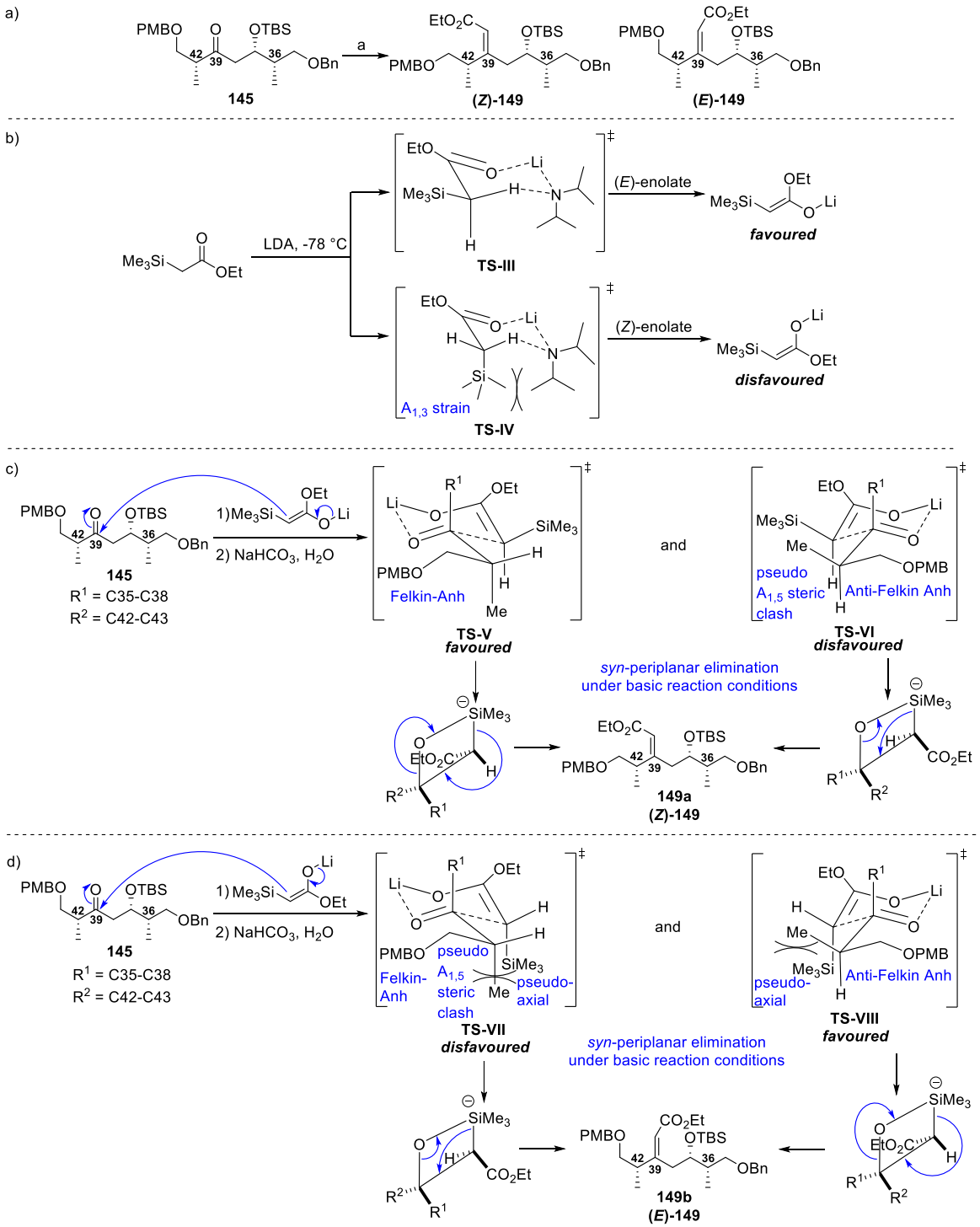

Reagents: (a) ETSA, LDA, –78°C *then* **145**, –78°C (1h) to rt, 63%:12% → 80%, *Z/E* 5:1 → >19:1

Scheme 25. a) Synthesis of enoates (*E*)- and (*Z*)-**149**; b) Formation of (*E*) and (*Z*)-enolates; c) Transition states arising from attack of (*E*)-enolate; and d) Transitions states arising from attack of (*Z*)-enolate.

A Peterson olefination, with ETSA, was conducted on ketone **145** (**Scheme 25a**). Encouragingly, on a test scale, the reaction proceeded to give a modest yield (44%) of enoates **149a** and **149b**, in a 5:1 ratio, with no other olefinic by-products observed. Initially, this result could not be reproduced on a larger scale, with no enoate products observed. However, through systematic modification of reaction conditions, it was found that an excess of the α-silylenolate was required. Furthermore, contrary to published conditions, it was necessary that the base (LDA) was present in substoichiometric amounts relative to the ETSA. This is likely necessary to avoid undesired side reactions of excess base with starting material **145**. Under these conditions, the reaction produced a good yield of enoates **149a** and **149b** (80%, *E*:*Z* = 1:4 to 1:19 condition dependent *vide infra*) (**Scheme 25a**). This represented a marked improvement over the previous two-step aldol/dehydration sequence (**Table 5**).

In cases of chelation control, the lithium cation acts as a Lewis acid, and a stepwise reaction pathway dominates.[146] The overall stereocontrol is governed in two stages: firstly, by enolisation geometry and, secondly, by carbonyl π-facial selectivity. Four diastereomeric intermediates are possible in Peterson olefination reactions involving ETSA enolate-addition into an unsymmetrical ketone. Two of these result in the (*E*)-enoate, while two result in the (*Z*)-enoate. In the formation of the lithium α-silylenolate with LDA, steric considerations favour one of the two possible transition states (**TS-III** and **TS-IV**, **Scheme 25b**). In the six-membered chair transition states, **TS-III** is strongly favoured over **TS-IV**, which experiences 1,3-diaxial strain between an *iso*-propyl group and the TMS substituent. This results in predominantly the (*E*)-enolate. The resulting (*E*)-enolate then attacks the ketone *via* a cyclic Zimmerman-Traxler transition state. The facial selectivity of this process will be discussed in the context of enolate attack into TBS ether **145** (**Scheme 25c-d**).

The (*E*)-lithium enolate can attack from either side of the C39 carbonyl, resulting in two possible transitions states (**TS-V** and **TS-VI**, **Scheme 25c**). In **TS-VI**, anti-Felkin approach leads to unfavourable 1,5-diaxial steric interactions between the TMS group of the enolate and Me42. In contrast, in **TS-V**, Felkin attack over the smallest group minimises steric interactions. As a result **TS-V** is believed to be favoured over **TS-VI**. It was important that the reaction mixture was allowed to warm to rt prior to quenching. This is because, during this process, both the basic conditions and the higher temperatures promote s*yn*-periplanar elimination. As **TS-V** and **TS-VI** are effectively mirror images of one another, under conditions favouring *syn*-periplanar elimination, both transition states eliminate to give enoate **149a** (note that the ethyl ester is on the same side as R^2 in both transition states in **Scheme 25c**).

The minor (*Z*)-lithium enolate can also attack from either face of the C39 ketone, giving rise to diastereomeric transitions states **TS-VII** and **TS-VIII** (**Scheme 25d**). Transition state **TS-VII** is unfavourable due to the 1,5-diaxial strain. Transition state **TS-VII** results in anti-Felkin Anh attack on the aldehyde and is, consequently, not as favourable as transition state **TS-V**. Again, as these transitions states are effectively mirror images of one another, they both undergo *syn*-periplanar elimination under the basic reaction conditions to give enoate **149b** (note that the ethyl ester is on the same side as R^1 in both transition states in **Scheme 25d**). The initial reaction gave the enoate products in a 5:1 ratio. The geometry was determined as discussed below (**Scheme 26a**).

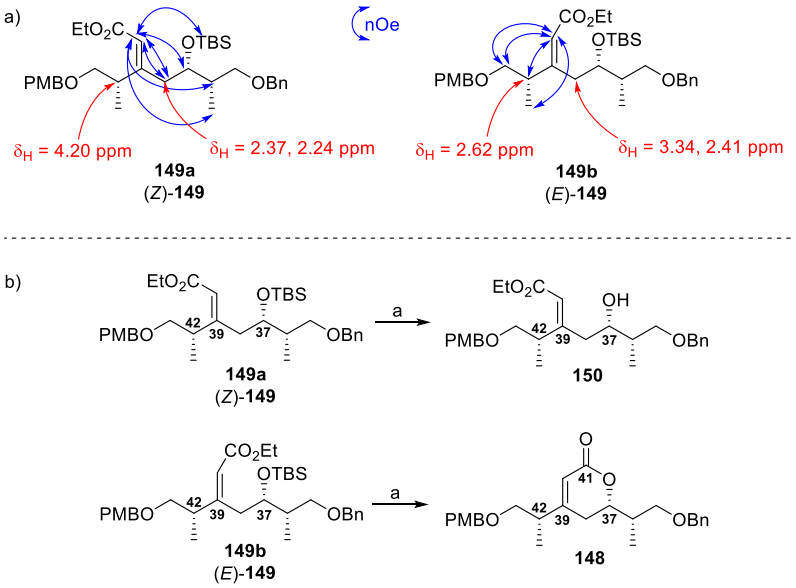

Reagents: (a) TsOH·H_2O, MeOH, rt, 97%-99%.
Scheme 26. a) Diagnostic spectroscopic features in Peterson olefination products **149a** and **149b**; b) Stereochemical confirmation by exposure of Peterson olefination products **149a** and **149b** to deprotection/lactonisation conditions

Mechanistic considerations would indicate that **149a** is the (*Z*)-enoate and **149b** is the (*E*)-enoate. NMR spectroscopic analysis further corroborated the stereochemical assignment (**Scheme 26a**). In **149a** compared to **149b**, H42 is shifted significantly downfield (+1.58 ppm), due to closer proximity to the ester carbonyl, in the (*Z*)-configuration. Conversely, in **149b** the diastereotopic H38 protons differ significantly from each other (0.93 ppm), as one is similarly shifted much further downfield compared to the corresponding signal in **149a** (+0.97 ppm), due to closer proximity to the ester carbonyl, in the (*E*)-configuration. NOe experiments also showed that in **149b** the olefinic proton, H37 shows correlations only with H42, Me42 and H43. Conversely, in **149a**, the olefinic proton shows strong correlations with only H38a and H38b, H36, Me36 and the TBS ether.

To corroborate the spectroscopic evidence, **149a** and **149b** were each exposed to the deprotection and lactonisation conditions used to give **148** (**Scheme 26b**). Under these conditions, the (*Z*)-olefin was not expected to lactonise, as the ester is geometrically locked in a configuration unable to engage with the C37 alcohol. Indeed compound **149b** underwent TBS deprotection and lactonisation to give a sample matching lactone **148**, whereas compound **149a** simply underwent TBS deprotection to give C37 alcohol **150**. These observations acted as further evidence to definitively confirm the stereochemistry of these enoates.

With the acyclic enoates in hand, reduction of the olefin to install the C39 stereocentre could be explored. A test scale conjugate reduction with Stryker's reagent ($[PPh_3CuH]_6$) gave no reaction (**Scheme 27, Table 6** entries 1-2). This is perhaps unsurprising, given the low reactivity of Stryker's reagent on the analogous unsaturated lactone system, which is more reactive due to ring strain (*vide supra*). More surprisingly, test scale conjugate reduction with the more reactive BDP-Styker's reagent (BDP-CuH), with a variety of different catalyst loadings and temperatures ranges (**Scheme 27, Table 6** entries 5-8), also gave no reaction with either of the enoates. This outcome is likely attributable to a combination of reduced reactivity of α,β-unsaturated esters compared to α,β-unsaturated ketones; unfavourable steric effects and loss of the rigidity and ring strain of a cyclic system. This prompted exploration of alternative strategies for installing the required C39 stereocentre.

Table 6. Test scale reduction reactions on enoate substrates

Entry	Starting Material	Conditions	Catalyst & Loading	Temperature (°C)	Result
1	(*E*)-**149**	TMDS, PhMe, 24 h	30 mol% $[PPh_3CuH]_6$	rt	NR
2	(*Z*)-**149**	TMDS, PhMe, 24 h	30 mol% $[PPh_3CuH]_6$	rt	NR
3	(*E*)-**149**	PMHS, PPh_3, PhMe, 48 h	0.05 %mol BDP-CuH	rt	NR
4	(*Z*)-**149**	PMHS, PPh_3, PhMe, 48 h	0.05 %mol BDP-CuH	rt	NR
5	(*E*)-**149**	PMHS, PPh_3, PhMe, 48 h	10 mol% BDP-CuH	40	NR
6	(*E*)-**149**	PMHS, PPh_3, PhMe, 48 h	10 mol% BDP-CuH	50	NR
7	(*E*)-**149**	PMHS, PPh_3, PhMe, 48 h	10 mol% BDP-CuH	60	NR
8	(*Z*)-**149**	PMHS, PPh_3, PhMe, 48 h	10 mol% BDP-CuH	70	NR

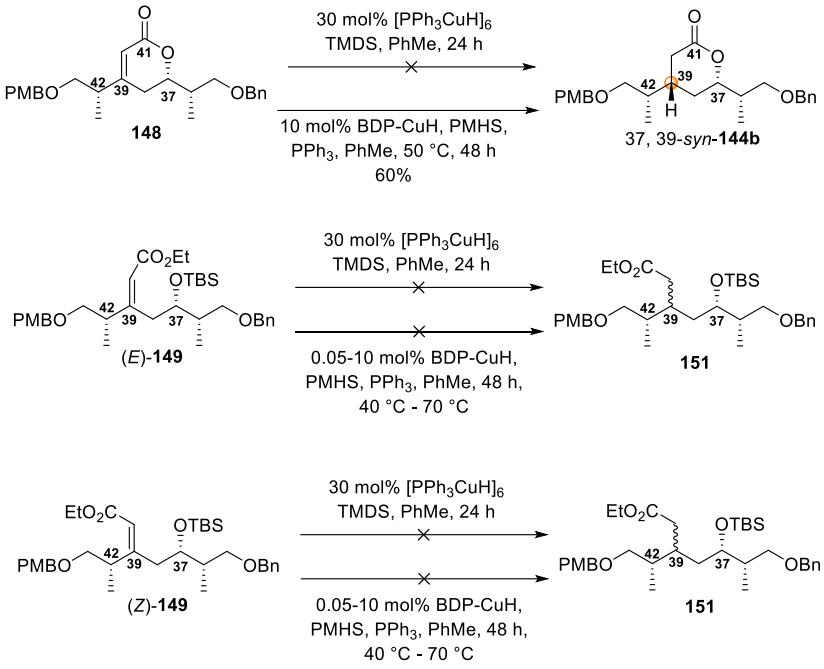

Scheme 27. Reduction conditions trialled on lactone **148** and the enoates (*E*)- and (*Z*)-**149**

Review of the literature disclosed good precedent that a hydroxyl-directed hydrogenation might allow selective installation of H39 in the desired configuration.[59,147,148] In such reactions, coordination of the catalyst to the alcohol directs reduction preferentially on one face of the olefin (e.g. **Figure 16a**).[149] Cationic iridium and rhodium complexes appear to be the most commonly used catalyst types. Of these, Crabtree's catalyst ([Ir(cod)py(PCy_3)]PF_6)[127] (**[Ir]-I**) appears to be particularly popular in hydroxyl-directed reductions (**Figure 16b-c**),[147] perhaps due to its ease of handling and wide applicability.

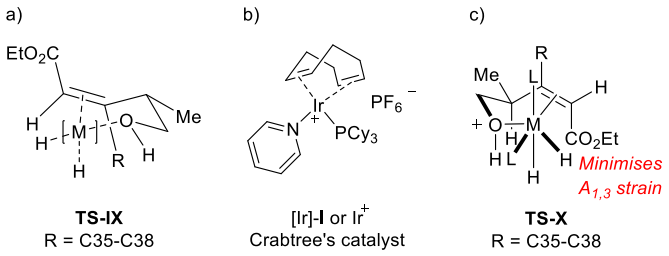

Figure 16. Cationic catalysts and their coordination to substrate homoallylic alcohol a) Example of chair-like coordination of homoallylic alcohol in the context of alcohol **152** (ligands excluded for clarity); b) Crabtree's catalyst; c) Possible transition state with Crabtree's catalyst.

In order to facilitate this approach, the PMB ether group of enoate (*Z*)-**149** was deprotected with DDQ, in good yields (78%) on the test scale, to give primary alcohol **152** (**Scheme 28a**). It was envisioned that the free hydroxyl in alcohol **152** would provide a coordinating group, chelating to the catalyst to form a pseudo-chair conformation (**Figure 16a**).[149] A test scale reaction with readily

available Wilkinson's catalyst showed no reduction to unsaturated ester **154** (**Scheme 28b**). This is perhaps unsurprising, given that attempted reduction of α-hydroxylactone **116b**, in the Cossy group synthesis of the C36-C42 stereocluster (section **1.4.5**), did not proceed under 1 atm of hydrogen with palladium on carbon catalysis.[59] Instead, it required forcing conditions using a H-cube flow reactor at 50 °C and 40 bar hydrogen. However, it was considered promising that a hydroxyl-directed reduction exploiting the C40 alcohol in the presence of Crabtree's catalyst ([Ir]-**I**) afforded both C42 epimers with moderate selectivity (*dr* 63:37, **117b:117d**, **Scheme 15**). Thus, on this reasoning, focus was shifted to hydroxyl-directed reductions using Crabtree's catalyst.

Unfortunately, alcohol **152** proved to be prone to translactonisation to give lactone **153**. This occured both under conditions employed during test reduction reactions, or when left under deprotection conditions for too long. In contrast, it was shown in the assignment of **149a** as (*Z*)-**149** and **149b** as (*E*)-**149** that (*Z*)-**149** does not readily lactonise when under mildly acidic deprotection conditions, but remains as C37 alcohol **150** (**Scheme 26b**). This provided a route to circumvent the translactonisation issue, while ensuring an appropriately positioned hydroxyl for directed reduction.

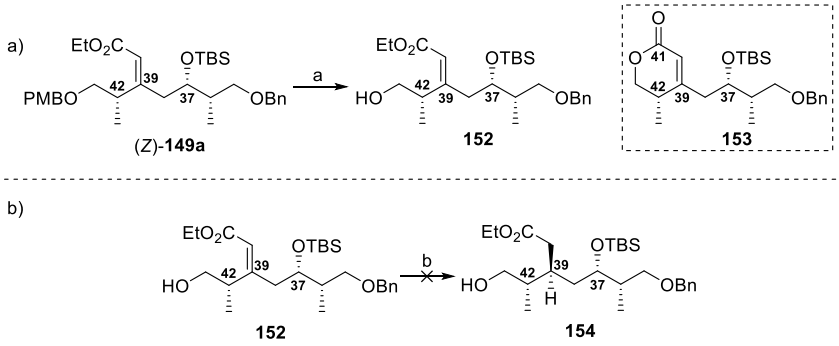

Reagents: (a) DDQ, CH_2Cl_2, pH 7 buffer, 0°C to rt, 78%; (b) $(PPh_3)_3RhCl$, Ph, H_2 (1 atm), rt, 0%.
Scheme 28. a) PMB deprotection of (*Z*)-enoate **149a**; and b) Test reduction with Wilkinson's catalyst on alcohol **152**.

After trialling a range of Crabtree's catalysed hydrogenation conditions on C37 alcohol **150**, it was shown, rather serendipitously, that this reaction gave the best diastereoselectivity for the desired product at lower temperatures and that longer reaction times were required on larger scales (**Table 7**). As the first reaction trialled indicated completion with 8 mol% catalyst loading, this variable was kept constant. Once reaction completion was shown by NMR (through absence of olefinic peaks), lactonisation could also be undertaken in the same pot by bringing the reaction to rt, adding a catalytic amount of *p*-toluenesulfonic acid and stirring for five minutes.

Table 7. Trial of reaction conditions for Crabtree catalysed hydroxyl-directed reduction at C39

Quantity (mg)	Solvent	Temperature (°C)	Reaction time	Diastereomeric ratio	Conversion SM:product
2.0	CH_2Cl_2	rt = *ca* 5-8	O/N	3:1	complete
14.0	CH_2Cl_2	rt = *ca* 26	O/N	1:1	complete
5.0	THF	rt = *ca* 12-18	O/N	3:1	50%:50%
5.0	PhMe	rt = *ca* 12-18	O/N	3:1	60%:40%
5.0	PhH	rt = *ca* 12-18	O/N	2:1	complete
5.0	CH_2Cl_2	0	O/N	3:1	complete
5.0	CH_2Cl_2	–20	O/N	4:1	complete
20.0	CH_2Cl_2	–40	O/N	-	NR
60.0	CH_2Cl_2	–20	O/N	4:1	~40% (NMR)
1000	CH_2Cl_2	–20	1 week	5:1	89%

An initial overnight test scale reaction (2.0 mg), undertaken at room temperature in dichloromethane, promisingly showed a new lactone product in a 3:1 ratio favouring the desired 37,39-*anti*-**144a**. Configurational assignment of the major product was made by NMR spectroscopic analysis, with particular reference to coupling constants and nOe interactions (**Figure 17a**). This showed that H39 of the new lactone showed a smaller coupling with H40a (6.0 Hz) and a larger coupling with H40b (11.2 Hz). This indicated a *trans*-relationship with H40b, which itself had nOe correlations with H37. On this basis, the major product, **144a**, was assigned as the desired 37,39-*anti* lactone diastereomer. It was proposed that the reaction proceeds through **TS-XI**, where the approach of the catalyst preferentially positions the larger C35-C36 portion of the molecule equatorially (**Figure 17b**).

After these promising initial results, repeating this reaction (14.0 mg), again at room temperature, gave only a 1:1 ratio of lactone products. Seeking to regain the desired diastereoselectivity, the reaction was trialled, again at room temperature, in a range of solvents. Running the reduction in THF and toluene allowed the 3:1 diastereoselectivity to be regained, but gave only 50-60% conversion of starting material to products by NMR. The reduction went effectively to completion in benzene, but with a reduced 2:1 diastereoselectivity.

At this point, the discrepancy between the two original reactions was reconsidered. Both had been run with no external heating or cooling, seemingly at room temperature. However, these reactions were conducted during winter, across a period where there had been heating issues in the lab.

The first reaction was run when the heating was completely off and only started late in the evening, when the lab was *ca.* 5-8°C. Whereas the second reaction was run when the heating had been fixed, but the thermostat had been set to maximum, so that it was *ca.* 26°C in the lab. This suggested that the desired diastereoselectivity improved when the reaction was cooled.

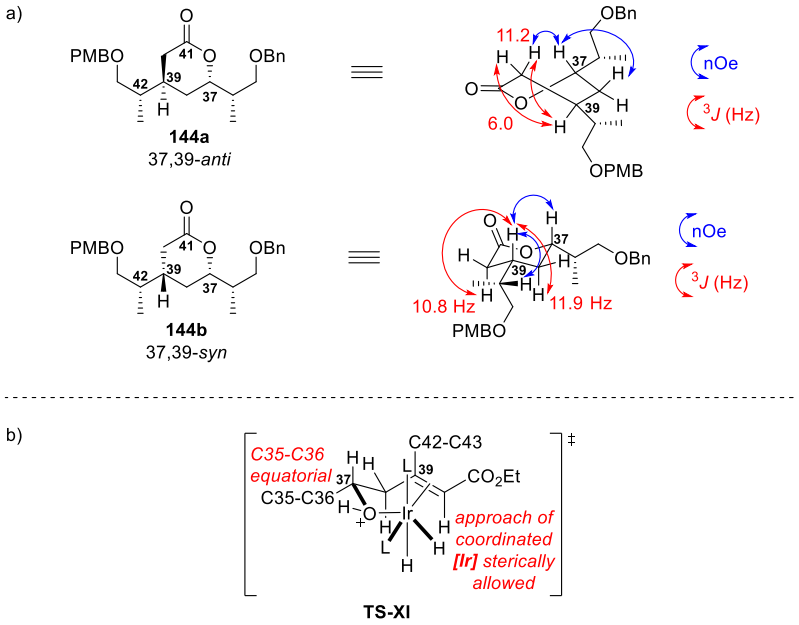

Figure 17. a) Assignment of C39 epimers **144a** and **144b**; b) Suggested transition state to give **144a**.

The overnight reduction was repeated, in dichloromethane, at 0°C, –20°C and –40°C, showing complete conversion at 0°C and –20°C, with diastereoselectivities of 3:1 and 4:1 for the desired lactone, respectively. However, the reaction stalled at –40°C, showing no conversion to product. Thus, –20°C was selected as the optimal reaction temperature to balance maximising diastereoselectivity while maintaining reactivity. The reaction scaled well and could be run on multigram scales, which bodes well for any future scale-up. Yet, with larger scale reactions it was necessary to extend the reaction time. Ultimately, all but very small reactions were best run at –20°C for 1 week. If scale up was repeated, catalyst dosing over the course of the reaction may assist in lowering reaction time. Workable diastereoselectivities of 5:1, in favour of the desired 37,39-*anti*-**144a**, could be achieved on the gram scale. However, at this stage the product diastereomers were not separable.

Following, C39 hydrogenation and lactonisation to give lactone 37,39-*anti*-**144a** (and inseparable 37,39-*syn*-**144b**) (**Scheme 29a**), diastereoselective α-hydroxylation of the lactone was achieved by addition of Davis oxaziridine[126] to lactone enolate **155** (**Scheme 29b**). The base used to generate the enolate was found to be important and yields could vary widely (25%-81%) depending on the

identity and quality of the base. Initially, a commercially available solution of NaHMDS in THF was used to enolise the lactone, but yields were quite low and irreproducible (25-50%). A number of other α-hydroxylation strategies were explored, but none gave satisfactory results.

Finally, freshly prepared solutions of KHMDS in THF were found to reproducibly give high yields (*ca.* 80%) and excellent diastereoselectivities for α-hydroxylactone **133a**, providing only the desired C40 diastereomer. This is likely due to the transdiaxial effect favouring reaction through the lower energy chair conformation in a form that avoids unfavourable 1,3-diaxial interactions (**Scheme 29b**). Protection of α-hydroxylactone **133a** as its TES ether (TESOTf, 2,6-lutidine) proceeded quantitatively. At this point, careful purification allowed separation of the C39 diastereomers to give TES ether **156** in 85% yield.

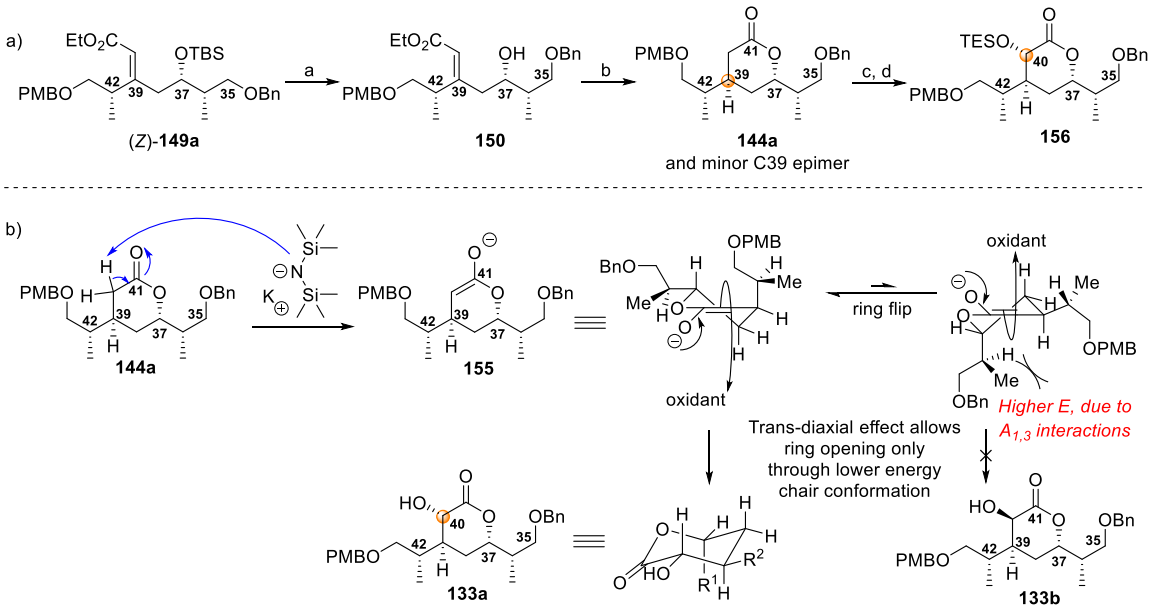

Reagents: (a) TsOH·H_2O, MeOH, rt, 97%; (b) [Ir(cod)py(PCy_3)]-PF_6, H_2 (1 atm), –20°C to rt *then* TsOH·H_2O, 89%; (c) KHMDS, 2-(phenylsulfonyl)-3-phenyloxaziridine, THF, –78°C, 81%, *dr* >20:1; (d) TESOTf, 2,6-lutidine, CH_2Cl_2, –78°C, quant., 85% 37,39-*anti*.
Scheme 29. a) Synthesis of TES ether **156** from (Z)-enoate **149a**; b) Mechanism of α-hydroxylation of enolate **155** to give only the desired C40 diastereomer.

In light of the problems faced by Ardisson/Cossy in their global deprotection of hemicalide stereoisomer **121** and their uncertainty regarding the C40 or C45 location of the remaining TBS protecting group (**Scheme 17**), a more labile TES ether was specifically chosen to balance the necessity of surviving subsequent synthetic manipulations with ease of eventual global desilylation. Although Han and Lam experienced some issues with *bis*-TES deprotection of the dihydroxylactone in their synthesis of the C1-C28 diastereomers 13,18-*syn*-**83a** and 13,18-*anti*-

83b (**Scheme 12**),[62] it was reasoned that this was due to the greater steric demands of the α,β-dihydroxylactone, which are not applicable in the present α-hydroxylactone system.

With protected α-hydroxylactone **156** in hand, it was now time to extend the carbon backbone at C43 (**Scheme 30a**). Oxidative PMB deprotection (DDQ) (**157**) and Swern oxidation[69–72] (**Scheme 30a**) gave aldehyde **158.** Although a DMP oxidation was trialled for this transformation, it was found that aldehyde **158** could be more reproducibly obtained, with greater yield in the subsequent HWE olefination, under Swern conditions. To avoid epimerisation at C42, aldehyde **158** was immediately subjected to mild HWE olefination[150] with dimethyl (2-oxopropyl)phosphonate (ketophosphonate **159**) and $Ba(OH)_2$ (**Scheme 30b**). Utilisation of $Ba(OH)_2$ permits an unusually mild HWE reaction. Initially Ba^{2+} coordinates both the carbonyl and phosphoryl oxygens, thereby lowering the pK_a of the methylene protons. This facilitates deprotonation to generate the corresponding carbanion, which swiftly and reversibly attacks into the C42 aldehyde carbonyl to give a mixture of *syn*- and *anti*- diastereomers. Formation of the oxaphosphetane occurs more slowly, but also reversibly. During the formation of the oxaphosphetane repulsion occurs between the polarised aldehyde carbonyl bond and the electronegative methyl ketone stabilising group. The four-membered ring then flattens, with the methyl ketone and C35-C42 chain being placed on opposite sides of the ring.[151] Consequently, the *anti*-oxaphosphetane forms more rapidly than the *syn*-oxaphosphetane, and irreversibly collapses to deliver (*E*)-enone **160**. In the present reaction, these factors result in the generation of exclusively (*E*)-enone **160** in good yields (74% over two steps).

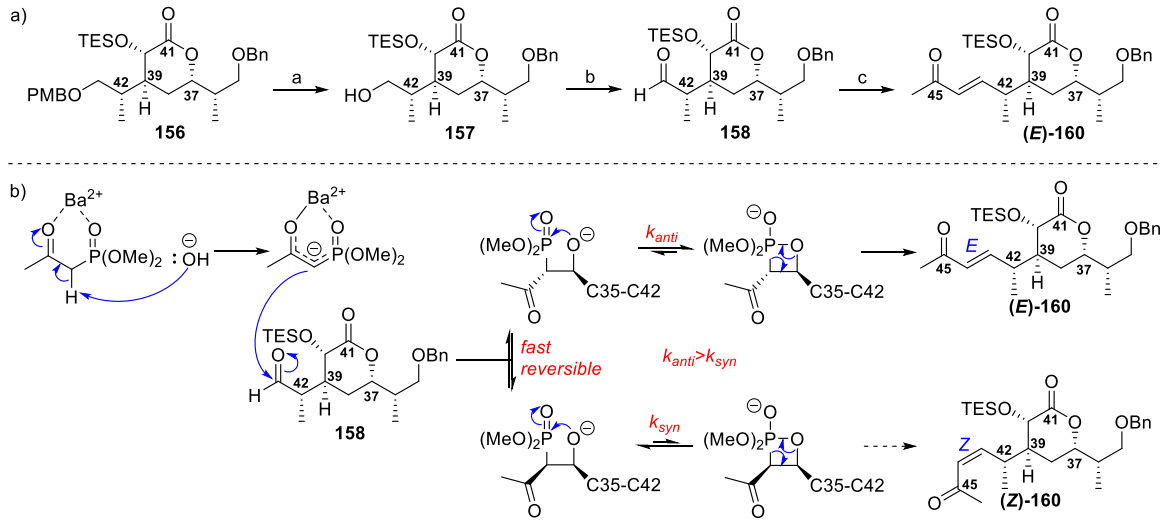

Reagents: (a) DDQ, CH_2Cl_2/pH 9.2 buffer (4:1), rt, 97%; (b) $(COCl)_2$, DMSO, CH_2Cl_2 *then* **157** *then* Et_3N, –78°C; (c) dimethyl(2-oxopropyl)phosphonate, $Ba(OH)_2$, rt to 0°C *then* **158**, THF:H_2O (40:1), 0°C to rt, 74% (2 steps).
Scheme 30. a) Synthesis of enone (*E*)-**160** from TES ether **156**; b) Mechanism of HWE olefination of C43 aldehyde **158**.

The next goal was reduction of the C45 enone carbonyl to install the final stereocentre of this region, producing the 42,45-*anti* and 42,45-*syn* diastereomers and permitting the eventual assignment of the relative configuration of this fragment. The reduction of the C45 carbonyl was planned to be performed on the enone in order to allow greater steric and electronic facial distinction of this prochiral carbonyl. With the enone there is the steric difference between the methyl on one side and the conjugated alkene on the other side. However, if reduction were performed first, there would only be the difference between a methyl on one side and a methylene on the other side. To this end, a number of asymmetric strategies were investigated, firstly CBS reduction. Exploratory studies by Han and Lam on the C16-C28 region showed that a CBS reduction[152] on analogous C28 enone **161** could give useful levels of diastereoselectivity (*dr* 5:1). However, subsequent directed hydrogenation on allylic alcohol **162**, mediated by suitable catalysts, did not result in any reaction to allow the selective removal of the allylic olefin.

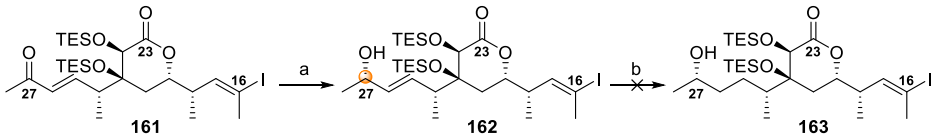

Reagents: (a) (*R*)-MeCBS, $BH_3{\cdot}SMe_2$, THF, –78°C, 80%, *ca dr* 5:1; (b) $RhCl(PPh_3)_3$ *or* $[Irpy(cod)PCy_3]PF_6$, H_2, 0%.

Scheme 31. Model enone reduction by Han and Lam[153,154]

CBS reduction showed some promise (*dr* 5:1) on test scale reductions (<10 mg) of enone (*E*)-**160**, with equimolar loading of methyl CBS catalysts, trialling multiple substituents on the boron (Error! R eference source not found.**a**, example reaction catalyst shown). The mechanism and stereomodel of CBS reduction are well established (Error! Reference source not found.**b**, catalyst with methyl substituent shown).[152] CBS catalysts are boron heterocycles, the most simple of which has a methyl substituent on the heterocyclic boron. Upon exposure to borane, the basic heterocyclic nitrogen complexes with the newly introduced reductant to give the active reducing agent. The active species then also complexes with the carbonyl compound, through the Lewis-acidic heterocyclic boron atom. This effectively activates both the borane and the carbonyl. The borane hydrogen is made more hydridic by donation of electron density from the nitrogen, while the carbonyl is made more electrophilic by withdrawal of electron density from the heterocyclic boron. Delivery of the hydride occurs through a cyclic six-membered transition state, where enantioselectivity is derived from the preference of the larger carbonyl substituent to occupy the pseudoequatorial position. Unfortunately, these preliminary results were not reproducible on practical scales. Excess loading of CBS catalysts, changing the catalyst structure (e.g. from Me to phenyl) and running them for extended timescales (up to 1 week) did not improve yields. Lowering

the temperature below –78°C offered no improvement, while raising the temperature of the reactions above –78°C resulted in deterioration of selectivity.

Review of the literature suggested that the Terashima reduction, which utilises a partially decomposed lithium aluminium hydride reductant, could provide an alternative approach for asymmetric reduction of prochiral carbonyls.[155,156] The reductant is created by refluxing lithium aluminium hydride in diethyl ether with either (+) or (–)-*N*-methylephedrine then adding *N*-ethylaniline. Although the reaction mechanism has not been established, it has been suggested that the lithium aluminium hydride partially decomposes during reflux. One of the aluminium-hydrogen bonds is replaced with a bond to diethyl ether. Aluminium also takes on additional bonds with the nitrogens of two *N*-ethylaniline molecules as well as the nitrogen and oxygen molecules of either (+) or (–)-*N*-methylephedrine (Error! Reference source not found.**d**).

The lithium cation also played an essential role, such that, if tetraethylenediamine was added, yields and stereoselectivity dropped dramatically. It was proposed that the steric interaction of the substituents of the enone with the methyl and phenyl groups of the ephedrine and ethylaniline, and the electronic interaction of the carbonyl oxygen with the lithium cation, controlled the face from which the reducing agent approached the enone. The enone is proposed to approach from the side of the octahedral complex that bears the hydrogen in the axial position, with the smaller group of the prochiral carbonyl closer to the phenyl group to minimise steric interactions.

The reaction product configuration was able to be predicted from ample precedent with 42,45-*anti*-**164a** or 42,45-*syn*-**164b** resulting from the (+) or (–)-*N*-methylephedrine additive, respectively. Formation of Mosher's esters **165** and **166** was also undertaken to assess and, ultimately, confirm the absolute stereochemistry of C45 (Error! Reference source not found.**e**). T his reaction produced consistently high yields of the desired allylic alcohols (*ca.* 90%, quantitative *brsm*) (Error! Reference source not found.**c**). The diastereoselectivity was optimised to 6:1 *dr*. H owever, although the diastereomers were separable by chromatography, it was a very challenging separation. As a result, only 62% yield of pure product 42,45-*anti*-**164a**, free from the other diastereomer, was obtained after rigorous purification.

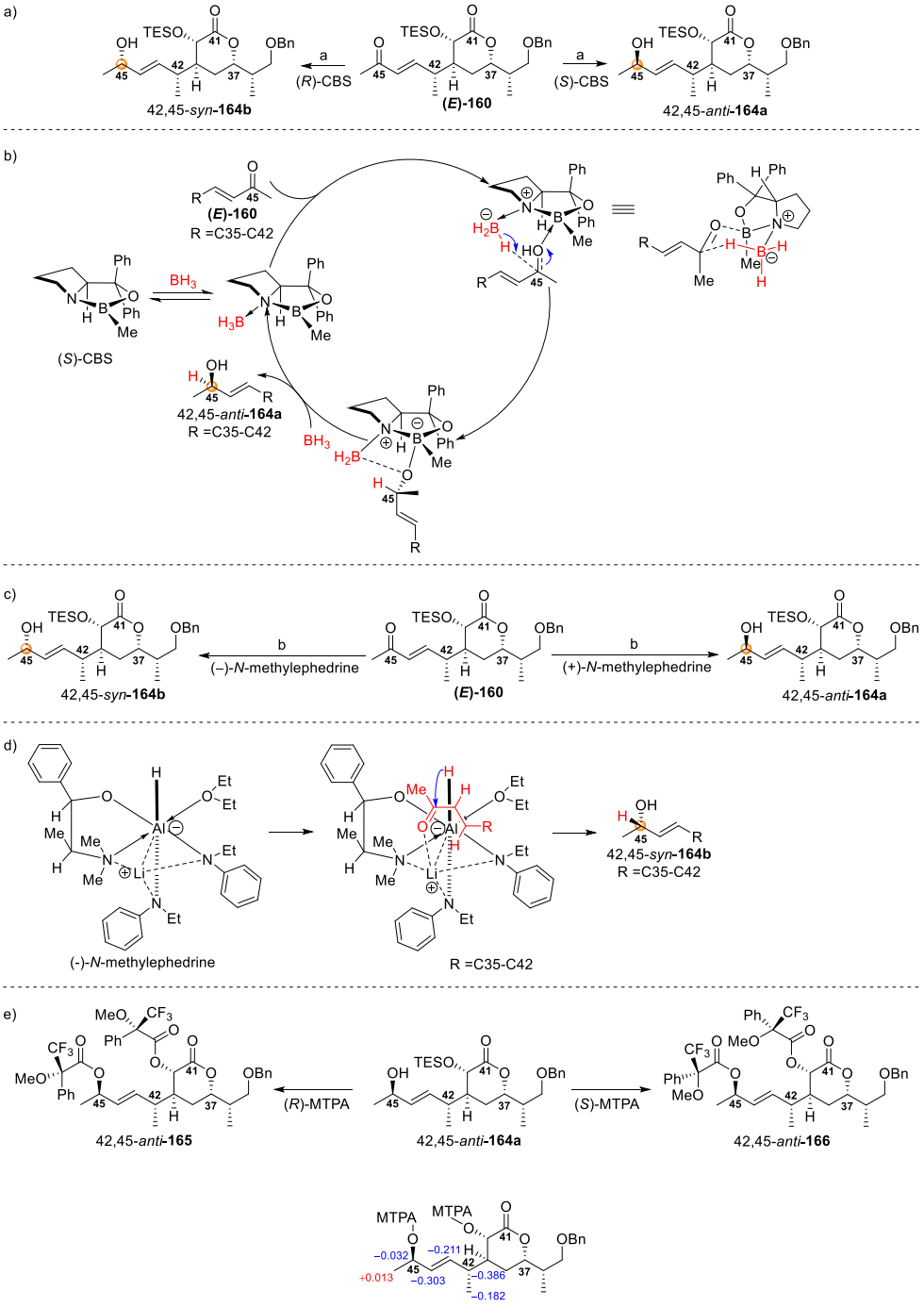

Reagents: (a) (*R*) or (*S*)-MeCBS, $BH_3{\cdot}SMe_2$, THF, –78°C, 80%, *ca dr* 5:1; (b) $LiAlH_4$, (–) or (+)-*N*-methylephedrine, Et_2O, reflux *then N*-ethylaniline, reflux *then* (*E*)-**160**, –94°C, 93%, *dr ca.* 6:1; (c) DCC, DMAP, (*R*)- or (*S*)-MTPA, CH_2Cl_2, rt.

Scheme 32. a) Example CBS-reduction with (*R*) or (*S*)-MeCBS; b) Reduction mechanism with (*S*)-MeCBS; c) Terashima reduction with (+) or (–)-*N*-methylephedrine ligand; d) Suggested Terashima reduction complex; e) Mosher ester formation and analysis of C45.

With the C45 diastereomers obtained, focus was turned to the concomitant olefin reduction and benzyl ether cleavage, to allow chain extension at C35. To facilitate these manipulations, allylic alcohol 42,45-*syn*-**164b** was protected as TES ether 42,45-*syn*-**167** (**Scheme 33a**). Analogously to the C40 hydroxyl, given the deprotection issues faced by Ardisson/Cossy in their deprotection of

hemicalide stereoisomer **121**, a TES group was initially considered to be preferable to a TBS group at the C45 hydroxyl.

As discussed above, Han and Lam were not able to reduce the analogous C25-C26 allylic olefin with Wilkinsons's catalyst ($RhCl(PPh_3)_3$) or Crabtree's catalyst ($[Irpy(cod)PCy_3]PF_6$) (**Scheme 31**). On this rationale, concomitant reduction and benzyl ether cleavage was explored using hydrogen and palladium on carbon. Although these conditions did allow for the desired alkene reduction and benzyl ether cleavage, desilylation at C40 and C45 was also observed. This persisted despite screening a range of reaction times, solvents, catalyst loadings and temperatures. Use of $NaHCO_3$, as an additive to buffer the potentially mildly acidic reaction conditions with the palladium on carbon, or switching to palladium hydroxide, as a milder catalyst, failed to solve these issues. Thus, alternative reduction and debenzylation strategies were explored.

As part of the evolution of the spirastellolide A methyl ester synthetic strategy, Raney nickel (Ra-Ni) was used to debenzylate an advanced intermediate containing secondary TES groups.[157] Stirring the substrate with Ra-Ni, under a hydrogen atmosphere for 14h, resulted in debenzylation, without loss of TES groups. It was noted that freshly prepared Ra-Ni was required, although for other debenzylations this was not necessary. It was also observed that this was a slow and low yielding reaction, with full conversion rarely seen.

Initial test scale reactions with commercial Ra-Ni gave no reactivity. Extensive screening was required to show that quantitative reduction and cleavage was possible, in overnight reactions, only when the Ra-Ni was prepared[158] and used on the same day. Use of Ra-Ni, prepared in this manner, after 1 week, resulted in no reactivity. Use of Ra-Ni after 2-3 days resulted in alkene hydrogenation, but no benzyl ether cleavage. Longer reaction times (~16-24h) with fresh Ra-Ni resulted in *bis*-desilylation at C40 and C45. Shortening the reaction time allowed C40-TES ether retention. Unfortunately, despite trialling a range of reaction times, complete alkene reduction and benzyl ether cleavage was not possible without significant amounts of undesired C45 desilyation (**168**) (>50%). Indeed, *bis*-TES ether **167** was only able to be carried through to 42,45-*syn*-**169** in 40% yield (**Scheme 33a**). DMP oxidation at C35[83,84] (**Scheme 33b**) and Wittig methylenation[159] (**Scheme 33c**) gave 42,45-*syn*-*bis*-TES olefin **170** in workable yields (66% over two steps). This compound was able to be smoothly desilylated (HF·py, py) to 42,45-*syn*-diol **171b**, in quantitative yield. This constituted the first C34-C46 diastereomer ready for comparison with the natural product.

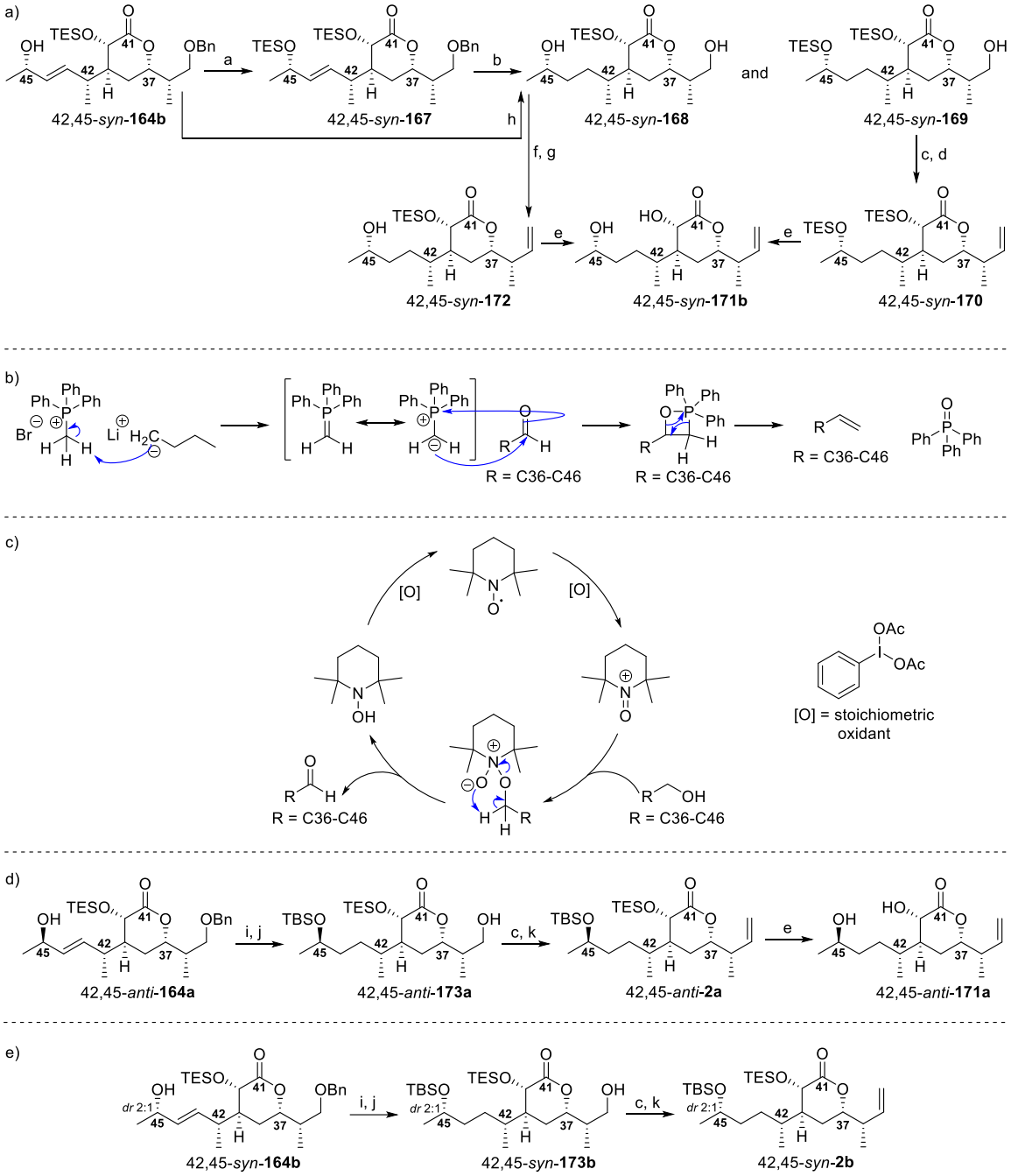

Reagents: (a) TESOTf, 2,6-lutidine, CH_2Cl_2, –78°C, 89%; (b) Ra-Ni, H_2, EtOAc, rt, 42% 42,45-*syn*-**169**, 50% diol-*syn*-**168**; (c) DMP, $NaHCO_3$, rt; (d) $MePPh_3Br$, *n*BuLi, THF, 0°C to rt *then* aldehyde, –78°C, 66% (over two steps); (e) HF·py, py, THF, 0°C, quant.; (f) TEMPO (40 mol %), BAIB, CH_2Cl_2, rt; (g) $MePPh_3Br$, *n*BuLi, THF, 0°C to rt *then* aldehyde, –78°C, 39% (over two steps); (h) Ra-Ni, H_2, EtOAc, rt, 90% 42,45-*syn*-**164b**; (i) TBSOTf, 2,6-lutidine, CH_2Cl_2, –78°C, 92%; (j) Ra-Ni, H_2, EtOAc, rt, quant.; (k) $MePPh_3Br$, *n*BuLi, THF, 0°C to rt *then* aldehyde, 89% (over two steps).

Scheme 33. a) Synthesis of diol 42,45-syn-**171b** from 42,45-*syn*-allylic alcohol **164b**; b) Mechanism of Wittig methylenation; c) Mechanisms of TEMPO BAIB oxidation; (d) Revised synthesis of diol 42,45-*anti*-**171a** from allylic alcohol 42,45-*anti*-**164a**; (e) Synthesis of TBS-protected terminal olefin 42,45-*syn*-**173b**.

An alternative pathway was also followed whereby allylic alcohol 42,45-*syn*-**164b** was directly subjected to Ra-Ni treatment for concurrent olefin hydrogenation and benzyl ether cleavage. This

proceeded to give 42,45-*syn*-**168** in high yield (90%), but required a selective TEMPO/BAIB oxidation[160] (**Scheme 33d**) at the C35 primary alcohol. Following Wittig methylenation, 42,45-*syn*-olefin **172** was obtained in only 39% yield (over two steps). This lower yield is attributed to inefficiency at the TEMPO/BAIB oxidation stage. These two approaches demonstrated that a TES ether protecting group at C45 was labile under the proposed synthetic sequence, but that carrying through the C45 free alcohol to avoid these issues, resulted in inefficient oxidation.

Given the challenges inherent to both of these pathways, the protecting group strategy was revised to minimise lability, while still taking heed of the necessity of efficient final global deprotection. On this basis, allylic alcohol 42,45-*anti*-**164a** was protected as its TBS ether (**Scheme 33e**). With this more robust protecting group, treatment with freshly prepared Ra-Ni allowed quantitative hydrogenation and benzyl ether cleavage to give C35-alcohol 42,45-*anti*-**173a** without competitive desilylation. DMP oxidation and Wittig methylenation gave 42,45-*anti*-olefin **2a** in high yield (89% over two steps). Global desilylation (HF·py, py) was able to be conducted without issues to smoothly deliver 42,45-a*nti*-diol **171a**, in quantitative yield. This constituted the second C34-C46 diastereomer for comparison with the natural product.

2.4 NMR Comparison with Hemicalide and Assignment of C45

With diols 42,45-*anti*-**171a** and 42,45-*syn*-**171b** in hand, NMR spectroscopic comparison was now able to be undertaken with hemicalide. The C34-C35 terminal olefin caused structural deviations from the NP and on this basis the H/C34-H/C38 shifts were excluded from the analysis. Based on currently published hemicalide data,[131] there were very few ^{1}H NMR data comparison points remaining (**Figure 18** top graph). Fortunately, Georges Massiot kindly provided the raw spectroscopic data, which was reprocessed for this work and both the ^{1}H and ^{13}C chemical shift data were tabulated *de novo* to two decimal places (**Figure 19**, **Table 10**). Furthermore, Massiot provided a draft manuscript containing additional hemicalide ^{1}H NMR (**Figure 18** bottom graph and **Table 9**). Analysis of the shift differences between 42,45-*anti*-**171a** and 42,45-*syn*-**171b** compared to hemicalide indicated that 42,45-*anti*-**171a** was a better match for the relative configuration of hemicalide (42,45-*anti*-**171a**: $\sum|\Delta\delta_H|$= 0.05 ppm; $\sum|\Delta\delta_C|$= 0.38 ppm; 42,45-*syn*-**171b**: $\sum|\Delta\delta_H|$= 0.13 ppm; $\sum|\Delta\delta_C|$= 0.67 ppm) (**Table 8**). This assignment is consistent with MacGregor's DP4f analysis of the C36-C45 stereocluster (**Figure 13**), which predicted that the 42,45-*anti* relative configuration was the best fit for the combined ^{1}H and ^{13}C NMR data, with a probability >95%.[101]

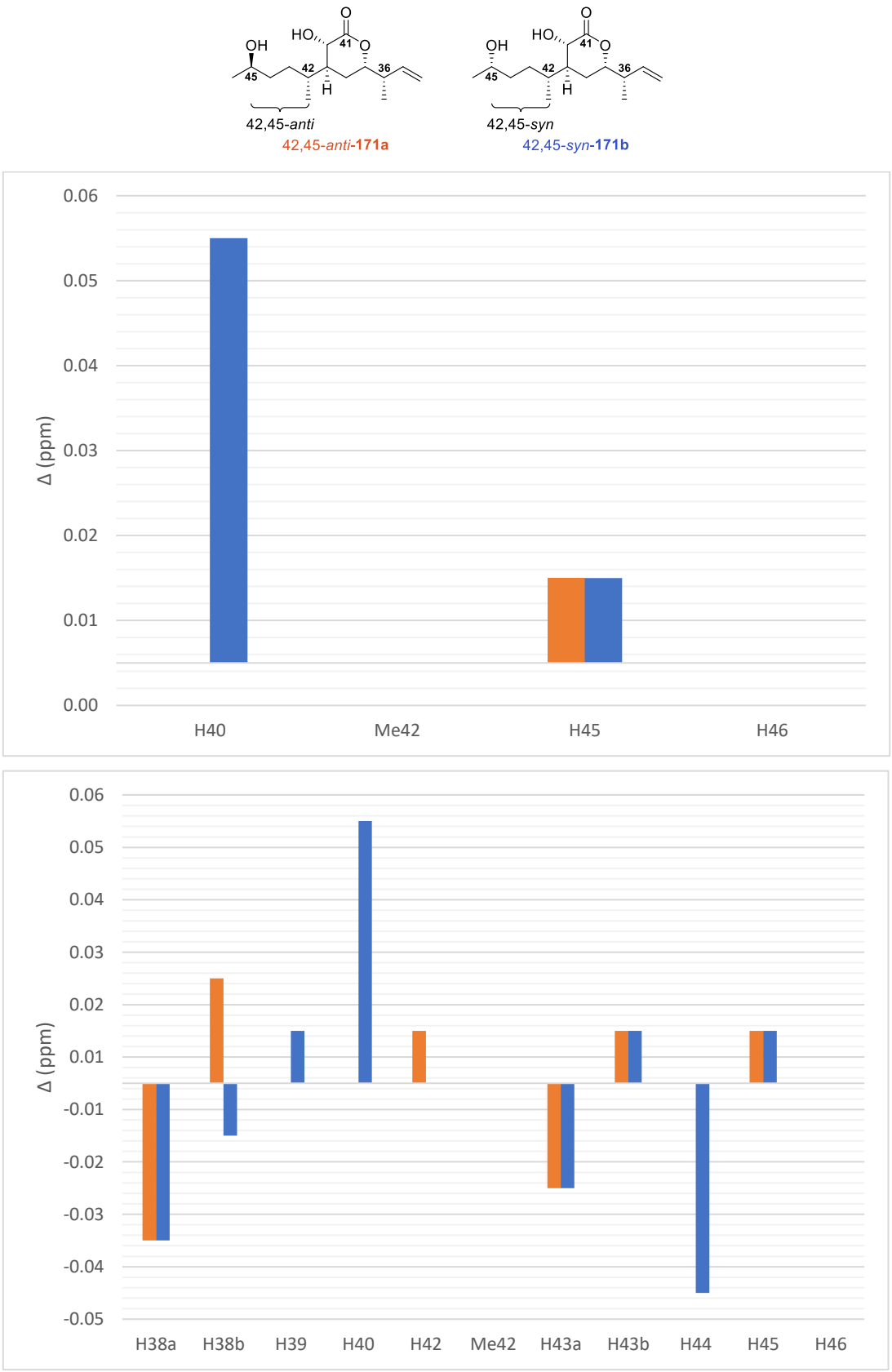

Figure 18. Bar graphs top: showing the currently published ^{1}H chemical shift difference between diol diastereomers 42,45-*anti*-**171a** (orange) and 42,45-*syn*-**171b** (blue) and hemicalide; bottom: ^{1}H chemical shift difference between diol diastereomers 42,45-*anti*-**171a** (orange) and 42,45-*syn*-**171b** (blue) and hemicalide including the additional unpublished data from Georges Massiot.

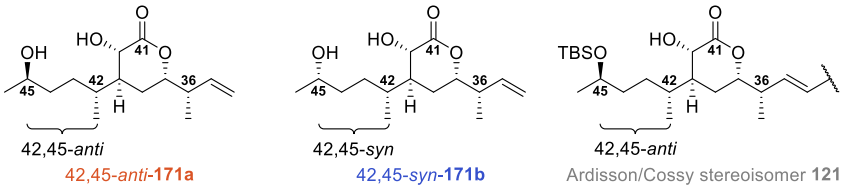

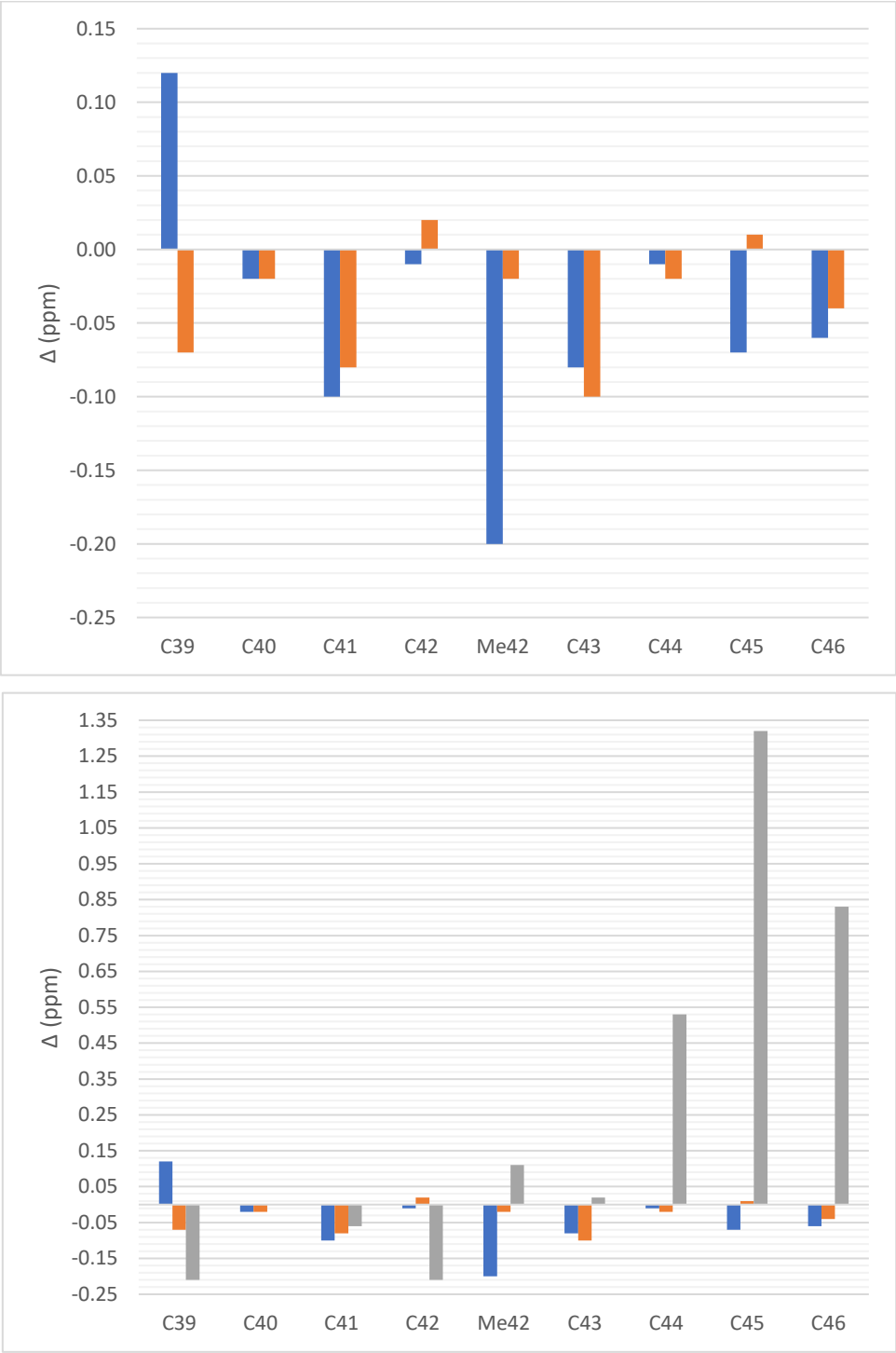

Figure 19. Bar graphs top: showing the ^{13}C chemical shift difference between diol diastereomers 42,45-*anti*-**171a** (orange), 42,45-*syn*-**171b** (blue) and hemicalide; bottom: ^{13}C chemical shift difference between diol diastereomers 42,45-*anti*-**171a** (orange), 42,45-*syn*-**171b** (blue) and hemicalide, also including comparison with Ardisson/Cossy stereoisomer **121** (grey).

Given that Ardisson/Cossy backbone stereoisomer **121** also bore a 42,45-*anti* arrangement, comparison was also made with this molecule. However, analysis of the shift differences indicated that the residual protecting group, which they had indicated remained at C40 or C45, disrupted the chemical shifts too much for reasonable comparison to be made (Ardisson/Cossy **121**: $\sum|\Delta\delta_H|$= 0.17 ppm; $\sum|\Delta\delta_C|$= 3.29 ppm). It did, however, strongly indicate that the remaining TBS ether was located at C45 ($|\Delta\delta_{H45}|$= 0.14 ppm; $|\Delta\delta_{C45}|$= 1.32 ppm), rather than at C40 ($|\Delta\delta_{H40}|$= 0.00 ppm; $|\Delta\delta_{C40}|$= 0.00 ppm).

To enable later reassessment of the C45 assignment, in the context of the larger C29-C46 region of hemicalide, it was considered wise to also take some of the 42,45-*syn* material through to coupling with the C29-C35 olefin **3**. On this basis, additional allylic alcohol **164** with largely 42,45-*syn* configuration (**164b**) (*ca. dr* 2:1) was also taken through to olefin 42,45-*syn*-**2b**, with the TBS ether at C45 (**Scheme 33f**). This provided sufficient material for coupling studies with C29-C35 olefin **3**.

Table 8. Summary of ^{1}H and ^{13}C spectroscopic differences, represented as total sum of errors and maximum errors, between diols 42,45-*anti*-**171a**, 42,45-*syn*-**171b** and and hemicalide (**1**)

	$\sum\|\Delta\delta_H\|$(ppm)*	Max$\|\Delta\delta_H\|$(ppm)*	$\sum\|\Delta\delta_C\|$(ppm)	Max$\|\Delta\delta_C\|$(ppm)
42,45-*anti*-**171a**	0.05	0.02	0.38	0.10
42,45-*syn*-**171b**	0.13	0.05	0.67	0.20

* Including data courtesy of personal communication with Georges Massiot (publication forthcoming).

Table 9. Proton (^{1}H) NMR comparisons between diol diastereomers 42,45-*anti*-**171a**, 42,45-*syn*-**171b** and hemicalide

Signal	^{1}H Shift in CD_3OD (ppm)				
	Hemicalide	42, 45-*anti*-**171a**	Δ	42, 45-*syn*-**171b**	Δ
H38a (m)*	1.80	1.77	-0.03	1.77	-0.03
H38b (m)*	1.67	1.69	0.02	1.66	-0.01
H39 (m)*	1.89	1.88	0.00	1.89	0.01
H42 (m)*	1.97	1.98	0.01	1.97	0.00
H43a (m)*	1.41	1.39	-0.02	1.39	-0.02
H43b (m)*	1.26	1.27	0.01	1.27	0.01
H44 (m)*	1.43	1.43	0.00	1.39	-0.04
H40 d (J Hz)	4.32 (*11.3*)	4.32	0.00	4.37	0.05
Me42 d (J Hz)	0.91 (*7.0*)	0.91 (*6.8*)	0.00	0.91 (*6.7*)	0.00
H45 (m)	3.69	3.70	0.01	3.70	0.01
H46 d (J Hz)	1.15 (*6.4*)	1.15 (*6.2*)	0.00	1.15 (*6.2*)	0.00

* Data courtesy of personal communication with Georges Massiot (publication forthcoming).

Table 10. Carbon (^{13}C) NMR comparisons between diol diastereomers 42,45-*anti*-**171a**, 42,45-*syn*-**171b** and hemicalide

Signal	^{1}H Shift in CD_3OD (ppm)				
	Hemicalide	42, 45-*anti*-**171a**	Δ	42, 45-*syn*-**171b**	Δ
C39	41.41	41.34	-0.07	41.53	0.12
C40	68.20	68.18	-0.02	68.18	-0.02
C41	178.36	178.28	-0.08	178.26	-0.10
C42	33.71	33.73	0.02	33.70	-0.01
Me42	13.39	13.37	-0.02	13.19	-0.20
C43	32.08	31.98	-0.10	32.00	-0.08
C44	37.97	37.95	-0.02	37.96	-0.01
C45	68.68	68.69	0.01	68.61	-0.07
C46	23.57	23.53	-0.04	23.51	-0.06

2.5 Conclusions

The 42,45-*anti*-olefin **2a**, ready for coupling to other regions of hemicalide, has been prepared in 16% yield and 15 steps (LLS) from ketone **73**. The 42,45-*syn*-olefin **170** was also prepared in 11% yield and 14 steps (LLS) from ketone **73**. Desilylation of both of these diastereomers quantitatively gave the C34-C46 olefin diols 42,45-*anti*-**171a** and 42,45-*syn*-**171b** for comparison with hemicalide NMR spectroscopic data. Analysis of ^{1}H and ^{13}C NMR chemical shift differences between the diastereomers and hemicalide indicated that the 42,45-*anti* diastereomer is a better match for the relative configuration of the natural product. This assigns one of the five remaining unassigned stereocentres, leaving the relative configuration unassigned for only four stereocentres. This assignment also reduces the hemicalide stereochemical possibilities from 128 to 64 arrangements, further narrowing down from the original over two million possibilities.

3. Results and Discussion: Synthesis of Selected C29-C35 Diastereomers

With C45 assigned and the C34-C46 terminal olefin 42,45-*anti*-**2** in hand, the remaining portion of the hemicalide carbon backbone is accounted for by C29-C35 olefin **3** (**Scheme 34a**). The C26-C33 region ecompasses the four remaining unassigned stereocentres (C27, C29, C31 and C32). As the relative configuration remains unassigned for all four stereocentres, there are 16 possible stereoisomers (**Scheme 34b**).

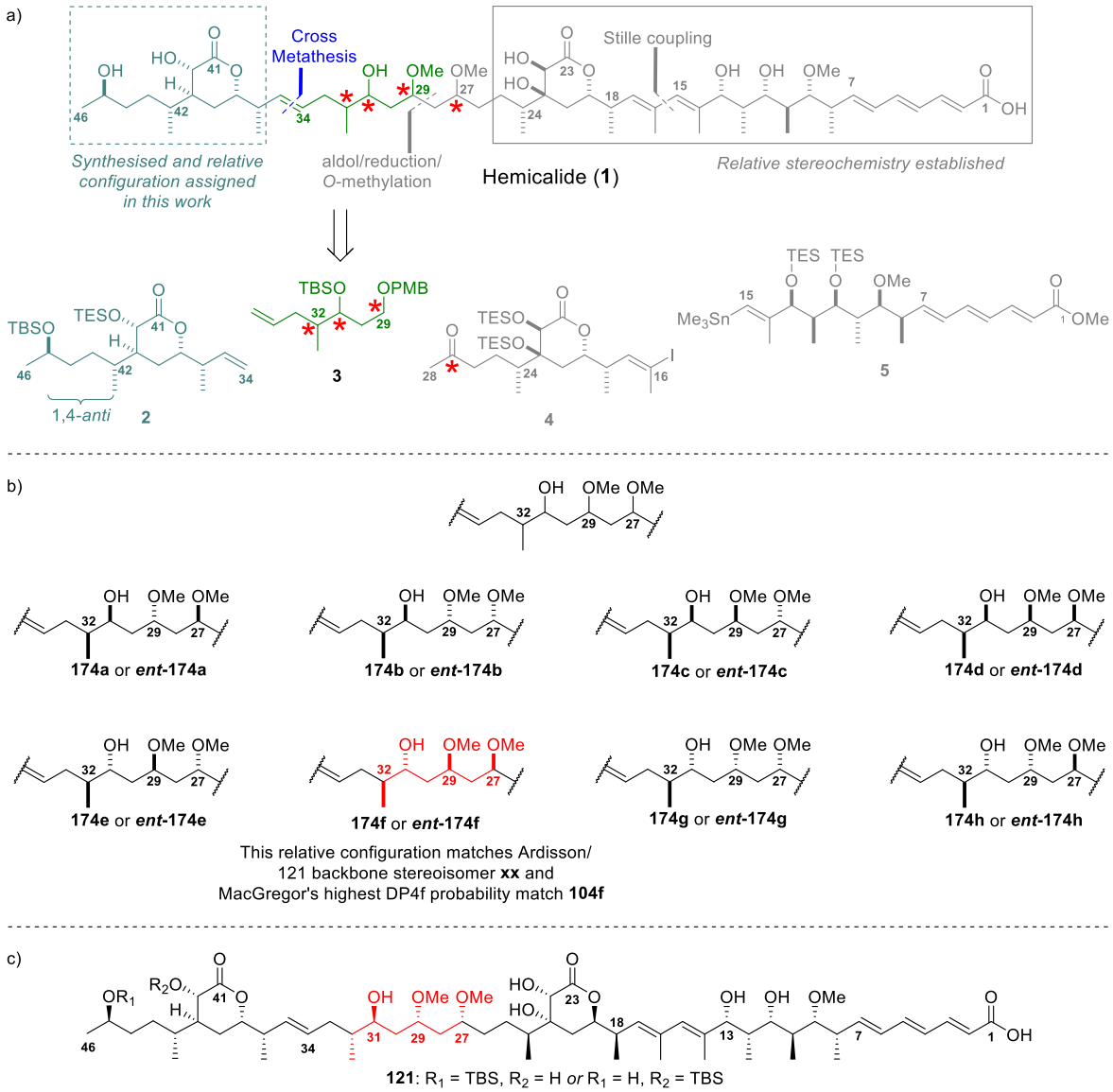

Scheme 34. a) Overview of the Paterson group approach to hemicalide, highlighting the portion of the carbon backbone and related stereocentres yet to be completed; b) Possible C27-C32 diastereomers; c) Ardisson/Cossy hemicalide backbone stereoisomer.

3.1 Narrowing the Diastereomeric Possibilities within the C27-C32 Stereocluster

As previously discussed (section **1.4.6**), detailed analysis of the ^{1}H and ^{13}C NMR spectroscopic data of hemicalide backbone stereoisomer **121** synthesised by Ardisson/Cossy reveals a number of significant deviations from the natural product data, with the result that stereoisomer **121** is highly unlikely to reflect the relative configuration of the natural product. Indeed, it is across the C26-C35 region, which encompasses the C27-C32 stereotetrad, that the observed spectroscopic deviations are especially apparent (**Figure 20a**). These stereocentres, as well as the C45 stereocentre, were randomly assigned in the Ardisson/Cossy synthesis of stereoisomer **121**.

During analysis of this data, it was discovered that a number of errors were present in Ardisson/Cossy's original data tabulation for this region. Firstly, the ^{13}C NMR shift difference for MeO29, originally calculated as 0.2 ppm, should actually be 0.8 ppm, given that the signals for hemicalide and stereoisomer **121** are 57.9 ppm and 57.1 ppm, respectively. Secondly, the ^{13}C NMR shift difference for C34 (133.2 ppm for hemicalide vs 132.2 ppm for stereoisomer **121**) was calculated to be 0 ppm rather than 1 ppm. Thirdly, reanalysing the raw NMR data showed that the signals for C34 and C35 had been reversed, with the result that C34 incorrectly appeared to have a 1 ppm error, while C35 had a 0.6 ppm error. Correcting this assignment resulted in ^{13}C shift deviations of less than 0.3 ppm across C34-C35. This correction also had the consequential effect that, in the later data analysis of C29-C46 diastereomers constructed in this work, smaller shift deviations were observed across C34-C35 (section **4.3**), than initially appeared.

With all signal assignments and shift difference calculations in this region double checked, four significant ^{13}C shift differences (>1ppm) at C26, C28, Me32 and C33 were apparent (**Figure 20a**). On this basis, it is reasonable to conclude that stereoisomer **121** is unlikely to reflect the relative configuration of the natural product. Indeed, the magnitude of the C26, C28, Me32 and C33 deviations likely indicates that hemicalide bears the opposite relative configuration at these points, namely 27,29-*anti* and 31,32-*syn*. The largest chemical shift deviations occur around C31-C32. If, on these grounds, a 31,32-*anti* relationship alone is excluded, this allows the possible diastereomers within this region to be narrowed from 16 to eight possibilities (**Figure 20b**).

Interestingly, the unusually low C30 shift (δ_C = 33.0 ppm), noted to be potentially diagnostic by MacGregor (section **1.4.4**),[101] was captured by stereoisomer **121**. This may provide some support for the presence of a 29,31-*anti* relationship. In this vein, it may be noted that, in Macgregor's

DP4f analysis, all diastereomers bearing a 29,31-*syn* relationship were of the lowest probability (2.3%-3.3%), whereas all diastereomers bearing a 29,31-*anti* relationship were of comparatively higher probability (16.7%-29.4%) (**Figure 11**). In the context of DP4f calculations, the inherent flexibility within this region results in multiple low energy conformers and their solvated structures make it extraordinarily hard to then average and provide accurate computational predictions of relative configuration. Consequently, a synthetic approach is necessary to provide the relevant fragment for stereochemical corroboration. Overall, diastereomer **174a** or ***ent*-174a** (**Figure 20b**), bearing 27,29-*anti*-29,31-*anti*-31,32-*syn*, is perhaps the most likely relative configuration. However spectroscopic evidence is necessary to substantiate this hypothesis.

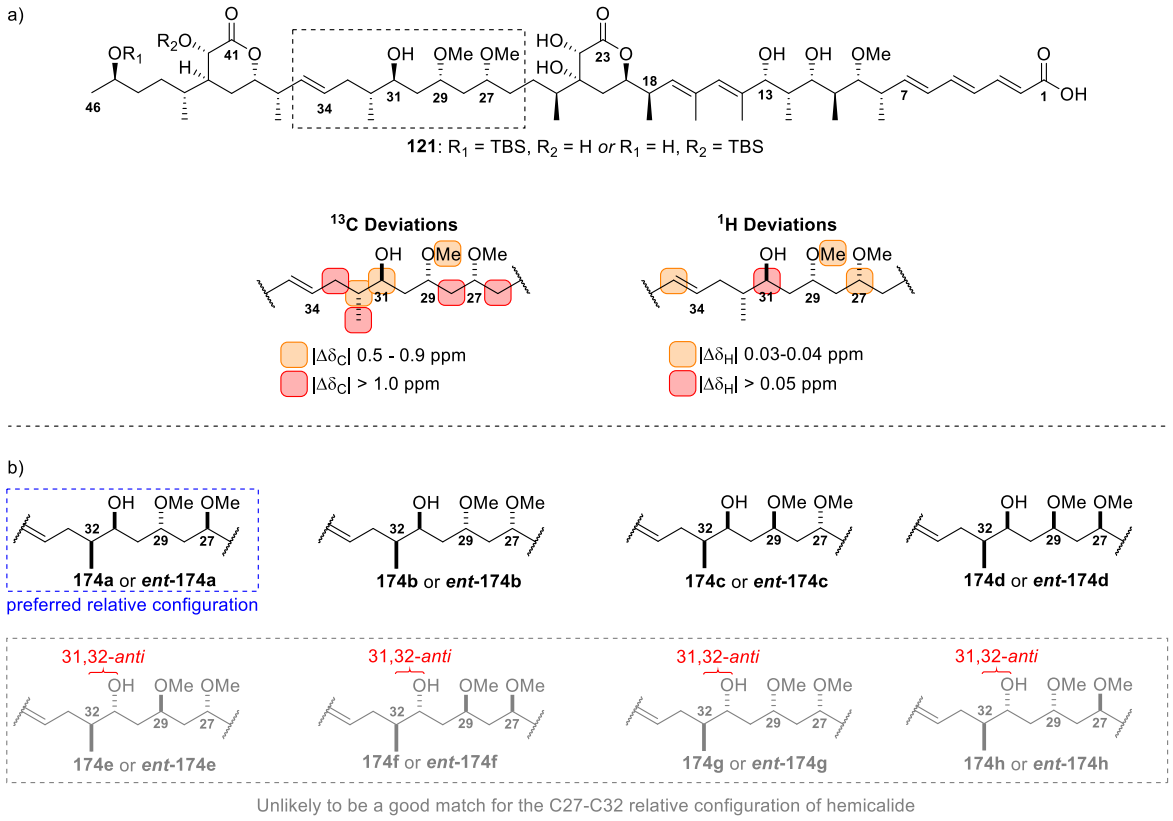

Figure 20. a) Summary of spectroscopic differences between hemicalide (**1**) and stereoisomer **121** across the C26-C35 region; b) Relative configurations able to be excluded on the basis of the shift deviations present in stereoisomer **121**.

3.2 Retrosynthetic Analysis of the C29-C35 Region

A flexible synthetic strategy was necessary to access fragments **174a-d** and their enantiomers. Disconnection of olefin **3** across the olefinic C34-C35 coupling handle, *via* a hydroboration, oxidation, Wittig methylenation sequence, reveals homoallylic alcohol **175** (**Scheme 35**).

Disconnection across C31-C32, *via* a Brown crotylboration approach, discloses aldehyde **176**, which can be readily accessed from 1,3-propandiol.

The C29-C35 olefin **3** contains two of the four remaining stereocentres (C31 and C32), with the remaining two set during later aldol coupling (C29) and reduction (C27), respectively (**Scheme 34a**). A Brown crotylboration approach allows C31 and C32 to be pre-installed during synthesis of the fragment, with high diastereoselectivity and enantioselectivity.[161–164] The desired 31,32-*syn* relationship can be accessed using *cis*-butene as a starting material. Furthermore, should a 31,32-*syn* relationship come into question, this route would be amenable to installation of 31,32-*anti* centres, simply by instead utilising *trans*-butene as a starting material. The enantioselectivity can also be predictably controlled by choice of the appropriate (+) or (–)-diisopinocampheylmethoxyborane reagent.

The stereocontrol possible in the planned boron-mediated aldol coupling of the two fragments depends directly upon reagent control provided by the chiral ligands on the Lewis acidic boron. Such reagent control can be disrupted by substrate stereoinduction, namely 1,3- and 1,5-stereoelectronic effects, in the cyclic aldol transition state.[68,165,166] Thus, it was necessary to select a protecting group that contributes as little to these effects as possible. On this basis, a silyl protecting group, rather than a benzoyl or PMB group, was chosen for C31 (contrast **TS-I** and **TS-II Scheme 21c**). Given the deprotection issues faced by the Ardisson and Cossy groups in their deprotection of hemicalide stereoisomer **121**, a TES group was initially considered to be preferable to a TBS group. However, similarly to the issues experienced with TES protection of C45, exploratory synthetic work revealed that this TES ether was susceptible to undesired desilylation during eventual attempted cross metathesis coupling with olefin 42,45-*syn*-**2b**. On this basis, a more robust TBS protecting group was installed at C31.

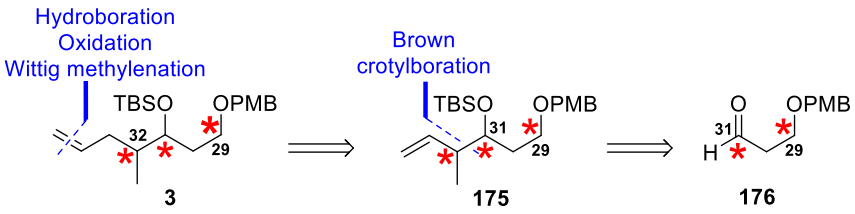

Scheme 35. Retrosynthesis of C29-C35 region of hemicalide

3.3 Synthesis of the C29-C35 Region

Pursuing a Brown crotylboration strategy to install the C31 and C32 stereocentres provides stereoflexibility, in addition to a high degree of diastereo- and enantiocontrol.[161–164] This stereocontrol, as well as the robustness and predictability of this methodology, has led to this strategy being utilised in many NP synthetic endeavours.[164] In Brown crotylboration the *syn*- or *anti*-configuration is determined by the *cis*- or *trans*-geometry of the starting butene (**Scheme 36**). Use of *cis*-butene gives rise to (*Z*)-crotylboranes (**TS-(Z)-XIIa-b**), resulting in *syn*-products, whereas use of *trans*-butene gives rise to (*E*)-crotylboranes (**TS-(E)-XIIa-b**), resulting in *anti*-products. On the other hand, the enantioselectivity is determined by the facial selectivity imposed by the chosen enantiomer of the chiral ligands on the boron reagent ((+)- or (–)-diisopinocampheylmethoxyborane), with the favoured transition state minimising steric interactions (*vide infra* **Scheme 37d**).

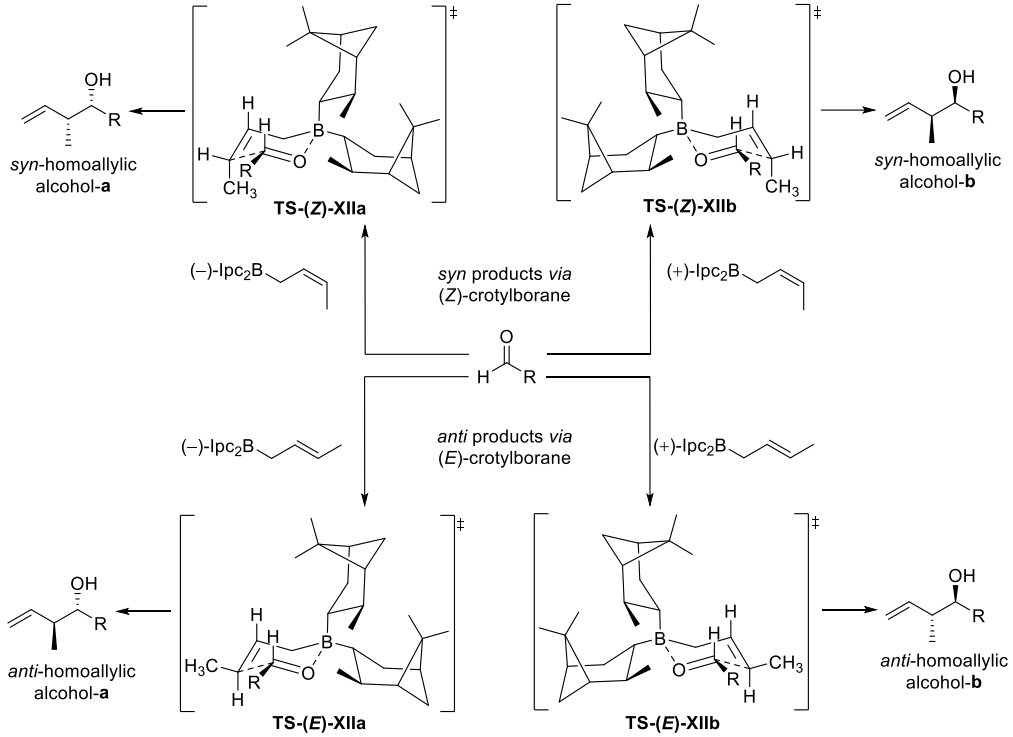

Scheme 36. Brown crotylboration transition states accounting for the high levels of diastereo- and enantiocontrol.

The necessary aldehyde starting material for Brown crotylboration was readily produced in two steps. 1,3-Propandiol was mono-PMB protected as alcohol **177** and a Swern oxidation[69–72] undertaken to produce aldehyde **176** (**Scheme 37a**). The reaction of crotylboranes with aldehydes is essentially instantaneous between –78°C to –100°C.[167] In order to avoid crotyl isomerisation,

the crotylboranes generated after decomplexation of methoxide from the –ate complex, by addition of $BF_3{\cdot}OEt_2$ must be immediately reacted with the intended aldehyde (see **178** to **179 Scheme 37b**).[163] For this reason, the necessary chiral crotylboranes were produced *in situ*. However, the precursor methoxyboranes are reasonably stable and are able to be made in advance and stored.

Brown crotylboration proceeded smoothly with aldehyde **176** and diastereoselectivities and enantioselectivities matching literature precedent (*dr* and *ee* >95:5) could be replicated. This demonstrated access to the desired stereochemistry with high enantiocontrol, which is key to validating the synthetic route and allowing highly stereopure material to be brought through, once the relative configuration within this region is assigned. In the Brown crotylboration of aldehyde **176** with (+)-diisopinocampheyl-(*Z*)-crotylborane to give homoallylic alcohol 31,32-*syn*-**180a** as the major product, **TS-XIII** is the favoured transition state. This is because it minimises steric interactions with the (+)-isopinocampheyl ligands. In contrast, **TS-XIV** is disfavoured, because of increased steric interactions, specifically between the methyl of one of the the (+)-isopinocampheyl ligands on boron and a methylene of the crotyl group. Following Brown crotylboration (**Scheme 37a**), the expected absolute stereochemistry of the C31 homoallylic alcohol in 31,32-*syn*-**180a** was confirmed by generating Mosher's esters **181a** and **182a (Scheme 37a, d**). The *ent*-31,32-*syn*-**180b** series, including Mosher's esters (**181b** and **182b**), was generated in the same manner, instead using (–)-diisopinocampheyl-(*Z*)-crotylborane (**Scheme 37**).

Unfortunately, purification of homoallylic alcohol 31,32-*syn*-**180a** proved extremely challenging, as the R_f values of any remaining aldehyde starting material and the IpcOH by-product were only slightly above and below that of the product, respectively, in every solvent system explored. To promote better separation of the desired product from other compounds, TBS protection was undertaken on the crude product mixture. This telescoping approach gave a much improved 88% yield of TBS ether 31,32-*syn*-**175a** over the Brown crotylboration and silyl protection steps (**Scheme 37a**).

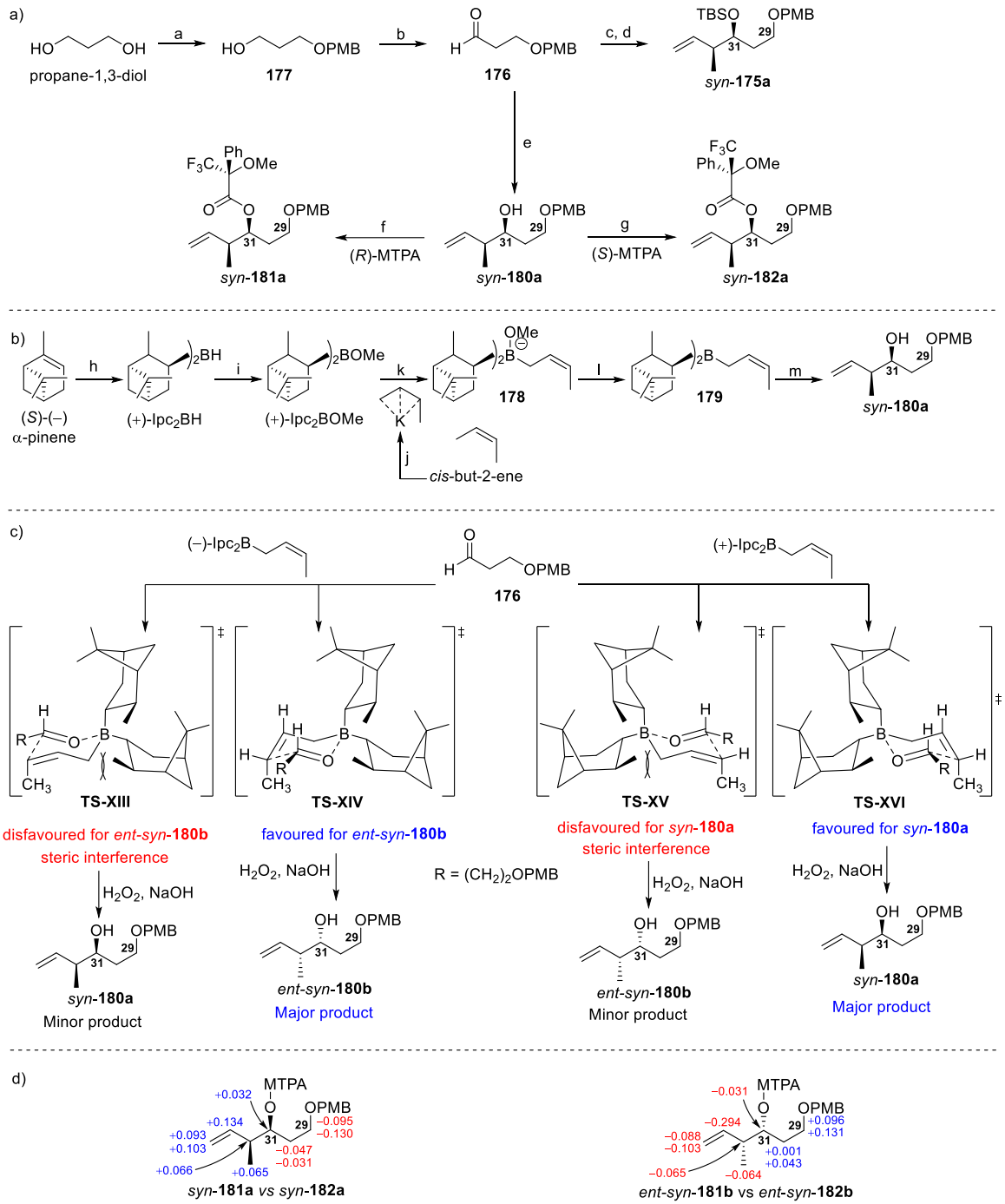

Reagents: (a) NaH, TBAI (10 mol%), THF 0°C *then* propan-1,3-diol, 0°C to rt *then* PMBCl, 0°C to reflux, 72%; (b) $(COCl)_2$, CH_2Cl_2, –78°C *then* DMSO *then* 3-((4-methoxybenzyl)oxy)propan-1-ol *then* Et_3N, –78°C to rt, 88%; (c) *t*BuOK, THF, rt to –78°C *then* *cis*-2-butene, *n*BuLi, –78°C to –45°C to –78°C, (+) or (–)-Ipc_2BOMe *then* $BF_3{\cdot}OEt_2$ *then* 3-((4-methoxybenzyl)oxy)propanal *then* H_2O_2, NaOH or $NaHCO_3$; (d) TBSOTf, 2,6-lutidine, CH_2Cl_2, –78°C, 88% (over 2 steps), *dr* >95:5, *ee* >95:5; (e) *t*BuOK, THF, rt to –78°C *then* *cis*-2-butene, *n*BuLi, –78°C to –45°C to –78°C, (+) or (–)-Ipc_2BOMe *then* $BF_3{\cdot}OEt_2$ *then* 3-((4-methoxybenzyl)oxy)propanal *then* H_2O_2, NaOH or $NaHCO_3$, 21%-27%; (f) DCC, DMAP, (*R*)-MTPA, CH_2Cl_2, rt, 93%; (g) DCC, DMAP, (*R*)-MTPA, CH_2Cl_2, rt, quant.; (h) $BH_3{\cdot}SMe_2$, THF, 0°C; (i) MeOH, Et_2O, 0°C (90% over two steps); (j) *n*BuLi, *t*BuOK, THF, –78°C to –45°C; (k) (*Z*)-but-2-en-1-ylpotassium, THF, –78°C *then* (+) or (–)-Ipc_2BOMe; (l) $BF_3{\cdot}OEt_2$, THF, –78°C; (m) 3-((4-methoxybenzyl)oxy)propanal, THF, –78°C *then* H_2O_2, NaOH or $NaHCO_3$.

Scheme 37. a) Synthesis of the C29-C35 *syn*-**180a** and *ent-syn*-**180b** from propandiol; b) Brown crotylboration of 3-((4-methoxybenzyl)oxy)propanal with (+)-Ipc_2 (*Z*)-crotylborane; c) Competing transition states for reaction of 3-((4-methoxybenzyl)oxy)propanal with (+)- and (–)-Ipc_2 (*Z*)-crotylborane.

The necessary homologation of 31,32-*syn*-**175a** to obtain the desired C29-C35 fragment 31,32-*syn*-**3a** was achieved by a sequence of hydroboration, oxidation, and methylenation, which proceeded largely without incident (**Scheme 38a**). Hydroboration with borane dimethyl sulfide[168] gave clean conversion to the desired alcohol 31,32-*syn*-**184a** (**Scheme 38b**). After oxidative cleavage, the resulting higher polarity of the alcohol product allowed for separation of the desired 31,32-*syn*-**184a** product from any minor secondary alcohol, as well as any trace diastereomeric product from the Brown crotylboration. On gram scale, Swern oxidation[69–72] and Wittig methylenation[159] gave quantitative yield (over two steps) to deliver terminal olefin 31,32-*syn*-**3a**, ready for coupling with the C34-C46 region of hemicalide. The same transformations were carried out on *ent*-31,32-*syn*-**175b** to give terminal olefin *ent*-31,32-*syn*-**3b**.

Reagents: (a) $BH_3{\cdot}SMe_2$, THF, 0°C to rt *then* MeOH, NaOH, H_2O_2, 0°C, 81%; (b) $(COCl)_2$, CH_2Cl_2, –78°C *then* DMSO *then syn*-**184a** *then* Et_3N, –78°C to rt; (c) $MePPh_3Br$, *n*BuLi, THF, 0°C to rt *then syn*-**185a**, quant. (over two steps).

Scheme 38. Completion of the C29-C35 fragment from homoallylic ethers *syn*-**175a** or *ent-syn*-**175b** to terminal olefins *syn*-**3a** or *ent-syn*-**3b**.

3.4 Conclusions

The C29-C35 terminal olefins 31,32-*syn*-**3a** and *ent*-31,32-*syn*-**3b** were delivered in comparable yields of 45% and 42%, over seven steps, respectively. This reaction sequence was able to be performed in a highly diastereoselective manner. High enantioselectivity in the crucial Brown crotylboration step was also validated. This will be important in any future scale up once the stereochemistry in this region is assigned. These intermediates were suitable to couple with the C34-C46 region, which would allow assessment of the relative configuration of the C31 and C32 centres as well as evaluation of the relationship between the C27-C32 and C36-C45 stereoclusters.

4. Results and Discussion: Fragment Union, Elaboration and Assignment of the C29-C46 Region

4.1 Forging the C34-C35 Bond

With C34-C46 olefins 42,45-*anti*-**2a** and 42,45-*syn*-**2b** in addition to both C29-C35 olefins 31,32-*syn*-**3a** and *ent*-31,32-*syn*-**3b** in hand, fragment union and elaboration of the resulting diastereomers for NMR spectroscopic comparison with hemicalide, as well as production of an advanced intermediate ready for coupling to the remainder of the molecule, became the primary goals. At this point, it was noted that if the relative configuration between the C27-C32 and C36-C45 stereoclusters could be established, one possible groups of enantiomers for the C27-C32 region would be able to be excluded, halving the possibilities within this region from eight to four.

4.1.1 Evolution of the Fragment Union Strategy

Initially, various fragment coupling strategies were considered, primary among them a Suzuki-Miyaura cross coupling[117] between C34-C46 vinyl-iodide **186** and C29-C33 dialkyl borane **187** to provide olefin **188** (**Scheme 39a**).[101,153,154] This approach would have necessitated creation of vinyl-iodide **186** by Takai-Utimoto olefination[169] of aldehyde **189** or an alternative olefination strategy. However, during some preliminary exploratory studies, conducted by Han,[153] slow conversion of olefin **190** to borane **191** during the synthesis of olefin **192**, as well as instability of borane **191** raised some concerns (**Scheme 39b**). These considerations, in conjunction with a successful example of a challenging olefin metathesis in the synthesis of actinoallolide within the Paterson group,[170] inspired a change in synthetic strategy to a cross metathesis approach.

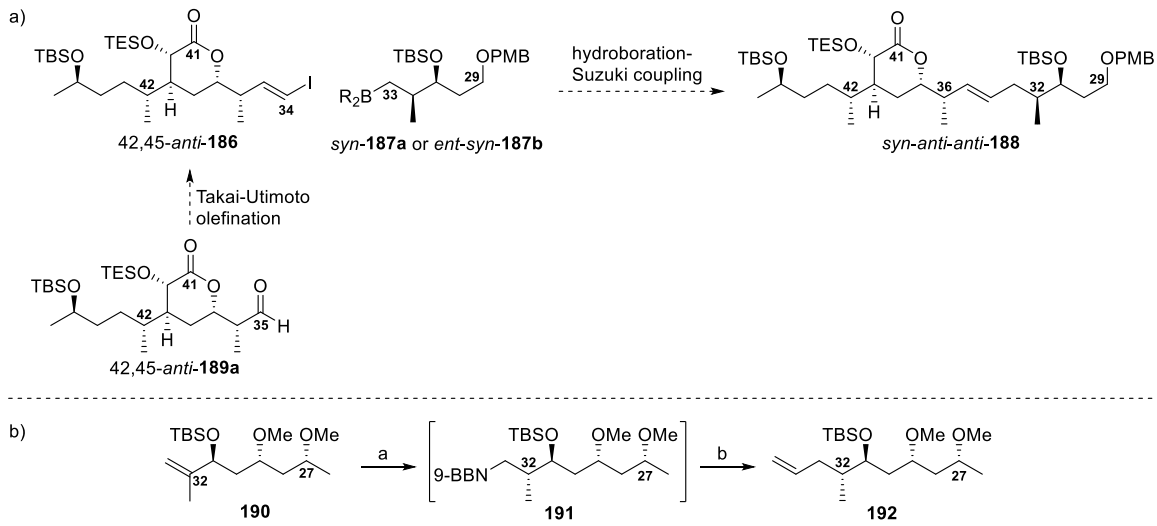

Reagents: (a) 9-BBN, THF, rt; (b) $PdCl_2$(dppf), Ph_3As, CH_2=CHI, Cs_2CO_3, H_2O, DMF, rt, *ca*. 50% (over two steps).
Scheme 39. a) Suzuki approach to fragment coupling; b) Model studies by Han.[153]

4.1.2 Cross Metathesis Studies between C29-C35 and C34-C46 Fragments

Having all necessary terminal olefin substrates (**2a**/**2b** and **3a**/**3b**) in hand, attention was focussed on cross metathesis as a strategy for forging the C34-C35 bond. During a metathesis reaction there are two main phases, the precatalyst initiation phase and the catalyst turnover phase, which generates product (**Scheme 40a**). Most pre-catalysts are 16 electron species.[171] To become active, these species must first lose a ligand to generate a (normally unobservable) 14 electron alkylidene species. For second generation Hoveyda-Grubbs (HG-II) catalysts an interchange mechanism (shown in **Scheme 40a**) appears to be the mechanism of pre-catalyst activation.[172] This involves association of one of the substrate alkenes concurrently with dissociation of a ligand. However, it has also been suggested that a dissociative mechanism is possible, depending on the identity and concentration of the substrate.[173,174] After the ligand is lost, carbene exchange occurs between *p*-substituted styrene metal carbene ligand and the newly associated alkene. This proceeds *via* a well characterised process of [2+2] cycloaddition and retro[2+2]cycloaddition in the metallacyclobutane intermediate species.[171,175] The catalyst turnover phase involves a similar process of the alkene ligand being replaced by another substrate alkene molecule, carbene exchange leading to homodimerisation or cross metathesis and ethylene being replaced by a new substrate alkene molecule to start the catalytic turnover cycle again.

Formation of (*E*)-olefins is generally thermodynamically favoured in cross metathesis,[176] allowing fragment union with installation of the desired C34-C35 bond geometry (**Scheme 40a**). In this instance, as (*E*)-selectivity was desired, specialised catalysts that promote (*Z*)-selectivity will not

be discussed. A reasonable degree of thermodynamic control in cross metathesis depends on the pre-catalyst system.[171] It also depends on product energetics, especially if the cross metathesis is reversible, and/or the selectivity determining step happens very late in the reaction coordinate. Second generation pre-catalysts, including HG-II, typically lead to higher (*E*)-selectivities in cross metathesis because of their ability to equilibrate (*E*)/(*Z*)- mixtures of products to the thermodynamically favoured (*E*)-isomer.[177] In fact, it is due to the ability of second generation catalysts to react with both starting materials and products that they are able to approach the thermodynamic endpoint.[177,178]

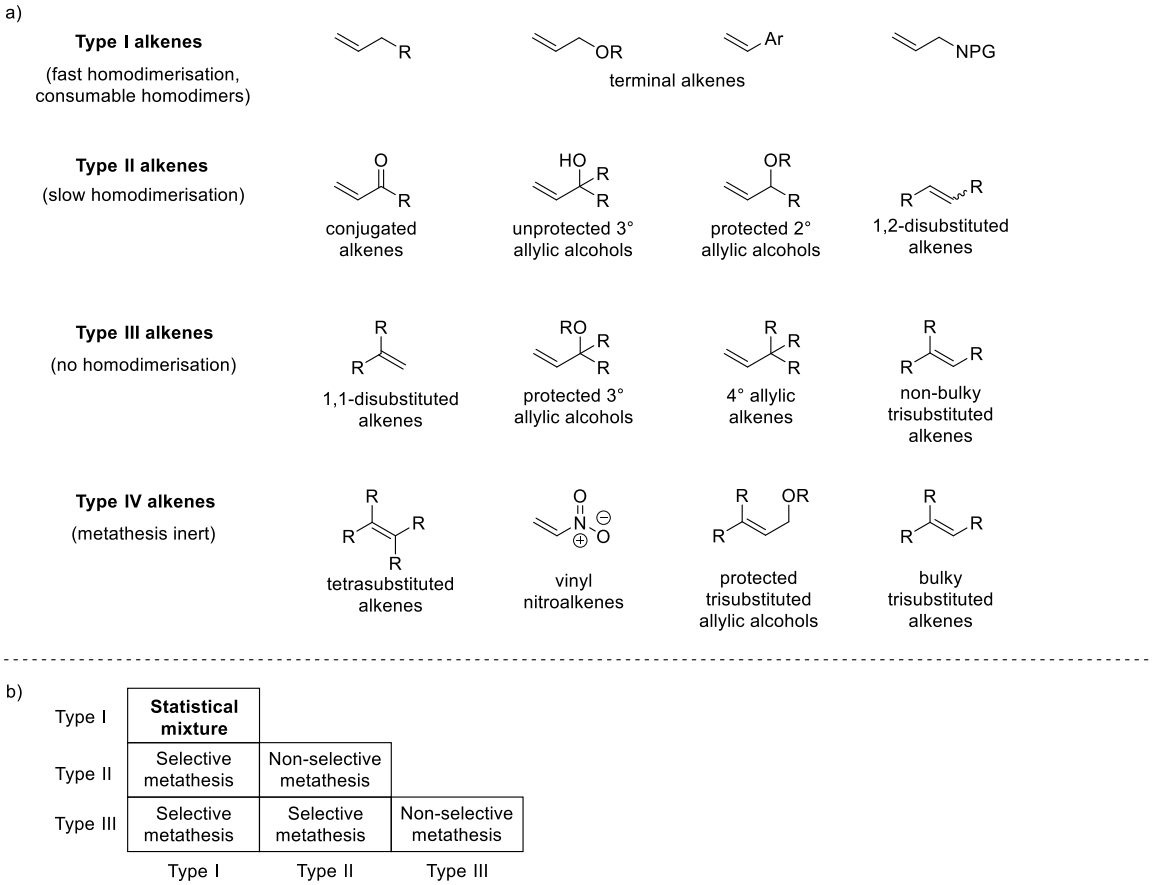

Figure 21. (a) Olefin types in cross metathesis; (b) Metathesis results with different olefin type combinations.

For cross metathesis, categorising each olefinic reaction partner allows the reaction outcome to be predicted (***Figure 21*a**).[176] There are four types of olefins for this purposes, I-IV, in order of decreasing reactivity, predicted by increased steric hinderance or being electron-deficient. Thus, Type I alkenes react and dimerise quickly, with dimers that are also cross metathesis active. Type II alkenes react and dimerise more slowly, with dimers reacting more slowly. Type III alkenes are still reactive, but will not dimerise. Type IV alkenes are not reactive, but will not poison the

catalyst. Although the exact categorisation of some alkenes depends on the catalyst used in the metathesis, unconjugated monosubstituted terminal alkenes, are typically classed as Type I alkenes.[176] Reaction of two different type I alkenes will lead to a statistical mixture of reaction products (***Figure 21*b**).[176] That is a mixture of the homodimers of each alkene and the cross metathesis product. In this situation, to bias the reaction towards the cross metathesis product, one alkene must be used in excess.

All possible variants of the C29-C35 and C34-C46 alkenes that may be used in cross metathesis are unconjugated monosubstituted terminal alkenes. Thus, they are best categorised as Type I alkenes. In order to bias the reaction to the desired cross metathesis product, the C29-C35 alkene partner was used in excess. Under these circumstances, the reaction products are expected to be the homodimer of the C29-C35 alkene and the cross metathesis product.

The tolerance of free alcohols in cross metathesis reactions is supported by literature precedent.[179,180] Thus, to reduce the necessity of protecting group manipulations on late stage materials, cross metathesis was originally planned to occur between C34-C46 olefin 42,45-*syn*-**170** and C29-primary alcohol *ent*-31,32-*syn*-**193** or, alternatively, C31-secondary alcohol *ent*-31,32-*syn*-**194** or C29,C31-diol *ent*-31,32-*syn*-**195** (**Scheme 40b**).

An initial overnight test reaction at rt with 5 mol% HG-II was encouraging, showing homodimerisation of olefin *ent*-31,32-*syn*-**193** to dimer *ent*-**196b**, but no cross metathesis (**Scheme 40b**, **Table 11** entry 1). Unfortunately, trialling long reaction times, increased temperature and higher catalyst loadings merely promoted double bond migration in olefin 42,45-*syn*-**170**, giving olefin **197** (**Scheme 40b**, **Table 11** entry 2). Isomerisation is a known issue under the aforementioned conditions, especially in conjunction with high dilution, which was unavoidable in small-scale test reactions.[181] Such isomerisation is thought to be catalysed by ruthenium hydride catalyst decomposition products, under metathesis conditions. Substrate isomerisation can be suppressed by the presence of *p*-benzoquinone, an additive that does not reduce catalyst activity.[181] Although *p*-benzoquinone successfully suppressed isomerisation, without suppressing homodimerisation of *ent*-31,32-*syn*-**193**, cross metathesis was still not observed (**Scheme 40b**, **Table 11** entry 3). Long reaction times (1 week) were also found to lead to desilylation of C31 giving C29,C31-diol *ent*-31,32-*syn*-**195** and C40 giving alcohol 42,45-*anti*-**200** (**Scheme 40b**, **Table 11** entry 4). Consequently, reaction times were capped at 16 hours (O/N).

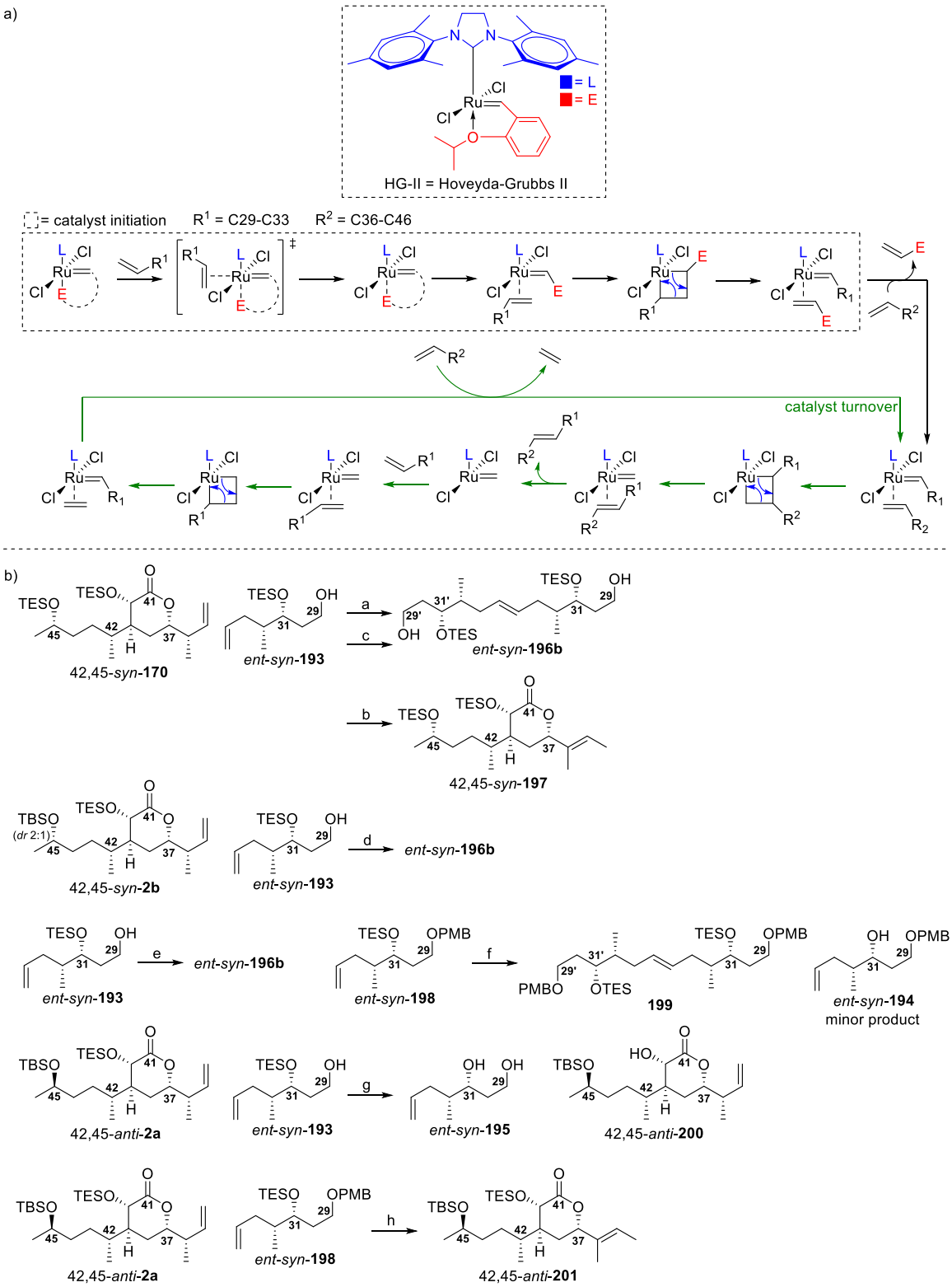

Reagents: (a) HG-II (5 mol %), CH_2Cl_2, rt, O/N, *ca.* 66% conversion to **196** (by NMR); (b) HG-II (10 mol %), PhMe, reflux, O/N, *ca.* full conversion to 42,45-*syn*-**197** (by NMR); (c) HG-II (5 mol %), *p*-benzoquinone, CD_2Cl_2, 40°C, 4 days, *ca.* 33% conversion to **196** (by NMR); (d) HG-II (5 mol %), *p*-benzoquinone, PhMe, 40°C, *ca.* 15% conversion to **196** (by NMR); (e) HG-II (20 mol %), *p*-benzoquinone, PhMe, 80°C, *ca.* full conversion to **196** (by NMR); (f) HG-II (20 mol %), *p*-benzoquinone, PhMe, 80°C, *ca.* 50% conversion to **199** (by NMR); (g) HG-II (10 mol %), *p*-benzoquinone, PhMe, 80°C, O/N, 75% diol *ent-syn*-**195** (by NMR), alcohol 42,45-*anti*-**200** (by NMR); (h) HG-II (5 mol%), *p*-benzoquinone (10 mol%), PhMe, 80°C, largely RSM, some isomerisation.
Scheme 40. a) Cross metathesis catalytic cycle with HG-II; b) Cross metathesis substrates with HG-II.

None of the C29-C35 intermediates bearing free hydroxyl groups (C29-primary alcohol *ent*-31,32-*syn*-**193** or, alternatively, C31-secondary alcohol *ent*-31,32-*syn*-**194** or C29,C31-diol *ent*-31,32-*syn*-**195**) were competent in cross metathesis, and competitive desilylation was observed in intermediates bearing TES protecting groups (C31-secondary alcohol *ent*-31,32-*syn*-**194** or olefin *ent*-31,32-*syn*-**198**) (**Scheme 40b**, **Table 11** entries 1-7, 9-10). It was hypothesised that, in the presence of free alcohols, isomerisation inducing catalyst decomposition was potentially caused by β-hydride elimination of OH–CH. Given these experimental results and the hypothesised cause of catalyst decomposition it was concluded that, despite literature precedent, the presence of free alcohols seemed not to be tolerated in the formation of the C34-C35 bond.

Table 11. Cross metathesis condition screening

Entry	Substrates	Conditions	Reaction outcome	Yield
1	42,45-*syn*-**170**, *ent*-31,32-*syn*-**193**	HG-II (5 mol%), CH_2Cl_2, rt, O/N	Homodimerisation: *ent-syn*-**196b**	Quant.
2	42,45-*syn*-**170**, *ent*-31,32-*syn*-**193**	HG-II (10 mol%), PhMe, reflux, O/N	Isomerisation: 42,45-*syn*-**197**	Quant.
3	42,45-*syn*-**170**, *ent*-31,32-*syn*-**193**	HG-II (5 mol%), *p*-benzoquinone (10 mol%), CD_2Cl_2, 40°C, O/N	Homodimerisation: *ent-syn*-**196b**	Quant.
4	42,45-*anti*-**2b**, *ent*-31,32-*syn*-**193**	HG-II (5 mol%), *p*-benzoquinone (10 mol%), PhMe, rt, 1 week	C31 desilylation: *ent*-31,32-*syn*-**195** C40 desilylation: 42,45-a*nti*-**200**	50%
5	*ent*-31,32-*syn*-**193**	G-II (20 mol%), *p*-benzoquinone (10 mol%), PhMe, 80°C, O/N	Homodimerisation: *ent-syn*-**196b**	Quant.
6	*ent*-31,32-*syn*-**198**	G-II (20 mol%), *p*-benzoquinone (10 mol%), PhMe, 80°C, O/N	Homodimerisation: *ent-syn*-**199b**	50%
7	42,45-*syn*-**2b**, *ent*-31,32-*syn*-**193**	HG-II (5 mol%), *p*-benzoquinone (10 mol%), PhMe, 40°C, O/N	Homodimerisation: *ent-syn*-**196b**	Quant.
8	42,45-*syn*-**2b**, *ent*-31,32-*syn*-**3b**	HG-II (5 mol%), *p*-benzoquinone (10 mol%), PhMe, 80°C, 8h	Cross metathesis: *syn-syn-syn*-**188c** homodimerisation: *ent-syn*-**196b**	Insep. mix
9	42,45-a*nti*-**2a**, *ent*-31,32-*syn*-**196**	HG-II (5 mol%), *p*-benzoquinone (10 mol%), PhMe, 80°C, 8h	Some isomerisation: 42,45-a*nti*-**201**	NA
10	42,45-a*nti*-**2a**, *ent*-31,32-*syn*-**198**	HG-II (5 mol%), *p*-benzoquinone (10 mol%), PhMe, 80°C, 8h	Isomerisation: 42,45-*anti*-**197**	Quant.
11	42,45-a*nti*-**2a**, *ent*-31,32-*syn*-**3b**	HG-II (5 mol%), *p*-benzoquinone (10 mol%), PhMe, 60°C, 6h	Cross metathesis & homodimerization: *syn-syn-anti*-**188b**, *ent-syn*-**196b**	Insep. mix
12	42,45-a*nti*-**2a**, 31,32-*syn*-**3a**	HG-II (5 mol%), *p*-benzoquinone (10 mol%), PhMe, 60°C, 6h	Cross metathesis & homodimerization: *syn-anti-anti*-**188c**, *syn*-**196a**	Insep. mix

These observations led to exploration of cross metathesis using the fully protected C34-C46 fragment **2b** and more robust C29-C35 TBS ethers 31,32-*syn*-**3a** and *ent*-31,32-*syn*-**3b** (**Scheme 40**, **Table 11** entries 8, 11-12). Under the optimised cross metathesis conditions (5 mol% HG-II, 10 mol% *p*-benzoquinone, 80°C, 8h), consumption of the olefin 42,45-*syn*-**2b** starting material, only trace amounts of isomerisation product **201** and presence of the *ent*-31,32-*syn*-**3b** homodimerisation product (*ent*-**196b**), suggested that C34-C35 bond formation may have occurred (**Scheme 41**, **Table 11** entry 8). However, chromatographic purification did not result in clean cross metathesis product fractions. Analysis of the homodimerisation product fractions by mass spectrometry revealed the presence of the cross metathesis product olefin *syn-syn-syn*-**188c**, which was not immediately evident in NMR analysis, due to the large excess of homodimer *ent*-**196b**. Oxidative PMB deprotection (DDQ) of this mixture allowed separation of primary alcohol *syn-syn-syn*-**202c** from diol *ent*-**203b**. Analogous conditions (5 mol% HG-II, 10 mol% *p*-benzoquinone, 60°C, 6h) were employed to achieve the successful cross metathesis between 42,45-*anti*-**2a** and *ent*-31,32-*syn*-**3b** (**Table 11** entry 11), with subsequent deprotection allowing separation of primary alcohol *syn-syn-anti*-**202b** from diol *ent*-**203b** (**Scheme 41**). Similarly, cross metathesis between 42,45-*anti*-**2a** and 31,32-*syn*-**3a** (**Table 11** entry 12) and deprotection allowed separation of primary alcohol *syn-anti-anti*-**202a** from diol-**203a** (**Scheme 41**).

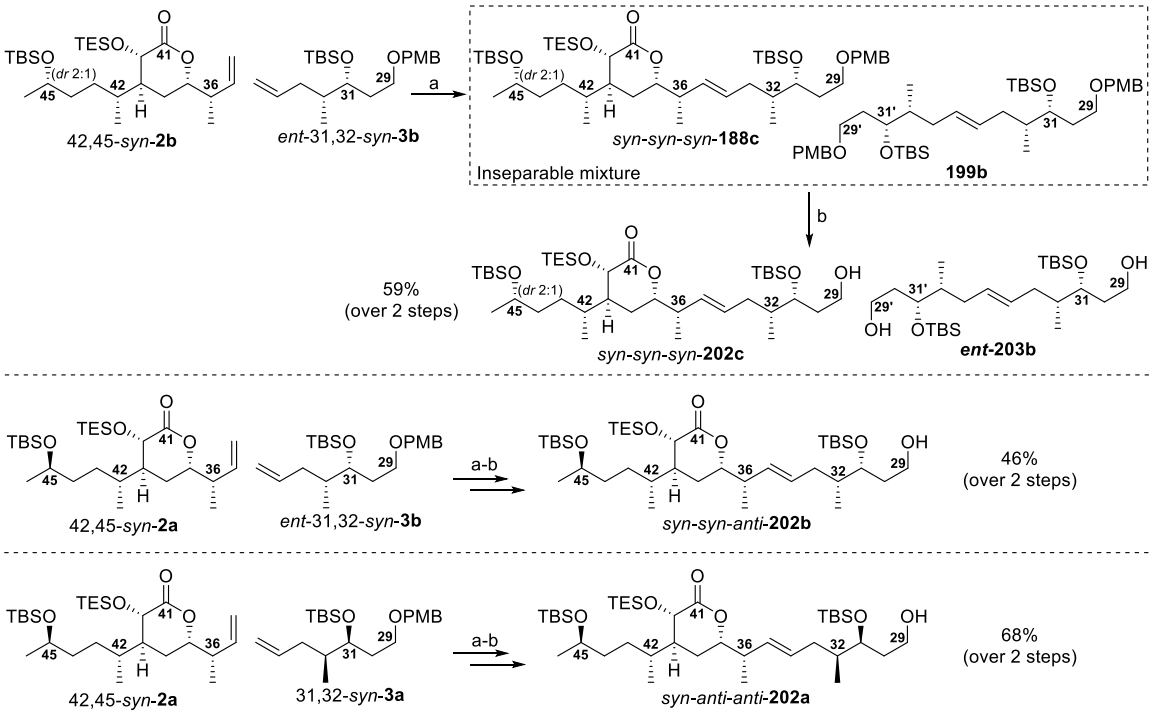

Reagents: (a) HG-II (5 mol % wrt total olefin), *p*-benzoquinone, PhMe, 80°C; (b) DDQ, CH_2Cl_2:pH 9.2 buffer (4:1), 0°C to rt, 59% (over two steps).

Scheme 41. Cross metathesis fragment coupling and deprotection of C29-C46 diastereomers to give primary alcohols *syn-syn-syn*-**202c**, *syn-syn-anti*-**202b** and *syn-anti-anti*-**202a** as well as diols **203a** and *ent*-**203b**.

4.2 Global Deprotection of the C29-C46 Diastereomers

Conditions were then tested to achieve global deprotection of primary alcohols *syn-anti-anti*-**202a**, *syn-syn-anti*-**202b** and *syn-syn-syn*-**202c**, thereby allowing comparison of the resulting tetraols, *syn-anti-anti*-**204a**, *syn-syn-anti*-**204b** and *syn-syn-syn*-**204c**, to hemicalide. There is good precedent within the Paterson group[68] and elsewhere[182,183] to support the use of pyridine buffered HF in pyridine (HF·py/py) to achieve global desilylation in polyketide natural products or their advanced intermediates. However, exposing *syn-syn-syn*-**202c** to initial deprotection conditions, utilising HF·py/py, did not result in full deprotection (**Scheme 42a**). Even after prolonged reaction times (3.5h), one TBS ether remained giving *syn-syn-syn*-**205c**.

This outcome was perhaps foreshadowed by a similar result obtained by Ardisson/Cossy, who found themselves unable to remove the final TBS ether from their carbon backbone stereoisomer **121** (*vide supra* **1.4.6**).[131] Furthermore, in the synthesis by Han and Lam of C1-C28 fragments 13,18-*syn*-**83a** and 13,18-*anti*-**83b**, global desilylation (to give 13,18-*syn*-**100a** and 13,18-*anti*-**100b**) could not be achieved in a single step.[62] This prompted the suggestion that TMS ethers should be used in place of TES ethers in the protection of the dihydroxylactone moiety.[153,154] Indeed, it was for these reasons, hoping to avoid final deprotection issues, that TES ethers were initially selected for both the C31 and C45 hydroxyls in this work. However, as discussed (*vide supra*), the TES ethers trialled on both of these hydroxyls were subject to unwanted early cleavage, during concomitant hydrogenation-debensylation and cross metathesis, respectively, and had to be replaced by more robust TBS ethers.

There is ample literature precedent for the use of aqueous HF in acetonitrile to achieve global desilylation, without causing undesired degradation of late-stage material.[184–187] However, when these conditions were tested by Heathcock in the final global deprotection of the marine polyketide spongistatin-2 it was discovered that starting material remained and spongistatin-2 was isolated from the products in low yield.[182] Testing various conditions revealed that using higher acid concentrations, shorter reaction times, low temperature (–20 °C) and conducting a cold initial quench, with Et_3N, allowed spongistatin-2 to be isolated in 92% yield. Application of these conditions to partially deprotected *syn-syn-syn*-**205c** gave tetraol *syn-syn-syn*-**204c** in good yield (82% over two steps) (**Scheme 42a**). Analogously, application of these conditions to primary alcohols *syn-anti-anti*-**202a** or *syn-syn-anti*-**202b** provided the corresponding tetraols *syn-anti-anti*-**204a** or *syn-syn-anti*-**204b** in quantitative yields (**Scheme 42b-c**).

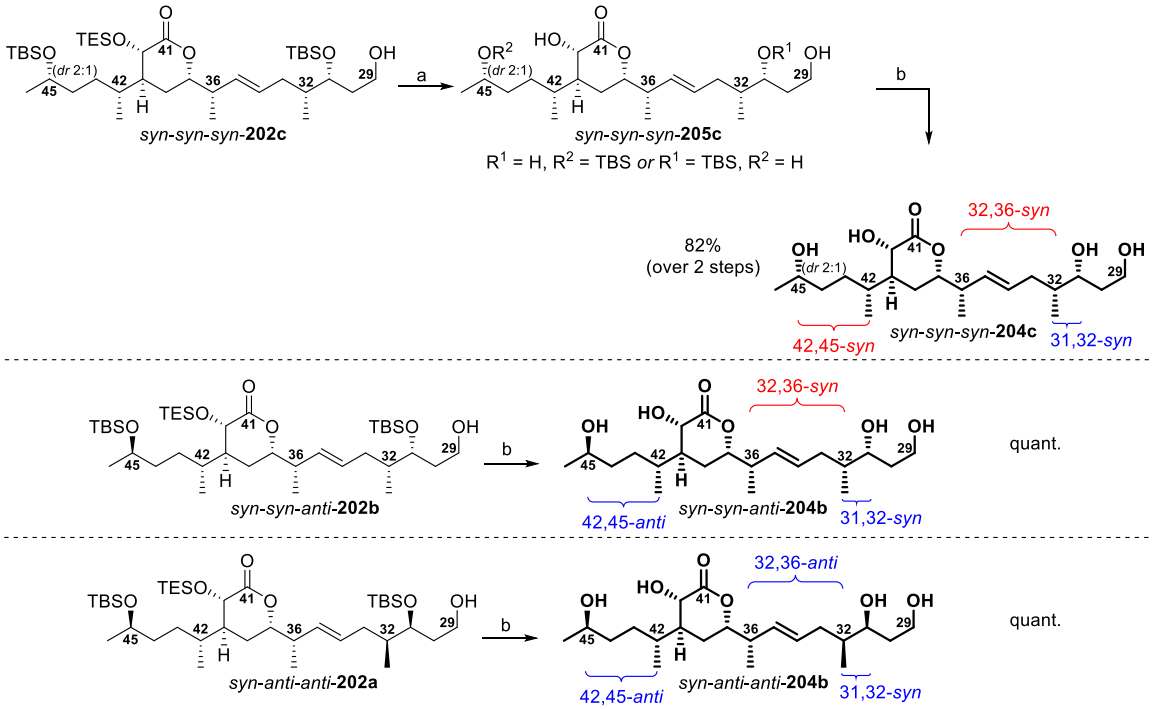

Reagents: (a) HF·py, py, THF, 0°C to rt; (b) HF (48% aq.) 10% in MeCN, –20°C *then* Et_3N, 82% (over two steps).
Scheme 42. Global desilylation of C29-C46 diastereomers (**202a-c**) to give tetraols *syn-anti-anti*-**204a**, *syn-syn-anti*-**204b** and *syn-syn-syn*-**204c**.

4.3 Relative Stereochemical Assignment of the C29-C46 Region

Brown crotylboration can be conducted with high diastereoselectivity (>95%) and enantioselectivity (>95%).[161–164] However, to facilitate direct comparison given the potentially minute spectroscopic differences, not only between fully elaborated C29-C46 tetraols (*syn-anti-anti*-**204a** or *syn-syn-anti*-**204b**) and hemicalide, but also between the tetraols themselves, it was considered desirable that a somewhat lower enantiomeric purity was employed. This approach effectly dopes each compound with a small amount of the diastereomer, to allow direct overlay between major and minor components. The same strategy was successfully employed in the Aggarwal synthesis-enabled assignment of baulamycin structures.[188] This can be achieved by faster addition of the aldehyde, with a conseqent slight raise in temperature, during the crotylboration (*vide supra*). As a consequence, tetraol *syn-anti-anti*-**204a** is produced largely as the named *syn-anti-anti* configuration, but also contains *syn-syn-anti*-**204b** as a minor component and *vice versa*. This allowed straightforward comparison of each tetraol to one other and hemicalide for the purposes of stereochemical assignment (**Figure 22**).

Lower enantioselectivity in the Brown crotylboration was achieved by faster addition of the aldehyde, with a conseqent slight raise in temperature. The extent of the energetic difference

between competing transition states is temperature dependent.[167] By slightly raising the temperature of the reaction, by faster addition of the aldehyde, the energy difference between **TS-XIII** and **TS-XIV** (or **TS-XV** and **TS-XVI**) is reduced and somewhat more *ent*-31,32-*syn*-**108a** (or 31,32-*syn*-**108b**) is created, decreasing the enantiomeric excess of the reaction. Following Brown crotylboration (**Scheme 37a**), the absolute stereochemistry of C31 homoallylic alcohol 31,32-*syn*-**108a** was validated by generating Mosher's esters **181a** and **182a** (**Scheme 37a, d**). This confirmed the expected absolute stereochemistry and verified that, while high diastereoselectivity (>95:5) was generally able to be maintained, faster addition of aldehyde **176** resulted in a lower enantiomeric excess of *ca*. 70%. Although Mosher's ester generation is not a typical method of determining enantiomeric excess, these reactions were pushed to completion, thereby reducing the risk of misleading results due to kinetic resolution. The estimate of enantiomeric excess made here also matches that indicated by the diastereomeric ratio resulting when the C29-C35 and C34-C46 terminal olefins are coupled to give the C29-C46 diastereomers.

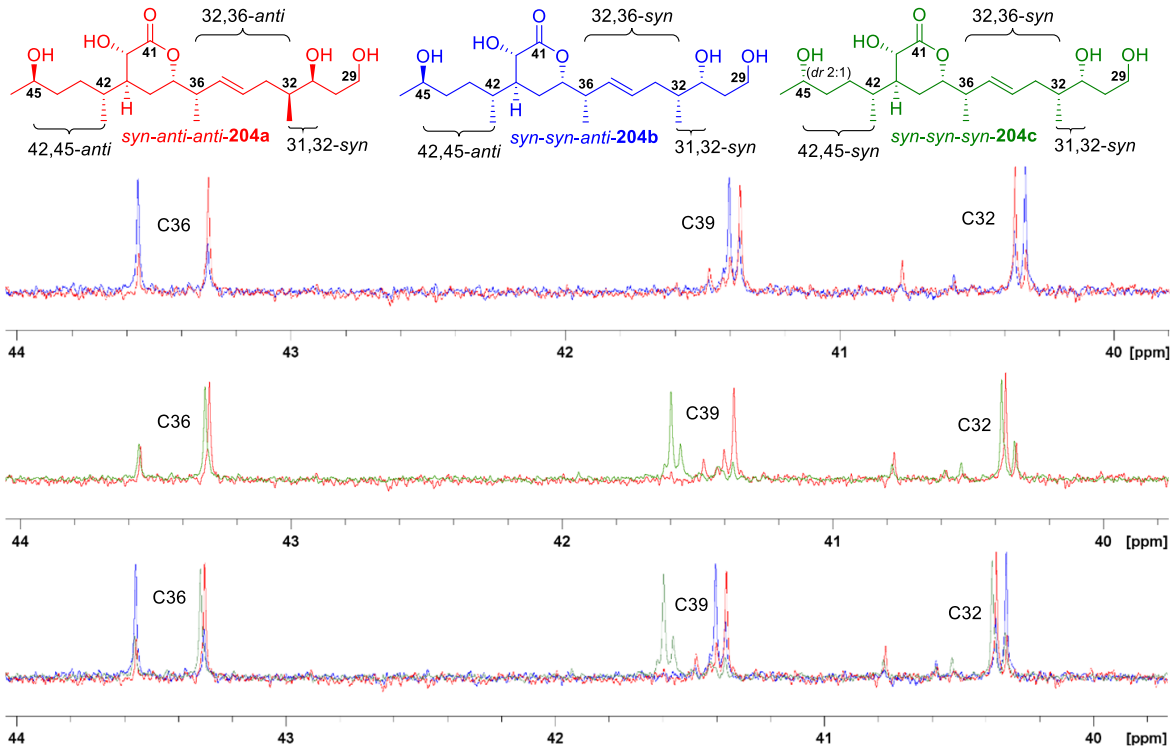

Figure 22. Example excerpt of ^{13}C NMR spectra overlay for: (top) *syn-anti-anti*-**204a** (red) and *syn-syn-anti*-**204b** (blue); (middle) *syn-syn-anti*-**204b** (blue) and *syn-syn-syn*-**204c** (green); (bottom) *syn-anti-anti*-**204a** (red), *syn-syn-anti*-**204b** (blue) and *syn-syn-syn*-**204c** (green).

Two other compounds were included in the NMR comparisons for the sake of completeness. Firstly, the *syn-syn-syn*-**204c** tetraol is a *ca.* 2:1 diastereomeric mixture of 42,45-*syn*:*anti* at C45. The utility of this diastereomeric mixture lay in the fact that comparison of this tetraol to tetraols

syn-anti-anti-**204a** and *syn-syn-anti*-**204b** as well as hemicalide, acts as a further test of the stereochemical assignment at C45 (**Figure 22b-c**). Secondly, chemical shift comparison could be made between the Ardisson/Cossy hemicalide backbone stereoisomer **121**,[131] and the C29-C46 *syn-anti-anti*-**204a**, *syn-syn-anti*-**204b** and *syn-syn-syn*-**204c** tetraols. This allowed evaluation of whether the C29-C46 diastereomers created in this work are an improvement upon the randomly assigned C31, C32, and C45 stereocentres present in that system.

Initially, it appeared that there were quite significant ^{13}C shift differences (0.6-1.0 ppm) for all tetraol diastereomers across both C34 and C35. This was odd, given that originally, Ardisson/Cossy had reported a 0 ppm shift deviation for C34.[131] Closer inspection of the data tables showed two calculation errors in this region. Relevant to this analysis was that the error for C34 (133.2 ppm for hemicalide vs 132.2 ppm for stereoisomer **121**). However, given that in all tetraol diastereomers created in this work, as well as in Ardisson/Cossy stereoisomer **121**, C34 was assigned as *ca* 132 ppm and C35 was assigned as *ca* 133 ppm, it appeared that these carbons had been incorrectly assigned. Reanalysis of the raw hemicalide NMR data files allowed correction of the C34 and C35 values, which had been reversed in Ardisson/Cossy's data tabulation. Thus, the actual C34 and C35 ^{13}C shift differences for Ardisson/Cossy stereoisomer **121** were 0.1 ppm and 0.3 ppm, respectively. This correction also had the consequential effect that all C29-C46 diastereomers constructed in this work have very low shift deviations (0.0-0.2 ppm) across C34-C35, rather than a quite a high shift differences as it initially appeared.

Comparison of the chemical shift differences between these five compounds not only confirmed the 42,45-*anti* assignment, it also revealed that a 32,36-*anti* assignment between the stereoclusters was the best fit, and favourably supported the 31,32-*syn* assignment as a better match than the 31,32-*anti* relative configuration in Ardisson/Cossy stereoisomer **121** (**Table 13**, **Table 14**, **Figure 23** and **Figure 24**). All 31,32-*syn* diastereomers synthesised (**204a-c**) have lower errors than the 31,32-*anti* Ardisson/Cossy diastereomer **121**, particularly over the C31-C33 region. This provides strong evidence in support of a 31,32-*syn* assignment. Comparison between *syn-syn-anti*-**204b** and *syn-syn-syn*-**204c**, shows a lower deviation for the *syn-syn-anti*-**204b** diastereomer. This validates the 42,45-*anti* relationship. Overall *syn-anti-anti*-**204a** is a much closer fit to the spectroscopic date for hemicalide than any of the other candidates (*syn-anti-anti*-**204a**: $\sum|\Delta\delta_H| = 0.06$ ppm; $\sum|\Delta\delta_C| = 1.57$ ppm; *syn-syn-anti*-**204b**: $\sum|\Delta\delta_H| = 0.11$ ppm; $\sum|\Delta\delta_C| = 2.72$ ppm; *syn-syn-syn*-**204c**: $\sum|\Delta\delta_H| = 0.10$ ppm; $\sum|\Delta\delta_C| = 2.86$ ppm; Cossy/Ardisson stereoisomer-**121**: $\sum|\Delta\delta_H| = 0.33$ ppm; $\sum|\Delta\delta_C| = 8.48$ ppm) (**Figure 23**, **Table 12**). Comparison with Cossy/Ardisson

stereoisomer **121** is not able to be made with the additional ^{1}H NMR data provided by Massiot as these shifts were not reported for stereoisomer **121**. Inclusion of these ten additional ^{1}H NMR data points in the spectroscopic comparison between hemicalide and tetraols *syn-anti-anti*-**204a**, *syn-syn-anti*-**204b** and *syn-syn-syn*-**204c** did not alter any of the above conclusions and is noted below where relevant (*syn-anti-anti*-**204a**: $\sum|\Delta\delta_H|$= 0.16 ppm; *syn-syn-anti*-**204b**: $\sum|\Delta\delta_H|$= 0.24 ppm; *syn-syn-syn*-**204c**: $\sum|\Delta\delta_H|$= 0.25 ppm) (**Figure 24** top graph, **Table 12**).

Table 12. Summary of ^{1}H and ^{13}C spectroscopic differences, represented as total sum of errors and maximum errors, between tetraols *syn-anti-anti*-**204a**, *syn-syn-anti*-**204b** and *syn-syn-syn*-**204c**, Ardisson/Cossy stereoisomer **121** and hemicalide (**1**)

	$\sum\|\Delta\delta_H\|$(ppm)	Max$\|\Delta\delta_H\|$(ppm)	$\sum\|\Delta\delta_C\|$(ppm)	Max$\|\Delta\delta_C\|$(ppm)
syn-anti-anti-**204a**	0.06 (0.16)*	0.04 (0.04)*	1.57	0.81
syn-syn-anti-**204b**	0.11 (0.24)*	0.04 (0.04)*	2.72	0.72
syn-syn-syn-**204c**	0.10 (0.25)*	0.03 (0.04)*	2.86	0.73
Stereoisomer **121**	0.33	0.14	8.48	1.32

* Including data courtesy of personal communication with Georges Massiot (publication forthcoming).

It should be noted that comparison with Cossy/Ardisson diastereomer **121** is troublesome, in the C44-C46 region. The original paper stated only that the remaining silyl group was attached at OH40 or OH45. However, comparison to hemicalide and tetraols *syn-anti-anti*-**204a**, *syn-syn-anti*-**204b** and *syn-syn-syn*-**204c**, show the highest ^{13}C deviations in the C44-C46 region, ranging from 0.53-1.32 ppm. By comparison, ^{13}C deviations in the C39-C41 region range from 0.00-0.21 ppm. These deviations strongly indicate that the TBS ether likely remains attached to C45 (*vide supra* section **2.4**). Nonetheless, exclusion of these data points from the overall evaluation (Cossy/Ardisson stereoisomer **121**: $\sum|\Delta\delta_H|$= 0.17 ppm; $\sum|\Delta\delta_C|$= 5.80 ppm) does not alter the conclusions made for the relative configurational assignment of C31 or C32. Importantly, this NMR spectroscopic comparison, further narrows down the possible diastereomeric candidates from eight to four in the C27-C32 stereotetrad, from 64 to four across the C27-C46 region, and from 128 to eight for hemicalide itself.

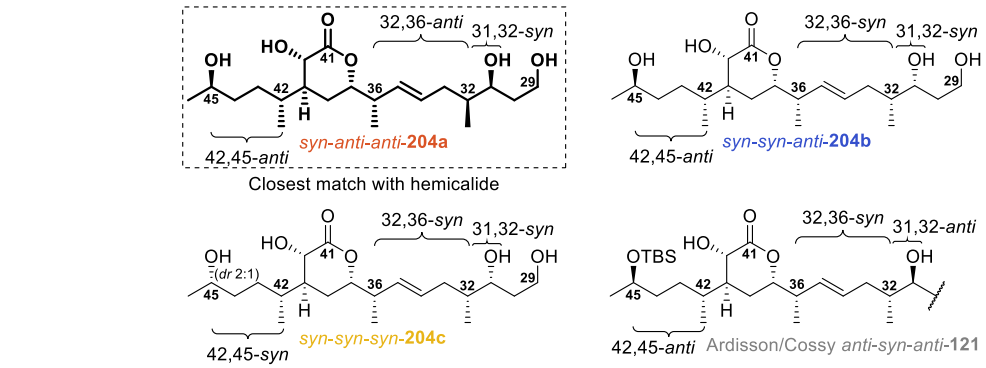

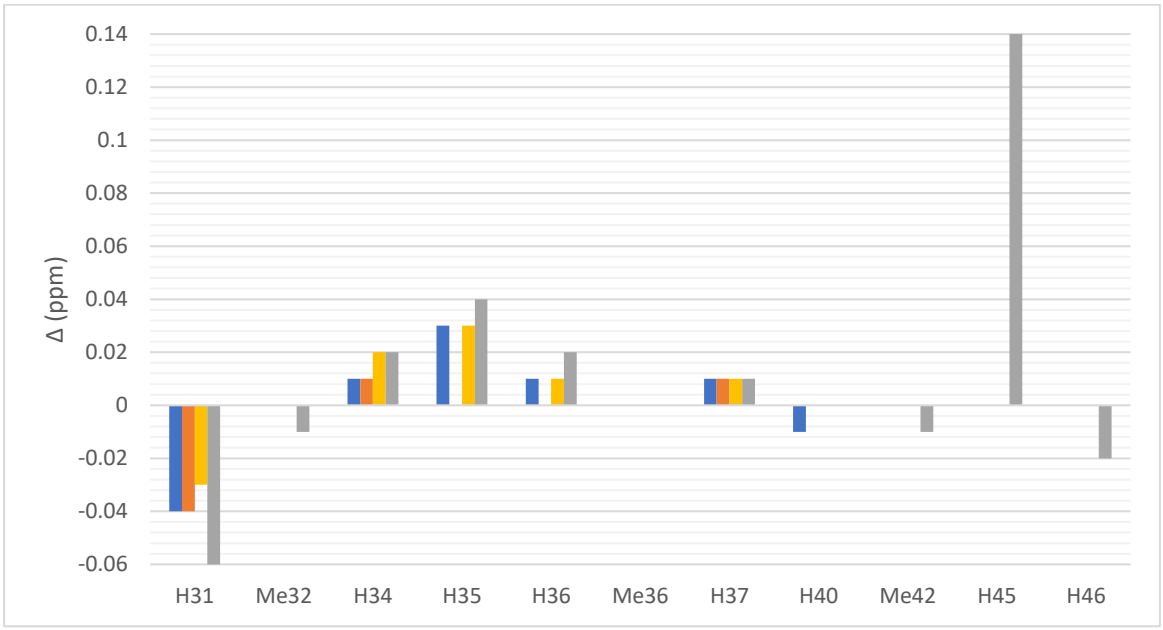

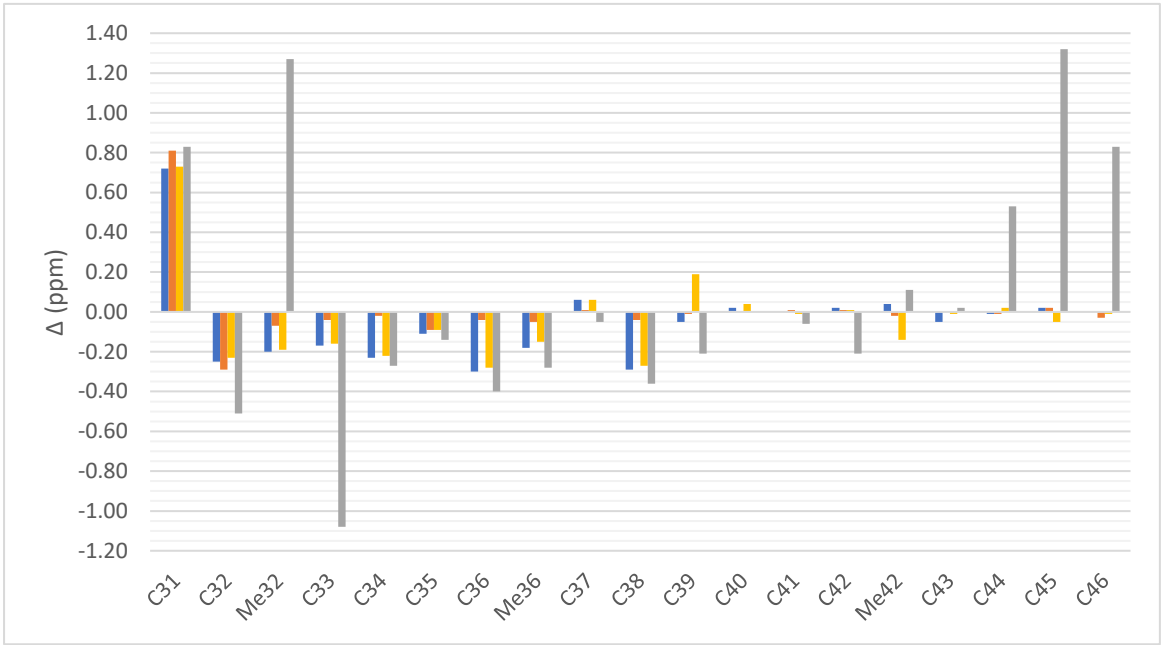

Figure 23. Bar graphs top: showing the ^{1}H chemical shift difference between tetraol diastereomers *syn-anti-anti*-**204a** (orange), *syn-syn-anti*-**204b** (blue); *syn-syn-syn*-**204c** (yellow); Ardisson/Cossy stereoisomer **121** (grey) and hemicalide; bottom: showing the ^{13}C chemical shift difference between tetraol diastereomers *syn-anti-anti*-**204a** (orange), *syn-syn-anti*-**204b** (blue); *syn-syn-syn*-**204c** (yellow); Ardisson/Cossy stereoisomer **121** (grey) and hemicalide.

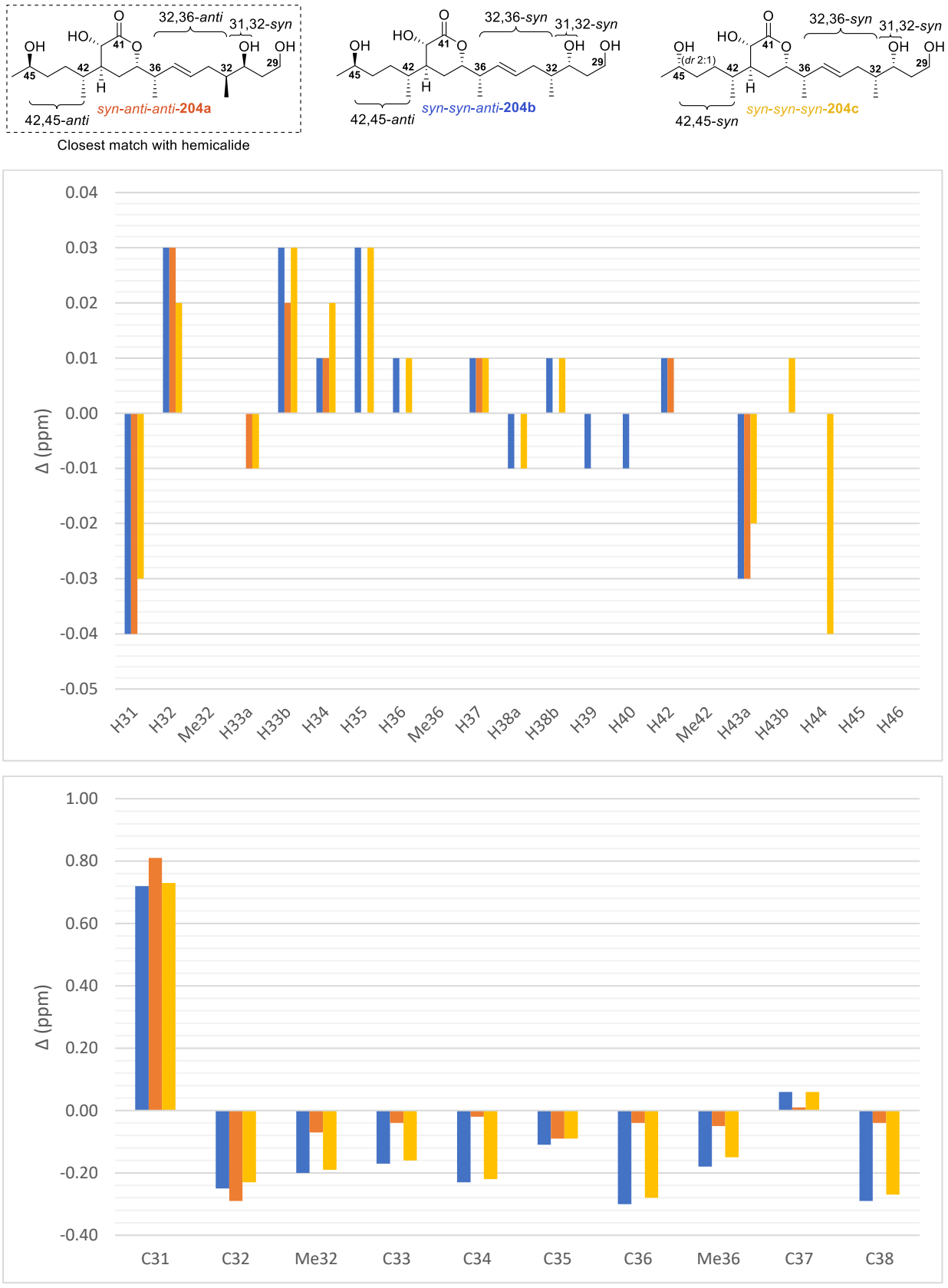

Figure 24. Bar graphs top: showing the ^{1}H chemical shift difference between tetraol diastereomers *syn-anti-anti*-**204a** (orange), *syn-syn-anti*-**204b** (blue); *syn-syn-syn*-**204c** (yellow) and hemicalide including the additional unpublished data from Georges Massiot; bottom: showing the ^{13}C chemical shift difference between tetraol diastereomers *syn-anti-anti*-**204a** (orange), *syn-syn-anti*-**204b** (blue); *syn-syn-syn*-**204c** (yellow)and hemicalide.

Table 13. Proton (^{1}H) NMR comparisons between tetraol diastereomers (**204a-c**),Cossy/Ardisson hemicalide stereoisomer **121** and hemicalide (**1**)

Signal	^{1}H Shift in CD_3OD (ppm)								
	Hemicalide (**1**)	*Syn, anti, anti*-**204a**	Δ	*Syn, syn, anti*-**204b**	Δ	*Syn, syn, syn*-**204c**	Δ	Cossy/Ardisson stereoisomer-**121**	Δ
H31 ddd (*J* Hz)	3.69 (m)	3.65 (*7.6, 4.2, 3.7*)	-0.04	3.65 (*7.7, 4.2, 3.6*)	-0.04	3.66 (*8.5, 4.1, 3.8*)	-0.03	3.63 (m)	-0.06
H31 ddd (*J* Hz)	3.69 (m)	3.65 (*7.6, 4.2, 3.7*)	-0.04	3.65 (*7.7, 4.2, 3.6*)	-0.04	3.66 (*8.5, 4.1, 3.8*)	-0.03	3.63 (m)	-0.06
H32 (m)*	1.51	1.54	0.03	1.54	0.03	1.53	0.02		
Me32 d (*J* Hz)	0.89 (*6.7*)	0.89 (*6.9*)	0.00	0.89 (*6.9*)	0.00	0.89 (*6.8*)	0.00	0.88 (*7.0*)	-0.01
H33a (m)*	2.22	2.21	-0.01	2.22	0.00	2.21	-0.01		
H33b (m)*	1.86	1.88	0.02	1.89	0.03	1.89	0.03		
H34 ddd (*J* Hz)	5.55 (14.6, 7.2, 7.2)	5.56 (*15.3, 7.8, 7.0*)	0.01	5.56 (*15.3, 7.8, 7.0*)	0.01	5.57 (m)	0.02	5.57 dt (*14.8, 7.3*)	0.02
H35 dd (*J* Hz)	5.33 (*15.3, 8.5*)	5.33 (*15.3, 8.3*)	0.00	5.36 (*15.3, 8.3*)	0.03	5.36 (*15.3, 8.3*)	0.03	5.37 (*15.3, 8.5*)	0.04
H36 (m)	2.34	2.34	0.00	2.35	0.01	2.35	0.01	2.36	0.02
Me36 d (*J* Hz)	1.11 (*6.7*)	1.11 (*6.7*)	0.00	1.11 (*6.7*)	0.00	1.11 (*6.8*)	0.00	1.11 (*6.7*)	0.00
H37 ddd (*J* Hz)	4.11 (*11.1, 7.7, 3.5*)	4.12 (*11.2, 7.8, 3.7*)	0.01	4.12 (*10.9, 7.5, 3.8*)	0.01	4.12 (*11.1, 7.9, 4.0*)	0.01	4.12 (*11.0, 7.6, 3.7*)	0.01
H38a (m)*	1.80	1.80	0.00	1.79	-0.01	1.79	-0.01	Not reported	
H38b (m)*	1.67	1.67	0.00	1.68	0.01	1.68	0.01	Not reported	
H39 (m)*	1.89	1.88	0.00	1.87	-0.01	1.88	0.00	Not reported	
H40 d (*J* Hz)	4.32 (*11.3*)	4.32 (*11.3*)	0.00	4.31 (*11.3*)	-0.01	4.32 (*11.3*)	0.00	4.32 (*11.3*)	0.00
H42 (m)*	1.97	1.98	0.01	1.98	0.01	1.97	0.00	Not reported	
Me42 d (*J* Hz)	0.91 (*7.0*)	0.91 (*6.9*)	0.00	0.91 (*6.9*)	0.00	0.91 (*6.8*)	0.00	0.90 (*7.0*)	-0.01
H43a (m)*	1.41	1.38	-0.03	1.38	-0.03	1.39	-0.02	Not reported	
H43b (m)*	1.26	1.26	0.00	1.26	0.00	1.27	0.01	Not reported	
H44 (m)*	1.43	1.43	0.00	1.43	0.00	1.39	-0.04	Not reported	
H45 (m)	3.69	3.69	0.00	3.69	0.00	3.69	0.00	3.83	0.14
H46 d (*J* Hz)	1.15 (*6.4*)	1.15 (*6.2*)	0.00	1.15 (*6.2*)	0.00	1.15 (*6.2*)	0.00	1.13 (*6.0*)	-0.02

Table 14. Carbon (^{13}C) NMR comparisons between tetraol diastereomers (**204a-c**), Cossy/Ardisson hemicalide stereoisomer **121** and hemicalide (**1**)

Signal	^{13}C Shift in CD_3OD (ppm)								
	Hemicalide (**1**)	*Syn, anti, anti*-**204a**	Shift deviations	*Syn, syn, anti*-**204b**	Shift deviations	*Syn, syn, syn*-**204c**	Shift deviations	Cossy/Ardisson stereoisomer-**121**	Shift deviations
C31	71.97	72.78	0.81	72.69	0.72	72.70	0.73	72.8	0.83
C32	40.61	40.32	-0.29	40.36	-0.25	40.38	-0.23	40.1	-0.51
Me32	14.43	14.36	-0.07	14.23	-0.20	14.24	-0.19	15.7	1.27
C33	37.68	37.64	-0.04	37.51	-0.17	37.52	-0.16	36.6	-1.08
C34	132.47	132.45	-0.02	132.24	-0.23	132.25	-0.22	132.2	-0.27
C35	133.24	133.15	-0.09	133.13	-0.11	133.15	-0.09	133.1	-0.14
C36	43.60	43.56	-0.04	43.30	-0.30	43.32	-0.28	43.2	-0.40
Me36	17.18	17.13	-0.05	17.00	-0.18	17.03	-0.15	16.9	-0.28
C37	80.85	80.86	0.01	80.91	0.06	80.91	0.06	80.8	-0.05
C38	26.76	26.72	-0.04	26.47	-0.29	26.49	-0.27	26.4	-0.36
C39	41.41	41.40	-0.01	41.36	-0.05	41.60	0.19	41.2	-0.21
C40	68.20	68.20	0.00	68.22	0.02	68.24	0.04	68.2	0.00
C41	178.36	178.37	0.01	178.36	0.00	178.35	-0.01	178.3	-0.06
C42	33.71	33.72	0.01	33.73	0.02	33.72	0.01	33.5	-0.21
Me42	13.39	13.37	-0.02	13.43	0.04	13.25	-0.14	13.5	0.11
C43	32.08	32.08	0.00	32.03	-0.05	32.07	-0.01	32.1	0.02
C44	37.97	37.96	-0.01	37.96	-0.01	37.99	0.02	38.5	0.53
C45	68.68	68.70	0.02	68.70	0.02	68.63	-0.05	70.0	1.32
C46	23.57	23.54	-0.03	23.57	0.00	23.56	-0.01	24.4	0.83
C31	71.97	72.78	0.81	72.69	0.72	72.70	0.73	72.8	0.83
C32	40.61	40.32	-0.29	40.36	-0.25	40.38	-0.23	40.1	-0.51

Confident in the best fitting assignment of the relative configuration in the C29-C46 region, DMP oxidation of primary alcohol *syn-anti-anti*-**202a** was undertaken to quantitatively provide the corresponding C29 aldehyde **131** (**Scheme 43**). This provides the necessary coupling handle for the planned asymmetric boron aldol reaction to forge the C28-C29 bond.

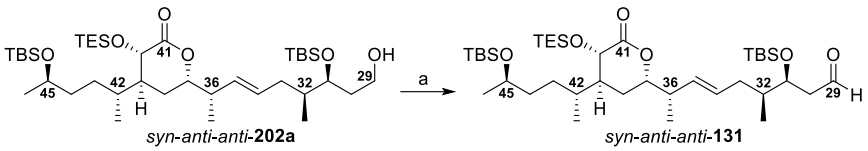

Reagents: (a) DMP, CH_2Cl_2, rt, quant.
Scheme 43. Oxidation of primary alcohol *syn-anti-anti*-**202a** to give aldehyde *syn-anti-anti*-**131**.

4.4 Conclusions

Cross metathesis was successfully used to forge the C34-C35 (*E*)-olefin, coupling the C29-C35 and C34-C46 fragments and providing access to the C29-C46 region of hemicalide. By coupling 42,45-*anti*-**2a** and 42,45-*syn*-**2b** with *ent*-31,32-*syn*-**3b**, the 42,45-relationship between stereoclusters was able to be reassessed in the context of a larger fragment of the natural product. By coupling 42,45-*anti*-**2a** with 31,32-*syn*-**3a** and *ent*-31,32-*syn*-**3b**, the 32,36-relationship between the stereoclusters was able to be explored as well as the 31,32-relationship.

Global deprotection gave access to diastereomeric tetraols that were able to be compared to the reprocessed natural product NMR data and Ardisson/Cossy stereoisomer **121**. Diastereomer *syn-syn-anti*-**204b** bearing the 42,45-*anti* relationship was a better overall match for the natural product data than diastereomer *syn-syn-syn*-**204c** bearing the 42,45-*syn* relationship. This confirms that a 42,45-*anti* relationship best represents the relative configuration of hemicalide. Furthermore, all three C29-C46 diastereomers produced in this work, bearing a 31,32-*syn* relationship, were a much better match for the natural product data than Ardisson/Cossy stereoisomer **121**, bearing the 31,32-*anti* relationship. This indicates that a 31,32-*syn* relationship best represents the relative configuration of hemicalide. Overall, assessment of the *syn-anti-anti*-**204a**, *syn-syn-anti*-**204b** and *syn-syn-syn*-**204c** diastereomers showed that *syn-anti-anti*-**204a** is the closest match for the natural product. Altogether, this indicates that a 32,36-*anti* relationship best represents the relative configuration of hemicalide and adds further support for assignment of the 31,32-*syn* and 42,45-*anti* relationships.

The creation of the advanced intermediate aldehyde **131** places the synthesis at a stage where the next step would be an aldol coupling with the remainder of the carbon backbone of hemicalide. This leaves the project well poised for the final synthetic steps (*vide infra*). It also positions the project with only two remaining unknown stereocentres and the relationship between the C29-C46 and C1-C28 stereoclusters to be determined (**Figure 25**).

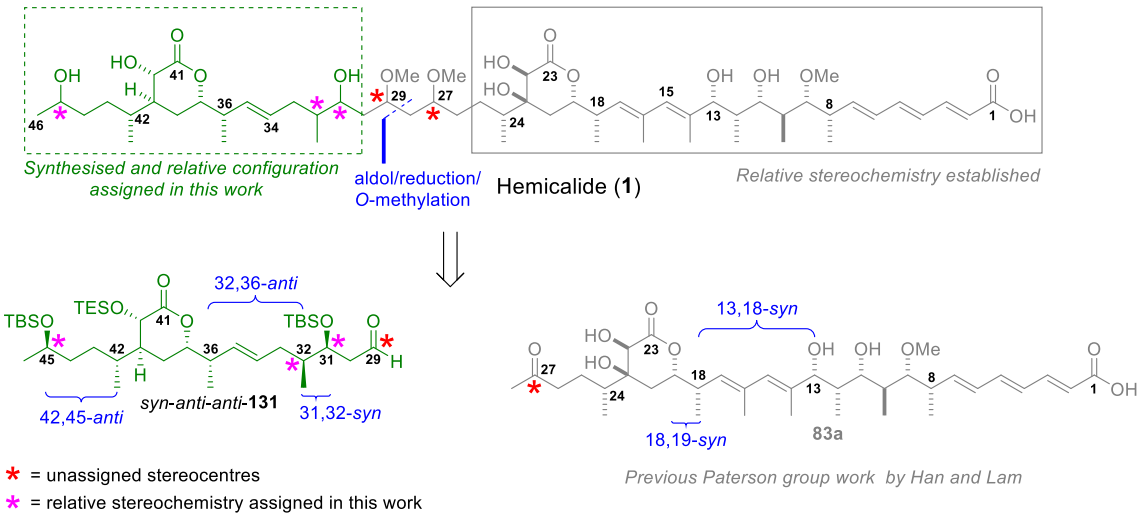

Figure 25. C29-C46 tetraol comparison fragments and advanced intermediate aldehyde **131**.

5. Conclusions and Future Work

5.1 Overall Conclusions

In the present work, significant progress has been made towards assigning the remaining five unassigned stereocentres and ascertaining the relationship between the stereoclusters of hemicalide. Furthermore, a highly stereoselective route for the synthesis and modular assembly of key fragments of hemicalide has been validated. This constitutes valuable progress towards the total synthesis of this intriguing and potently bioactive marine natural product. Prior to this project, the initial two million plus candidate enantiomers had been narrowed to 128 stereochemical permutations. The current project synthesised two possible enantiomers of the C29-C35 region (31,32-*syn*-**3a** and *ent*-31,32-*syn*-**3b**) and both of the two possible diastereomers of the C34-C46 region of hemicalide (42,45-*anti*-**2a** and 42,45-*syn*-**2b**), the coupling of which gave rise to C29-C46 diastereomers (*syn-anti-anti*-**204a**, *syn-syn-anti*-**204b** and *syn-syn-syn*-**204c**) that were able to be compared to natural product data (**Figure 26**).

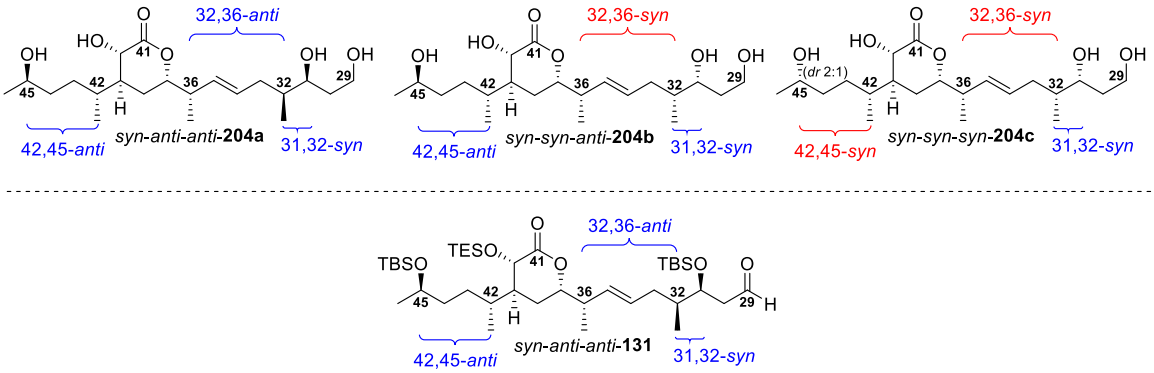

Figure 26. C29-C46 tetraol comparison fragments **204a-c** and advanced intermediate aldehyde **131**.

Synthesis of the C34-C46 region of hemicalide was conducted with an emphasis on diastereoselectivity, allowing confidence in the high fidelity creation of the desired configuration at each stereocentre, and scaleability, facilitiating future scale-up endeavours (**Scheme 44**). This region contains six stereocentres, with the original two (C36 and C42) sourced from the chiral pool from Roche ester (*S*-**24** and *R*-**25**). These stereocentres form the foundation for the substrate-controlled installation of the next three stereocentres (C37, C39 and C40). Chiral ligands are employed to enhance diastereoselectivity in the boron-mediated aldol reaction at C37.[138] The hydroxyl-directed reduction[127,189] and α-hydroxylation[126] that set C39 and C40, respectively, are wholly under substrate control. On the other hand, the only wholly reagent-controlled reaction is

found in the creation of the C45 stereocentre by Terashima reduction,[156] which gives rise to the 42,45-*syn* and 42,45-*anti* diastereomers intended for comparison with natural product data.

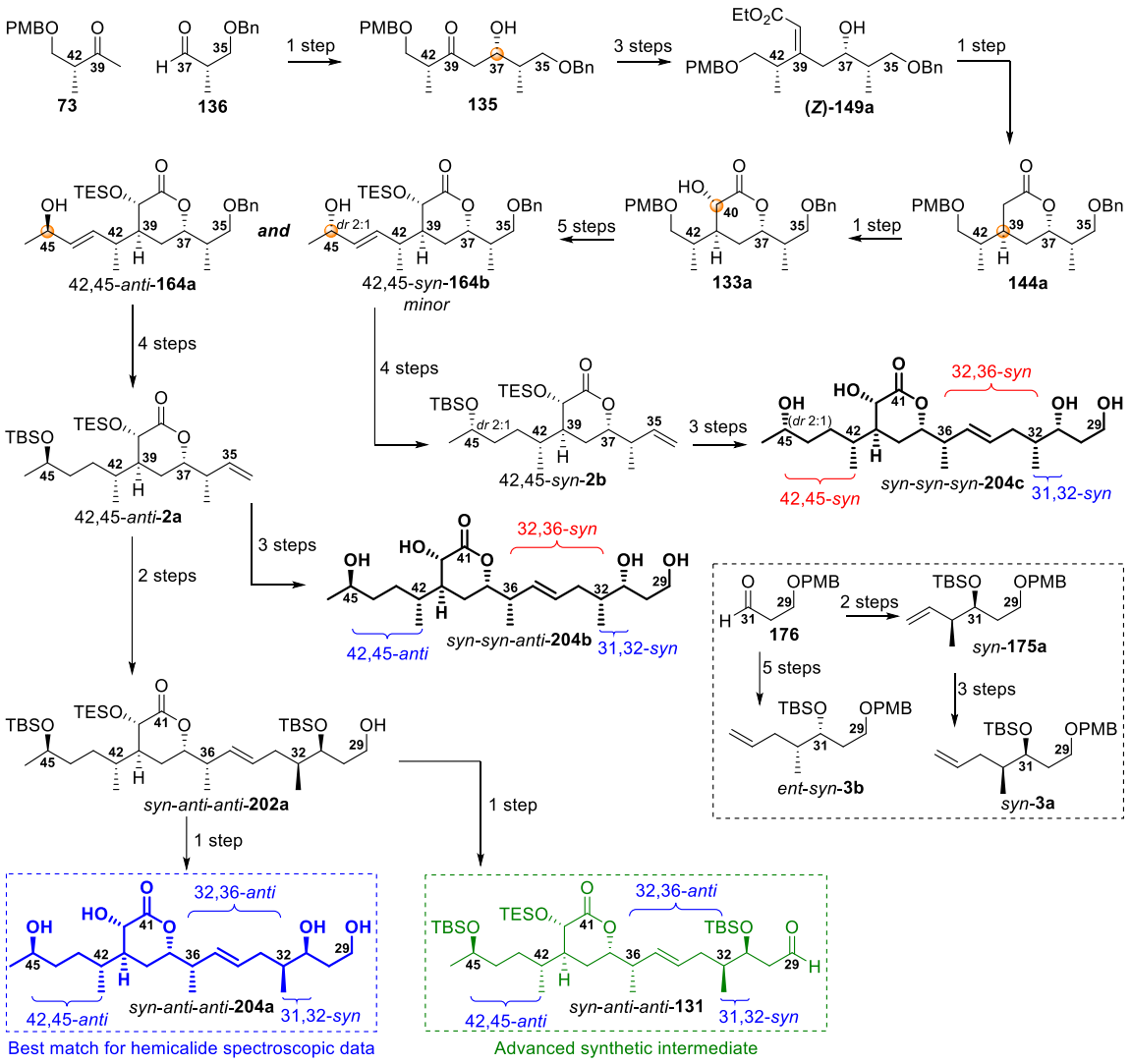

Scheme 44. Summary of the synthesis of C29-C46 diastereomers

Overall, the 42,45-*anti*-**2a** diastereomer was accessed *via* a scaleable synthesis in 16% yield, over 15 steps (LLS) from ketone **73**. Global desilylation was conducted to quantitatively provide the corresponding diol, 42,45-*anti*-**171a**, for comparison to hemicalide spectroscopic data. Analogous synthesis of diastereomer 42,45-*syn*-**170** (11% yield over 14 steps (LLS)) and quantitative desilylation gave the corresponding diol, 42,45-*syn*-**171b**, for comparison to hemicalide NMR spectroscopic data. This detailed comparison showed that the 42,45-*anti* diastereomer was a better match for the relative configuration of hemicalide.

Synthesis of the C29-C35 region of hemicalide was conducted in such a way as to secure a scaleable and highly diastereoselective and enantioselective route. Assessment of the chemical shift deviations in this region for Ardisson/Cossy stereoisomer **121** indicated that hemicalide was highly unlikely to bear a 31,32-*anti* relationship. Brown crotylboration provided a way to simultaneously set both of the C31 and C32 stereocentres with high diastereoselectivity and enantioselectivity. By employing *cis*-butene in this reaction and either (+) or (–)-diisopinocampheylmethoxyborane followed by homologation, 31,32-*syn*-**3a** and 31,32-*ent*-*syn*-**3b** were able to be accessed in seven steps and 45% or 42% yield, respectively.

The final diastereomeric tetraols of the C29-C46 region of hemicalide were synthesised by olefin cross metathesis between the C34-C46 and C29-C35 fragments and PMB deprotection to give C29-C46 primary alcohols *syn*-*anti*-*anti*-**202a**, *syn*-*syn*-*anti*-**202b** and *syn*-*syn*-*syn*-**202c**. Global desilylation provided the corresponding tetraols *syn*-*anti*-*anti*-**204a** (11%, 18 steps (LLS)), *syn*-*syn*-*anti*-**204b** (7%, 18 steps (LLS)) and *syn*-*syn*-*syn*-**204c** (8%, 19 steps (LLS)) for comparison to hemicalide data. This evaluation showed that tetraol *syn*-*anti*-*anti*-**204a** was noticeably the best match for the natural product data and, as such, that 31,32-*syn*, 32,36-*anti* and 42,45-*anti* relationships best reflect the relative configuration of hemicalide. Primary alcohol *syn*-*anti*-*anti*-**202a** was quantitively oxidised to aldehyde **131**, installing the coupling handle necessary for joining the C29-C46 region with the C1-C28 region of hemicalide.

This work permitted the assignment of the relative configuration of a further three previously unassigned stereocentres of hemicalide (C31, C32 and C45). It also determined the relationship between the C27-C32 and C36-C45 stereoclusters. This has the effect of narrowing the possible relative configurational permutations from 128 to only eight possible diastereomeric candidates. Furthermore, it has validated the synthesis of C29-C46 aldehyde **131** and positions the synthesis at the stage ready for coupling to the remainder of hemicalide, with only five synthetic steps necessary to access each of the remaining candidate diastereomers.

5.2 Future Work

The successful synthesis of the C29-C46 region of hemicalide validates a number of crucial steps central to the total synthesis of the natural product. This work by narrowing down the relative configuration to a single diastereomer in the C31-C36 region also represents significant progress towards the synthesis-enabled stereochemical elucidation of hemicalide. Nonetheless, further

work is necessary to establish the full relative and absolute stereochemistry of this natural product and complete the total synthesis of hemicalide. NMR spectroscopic comparison of candidate diastereomers with the natural product has and should continue to enable determination of the relative configuration of hemicalide. However, to determine the absolute stereochemistry, as well as to permit future analogue generation, both enantiomers of the full carbon skeleton with the correct relative configuration would need to be subjected to bioactivity studies.

5.2.1 Proposed Endgame Sequence

Five more steps are required to access each of the eight possible hemicalide diastereomers. With C29-C46 aldehyde **131** in hand, a boron-mediated aldol reaction with (+) or (–)-Ipc_2BCl could be undertaken with previously synthesised C1-C28 ketone **83a** or its enantiomer to give the corresponding β-hydroxy ketone (e.g. **206a**) (**Scheme 45**).[62] This step would complete the carbon backbone of hemicalide. Each of these diastereomers could then be subjected to 1,3-*syn* or 1,3-*anti* reduction of the C29 ketone and *bis*-*O*-methylation to provide access to the eight possible diastereomers (e.g. **207a**). This step would set the last of the 21 stereocentres in the molecule. Lastly, global deprotection *via* methyl ester hydrolysis and desilylation would enable detailed NMR comparison of the eight candidate diastereomers (e.g. **208a**) to the natural product.

It should be noted that the relative stereochemistry of C27 and C29, as well as the relationship between the C1-C24 and C27-C46 regions, can also be determined by coupling C29-C46 aldehyde **131** with the truncated C16-C28 ketone **4** or *ent*-**4** and elaborating the fragment as described above. This is less demanding on material as it allows use of a smaller truncate during work to determine relative stereochemistry.

5.2.2 Assessing the Eight Final Hemicalide Diastereomers

Once the eight candidate diastereomers are obtained, detailed NMR spectroscopic comparison with the natural product data can be undertaken to determine the closest matches with hemicalide. This assessment should focus particularly on the C27-C32 region, where the C27 and C29 centres remain unassigned, as well as the relationship between C29 and C31. The C24/Me24 shifts should also be noted, given that the relationship between C24 and C27 remains undetermined. It was noted, by Han and Lam,[62] that the chemical shifts in proximity to the carboxylic acid, especially C1-C7, are particularly sensitive to pH. As such, it may be necessary to

adjust the pH when data for the hemicalide diastereomers is collected or to exclude some of these signals from analysis.

5.2.3 Bioactivity Screening

Biological testing on the best matching hemicalide diastereomer and its enantiomer will be the final determinant of the absolute configuration, as it is highly likely that only one enantiomer of hemicalide is potently bioactive. Thus, the enantiomer matching the bioactivity and the absolute configuration of hemicalide is expected to be evident through display of differing biological activities. Screening against the original panel of cancer cells lines may be particularly illustrative.

Preliminary biological studies on the advanced C1-C15, C16-C28, C29-C35, C34-C46, C1-C28 and C29-C46 intermediates may also allow evaluation of fragment bioactivity, which may indicate the diastereomer candidates that are more likely to represent the correct relative configuration. It could also permit identification of a truncated pharmacophore that retains bioactivity. This would be highly valuable, especially given the major synthetic effort needed to produce a full natural product of this size and complexity.

This work describes the synthesis and configurational assignment of the C29-C46 region of hemicalide. It marks significant progress in the journey towards the total synthesis of this potent natural product, while illustrating the utility of synthesis and detailed spectroscopic examination in determining the relative configuration of complex molecules. This contribution to the ongoing narrative of the hemicalide project provides further evidence of the power of total synthesis in elucidating the full stereochemical assignment of structurally intriguing natural products even from minimal initial spectroscopic data.

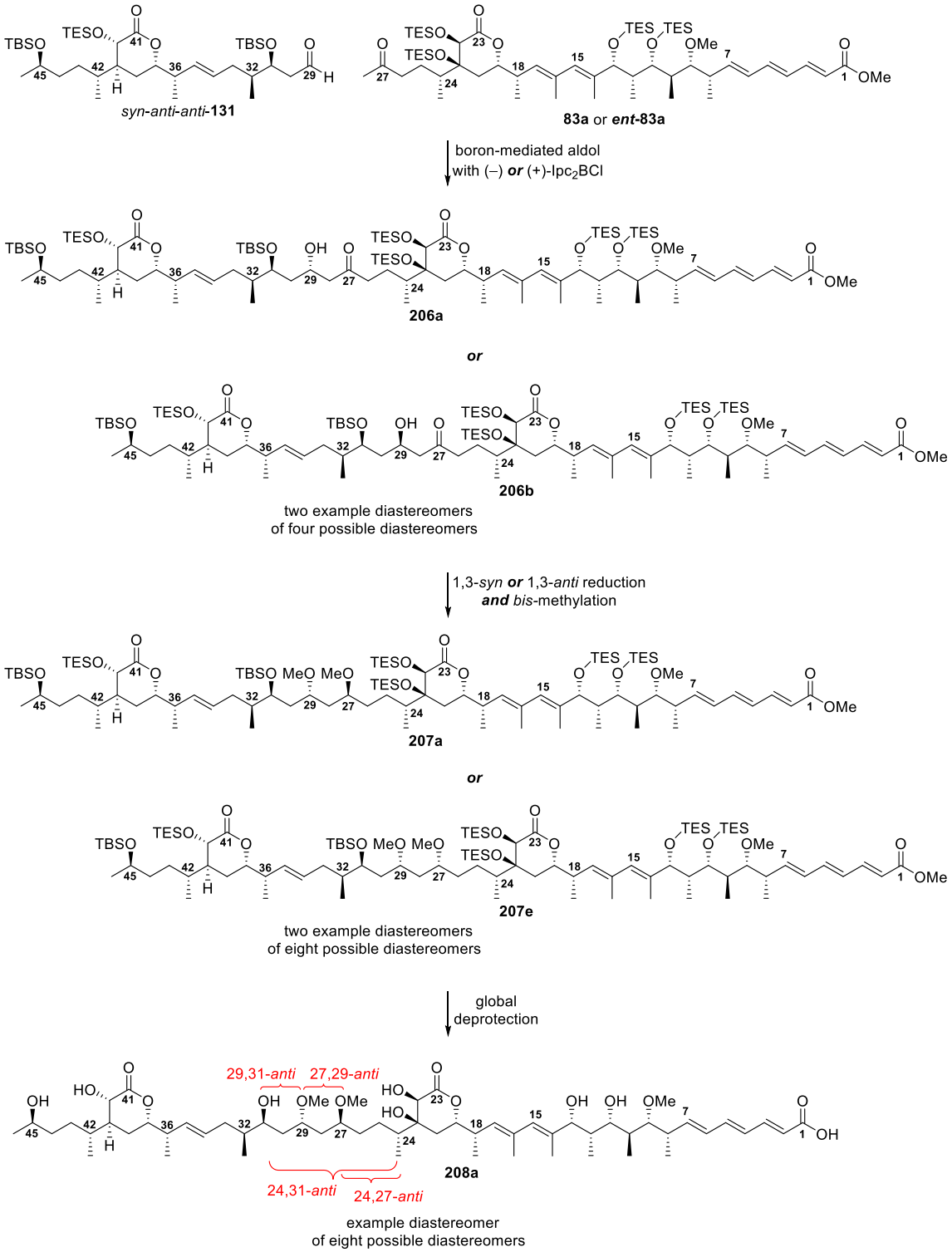

Scheme 45. Future work towards completing the total synthesis and stereochemical assignment of hemicalide.

Appendix 1: Experimental Procedures and Data

I. General Procedures

Unless the reaction contained aqueous reagents or otherwise stated, all reactions were carried out under an atmosphere of argon, using oven dried glassware and standard techniques for handling air sensitive chemicals. Reagents were purified using standard laboratory procedures; benzene and CH_2Cl_2 were distilled from CaH_2 and stored under argon. THF and Et_2O were distilled from potassium or sodium wire/benzophenone ketyl radical and stored under argon. DMSO, 2,6-lutidine, *i*Pr_2NH, DIPEA, trimethylamine, ETSA and were distilled from CaH_2 and stored over CaH_2 under argon. DMF was distilled from $MgSO_4$ and stored over 4 Å molecular sieves. EtOAc was distilled from $MgSO_4$, DDQ was recrystallised from $CHCl_3$. Oxalyl chloride was distilled. Solvents used for extraction and chromatography were distilled. All other chemicals were used as received from the supplier unless otherwise stated.

Aqueous solutions of ammonium chloride (NH_4Cl), sodium bicarbonate ($NaHCO_3$), sodium thiosulfate ($Na_2S_2O_3$) and brine (NaCl) were saturated. Buffer solutions were prepared as directed from stock tablets. Purification by flash column chromatography was carried out using Kieselgel 60 (230 – 400 mesh) and a positive solvent pressure. Chromatographic purification over alumina was carried out using Merck Millipore Aluminium oxide 90 and a positive solvent pressure.

II. Analytical Procedures

TLC was carried out using Merck Kieselgel 60 F_{254} or Aluminium oxide 60 F_{254} plates, which were visualised under UV light (254 nm) and stained with potassium permanganate or phosphomolybdic acid/$Ce_2(SO_4)_3$ dips.

NMR spectra were recorded using the following machines: Bruker (700 MHz), Bruker (600 MHz), Bruker Avance 500 BB (500 MHz), Avance TCI cryoprobe (500 MHz) and Avance 400 DRX (400 MHz). ^{1}H NMR spectra were recorded at 298 K with an internal deuterium lock for the residual undeuterated solvent: $CDCl_3$ (δ_H = 7.26 ppm), CD_3OD (δ_H = 3.31 ppm) and DMSO-d_6 (δ_H = 2.50 ppm). ^{1}H NMR data are presented as: chemical shift (δ/ppm), relative to tetramethylsilane (δ_{TMS} = 0 ppm), integration, multiplicity and coupling constants (*J* in Hz). Signals are assigned according to the

numbering scheme for hemicalide (**Figure 1**) unless otherwise indicated. Assignments have been made based on 1D data presented along with 2D spectra and comparison with fully assigned spectra for similar compounds. ^{13}C NMR spectra were recorded at 298 K with broadband proton decoupling and an internal carbon lock for ^{13}C: $CDCl_3$ (δ_C = 77.0 ppm), CD_3OD (δ_C = 49.0 ppm) or DMSO-d_6 (δ_C = 39.5 ppm). Data are listed by chemical shift (δ/ppm) relative to tetramethylsilane (δ_{TMS} = 0 ppm). All multiplets are assigned by their midpoint in COSY and HSQC spectra.

Fourier transform IR spectroscopy (FT-IR) was carried out using a Perkin-Elmer Spectrum-One spectrometer and spectra were recorded as a thin film. Wavelengths of maximum absorption (ν_{max}) are reported in integral wavenumbers (cm^{-1}).

Optical rotations were measured using an Anton Paar MCP 100 at the sodium D-line (589 nm) and are reported as $[\alpha]_D^{20}$, concentration (c in g/100 mL) in $CHCl_3$.

High resolution mass spectrometry (HRMS) was carried out by the EPSRC National Mass Spectrometry Facility (Swansea, UK) or departmental facilities using electrospray ionisation (ESI). The parent ion $[M+H]^+$ or $[M+Na]^+$ is quoted.

III. Preparation of Reagents

Benzyl 2,2,2-trichloroacetimidate

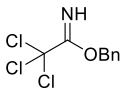

Benzyl alcohol (14.5 mL, 139 mmol), tetra-*n*-butylammonium hydrogen sulphate (407 mg, 1.20 mmol) and potassium hydroxide (70 g, 1.25 mol) were added to CH_2Cl_2:H_2O (1:1, 280 mL) stirring at –10 °C. Trichloroacetonitrile (29.1 mL, 140 mmol) was added dropwise to the reaction flask (15 min). The reaction was allowed to warm to rt (stirred, 2 h). The layers were separated and the aqueous layer extracted with Et_2O (5 x 20 mL). The combined organic extracts were dried (Na_2SO_4), filtered and concentrated *in vacuo*. Flash column chromatography (alumina 25% EtOAc/PE 40-60) afforded the benzyl trichloroacetimidate (32.0 g, 127 mmol, 91%), as a pale yellow oil, consistent with literature data[190]: $\mathbf{R_f}$ (25% EtOAc/P.E. 40-60) = 0.69; **^{1}H NMR** (500 MHz, $CDCl_3$) δ 8.40 (s, 1H, N<u>H</u>), 7.46-7.32 (m, 5H, Ar<u>H</u>), 5.35 (s, 2H, C<u>H$_2$</u>).

1,2-Bis(diphenylphosphino)benzene-CuH (BDP-Stryker's Reagent) Solution[143]

Copper (II) acetate monohydrate (20.0 mg, 0.1 mmol), 1,2-bis(diphenylphosphino)benzene (BDP) (4.46 mg, 0.01 mmol) and triphenylphosphine (27 mg, 0.1 mmol) were dissolved in freshly distilled toluene (8.00 mL), under an argon atmosphere. Polymethyldisiloxane (PMHS) (2.00 mL, 30 mmol) was added dropwise and the bright blue mixture stirred (16-48 h) to produce a deep red solution of BDP-CuH (0.01 M in copper, 3 M in hydride).

(+)-β-Chlorodiisopinocampheylborane ((+)-Ipc_2BCl)[191]

Monochloroborane dimethyl sulfide complex (4.16 mmol, 430 µL) was added dropwise to a stirred solution of freshly distilled (–)-α-pinene (1.33 mL, 8.38 mmol) in Et_2O (2.4 mL) at –10 °C. The reaction was slowly warmed to 10°C and stirred (16 h) to afford a colourless, ethereal solution of (+)-Ipc_2BCl (*ca*. 1.0 M).

LiAlH(*N*-ethylaniline)$_2$(EtO)((–)-*N*-methylephedrine)(Terashima Reagent) Suspension[155,156]

(–)-*N*-methylephedrine (458 mg, 2.55 mmol) in Et_2O (5 mL) was added to a stirred suspension of $LiAlH_4$ (94.0 mg, 2.48 mmol) in Et_2O (2.5 mL) at rt under $Ar_{(g)}$. The mixture was brought to reflux and, after 1 h, a solution of *N*-ethylaniline (640 µL, 5.10 mmol) was added. After an additional 1 h, at reflux, the reaction mixture was allowed to cool to rt, to give a suspension of the reducing agent LiAlH(*N*-ethylaniline)$_2$(EtO)((–)-*N*-methylephedrine) (10mL, ca. 0.248 M $LiAlH_4$). This can be stored at –20 °C, under $Ar_{(g)}$, parafilmed and wrapped in aluminium foil, for up to 1 week.

[PPh_3CuH]$_6$ (Stryker's Reagent) Solution[110]

Copper (II) acetate monohydrate (25.0 mg, 0.125 mmol) and triphenylphosphine (65.0 mg, 0.25 mmol) were dissolved in freshly distilled toluene (4.66 mL), under $Ar_{(g)}$. Tetramethyldisiloxane (TMDS) (0.330 mL, 1.87 mmol) was added and the bright blue mixture stirred (16-48 h) to produce a deep red solution (0.025 M in copper, 0.46 M in hydride).

Raney-Nickel (Ra-Ni) Catalyst [158]

Nickel aluminium alloy (1.00 g) was added portion-wise to a stirring solution of NaOH (1.27g) in H_2O (25 mL) at 0 °C, keeping the temperature below 20 °C, during additions and stirring. Stirring should be rapid, but not such much as to incorporate air into the reaction. The suspension was then allowed to warm slowly to rt, while stirring, cooling if the reaction became too vigorous. Once $H_{2(g)}$ evolution had slowed, the temperature was raised to 80 °C and the reaction stirred for 5h. Once the reaction had been allowed to cool to rt, the liquid was decanted, the solid rinsed with H_2O (10 mL) and the liquid decanted. The solid was then rinsed with NaOH (10 mL, 10%) and the liquid decanted. The solid was lastly rinsed repeatedly with H_2O (10 mL) until reaching neutral pH (ca. 20 times). The solid was then transferred to an airtight amber bottle and stored under EtOH (abs) in an $Ar_{(g)}$ atmosphere. The sample should be used within 24 hours and can be tested by placing a small amount on filter paper to see if it sparks.

IV. Experimental Protocols

Benzyl ether 139

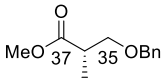

Trifluoromethanesulfonic acid (370 µL, 4.13 mmol) was added dropwise to stirred benzyl trichloroacetimidate (25 g, 110 mmol) and (*S*)-(+)-methyl L-β-hydroxyisobutyrate ((*S*)-**24**) (10.8 g, 91.7 mmol) in cyclohexane:CH_2Cl_2 (2:1, 414 mL) and stirred (–15 °C, 2h). The solution was allowed to warm to rt and stirred (16 h). The reaction mixture was filtered through Celite®, rinsing with PE 40-60 (10 mL), quenched with $NaHCO_3$ (25 mL), washed with brine (50 mL), dried (Na_2SO_4), filtered and concentrated *in vacuo*. The residue was titurated with additional PE, refiltered through Celite®, rinsing with PE (10 mL) and concentrated *in vacuo*. Purification by flash column chromatography (SiO_2, 10% EtOAc/PE 40-60) afforded benzyl ether **139** (15.7 g, 75.5 mmol, 82%) as a colourless oil, consistent with literature data[192]: $\mathbf{R_f}$ (10% EtOAc/PE 40-60) = 0.31; **^{1}H NMR** (500 MHz, $CDCl_3$) δ 7.36-7.27 (m, 5H, Ar<u>H</u>), 4.52 (ABq, 2H, J_{AB} = 12.2 Hz, PhC<u>H_2</u>), 3.70 (s, 3H, -OC<u>H_3</u>), 3.66 (dd, 1H, *J* = 9.2, 7.3 Hz, H35a), 3.50 (dd, 1H, *J* = 9.2, 5.9 Hz, H35b), 2.78 (m, 1H, H36), 1.18 (d, 3H, *J* = 7.1 Hz, Me36).

Alcohol 140

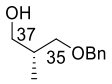

$LiAlH_4$ (8.77 g, 23.1 mmol) was added portionwise to a solution of benzyl ether **139** (3.21 g, 15.4 mmol) in THF (155 mL) at 0 °C. After 3 h, the reaction was carefully quenched with H_2O (50 mL) followed by NaOH (7.5 mL, 1M). The layers were separated and the aqueous layer extracted with Et_2O (4 x 10 mL). The combined organic phases were washed with brine (30 mL), dried (Na_2SO_4), filtered and concentrated *in vacuo*. Purification by flash column chromatography (SiO_2, 2-5% MeOH/CH_2Cl_2) afforded alcohol **140** (2.67 g, 14.8 mmol, 96%) as a colourless oil, consistent with literature data[192]: $\mathbf{R_f}$ (20% EtOAc/PE 40-60) = 0.31, (2% MeOH in CH_2Cl_2) = 0.42; **^{1}H NMR** (500 MHz, $CDCl_3$) δ 7.38-7.27 (m, 5H, ArH), 4.52 (s, 2H, PhC$\underline{H}_2$), 3.64-3.60 (m, 2H, H37), 3.56 (dd, 1H, *J* = 9.0, 4.6 Hz, H35a), 3.43 (dd, 1H, *J* = 9.0, 8.1 Hz, H35b), 2.50 (br s, 1H, OH), 2.08 (m, 1H, H36), 0.89 (d, 3H, *J* = 7.0 Hz, Me36).

Aldehyde 136

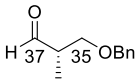

Note: This α-chiral aldehyde is prone to epimerisation at C36 and must be immediately used, without purification, in the (+)-Ipc_2BCl or *c*Hex_2BCl aldol reaction.

DMSO (200 µL, 2.77 mmol) was added dropwise to a stirred solution of oxalyl chloride (180 µL, 2.08 mmol) in CH_2Cl_2 (3.0 mL) and stirred (–78 °C, 15 min). A solution of alcohol **140** (250 mg, 1.39 mmol) in CH_2Cl_2 (2 x 2.5 mL) was added, dropwise *via* cannula, and the mixture stirred (–78 °C, 15 min). Distilled Et_3N (580 µL, 4.16 mmol) was added dropwise and the suspension was allowed to warm slowly to –20 °C and stirred (30 min). The reaction was quenched with NH_4Cl (2.0 mL), the organic layer separated and the aqueous layer extracted with Et_2O (3 x 20 mL). The combined organic extracts were dried over ($MgSO_4$), filtered and concentrated *in vacuo* to give crude aldehyde **136** as a slightly yellow oil, consistent with literature data[193]: $\mathbf{R_f}$ (20% EtOAc/PE 40-60) = 0.41; **^{1}H NMR** (500 MHz, $CDCl_3$) δ 9.73 (d, 1H, *J* = 1.6 Hz, H37), 7.37-7.28 (m, 5H, ArH), 4.53 (s, 2H, PhC$\underline{H}_2$), 3.64-3.60 (m, 2H, H37), 3.69 (dd, 1H, *J* = 9.4, 6.8 Hz, H35a), 3.64 (dd, 1H, *J* = 9.4, 5.3 Hz, H35b), 2.67 (m, 1H, H36), 1.14 (d, 3H, *J* = 7.2 Hz, Me36).

Methyl ketone 73

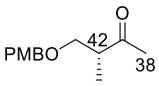

Methylmagnesium bromide (25.0 mL, 75.0 mmol, 3 M in Et_2O) was added dropwise, over 5 min, to a solution of the Weinreb amide **137** (10.0 g, 37.5 mmol) in Et_2O (100 mL) and stirred (0 °C, 20 min). The reaction was carefully quenched with NH_4Cl (8 mL), the layers separated and the aqueous layer extracted with Et_2O (3 x 20 mL). The combined extracts were washed with brine (3 x 20 mL), dried ($MgSO_4$), filtered and concentrated *in vacuo*. Purification by flash column chromatography (SiO_2, 10-30% EtOAc/PE 40-60) afforded methyl ketone **73** (5.92 g, 26.6 mmol, 71%) as a pale yellow oil, consistent with literature data[113]: $\mathbf{R_f}$ (20% EtOAc/PE 40-60) = 0.24; **^{1}H NMR** (500 MHz, $CDCl_3$) δ 7.22 (d, 2H, *J* = 8.7 Hz, ArH), 6.87 (d, 2H, *J* = 8.7 Hz, ArH), 4.42 (ABq, 2H, J_{AB} = 11.8 Hz, ArCH_2), 3.80 (s, 3H, ArOCH_3), 3.59 (dd, 1H, *J* = 9.2, 7.6 Hz, H43a), 3.45 (dd, 1H, *J* = 9.2, 5.5 Hz, H43b), 2.83 (m, 1H, H42), 2.17 (s, 3H, H38), 1.08 (d, 3H, *J* = 7.1 Hz, Me42).

β-Hydroxy ketone 135

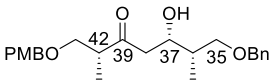

Method 1: (+)-Ipc$_2$BCl mediated aldol reaction

Distilled Et_3N (7.96 mL, 57.1 mmol) was added to a stirred solution of (+)-Ipc$_2$BCl (32.0 mL, 32.0 mmol, ~1M in Et_2O) in Et_2O (100 mL) at 0 °C, to give a clear solution. Subsequent addition of methyl ketone **73** (6.35 g, 28.5 mmol) in Et_2O (4 x 2.75 mL), *via* cannula, resulted in a white suspension (stirred, 1 h, 0 °C). The reaction mixture was cooled to –78 °C and a solution of the crude aldehyde **136** (*ca*. 34.3 mmol) in Et_2O (2 x 2.5 mL) was added, *via* cannula, to the reaction mixture, resulting in a pale yellow solution (stirred, –78 °C, 2 h). The reaction was allowed to warm to –20 °C and stirred (~16 h) before being quenched (–20 °C) by sequential addition of MeOH (23 mL), pH buffer solution (23 mL) and H_2O_2 (16 mL, 30% w/w) and allowed to warm to rt (stirred, 30 min). The layers were separated and the aqueous layer extracted with Et_2O (4 x 20 mL). The combined organic extracts were washed with $Na_2S_2O_3$ (3 x 10 mL) and brine (20 mL), dried ($MgSO_4$), filtered and concentrated *in vacuo*. Purification by flash column chromatography (SiO_2, 10-20% EtOAc/PE 40-

60) afforded β-hydroxy ketone **135** (10.42 g, 26.0 mmol, 91%, >20:1 *dr*) as a pale yellow oil: $\mathbf{R_f}$ (20% EtOAc/PE 40-60) = 0.11; **^{1}H NMR** (500 MHz, $CDCl_3$) δ 7.38-7.27 (m, 5H, PhH), 7.20 (d, 2H, *J* = 8.7 Hz, ArH), 6.86 (d, 2H, *J* = 8.7 Hz, ArH), 4.49 (s, 2H, $PhCH_2$), 4.40 (ABq, 2H, J_{AB} = 11.7 Hz, $ArCH_2$), 4.24 (dq, 1H, *J* = 9.1, 2.4 Hz, H37), 3.79 (s, 3H, $ArOCH_3$), 3.57 (dd, 1H, *J* = 9.0, 8.1 Hz, H43a), 3.45 (m, 1H, H35a), 3.44 (m, 1H, H43b), 3.49 (dd, 1H, *J* = 9.1, 6.5 Hz, H35b), 3.14 (d, 1H, *J* = 3.5 Hz, OH), 2.87 (m, 1H, H42), 2.67 (dd, 1H, *J* = 17.2, 9.1 Hz, H38a), 2.59 (dd, 1H, *J* = 17.2, 3.3 Hz, H38b), 1.84 (m, 1H, H36), 1.05 (d, 3H, *J* = 7.0 Hz, Me42), 0.93 (d, 3H, *J* = 7.0 Hz, Me36); **^{13}C NMR** (100 MHz, $CDCl_3$) δ 214.0 (C=O), 159.3, 138.3, 130.0, 129.3, 128.4, 127.6 (3C), 113.8, 73.6, 73.3, 73.0, 71.9, 68.8, 55.3, 46.8, 46.6, 38.0, 13.2, 11.4; **FTIR ν_{max}** 3494 (w, OH str), 2857 (w, sp^3 CH str), 1707 (s, sh, C=O str), 1613, 1587, 1513, 1455, 1363, 1303, 1246 (s, sh, C-O str), 1174, 1092, 1031, 820, 735, 699, 668; $[\boldsymbol{\alpha}]_{\mathbf{D}}^{\mathbf{20}}$ –26.9 (*c* 1.0, $CHCl_3$); **HRMS** (ESI^+): calculated for $C_{24}H_{32}O_5Na$ $[M+Na]^+$ 423.2147, found 423.2144.

Method 2: $cHex_2BCl$ mediated aldol reaction

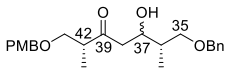

Distilled Et_3N (160 µL, 1.10 mmol) was added to a stirred solution of $cHex_2BCl$ (140 µL, 527 µmol) in Et_2O (2.5 mL) at 0 °C, to give a clear solution. Subsequent addition of methyl ketone **73** (146 mg, 656 µmol) in Et_2O (2.5 mL), *via* cannula, resulted in a white suspension (stirred, 1 h, 0 °C). The reaction mixture was cooled to –78 °C and a solution of the crude aldehyde **136** (*ca*. 490 µmol) in Et_2O (2.5 mL) was added, *via* cannula, to the reaction mixture, resulting in a pale yellow solution (stirred, –78 °C, 2 h). The reaction was allowed to warm to –20 °C and stirred (~16 h) before being quenched (–20 °C) by sequential addition of MeOH (3.0 mL), pH buffer solution (3.0 mL) and H_2O_2 (2.5 mL, 30% w/w) and allowed to warm to rt (stirred, 30 min). The layers were separated and the aqueous layer extracted with Et_2O (3 x 10 mL). The combined organic extracts were washed with $Na_2S_2O_3$ (3 x 10 mL) and brine (3 x 10 mL), dried ($MgSO_4$), filtered and concentrated *in vacuo*. Purification by flash column chromatography (SiO_2, 10-20% EtOAc/PE 40-60) afforded β-hydroxy ketone **135** (146mg, 66%, 2:1 *dr*) as a pale yellow oil, with spectra consistent with previous samples, but showing the presence of the undesired C37 diastereomer.

(*R*)-Mosher ester 141

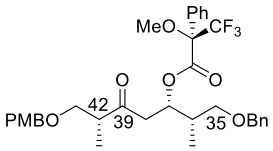

DCC (10 µL, 8 µmol, 1 M in CH_2Cl_2) was added dropwise to a stirred solution of aldol adduct **135** (6 mg, 1.49 µmol), (*R*)-MTPA (1.8 mg, 7.49 µmol) and DMAP (0.9 mg, 7.49 µmol) in CH_2Cl_2 (250 µL). The reaction was stirred and monitored by TLC, until the starting material was consumed or any elimination product was indicated (*ca.* 2.5 h, rt). The reaction mixture was filtered through cotton wool and the filtrate concentrated *in vacuo*. Purification by flash column chromatography (SiO_2, 5-20% EtOAc/PE 40-60) afforded (*R*)-Mosher ester **141** (4.3 mg, 6.97 µmol, 47%) as a colourless oil. $\mathbf{R_f}$ (20% EtOAc/PE 40-60) = 0.22; **^{1}H NMR** (500 MHz, $CDCl_3$) δ 7.49 (d, 2H, *J* = 7.0 Hz, PhH), 7.38-7.27 (m, 8H, PhH), 7.19 (d, 2H, *J* = 8.7 Hz, ArH), 6.84 (d, 2H, *J* = 8.6 Hz, ArH), 5.71 (ddd, 1H, *J* = 8.0, 6.5, 3.5 Hz, H37), 4.38 (ABq, 2H, J_{AB} = 11.9 Hz, PhCH_2), 4.37 (ABq, 2H, J_{AB} = 11.5 Hz, ArCH_2), 3.78 (s, 3H, ArOCH_3), 3.47 (s, 3H, -OMe), 3.52 (dd, 1H, *J* = 9.0, 8.2 Hz, H43a), 3.42 (dd, 1H, *J* = 9.0, 5.2 Hz, H43b), 3.23 (dd, 1H, *J* = 9.3, 6.6 Hz, H35a), 3.18 (dd, 1H, *J* = 9.3, 6.3 Hz, H35b), 2.91 (dd, 1H, *J* = 17.9, 8.0 Hz, H38a), 2.80 (m, 1H, H42), 2.79 (dd, 1H, *J* = 17.9, 4.8 Hz, H38b), 2.14 (m, 1H, H36), 0.98 (d, 3H, *J* = 7.1 Hz, Me42), 0.89 (d, 3H, *J* = 7.0 Hz, Me36).

(*S*)-Mosher ester 142

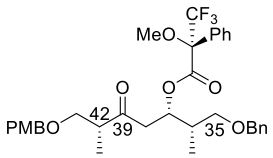

The diastereomeric (*S*)-Mosher ester **142** was prepared analogously to (*R*)-Mosher ester **141** (*vide supra*) from aldol adduct **135** (6 mg, 1.49 µmol), (*S*)-MTPA (1.8 mg, 7.49 µmol), DCC (10 µL, 8 µmol, 1 M in CH_2Cl_2), DMAP (0.9 mg, 7.49 µmol) in CH_2Cl_2 (250 µL). Purification by flash column chromatography (5-20% EtOAc/PE 40-60) afforded (*S*)-Mosher ester **142** (2.9 mg, 4.70 µmol, 32 %), as a colourless oil. $\mathbf{R_f}$ (20% EtOAc/PE 40-60) = 0.25; **^{1}H NMR** (500 MHz, $CDCl_3$) δ 7.49 (d, 2H, *J* = 7.0 Hz, PhH), 7.38-7.27 (m, 8H, PhH), 7.18 (d, 2H, *J* = 8.7 Hz, ArH), 6.85 (d, 2H, *J* = 8.7 Hz, ArH), 5.73 (ddd, 1H, *J* = 8.0, 4.9, 3.4 Hz, H37), 4.45 (ABq, 2H, J_{AB} = 12.1 Hz, PhCH_2), 4.36 (ABq, 2H, J_{AB} = 11.5 Hz, ArCH_2), 3.78 (s, 3H, ArOCH_3), 3.45 (s, 3H, -OMe), 3.50 (dd, 1H, *J* = 9.0, 8.2 Hz, H43a), 3.39

(dd, 1H, *J* = 9.0, 5.3 Hz, H43b), 3.35 (dd, 1H, *J* = 9.4, 7.0 Hz, H35a), 3.29 (dd, 1H, *J* = 9.4, 6.3 Hz, H35b), 2.90 (dd, 1H, *J* = 17.8, 7.7 Hz, H38a), 2.76 (m, 1H, H42), 2.72 (dd, 1H, *J* = 17.9, 5.1 Hz, H38b), 2.17 (m, 1H, H36), 0.93 (d, 3H, *J* = 7.0 Hz, Me42), 0.90 (d, 3H, *J* = 6.9 Hz, Me36).

TBS ether 145

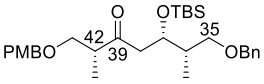

2,6-Lutidine (4.54 mL, 39.0 mmol) was added to a stirred solution of β-hydroxy ketone **135** (10.4 g, 26.0 mmol) in CH_2Cl_2 (240 mL). The reaction mixture was cooled to –78 °C and stirred for 5 min before TBSOTf (4.90 mL, 32.5 mmol) was slowly added dropwise. After 2 h, the reaction was checked by TLC and a further aliquot of TBSOTf (1.00 mL, 6.62 mmol) was slowly added dropwise. After 30 mins, the reaction mixture was quenched with sequentially with MeOH (17.7 mL) and $NaHCO_3$ (20 mL), allowed to warm to rt, the layers separated and the aqueous layer extracted with CH_2Cl_2 (4 x 20 mL). The combined organic extracts were washed with brine (50 mL), dried (Na_2SO_4), filtered and concentrated *in vacuo*. Purification by flash column chromatography (SiO_2, 10% EtOAc/PE 40-60) afforded the TBS ether **145** (13.4 g, 26.0 mmol, quant.) as a pale yellow oil: $\mathbf{R_f}$ (20% EtOAc/PE 40-60) = 0.50; **^{1}H NMR** (500 MHz, $CDCl_3$) δ 7.34-7.27 (m, 5H, PhH), 7.20 (d, 2H, *J* = 8.7 Hz, ArH), 6.85 (d, 2H, *J* = 8.7 Hz, ArH), 4.48 (ABq, 2H, J_{AB} = 12.0 Hz, PhCH_2), 4.39 (ABq, 2H, J_{AB} = 11.7 Hz, ArCH_2), 4.38 (dq, 1H, *J* = 9.0, 3.0 Hz, H37), 3.79 (s, 3H, ArOCH_3), 3.57 (dd, 1H, *J* = 9.1, 7.5 Hz, H43a), 3.49 (dd, 1H, *J* = 9.0, 6.3 Hz, H35a), 3.42 (dd, 1H, *J* = 9.1, 5.5 Hz, H43b), 3.27 (dd, 1H, *J* = 9.0, 7.1 Hz, H35b), 2.79 (dq, 1H, *J* = 12.6, 7.1 Hz, H42), 2.66 (dd, 1H, *J* = 17.2, 6.9 Hz, H38a), 2.58 (dd, 1H, *J* = 17.2, 6.9 Hz, H38b), 1.88 (d sex, 1H, *J* = 7.0, 2.9 Hz, H36), 1.04 (d, 3H, *J* = 7.0 Hz, Me42), 0.87 (d, 3H, *J* = 6.9 Hz, Me36) , 0.83 (s, 9H, Si$(CH_3)_2$C(CH_3)$_3$), 0.05 (s, 3H, Si(CH_3)$_2$C$(CH_3)_3$), -0.03 (s, 3H, Si(CH_3)$_2$C$(CH_3)_3$); **^{13}C NMR** (125 MHz, $CDCl_3$) δ 211.2 (C39=O), 159.2 (ArC), 138.7 (ArC), 130.1 (ArC), 129.2 (ArCH), 128.3 (ArCH), 127.5 (ArCH), 127.4 (ArCH), 113.7 (ArCH), 72.92 (PhCH_2), 72.85 (ArCH_2), 72.3 (C35), 71.8 (C43), 68.2 (C37), 55.2 (ArOCH_3), 47.4 (C38), 47.1 (C42), 38.9 (C36), 25.9 (Si$(CH_3)_2$C(CH_3)$_3$), 18.1 (Si$(CH_3)_2$C$(CH_3)_3$), 13.1 (Me42), 11.6 (Me36), -4.4 (Si(CH_3)$_2$C$(CH_3)_3$), -5.0 (Si(CH_3)$_2$C$(CH_3)_3$); **FTIR ν_{max}** 2929 (w, sp^3 CH str), 2855 (w, sp^3 CH str), 1715 (s, sh, C=O str), 1613, 1588, 1514, 1456, 1361, 1303, 1248 (s, sh, C-O str), 1173, 1089, 1037, 832, 776, 736, 698, 668; $[\alpha]_D^{20}$ –25.8 (*c* 1.0, $CHCl_3$); **HRMS** (ESI$^+$): calculated for $C_{30}H_{46}O_5SiNa$ $[M+Na]^+$ 537.3012, found 537.3011.

Ester 146

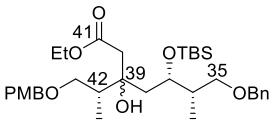

*n*BuLi (8.96 mL, 14.3 mmol, 1.6 M in hexanes) was added dropwise to a stirred solution of distilled *i*Pr_2NH (1.50 mL, 14.8 mmol) in THF (5.00 mL) and stirred (0 °C, 30 min). The mixture was cooled to –78 °C and distilled EtOAc (1.45 mL, 14.8 mmol) was added dropwise. Stirring was continued at –78 °C (1 h) to give a c.a. 1.0 M solution. The lithium enolate solution (8.40 mL, 8.40 mmol, *ca*. 1.0 M in THF) was added dropwise to a stirred solution of TBS ether **145** (865 mg, 1.68 mmol) in THF (2.00 mL) and stirred (–78 °C, 3 h). The reaction was quenched with $NaHCO_3$ (4.4 mL), allowed to warm to rt and diluted with Et_2O (5 mL). The layers were separated and the aqueous layer extracted with Et_2O (4 x 10 mL). The combined organic phases were washed with brine (3 x 10 mL), dried ($MgSO_4$), filtered and concentrated *in vacuo* to afford ester **146** (1.01 g, 1.68 mmol, 99%, inconsequential 5:1 mix of diastereomers), as a colourless oil. Major diastereomer: $\mathbf{R_f}$ (20% EtOAc/PE 40-60) = 0.40; **^{1}H NMR** (500 MHz, $CDCl_3$) δ 7.34-7.27 (m, 5H, PhH), 7.24 (d, 2H, *J* = 8.6 Hz, ArH), 6.86 (d, 2H, *J* = 8.6 Hz, ArH), 4.48 (ABq, 2H, J_{AB} = 12.0 Hz, $PhCH_2$), 4.40 (ABq, 2H, J_{AB} = 11.6 Hz, $ArCH_2$), 4.17 (m, 1H, H37), 4.09 (dq, 2H, *J* = 7.2, 5.6 Hz, $-OCH_2CH_3$), 3.80 (s, 3H, $ArOCH_3$), 3.66 (dd, 1H, *J* = 9.3, 4.9 Hz, H43a), 3.58 (dd, 1H, *J* = 8.8, 5.1 Hz, H35a), 3.35 (dd, 1H, *J* = 9.3, 6.7 Hz, H43b), 3.26 (dd, 1H, *J* = 8.7, 8.0 Hz, H35b), 2.66 (d, 1H, *J* = 15.3 Hz, H40a), 2.54 (d, 1H, *J* = 15.3 Hz, H40b), 2.07 (m, 1H, H42), 2.03 (m, 1H, H36), 1.81 (dd, 1H, *J* = 14.8, 4.7 Hz, H38a), 1.59 (dd, 1H, *J* = 14.7, 7.4 Hz, H38b), 1.22 (t, 3H, *J* = 7.2 Hz, $-OCH_2CH_3$), 0.99 (d, 3H, *J* = 7.0 Hz, Me42), 0.93 (d, 3H, *J* = 7.0 Hz, Me36) , 0.87 (s, 9H, $Si(CH_3)_2C(CH_3)_3$) , 0.10 (s, 3H, $Si(CH_3)_2C(CH_3)_3$) , 0.08 (s, 3H, $Si(CH_3)_2C(CH_3)_3$); **^{13}C NMR** (125 MHz, $CDCl_3$) δ 172.1 (C41=O), 159.1 (ArC), 138.7 (ArC), 130.6 (ArC), 129.2 (ArCH), 128.3 (ArCH), 127.6 (ArCH), 127.4 (ArCH), 113.7 (ArCH), 74.5 (C39), 73.2 ($PhCH_2$), 72.7 ($ArCH_2$), 72.0 (2C, C43, C35), 71.2 (C37), 60.4 ($-OCH_2CH_3$), 55.3 ($ArOCH_3$), 41.6 (C40), 40.8 (C42), 40.0 (C36), 37.9 (C38), 26.0 ($Si(CH_3)_2C(CH_3)_3$), 18.1 ($Si(CH_3)_2C(CH_3)_3$), 14.2 ($-OCH_2CH_3$), 12.74/12.71 (Me42/Me36), -4.2 ($Si(CH_3)_2C(CH_3)_3$), -4.3 ($Si(CH_3)_2C(CH_3)_3$); **FTIR ν_{max}** 3478 (w, OH str), 2929 (w, sp^3 CH str), 2857 (w, sp^3 CH str), 1732 (s, sh, C=O str), 1614, 1589, 1515, 1464, 1370, 1303, 1249 (s, sh, C-O str), 1188, 1097, 1038, 836, 776, 736, 699, 669; $[\alpha]_D^{20}$ –4.6 (*c* 1.0, $CHCl_3$); **HRMS** (ESI$^+$): calculated for $C_{34}H_{54}O_7SiNa$ $[M+Na]^+$ 625.3537, found 625.3531.

β-Hydroxy lactone 147

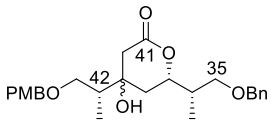

Tosylic acid monohydrate (22 mg, 116 µmol) was added to a stirred solution of aldol adduct **146** (175 mg, 290 µmol) in MeOH (3.3 mL) and stirred (rt, 1 h). The reaction was quenched with $NaHCO_3$ (1 mL) and diluted with EtOAc (5 mL). The layers were separated and the aqueous layer extracted with EtOAc (4 x 10 mL). The combined organic phases were washed with brine (3 x 10 mL), dried ($MgSO_4$), filtered and concentrated *in vacuo*. Purification by flash column chromatography (SiO_2, 15%-40% EtOAc/PE 40-60) afforded β-hydroxy lactone **147** (120.2 mg, 272 µmol, 94%, inconsequential 5:1 mix of diastereomers) as a pale yellow oil: Minor diastereomer - $\mathbf{R_f}$ (40% EtOAc/PE 40-60) = 0.22; **^{1}H NMR** (500 MHz, $CDCl_3$) δ 7.35-7.27 (m, 5H, ArH), 7.21 (d, 2H, *J* = 8.6 Hz, ArH), 6.88 (d, 2H, *J* = 8.7 Hz, ArH), 4.88 (ddd, 1H, *J* = 8.4, 6.3, 3.7 Hz, H37), 4.50 (ABq, 2H, J_{AB} = 12.0 Hz, PhCH_2), 4.43 (ABq, 2H, J_{AB} = 11.6 Hz, ArCH_2), 4.14 (s, 1H, OH), 3.80 (s, 3H, ArOCH_3), 3.64 (dd, 1H, *J* = 9.7, 3.9 Hz, H43a), 3.55 (dd, 1H, *J* = 9.3, 7.1 Hz, H35a), 3.44 (dd, 1H, *J* = 9.3, 6.0 Hz, H35b), 3.42 (dd, 1H, *J* = 9.5, 7.7 Hz, H43b), 2.57 (d, 1H, *J* = 17.4 Hz, H40a), 2.38 (d, 1H, *J* = 17.5 Hz, H40b), 1.68 (d, 2H, *J* = 8.1 Hz, H38), 1.97 (m, 1H, H36), 1.90 (m, 1H, H42), 0.99 (d, 3H, *J* = 6.9 Hz, Me36), 0.93 (d, 3H, *J* = 7.2 Hz, Me42); **^{13}C NMR** (125 MHz, $CDCl_3$) δ 171.3 (C41=O), 159.6 (ArC), 138.4 (ArC), 129.5 (ArCH), 128.9 (ArC), 128.4 (ArCH), 127.63 (ArCH), 127.56 (ArCH), 114.0 (ArCH), 76.6 (C37), 73.4 (ArCH_2), 73.2 (PhCH_2), 72.3 (C39), 72.2 (C43), 72.0 (C35), 55.3 (ArOCH_3), 41.5 (C42), 39.4 (C40), 37.8 (C36), 36.9 (C38**)**, 12.3 (Me42), 11.4 (Me36); **FTIR ν_{max}** 3475 (w, OH str), 2926 (w, sp^3 CH str), 1728 (s, sh, C=O str), 1613, 1514, 1456, 1363, 1303, 1249 (s, sh, C-O str), 1175, 1091, 1033, 822, 740, 700, 668; $[\alpha]_D^{20}$ –19.6 (*c* 1.0, $CHCl_3$); **HRMS** (ESI^+): calculated for $C_{26}H_{34}O_6Na$ $[M+Na]^+$ 465.2253, found 465.2257.

Major diastereomer: $\mathbf{R_f}$ (40% EtOAc/PE 40-60) = 0.19; **^{1}H NMR** (500 MHz, $CDCl_3$) δ 7.35-7.27 (m, 5H, ArH), 7.22 (d, 2H, *J* = 8.6 Hz, ArH), 6.88 (d, 2H, *J* = 8.6 Hz, ArH), 4.48 (ABq, 2H, J_{AB} = 12.0 Hz, PhCH_2), 4.43 (ABq, 2H, J_{AB} = 11.6 Hz, ArCH_2), 4.88 (dt, 1H, *J* = 11.9, 4.2 Hz, H37), 3.85 (s, 1H, OH), 3.81 (s, 3H, ArOCH_3), 3.68 (dd, 1H, *J* = 9.6, 3.6 Hz, H35a), 3.50 (dd, 1H, *J* = 9.2, 7.7 Hz, H43a), 3.42 (m, 2H, H43b & H35b), 2.60 (d, 1H, *J* = 14.9 Hz, H40), 2.55 (d, 1H, *J* = 14.9 Hz, H40), 1.94 (m, 1H, H42), 1.93 (dd, 1H, *J* = 14.5, 4.4 Hz, H38a), 1.83 (m, 1H, H36), 1.76 (dd, 1H, *J* = 14.4, 12.0 Hz, H38b), 1.02 (d, 3H, *J* = 7.0 Hz, Me42), 1.01 (d, 3H, *J* = 7.1 Hz, Me36).

α,β-Unsaturated Lactone 148

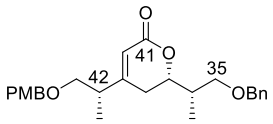

Method 1: Acetic anhydride dehydration of β-hydroxy lactone

Benzene, pyridine and acetic anhydride (5:5:1, 2.57 mL) were sequentially added to a flask containing DMAP (27.6 mg, 226 µmol) and β-hydroxy lactone **147** (100 mg, 226 µmol). The resulting solution was stirred and the mixture heated to reflux (16 h). The reaction was then allowed to cool to rt, diluted with CH_2Cl_2 (5 mL) and carefully quenched with $NaHCO_3$ (1 mL). The layers were separated and the reaction solution extracted with CH_2Cl_2 (4 x 10 mL). The combined organic extracts were washed with brine (3 x 10 mL), dried ($MgSO_4$), filtered and concentrated *in vacuo*. Purification by flash column chromatography (SiO_2, 20% EtOAc/PE 40-60) afforded α,β-unsaturated lactone **148** (86.1 mg, 272 µmol, 94%) as a pale yellow oil: $\mathbf{R_f}$ (40% EtOAc/PE 40-60) = 0.22; **^{1}H NMR** (500 MHz, $CDCl_3$) δ 7.35-7.27 (m, 5H, ArH), 7.20 (d, 2H, *J* = 8.6 Hz, ArH), 6.87 (d, 2H, *J* = 8.8 Hz, ArH), 5.81 (s, 1H, *J* = 2.3 Hz, H40), 4.49 (ABq, 2H, J_{AB} = 11.9 Hz, PhCH_2), 4.47 (m, 1H, H37), 4.40 (ABq, 2H, J_{AB} = 11.6 Hz, ArCH_2), 3.79 (s, 3H, ArOCH_3), 3.54 (dd, 1H, *J* = 9.2, 7.5 Hz, H35a), 3.43 (dd, 1H, *J* = 9.2, 5.2 Hz, H35b), 3.40 (m, 2H, H43), 2.63 (dq, 1H, *J* = 13.5, 6.7 Hz, H42), 2.38 (ddd, 1H, *J* = 17.7, 12.8, 2.3 Hz, H38a), 2.15 (dd, 1H, *J* = 17.6, 3.5 Hz, H38b), 2.00 (m, 1H, H36), 1.08 (d, 3H, *J* = 7.0 Hz, Me42), 1.02 (d, 3H, *J* = 7.0 Hz, Me36); **^{13}C NMR** (125 MHz, $CDCl_3$) δ 171.1 (C41=O), 165.7 (C39), 159.3 (ArC), 138.2 (ArC), 129.9 (ArC), 129.3 (ArCH), 127.68 (ArCH), 127.67 (ArCH), 115.5 (C40), 113.8 (ArCH), 77.8 (C37), 73.3 (PhCH_2), 72.8 (ArCH_2), 72.2 (C43), 71.6 (C35), 55.3 (ArOCH_3), 40.3 (C42), 37.5 (C36), 29.2 (C38**)**, 15.6 (Me42), 11.7 (Me36); **FTIR ν_{max}** 2924 (w, sp^3 CH str), 2854 (w, sp^3 CH str), 1714 (s, sh, C=O str), 1612, 1513, 1456, 1363, 1247 (s, sh, C-O str), 1174, 1091, 1030, 869, 819, 739, 699, 668; $[\alpha]_D^{20}$ –33.2 (*c* 1.0, $CHCl_3$); **HRMS** (ESI$^+$): calculated for $C_{26}H_{33}O_5$ $[M+H]^+$ 425.2323, found 425.2320.

Method 2: Deprotection and lactonisation of (E)-enoate

Tosylic acid monohydrate (0.7 mg, 3.5 µmol) was added to a stirred solution of enoate (*E*)-**149b** (5.0 mg, 8.5 µmol) in MeOH (100 µL) and stirred (rt, 2 h). The reaction was quenched with $NaHCO_3$ (1 mL) and diluted with EtOAc (1 mL). The layers were separated and the aqueous layer extracted with EtOAc (4 x 1 mL). The combined organic phases were washed with brine (3 x 1 mL), dried

($MgSO_4$), filtered and concentrated *in vacuo*, to afford lactone enoate **148** (3.5 mg, 8.2 µmol, 96%) as a colourless oil, with spectra matching previously prepared samples.

Enoates (*Z*)-149a and (*E*)-149b

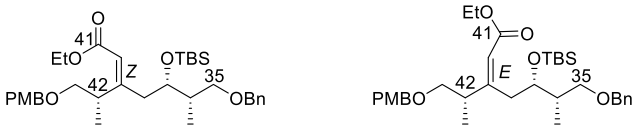

*Method 1: Burgess dehydration of aldol adduct **146***

Burgess reagent (225 mg, 945 µmol) was added to a stirred solution of aldol adduct **146** (475 mg, 788 µmol) in THF (4.73 mL) and stirred, at rt, for 16 h. The reaction was carefully quenched with $NaHCO_3$ (2.0 mL). The layers were separated and the aqueous layer extracted with CH_2Cl_2 (4 x 5 mL), washed with brine (3 x 5 mL), dried ($MgSO_4$), filtered and concentrated *in vacuo*. The crude product was purified by flash column chromatography (SiO_2, 5-20% EtOAc/PE 40-60) afforded enoate (*E*)-**149b** (69.1 mg, 118 µmol, 15%) as a colourless oil. Enoate isomer (*Z*)-**149a** was inseparable from other olefin isomers. (*E*)-**149b**: $\mathbf{R_f}$ (10% EtOAc/PE 40-60) = 0.24; **^{1}H NMR** (500 MHz, $CDCl_3$) δ 7.34-7.27 (m, 5H, PhH), 7.22 (d, 2H, *J* = 8.7Hz, ArH), 6.86 (d, 2H, *J* = 8.7 Hz, ArH), 5.68 (s, 1H, H40), 4.45 (ABq, 2H, J_{AB} = 12.0 Hz, PhCH_2), 4.41 (ABq, 2H, J_{AB} = 11.7 Hz, ArCH_2), 4.14 (m, 1H, H37), 4.13 (q, 2H, *J* = 7.1 Hz, -OCH_2CH$_3$), 3.80 (s, 3H, ArOCH$_3$), 3.48 (dd, 1H, *J* = 8.9, 7.1 Hz, H35a), 3.45 (dd, 1H, *J* = 9.2, 5.2 Hz, H43a), 3.34 (dd, 1H, *J* = 12.6, 7.6 Hz, H38a), 3.27 (dd, 1H, *J* = 9.2, 7.2 Hz, H43b), 3.26 (dd, 1H, *J* = 8.9, 6.6 Hz, H35b), 2.62 (m, 1H, H42), 2.41 (dd, 1H, *J* = 12.6, 6.6 Hz, H38b), 1.83 (m, 1H, H36), 1.27 (t, 3H, *J* = 7.1 Hz, -OCH$_2$CH$_3$), 1.11 (d, 3H, *J* = 6.8 Hz, Me42), 0.94 (d, 3H, *J* = 6.9 Hz, Me36) , 0.86 (s, 9H, Si(CH$_3$)$_2$C(CH$_3$)$_3$) , 0.01 (s, 6H, Si(CH$_3$)$_2$C(CH$_3$)$_3$); **^{13}C NMR** (125 MHz, $CDCl_3$) δ 166.4 (C41=O), 163.0 (C39), 159.1 (ArC), 138.8 (ArC), 130.4 (ArC), 129.1 (ArCH), 128.2 (ArCH), 127.4 (ArCH), 127.3 (ArCH), 116.5 (C40), 113.7 (ArCH), 74.2 (C43), 72.8 (C35), 72.64 (PhCH$_2$), 72.60 (ArCH$_2$), 71.6 (C37), 59.6 (-OCH$_2$CH$_3$), 55.2 (ArOCH$_3$), 41.2 (C42), 38.1 (C36), 37.0 (C38), 25.9 (Si(CH$_3$)$_2$C(CH$_3$)$_3$), 18.0 (Si(CH$_3$)$_2$C(CH$_3$)$_3$), 16.9 (Me42), 14.3 (-OCH$_2$CH$_3$), 11.2 (Me36), 4.3 (Si(CH$_3$)$_2$C(CH$_3$)$_3$), -4.8 (Si(CH$_3$)$_2$C(CH$_3$)$_3$); **FTIR ν_{max}** 2929 (w, sp^3 CH str), 2856 (w, sp^3 CH str), 1714 (s, sh, C=O str), 1640, 1614, 1513, 1462, 1363, 1303, 1249 (s, sh, C-O str), 1158, 1090, 1036, 939, 836, 774, 736, 698, 670; $[\alpha]_D^{20}$ –38.3 (*c* 1.0, $CHCl_3$); **HRMS** (ESI$^+$): calculated for $C_{34}H_{53}O_6Si$ $[M+H]^+$ 585.3611, found 585.3588.

*Method 2: Thionyl chloride dehydration of aldol adduct **146***

Pyridine (130 µL, 1.59 mmol) and $SOCl_2$ (70 µL, 858 µmol) were successively added to a stirred solution of aldol adduct **146** (20 mg, 33.2 µmol) in CH_2Cl_2 (1.7 mL) at 0 °C (stirred, 1 h). The reaction was carefully quenched with $NaHCO_3$ (2.0 mL). The layers were separated and the aqueous layer extracted with CH_2Cl_2 (4 x 5 mL), washed with brine (3 x 5 mL), dried ($MgSO_4$), filtered and concentrated *in vacuo*. The crude product was purified by flash column chromatography (SiO_2, 5-20% EtOAc/PE 40-60) afforded enoate (*E*)-**149b** (6.8 mg, 11.6 µmol, 35%) as a colourless oil, with spectra matching previously prepared samples. Enoate isomer (*Z*)-**149a** was inseparable from other olefin isomers.

*Method 3: Peterson Olefination of TBS ether **145***

*n*BuLi (56.3 mL, 89.9 mmol, 1.6 M in hexanes) was added dropwise to a stirred solution of distilled *i*Pr_2NH (12.7 mL, 89.9 mmol) in THF (160 mL), at –78 °C, and stirred for 15 min. Distilled ETSA (17.3 mL, 94.7 mmol) was added dropwise and stirred (20 min) to give the lithium enolate. 114 mL of this solution (75%) was added dropwise to a stirred solution of TBS ether **145** (9.75 g, 18.9 mmol) in THF (330 mL), at –78 °C, and stirred for 30 min. The remaining 39 mL (25%) of the lithium enolate solution was added, dropwise, to the reaction mixture and stirred for an additional 30 min. The reaction was warmed to –25 °C and then allowed to warm slowly to rt., before being quenched with NH_4Cl. The layers were separated and the aqueous layer extracted with CH_2Cl_2 (4 x 50 mL). The combined organic phases were washed with brine (200 mL), dried ($MgSO_4$), filtered and concentrated *in vacuo*. Purification by flash column chromatography (SiO_2, 20% EtOAc/PE 40-60) afforded enoate (*Z*)-**149a** (8.87 g, 15.2 mmol, 80%, 96% *brsm*, *Z*/*E* >19:1), as a colourless oil: **R_f** (10% EtOAc/PE 40-60) = 0.22; **^{1}H NMR** (500 MHz, $CDCl_3$) δ 7.33-7.27 (m, 5H, PhH), 7.21 (d, 2H, *J* = 8.6 Hz, ArH), 6.85 (d, 2H, *J* = 8.6 Hz, ArH), 5.74 (s, 1H, H40), 4.46 (ABq, 2H, J_{AB} = 11.9 Hz, $PhCH_2$), 4.39 (ABq, 2H, J_{AB} = 11.8 Hz, $ArCH_2$), 4.20 (m, 1H, H42), 4.12 (m, 1H, H37), 4.11 (q, 2H, *J* = 7.1 Hz, -OCH_2CH_3), 3.79 (s, 3H, $ArOCH_3$), 3.46 (dd, 1H, *J* = 9.5, 7.8 Hz, H43a), 3.43 (dd, 1H, *J* = 8.8, 7.4 Hz, H35a), 3.37 (dd, 1H, *J* = 9.5, 6.7 Hz, H43b), 3.25 (dd, 1H, *J* = 8.8, 6.8 Hz, H35b), 2.37 (dd, 1H, *J* = 15.3, 8.2 Hz, H38a), 2.24 (dd, 1H, *J* = 15.3, 5.7, 1.2 Hz, H38b), 1.95 (m, 1H, H36), 1.25 (t, 3H, *J* = 7.1 Hz, -OCH_2CH_3), 1.06 (d, 3H, *J* = 7.0 Hz, Me42), 0.87 (s, 9H, $Si(CH_3)_2C(CH_3)_3$), 0.86 (d, 3H, *J* = 7.0 Hz, Me36), 0.02 (s, 6H, $Si(CH_3)_2C(CH_3)_3$); **^{13}C NMR** (125 MHz, $CDCl_3$) δ 166.1 (C41=O), 161.1 (C39), 159.0 (ArC), 138.7 (ArC), 130.7 (ArC), 129.1 (ArCH), 128.2 (ArCH), 127.4 (ArCH), 127.3 (ArCH), 118.8 (C40), 113.6 (ArCH), 73.0 (C43), 72.9 ($PhCH_2$), 72.7 (C35), 72.2 ($ArCH_2$), 70.0 (C37), 59.5 (-OCH_2CH_3),

55.2 (ArO<u>C</u>H$_3$), 37.7 (C38), 37.1 (C36), 35.1 (C42), 25.9 (Si(CH$_3$)$_2$C(<u>C</u>H$_3$)$_3$), 18.0 (Si(CH$_3$)$_2$<u>C</u>(CH$_3$)$_3$), 15.4 (Me42), 14.3 (-OCH$_2$C<u>H</u>$_3$), 10.4 (Me36), -4.1 (Si(<u>C</u>H$_3$)$_2$C(CH$_3$)$_3$), -4.8 (Si(<u>C</u>H$_3$)$_2$C(CH$_3$)$_3$); **FTIR ν_{max}** 2930 (w, sp^3 CH str), 2856 (w, sp^3 CH str), 1714 (s, sh, C=O str), 1637, 1614, 1514, 1463, 1362, 1302, 1249 (s, sh, C-O str), 1211, 1156, 1097, 1039, 836, 776, 736, 698, 668; $[\alpha]_D^{20}$ –14.2 (*c* 1.0, CHCl$_3$); **HRMS** (ESI$^+$): calculated for C$_{34}$H$_{52}$O$_6$SiNa [M+Na]$^+$ 607.3431, found 607.3435. Data for enoate (*E*)-**149b** matched that previously obtained.

Alcohol 150

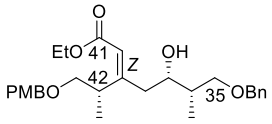

Tosylic acid monohydrate (1.1 mg, 5.68 µmol) was added to a stirred solution of enoate (*Z*)-**149a** (8.3 mg, 14.2 µmol) in MeOH (100 µL) and stirred (rt, 16 h). The reaction was quenched with NaHCO$_3$ (1 mL) and diluted with CH$_2$Cl$_2$ (1 mL). The layers were separated and the aqueous layer extracted with CH$_2$Cl$_2$ (3 x 5 mL). The combined organic phases were washed with brine (20 mL), dried (MgSO$_4$), filtered and concentrated *in vacuo*. Purification by flash column chromatography (SiO$_2$, 20% EtOAc/PE 40-60) afforded alcohol **150** (6.5 mg, 13.8 µmol, 97%), as a colourless oil. **R$_f$** (20% EtOAc/PE 40-60) = 0.14; **^{1}H NMR** (500 MHz, CDCl$_3$) δ 7.37-7.27 (m, 5H, Ph<u>H</u>), 7.22 (d, 2H, *J* = 8.7 Hz, Ar<u>H</u>), 6.85 (d, 2H, *J* = 8.7 Hz, Ar<u>H</u>), 5.89 (s, 1H, H40), 4.50 (s, 2H, PhC<u>H</u>$_2$), 4.42 (ABq, 2H, J_{AB} = 11.7 Hz, ArC<u>H</u>$_2$), 4.27 (m, 1H, H42), 4.13 (q, 2H, *J* = 7.1 Hz, -OC<u>H</u>$_2$CH$_3$), 3.99 (ddd, 1H, *J* = 9.1, 6.8, 3.4 Hz, H37), 3.79 (s, 3H, ArOC<u>H</u>$_3$), 3.58 (dd, 1H, *J* = 9.8, 9.3 Hz, H43a), 3.51 (dd, 1H, *J* = 9.1, 6.3 Hz, H35a), 3.45 (dd, 1H, *J* = 9.1, 5.2 Hz, H35b), 3.41 (dd, 1H, *J* = 9.9, 5.5 Hz, H43b), 3.14 (d, 1H, *J* = 3.3 Hz, -O<u>H</u>), 2.29 (dd, 1H, *J* = 14.8, 9.2 Hz, H38a), 2.23 (ddd, 1H, *J* = 14.8, 3.6, 1.0 Hz, H38b), 1.88 (m, 1H, H36), 1.27 (t, 3H, *J* = 7.1 Hz, -OCH$_2$C<u>H</u>$_3$), 1.02 (d, 3H, *J* = 7.0 Hz, Me42), 0.95 (d, 3H, *J* = 7.0 Hz, Me36); **^{13}C NMR** (100 MHz, CDCl$_3$) δ 166.2 (C41=O), 162.6 (C39), 159.1 (ArC), 138.3 (ArC), 130.0 (ArC), 129.4 (ArCH), 128.4 (ArCH), 127.6 (x ArCH), 119.0 (C40), 113.7 (ArCH), 73.8 (C35), 73.3 (Ph<u>C</u>H$_2$), 72.4 (C37), 72.14 (Ar<u>C</u>H$_2$), 72.08 (C43), 59.6 (-OC<u>H</u>$_2$CH$_3$), 55.2 (ArO<u>C</u>H$_3$), 38.7 (C36), 37.5 (C38), 34.7 (C42), 15.3 (Me42), 14.3 (-OCH$_2$C<u>H</u>$_3$), 11.2 (Me36); **FTIR ν_{max}** 3453 (w, OH str), 2920 (w, sp^3 CH str), 2851 (w, sp^3 CH str), 1710 (s, sh, C=O str), 1638, 1613, 1589, 1514, 1455, 1366, 1302, 1247 (s, sh, C-O str), 1210, 1154, 1092, 1034, 819, 735, 699, 668; $[\alpha]_D^{20}$ –15.0 (*c* 1.0, CHCl$_3$); **HRMS** (ESI$^+$): calculated for C$_{28}$H$_{39}$O$_6$ [M+H]$^+$ 471.2747, found 471.2728.

N.b. On larger scale (e.g. 0.864 g, 1.48 mmol), to avoid the accumulation of by-products, it was better to stop the reaction after 6 h, purify the product (0.544 g, 1.16 mmol, 78% or 96% *brsm*) and resubmit the recovered starting material (0.180 g, 0.307 mmol).

Alcohol 152

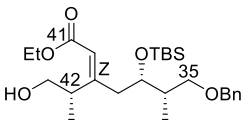

DDQ (3.9 mg, 17 µmol) was added to a stirred solution of enoate (*Z*)-**149a** (5.0 mg, 8.6 µmol) in CH_2Cl_2 and pH 7 buffer (9:1, 90 µL:10 µL) at 0 °C, giving a dark green solution. The mixture was stirred for 10 min at 0 °C, then allowed to warm to rt. The reaction slowly turned to red over 25 min, and TLC analysis also indicated completion. The mixture was diluted with CH_2Cl_2 (1 mL) and quenched with $NaHCO_3$ (1 mL). The layers were separated and the aqueous layer extracted with CH_2Cl_2 (3 x 1 mL). The combined organic phases were washed with brine (20 mL), dried ($MgSO_4$), filtered and concentrated *in vacuo*. Purification by flash column chromatography (SiO_2, 20% EtOAc/PE 40-60) afforded alcohol **152** (3.0 mg, 6.5 µmol, 75%), as a colourless oil. $\mathbf{R_f}$ (20% EtOAc/PE 40-60) = 0.26; **^{1}H NMR** (500 MHz, $CDCl_3$) δ 7.35-7.27 (m, 5H, PhH), 5.86 (s, 1H, H40), 4.49 (ABq, 2H, J_{AB} = 11.9 Hz, PhCH_2), 4.14 (m, 3H, H37 and -OCH_2CH$_3$), 3.93 (m, 1H, H42), 3.65 (ddd, 1H, *J* = 10.8, 5.2, 4.3 Hz, H43a), 3.51 (ddd, 1H, *J* = 10.8, 9.6, 7.7 Hz, H43b), 3.45 (dd, 1H, *J* = 8.8, 7.7 Hz, H35a), 3.28 (dd, 1H, *J* = 8.8, 6.2 Hz, H35b), 2.73 (dd, 1H, *J* = 7.6, 4.2 Hz, -OH), 2.32 (d, 2H, *J* = 7.1, H38), 2.01 (m, 1H, H36), 1.27 (t, 3H, *J* = 7.1 Hz, -OCH$_2$CH$_3$), 1.03 (d, 3H, *J* = 7.0 Hz, Me42), 0.88 (d, 3H, *J* = 7.0 Hz, Me36), 0.87 (s, 9H, Si(CH$_3$)$_2$C(CH$_3$)$_3$) , 0.03 (s, 6H, Si(CH$_3$)$_2$C(CH$_3$)$_3$); **^{13}C NMR** (125 MHz, $CDCl_3$) δ 167.4 (C41=O), 160.6 (C39), 138.5 (ArC), 128.3 (ArCH), 127.5 (ArCH), 127.4 (ArCH), 120.5 (C40), 73.0 (PhCH$_2$), 72.2 (C35), 70.4 (C37), 66.6 (C43), 60.1 (-OCH$_2$CH$_3$), 37.9 (C42), 37.8 (C38), 37.3 (C36), 25.9 (Si(CH$_3$)$_2$C(CH$_3$)$_3$), 18.1 (Si(CH$_3$)$_2$C(CH$_3$)$_3$), 14.7 (Me42), 14.2 (-OCH$_2$CH$_3$), 10.7 (Me36), -4.0 (Si(CH$_3$)$_2$C(CH$_3$)$_3$), -4.8 (Si(CH$_3$)$_2$C(CH$_3$)$_3$); **HRMS** (ESI$^+$): calculated for $C_{26}H_{45}O_5Si$ $[M+H]^+$ 465.3031, found 465.3021.

Lactones 35,37-*anti*-144a and 35,37-*syn*-144b

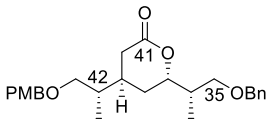

35,37-*anti*-**144a**

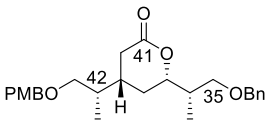

35,37-*syn*-**144b**

Method 1 – Catalytic reduction with $[PPh_3CuH]_6$

$[PPh_3CuH]_6$ reagent solution (50 µL, 1.04 µmol copper) was added to a stirred solution of lactone enoate **148** (2.2 mg, 5.18 µmol) in toluene (20 µL) and stirred at rt for 3 h, a further aliquot of $[PPh_3CuH]_6$ reagent solution (20 µL, 0.518 µmol copper equivalent, 10% mol cat.) and the reaction stirred for 16h. Direct application of the product to flash column chromatography (25-66% EtOAc/PE 40-60) afforded an inseparable 1:1 mixture of starting material and a non-olefinic product (shown to be reduced product, see method 2 below).

Method 2 – Catalytic reduction with BDP-CuH

BDP-CuH reagent solution (50 µL, 0.50 µmol copper) and *t*BuOH (1 drop in 3 drops toluene) were added to a stirred solution of lactone enoate **148** (2.0 mg, 4.71 µmol) in toluene (100 µL) and stirred at rt for 72 h. Direct application of the product to flash column chromatography (20% EtOAc/PE 40-60) afforded lactone 35,37-*syn*-**144b** (1.2 mg, 2.81 µmol, 60%) as a colourless oil. $\mathbf{R_f}$ (20% EtOAc/PE 40-60) = 0.08; **^{1}H NMR** (500 MHz, $CDCl_3$) δ 7.35-7.27 (m, 5H, Ar<u>H</u>), 7.22 (d, 2H, *J* = 8.6 Hz, Ar<u>H</u>), 6.87 (d, 2H, *J* = 8.6 Hz, Ar<u>H</u>), 4.50 (ABq, 2H, J_{AB} = 11.9 Hz, PhC<u>H_2</u>), 4.50 (m, 1H, H37), 4.40 (s, 2H, ArC<u>H_2</u>), 3.80 (s, 3H, ArOC<u>H_3</u>), 3.54 (dd, 1H, *J* = 9.2, 5.7 Hz, H35a), 3.40 (dd, 1H, *J* = 9.2, 5.4 Hz, H35b), 3.31 (dd, 1H, *J* = 9.4, 5.5 Hz, H43a), 3.28 (dd, 1H, *J* = 9.4, 6.6 Hz, H43b), 2.58 (ddd, 1H, *J* = 17.3, 5.8, 1.7 Hz, H40a), 2.18 (dd, 1H, *J* = 17.3, 10.8 Hz, H40b), 2.11 (m, 1H, H39), 1.95 (m, 1H, H36), 1.73 (m, 2H, H42 and H38a), 1.42 (dt, 1H, *J* = 13.7, 11.9 Hz, H38b), 0.96 (d, 3H, *J* = 7.0 Hz, Me36), 0.89 (d, 3H, *J* = 7.0 Hz, Me42); **FTIR ν_{max}** 2856 (w, sp^3 CH str), 1707 (s, sh, C=O str), 1612, 1587, 1513, 1455, 1363, 1303, 1246 (s, sh, C-O str), 1173, 1090, 1030, 819, 736, 699; $[\boldsymbol{\alpha}]_{\mathbf{D}}^{\mathbf{20}}$ –13.3 (*c* 1.0, $CHCl_3$); **HRMS** (ESI^+): **HRMS** (ESI^+): calculated for $C_{26}H_{34}O_5Na$ $[M+Na]^+$ 449.2304, found 449.2288.

Method 3 – Hydroxyl directed hydrogenation catalysed by [Ir(COD)(PCy$_3$)(py)]PF$_6$

[Ir(COD)(PCy$_3$)(py)]PF$_6$ (137 mg, 0.170 mmol) in CH_2Cl_2 (6.2 mL) was added to a stirred solution of alcohol **150** (620 mg, 1.32 mmol) in CH_2Cl_2 (8.2 mL), at –20 °C, under $Ar_{(g)}$. The reaction flask was immediately flushed and $H_{2(g)}$ bubbled through the reaction mixture. The reaction was stirred, under a triple skinned balloon of $H_{2(g)}$ for 1 week. When consumption of alcohol **150** was indicated by ^{1}H NMR, the reaction was allowed to come to rt and tosylic acid monohydrate (100 mg, 0.527 mmol) was added. The solution was stirred for 30 min before being carefully quenched with $NaHCO_3$ (10 mL). The layers were separated and the reaction solution extracted with CH_2Cl_2 (4 x 10 mL). The combined organic extracts were washed with brine (20 mL), dried ($MgSO_4$), filtered and concentrated *in vacuo*. Purification by flash column chromatography (SiO_2, 30% EtOAc/PE 40-60) afforded lactone 35,37-*anti*-**144a** (521 mg, 1.22 mmol, 93%, *dr* 5:1) as a pale yellow oil: $\mathbf{R_f}$ (30% EtOAc/PE 40-60) = 0.24; **^{1}H NMR** (500 MHz, $CDCl_3$) δ 7.36-7.27 (m, 5H, ArH), 7.22 (d, 2H, *J* = 8.6 Hz, ArH), 6.87 (d, 2H, *J* = 8.6 Hz, ArH), 4.47 (ABq, 2H, J_{AB} = 12.0 Hz, PhCH_2), 4.39 (m, 2H, ArCH_2), 4.36 (m, 1H, H37), 3.80 (s, 3H, ArOCH_3), 3.46 (dd, 1H, *J* = 9.2, 7.1 Hz, H35a), 3.39 (dd, 1H, *J* = 9.3, 5.2 Hz, H35b), 3.32 (dd, 1H, *J* = 9.5, 5.5 Hz, H43a), 3.29 (dd, 1H, *J* = 9.6, 5.9 Hz, H43b), 2.44 (dd, 1H, *J* = 15.4, 6.0 Hz, H40a), 2.36 (dd, 1H, *J* = 15.3, 11.2 Hz, H40b), 2.11 (m, 1H, H39), 1.92 (m, 1H, H36), 1.77 (m, 2H, H38a, H42), 1.60 (ddd, 1H, *J* = 14.3, 5.4, 4.5 Hz, H38b), 1.01 (d, 3H, *J* = 6.9 Hz, Me36), 0.91 (d, 3H, *J* = 6.9 Hz, Me36); **^{13}C NMR** (125 MHz, $CDCl_3$) δ 174.0 (C41=O), 159.2 (ArC), 138.2 (ArC), 130.2 (ArC), 129.2 (ArCH), 128.4 (ArCH), 127.7 (ArCH), 113.8 (ArCH), 77.5 (C37), 73.3 (PhCH_2), 72.8 (ArCH_2), 72.5 (C43), 71.8 (C35), 55.3 (ArOCH_3), 37.7 (C36), 37.4 (C40), 33.3 (C42), 31.3 (C39), 27.7 (C38), 13.8 (Me42), 11.8 (Me36); **FTIR ν_{max}** 2958 (w, sp^3 CH str), 2933 (w, sp^3 CH str), 2857 (w, sp^3 CH str), 1736 (s, sh, C=O str), 1611, 1585, 1512, 1454, 1364, 1244 (s, sh, C-O str), 1172, 1089, 1029, 818, 738, 698; $[\alpha]_D^{20}$ +21.1 (*c* 1.0, $CHCl_3$); **HRMS** (ESI$^+$): calculated for $C_{26}H_{34}O_5Na$ $[M+Na]^+$ 449.2304, found 449.2296.

α-Hydroxy lactone 133

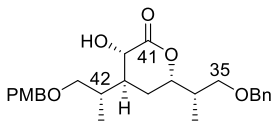

KHMDS (561 mg, 2.81 mmol µmol) was added to a stirred solution of lactone 35,37-*anti*-**144a** (0.960 g, 2.25 mmol) in THF (20 mL) at –78 °C. After 15 min (±)-*trans*-2-(phenylsulfonyl)-3-phenyloxaziridine[126,194] (736 mg, 2.81 mmol) in THF (5 mL) was added dropwise. After 5 h, the reaction mixture was quenched with $NH_4Cl_{(aq)}$ (25 mL), diluted with CH_2Cl_2 and allowed to warm

to rt. The layers were separated and the aqueous layer extracted with CH_2Cl_2 (4 x 10 mL). The combined organic extracts were washed with brine (50 mL), dried ($MgSO_4$), filtered and concentrated *in vacuo*. Purification by flash column chromatography (SiO_2, 3% Et_3N and 25% EtOAc/PE 40-60) afforded α-hydroxy lactone **133** (0.804 g, 1.82 mmol, 81%) as a pale yellow oil: **R_f** (30% EtOAc/PE 40-60) = 0.16; **^{1}H NMR** (500 MHz, $CDCl_3$) δ 7.36-7.27 (m, 5H, ArH), 7.27 (d, 2H, *J* = 8.4 Hz, ArH), 6.87 (d, 2H, *J* = 8.4 Hz, ArH), 4.46 (ABq, 2H, J_{AB} = 12.2 Hz, PhCH_2), 4.41 (ABq, 2H, J_{AB} = 11.7 Hz, ArCH_2), 4.38 (m, 1H, H37), 4.22 (dd, 1H, *J* = 11.4, 3.6 Hz, H40), 3.80 (s, 3H, ArOCH_3), 3.44-3.37 (m, 2H, 2 x H35), 3.36-3.27 (m, 2H, 2 x H43), 3.23 (d, 1H, *J* = 3.5 Hz, OH), 2.36 (m, 1H, H42), 2.07 (m, 1H, H39), 1.89 (m, 1H, H36), 1.77 (m, 1H, H38a), 1.64 (m, 1H, H38b), 0.99 (d, 3H, *J* = 6.9 Hz, Me36), 0.91 (d, 3H, *J* = 7.0 Hz, Me42); **^{13}C NMR** (125 MHz, $CDCl_3$) δ 177.0 (C41=O), 159.2 (ArC), 138.1 (ArC), 130.4 (ArC), 129.3 (ArCH), 128.4 (ArCH), 127.8 (ArCH), 127.7 (ArCH), 113.8 (ArCH), 76.4 (C37), 73.3 (PhCH_2), 72.7 (ArCH_2), 72.5 (C43), 71.5 (C35), 55.3 (ArOCH_3), 66.8 (C40), 38.2 (C39), 37.8 (C36), 33.2 (C42), 25.5 (C38) , 11.4 (Me36), 11.0 (Me42); **FTIR ν_{max}** 3459 (w, br, OH str), 2916 (w, sp^3 CH str), 2852 (w, sp^3 CH str), 1734 (s, sh, C=O str), 1611, 1586, 1512, 1454, 1364, 1301, 1245 (s, sh, C-O str), 1172, 1090 (s, sh, C-O str), 1029, 846, 818, 736, 698; $[\alpha]_D^{20}$ +16.4 (*c* 1.0, $CHCl_3$); **HRMS** (ESI^+): calculated for $C_{26}H_{34}O_6Na$ $[M+Na]^+$ 465.2253, found 465.2245.

α-OTES lactone 156

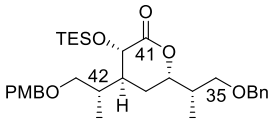

2,6-Lutidine (320 µL, 2.71 mmol) was added to a stirred solution of α-hydroxy lactone **133** (400 mg, 0.904 mmol) in CH_2Cl_2 (9 mL). The reaction mixture was cooled to –78 °C and stirred for 5 min before TESOTf (410 µL, 1.81 mmol) was slowly added dropwise. After 30 min, the reaction mixture was quenched sequentially with MeOH (100 µL) and $NaHCO_3$ (15 mL), allowed to warm to rt, the layers separated and the aqueous layer extracted with CH_2Cl_2 (4 x 10 mL). The combined organic extracts were washed with brine (50 mL), dried ($MgSO_4$), filtered and concentrated *in vacuo*. Purification by flash column chromatography (SiO_2, 5-40% EtOAc/PE 40-60) afforded the α-TES ether lactone (500 mg, 0.904 mmol, quant.) and also allowed separation of the desired C39 diastereomer **156** (0.428 mg, 0.787 mmol, 85%) as a colourless oil: **R_f** (20% EtOAc/PE 40-60) = 0.34; **^{1}H NMR** (500 MHz, $CDCl_3$) δ 7.35-7.27 (m, 5H, ArH), 7.23 (d, 2H, *J* = 8.6 Hz, ArH), 6.87 (d, 2H, *J* = 8.6 Hz, ArH), 4.47 (ABq, 2H, J_{AB} = 12.0 Hz, PhCH_2), 4.40 (ABq, 2H, J_{AB} = 11.6 Hz, ArCH_2), 4.30 (ddd, 1H, *J* = 11.7, 4.5, 4.2 Hz, H37), 4.28 (d, 1H, *J* = 10.7 Hz, H40), 3.80 (s, 3H, ArOCH_3), 3.44 (dd, 1H, *J* =

9.3, 6.9 Hz, H35a), 3.38 (dd, 1H, *J* = 9.3, 5.2 Hz, H35b), 3.31 (dd, 1H, *J* = 9.6, 6.4 Hz, H43a), 3.27 (dd, 1H, *J* = 9.6, 7.8 Hz, H43b), 2.34 (m, 1H, H42), 2.17 (dddd, 1H, *J* = 10.5, 10.4, 4.9. 3.5, H39), 1.87 (m, 1H, H36), 1.74 (ddd, 1H, *J* = 14.4, 11.6, 10.5 Hz, H38a), 1.61 (ddd, 1H, *J* = 14.5, 4.5, 4.3 Hz, H38b), 1.00 (d, 3H, *J* = 6.8 Hz, Me36), 0.99 (t, 9H, *J* = 8.0 Hz, Si($CH_2\underline{CH_3}$)$_3$), 0.87 (d, 3H, *J* = 7.0 Hz, Me36), 0.70 (m, 6H, Si($\underline{CH_2}CH_3$)$_3$); **^{13}C NMR** (100 MHz, $CDCl_3$) δ 174.4 (C41=O), 159.1 (Ar$\underline{C}$), 138.2 (Ar$\underline{C}$), 130.4 (Ar$\underline{C}$), 129.2 (Ar$\underline{C}$H), 128.4 (Ar$\underline{C}$H), 127.7 (Ar$\underline{C}$H), 113.7 (Ar$\underline{C}$H), 75.9 (C37), 73.2 (Ph$\underline{C}H_2$), 73.0 (C43), 72.4 (Ar$\underline{C}H_2$), 71.8 (C35), 68.2 (C40), 55.2 (ArO$\underline{C}H_3$), 38.2 (C39), 37.9 (C36), 32.2 (C42), 24.8 (C38**)**, 11.6 (Me36), 10.4 (Me42), 6.9 (Si($CH_2\underline{CH_3}$)$_3$), 5.0 (Si($\underline{CH_2}CH_3$)$_3$); **FTIR ν_{max}** 2956 (w, sp^3 CH str), 2912 (w, sp^3 CH str), 2875 (w, sp^3 CH str), 1739 (s, sh, C=O str), 1604, 1513, 1496, 1455, 1412, 1365, 1234 (s, sh, C-O str), 1217, 1095, 1028, 1004, 836, 733, 697; $[\boldsymbol{\alpha}]_{\mathbf{D}}^{\mathbf{20}}$ +11.0 (*c* 1.0, $CHCl_3$); **HRMS** (ESI^+): calculated for $C_{32}H_{48}O_6SiNa$ $[M+Na]^+$ 579.3118, found 579.3100.

Alcohol 157

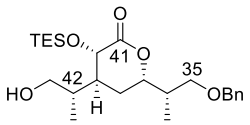

DDQ (32.6 mg, 144 µmol) was added to a stirred solution of α-TES ether lactone **156** (40.0 mg, 71.8 µmol) in CH_2Cl_2 and pH 7 buffer (9:1, 900 µL:100 µL) at 0 °C, giving a dark green solution. The mixture was stirred for 10 min at 0 °C, then allowed to warm to rt. The reaction slowly turned to red over 1h 15 min, and TLC analysis also indicated completion. The mixture was diluted with CH_2Cl_2 (2 mL) and quenched with $NaHCO_3$ (2 mL). The layers were separated and the aqueous layer extracted with CH_2Cl_2 (3 x 2 mL). The combined organic phases were washed with brine (2 x 2 mL), dried ($MgSO_4$), filtered and concentrated *in vacuo*. Purification by flash column chromatography (SiO_2, 15-25% EtOAc/PE 40-60) afforded alcohol **157** (30.6 mg, 70.1 µmol, 97%), as a colourless oil: **R_f** (20% EtOAc/PE 40-60) = 0.07; **^{1}H NMR** (500 MHz, $CDCl_3$) δ 7.36-7.28 (m, 5H, Ar$\underline{H}$), 4.46 (ABq, 2H, J_{AB} = 12.0 Hz, PhC$\underline{H}_2$), 4.33 (ddd, 1H, *J* = 11.5, 4.8, 3.7 Hz, H37), 4.28 (d, 1H, *J* = 10.3 Hz, H40), 3.55 (dd, 1H, *J* = 10.8, 5.7 Hz, H43a), 3.46 (dd, 1H, *J* = 10.9, 6.8 Hz, H43b), 3.45 (dd, 1H, *J* = 9.3, 7.0 Hz, H35a), 3.41(dd, 1H, *J* = 9.3, 5.1 Hz, H35b), 2.14 (m, 1H, H42), 2.11 (m, 1H, H39), 1.91 (m, 1H, H36), 1.86 (ddd, 1H, *J* = 14.4, 11.5, 9.9 Hz, H38a), 1.65 (ddd, 1H, *J* = 14.4, 4.6, 3.7 Hz, H38b), 1.01 (d, 3H, *J* = 6.9 Hz, Me36), 0.98 (t, 9H, *J* = 7.9 Hz, 3 x Si($CH_2\underline{CH_3}$)$_3$), 0.89 (d, 3H, *J* = 6.8 Hz, Me42), 0.70 (m, 6H, 3 x Si($\underline{CH_2}CH_3$)$_3$); **^{13}C NMR** (125 MHz, $CDCl_3$) δ 174.2 (C41=O), 138.1 (Ar$\underline{C}$), 128.4 (Ar$\underline{C}$H), 127.75 (Ar$\underline{C}$H), 127.74 (Ar$\underline{C}$H), 76.0 (C37), 73.3 (Ph$\underline{C}H_2$), 71.8 (C35), 68.6 (C40), 66.1 (C43), 38.2 (C39), 37.9 (C36), 35.4 (C42), 25.4 (C38) , 11.7 (Me36), 10.7 (Me42), 7.9 (Si($CH_2\underline{CH_3}$)$_3$), 5.1 (Si($\underline{CH_2}CH_3$)$_3$); **FTIR ν_{max}** 3459 (w, br, OH str), 2964 (w, sp^3 CH str), 2877 (w, sp^3 CH str), 1717 (s, sh,

C=O str), 1602, 1512, 1453, 1379, 1379, 1273 (s, sh, C-O str), 1217, 1176, 1096 (s, sh, C-O str), 1070, 1026, 848, 807, 751, 713, 666; $[\alpha]_D^{20}$ +11.3 (*c* 1.0, $CHCl_3$); **HRMS** (ESI^+): calculated for $C_{24}H_{40}O_5SiNa$ $[M+Na]^+$ 459.2543, found 459.2538.

Aldehyde 158

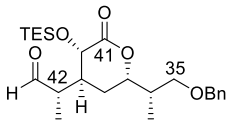

Note: This α-chiral aldehyde is prone to epimerisation at C42 and must be immediately used, without purification, in the HWE olefination reaction.

Method 1 – DMP Oxidation

DMP (117 mg, 275 µmol) was added to a stirred solution of alcohol **157** (20.0 mg, 45.8 µmol) and $NaHCO_{3(s)}$ (46.2 mg, 0.550 mmol) in CH_2Cl_2 (460 µL) at rt. The mixture was stirred for 1h and quenched with premixed $NaHCO_3$ (1 mL) and $Na_2S_2O_3$ (1 mL), by stirring for 30 min. The layers were separated and the aqueous layer extracted with CH_2Cl_2 (3 x 2 mL). The combined organic phases were washed with brine (2 x 2 mL), dried ($MgSO_4$), filtered and concentrated *in vacuo* to afford crude aldehyde **158** (~18 mg, ~41 µmol, ~90%), as a pale yellow oil: $\mathbf{R_f}$ (20% EtOAc/PE 40-60) = 0.35; **^{1}H NMR** (500 MHz, $CDCl_3$) δ 9.62 (d, 1H, *J* = 0.9 Hz, H43), 7.37-7.27 (m, 5H, Ar<u>H</u>), 4.47 (m, 2H, PhC<u>H</u>$_2$), 4.34 (ddd, 1H, *J* = 11.6, 4.6, 4.2 Hz, H37), 4.28 (d, 1H, *J* = 11.0 Hz, H40), 3.43 (dd, 1H, *J* = 9.3, 6.9 Hz, H35a), 3.40 (dd, 1H, *J* = 9.3, 5.0 Hz, H35b), 2.83 (m, 1H, H42), 2.51 (m, 1H, H39), 1.89 (m, 1H, H36), 1.94 (m, 1H, H38a), 1.62 (m, 1H, H38b), 1.10 (d, 3H, *J* = 7.1 Hz, Me36), 1.01 (d, 3H, *J* = 6.9 Hz, Me36), 0.98 (t, 9H, *J* = 7.9 Hz, 3 x Si(CH_2<u>CH_3</u>)$_3$), 0.69 (m, 6H, 3 x Si(<u>CH_2</u>CH_3)$_3$).

Method 2 – Swern Oxidation

DMSO (120 µL, 1.60 mmol) was added dropwise to a stirred solution of oxalyl chloride (70 µL, 0.802 mmol) in CH_2Cl_2 (5.4 mL) and stirred (–78 °C, 15 min). A solution of alcohol **157** (280 mg, 0.641 mmol) in CH_2Cl_2 (2 x 0.5 mL) was added, dropwise *via* cannula, and the mixture stirred (–78 °C, 15 min). Distilled Et_3N (450 µL, 3.21 mmol) was added dropwise and the suspension stirred (30 min – 1 h). The reaction was quenched with NH_4Cl (2.0 mL), the organic layer separated and the aqueous layer extracted with Et_2O (3 x 20 mL). The combined organic extracts were dried over

($MgSO_4$), filtered and concentrated *in vacuo* to give crude aldehyde **158** as a slightly yellow oil (265 mg, ca. 0.609 mmol, ca. 95%).

Enone (*E*)-160

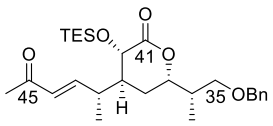

A solution of anhydrous $Ba(OH)_2$ (471 mg, 2.75 mmol) and dimethyl (2- oxopropyl)phosphonate (ketophosphonate **159**) (640 µL, 4.63 mmol) in THF (10 mL) was stirred for 2 h at rt then lowered to 0 °C. Aldehyde **158** (crude from Swern oxidation) in THF:H_2O (40:1, 3 x 2.4 mL) was added to the solution and stirred overnight at rt. If necessary, the reaction was diluted with CH_2Cl_2 before being quenched with NH_4Cl (5 mL). The layers were separated and the aqueous layer extracted with CH_2Cl_2 (3 x 2 mL). The combined organic phases were washed with brine (2 x 2 mL), dried ($MgSO_4$), filtered and concentrated *in vacuo*. Purification by flash column chromatography (SiO_2, 15-25% EtOAc/PE 40-60) afforded enone (*E*)-**160** (242.8 mg, 511 µmol, 74% over two steps), as a colourless oil: $\mathbf{R_f}$ (30% EtOAc/PE 40-60) = 0.63; **^{1}H NMR** (500 MHz, $CDCl_3$) δ 7.36-7.28 (m, 5H, ArH), 6.73 (dd, 1H, *J* = 16.1, 6.2 Hz, H43), 6.08 (dd, 1H, *J* = 16.1, 1.6 Hz, H44), 4.48 (ABq, 2H, J_{AB} = 12.0 Hz, PhCH_2), 4.33 (ddd, 1H, *J* = 11.9, 4.3, 4.0 Hz, H37), 4.28 (d, 1H, *J* = 10.4 Hz, H40), 3.44 (dd, 1H, *J* = 9.3, 7.0 Hz, H35a), 3.41 (dd, 1H, *J* = 9.3, 5.1 Hz, H35b), 2.87 (m, 1H, H42), 2.25 (m, 1H, H46), 2.11 (m, 1H, H39), 1.89 (m, 1H, H36), 1.83 (ddd, 1H, *J* = 14.6, 11.9, 10.6 Hz, H38a), 1.56 (ddd, 1H, *J* = 14.6, 4.3, 3.9 Hz, H38b), 1.05 (d, 3H, *J* = 6.8 Hz, Me42), 1.00 (d, 3H, *J* = 6.9 Hz, Me36), 0.98 (t, 9H, *J* = 7.9 Hz, 3 x Si(CH_2CH_3)$_3$), 0.69 (m, 6H, 3 x Si(CH_2CH_3)$_3$); **^{13}C NMR** (125 MHz, $CDCl_3$) δ 192 (C45), 173.5 (C41=O), 150.6 (C43), 138.2 (ArC), 130.5 (C44), 128.4 (ArCH), 127.8 (ArCH), 127.7 (ArCH), 75.8 (C37), 73.3 (PhCH_2), 71.6 (C35), 68.2 (C40), 11.2 (C39), 37.9 (C36), 35.5 (C42), 27.3 (C46), 25.4 (C38), 11.60 (Me36), 11.56 (Me42), 6.9 (Si(CH_2CH_3)$_3$), 5.0 (Si(CH_2CH_3)$_3$); **FTIR ν_{max}** 2956 (w, sp^3 CH str), 2908 (w, sp^3 CH str), 2876 (w, sp^3 CH str), 1757 (s, sh, C=O str), 1697, 1673 (s, sh, C=O str), 1624, 1496, 1455, 1414, 1359, 1254 (s, sh, C-O str), 1202, 1149, 1100, 1057, 1005, 976, 906, 868, 731, 697; $[\alpha]_D^{20}$ +18.8 (*c* 1.0, $CHCl_3$); **HRMS** (ESI$^+$): calculated for $C_{27}H_{42}O_5SiNa$ $[M+Na]^+$ 497.2699, found 497.2692.

Allylic alcohols C42, C45-*anti*-164a and C42, C45-*syn*-164b

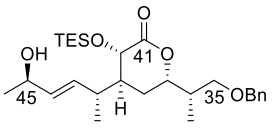

anti-**164a**

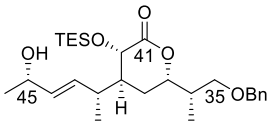

syn-**164b**

Method 1 – CBS Reduction

(*S*)-Me-CBS-oxazaborolidine (90 µL, 84.3 µmol, 1 M in PhMe) and borane dimethyl sulphide (20 µL, 169 µmol) were sequentially added to a stirred solution of enone (*E*)-**160** (20 mg, 42.1 µmol) in THF (740 mL) and stirred (–85 °C, 4 days). The mixture was quenched with MeOH and allowed to return to rt before being concentrated *in vacuo*. Addition of MeOH and *in vacuo* evaporation was repeated three additional times. Purification by flash column chromatography (SiO_2, 10-20% EtOAc/PE 40-60) afforded C42, C45-*anti*-allylic alcohol **144a** (4.8 mg, 10.1 µmol, 24%, 62% *brsm*, *dr* 3:1), as a colourless oil. See below for full data.

Use of (*R*)-*n*-Butyl-CBS-oxazaborolidine with enone (*E*)-**160** (10 mg, 21.1 µmol), under the same conditions, afforded C42, C45-*syn*-allylic alcohol **144b** (6.9 mg, 14.5 µmol, 69%, *dr* 2:1), as a colourless oil. See below for full data.

*Method 2 – Terashima Reduction with LiAlH(*N*-ethylaniline)$_2$(EtO)((–)/(+)*-N*-methylephedrine)*

An aliquot of a pre-prepared suspension of LiAlH(*N*-ethylaniline)$_2$(EtO)((–)-*N*-methylephedrine) in Et_2O (1.40 mL, 348 µmol, ca. 0.248M $LiAlH_4$) was added to a stirred solution of enone (*E*)-**160** (50.0 mg, 105 µmol) in Et_2O (2.1 mL) and stirred (–90 °C, 3 h, then –78 °C, 3 h). The mixture was quenched with NH_4Cl and allowed to return to rt. The layers were separated and the aqueous layer extracted with CH_2Cl_2 (3 x 2 mL). The combined organic phases were washed with brine (10 mL), dried ($MgSO_4$), filtered and concentrated *in vacuo*. Purification by flash column chromatography (SiO_2, 20% EtOAc/Hexane) afforded allylic alcohol *syn*-**144b** (46.9 mg, 98.4 µmol, 93%, *dr* 6:1), as a colourless oil : $\mathbf{R_f}$ (30% EtOAc/PE 40-60) = 0.26; **^{1}H NMR** (700 MHz, $CDCl_3$) δ 7.37-7.28 (m, 5H, Ar<u>H</u>), 5.56 (dd, 1H, *J* = 15.6, 5.7 Hz, H43), 5.53 (dd, 1H, *J* = 15.6, 5.2 Hz, H44), 4.49 (ABq, 2H, J_{AB} = 12.0 Hz, PhC<u>H</u>$_2$), 4.34 (ddd, 1H, *J* = 11.8, 4.1, 3.3 Hz, H37), 4.27 (m, 1H, H45), 4.26 (d, 1H, *J* = 9.7 Hz, H40), 3.46 (dd, 1H, *J* = 9.3, 7.2 Hz, H35a), 3.41 (dd, 1H, *J* = 9.3, 5.4 Hz, H35b), 2.62 (m, 1H, H42), 1.98 (m, 1H, H39), 1.89 (m, 1H, H36), 1.84 (ddd, 1H, *J* = 14.5, 11.9, 9.8 Hz, H38a), 1.60 (ddd, 1H, *J* = 14.5, 4.1, 3.5 Hz, H38b), 1.26 (d, 3H, *J* = 6.3 Hz, H46), 1.000 (d, 3H, *J* = 6.9 Hz, Me36), 0.996 (d, 3H, *J* = 6.9 Hz, Me42), 0.98 (t, 9H, *J* = 6.9 Hz, Si(CH$_2$<u>CH$_3$</u>)$_3$), 0.67 (m, 6H,

Si(C<u>H</u>$_2$CH$_3$)$_3$); **^{13}C NMR** (125 MHz, $CDCl_3$) δ 173.8 (C41=O), 138.2 (Ar<u>C</u>), 134.4 (C44), 133.6 (C43), 128.4 (Ar<u>C</u>H), 127.71 (Ar<u>C</u>H), 127.66 (Ar<u>C</u>H), 76.1 (C37), 73.3 (Ph<u>C</u>H$_2$), 71.8 (C35), 68.7 (C45), 68.5 (C40), 41.8 (C39), 37.9 (C36), 35.1 (C42), 25.3 (C38), 23.6 (C46), 13.0 (Me42), 11.5 (Me36), 6.9 (Si(CH$_2$<u>C</u>H$_3$)$_3$), 5.0 (Si(<u>C</u>H$_2$CH$_3$)$_3$); **FTIR ν_{max}** 3454 (w, br OH str), 2970 (w, sp^3 CH str), 2917 (w, sp^3 CH str), 2850 (w, sp^3 CH str), 1745 (s, sh, C=O str), 1673, 1632, 1536, 1455, 1415, 1365, 1229 (s, sh, C-O str), 1217, 1205, 1150, 1099, 1009, 870, 837, 732, 698, 663; $[\alpha]_D^{20}$ +7.8 (*c* 1.0, $CHCl_3$); **HRMS** (ESI$^+$): calculated for $C_{27}H_{44}O_5SiNa$ $[M+Na]^+$ 499.2856, found 499.2837.

Use of LiAlH(*N*-ethylaniline)$_2$(EtO)((+)-*N*-methylephedrine) on enone (*E*)-**160** (45 mg, 94.9 µmol), under the same conditions and after purification, afforded allylic alcohol *anti*-**144a** (27.8 mg, 58.3 µmol, 62%, *dr* 6:1), as a colourless oil: **R_f** (30% EtOAc/PE 40-60) = 0.26; **^{1}H NMR** (700 MHz, $CDCl_3$) δ 7.36-7.28 (m, 5H, Ar<u>H</u>), 5.56 (dd, 1H, *J* = 15.7, 5.6 Hz, H43), 5.52 (dd, 1H, *J* = 15.6, 6.0 Hz, H44), 4.49 (ABq, 2H, J_{AB} = 11.9 Hz, PhC<u>H</u>$_2$), 4.34 (ddd, 1H, *J* = 11.9, 4.4, 3.4 Hz, H37), 4.27 (d, 1H, *J* = 9.7 Hz, H40), 4.25 (m, 1H, H45), 3.45 (dd, 1H, *J* = 9.3, 7.3 Hz, H35a), 3.40 (dd, 1H, *J* = 9.3, 5.0 Hz, H35b), 2.62 (m, 1H, H42), 2.00 (m, 1H, H39), 1.89 (m, 1H, H36), 1.84 (ddd, 1H, *J* = 14.5, 11.8, 10.1 Hz, H38a), 1.58 (ddd, 1H, *J* = 14.3, 3.8, 3.8 Hz, H38b), 1.25 (d, 3H, *J* = 6.4 Hz, H46), 1.00 (d, 3H, *J* = 6.7 Hz, Me42), 0.99 (d, 3H, *J* = 6.9 Hz, Me36), 0.98 (t, 9H, *J* = 6.9 Hz, Si(CH$_2$<u>C</u>H$_3$)$_3$), 0.69 (m, 6H, Si(<u>C</u>H$_2$CH$_3$)$_3$); **^{13}C NMR** (125 MHz, $CDCl_3$) δ 173.9 (C41=O), 138.1 (Ar<u>C</u>), 134.4 (C44), 133.5 (C43), 128.4 (Ar<u>C</u>H), 127.73 (Ar<u>C</u>H), 127.71 (Ar<u>C</u>H), 76.0 (C37), 73.3 (Ph<u>C</u>H$_2$), 71.7 (C35), 68.7 (C45), 68.5 (C40), 41.8 (C39), 37.9 (C36), 35.4 (C42), 25.7 (C38), 25.3 (C46), 13.2 (Me42), 11.4 (Me36), 6.9 (Si(CH$_2$<u>C</u>H$_3$)$_3$), 5.0 (Si(<u>C</u>H$_2$CH$_3$)$_3$); **FTIR ν_{max}** 3454 (w, br OH str), 2970 (w, sp^3 CH str), 2917 (w, sp^3 CH str), 2850 (w, sp^3 CH str), 1745 (s, sh, C=O str), 1673, 1632, 1536, 1455, 1415, 1365, 1229 (s, sh, C-O str), 1217, 1205, 1150, 1099, 1009, 870, 837, 732, 698, 663; $[\alpha]_D^{20}$ –9.2 (*c* 1.0, $CHCl_3$); **HRMS** (ESI$^+$): calculated for $C_{27}H_{44}O_5SiNa$ $[M+Na]^+$ 499.2856, found 499.2842.

(*R, R*)-Mosher ester 165

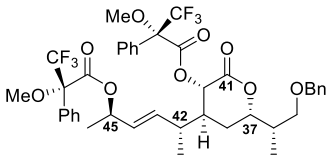

DCC (20 µL, 18.9 µmol, 1 M in CH_2Cl_2) was added dropwise to a stirred solution of allylic alcohol *anti*-**144a** (1.8 mg, 3.78 µmol), (*R*)-MTPA (4.4 mg, 18.9 µmol) and DMAP (2.3 mg, 18.9 µmol) in CH_2Cl_2 (400 µL). The reaction was stirred and monitored by TLC, until the starting material was consumed (*ca.* 8 h, rt). The reaction mixture was filtered through cotton wool and the filtrate

concentrated *in vacuo*. Purification by flash column chromatography (SiO_2, 5-20% EtOAc/PE 40-60) afforded (*R, R*)-Mosher ester **165** (2.6 mg, 3.27 µmol, 87%) as a colourless oil. $\mathbf{R_f}$ (30% EtOAc/PE 40-60) = 0.68; **^{1}H NMR** (500 MHz, $CDCl_3$) δ 7.67 (m, 2H, PhH), 7.51-7.29 (m, 13H, PhH), 5.66 (m, 1H, H43), 5.53 (m, 1H, H44), 5.51 (m, 1H, H45), 5.40 (d, 1H, *J* = 11.3 Hz, H40), 4.49 (ABq, 2H, J_{AB} = 12.0 Hz), 4.44 (m, 1H, H37), 3.54 (s, 3H, -OMe), 3.51 (s, 3H, -OMe), 3.41 (m, 2H, H35), 2.49 (m, 1H, H42), 2.28 (m, 1H, H39), 1.90 (m, 1H, H36), 1.85 (m, 1H, H38a), 1.67 (m, 1H, H38b), 1.33 (d, 3H, *J* = 6.1 Hz, H46), 0.99 (d, 3H, *J* = 6.9 Hz, Me42), 0.98 (d, 3H, *J* = 6.9 Hz, Me36).

(*S, S*)-Mosher ester 166

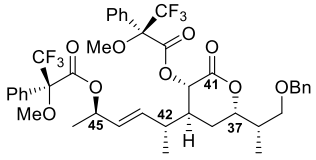

The diastereomeric (*S, S*)-Mosher ester **166** was prepared analogously to (*R, R*)-Mosher ester **165** (*vide supra*) from allylic alcohol *anti*-**144a** (1.8 mg, 3.78 µmol), (*S*)-MTPA (4.4 mg, 18.9 µmol), DCC (20 µL, 18.9 µmol, 1 M in CH_2Cl_2) DMAP (2.3 mg, 18.9 µmol) in CH_2Cl_2 (400 µL). Purification by flash column chromatography (5-20% EtOAc/PE 40-60) afforded (*S, S*)-Mosher ester **166** (2.5 mg, 3.15 µmol, 83%), as a colourless oil. $\mathbf{R_f}$ (30% EtOAc/PE 40-60) = 0.73; **^{1}H NMR** (500 MHz, $CDCl_3$) δ 7.72 (m, 2H, PhH), 7.48-7.30 (m, 13H, PhH), 5.48 (m, 1H, H45), 5.45 (m, 1H, H43), 5.43 (d, 1H, *J* = 11.7 Hz, H40), 5.23 (m, 1H, H44), 4.49 (ABq, 2H, J_{AB} = 12.0 Hz), 4.43 (m, 1H, H37), 3.70 (s, 3H, -OMe), 3.53 (s, 3H, -OMe), 3.43 (dd, 1H, *J* = 9.3, 6.9 Hz, H35a), 3.40 (dd, 1H, *J* = 9.3, 5.2 Hz, H35b), 2.15 (m, 1H, H39), 2.11 (m, 1H, H42), 1.90 (m, 1H, H36), 1.80 (m, 1H, H38a), 1.58 (m, 1H, H38b), 1.34 (d, 3H, *J* = 6.4 Hz, H46), 0.99 (d, 3H, *J* = 6.9 Hz, Me36), 0.80 (d, 3H, *J* = 6.9 Hz, Me42).

Bis-TES ethers C42, C45-*anti*-167a and C42, C45-*syn*-167b

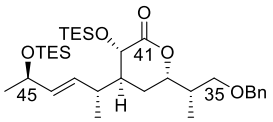

anti-**167a**

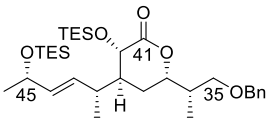

syn-**167b**

2,6-Lutidine (10 µL, 94.4 µmol) was added to a stirred solution of allylic alcohol *anti*-**144a** (15.0 mg, 31.5 µmol) in CH_2Cl_2 (300 µL). The reaction mixture was cooled to –78 °C and stirred for 5 min before TESOTf (20 µL, 62.9 µmol) was slowly added dropwise. After 30 min, the reaction mixture was quenched with $NaHCO_3$ (10 mL), allowed to warm to rt, the layers separated and the aqueous layer extracted with CH_2Cl_2 (3 x 2 mL). The combined organic extracts were washed with brine (10 mL), dried ($MgSO_4$), filtered and concentrated *in vacuo*. Purification by flash column

chromatography (SiO_2, 2.5% EtOAc/PE 40-60) afforded *bis* TES ether *anti*-**167a** (18.6 mg, 31.5 µmol, quant.), as a colourless oil: $\mathbf{R_f}$ (30% EtOAc/PE 40-60) = 0.70; **^{1}H NMR** (700 MHz, $CDCl_3$) δ 7.36-7.27 (m, 5H, ArH), 5.51 (dd, 1H, *J* = 15.6, 5.6 Hz, H43), 5.47 (dd, 1H, *J* = 15.6, 4.6 Hz, H44), 4.48 (ABq, 2H, J_{AB} = 12.0 Hz, PhCH_2), 4.31 (ddd, 1H, *J* = 12.0, 4.2, 3.9 Hz, H37), 4.27 (d, 1H, *J* = 10.2 Hz, H40), 4.25 (m, 1H, H45), 3.45 (dd, 1H, *J* = 9.2, 6.9 Hz, H35a), 3.39 (dd, 1H, *J* = 9.3, 5.2 Hz, H35b), 2.65 (m, 1H, H42), 2.00 (m, 1H, H39), 1.88 (m, 1H, H36), 1.79 (ddd, 1H, *J* = 14.5, 12.0, 10.2 Hz, H38a), 1.58 (ddd, 1H, *J* = 14.5, 4.1, 3.8 Hz, H38b), 1.20 (d, 3H, *J* = 6.3 Hz, H46), 1.00 (d, 3H, *J* = 6.9 Hz, Me42), 0.98 (t, 9H, *J* = 7.9 Hz, Si(CH_2CH_3)$_3$), 0.97 (d, 3H, *J* = 6.9 Hz, Me36), 0.69 (m, 6H, Si(CH_2CH_3)$_3$); **^{13}C NMR** (125 MHz, $CDCl_3$) δ 174.0 (C41=O), 138.2 (ArC), 134.7 (C44), 132.0 (C43), 128.4 (ArCH), 127.7 (ArCH), 127.6 (ArCH), 76.1 (C37), 73.3 (PhCH_2), 71.8 (C35), 68.9 (C45), 68.4 (C40), 41.7 (C39), 38.0 (C36), 34.6 (C42), 25.1 (C38), 24.8 (C46), 12.5 (Me42), 11.5 (Me36), 6.9 and 6.8 (2 x Si(CH_2CH_3)$_3$), 5.0 and 4.8 (2 x Si(CH_2CH_3)$_3$); **FTIR ν_{max}** 2953 (w, sp^3 CH str), 2927 (w, sp^3 CH str), 2875 (w, sp^3 CH str), 1762 (s, sh, C=O str), 1672, 1457, 1415, 1377, 1238, 1201, 1136 (s, sh, C-O str), 1086, 1052, 1004 (s, sh, C-O str), 918, 875, 833, 805, 724; $[\alpha]_D^{20}$ +10.6 (*c* 1.0, $CHCl_3$); **HRMS** (ESI^+): calculated for $C_{33}H_{58}O_5Si_2Na$ $[M+Na]^+$ 613.3720, found 613.3711.

Analogous conditions were used to protect allylic alcohol *syn*-**144b** (57.0 mg, 0.120 mmol) and afforded *bis* TES ether *syn*-**167b** (62.8 mg, 106 µmol, 89%), as a colourless oil: $\mathbf{R_f}$ (30% EtOAc/PE 40-60) = 0.70; **^{1}H NMR** (500 MHz, $CDCl_3$) δ 7.36-7.28 (m, 5H, ArH), 5.48 (m, 2H, H43 and H44), 4.49 (ABq, 2H, J_{AB} = 12.2 Hz, PhCH_2), 4.33 (ddd, 1H, *J* = 11.8, 4.1, 3.9 Hz, H37), 4.26 (d, 1H, *J* = 9.8 Hz, H40), 4.25 (m, 1H, H45), 3.46 (dd, 1H, *J* = 9.2, 7.0 Hz, H35a), 3.39 (dd, 1H, *J* = 9.2, 5.3 Hz, H35b), 2.62 (m, 1H, H42), 1.98 (m, 1H, H39), 1.88 (m, 1H, H36), 1.81 (ddd, 1H, *J* = 14.4, 12.1, 10.2 Hz, H38a), 1.60 (ddd, 1H, *J* = 14.5, 4.1, 3.8 Hz, H38b), 1.21 (d, 3H, *J* = 6.3 Hz, H46), 0.99 (d, 3H, *J* = 6.9 Hz, Me36), 0.98 (t, 9H, *J* = 7.9 Hz, Si(CH_2CH_3)$_3$), 0.97 (d, 3H, *J* = 6.9 Hz, Me42), 0.68 (m, 6H, Si(CH_2CH_3)$_3$); **^{13}C NMR** (125 MHz, $CDCl_3$) δ 173.90 (C41=O), 138.2 (ArC), 134.9 (C44), 132.1 (C43), 128.4 (ArCH), 127.7 (ArCH), 127.6 (ArCH), 76.0 (C37), 73.3 (PhCH_2), 71.7 (C35), 69.1 (C45), 68.5 (C40), 41.8 (C39), 37.9 (C36), 34.8 (C42), 25.1 (C38), 24.8 (C46), 12.5 (Me42), 11.4 (Me36), 6.9 and 6.8 (2 x Si(CH_2CH_3)$_3$), 5.0 and 4.8 (2 x Si(CH_2CH_3)$_3$); **FTIR ν_{max}** 2953 (w, sp^3 CH str), 2927 (w, sp^3 CH str), 2875 (w, sp^3 CH str), 1762 (s, sh, C=O str), 1672, 1457, 1415, 1377, 1238, 1201, 1136 (s, sh, C-O str), 1086, 1052, 1004 (s, sh, C-O str), 918, 875, 833, 805, 724; $[\alpha]_D^{20}$ –16.2 (*c* 1.0, $CHCl_3$); **HRMS** (ESI^+): calculated for $C_{33}H_{58}O_5Si_2Na$ $[M+Na]^+$ 613.3720, found 613.3704.

Primary alcohol C42, C45-*syn*-169b

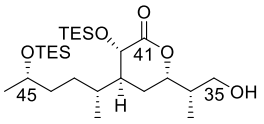

syn-**169b**
desired product

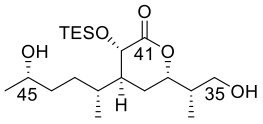

syn-**168b**
by-product 1

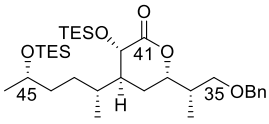

syn-**209b**
by-product 2

A spatula tip of freshly prepared Ra-Ni slurry was added to a stirred solution of allylic TES ether *syn*-**167b** (15.5 mg, 26.2 µmol) in EtOAc (3 mL), under $Ar_{(g)}$. The reaction mixture was flushed with $H_{2(g)}$, the suba seal rapidly changed for a fresh seal and a fresh $H_{2(g)}$ balloon fitted. The reaction was stirred for 13h, with careful monitoring, then filtered and concentrated *in vacuo*. Purification by flash column chromatography (SiO_2, 2.5% - 100% EtOAc/PE 40-60) afforded two by-products, diol *syn*-**168b** (5.1 mg, 13.1 µmol, 50%) and TES ether *syn*-**169b** (1.2 mg, 2.1 µmol, 8%.),as well as the desired *syn*-primary alcohol **169b** (5.6 mg, 11.1 µmol, 42%.), as a colourless oil: $\mathbf{R_f}$ (30% EtOAc/PE 40-60) = 0.44; **^{1}H NMR** (700 MHz, $CDCl_3$) δ 4.35 (ddd, 1H, *J* = 11.9, 3.9, 3.8 Hz, H37), 4.28 (d, 1H, *J* = 10.5 Hz, H40), 3.77 (m, 1H, H45), 3.68 (dd, 1H, *J* = 10.6, 7.1 Hz, H35a), 3.61 (dd, 1H, *J* = 10.6, 5.1 Hz, H35b), 1.97 (m, 1H, H39), 1.94 (m, 1H, H42), 1.82 (m, 1H, H36), 1.81 (m, 1H, H38a), 1.62 (ddd, 1H, *J* = 14.4, 4.1, 3.9 Hz, H38b), 1.46 (m, 1H, H44a), 1.36 (m, 1H, H44b), 1.34 (m, 1H, H43a), 1.20 (m, 1H, H43b), 1.14 (d, 3H, *J* = 6.1 Hz, H46), 1.00 (d, 3H, *J* = 7.0 Hz, Me36), 0.98 (t, 9H, *J* = 7.9 Hz, $Si(CH_2\underline{CH_3})_3$), 0.96 (t, 9 H, *J* = 7.9 Hz, $Si(CH_2\underline{CH_3})_3$), 0.86 (d, 3H, *J* = 6.8 Hz, Me42), 0.68 (m, 6H, $Si(\underline{CH_2}CH_3)_3$), 0.59 (q, 6H, *J* = 8.0 Hz, $Si(\underline{CH_2}CH_3)_3$); **^{13}C NMR** (125 MHz, $CDCl_3$) δ 174.4 (C41=O), 75.8 (C37), 68.41 (C45), 68.35 (C40), 64.4 (C35), 41.0 (C39), 39.5 (C36), 37.4 (C44), 32.0 (C42), 30.9 (C43), 24.4 (C38), 23.8 (C46), 13.0 (Me42), 11.0 (Me36), 6.88 and 6.85 (2 x $Si(CH_2\underline{CH_3})_3$), 5.0 and 4.9 (2 x $Si(\underline{CH_2}CH_3)_3$); **FTIR ν_{max}** 3459 (w, br, OH str), 2954 (w, sp^3 CH str), 2928 (w, sp^3 CH str), 2857 (w, sp^3 CH str), 1741 (s, sh, C=O str), 1668, 1461, 1413, 1374, 1217, 1150 (s, sh, C-O str), 1085, 1040, 1004, 939, 833, 810, 773, 731, 680, 662; $[\alpha]_D^{20}$ +7.1 (*c* 1.0, $CHCl_3$); **HRMS** (ESI^+): calculated for $C_{26}H_{54}O_5Si_2Na$ $[M+Na]^+$ 525.3407, found 525.3402.

Aldehyde C42, C45-*syn*-210b

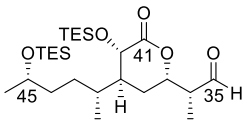

DMP (7.8 mg, 17.9 µmol) was added to a stirred solution of primary alcohol *syn*-**169b** (1.5 mg, 2.98 µmol) and $NaHCO_{3(s)}$ (3.0 mg, 35.8 µmol) in CH_2Cl_2 (1 mL) at rt. The mixture was stirred for 1h and quenched with premixed $NaHCO_3$ (100 µL) and $Na_2S_2O_3$ (100 µL), by stirring for 30 min. The layers were separated and the aqueous layer extracted with CH_2Cl_2 (3 x 2 mL). The combined organic

phases were washed with brine (10 mL), dried ($MgSO_4$), filtered and concentrated *in vacuo* to afford crude aldehyde *syn*-**210b** (~1.5 mg, ~2.98 µmol, ~quant.), as a colourless oil: $\mathbf{R_f}$ (30% EtOAc/PE 40-60) = 0.40; **^{1}H NMR** (700 MHz, $CDCl_3$) δ 9.71 (s, 1H, H35), 4.51 (m, 1H, H37), 4.29 (d, 1H, *J* = 10.5 Hz, H40), 3.76 (m, 1H, H45), 2.61 (m, 1H, H36), 2.00 (m, 1H, H39), 1.95 (m, 1H, H42), 1.8-1.6 (m, 2H, H38), 1.5-1.3 (m, 4H, H44 and H43), 1.26 (d, 3H, *J* = 5.7 Hz Me36), 1.13 (d, 3H, *J* = 6.0 Hz, H46), 0.98 (t, 9 H, *J* = 7.9 Hz, $Si(CH_2\underline{CH_3})_3$), 0.95 (t, 9 H, *J* = 7.9 Hz, $Si(CH_2\underline{CH_3})_3$), 0.89 (d, 3H, *J* = 6.8 Hz, Me42), 0.68 (m, 6H, $Si(\underline{CH_2}CH_3)_3$), 0.58 (q, 6H, *J* = 7.8 Hz, $Si(\underline{CH_2}CH_3)_3$).

Olefin C42, C45-*syn*-170b

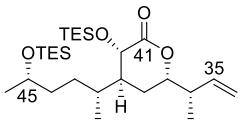

*n*BuLi (80 µL, 121 µmol) was added, dropwise, to a suspension of methyltriphenylphosphonium bromide (45.5 mg, 127 µmol) in THF (5 mL), at 0 °C, and stirred for 30 min. The reaction was then allowed to warm to rt and stirred for 1h, after which the temperature was lowered to –78 °C. Stirred crude aldehyde *syn*-**210b** (ca. 2.3 mg, 4.6 µmol) in THF (5 mL), at –78 °C, was cannulated into the solution and stirred for 30 min. The reaction was quenched with NH_4Cl (10 mL) and allowed to warm to rt. The layers were separated and the aqueous layer extracted with CH_2Cl_2 (3 x 2 mL). The combined organic phases were washed with brine (10 mL), dried ($MgSO_4$), filtered and concentrated *in vacuo*. Purification by flash column chromatography (SiO_2, 2.5-25% EtOAc/PE 40-60) afforded olefin *syn*-**170b** (2.1 mg, 4.21 µmol, 66% over two steps), as a colourless oil: $\mathbf{R_f}$ (15% EtOAc/PE 40-60) = 0.60; **^{1}H NMR** (700 MHz, $CDCl_3$) δ 5.69 (ddd, 1H, *J* = 17.2, 10.3, 8.0 Hz, H35), 5.09 (m, 2H, H34), 4.22 (d, 1H, *J* = 10.6 Hz, H40), 3.94 (ddd, 1H, *J* = 10.3, 7.4, 4.5 Hz, H37), 3.76 (m, 1H, H45), 2.38 (m, 1H, H36), 1.95 (m, 1H, H39), 1.92 (m, 1H, H42), 1.64 (m, 2H, H38), 1.46 (m, 1H, H44a), 1.34 (m, 2H, H44b and H43a), 1.17 (m, 1H, H43b), 1.13 (d, 3H, *J* = 6.1 Hz, H46), 1.12 (d, 3H, *J* = 7.0 Hz, Me36), 0.98 (t, 9 H, *J* = 7.9 Hz, $Si(CH_2\underline{CH_3})_3$), 0.95 (t, 9 H, *J* = 7.9 Hz, $Si(CH_2\underline{CH_3})_3$), 0.83 (d, 3H, *J* = 6.8 Hz, Me42), 0.68 (m, 6H, $Si(\underline{CH_2}CH_3)_3$), 0.58 (q, 6H, *J* = 7.8 Hz, $Si(\underline{CH_2}CH_3)_3$); **^{13}C NMR** (125 MHz, $CDCl_3$) δ 174.4 (C41=O), 138.6 (C35), 116.3 (C34), 78.9 (C37), 68.5 (C40), 68.4 (C45), 42.9 (C36), 40.9 (C39), 37.5 (C44), 32.0 (C42), 31.0 (C43), 24.9 (C38), 23.8 (C46), 16.0 (Me36), 12.9 (Me42), 6.88 and 6.86 (2 x $Si(CH_2\underline{CH_3})_3$), 5.0 and 4.9 (2 x $Si(\underline{CH_2}CH_3)_3$); **FTIR ν_{max}** 2953 (w, sp^3 CH str), 2927 (w, sp^3 CH str), 2875 (w, sp^3 CH str), 1762 (s, sh, C=O str), 1672, 1457, 1415, 1377, 1238, 1136 (s, sh, C-O str), 1086, 1004, 918, 833, 805, 724; $[\boldsymbol{\alpha}]_{\mathbf{D}}^{\mathbf{20}}$ –10.2 (*c* 1.0, $CHCl_3$); **HRMS** (ESI^+): calculated for $C_{27}H_{54}O_4Si_2Na$ $[M+Na]^+$ 521.3458, found 521.3451.

Diols C42, C45-*anti*-168a and C42, C45-*syn*-168b

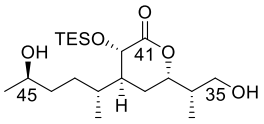

anti-**168a**

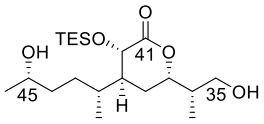

syn-**168b**

A spatula tip of freshly prepared Ra-Ni slurry was added to a stirred solution of allylic alcohol *anti*-**164a** (19.9 mg, 41.7 µmol) in EtOAc (3 mL), under $Ar_{(g)}$. The reaction mixture was flushed with $H_{2(g)}$, the suba seal rapidly changed for a fresh seal and a fresh $H_{2(g)}$ balloon fitted. The reaction was stirred for ~18h, then filtered and concentrated *in vacuo*. Purification by flash column chromatography (SiO_2, 30% - 100% EtOAc/PE 40-60) afforded diol *anti*-**168a** (16.2 mg, 41.7 µmol, quant.), as a colourless oil: $\mathbf{R_f}$ (100% EtOAc) = 0.49; **^{1}H NMR** (700 MHz, $CDCl_3$) δ 4.35 (ddd, 1H, *J* = 11.8, 4.4, 3.5 Hz, H37), 4.28 (d, 1H, *J* = 10.4 Hz, H40), 3.79 (m, 1H, H45), 3.67 (ddd, 1H, *J* = 10.5, 7.0, 5.2 Hz, H35a), 3.62 (ddd, 1H, *J* = 10.6, 5.1, 4.5 Hz, H35b), 1.99 (m, 1H, H39), 1.98 (m, 1H, H42), 1.84 (m, 1H, H38a), 1.83 (m, 1H, H36), 1.63 (ddd, 1H, *J* = 14.5, 4.3, 3.7 Hz, H38b), 1.52 (dd, 1H, *J* = 5.3, 5.1 Hz, C35O<u>H</u>), 1.45 (m, 2H, H44), 1.39 (m, 1H, H43a), 1.29 (d, 1H, *J* = 4.7 Hz, C45O<u>H</u>), 1.27 (m, 1H, H43b), 1.20 (d, 3H, *J* = 6.2 Hz, H46), 1.00 (d, 3H, *J* = 7.0 Hz, Me42), 0.98 (t, 9H, *J* = 7.9 Hz, Si($CH_2\underline{CH_3}$)$_3$), 0.89 (d, 3H, *J* = 6.8 Hz, Me36), 0.68 (m, 6H, Si($\underline{CH_2}CH_3$)$_3$); **^{13}C NMR** (125 MHz, $CDCl_3$) δ 174.4 (C41=O), 75.6 (C37), 68.3 (C40), 68.2 (C45), 64.4 (C35), 40.7 (C39), 39.5 (C36), 37.0 (C44), 32.0 (C42), 31.0 (C43), 24.4 (C38), 23.7 (C46), 13.1 (Me42), 11.0 (Me36), 6.9 (Si($CH_2\underline{CH_3}$)$_3$), 5.0 (Si($\underline{CH_2}CH_3$)$_3$); **FTIR ν_{max}** 3300 (br, s) 2954 (w, sp^3 CH str), 2875 (w, sp^3 CH str), 1740, 1638 (s, sh, C=O str), 1457, 1406, 1257, 1153 (s, sh, C-O str), 1004 (s, sh, C-O str), 673; $[\alpha]_D^{20}$ –7.2 (*c* 1.0, $CHCl_3$); **HRMS** (ESI^+): calculated for $C_{20}H_{40}O_5SiNa$ $[M+Na]^+$ 411.2543, found 411.2540.

Analogous conditions were used to concurrently hydrogenate and debenzylate allylic alcohol *syn*-**164b** (19.2 mg, 40.3 µmol) and afforded diol *syn*-**168b** (14.1 mg, 36.6 µmol, 90%), as a colourless oil: $\mathbf{R_f}$ (100% EtOAc) = 0.49; **^{1}H NMR** (600 MHz, $CDCl_3$) δ 4.35 (ddd, 1H, *J* = 11.9, 4.4, 3.4 Hz, H37), 4.28 (d, 1H, *J* = 10.4 Hz, H40), 3.78 (m, 1H, H45), 3.66 (dd, 1H, *J* = 10.6, 7.2 Hz, H35a), 3.61 (dd, 1H, *J* = 10.7, 5.1 Hz, H35b), 1.98 (m, 1H, H39), 1.97 (m, 1H, H42), 1.84 (m, 1H, H38a), 1.83 (m, 1H, H36), 1.64 (ddd, 1H, *J* = 14.5, 4.5, 3.7 Hz, H38b), 1.62 (m, 1H, C35O<u>H</u>), 1.48 (m, 1H, H44a), 1.41 (m, 1H, H44b), 1.39 (m, 1H, H43a), 1.25 (m, 1H, H43b), 1.24 (d, 1H, *J* = 4.7 Hz, C45O<u>H</u>), 1.20 (d, 3H, *J* = 6.2 Hz, H46), 0.99 (d, 3H, *J* = 7.0 Hz, Me42), 0.97 (t, 9H, *J* = 7.9 Hz, Si($CH_2\underline{CH_3}$)$_3$), 0.88 (d, 3H, *J* = 6.7 Hz, Me36), 0.68 (m, 6H, Si($\underline{CH_2}CH_3$)$_3$); **^{13}C NMR** (125 MHz, $CDCl_3$) δ 174.4 (C41=O), 75.8 (C37), 68.3 (C40), 68.2 (C45), 64.3 (C35), 41.0 (C39), 39.5 (C36), 37.1 (C44), 32.0 (C42), 31.1 (C43), 24.5 (C38), 23.7 (C46), 12.9 (Me42), 11.0 (Me36), 6.8 (Si($CH_2\underline{CH_3}$)$_3$), 4.9 (Si($\underline{CH_2}CH_3$)$_3$); **FTIR ν_{max}** 3300 (br, s) 2954 (w, sp^3 CH str), 2875 (w, sp^3 CH str), 1740, 1638 (s, sh, C=O str), 1457, 1406, 1257, 1153 (s,

sh, C-O str), 1004 (s, sh, C-O str), 673; $[\alpha]_D^{20}$ +3.7 (*c* 1.0, $CHCl_3$); **HRMS** (ESI^+): calculated for $C_{20}H_{40}O_5SiNa$ $[M+Na]^+$ 411.2543, found 411.2546.

Aldehydes C42, C45-*anti*-210a and C42, C45-*syn*-210b

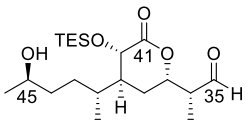

anti-**210a**

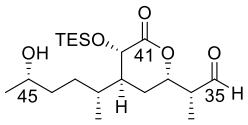

syn-**210b**

Iodobenzene diacetate (6.2 mg, 19.3 µmol) and TEMPO (0.8 mg, 5.15 µmol) were added to a stirred solution of diol *syn*-**168b** (5.0 mg, 12.9 µmol) in CH_2Cl_2 (1 mL) at rt. The mixture was stirred for 3h and quenched with $Na_2S_2O_3$ (1 mL), by stirring for 30 min. The layers were separated and the aqueous layer extracted with CH_2Cl_2 (3 x 2 mL). The combined organic phases were washed with brine (10 mL), dried ($MgSO_4$), filtered and concentrated *in vacuo* to afford crude aldehyde *syn*-**210b** (~ca. quant) as a slightly yellow oil: $\mathbf{R_f}$ (30% EtOAc/PE 40-60) = 0.19; **^{1}H NMR** (600 MHz, $CDCl_3$) δ 9.72 (s, 1H, H35), 4.52 (m, 1H, H37), 4.31 (d, 1H, *J* = 10.5 Hz, H40), 3.79 (m, 1H, H45), 2.62 (m, 1H, H36), 2.01 (m, 1H, H39), 1.98 (m, 1H, H42), 1.8-1.7 (m, 2H, H38), 1.5-1.3 (m, 4H, H44 and H43), 1.27 (d, 3H, *J* = 7.3 Hz, Me36), 1.21 (d, 3H, *J* = 6.1 Hz, H46), 0.99 (t, 9 H, *J* = 7.9 Hz, $Si(CH_2\underline{CH_3})_3$), 0.92 (d, 3H, *J* = 6.8 Hz, Me42), 0.69 (m, 6H, $Si(\underline{CH_2}CH_3)_3$).

Analogous conditions were used to oxidise diol *anti*-**168a** (15.0 mg, 38.6 µmol) to afford crude aldehyde *anti*-**210a** (~ca. quant) as a slightly yellow oil: $\mathbf{R_f}$ (30% EtOAc/PE 40-60) = 0.19, reaction conversion assessed by TLC comparison to *syn*-aldehyde **210b**.

Terminal Olefins C42, C45-*anti*-212a and C42, C45-*syn*-212b

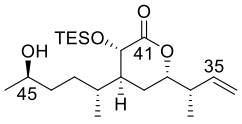

anti-**212a**

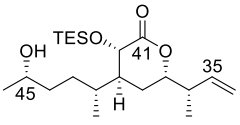

syn-**212b**

*n*BuLi (150 µL, 244 µmol) was added, dropwise, to a suspension of methyltriphenylphosphonium bromide (91.9 mg, 257 µmol) in THF (10 mL), at 0 °C, and stirred for 30 min. The reaction was then allowed to warm to rt and stirred for 1h, after which the temperature was lowered to –78 °C. Stirred aldehyde *syn*-**210b** (crude) in THF (5 mL), at –78 °C, was cannulated into the solution and stirred for 30 min. The reaction was quenched with NH_4Cl (10 mL) and allowed to warm to rt. The layers were separated and the aqueous layer extracted with CH_2Cl_2 (3 x 2 mL). The combined organic phases were washed with brine (10 mL), dried ($MgSO_4$), filtered and concentrated *in*

vacuo. Purification by flash column chromatography (SiO_2, 2.5-100% EtOAc/PE 40-60) afforded olefin *syn*-**212b** (1.9 mg, 4.94 µmol, 39% over two steps), as a colourless oil: $\mathbf{R_f}$ (15% EtOAc/PE 40-60) = 0.40; **^{1}H NMR** (700 MHz, $CDCl_3$) δ 5.70 (ddd, 1H, *J* = 17.3, 10.3, 8.0 Hz, H35), 5.11 (d, 1H, *J* = 17.3 Hz, H34a), 5.09 (d, 1H, *J* = 10.3 Hz, H34b), 4.23 (d, 1H, *J* = 10.6 Hz, H40), 3.95 (ddd, 1H, *J* = 10.1, 7.3, 4.8 Hz, H37), 3.77 (m, 1H, H45), 2.39 (m, 1H, H36), 1.96 (m, 1H, H39), 1.95 (m, 1H, H42), 1.7-1.6 (m, 2H, H38), 1.47 (m, 1H, H44a), 1.40 (m, 1H, H44b), 1.38 (m, 1H, H43a), 1.23 (m, 1H, H43b), 1.20 (d, 3H, *J* = 6.2 Hz, H46), 1.12 (d, 3H, *J* = 6.8 Hz, Me36), 0.98 (t, 9 H, *J* = 7.9 Hz, $Si(CH_2\underline{CH_3})_3$), 0.85 (d, 3H, *J* = 6.8 Hz, Me42), 0.68 (m, 6H, $Si(\underline{CH_2}CH_3)_3$); **^{13}C NMR** (125 MHz, $CDCl_3$) δ 174.2 (C41=O), 138.6 (C35), 116.4 (C34), 78.9 (C37), 68.5 (C40), 68.2 (C45), 42.8 (C36), 40.9 (C39), 37.2 (C44), 32.0 (C42), 31.2 (C43), 24.9 (C38), 23.7 (C46), 15.9 (Me36), 12.9 (Me42), 6.9 ($Si(CH_2\underline{CH_3})_3$), 5.0 ($Si(\underline{CH_2}CH_3)_3$); **FTIR ν_{max}** 3445 (w, br, OH str), 2959 (w, sp^3 CH str), 2931 (w, sp^3 CH str), 2875 (w, sp^3 CH str), 1751 (s, sh, C=O str), 1643, 1457, 1414, 1379, 1241, 1145 (s, sh, C-O str), 1004 (s, sh, C-O str), 918, 833, 801, 727, 695; $[\alpha]_D^{20}$ –4.9 (*c* 1.0, $CHCl_3$); **HRMS** (ESI^+): calculated for $C_{21}H_40O_4SiNa$ $[M+Na]^+$ 407.2594, found 407.2587.

Analogous conditions were used to olefinate crude aldehyde *anti*-**210a** to afford olefin *anti*-**212a** (4.4 mg, 11.4 µmol, 30% over 2 steps) as a slightly yellow oil: $\mathbf{R_f}$ (30% EtOAc/PE 40-60) = 0.42; **^{1}H NMR** (700 MHz, $CDCl_3$) δ 5.70 (ddd, 1H, *J* = 17.3, 10.3, 7.8 Hz, H35), 5.12 (d, 1H, *J* = 17.3 Hz, H34a), 5.09 (d, 1H, *J* = 10.3 Hz, H34b), 4.23 (d, 1H, *J* = 10.5 Hz, H40), 3.95 (ddd, 1H, *J* = 10.0, 7.2, 4.8 Hz, H37), 3.78 (m, 1H, H45), 2.39 (m, 1H, H36), 1.97 (m, 1H, H39), 1.96 (m, 1H, H42), 1.7-1.6 (m, 2H, H38), 1.46 (m, 1H, H44a), 1.43 (m, 1H, H44b), 1.35 (m, 1H, H43a), 1.24 (m, 1H, H43b), 1.20 (d, 3H, *J* = 6.2 Hz, H46), 1.12 (d, 3H, *J* = 6.8 Hz, Me36), 0.98 (t, 9 H, *J* = 7.9 Hz, $Si(CH_2\underline{CH_3})_3$), 0.86 (d, 3H, *J* = 6.7 Hz, Me42), 0.68 (m, 6H, $Si(\underline{CH_2}CH_3)_3$); **^{13}C NMR** (125 MHz, $CDCl_3$) δ 174.3 (C41=O), 138.6 (C35), 116.4 (C34), 78.9 (C37), 68.5 (C40), 68.2 (C45), 42.8 (C36), 40.6 (C39), 37.0 (C44), 31.9 (C42), 30.9 (C43), 24.9 (C38), 23.6 (C46), 15.9 (Me36), 13.0 (Me42), 6.9 ($Si(CH_2\underline{CH_3})_3$), 5.0 ($Si(\underline{CH_2}CH_3)_3$); **FTIR ν_{max}** 3445 (w, br, OH str), 2959 (w, sp^3 CH str), 2931 (w, sp^3 CH str), 2875 (w, sp^3 CH str), 1751 (s, sh, C=O str), 1643, 1457, 1414, 1379, 1241, 1145 (s, sh, C-O str), 1004 (s, sh, C-O str), 918, 833, 801, 727, 695; $[\alpha]_D^{20}$ –8.6 (*c* 1.0, $CHCl_3$); **HRMS** (ESI^+): calculated for $C_{21}H_40O_4SiNa$ $[M+Na]^+$ 407.2594, found 407.2583.

Diols C42, C45-*anti*-171a and C42, C45-*syn*-171b

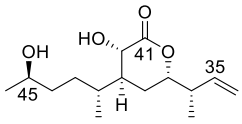

anti-**171a**

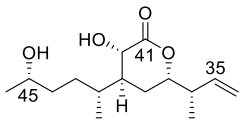

syn-**171b**

HF·pyridine (50 µL) was added, dropwise, to stirring pyridine (150 µL), at 0 °C, to create HF·py/py (200 µL, 1:3 v/v). This solution was stirred for 15 min and then added, dropwise, to a solution of olefin *syn*-**170b** (2.1 mg, 4.21 µmol) in THF (1 mL), at 0 °C, and stirred for 30 min. The reaction was then allowed to warm to rt and stirred for an additional 30-45 min. The reaction was quenched with $NaHCO_3$ (10 mL). The layers were separated and the aqueous layer extracted with CH_2Cl_2 (3 x 2 mL). The combined organic phases were washed with brine (10 mL), dried ($MgSO_4$), filtered and concentrated *in vacuo*. Purification by flash column chromatography (SiO_2, 30-100% EtOAc/PE 40-60) afforded diol *syn*-**171b** (1.1 mg, 4.21 µmol, quant.), as a colourless oil: $\mathbf{R_f}$ (30% EtOAc/PE 40-60) = 0.05; **^{1}H NMR** (700 MHz, $CDCl_3$) δ 5.71 (ddd, 1H, *J* = 17.2, 10.3, 7.9 Hz, H35), 5.14 (ddd, 1H, *J* = 17.2, 1.5, 1.1 Hz, H34a), 5.10 (ddd, 1H, *J* = 10.4, 1.5, 0.8 Hz, H34b), 4.21 (dd, 1H, *J* = 11.2, 2.0 Hz, H40), 4.05 (m, 1H, H37), 3.79 (m, 1H, H45), 2.43 (m, 1H, H36), 2.02 (m, 1H, H42), 2.00 (m, 1H, H39), 1.89 (m, 1H, H38a), 1.63 (m, 1H, H38b), 1.45-1.38 (m, 4H, H44 and H43), 1.20 (d, 3H, *J* = 6.2 Hz, H46), 1.13 (d, 3H, *J* = 6.8 Hz, Me36), 0.91 (d, 3H, *J* = 6.8 Hz, Me42); **^{13}C NMR** (125 MHz, $CDCl_3$) δ 176.8 (C41=O), 138.1 (C35), 116.7 (C34), 79.6 (C37), 68.2 (C40), 67.1 (C45), 42.6 (C36), 40.8 (C39), 36.9 (C44), 32.7 (C42), 30.9 (C43), 25.3 (C38), 23.8 (C46), 15.8 (Me36), 13.0 (Me42); **^{1}H NMR** (700 MHz, CD_3OD) δ 5.76 (ddd, 1H, *J* = 17.2, 10.4, 8.0 Hz, H35), 5.15 (ddd, 1H, *J* = 17.2, 1.7, 1.1 Hz, H34a), 5.10 (ddd, 1H, *J* = 10.4, 1.7, 0.7 Hz, H34b), 4.37 (d, 1H, *J* = 11.3 Hz, H40), 4.17 (ddd, 1H, *J* = 10.5, 7.4, 4.2 Hz, H37), 3.70 (m, 1H, H45), 2.40 (m, 1H, H36), 1.97 (m, 1H, H42), 1.89 (m, 1H, H39), 1.77 (ddd, 1H, *J* = 14.6, 5.1, 3.9 Hz, H38a), 1.66 (ddd, 1H, *J* = 14.5, 10.6, 3.8 Hz, H38b), 1.48 (m, 1H, H44a), 1.40 (m, 1H, H44b), 1.39 (m, 1H, H43b), 1.27 (m, 1H, H43b), 1.15 (d, 3H, *J* = 6.2 Hz, H46), 1.12 (d, 3H, *J* = 6.7 Hz, Me36), 0.91 (d, 3H, *J* = 6.7 Hz, Me42); **^{13}C NMR** (125 MHz, CD_3OD) δ 178.3 (C41=O), 140.1 (C35), 116.7 (C34), 80.4 (C37), 68.6 (C40), 68.2 (C45), 44.1 (C36), 41.5 (C39), 38.0 (C44), 33.7 (C42), 32.0 (C43), 26.3 (C38), 23.5 (C46), 16.2 (Me36), 13.2 (Me42); **FTIR ν_{max}** 3422 (w, br, OH str), 2924 (w, sp^3 CH str), 2926 (w, sp^3 CH str), 2853 (w, sp^3 CH str), 1737 (s, sh, C=O str), 1666, 1457, 1418, 1376, 1257 (s, sh, C-O str), 1208, 1104 (s, sh, C-O str), 1003, 920, 878, 847, 801, 757, 687; $[\alpha]_D^{20}$ –2.3 (*c* 1.0, $CHCl_3$); **HRMS** (ESI^+): calculated for $C_{15}H_{26}O_4Na$ $[M+Na]^+$ 293.1729, found 293.1727.

Analogous conditions were used to deprotect olefin *anti*-**170a** (2.1 mg, 5.46 mmol) and afforded diol *anti*-**171a** (1.5 mg, 5.46 µmol, quant.), as a colourless oil: $\mathbf{R_f}$ (30% EtOAc/PE 40-60) = 0.05; **^{1}H**

NMR (700 MHz, CD_3OD) δ 5.76 (ddd, 1H, *J* = 17.2, 10.4, 8.0 Hz, H35), 5.15 (ddd, 1H, *J* = 17.2, 1.7, 1.1 Hz, H34a), 5.10 (ddd, 1H, *J* = 10.4, 1.7, 0.7 Hz, H34b), 4.37 (d, 1H, *J* = 11.3 Hz, H40), 4.17 (ddd, 1H, *J* = 10.5, 7.4, 4.2 Hz, H37), 3.70 (m, 1H, H45), 2.40 (m, 1H, H36), 1.97 (m, 1H, H42), 1.89 (m, 1H, H39), 1.77 (ddd, 1H, *J* = 14.6, 5.1, 3.9 Hz, H38a), 1.66 (ddd, 1H, *J* = 14.5, 10.6, 3.8 Hz, H38b), 1.48 (m, 1H, H44a), 1.40 (m, 1H, H44b), 1.39 (m, 1H, H43b), 1.27 (m, 1H, H43b), 1.15 (d, 3H, *J* = 6.2 Hz, H46), 1.12 (d, 3H, *J* = 6.7 Hz, Me36), 0.91 (d, 3H, *J* = 6.7 Hz, Me42); **^{13}C NMR** (125 MHz, CD_3OD) δ 178.3 (C41=O), 140.1 (C35), 116.7 (C34), 80.4 (C37), 68.6 (C40), 68.2 (C45), 44.1 (C36), 41.5 (C39), 38.0 (C44), 33.7 (C42), 32.0 (C43), 26.3 (C38), 23.5 (C46), 16.2 (Me36), 13.2 (Me42); **FTIR ν_{max}** 3422 (w, br, OH str), 2924 (w, sp^3 CH str), 2926 (w, sp^3 CH str), 2853 (w, sp^3 CH str), 1737 (s, sh, C=O str), 1666, 1457, 1418, 1376, 1257 (s, sh, C-O str), 1208, 1104 (s, sh, C-O str), 1003, 920, 878, 847, 801, 757, 687; $[\alpha]_D^{20}$ –3.4 (*c* 1.0, $CHCl_3$); **HRMS** (ESI^+): calculated for $C_{15}H_{26}O_4Na$ $[M+Na]^+$ 293.1729, found 293.1726.

TBS ethers C42, C45-*anti*-211a and C42, C45-*syn(anti)*-211b

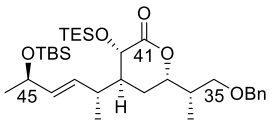

anti-**211a**

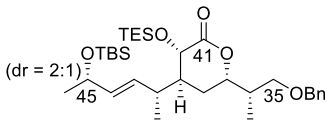

syn(anti)-**211b**

2,6-Lutidine (120 µL, 1.01 mmol) was added to a stirred solution of allylic alcohol *anti*-**164a** (160 mg, 336 µmol) in CH_2Cl_2 (3 mL). The reaction mixture was cooled to –78 °C and stirred for 5 min before TBSOTf (90 µL, 581 µmol) was slowly added dropwise. After 1.5 h, an additional aliquot of TBSOTf (40 µL, 258 µmol) was added dropwise and the reaction mixture stirred for an additional 30 min before the reaction was quenched with $NaHCO_3$ (10 mL), allowed to warm to rt, the layers separated and the aqueous layer extracted with CH_2Cl_2 (3 x 2 mL). The combined organic extracts were washed with brine (10 mL), dried ($MgSO_4$), filtered and concentrated *in vacuo*. Purification by flash column chromatography (SiO_2, 2.5-10% EtOAc/PE 40-60) afforded TBS ether *anti*-**211a** (183 mg, 0.310 mmol, 92%), as a colourless oil: **R_f** (15% EtOAc/PE 40-60) = 0.49; **^{1}H NMR** (700 MHz, $CDCl_3$) δ 7.36-7.27 (m, 5H, Ph), 5.51 (dd, 1H, *J* = 15.7, 5.3 Hz, H43), 5.45 (dd, 1H, *J* = 15.7, 4.5 Hz, H44), 4.48 (ABq, 2H, J_{AB} = 11.2 Hz, PhC$\underline{H}_2$), 4.32 (ddd, 1H, *J* = 12.0, 4.1, 4.0 Hz, H37), 4.27 (d, 1H, *J* = 9.8 Hz, H40), 4.26 (m, 1H, H45), 3.46 (dd, 1H, *J* = 9.2, 6.9 Hz, H35a), 3.39 (dd, 1H, *J* = 9.2, 5.2 Hz, H35b), 2.64 (m, 1H, H42), 1.99 (m, 1H, H39), 1.88 (m, 1H, H36), 1.79 (ddd, 1H, *J* = 14.4, 11.9, 10.2 Hz, H38a), 1.58 (ddd, 1H, *J* = 14.5, 4.0, 3.9 Hz, H38b), 1.19 (d, 3H, *J* = 6.3 Hz, H46), 1.00 (d, 3H, *J* = 6.9 Hz, Me42), 0.98 (t, 9H, *J* = 8.0 Hz, Si($CH_2\underline{CH}_3$)$_3$), 0.96 (d, 3H, *J* = 6.7 Hz, Me36), 0.89 (s, 9H, Si(CH_3)$_2$C($C\underline{H}_3$)$_3$), 0.69 (m, 6H, Si($\underline{CH}_2CH_3$)$_3$), 0.04 (s, 3H, Si($C\underline{H}_3$)$_2$C(CH_3)$_3$), 0.03 (s, 3H, Si($C\underline{H}_3$)$_2$C(CH_3)$_3$); **^{13}C NMR** (125 MHz, $CDCl_3$) δ 174.0 (C41=O), 138.2 (Ph$\underline{C}$), 134.7 (C44), 131.8 (C43),

128.4 (Ph<u>C</u>H), 127.7 (Ph<u>C</u>H), 127.6 (Ph<u>C</u>H), 76.1 (C37), 73.3 (Ph<u>C</u>H_2), 71.8 (C35), 69.0 (C45), 68.5 (C40), 41.7 (C39), 38.0 (C36), 34.6 (C42), 25.9 (Si(CH_3)$_2$C(<u>C</u>H_3)$_3$), 25.1 (C38), 24.7 (C46), 18.3 (Si(CH_3)$_2$<u>C</u>(CH_3)$_3$), 12.6 (Me42), 11.6 (Me36), 6.9 (Si(CH_2<u>C</u>H_3)$_3$), 5.0 (Si(<u>C</u>$H_2$$CH_3$)$_3$), –4.6 (Si(<u>C</u>$H_3$)$_2$C($CH_3$)$_3$), –4.8 (Si(<u>C</u>$H_3$)$_2$C($CH_3$)$_3$); **FTIR ν_{max}** 2956 (w, sp^3 CH str), 2928 (w, sp^3 CH str), 2875 (w, sp^3 CH str), 1760 (s, sh, C=O str), 1454, 1410, 1365, 1250, 1216, 1150 (s, sh, C-O str), 1090 (s, sh, C-O str), 1003, 970, 905, 831, 809, 774, 731, 663; $[\alpha]_D^{20}$ –19.4 (*c* 1.0, $CHCl_3$); **HRMS** (ESI^+): calculated for $C_{33}H_{58}O_5Si_2Na$ $[M+Na]^+$ 613.3720, found 613.3717.

Analogous conditions were used to produce TBS ether *syn(anti)*-**211b** (50.6 mg, 85.6 µmol, 70%, *dr* remains ca. 2:1), from allylic alcohol *syn(anti)*-**164b** (58 mg, 122 µmol), as a colourless oil: **R_f** (30% EtOAc/PE 40-60) = 0.67; **^{1}H NMR** (700 MHz, $CDCl_3$) δ 7.36-7.28 (m, 5H, Ph), 5.49 (dd, 1H, *J* = 15.7, 5.1 Hz, H43), 5.46 (dd, 1H, *J* = 15.7, 4.2 Hz, H44), 4.49 (ABq, 2H, J_{AB} = 11.8 Hz, PhC<u>H_2</u>), 4.33 (ddd, 1H, *J* = 12.0, 3.8, 3.4 Hz, H37), 4.26 (d, 1H, *J* = 9.6 Hz, H40), 4.25 (m, 1H, H45), 3.47 (dd, 1H, *J* = 9.2, 6.7 Hz, H35a), 3.40 (dd, 1H, *J* = 9.2, 5.2 Hz, H35b), 2.62 (m, 1H, H42), 1.98 (m, 1H, H39), 1.89 (m, 1H, H36), 1.82 (ddd, 1H, *J* = 14.5, 12.0, 10.9 Hz, H38a), 1.61 (ddd, 1H, *J* = 14.5, 3.5, 3.3 Hz, H38b), 1.20 (d, 3H, *J* = 6.2 Hz, H46), 1.00 (d, 3H, *J* = 6.9 Hz, Me42), 0.98 (t, 9H, *J* = 8.0 Hz, Si(CH_2<u>C</u>H_3)$_3$), 0.98 (d, 3H, *J* = 6.8 Hz, Me36), 0.89 (s, 9H, Si(CH_3)$_2$C(C<u>H_3</u>)$_3$), 0.69 (m, 6H, Si(<u>C</u>$H_2$$CH_3$)$_3$), 0.05 (s, 3H, Si(C<u>$H_3$</u>)$_2$C($CH_3$)$_3$), 0.04 (s, 3H, Si(C<u>$H_3$</u>)$_2$C($CH_3$)$_3$); **^{13}C NMR** (125 MHz, $CDCl_3$) δ 173.9 (C41=O), 138.2 (Ph<u>C</u>), 134.8 (C44), 132.0 (C43), 128.4 (Ph<u>C</u>H), 127.7 (Ph<u>C</u>H), 127.6 (Ph<u>C</u>H), 76.1 (C37), 73.3 (Ph<u>C</u>H_2), 71.8 (C35), 69.1 (C45), 68.5 (C40), 41.8 (C39), 38.0 (C36), 34.7 (C42), 25.9 (Si(CH_3)$_2$C(<u>C</u>H_3)$_3$), 25.1 (C38), 24.8 (C46), 18.3 (Si(CH_3)$_2$<u>C</u>(CH_3)$_3$), 12.5 (Me42), 11.5 (Me36), 6.9 (Si(CH_2<u>C</u>H_3)$_3$), 5.0 (Si(<u>C</u>$H_2$$CH_3$)$_3$), –4.6 (Si(<u>C</u>$H_3$)$_2$C($CH_3$)$_3$), –4.8 (Si(<u>C</u>$H_3$)$_2$C($CH_3$)$_3$).

Primary alcohol C42, C45-*anti*-173a and C42, C45-*syn(anti)*-173b

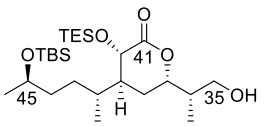

anti-**173a**

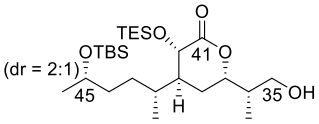

syn(anti)-**173b**

A spatula tip of freshly prepared Ra-Ni slurry was added to a stirred solution of *anti*-TBS ether **211a** (133 mg, 225 µmol) in EtOAc (3 mL), under $Ar_{(g)}$. The reaction mixture was flushed with $H_{2(g)}$, the suba seal rapidly changed for a fresh seal and a fresh $H_{2(g)}$ balloon fitted. The reaction was stirred for 24h, with careful monitoring, then filtered and concentrated *in vacuo*. Purification by flash column chromatography (SiO_2, 15% EtOAc/PE 40-60) primary alcohol *anti*-**173a** (113 mg, 225 µmol, quant.), as a colourless oil: **R_f** (30% EtOAc/PE 40-60) = 0.22; **^{1}H NMR** (700 MHz, $CDCl_3$) δ 4.35

(ddd, 1H, *J* = 11.9, 4.0, 3.9 Hz, H37), 4.28 (d, 1H, *J* = 10.7 Hz, H40), 3.76 (m, 1H, H45), 3.67 (ddd, 1H, *J* = 10.6, 7.0, 5.5 Hz, H35a), 3.61 (m, 1H, H35b), 1.97 (m, 1H, H39), 1.93 (m, 1H, H42), 1.83 (m, 1H, H36), 1.81 (ddd, 1H, *J* = 14.4, 11.8, 10.7 Hz, H38a), 1.61 (ddd, 1H, *J* = 14.4, 4.2, 4.1 Hz, H38b), 1.56 (dd, 1H, *J* = 4.9, 4.9 Hz, -OH), 1.40 (m, 2H, H44), 1.31 (m, 1H, H43a), 1.21 (m, 1H, H43b), 1.11 (d, 3H, *J* = 6.1 Hz, H46), 0.99 (d, 3H, *J* = 6.8 Hz, Me36), 0.98 (t, 9H, *J* = 7.9 Hz, $Si(CH_2\underline{CH_3})_3$), 0.88 (s, 9H, $Si(CH_3)_2C(C\underline{H_3})_3$), 0.86 (d, 3H, *J* = 6.8 Hz, Me42), 0.68 (m, 6H, $Si(\underline{CH_2}CH_3)_3$), 0.042 (s, 3H, $Si(C\underline{H_3})_2C(CH_3)_3$), 0.037 (s, 3H, $Si(C\underline{H_3})_2C(CH_3)_3$); **^{13}C NMR** (125 MHz, $CDCl_3$) δ 174.5 (C41=O), 75.8 (C37), 68.5 (C45), 68.4 (C40), 64.4 (C35), 40.7 (C39), 39.5 (C36), 37.3 (C44), 31.8 (C42), 30.9 (C43), 25.9 ($Si(CH_3)_2C(\underline{C}H_3)_3$), 24.4 (C38), 23.8 (C46), 18.1 ($Si(CH_3)_2\underline{C}(CH_3)_3$), 13.2 (Me42), 10.9 (Me36), 6.8 ($Si(CH_2\underline{CH_3})_3$), 5.0 ($Si(\underline{CH_2}CH_3)_3$), –4.4 ($Si(\underline{C}H_3)_2C(CH_3)_3$), –4.8 ($Si(\underline{C}H_3)_2C(CH_3)_3$); **FTIR ν_{max}** 3459 (w, br, OH str), 2954 (w, sp^3 CH str), 2928 (w, sp^3 CH str), 2857 (w, sp^3 CH str), 1741 (s, sh, C=O str), 1668, 1461, 1413, 1374, 1217, 1150 (s, sh, C-O str), 1085, 1040, 1004, 939, 833, 810, 773, 731, 680, 662; $[\boldsymbol{\alpha}]_{\mathbf{D}}^{\mathbf{20}}$ –2.7 (*c* 1.0, $CHCl_3$); **HRMS** (ESI^+): calculated for $C_{26}H_{54}O_5Si_2Na$ $[M+Na]^+$ 525.3407, found 525.3402.

Analogous conditions were used to produce primary alcohol *syn(anti)*-**173b** (10.4 mg, 20.7 µmol, 90%, *dr* remains ca. 2:1), from TBS ether *syn(anti)*-**211b** (13.5 mg, 22.8 µmol), as a colourless oil: **R_f** (30% EtOAc/PE 40-60) = 0.22; **^{1}H NMR** (700 MHz, $CDCl_3$) δ 4.35 (ddd, 1H, *J* = 11.9, 4.0, 3.9 Hz, H37), 4.28 (d, 1H, *J* = 10.6 Hz, H40), 3.77 (m, 1H, H45), 3.68 (m, 1H, H35a), 3.61 (m, 1H, H35b), 1.97 (m, 1H, H39), 1.94 (m, 1H, H42), 1.83 (m, 1H, H36), 1.82 (m, 1H, H38a), 1.61 (ddd, 1H, *J* = 14.34, 4.0, 3.7 Hz, H38b), 1.56 (dd, 1H, *J* = 4.9, 4.9 Hz, -OH), 1.44 (m, 1H, H44a), 1.40 (m, 1H, H44b), 1.33 (m, 1H, H43a), 1.20 (m, 1H, H43b), 1.12 (d, 3H, *J* = 6.0 Hz, H46), 0.99 (d, 3H, *J* = 6.8 Hz, Me36), 0.98 (t, 9H, *J* = 7.9 Hz, $Si(CH_2\underline{CH_3})_3$), 0.88 (s, 9H, $Si(CH_3)_2C(C\underline{H_3})_3$), 0.86 (d, 3H, *J* = 6.7 Hz, Me42), 0.68 (m, 6H, $Si(\underline{CH_2}CH_3)_3$), 0.044 (s, 3H, $Si(C\underline{H_3})_2C(CH_3)_3$), 0.036 (s, 3H, $Si(C\underline{H_3})_2C(CH_3)_3$); **^{13}C NMR** (125 MHz, $CDCl_3$) δ 174.4 (C41=O), 75.8 (C37), 68.5 (C45), 68.4 (C40), 64.4 (C35), 40.9 (C39), 39.5 (C36), 37.4 (C44), 31.9 (C42), 30.9 (C43), 25.9 ($Si(CH_3)_2C(\underline{C}H_3)_3$), 24.4 (C38), 23.8 (C46), 18.1 ($Si(CH_3)_2\underline{C}(CH_3)_3$), 13.1 (Me42), 10.9 (Me36), 6.8 ($Si(CH_2\underline{CH_3})_3$), 5.0 ($Si(\underline{CH_2}CH_3)_3$), –4.4 ($Si(\underline{C}H_3)_2C(CH_3)_3$), –4.8 ($Si(\underline{C}H_3)_2C(CH_3)_3$).

Aldehydes C42, C45-*anti*-213a and C42, C45-*syn(anti)*-213b

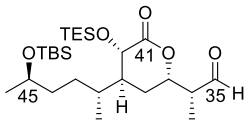

anti-**213a**

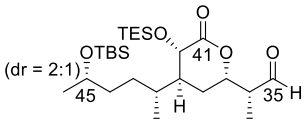

syn(anti)-**213b**

DMP (162 mg, 382 µmol) was added to a stirred solution of primary alcohol *anti*-**173a** (32.0 mg, 63.6 µmol) and $NaHCO_{3(s)}$ (64.1 mg, 764 µmol) in CH_2Cl_2 (1 mL) at rt. The mixture was stirred for 1h, diluted with CH_2Cl_2 (3 mL) and quenched with premixed $NaHCO_3$ (3 mL) and $Na_2S_2O_3$ (3 mL), by stirring for 30 min. The layers were separated and the aqueous layer extracted with CH_2Cl_2 (4 x 2 mL). The combined organic phases were washed with brine (10 mL), dried ($MgSO_4$), filtered and concentrated *in vacuo* to afford crude aldehyde *anti*-**213a** (32 mg, 63.6 µmol, quant.), as a colourless oil: $\mathbf{R_f}$ (30% EtOAc/PE 40-60) = 0.62; ^{1}**H NMR** (700 MHz, $CDCl_3$) δ 9.71 (s, 1H, H35), 4.51 (ddd, 1H, *J* = 11.3, 5.6, 4.2 Hz, H37), 4.29 (d, 1H, *J* = 10.6 Hz, H40), 3.75 (m, 1H, H45), 2.60 (m, 1H, H36), 2.00 (m, 1H, H39), 1.93 (m, 1H, H42), 1.76 (m, 1H, H38a), 1.71 (m, 1H, H38b), 1.40 (m, 1H, H44a), 1.39 (m, 1H, H44b), 1.30 (m, 1H, H43a), 1.26 (d, 3H, *J* = 7.3 Hz, Me36), 1.20 (m, 1H, H43b), 1.11 (d, 3H, *J* = 6.1 Hz, H46), 0.98 (t, 9 H, *J* = 7.9 Hz, $Si(CH_2\underline{CH_3})_3$), 0.90 (d, 3H, *J* = 6.8 Hz, Me42), 0.88 (s, 9H, $Si(CH_3)_2C(C\underline{H_3})_3$), 0.68 (m, 6H, $Si(\underline{CH_2}CH_3)_3$), 0.04 (s, 3H, $Si(C\underline{H_3})_2C(CH_3)_3$), 0.03 (s, 3H, $Si(C\underline{H_3})_2C(CH_3)_3$).

Analogous conditions were used to produce aldehyde *syn(anti)*-**213b** (ca. 18 mg, 35.8 µmol, quant.), from TBS ether *syn(anti)*-**173b** (18.0 mg, 35.8 µmol, *dr* remains ca. 2:1), as a colourless oil: $\mathbf{R_f}$ (30% EtOAc/PE 40-60) = 0.62; ^{1}**H NMR** (700 MHz, $CDCl_3$) δ 9.71 (s, 1H, H35), 4.51 (ddd, 1H, *J* = 11.3, 5.6, 4.2 Hz, H37), 4.29 (d, 1H, *J* = 10.6 Hz, H40), 3.76 (m, 1H, H45), 2.60 (m, 1H, H36), 1.99 (m, 1H, H39), 1.92 (m, 1H, H42), 1.76 (ddd, 1H, *J* = 14.5, 4.4, 4.3 Hz, H38a), 1.71 (ddd, 1H, *J* = 14.5, 11.1, 10.7 Hz, H38b), 1.44 (m, 1H, H44b), 1.38 (m, 1, H44b), 1.34 (m, 1H, H43a), 1.25 (d, 3H, *J* = 7.2 Hz, Me36), 1.18 (m, 1H, H43b), 1.11 (d, 3H, *J* = 6.1 Hz, H46), 0.97 (t, 9 H, *J* = 7.9 Hz, $Si(CH_2\underline{CH_3})_3$), 0.89 (d, 3H, *J* = 6.8 Hz, Me42), 0.87 (s, 9H, $Si(CH_3)_2C(C\underline{H_3})_3$), 0.68 (m, 6H, $Si(\underline{CH_2}CH_3)_3$), 0.04 (s, 3H, $Si(C\underline{H_3})_2C(CH_3)_3$), 0.03 (s, 3H, $Si(C\underline{H_3})_2C(CH_3)_3$).

Terminal Olefins C42, C45-*anti*-2a and C42, C45-*syn(anti)*-2b

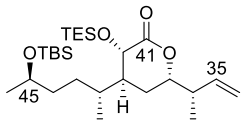

anti-**2a**

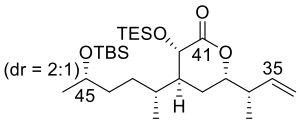

syn(anti)-**2b**

*n*BuLi (760 µL, 1.21 mmol) was added, dropwise, to a suspension of methyltriphenylphosphonium bromide (455 mg, 1.27 mmol) in THF (5 mL), at 0 °C, and stirred for 30 min. The reaction was then allowed to warm to rt and stirred for 1h, after which the temperature was lowered to –78 °C. Stirred aldehyde *anti*-**213a** (ca. 32mg, 63.6 µmol) in THF (5 mL), at –78 °C, was cannulated into the solution and stirred for 30 min. The reaction was quenched with NH_4Cl (10 mL) and allowed to warm to rt. The layers were separated and the aqueous layer extracted with CH_2Cl_2 (4 x 2 mL). The combined organic phases were washed with brine (10 mL), dried ($MgSO_4$), filtered and concentrated *in vacuo*. Purification by flash column chromatography (SiO_2, 1-2.5% EtOAc/PE 40-60) afforded terminal olefin *anti*-**2a** (25.7 mg, 51.5 µmol, 81% over two steps), as a colourless oil: $\mathbf{R_f}$ (30% EtOAc/PE 40-60) = 0.76; **^{1}H NMR** (700 MHz, $CDCl_3$) δ 5.69 (ddd, 1H, *J* = 17.1, 10.1, 8.2 Hz, H35), 5.11 (d, 1H, *J* = 17.3 Hz, H34a), 5.08 (d, 1H, *J* = 10.5 Hz, H34b), 4.22 (d, 1H, *J* = 10.8 Hz, H40), 3.94 (ddd, 1H, *J* = 10.4, 7.3, 4.6 Hz, H37), 3.75 (m, 1H, H45), 2.38 (m, 1H, H36), 1.95 (m, 1H, H39), 1.92 (m, 1H, H42), 1.67 (ddd, 1H, *J* = 14.6, 4.9, 4.9 Hz, H38a), 1.64 (ddd, 1H, *J* = 14.6, 10.4, 10.1 Hz, H38b), 1.39 (m, 2H, H44), 1.29 (m, 1H, H43a), 1.20 (m, 1H, H43b), 1.12 (d, 3H, *J* = 6.8 Hz, Me36), 1.11 (d, 3H, *J* = 6.1 Hz, H46), 0.98 (t, 9H, *J* = 7.9 Hz, $Si(CH_2\underline{CH_3})_3$), 0.88 (s, 9H, $Si(CH_3)_2C(C\underline{H_3})_3$), 0.84 (d, 3H, *J* = 6.7 Hz, Me42), 0.68 (m, 6H, $Si(\underline{CH_2}CH_3)_3$), 0.04 (s, 3H, $Si(C\underline{H_3})_2C(CH_3)_3$), 0.03 (s, 3H, $Si(C\underline{H_3})_2C(CH_3)_3$); **^{13}C NMR** (125 MHz, $CDCl_3$) δ 174.3 (C41=O), 138.6 (C35), 116.3 (C34), 79.0 (C37), 68.6 (C45), 68.4 (C40), 42.8 (C36), 40.5 (C39), 37.3 (C44), 31.8 (C42), 30.9 (C43), 25.9 ($Si(CH_3)_2C(\underline{C}H_3)_3$), 24.8 (C38), 23.8 (C46), 18.1 ($Si(CH_3)_2\underline{C}(CH_3)_3$), 15.9 (Me36), 13.2 (Me42), 6.9 ($Si(CH_2\underline{CH_3})_3$), 5.0 ($Si(\underline{CH_2}CH_3)_3$), –4.3 ($Si(\underline{C}H_3)_2C(CH_3)_3$), –4.8 ($Si(\underline{C}H_3)_2C(CH_3)_3$); **FTIR ν_{max}** 2956 (w, sp^3 CH str), 2929 (w, sp^3 CH str), 2857 (w, sp^3 CH str), 1761 (s, sh, C=O str), 1460, 1414, 1374, 1252, 1136 (s, sh, C-O str), 1085, 1053, 1005 (s, sh, C-O str), 919, 834, 808, 773, 728, 663; $[\boldsymbol{\alpha}]_{\mathbf{D}}^{\mathbf{20}}$ –12.3 (*c* 1.0, $CHCl_3$); **HRMS** (ESI^+): calculated for $C_{27}H_{54}O_4Si_2Na$ $[M+Na]^+$ 521.3458, found 521.3453.

Analogous conditions were used to produce olefin *syn(anti)*-**2b** (15.9 mg, 31.9 µmol, 89% over 2 steps), from aldehyde *syn(anti)*-**213b** (ca. 18 mg, 35.8 µmol, *dr* remains ca. 2:1), as a colourless oil: $\mathbf{R_f}$ (30% EtOAc/PE 40-60) = 0.76; **^{1}H NMR** (700 MHz, $CDCl_3$) δ 5.69 (ddd, 1H, *J* = 17.2, 10.5, 8.1 Hz, H35), 5.11 (d, 1H, *J* = 17.2 Hz, H34a), 5.08 (d, 1H, *J* = 10.4 Hz, H34b), 4.23 (d, 1H, *J* = 10.7 Hz, H40), 3.95 (ddd, 1H, *J* = 10.6, 7.4, 4.1 Hz, H37), 3.76 (m, 1H, H45), 2.38 (m, 1H, H36), 1.95 (m, 1H, H39),

1.92 (m, 1H, H42), 1.68 (ddd, 1H, *J* = 14.7, 4.9, 4.6 Hz, H38a), 1.64 (ddd, 1H, *J* = 14.6, 10.6, 10.5 Hz, H38b), 1.39 (m, 2H, H44), 1.29 (m, 1H, H43a), 1.20 (m, 1H, H43b), 1.120 (d, 3H, *J* = 6.8 Hz, Me36), 1.115 (d, 3H, *J* = 6.0 Hz, H46), 0.98 (t, 9H, *J* = 7.9 Hz, $Si(CH_2\underline{CH_3})_3$), 0.88 (s, 9H, $Si(CH_3)_2C(C\underline{H_3})_3$), 0.83 (d, 3H, *J* = 6.8 Hz, Me42), 0.68 (m, 6H, $Si(\underline{CH_2}CH_3)_3$), 0.04 (s, 3H, $Si(C\underline{H_3})_2C(CH_3)_3$), 0.03 (s, 3H, $Si(C\underline{H_3})_2C(CH_3)_3$); **^{13}C NMR** (125 MHz, $CDCl_3$) δ 174.4 (C41=O), 138.6 (C35), 116.3 (C34), 78.9 (C37), 68.56 (C45), 68.4 (C40), 42.9 (C36), 40.8 (C39), 37.4 (C44), 31.9 (C42), 31.0 (C43), 25.9 ($Si(CH_3)_2C(\underline{C}H_3)_3$), 24.9 (C38), 23.8 (C46), 18.1 ($Si(CH_3)_2\underline{C}(CH_3)_3$), 16.0 (Me36), 13.0 (Me42), 6.9 ($Si(CH_2\underline{CH_3})_3$), 5.0 ($Si(\underline{CH_2}CH_3)_3$), –4.3 ($Si(\underline{C}H_3)_2C(CH_3)_3$), –4.8 ($Si(\underline{C}H_3)_2C(CH_3)_3$).

3-((4-methoxybenzyl)oxy)propan-1-ol

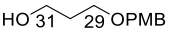

TBAI (1.03 g, 2.78 mmol) was added to a stirred solution of NaH (60% in mineral oil) (1.22 g, 30.6 mmol) in THF (50 mL) at 0 °C and stirred for 5 min. 1,3-Propandiol (2.00 mL, 27.8 mmol) was added dropwise, the mixture allowed to come to rt and stirred for 30 min before returning the temperature to 0 °C. PMBCl (3.78 mL, 27.9 mmol) was added dropwise to the mixture before it was heated to reflux for 3 h. The reaction was allowed to cool to rt and quenched with NH_4Cl. The layers were separated and the aqueous layer extracted with Et_2O (3 x 5 mL). The combined organic phases were washed with brine (50 mL), dried ($MgSO_4$), filtered and concentrated *in vacuo*. Purification by flash column chromatography (SiO_2, 30% EtOAc/PE 40-60) afforded 3-((4-methoxybenzyl)oxy)propan-1-ol (3.94 g, 20.1 mmol, 72%), as a colourless oil: $\mathbf{R_f}$ (50% EtOAc/PE 40-60) = 0.22; **^{1}H NMR** (500 MHz, $CDCl_3$) δ 7.25 (d, 2H, *J* = 8.7 Hz, Ar$\underline{H}$), 6.88 (d, 2H, *J* = 8.7 Hz, Ar$\underline{H}$), 4.45 (s, 2H, $ArC\underline{H_2}$), 3.81 (s, 3H, $ArOC\underline{H_3}$), 3.78 (dt, 2H, *J* = 5.7, 5.6 Hz, H31), 3.64 (t, 2H, *J* = 5.8 Hz, H29), 2.28 (t, 1H, *J* = 5.5 Hz, -O$\underline{H}$), 1.85 (qn, 2H, *J* = 5.7 Hz, H30).

Data in agreement with literature values.[195]

3-((4-Methoxybenzyl)oxy)propanal

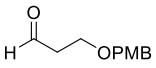

DMSO (2.85 mL, 40.2 mmol) was added dropwise to a stirred solution of oxalyl chloride (2.59 mL, 30.1 mmol) in CH_2Cl_2 (150 mL) at –78 °C and stirred for 30 mins. 3-((4-Methoxybenzyl)oxy)propan-1-ol (3.94 g, 20.1 mmol) in 25 mL was cannulated into the reaction and stirred for 1 h. Et_3N (8.40 mL, 60.2 mmol) was added dropwise, the reaction allowed to come to rt and stirred for 30 min before being quenched with HCL (1M). The layers were separated and the aqueous layer extracted with CH_2Cl_2 (4 x 10 mL). The combined organic phases were washed with brine (100 mL), dried ($MgSO_4$), filtered and concentrated *in vacuo*. Purification by flash column chromatography (SiO_2,

30% EtOAc/PE 40-60) afforded 3-((4-Methoxybenzyl)oxy)propanal (3.50 g, 18.0 mmol, 88%), as a colourless oil: $\mathbf{R_f}$ (30% EtOAc/PE 40-60) = 0.30; **^{1}H NMR** (700 MHz, $CDCl_3$) δ 9.79, (t, 1H, *J* = 1.7 Hz, H31), 7.25 (d, 2H, *J* = 8.6 Hz, ArH), 6.88 (d, 2H, *J* = 8.6 Hz, ArH), 4.46 (s, 2H, $ArCH_2$), 3.80 (s, 3H, $ArOCH_3$), 3.79 (t, 2H, *J* = 6.1 Hz, H29), 1.85 (dt, 2H, *J* = 6.1, 1.7 Hz, H30).

Data in agreement with literature values.[195]

Homoallylic Alcohols C31, 31-*syn*-180a and *ent*-C31, 31-*syn*-180b

syn-**180a** *ent-syn*-**180b**

Cis-2-butene (720 mg, 12.9 mmol) and nBuLi (2.48 mL, 4.12 mmol) were sequentially added, dropwise, to a stirring solution of potassium *tert*-butoxide (433 mg, 3.86 mmol) in THF (16 mL), at –78 °C. The temperature was raised to –45 °C and the reaction mixture stirred for 20 min before the temperature was again lowered to –78 °C. (+)-Ipc_2BOMe (1.38 g, 4.38 mmol) in THF (5 mL) was added, dropwise, and the reaction mixture stirred for 30 min. $BF_3{\cdot}OEt_2$ (0.730 mL, 5.92 mmol) was then added, dropwise, and the reaction mixture stirred for a further 5 min. 3-(4-Methoxybenzyloxy)propanal (500 mg, 2.57 mmol) in THF (5 mL) was added, dropwise, and the reaction stirred for 3 h. The reaction was quenched with $NaHCO_3$ (5 mL) and H_2O_2 (30% aq., 1 mL), allowed to warm to rt and stirred O/N. H_2O (2.5 mL) and Na_2SO_3 (50 mL) were added and the reaction stirred for 30 min. The layers were separated and the aqueous layer extracted with CH_2Cl_2 (3 x 5 mL). The combined organic phases were washed with brine (50 mL), dried ($MgSO_4$), filtered and concentrated *in vacuo*. Purification by flash column chromatography (SiO_2, 15% EtOAc/PE 40-60) afforded *syn*-homoallylic alcohol **180a** (293.2 mg, 1.17 mmol, 45%, *ee* 70%, >20:1 *dr*), as a colourless oil: $\mathbf{R_f}$ (30% EtOAc/PE 40-60) = 0.37; **^{1}H NMR** (700 MHz, $CDCl_3$) δ 7.25 (d, 2H, *J* = 8.7 Hz, ArH), 6.87 (d, 2H, *J* = 8.7 Hz, ArH), 5.78 (ddd, 1H, *J* = 17.2, 10.3, 7.6 Hz, H33), 5.05 (ddd, 1H, *J* = 17.2, 1.8, 1.2 Hz, H34a), 5.03 (ddd, 1H, *J* = 10.4, 1.8, 0.9 Hz, H34b), 4.45 (s, 2H, $ArCH_2$), 3.80 (s, 3H, $ArOCH_3$), 3.70 (ddd, 1H, *J* = 9.3, 5.7, 4.7 Hz, H31), 3.66 (ddd, 1H, *J* = 9.3, 6.2, 3.0 Hz, H29a), 3.61 (ddd, 1H, *J* = 9.2, 8.3, 4.4 Hz, H29b), 2.90 (d, 1H, *J* = 3.2 Hz, -OH), 2.25 (m, 1H, H32), 1.77 (dddd, 1H, *J* = 14.6, 5.7, 4.4, 2.5 Hz, H30a), 1.69 (ddd, 1H, *J* = 14.6, 9.4, 8.3, 4.7 Hz, H30b), 1.04 (d, 3H, *J* = 6.8 Hz, Me32).

Data in agreement with the enantiomeric compound reported by Brimble.[196]

N.b. *ee* was estimated from Mosher's ester analysis and comparison of diastereomers after cross metathesis.

Analogous conditions were used, with (–)-Ipc$_2$BOMe, to generate *ent-syn*-homoallylic alcohol **180b** (347.3 mg, 1.39 mmol, 27%) as a colourless oil with R_f and ^{1}H NMR data matching *syn*-homoallylic alcohol **180a**.

(*R*)-Mosher ester-181a

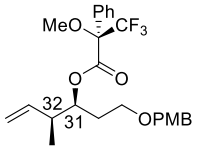

DCC (120 µL, 120 µmol, 1 M in CH_2Cl_2) was added dropwise to a stirred solution of *syn*-homoallylic alcohol **180a** (6.0 mg, 24.0 µmol), (*R*)-MTPA (28.1 mg, 120 µmol) and DMAP (14.6 mg, 120 µmol) in CH_2Cl_2 (120 µL). The reaction was stirred and monitored by TLC, until the starting material was consumed or any elimination product was indicated (*ca.* 5 h, rt). The reaction mixture was filtered through a silica plug and the filtrate concentrated *in vacuo*. Purification by flash column chromatography (SiO_2, 7.5-20% EtOAc/PE 40-60) afforded (*R*)-Mosher ester-**181a** (7.1 mg, 15.2 µmol, 63%) as a colourless oil. **R_f** (30% EtOAc/PE 40-60) = 0.66; Major diastereomer: **^{1}H NMR** (500 MHz, $CDCl_3$) δ 7.55-7.53 (m, 2H, PhH), 7.40-7.35 (m, 2H, PhH), 7.23 (d, 2H, *J* = 8.6 Hz, ArH), 6.87 (d, 2H, *J* = 8.7 Hz, ArH), 5.64 (ddd, 1H, *J* = 17.4, 10.4, 7.1 Hz, H33), 5.23 (ddd, 1H, *J* = 8.8, 5.0, 3.6 Hz, H31), 4.98 (ddd, 1H, *J* = 10.5, 1.3, 1.2 Hz, H34a), 4.94 (ddd, 1H, *J* = 17.3, 1.4, 1.4 Hz, H34b), 4.38 (ABq, 2H, J_{AB} = 11.6 Hz, ArCH_2), 3.80 (s, 3H, ArOCH_3), 3.49 (d, 3H, *J* = 1.1 Hz, -OCH_3), 3.44 (ddd, 1H, *J* = 9.3, 6.9, 5.1 Hz, H29a), 3.39 (ddd, 1H, *J* = 9.3, 8.0, 6.2 Hz, H29b), 2.49 (m, 1H, H32), 1.93 (ddd, 1H, *J* = 7.8, 7.0, 3.6 Hz, H30a), 1.89 (m, 1H, H30b), 0.97 (d, 3H, *J* = 6.9 Hz, Me32). Minor diastereomer: **^{1}H NMR** (500 MHz, $CDCl_3$) δ 7.55-7.53 (m, 2H, PhH), 7.40-7.35 (m, 2H, PhH), 7.22 (d, 2H, *J* = 8.4 Hz, ArH), 6.87 (d, 2H, *J* = 8.7 Hz, ArH), 5.78 (ddd, 1H, *J* = 17.3, 10.5, 6.9 Hz, H33), 5.26 (ddd, 1H, *J* = 8.8, 4.7, 3.7 Hz, H31), 5.07 (ddd, 1H, *J* = 10.1, 1.3, 1.3 Hz, H34a), 5.05 (ddd, 1H, *J* = 17.2, 1.5, 1.5 Hz, H34b), 4.32 (ABq, 2H, J_{AB} = 11.4 Hz, ArCH_2), 3.80 (s, 3H, ArOCH_3), 3.52 (d, 3H, *J* = 1.1 Hz, -OCH_3), 3.35 (ddd, 1H, *J* = 9.3, 6.8, 4.8 Hz, H29a), 3.26 (ddd, 1H, *J* = 9.3, 8.2, 6.1 Hz, H29b), 2.56 (m, 1H, H32), 1.96 (ddd, 1H, *J* = 7.8, 7.0, 3.6 Hz, H30a), 1.86 (m, 1H, H30b), 1.03 (d, 3H, *J* = 6.9 Hz, Me32).

(*S*)-Mosher ester-182a

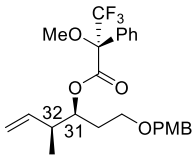

An analogous procedure, with (*S*)-MTPA and *syn*-homoallylic alcohol **180a** (6.0 mg, 24.0 µmol), was used to generate (*S*)-Mosher ester-**182a** (8.3 mg, 17.8 µmol, 74 %), as a colourless oil. $\mathbf{R_f}$ (20% EtOAc/PE 40-60) = 0.66; Major diastereomer: **^{1}H NMR** (500 MHz, $CDCl_3$) δ 7.55-7.54 (m, 2H, PhH), 7.40-7.35 (m, 2H, PhH), 7.22 (d, 2H, *J* = 8.7 Hz, ArH), 6.87 (d, 2H, *J* = 8.7 Hz, ArH), 5.78 (ddd, 1H, *J* = 17.3, 10.5, 6.9 Hz, H33), 5.26 (ddd, 1H, *J* = 9.1, 4.7, 3.7 Hz, H31), 5.07 (ddd, 1H, *J* = 10.5, 1.3, 1.3 Hz, H34a), 5.05 (ddd, 1H, *J* = 17.2, 1.5, 1.4 Hz, H34b), 4.32 (ABq, 2H, J_{AB} = 11.5 Hz, ArCH_2), 3.80 (s, 3H, ArOCH_3), 3.52 (d, 3H, *J* = 1.1 Hz, -OCH_3), 3.35 (ddd, 1H, *J* = 9.3, 6.8, 4.9 Hz, H29a), 3.26 (ddd, 1H, *J* = 9.3, 8.2, 6.1 Hz, H29b), 2.56 (m, 1H, H32), 1.88 (ddd, 1H, *J* = 8.0, 6.9, 3.5 Hz, H30a), 1.83 (ddd, 1H, *J* = 9.2, 6.0, 5.1 Hz, H30b), 1.03 (d, 3H, *J* = 6.9 Hz, Me32). Minor diastereomer: **^{1}H NMR** (500 MHz, $CDCl_3$) δ 7.55-7.54 (m, 2H, PhH), 7.40-7.35 (m, 2H, PhH), 7.24 (d, 2H, *J* = 8.2 Hz, ArH), 6.87 (d, 2H, *J* = 8.7 Hz, ArH), 5.48 (ddd, 1H, *J* = 17.4, 10.5, 7.1 Hz, H33), 5.23 (ddd, 1H, *J* = 9.0, 5.0, 3.6 Hz, H31), 4.99 (ddd, 1H, *J* = 10.5, 1.3, 1.2 Hz, H34a), 4.94 (ddd, 1H, *J* = 17.2, 1.4, 1.4 Hz, H34b), 4.38 (ABq, 2H, J_{AB} = 11.6 Hz, ArCH_2), 3.80 (s, 3H, ArOCH_3), 3.49 (d, 3H, *J* = 1.1 Hz, -OCH_3), 3.44 (ddd, 1H, *J* = 9.4, 6.9, 5.1 Hz, H29a), 3.39 (ddd, 1H, *J* = 9.3, 8.0, 6.2 Hz, H29b), 2.49 (m, 1H, H32), 1.96 (ddd, 1H, *J* = 7.8, 6.9, 3.6 Hz, H30a), 1.91 (m, 1H, H30b), 0.97 (d, 3H, *J* = 6.9 Hz, Me32).

TBS Ether C31, 31-*syn*-183a and *ent*-C31, 31-*syn*-183b

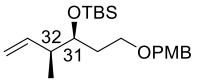

syn-**183a**

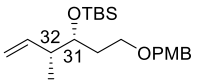

ent-syn-**183b**

Cis-2-butene (720 mg, 12.9 mmol) and nBuLi (2.48 mL, 4.12 mmol) were sequentially added, dropwise, to a stirring solution of potassium tert-butoxide (433 mg, 3.86 mmol) in THF (16 mL), at –78 °C. The temperature was raised to –45 °C and the reaction stirred for 20 min before the temperature was again lowered to –78 °C. (+)-Ipc_2BOMe (1.38 g, 4.38 mmol) in THF (5 mL) was added, dropwise, and the reaction stirred for 30 min. $BF_3{\cdot}OEt_2$ (0.730 mL, 5.92 mmol) was then added, dropwise, and the reaction stirred for a further 5 min. 3-(4-methoxybenzyloxy)propanal (500 mg, 2.57 mmol) in THF (5 mL) was added, dropwise, and the reaction stirred for 3 h. The reaction was quenched with $NaHCO_3$ (5 mL) and H_2O_2 (30% aq., 1 mL), allowed to warm to rt and

stirred O/N. H_2O (2.5 mL) and Na_2SO_3 (50 mL) were added and reaction stirred for 30 min. The layers were separated and the aqueous layer extracted with CH_2Cl_2 (3 x 5 mL). The combined organic phases were washed with brine (50 mL), dried ($MgSO_4$), filtered and concentrated *in vacuo* overnight to give the crude product mixture (3.77 g).

2,6-Lutidine (8.1 mL, 69.5 mmol) was added to the crude product mixture in CH_2Cl_2 (50 mL), at –78 °C, and stirred for 5 minutes. TBSOTf (6.75 mL, 44.7 mmol) was added dropwise and the mixture stirred, at –78 °C, for 1.5 h. Additional TBSOTf (2.00 mL, 13.2 mmol) was added dropwise and the mixture stirred, at –78 °C, for a further 30 mins. The reaction was quenched sequentially by dropwise addition of MeOH (1 mL), at –78 °C, followed by $NaHCO_3$ (50 mL) and allowed to warm to rt. H_2O (2.5 mL) and were added and reaction stirred for 30 min. The layers were separated and the aqueous layer extracted with CH_2Cl_2 (3 x 5 mL). The combined organic phases were washed with brine (50 mL), dried ($MgSO_4$), filtered and concentrated *in vacuo*. Purification by flash column chromatography (SiO_2, 5-10% EtOAc/PE 40-60) afforded TBS ether *syn*-**183a** (1.56 g, 4.28 mmol, 88% over 2 steps), as a colourless oil: $\mathbf{R_f}$ (5% EtOAc/PE 40-60) = 0.75; **^{1}H NMR** (700 MHz, $CDCl_3$) δ 7.25 (d, 2H, *J* = 8.6 Hz, Ar<u>H</u>), 6.87 (d, 2H, *J* = 8.7 Hz, Ar<u>H</u>), 5.88 (ddd, 1H, *J* = 17.2, 10.7, 6.9 Hz, H33), 5.01 (d, 1H, *J* = 10.5 Hz, H34a), 4.99 (dd, 1H, *J* = 17.3 Hz, H34b), 4.41 (AB_q, 2H, *J* = 11.5 Hz, Ar<u>C</u>H$_2$), 3.80 (s, 3H, ArO<u>C</u>H$_3$), 3.71 (m, 1H, H31), 3.50 (m, 2H, H29), 2.30 (m, 1H, H32), 1.73 (m, 1H, H30a), 1.65 (m, 1H, 30b), 0.96 (d, 3H, *J* = 6.9 Hz, Me32),), 0.88 (s, 9H, Si(CH$_3$)$_2$C(C<u>H</u>$_3$)$_3$), 0.04 (s, 3H, Si(C<u>H</u>$_3$)$_2$C(CH$_3$)$_3$), 0.03 (s, 3H, Si(C<u>H</u>$_3$)$_2$C(CH$_3$)$_3$); **^{13}C NMR** (125 MHz, $CDCl_3$) δ 159.1 (Ar<u>C</u>), 140.9 (C33), 130.7 (Ar<u>C</u>), 129.2 (Ar<u>C</u>H), 114.2 (C34), 113.7 (Ar<u>C</u>H), 73.0 (C31), 72.6 (Ar<u>C</u>H$_2$), 66.9 (C29), 55.3 (ArO<u>C</u>H$_3$), 43.0 (C32), 33.4 (C30), 25.9 (Si(CH$_3$)$_2$C(<u>C</u>H$_3$)$_3$), 18.1 (Si(CH$_3$)$_2$<u>C</u>(CH$_3$)$_3$), 14.8 (Me32), –4.3 (Si(<u>C</u>H$_3$)$_2$C(CH$_3$)$_3$), –4.6 (Si(<u>C</u>H$_3$)$_2$C(CH$_3$)$_3$); **FTIR ν_{max}** 2953 (w, sp^3 CH str), 2928 (w, sp^3 CH str), 2856 (w, sp^3 CH str), 1613, 1513, 1462, 1364, 1247 (s, sh, C-O str), 1172, 1090, 1038, 1004, 833, 773; $[\alpha]_D^{20}$ –2.3 (*c* 1.0, $CHCl_3$); **HRMS** (ESI$^+$): calculated for $C_{21}H_{36}O_3SiNa$ $[M+Na]^+$ 387.2331, found 387.2328.

Analogous conditions, with (–)-Ipc$_2$BOMe, were used to produce homoallylic alcohol *ent-syn*-**181b** and the crude reaction mixture analogously TBS protected to afford TBS ether *ent-syn*-**183b** (1.93 g, 5.30 mmol, 61% over 2 steps), as a colourless oil with R_f, ^{1}H NMR, ^{13}C NMR, FTIR and HRMS data matching homoallylic alcohol *syn*-**181a**: $[\alpha]_D^{20}$ +2.9° (*c* 1.0, $CHCl_3$).

Primary Alcohol C31, 31-*syn*-184a and *ent*-C31, 31-*syn*-184b

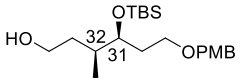

syn-**184a**

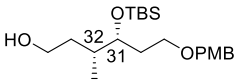

ent-syn-**184b**

$BH_3{\cdot}SMe_2$ (310 µL, 3.29 mmol) was added, dropwise, to a stirred solution of TBS ether *syn*-**183a** (200 mg, 0.549 mmol) at 0 °C. The reaction was allowed to come to rt and stirred for 3h before returning to 0 °C. MeOH (5mL) and NaOH (15 mL, 2.5 M) were added dropwise, followed by H_2O_2 (3 mL, 30% aq.), the mixture allowed to come to room temperature and stirred for 1 h. The layers were separated and the aqueous layer extracted with CH_2Cl_2 (3 x 5 mL). The combined organic phases were washed with brine (50 mL), dried ($MgSO_4$), filtered and concentrated *in vacuo*. Purification by flash column chromatography (SiO_2, 20% EtOAc/PE 40-60) afforded primary alcohol *syn*-**184a** (167.8 mg, 0.439 mmol, 80%), as a colourless oil: $\mathbf{R_f}$ (30% EtOAc/PE 40-60) = 0.27; **^{1}H NMR** (700 MHz, $CDCl_3$) δ 7.25 (d, 2H, *J* = 8.7 Hz, ArH), 6.88 (d, 2H, *J* = 8.7 Hz, ArH), 4.41 (AB_q, 2H, *J* = 11.5 Hz, $ArCH_2$), 3.80 (s, 3H, $ArOCH_3$), 3.77 (m, 1H, H31), 3.69 (ddd, 1H, *J* = 10.9, 7.9, 5.4 Hz, H34a), 3.60 (dd, 1H, *J* = 11.2, 8.7, 4.5 Hz, H34b), 3.49 (m, 2H, H29), 2.53 (dd, 1H, *J* = 7.8, 4.3 Hz, -OH), 1.79-1.72 (m, 4H, H30, H32, H33a), 1.37 (m, 1H, 33b), 0.89 (s, 9H, $Si(CH_3)_2C(CH_3)_3$), 0.87 (d, 3H, *J* = 6.9 Hz, Me32), 0.07 (s, 3H, $Si(CH_3)_2C(CH_3)_3$), 0.06 (s, 3H, $Si(CH_3)_2C(CH_3)_3$); **^{13}C NMR** (125 MHz, $CDCl_3$) δ 159.1 (ArC), 130.6 (ArC), 129.3 (ArCH), 113.7 (ArCH), 73.3 (C31), 72.6 ($ArCH_2$), 67.0 (C29), 55.3 ($ArOCH_3$), 62.0 (C34), 37.3 (C32), 35.3 (C33), 32.1 (C30), 25.9 ($Si(CH_3)_2C(CH_3)_3$), 18.1 ($Si(CH_3)_2C(CH_3)_3$), 17.1 (Me32), –4.3 ($Si(CH_3)_2C(CH_3)_3$), –4.8 ($Si(CH_3)_2C(CH_3)_3$); **FTIR ν_{max}** 3459 (w, br, -OH str), 2954 (w, sp^3 CH str), 2928 (w, sp^3 CH str), 2855 (w, sp^3 CH str), 1613, 1513, 1462, 1362, 1085, 1036 (s, sh, C-O str), 1004, 833, 772; $[\alpha]_D^{20}$ –8.0 (*c* 1.0, $CHCl_3$); **HRMS** (ESI^+): calculated for $C_{21}H_{38}O_4SiNa$ $[M+Na]^+$ 405.2432, found 405.2433.

Analogous conditions were used to produce primary alcohol *ent-syn*-**184b** (1.19 g, 3.12 mmol, 60%), from TBS ether *ent-syn*-**183b** (1.90 g, 5.21 mmol), as a colourless oil with R_f, ^{1}H NMR, ^{13}C NMR, FTIR and HRMS data identical to primary alcohol *syn*-**184a**: $[\alpha]_D^{20}$ +8.9° (*c* 1.0, $CHCl_3$).

Aldehyde C31, 31-*syn*-185a and *ent*-C31, 31-*syn*-185b

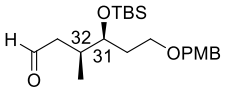

syn-**185a**

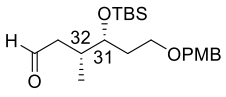

ent-syn-**185b**

DMSO (400 µL, 5.70 mmol) was added dropwise to a stirred solution of oxalyl chloride (370 µL, 4.27 mmol) in CH_2Cl_2 (21 mL) and stirred (–78 °C, 15 min). A solution of primary alcohol *ent-syn*-

184b (1.09 g, 2.85 mmol) in CH_2Cl_2 (4 x 2 mL) was added, dropwise *via* cannula, with rinsing and the mixture stirred (–78 °C, 15 min). Distilled Et_3N (1.19 mL, 8.55 mmol) was added dropwise and the suspension stirred (30 min). The reaction was quenched with NH_4Cl (excess), the organic layer separated and the aqueous layer extracted with CH_2Cl_2 (3 x 20 mL). The combined organic extracts were dried over ($MgSO_4$), filtered and concentrated *in vacuo* to give crude aldehyde *ent-syn*-**185b** as a slightly yellow oil (1.08 g, ca. 2.84 mmol, ca. quant.): $\mathbf{R_f}$ (30% EtOAc/PE 40-60) = 0.62; **^{1}H NMR** (700 MHz, $CDCl_3$) δ 9.75 (dd, 1H, *J* = 2.4, 1.8 Hz, H34), 7.25 (d, 2H, *J* = 8.7 Hz, Ar<u>H</u>), 6.88 (d, 2H, *J* = 8.7 Hz, Ar<u>H</u>), 4.41 (AB_q, 2H, *J* = 11.5 Hz, ArC<u>H_2</u>), 3.81 (s, 3H, ArOC<u>H_3</u>), 3.77 (m, 1H, ddd, 1H, *J* = 8.5, 4.0, 3.7 Hz, H31), 3.48 (m, 2H, H29), 2.62 (ddd, 1H, *J* = 15.8, 4.2, 1.7 Hz, H33a), 2.25 (m, 1H, C32), 2.18 (ddd, 1H, *J* = 15.8, 9.0, 2.5 Hz, H33b), 1.75 (m, 1H, H30a), 1.57 (m, 1H, 30b), 0.89 (d, 3H, *J* = 6.7 Hz, Me32), 0.87 (s, 9H, $Si(CH_3)_2C(C\underline{H_3})_3$), 0.039 (s, 3H, $Si(C\underline{H_3})_2C(CH_3)_3$), 0.036 (s, 3H, $Si(C\underline{H_3})_2C(CH_3)_3$); **^{13}C NMR** (125 MHz, $CDCl_3$) δ 202.7 (C34), 159.2 (Ar<u>C</u>), 130.5 (Ar<u>C</u>), 129.3 (Ar<u>C</u>H), 113.8 (Ar<u>C</u>H), 72.7 (Ar<u>C</u>H_2), 72.2 (C31), 66.9 (C29), 55.3 (ArO<u>C</u>H_3), 46.4 (C33), 33.7 (C32), 32.6 (C30), 25.8 ($Si(CH_3)_2C(\underline{C}H_3)_3$), 18.1 ($Si(CH_3)_2\underline{C}(CH_3)_3$), 15.4 (Me32), –4.3 ($Si(\underline{C}H_3)_2C(CH_3)_3$), –4.6 ($Si(\underline{C}H_3)_2C(CH_3)_3$); **FTIR ν_{max}** 2953 (w, sp^3 CH str), 2927 (w, sp^3 CH str), 2855 (w, sp^3 CH str), 1725 (s, sh, C=O str), 1613, 1513, 1462, 1362, 1247 (s, sh, C-O str), 1087 (s, sh, C-O str), 1035 (s, sh, C-O str), 1005, 834, 774; $[\alpha]_D^{20}$ +7.6 (*c* 1.0, $CHCl_3$); **HRMS** (ESI^+): not sufficiently stable for analysis.

Analogous conditions were used to produce aldehyde *syn*-**185a** (203 mg, 0.533 mmol, ca. 75%), from primary alcohol *syn*-**184a** (270 mg, 0.706 mmol), as a colourless oil with R_f, ^{1}H NMR, ^{13}C NMR and FTIR data identical to aldehyde *ent-syn*-**185a**: $[\alpha]_D^{20}$ –7.0° (*c* 1.0, $CHCl_3$).

Terminal Olefin C31, 31-*syn*-3a and *ent*-C31, 31-*syn*-3b

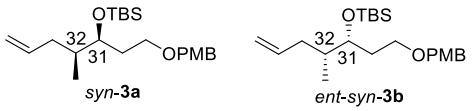

syn-**3a** *ent-syn*-**3b**

*n*BuLi (12.2 mL, 19.4 mmol, ca 1.6 M in hexanes) was added, dropwise, to a stirring suspension of methyltriphenylphosphonium bromide (7.7 g, 21.5 mmol) in THF (187 mL) at 0°C. After stirring for 30 mins, the bright yellow ylide solution was allowed to come to rt and stirred for 1h, before cooling to –78 °C. The ylide solution was cannulated, dropwise, into a stirring solution of aldehyde *ent-syn*-**185b** (1.08 g, ca. 2.84 mmol) in THF (35 mL) at –78 °C. After stirring for 30 mins, the reaction was allowed to come to rt, before being quenched with NH_4Cl (excess). The layers were separated and the aqueous layer extracted with CH_2Cl_2 (4 x 20 mL). The combined organic phases were washed with brine (50 mL), dried ($MgSO_4$), filtered and concentrated *in vacuo*. Purification

by flash column chromatography (SiO_2, 1-2% EtOAc/PE 40-60) afforded terminal olefin *ent-syn*-**3b** (1.08 g, 3.84 mmol, quant.), as a colourless oil: $\mathbf{R_f}$ (30% EtOAc/PE 40-60) = 0.75; , **^{1}H NMR** (500 MHz, $CDCl_3$) δ 7.26 (d, 2H, *J* = 8.6 Hz, ArH), 6.88 (d, 2H, *J* = 8.7 Hz, ArH), 5.76 (dddd, 1H, *J* = 17.0, 10.1, 7.8, 6.4 Hz, H34), 5.00 (d, 1H, *J* = 17.0 Hz, H35a), 4.97 (d, 1H, *J* = 10.1 Hz, H35b), 4.42 (AB_q, 2H, *J* = 11.5 Hz, $ArCH_2$), 3.81 (s, 3H, $ArOCH_3$), 3.74 (ddd, 1H, *J* = 8.0, 4.2, 3.7 Hz, H31), 3.48 (m, 2H, H29), 2.30 (m, 1H, H33a), 1.77 (m, 1H, H33b), 1.73 (ddd, 1H, *J* = 14.6, 7.3, 4.6 Hz, H30a), 1.66 (m, 1H, 30b), 1.59 (m, 1H, H32), 0.82 (d, 3H, *J* = 6.9 Hz, Me32), 0.88 (s, 9H, $Si(CH_3)_2C(CH_3)_3$), 0.033 (s, 3H, $Si(CH_3)_2C(CH_3)_3$), 0.026 (s, 3H, $Si(CH_3)_2C(CH_3)_3$); **^{13}C NMR** (125 MHz, $CDCl_3$) δ 159.1 (ArC), 138.2 (C34), 130.7 (ArC), 129.2 (ArCH), 115.4 (C35), 113.7 (ArCH), 72.64 (C31), 72.60 ($ArCH_2$), 67.3 (C29), 55.3 ($ArOCH_3$), 38.5 (C32), 36.4 (C33), 33.0 (C30), 25.9 ($Si(CH_3)_2C(CH_3)_3$), 18.1 ($Si(CH_3)_2C(CH_3)_3$), 14.4 (Me32), –4.4 ($Si(CH_3)_2C(CH_3)_3$), –4.5 ($Si(CH_3)_2C(CH_3)_3$); **FTIR ν_{max}** 2954 (w, sp^3 CH str), 2928 (w, sp^3 CH str), 2854 (w, sp^3 CH str), 1613, 1513, 1461, 1361, 1246 (s, sh, C-O str), 1172, 1087 (s, sh, C-O str), 1038 (s, sh, C-O str), 909, 833, 772; $[\alpha]_D^{20}$ +5.5 (*c* 1.0, $CHCl_3$); **HRMS** (ESI^+): calculated for $C_{22}H_{38}O_3SiNa$ $[M+Na]^+$ 401.2488, found 401.2486.

Analogous conditions were used to produce terminal olefin *syn*-**3a** (161 mg, 0.425 mmol, 60% over 2 steps), from aldehyde *syn*-**185a** (203 mg, 0.533 mmol), as a colourless oil with R_f, ^{1}H NMR, ^{13}C NMR, FTIR and HRMS data identical to primary alcohol *ent-syn*-**186a**: $[\alpha]_D^{20}$ –4.7° (*c* 1.0, $CHCl_3$).

Primary Alcohol C31, 31-*syn*, C32, C36-*anti,* C42, C45-*anti*-202a

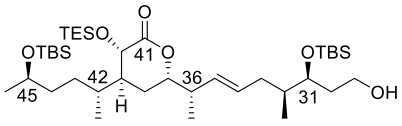

syn-anti-anti-**202a**

by-product

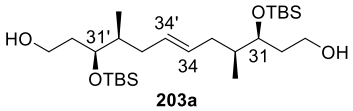

203a

Inseparable intermediates

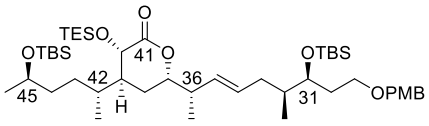

syn-anti-anti-**188a**

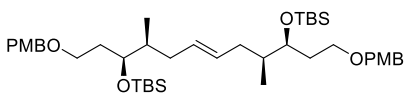

199a

Toluene (500 µL) was used to dissolve *p*-benzoquinone (0.2 mg, 1.8 µmol). The *p*-benzoquinone solution was then used to dissolve dichloro[1,3-bis(2,4,6-trimethylphenyl)-2-

imidazolidinylidene](2-isopropoxyphenylmethylene) ruthenium(II) (4.5 mg, 7.44 µmol, 3 mol % wrt total olefin). This resulting solution was added to terminal olefin 42,45-*anti*-**2a** (80 mg, 211 µmol) and terminal olefin 31,32-*syn*-**3a** (9.0 mg, 18.0 µmol). The reaction solution was carefully exposed to vacuum and flushed with $Ar_{(g)}$ four times. After stirring at 60 °C for 6 hours, the reaction mixture was filtered through a silica plug and concentrated *in vacuo*. Purification by flash column chromatography (SiO_2, 5% EtOAc/PE 40-60) afforded an inseparable mixture of the desired *syn-anti-anti*-olefin **188a** and olefin dimer by-product **199a** as a colourless oil (21.7 mg): $\mathbf{R_f}$ (5% EtOAc/PE 40-60) = 0.08.

DDQ (95.9 mg, 423 µmol) was added, in two portions, to a stirred solution of the inseparable *syn-anti-anti*-olefin **188a** and olefin dimer by-product **199a** mixture (21.7 mg) in CH_2Cl_2 and pH 7 buffer (4:1, 4 mL:1 mL) at 0 °C, giving a dark green solution. The mixture was allowed to come to rt and stirred for 15 min, until red in colour. After TLC analysis to check completion, the mixture was diluted with CH_2Cl_2 (6 mL) and carefully quenched with $NaHCO_3$ (9 mL). The layers were separated and the aqueous layer extracted with CH_2Cl_2 (4 x 2 mL). The combined organic phases were washed with brine (20 mL), dried ($MgSO_4$), filtered and concentrated *in vacuo*. Purification by flash column chromatography (SiO_2, 5-20% EtOAc/PE 40-60) afforded primary alcohol *syn-anti-anti*-olefin **202a** (7.8 mg, 10.7 µmol, 59% over two steps, 68% upon recycling returned starting material), as a colourless oil: $\mathbf{R_f}$ (30% EtOAc/PE 40-60) = 0.59; **^{1}H NMR** (500 MHz, $CDCl_3$) δ 5.45 (ddd, 1H, *J* = 15.3, 8.0, 6.9 Hz, H34), 5.25 (dd, 1H, *J* = 15.3, 8.3 Hz, H35), 4.22 (d, 1H, *J* = 10.6 Hz, H40), 3.89 (m, 1H, H37), 3.78 (m, 1H, H31), 3.75 (m, 1H, H45), 3.72 (m, 2H, H29), 2.33 (m, 1H, H36), 2.32 (m, 1H, H33a), 1.94 (m, 1H, H39), 1.91 (m, 1H, H42), 1.71 (m, 1H, H33b), 1.67 (m, 3H, H30, H38a), 1.65 (m, 1H, H32), 1.62 (m, 1H, H38b), 1.39 (m, 2H, H44), 1.27 (m, 1H, H43a), 1.19 (m, 1H, H43b), 1.10 (d, 3H, *J* = 6.1 Hz, H46), 1.09 (d, 3H, *J* = 6.8 Hz, Me36), 0.98 (t, 9H, 500 µL, $Si(CH_2\underline{CH_3})_3$), 0.90 (s, 9H, $Si(CH_3)_2C(C\underline{H_3})_3$), 0.88 (s, 9H, $Si(CH_3)_2C(C\underline{H_3})_3$), 0.831 (d, 3H, *J* = 6.8 Hz, Me42), 0.826 (d, 3H, *J* = 6.5 Hz, Me32), 0.68 (m, 6H, $Si(\underline{CH_2}CH_3)_3$), 0.09 (s, 3H, $Si(C\underline{H_3})_2C(CH_3)_3$), 0.07 (s, 3H, $Si(C\underline{H_3})_2C(CH_3)_3$) , 0.04 (s, 3H, $Si(C\underline{H_3})_2C(CH_3)_3$), 0.03 (s, 3H, $Si(C\underline{H_3})_2C(CH_3)_3$); **^{13}C NMR** (125 MHz, $CDCl_3$) δ 174.5 (C41=O), 131.58 (C35), 131.36 (C34), 79.26 (C37), 74.56 (C31), 68.49 (C40), 68.45 (C45), 60.67 (C29), 42.17 (C36), 40.63 (C39), 38.75 (C32), 37.33 (C44), 34.56 (C33), 34.37 (C30), 31.82 (C42), 30.88 (C43), 25.88 ($Si(CH_3)_2C(\underline{C}H_3)_3$), 25.87 ($Si(CH_3)_2C(\underline{C}H_3)_3$), 25.17 (C38), 23.76 (C46), 18.1 ($Si(CH_3)_2\underline{C}(CH_3)_3$), 18.0 ($Si(CH_3)_2\underline{C}(CH_3)_3$), 16.79 (Me36), 15.27 (Me32), 13.12 (Me42), 6.9 ($Si(CH_2\underline{CH_3})_3$), 5.0 ($Si(\underline{CH_2}CH_3)_3$), –4.3 ($Si(\underline{C}H_3)_2C(CH_3)_3$), –4.4 ($Si(\underline{C}H_3)_2C(CH_3)_3$), –4.6 ($Si(\underline{C}H_3)_2C(CH_3)_3$), –4.7 ($Si(\underline{C}H_3)_2C(CH_3)_3$) (nb: signals for the minor diastereomer matched primary alcohol *syn-syn-anti*-**202b**); **FTIR ν_{max}** 2956 (w, sp^3 CH str), 2928 (w, sp^3 CH str), 2857 (w, sp^3 CH str), 1740 (s, sh, C=O str), 1461, 1373, 1249, 1230, 1217, 1151 (s, sh, C-O str), 1081, 1057, 1005 (s,

sh, C-O str), 971, 834, 773, 741, 665; $[\alpha]_D^{20}$ –11.0 (*c* 1.0, $CHCl_3$); **HRMS** (ESI^+): calculated for $C_{39}H_{80}O_6Si_3Na$ $[M+Na]^+$ 752.5179, found 752.5171.

Dimer diol-**203a** (30.4 mg, 62.2 µmol) was separated as a colourless oil: $\mathbf{R_f}$ (30% EtOAc/PE 40-60) = 0.34; **^{1}H NMR** (700 MHz, $CDCl_3$) δ 5.36 (m, 2H, H34, H34'), 3.78 (m, 2H, H31, H31'), 3.73 (m, 4H, H29, H29'), 2.29 (m, 2H, H33a, H33a'), 1.96 (dd, 2H, *J* = 5.3, 5.0 Hz, -O<u>H</u>), 1.74-1.63 (m, 8H, H30, H32, H30', H32', H33b, H33b'), 0.90 (s, 18H, 2 x $Si(CH_3)_2C(C\underline{H_3})_3$), 0.84 (d, 6H, *J* = 6.7 Hz, Me32, Me32'), 0.09 (s, 6H, 2 x $Si(C\underline{H_3})_2C(CH_3)_3$), 0.07 (s, 6H, 2 x $Si(C\underline{H_3})_2C(CH_3)_3$).

Primary Alcohol C31, 31-*syn*, C32, C36-*syn,* C42, C45-*anti*-202b

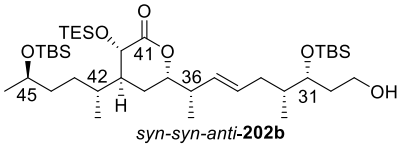

syn-syn-anti-**202b**

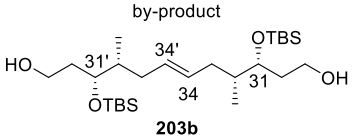

203b

Inseparable intermediates

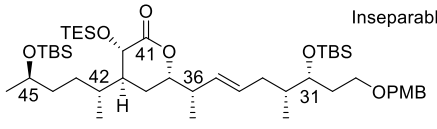

syn-syn-anti-**188b**

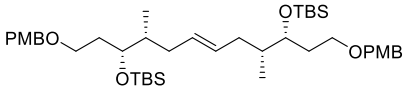

199b

Analogous conditions to olefin *syn-anti-anti*-**188a** (3 mol % catalyst loading wrt total olefin) were used to produce olefin *syn-syn-anti*-**188b** and the co-eluting olefin dimer by-product **199b** as a colourless oil (83.4 mg), from 42,45-*anti*-**2a** (9.9 mg, 19.8 µmol) and terminal olefin *ent-syn*-**3b** (88.3 mg, 233 µmol), as a colourless oil.

Analogous conditions to primary alcohol *syn-anti-anti*-**202a** were used to produce primary alcohol *syn-syn-anti*-**202b** (6.6 mg, 9.05 µmol, 46% over 2 steps), from olefin *syn-syn-anti*-**188b** and co-eluting olefin **199b** mixture (83.4 mg), as a colourless oil: $\mathbf{R_f}$ (30% EtOAc/PE 40-60) = 0.59; **^{1}H NMR** (700 MHz, $CDCl_3$) 5.47 (ddd, 1H, *J* = 15.3, 8.0, 6.2 Hz, H34), 5.29 (dd, 1H, *J* = 15.3, 8.1 Hz, H35), 4.22 (d, 1H, *J* = 10.6 Hz, H40), 3.91 (m, 1H, H37), 3.77 (m, 1H, H31), 3.75 (m, 1H, H45), 3.72 (m, 2H, H29), 2.34 (m, 1H, H36), 2.30 (m, 1H, H33a), 1.94 (m, 1H, H39), 1.91 (m, 1H, H42), 1.69 (m, 1H, H33b), 1.67 (m, 2H, H30), 1.65 (m, 1H, H38a), 1.64 (m, 1H, H32), 1.61 (m, 1H, H38b), 1.39 (m, 2H,

H44), 1.27 (m, 1H, H43a), 1.19 (m, 1H, H43b), 1.11 (d, 3H, *J* = 6.1 Hz, H46), 1.09 (d, 3H, *J* = 6.8 Hz, Me36), 0.98 (t, 9H, *J* = 7.9 Hz, $Si(CH_2\underline{CH_3})_3$), 0.90 (s, 9H, $Si(CH_3)_2C(C\underline{H_3})_3$), 0.88 (s, 9H, $Si(CH_3)_2C(C\underline{H_3})_3$), 0.832 (d, 3H, *J* = 6.8 Hz, Me42), 0.829 (d, 3H, *J* = 6.5 Hz, Me32), 0.68 (m, 6H, $Si(\underline{CH_2}CH_3)_3$), 0.09 (s, 3H, $Si(C\underline{H_3})_2C(CH_3)_3$), 0.06 (s, 3H, $Si(C\underline{H_3})_2C(CH_3)_3$) , 0.04 (s, 3H, $Si(C\underline{H_3})_2C(CH_3)_3$), 0.03 (s, 3H, $Si(C\underline{H_3})_2C(CH_3)_3$); **^{13}C NMR** (125 MHz, $CDCl_3$) δ 174.5 (C41=O), 131.57 (C35), 131.09 (C34), 79.26 (C37), 74.66 (C31), 68.49 (C40), 68.43 (C45), 60.67 (C29), 41.89 (C36), 40.59 (C39), 38.84 (C32), 37.29 (C44), 34.37 (C33), 34.33 (C30), 31.78 (C42), 30.87 (C43), 25.88 ($Si(CH_3)_2C(\underline{C}H_3)_3$), 25.87 ($Si(CH_3)_2C(\underline{C}H_3)_3$), 24.91 (C38), 23.78 (C46), 18.1 ($Si(CH_3)_2\underline{C}(CH_3)_3$), 18.0 ($Si(CH_3)_2\underline{C}(CH_3)_3$), 16.64 (Me36), 15.18 (Me32), 13.15 (Me42), 6.9 ($Si(CH_2\underline{CH_3})_3$), 5.0 ($Si(\underline{CH_2}CH_3)_3$), –4.2 ($Si(\underline{C}H_3)_2C(CH_3)_3$), –4.4 ($Si(\underline{C}H_3)_2C(CH_3)_3$), –4.6 ($Si(\underline{C}H_3)_2C(CH_3)_3$), –4.7 ($Si(\underline{C}H_3)_2C(CH_3)_3$) (nb: signals for the minor diastereomer matched (*S, S, R*)-primary alcohol **202a**); **FTIR ν_{max}** 2956 (w, sp^3 CH str), 2928 (w, sp^3 CH str), 2856 (w, sp^3 CH str), 1745 (s, sh, C=O str), 1461, 1412, 1374, 1250, 1150 (s, sh, C-O str), 1082, 1058, 1004 (s, sh, C-O str), 971, 833, 772, 7428, 664; $[\alpha]_D^{20}$ –7.1 (*c* 1.0, $CHCl_3$); **HRMS** (ESI^+): calculated for $C_{39}H_{80}O_6Si_3Na$ $[M+Na]^+$ 752.5179, found 752.5171.

Diol *ent*-**203b** (41.4 mg, 84.7 µmol) was separated as a colourless oil with R_f and ^{1}H NMR data matching diol **203a**.

Primary Alcohol C31, 31-*syn*, C32, C36-*syn,* C42, C45-*syn(anti)*-202c

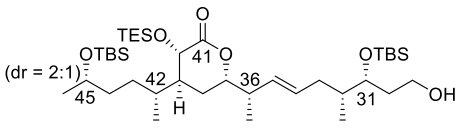

syn-syn-syn(anti)-**202c**

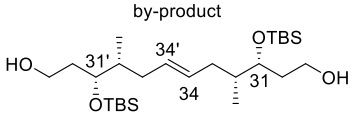

203b

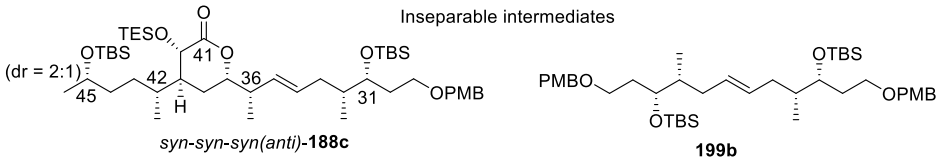

syn-syn-syn(anti)-**188c** **199b**

Analogous conditions to olefin *syn-anti-anti*-**188a** (5 mol % catalyst loading wrt total olefin) were used to produce olefin *syn-syn-syn(anti)*-**188c** and the co-eluting olefin **199b** dimer by-product as

a colourless oil (79.6 mg), from terminal olefin 42,45-*syn(anti)*-**2b** (15.0 mg, 30.1 µmol, *dr* at C45 remains ca 2:1) and terminal olefin *ent*-*syn*-**3b** (85.2 mg, 225 µmol), as a colourless oil.

Analogous conditions to primary alcohol *syn-anti-anti*-**202a** were used to produce olefin *syn-syn-syn(anti)*-**202c** (13.3 mg, 18.2 µmol, 60% over 2 steps, *dr* at C45 remains ca. 2:1), from olefin *syn-syn-syn(anti)*-**188c** and co-eluting olefin **199b** mixture (79.6 mg), as a colourless oil: $\mathbf{R_f}$ (30% EtOAc/PE 40-60) = 0.59; **^{1}H NMR** (700 MHz, $CDCl_3$) 5.47 (ddd, 1H, *J* = 15.1, 7.8, 7.0 Hz, H34), 5.28 (dd, 1H, *J* = 15.3, 8.1 Hz, H35), 4.22 (d, 1H, *J* = 10.6 Hz, H40), 3.90 (m, 1H, H37), 3.77 (m, 1H, H31), 3.75 (m, 1H, H45), 3.72 (m, 2H, H29), 2.34 (m, 1H, H36), 2.31 (m, 1H, H33a), 1.94 (m, 1H, H39), 1.91 (m, 1H, H42), 1.70-1.61 (m, 6H, H30, 32, 33b, H38), 1.43 (m, 1H, H44a), 1.35 (m, 1H, H44b), 1.31 (m, 1H, H43a), 1.17 (m, 1H, H43b), 1.11 (d, 3H, *J* = 6.1 Hz, H46), 1.09 (d, 3H, *J* = 6.8 Hz, Me36), 0.98 (t, 9H, *J* = 7.9 Hz, $Si(CH_2\underline{CH_3})_3$), 0.90 (s, 9H, $Si(CH_3)_2C(C\underline{H_3})_3$), 0.88 (s, 9H, $Si(CH_3)_2C(C\underline{H_3})_3$), 0.83 (d, 6H, *J* = 6.7 Hz, Me32, Me42), 0.68 (m, 6H, $Si(\underline{CH_2}CH_3)_3$), 0.09 (s, 3H, $Si(C\underline{H_3})_2C(CH_3)_3$), 0.06 (s, 3H, $Si(C\underline{H_3})_2C(CH_3)_3$) , 0.04 (s, 3H, $Si(C\underline{H_3})_2C(CH_3)_3$), 0.03 (s, 3H, $Si(C\underline{H_3})_2C(CH_3)_3$); **^{13}C NMR** (125 MHz, $CDCl_3$) δ 174.4 (C41=O), 131.57 (C35), 131.09 (C34), 79.25 (C37), 74.62 (C31), 68.48 (C40), 68.51 (C45), 60.66 (C29), 41.91 (C36), 40.84 (C39), 38.81 (C32), 37.36 (C44), 34.35 (C33), 34.40 (C30), 31.95 (C42), 30.87 (C43), 25.88 ($Si(CH_3)_2C(\underline{C}H_3)_3$), 25.87 ($Si(CH_3)_2C(\underline{C}H_3)_3$), 24.89 (C38), 23.72 (C46), 18.1 ($Si(CH_3)_2\underline{C}(CH_3)_3$), 18.0 ($Si(CH_3)_2\underline{C}(CH_3)_3$), 16.68 (Me36), 15.16 (Me32), 12.92 (Me42), 6.9 ($Si(CH_2\underline{CH_3})_3$), 5.0 ($Si(\underline{CH_2}CH_3)_3$), –4.2 ($Si(\underline{C}H_3)_2C(CH_3)_3$), –4.4 ($Si(\underline{C}H_3)_2C(CH_3)_3$), –4.6 ($Si(\underline{C}H_3)_2C(CH_3)_3$), –4.7 ($Si(\underline{C}H_3)_2C(CH_3)_3$).

Diol *ent*-**203b** (41.4 mg, 84.7 µmol) was separated as a colourless oil with R_f and ^{1}H NMR data matching diol-**203a**.

Tetraols C31, 31-*syn*, C32, C36-*anti,* C42, C45-*anti*-204a, C31, 31-*syn*, C32, C36-*syn,* C42, C45-*anti*-204b and C31, 31-*syn*, C32, C36-*syn,* C42, C45-*syn(anti)*-204c

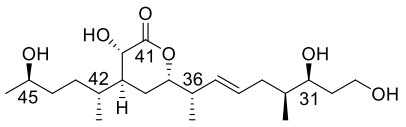

syn-anti-anti-**204a**

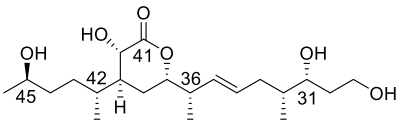

syn-syn-anti-**204b**

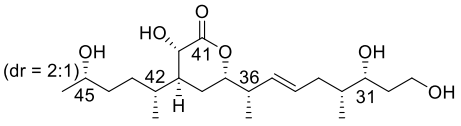

syn-syn-syn(anti)-**204c**

Hydrofluoric acid (60 µL, 48% aq.) in MeCN (240 µL) was carefully added, dropwise, to a stirring solution of primary alcohol *syn-anti-anti*-**202a** (2.0 mg, 2.74 µmol) and in MeCN (240 µL), at –20 °C, in a plastic eppendorf. The mixture was stirred for 6 h before being carefully quenched with Et_3N (3 drops). The mixture was allowed to come to room temperature and $NaHCO_3$ (2 mL) added. The layers were separated and the aqueous layer extracted with CH_2Cl_2 (4 x 2 mL). The combined organic phases were washed with brine (5 mL), dried ($MgSO_4$), filtered and concentrated *in vacuo*. Purification by flash column chromatography (SiO_2, 1-10% MeOH/CH_2Cl_2) afforded tetraol *syn-anti-anti*-**204a** (1.1 mg, 2.74 µmol, quant.), as a colourless oil: $\mathbf{R_f}$ (10% MeOH/CH_2Cl_2) = 0.21; **^{1}H NMR** (700 MHz, $CDCl_3$) δ 5.55 (m, 1H, H34), 5.25 (dd, 1H, *J* = 15.4, 8.0 Hz, H35), 4.19 (d, 1H, *J* = 11.2 Hz, H40), 4.02 (m, 1H, H37), 3.88 (m, 1H, H29a), 3.81 (m, 1H, H29b), 3.79 (m, 1H, H31), 3.78 (m, 1H, H45), 2.41 (m, 1H, H36), 2.21 (m, 1H, H33a), 2.00 (m, 1H, H42), 1.95 (m, 1H, H33b), 1.90 (m, 1H, H39), 1.73 (m, 1H, H30a), 1.70 (m, 2H, H38), 1.64 (m, 1H, H30b), 1.61 (m, 1H, H32), 1.50 (m, 1H, H44a), 1.42 (m, 1H, H43a), 1.41 (m, 1H, H44b), 1.25 (m, 1H, H43b), 1.20 (d, 3H, *J* = 6.2 Hz, H46), 1.11 (d, 3H, *J* = 6.7 Hz, Me36), 0.91 (d, 6H, *J* = 6.8 Hz, Me42, Me32); **^{13}C NMR** (125 MHz, $CDCl_3$) δ 176.9 (C41=O), 131.42 (C35), 131.06 (C34), 79.95 (C37), 74.69 (C31), 68.33 (C45), 67.04 (C40), 62.08 (C29), 41.75 (C36), 40.28 (C39), 38.92 (C32), 36.90 (C44), 36.33 (C33), 35.50 (C30), 32.65 (C42), 30.73 (C43), 25.10 (C38), 23.70 (C46), 16.46 (Me36), 14.11 (Me32), 13.26 (Me42); **^{1}H NMR** (700 MHz, CD_3OD) δ 5.56 (ddd, 1H, *J* = 15.3, 7.8, 7.0 Hz, H34), 5.33 (dd, 1H, *J* = 15.3, 8.3 Hz, H35), 4.32 (d, 1H, *J* = 11.3 Hz, H40), 4.11 (ddd, 1H, *J* = 11.2, 7.8, 3.7 Hz, H37), 3.69 (m, 3H, H29, H45), 3.65 (ddd, 1H, *J* = 7.6, 4.2, 3.7 Hz, H31), 2.34 (m, 1H, H36), 2.21 (m, 1H, H33a), 1.98 (m, 1H, H42), 1.89 (m, 2H, H33b, H39), 1.80 (m, 1H, H38a), 1.67 (m, 1H, H38b), 1.65 (m, 2H, H30), 1.54 (m, 1H, H32), 1.43 (m, 2H, H44), 1.38 (m, 1H, H43a), 1.26 (m, 1H, H43b), 1.15 (d, 3H, *J* = 6.2 Hz, H46), 1.11 (d, 3H, *J* = 6.7 Hz, Me36), 0.91 (d, 6H, *J* = 6.9 Hz, Me42), 0.89 (d, 6H, *J* = 6.9 Hz, Me32); **^{13}C NMR** (125 MHz, CD_3OD) δ 178.37 (C41=O), 133.15 (C35), 131.45 (C34), 80.86 (C37), 72.78 (C31), 68.70 (C45), 68.20 (C40), 60.71 (C29), 43.56 (C36), 41.40 (C39), 40.32 (C32), 37.96 (C44), 37.77

(C30), 37.64 (C33), 33.72 (C42), 32.08 (C43), 26.72 (C38), 23.54 (C46), 17.13 (Me36), 14.36 (Me32), 13.37 (Me42) (nb: signals for the minor diastereomer matched *syn-syn-anti*-**204b**; **FTIR ν_{max}** 3374 (w, br, -OH str), 2964 (w, sp^3 CH str), 2923 (w, sp^3 CH str), 2858 (w, sp^3 CH str), 1738 (s, sh, C=O str), 1457, 1415, 1365 (s, sh, C-O str), 1218 (s, sh, C-O str), 1107 (s, sh, C-O str), 1051 (s, sh, C-O str), 1003, 974, 872, 846, 795, 706, 666; $[\alpha]_D^{20}$ –11.1 (*c* 1.0, $CHCl_3$); **HRMS** (ESI^+): calculated for $C_{21}H_{37}O_6$ $[M-H]^-$ 386.2630, found 386.2631.

Analogous conditions were used to produce tetraol *syn-syn-anti*-**204b** (1.1 mg, 2.74 µmol, quant.), from primary alcohol *syn-syn-anti*-**202b** (2.0 mg, 2.74 µmol) as a colourless oil: **R_f** (30% EtOAc/PE 40-60) = 0.59; **^{1}H NMR** (700 MHz, $CDCl_3$) δ 5.54 (m, 1H, H34), 5.30 (dd, 1H, *J* = 15.3, 8.4 Hz, H35), 4.19 (d, 1H, *J* = 11.1 Hz, H40), 4.02 (m, 1H, H37), 3.88 (m, 1H, H29a), 3.81 (m, 1H, H29b), 3.79 (m, 1H, H31), 3.78 (m, 1H, H45), 2.41 (m, 1H, H36), 2.19 (m, 1H, H33a), 1.99 (m, 1H, H42), 1.96 (m, 1H, H33b), 1.90 (m, 1H, H39), 1.73 (m, 1H, H30a), 1.71 (m, 2H, H38), 1.63 (m, 1H, H30b), 1.61 (m, 1H, H32), 1.51 (m, 1H, H44a), 1.43 (m, 1H, H43a), 1.42 (m, 1H, H44b), 1.25 (m, 1H, H43b), 1.20 (d, 3H, *J* = 6.2 Hz, H46), 1.11 (d, 3H, *J* = 6.7 Hz, Me36), 0.92 (d, 6H, *J* = 6.8 Hz, Me42), 0.91 (d, 6H, *J* = 6.9 Hz, Me32); **^{13}C NMR** (125 MHz, $CDCl_3$) δ 176.9 (C41=O), 131.48 (C35), 131.22 (C34), 80.10 (C37), 74.11 (C31), 68.40 (C45), 67.09 (C40), 61.98 (C29), 42.04 (C36), 40.20 (C39), 38.75 (C32), 36.92 (C44), 36.41 (C33), 35.64 (C30), 32.80 (C42), 30.64 (C43), 25.14 (C38), 23.74 (C46), 16.86 (Me36), 14.08 (Me32), 13.40 (Me42); **^{1}H NMR** (700 MHz, CD_3OD) δ 5.56 (ddd, 1H, *J* = 15.3, 7.6, 7.0 Hz, H34), 5.30 (dd, 1H, *J* = 15.3, 8.3 Hz, H35), 4.31 (d, 1H, *J* = 11.3 Hz, H40), 4.12 (ddd, 1H, *J* = 10.9, 7.5, 3.8 Hz, H37), 3.69 (m, 3H, H29, H45), 3.65 (m, 1H, H31), 2.35 (m, 1H, H36), 2.22 (m, 1H, H33a), 1.98 (m, 1H, H42), 1.89 (m, 1H, H33b), 1.87 (m, 1H, H39), 1.79 (m, 1H, H38a), 1.68 (m, 1H, H38b), 1.65 (m, 2H, H30), 1.54 (m, 1H, H32), 1.43 (m, 2H, H44), 1.38 (m, 1H, H43a), 1.26 (m, 1H, H43b), 1.15 (d, 3H, *J* = 6.2 Hz, H46), 1.11 (d, 3H, *J* = 6.7 Hz, Me36), 0.91 (d, 6H, *J* = 6.9 Hz, Me42), 0.89 (d, 6H, *J* = 6.9 Hz, Me32); **^{13}C NMR** (125 MHz, CD_3OD) δ 178.36 (C41=O), 133.14 (C35), 131.24 (C34), 80.91 (C37), 72.69 (C31), 68.70 (C45), 68.22 (C40), 60.74 (C29), 43.30 (C36), 41.36 (C39), 40.36 (C32), 37.96 (C44), 37.80 (C30), 37.51 (C33), 33.73 (C42), 32.03 (C43), 26.47 (C38), 23.57 (C46), 17.00 (Me36), 14.23 (Me32), 13.43 (Me42) (nb: signals for the minor diastereomer matched *syn-anti-anti*-**204a**; **FTIR ν_{max}** 3384 (w, br, -OH str), 2960 (w, sp^3 CH str), 2927 (w, sp^3 CH str), 1736 (s, sh, C=O str), 1664, 1457, 1376 (s, sh, C-O str), 1216 (s, sh, C-O str), 1106 (s, sh, C-O str), 1051 (s, sh, C-O str), 1002, 972, 873, 847, 800, 752, 703, 666; $[\alpha]_D^{20}$ –8.0 (*c* 1.0, $CHCl_3$); **HRMS** (ESI^+): calculated for $C_{21}H_{37}O_6$ $[M-H]^-$ 386.2630, found 386.2631.

Analogous conditions were used to produce tetraol *syn-syn-syn(anti)*-**204c** (1.3 mg, 3.34 µmol, 81%, *dr* at C45 remains ca. 2:1), from primary alcohol *syn-syn-syn(anti)*-**202c** (3.0 mg, 4.11 µmol) as a colourless oil: $\mathbf{R_f}$ (30% EtOAc/PE 40-60) = 0.59; **^{1}H NMR** (700 MHz, $CDCl_3$) δ 5.53 (m, 1H, H34), 5.30 (dd, 1H, *J* = 15.3, 8.4 Hz, H35), 4.19 (d, 1H, *J* = 11.2 Hz, H40), 4.01 (ddd, 1H, *J* = 10.4, 7.4, 4.3 Hz, H37), 3.88 (m, 1H, H29a), 3.81 (m, 1H, H29b), 3.80 (m, 1H, H31), 3.79 (m, 1H, H45), 2.40 (m, 1H, H36), 2.20 (m, 1H, H33a), 2.00 (m, 1H, H42), 1.95 (m, 1H, H33b), 1.88 (m, 1H, H39), 1.74 (m, 1H, H30a), 1.72 (m, 1H, H38a), 1.67 (m, 1H, H38b), 1.61 (m, 1H, H32), 1.60 (m, 1H, H30b), 1.50 (m, 1H, H44a), 1.42 (m, 1H, H44b), 1.41 (m, 1H, H43a), 1.27 (m, 1H, H43b), 1.20 (d, 3H, *J* = 6.2 Hz, H46), 1.11 (d, 3H, *J* = 6.7 Hz, Me36), 0.91 (d, 6H, *J* = 6.8 Hz, Me32, Me42); **^{13}C NMR** (125 MHz, $CDCl_3$) δ 176.88 (C41=O), 131.50 (C35), 131.30 (C34), 80.08 (C37), 74.11 (C31), 68.27 (C45), 67.13 (C40), 62.01 (C29), 42.10 (C36), 40.93 (C39), 38.75 (C32), 36.86 (C44), 36.47 (C33), 35.66 (C30), 32.66 (C42), 30.94 (C43), 25.32 (C38), 23.88 (C46), 16.91 (Me36), 14.11 (Me32), 12.87 (Me42); **^{1}H NMR** (700 MHz, CD_3OD) δ 5.57 (m, 1H, H34), 5.36 (dd, 1H, *J* = 15.3, 8.3 Hz, H35), 4.32 (d, 1H, *J* = 11.3 Hz, H40), 4.12 (ddd, 1H, *J* = 11.1, 7.9, 4.0 Hz, H37), 3.69 (m, 3H, H29, H45), 3.66 (m, 1H, H31), 2.35 (m, 1H, H36), 2.21 (m, 1H, H33a), 1.97 (m, 1H, H42), 1.89 (m, 1H, H33b), 1.88 (m, 1H, H39), 1.79 (m, 1H, H38a), 1.68 (m, 1H, H38b), 1.65 (m, 2H, H30), 1.53 (m, 1H, H32), 1.49 (m, 1H, H44a), 1.40 (m, 1H, H44b), 1.39 (m, 1H, H43a), 1.27 (m, 1H, H43b), 1.15 (d, 3H, *J* = 6.2 Hz, H46), 1.11 (d, 3H, *J* = 6.8 Hz, Me36), 0.91 (d, 6H, *J* = 6.8 Hz, Me42), 0.89 (d, 6H, *J* = 6.9 Hz, Me32); **^{13}C NMR** (125 MHz, CD_3OD) δ 178.35 (C41=O), 133.15 (C35), 132.25 (C34), 80.91 (C37), 72.70 (C31), 68.63 (C45), 68.24 (C40), 60.75 (C29), 43.32 (C36), 41.60 (C39), 40.38 (C32), 37.99 (C44), 37.80 (C30), 37.52 (C33), 33.72 (C42), 32.07 (C43), 26.49 (C38), 23.56 (C46), 17.03 (Me36), 14.24 (Me32), 13.25 (Me42).

Aldehyde C31, 31-*syn*, C32, C36-*anti,* C42, C45-*anti*-131a

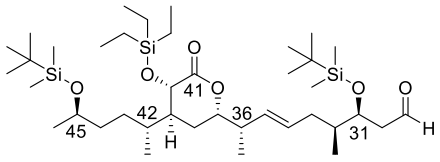

DMP (3.8 mg, 9.05 µmol) was added to a stirred solution of primary alcohol *syn-anti-anti*-**202a** (1.1 mg, 1.51 µmol) and $NaHCO_{3(s)}$ (1.5 mg, 18.1 µmol) in CH_2Cl_2 (0.5 mL) at rt. The mixture was stirred for 1h, diluted with CH_2Cl_2 (0.5 mL) and quenched with premixed $NaHCO_3$ (70 µL) and $Na_2S_2O_3$ (70 µL), by stirring for 30 min. The layers were separated and the aqueous layer extracted with CH_2Cl_2 (4 x 2 mL). The combined organic phases were washed with brine (5 mL), dried ($MgSO_4$), filtered and concentrated *in vacuo*. Purification by flash column chromatography (SiO_2, 5% EtOAc/PE 40-60) afforded aldehyde *syn-anti-anti*-**131a** (1.1 mg, 1.51 µmol, quant.), as a colourless oil: $\mathbf{R_f}$ (30% EtOAc/PE 40-60) = 0.70; **^{1}H NMR** (700 MHz, $CDCl_3$) δ 9.79 (dd, 1H, *J* = 2.8,

1.8 Hz, H29), 5.44 (ddd, 1H, *J* = 15.1, 7.6, 6.2 Hz, H34), 5.27 (dd, 1H, *J* = 15.2, 8.3 Hz, H35), 4.23 (d, 1H, *J* = 10.6 Hz, H40), 4.15 (m, 1H, H31), 3.90 (m, 1H, H37), 3.75 (m, 1H, H45), 2.53 (ddd, 1H, *J* = 15.9, 7.4, 2.8 Hz, H30a), 2.45 (ddd, 1H, *J* = 15.9, 4.6, 1.7 Hz, H30b), 2.33 (m, 1H, H36), 2.31 (m, 1H, H33a), 1.94 (m, 1H, H39), 1.91 (m, 1H, H42), 1.70 (m, 1H, H33b), 1.66 (m, 1H, H38a), 1.64 (m, 1H, H32), 1.62 (m, 1H, H38b), 1.39 (m, 2H, H44), 1.27 (m, 1H, H43a), 1.19 (m, 1H, H43b), 1.10 (d, 3H, *J* = 6.1 Hz, H46), 1.09 (d, 3H, *J* = 6.8 Hz, Me36), 0.98 (t, 9H, *J* = 7.9 Hz, $Si(CH_2\underline{CH_3})_3$), 0.879 (s, 9H, $Si(CH_3)_2C(C\underline{H_3})_3$), 0.875 (s, 9H, $Si(CH_3)_2C(C\underline{H_3})_3$), 0.84 (d, 3H, *J* = 6.6 Hz, Me32), 0.83 (d, 3H, *J* = 6.8 Hz, Me42), 0.68 (m, 6H, $Si(\underline{CH_2}CH_3)_3$), 0.07 (s, 3H, $Si(C\underline{H_3})_2C(CH_3)_3$), 0.04 (s, 6H, 2 x $Si(C\underline{H_3})_2C(CH_3)_3$), 0.03 (s, 3H, $Si(C\underline{H_3})_2C(CH_3)_3$); **^{13}C NMR** (125 MHz, $CDCl_3$) δ 202.14 (C29), 174.4 (C41=O), 131.96 (C35), 130.87 (C34), 79.18 (C37), 71.15 (C31), 68.48 (C40), 68.435 (C45), 47.48 (C30), 42.13 (C36), 40.62 (C39), 39.39 (C32), 37.33 (C44), 34.91 (C33), 31.80 (C42), 30.88 (C43), 25.88 ($Si(CH_3)_2C(\underline{C}H_3)_3$), 25.78 ($Si(CH_3)_2C(\underline{C}H_3)_3$), 25.13 (C38), 23.76 (C46), 18.1 ($Si(CH_3)_2\underline{C}(CH_3)_3$), 18.0 ($Si(CH_3)_2\underline{C}(CH_3)_3$), 16.71 (Me36), 14.81 (Me32), 13.13 (Me42), 6.9 ($Si(CH_2\underline{CH_3})_3$), 5.0 ($Si(\underline{CH_2}CH_3)_3$), –4.37 ($Si(\underline{C}H_3)_2C(CH_3)_3$), –4.40 ($Si(\underline{C}H_3)_2C(CH_3)_3$), –4.6 ($Si(\underline{C}H_3)_2C(CH_3)_3$), –4.7 ($Si(\underline{C}H_3)_2C(CH_3)_3$); **FTIR ν_{max}** 2955 (w, sp^3 CH str), 2928 (w, sp^3 CH str), 2856 (w, sp^3 CH str), 1760 (s, sh, C=O str), 1727 (s, sh, C=O str), 1461, 1376, 1361, 1251, 1150 (s, sh, C-O str), 1083, 1051, 1005 (s, sh, C-O str), 972, 834, 773; $[\alpha]_D^{20}$ –13.9 (*c* 1.0, $CHCl_3$); **HRMS** (ESI^+): not sufficiently stable for analysis.

Minor aldehyde diastereomer *syn-syn-anti*-**131b**: **^{13}C NMR** (125 MHz, $CDCl_3$) δ 202.17 (C29), 174.4 (C41=O), 131.98 (C35), 130.55 (C34), 79.19 (C37), 71.24 (C31), 68.48 (C40), 68.42 (C45), 47.44(C30), 41.82 (C36), 40.57 (C39), 39.48 (C32), 34.71 (C33), 31.76 (C42), 30.88 (C43), 25.88 ($Si(CH_3)_2C(\underline{C}H_3)_3$), 25.78 ($Si(CH_3)_2C(\underline{C}H_3)_3$), 24.88 (C38), 23.79 (C46), 18.1 ($Si(CH_3)_2\underline{C}(CH_3)_3$), 18.0 ($Si(CH_3)_2\underline{C}(CH_3)_3$), 16.52 (Me36), 14.721 (Me32), 13.16 (Me42), 6.9 ($Si(CH_2\underline{CH_3})_3$), 5.0 ($Si(\underline{CH_2}CH_3)_3$), –4.37 ($Si(\underline{C}H_3)_2C(CH_3)_3$), –4.40 ($Si(\underline{C}H_3)_2C(CH_3)_3$), –4.6 ($Si(\underline{C}H_3)_2C(CH_3)_3$), –4.7 ($Si(\underline{C}H_3)_2C(CH_3)_3$).

Appendix 2: Spectral Data

Spectrum 1. β-Hydroxy ketone **135**, $CDCl_3$, ^1H NMR, 400 MHz

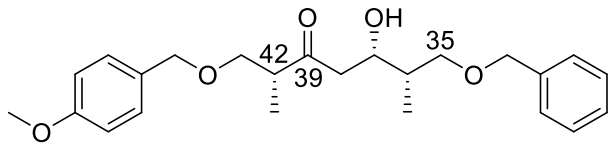

Spectrum 2. β-Hydroxy ketone **135**, $CDCl_3$, ^{13}C NMR, 125 MHz

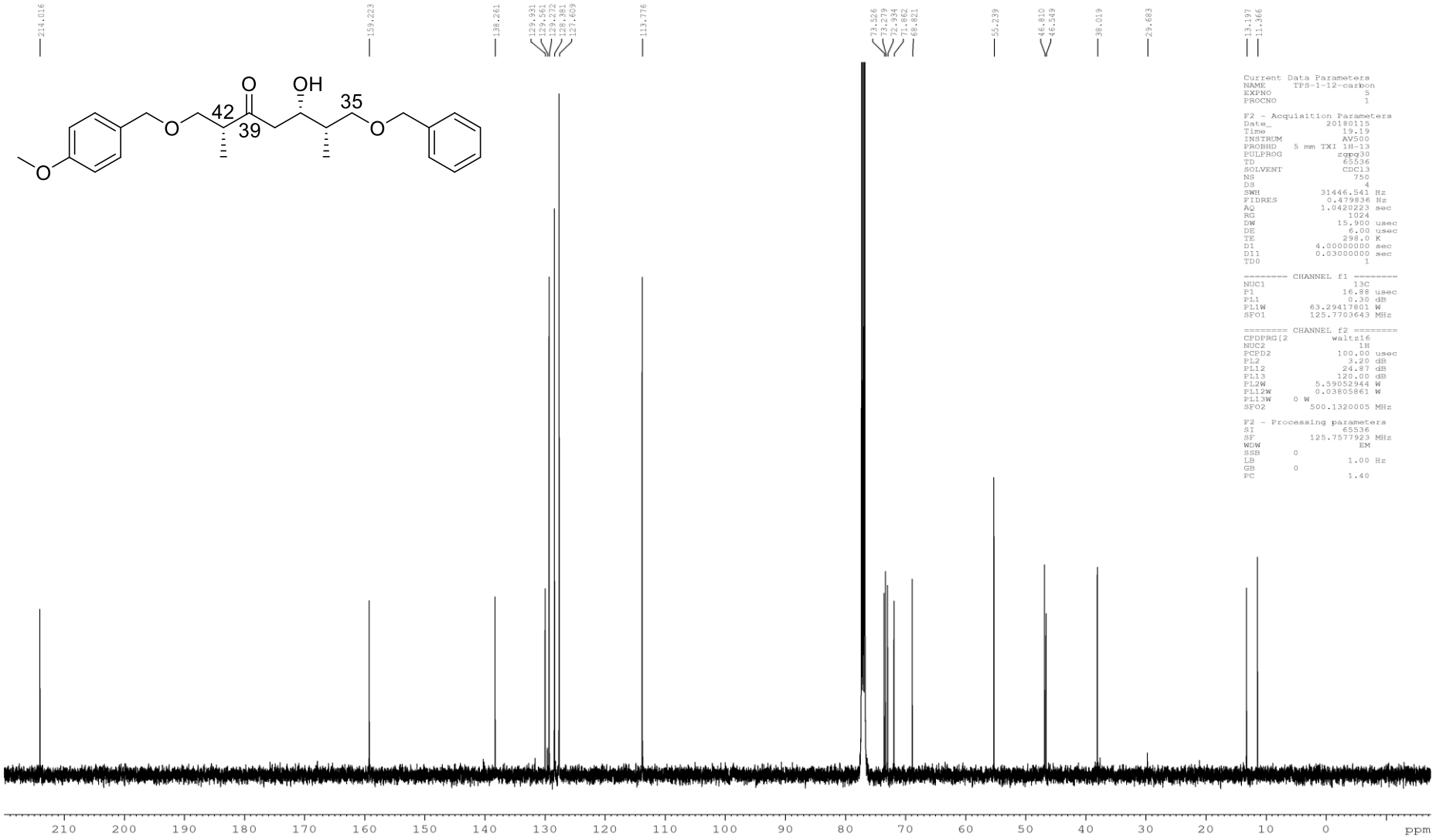

Spectrum 3. TBS ether **145**, $CDCl_3$, ^1H NMR, 500 MHz

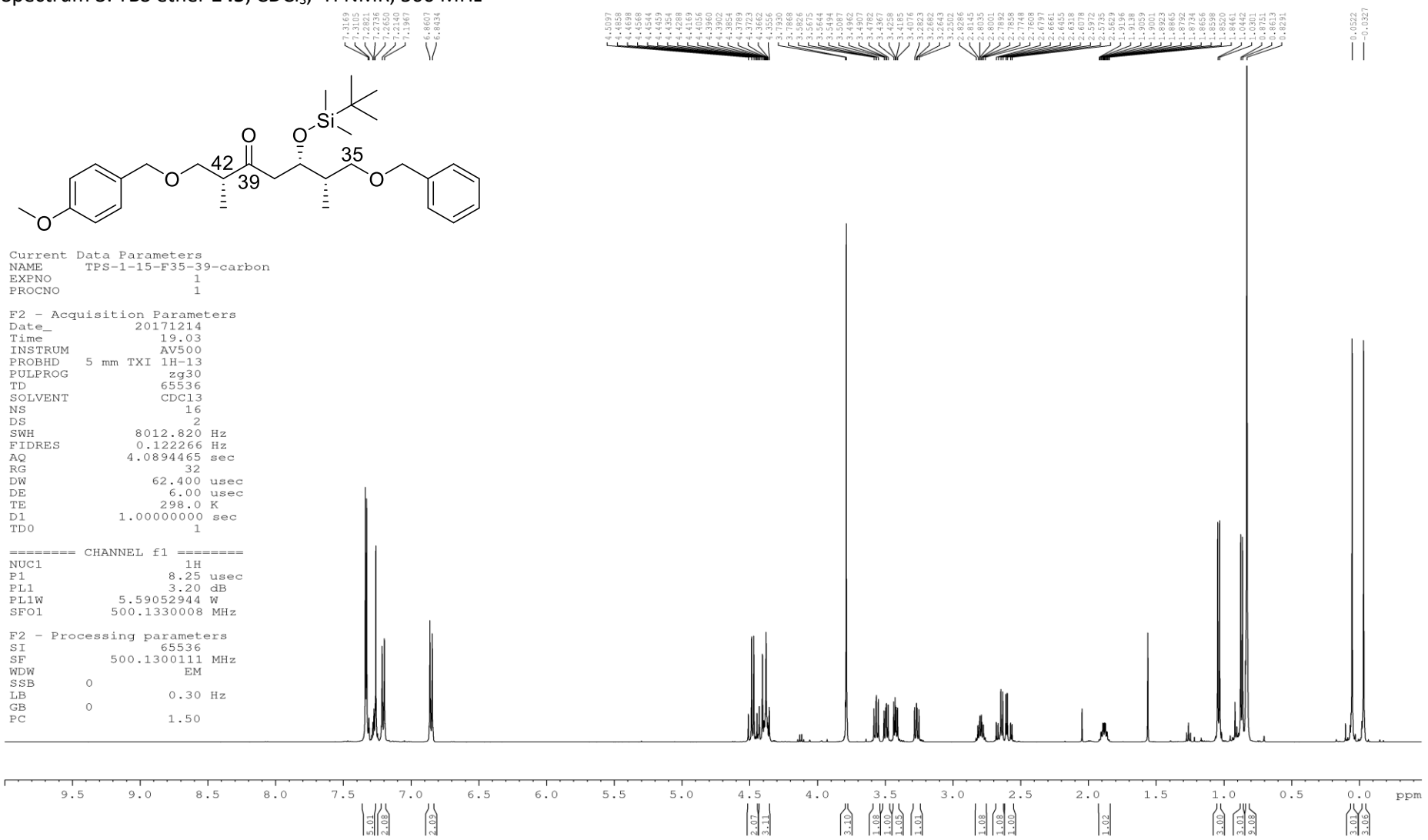

Spectrum 4. TBS ether **145**, $CDCl_3$, ^{13}C NMR, 125 MHz

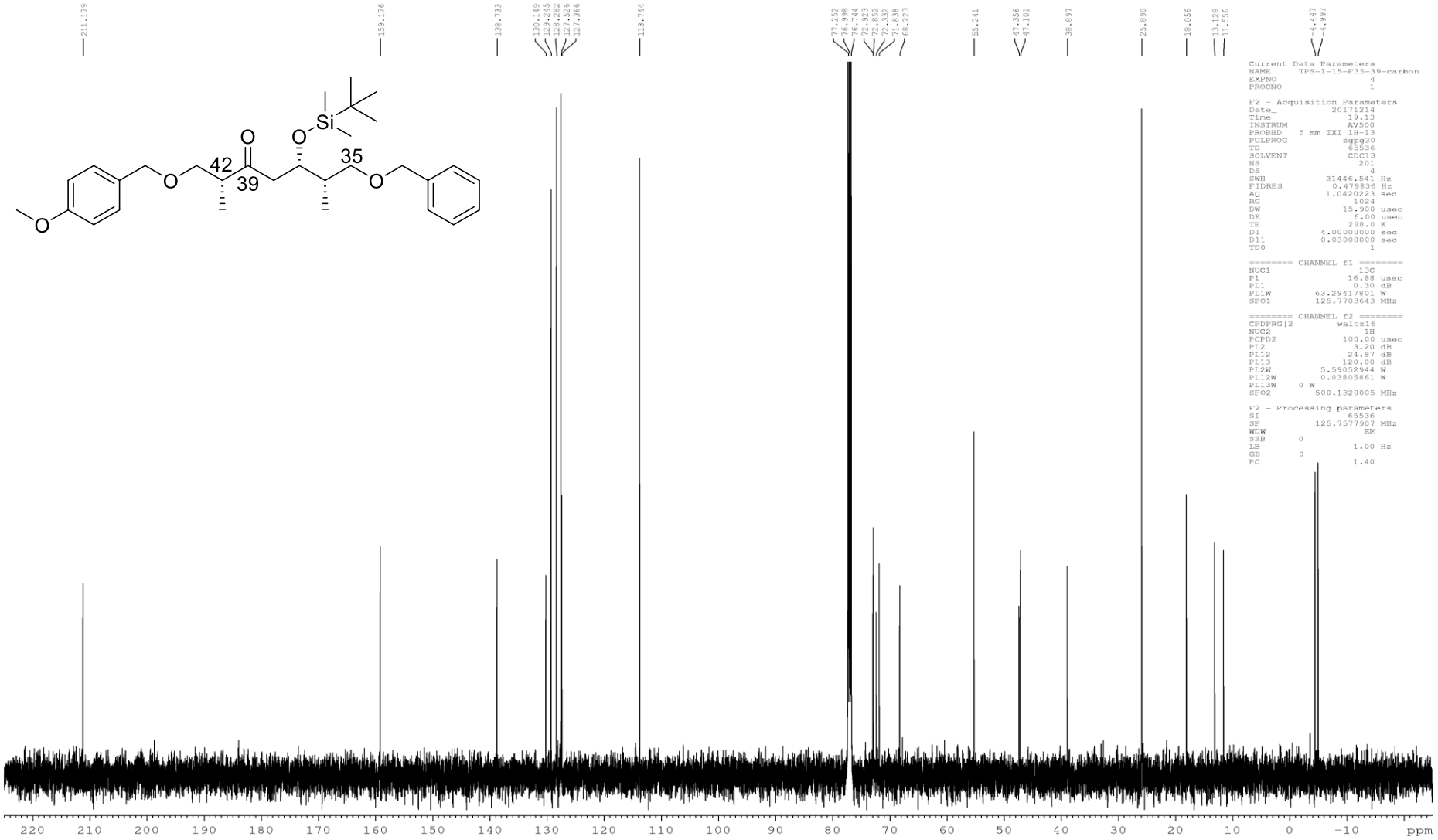

Spectrum 5. Enoate (*Z*)-**149a**, $CDCl_3$, ^1H NMR, 500 MHz

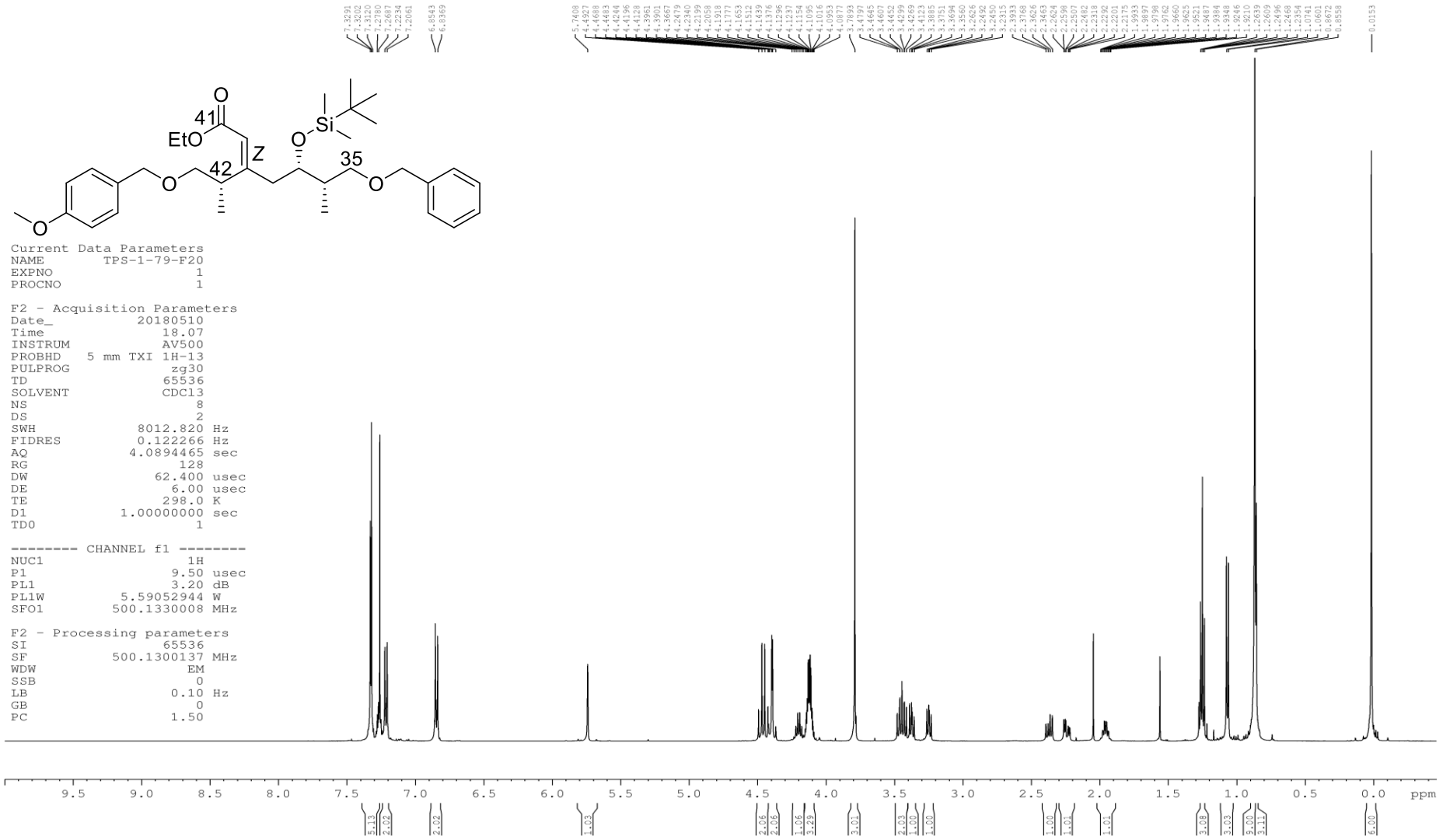

Spectrum 6. Enoate (*Z*)-**149a**, $CDCl_3$, ^{13}C NMR, 125 MHz

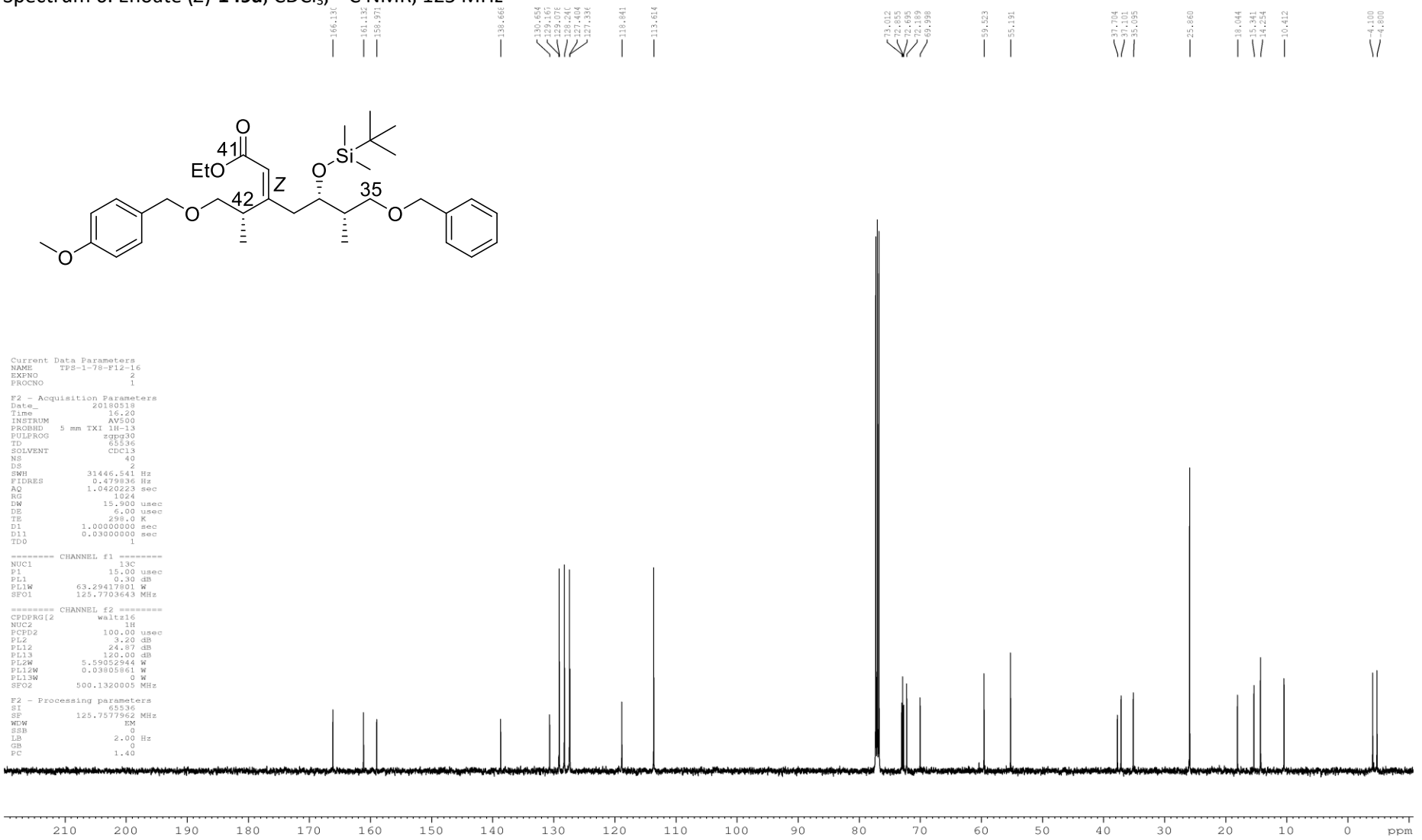

Spectrum 7. Enoate (*E*)-**149b**, $CDCl_3$, ^1H NMR, 500 MHz

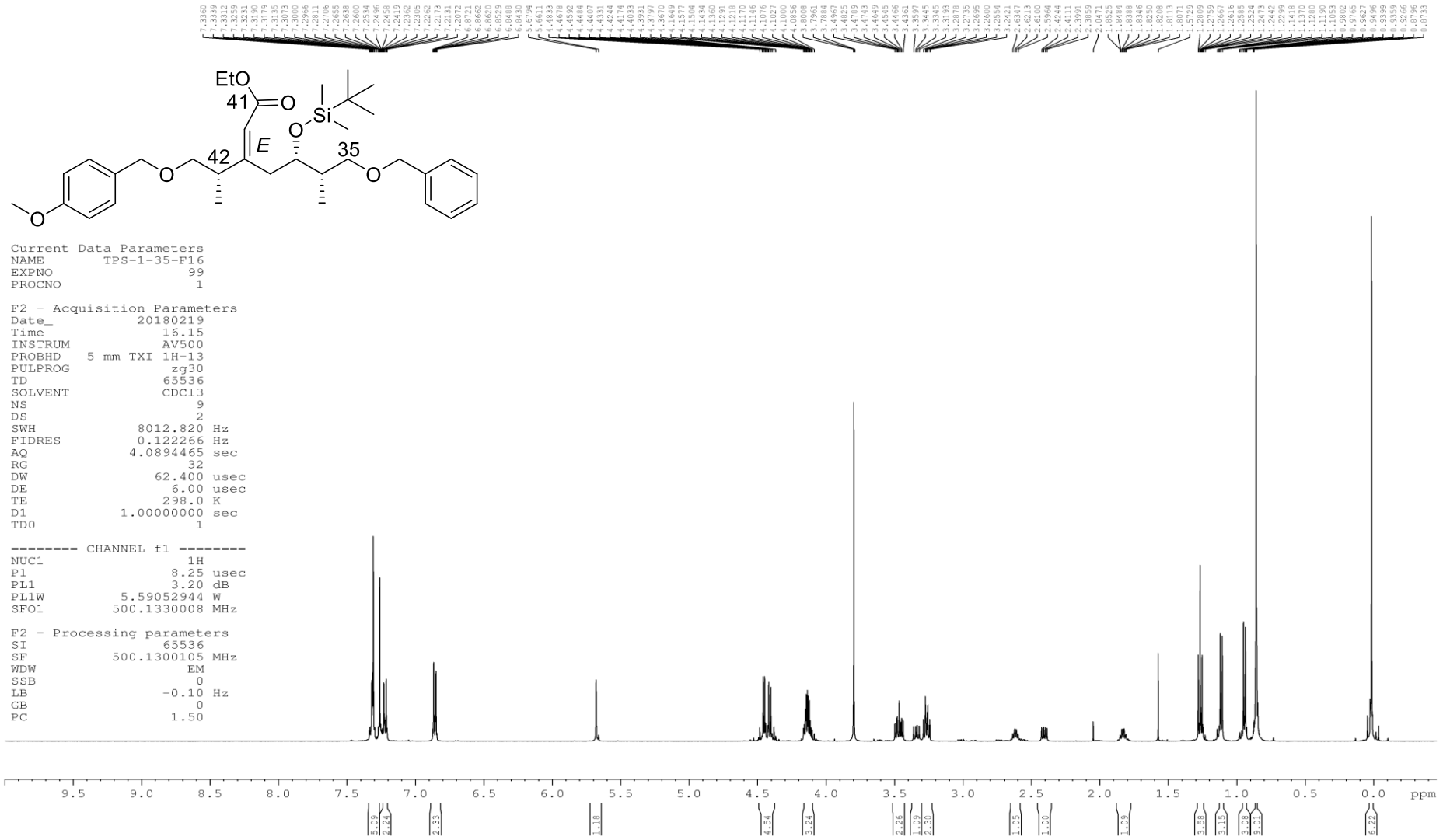

Spectrum 8. Enoate (*E*)-**149b**, $CDCl_3$, ^{13}C NMR, 125 MHz

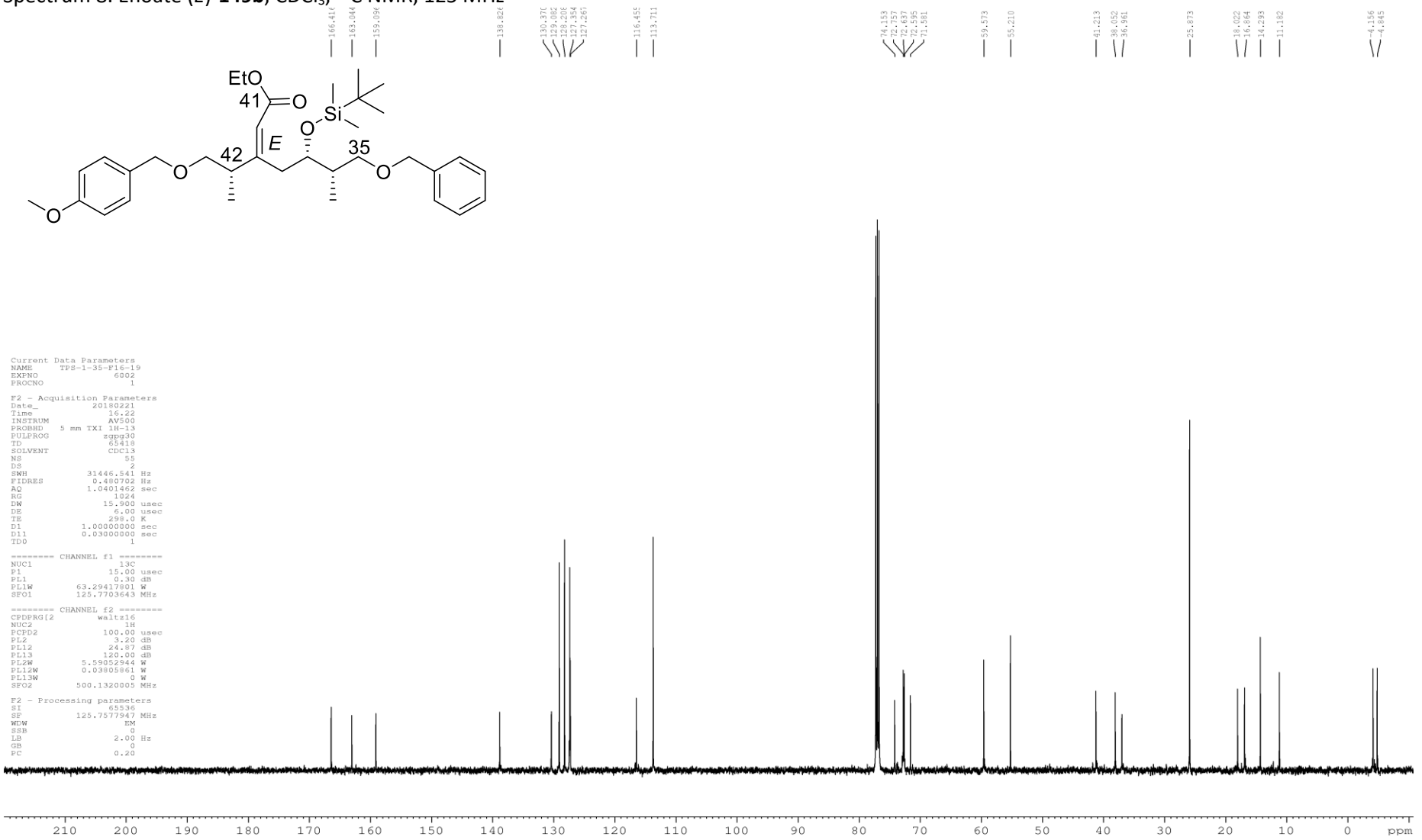

Spectrum 9. Alcohol **150**, $CDCl_3$, ^1H NMR, 500 MHz

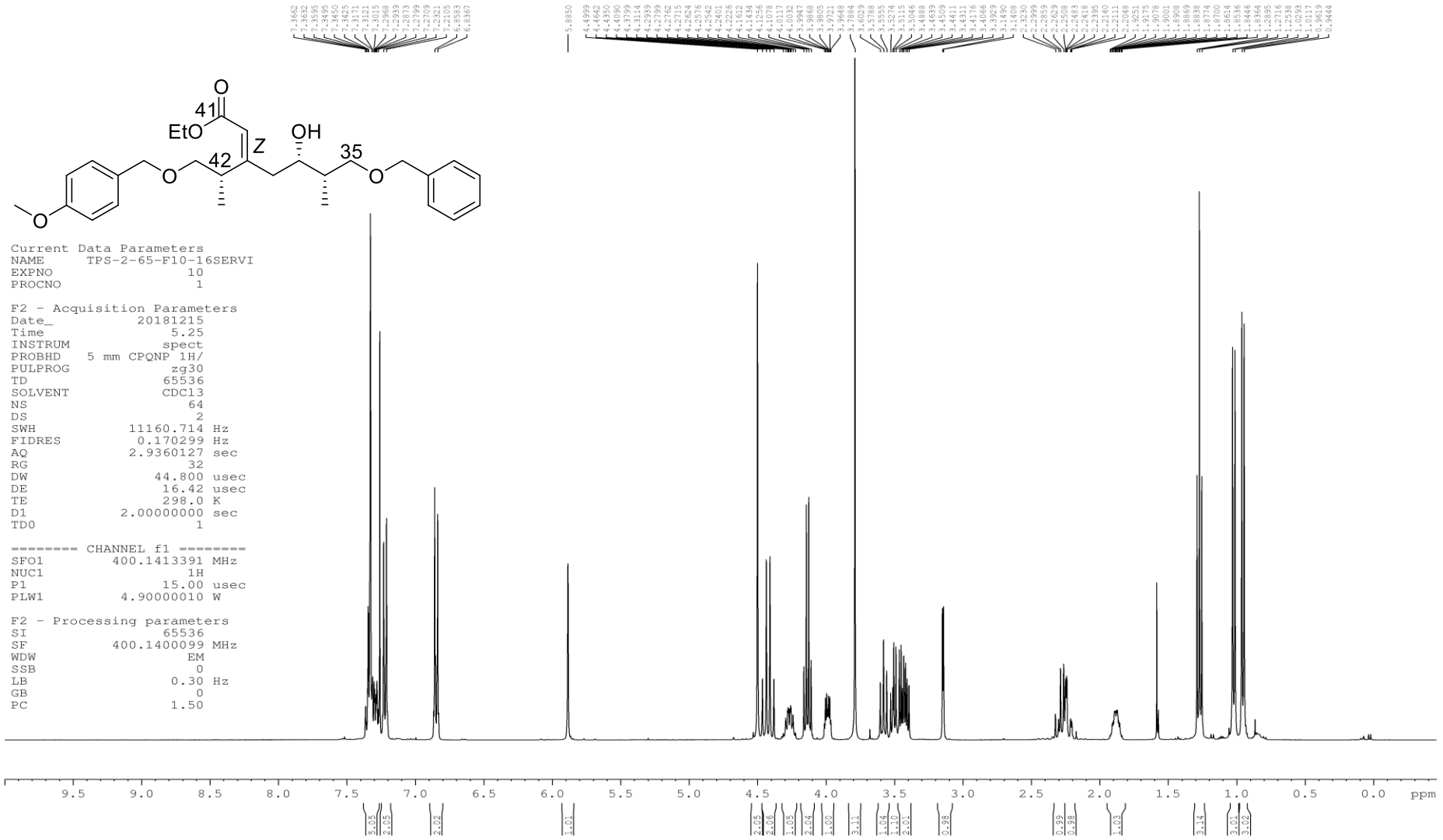

Spectrum 10. Alcohol **150**, $CDCl_3$, ^{13}C NMR, 125 MHz

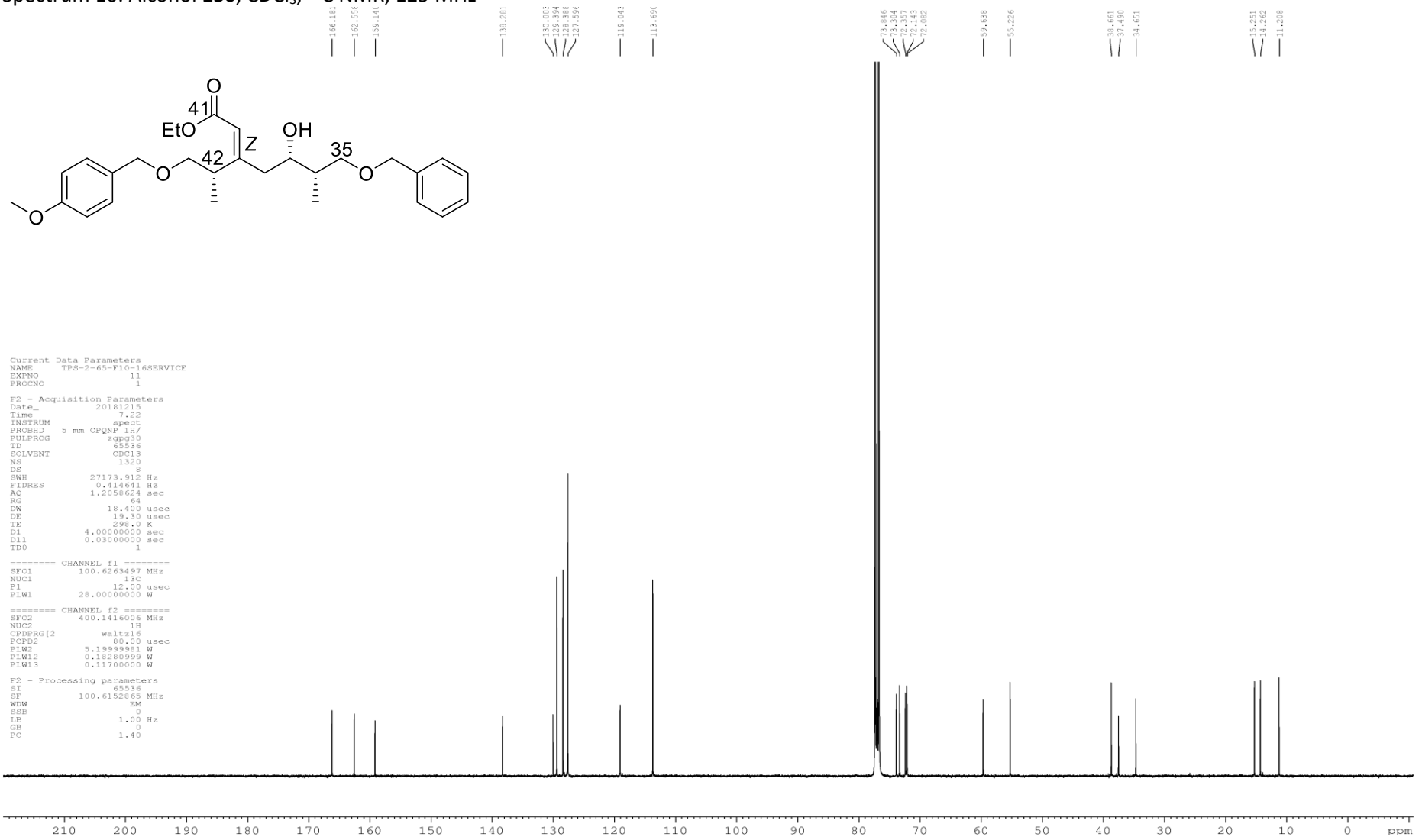

Spectrum 11. Lactone 37,39-*anti*-**144a**, $CDCl_3$, ^1H NMR, 500 MHz

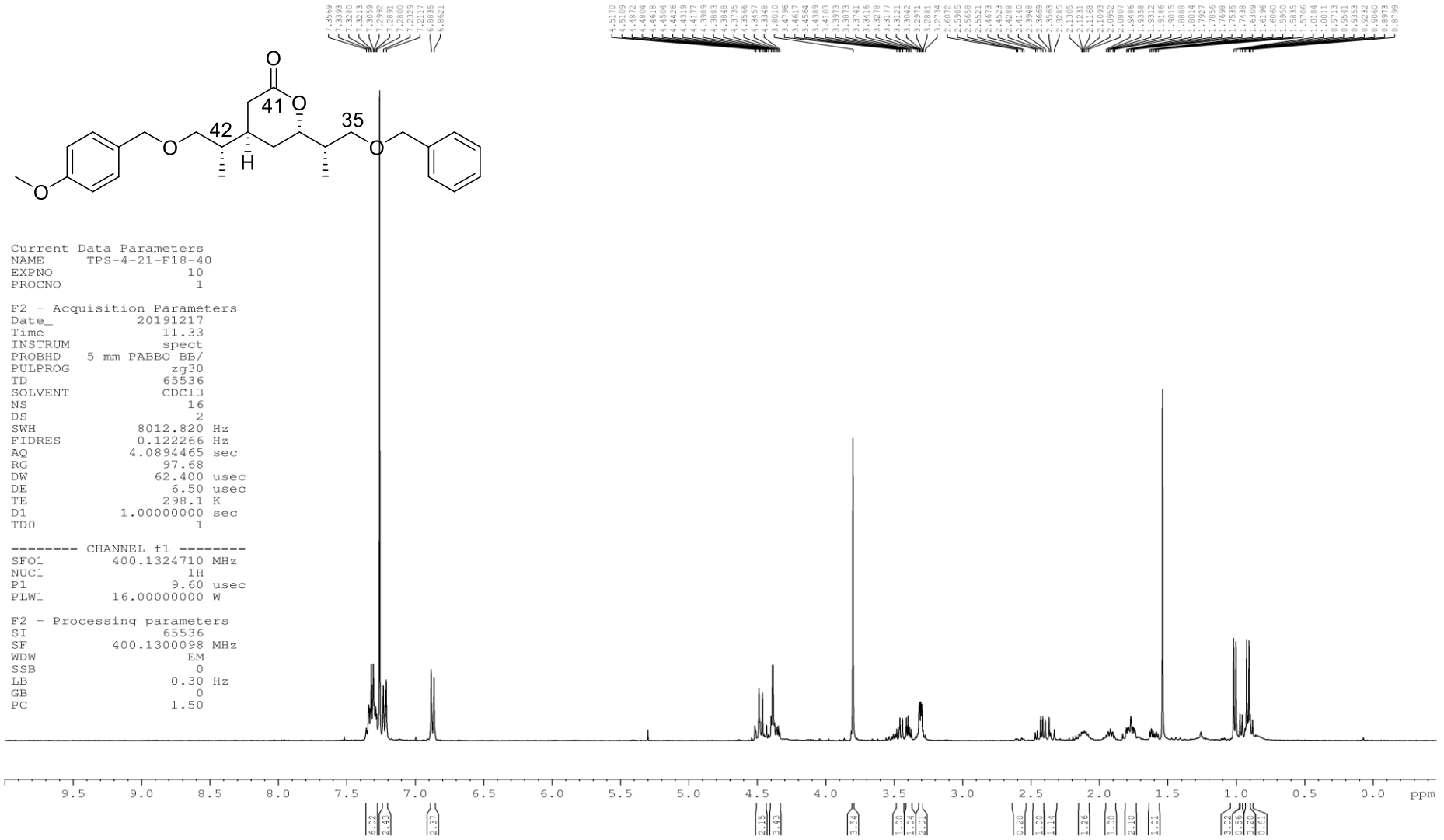

Spectrum 12. Lactone 37,39-*anti*-**144b**, $CDCl_3$, ^{13}C NMR, 125 MHz

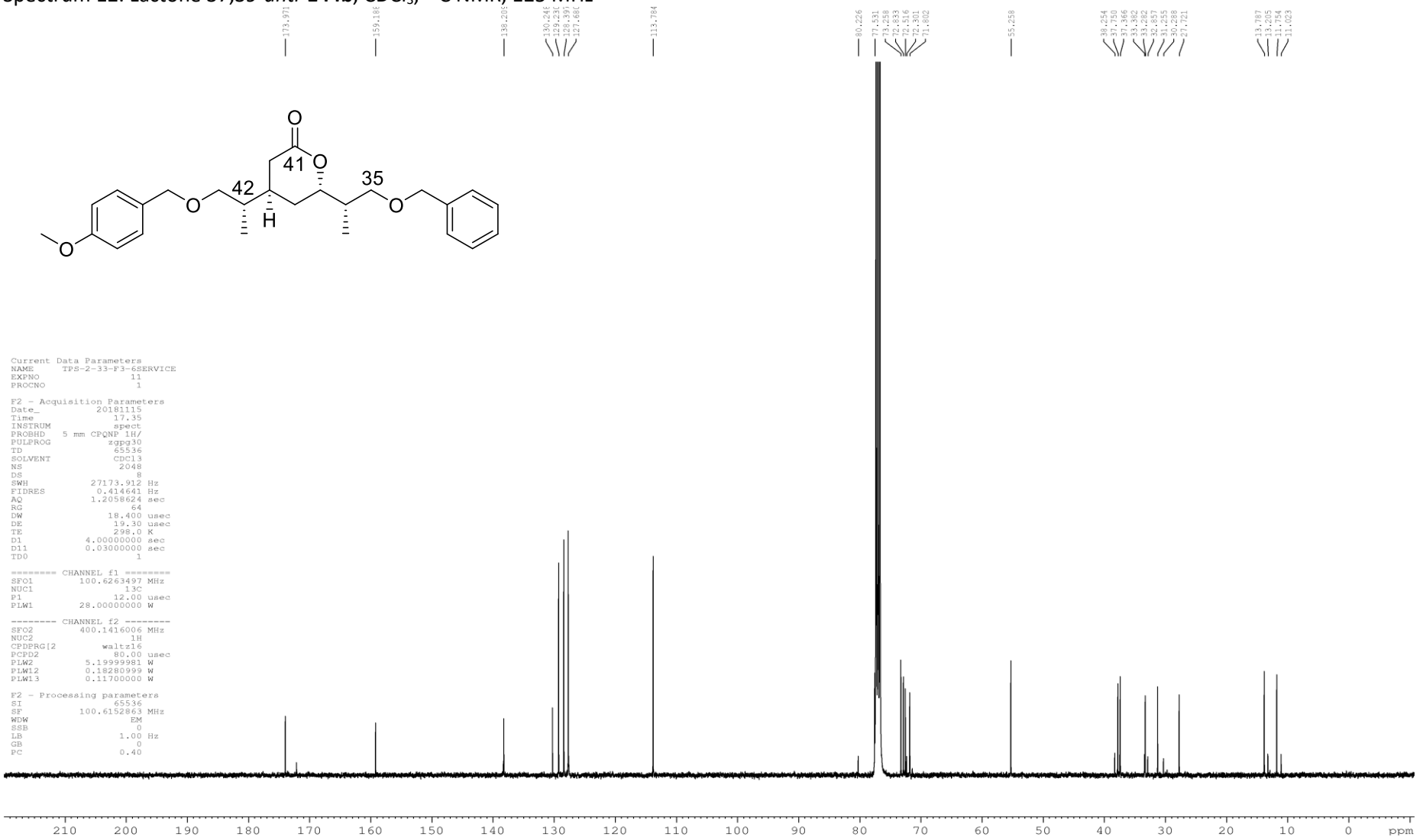

Spectrum 13. Lactone 37,39-*syn*-**144b**, $CDCl_3$, ^1H NMR, 500 MHz

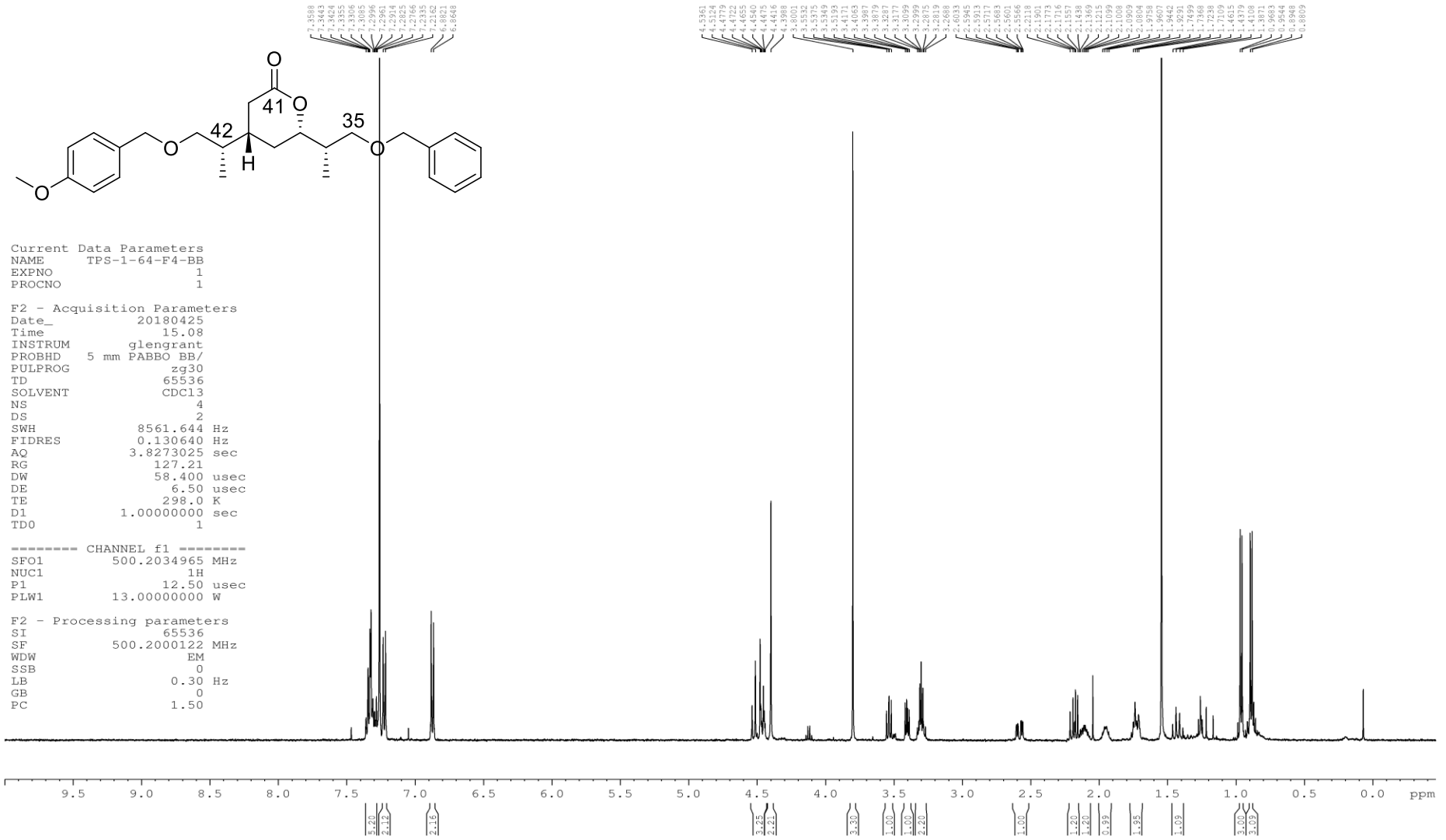

Spectrum 14. α-Hydroxy lactone **133**, $CDCl_3$, ^1H NMR, 500 MHz

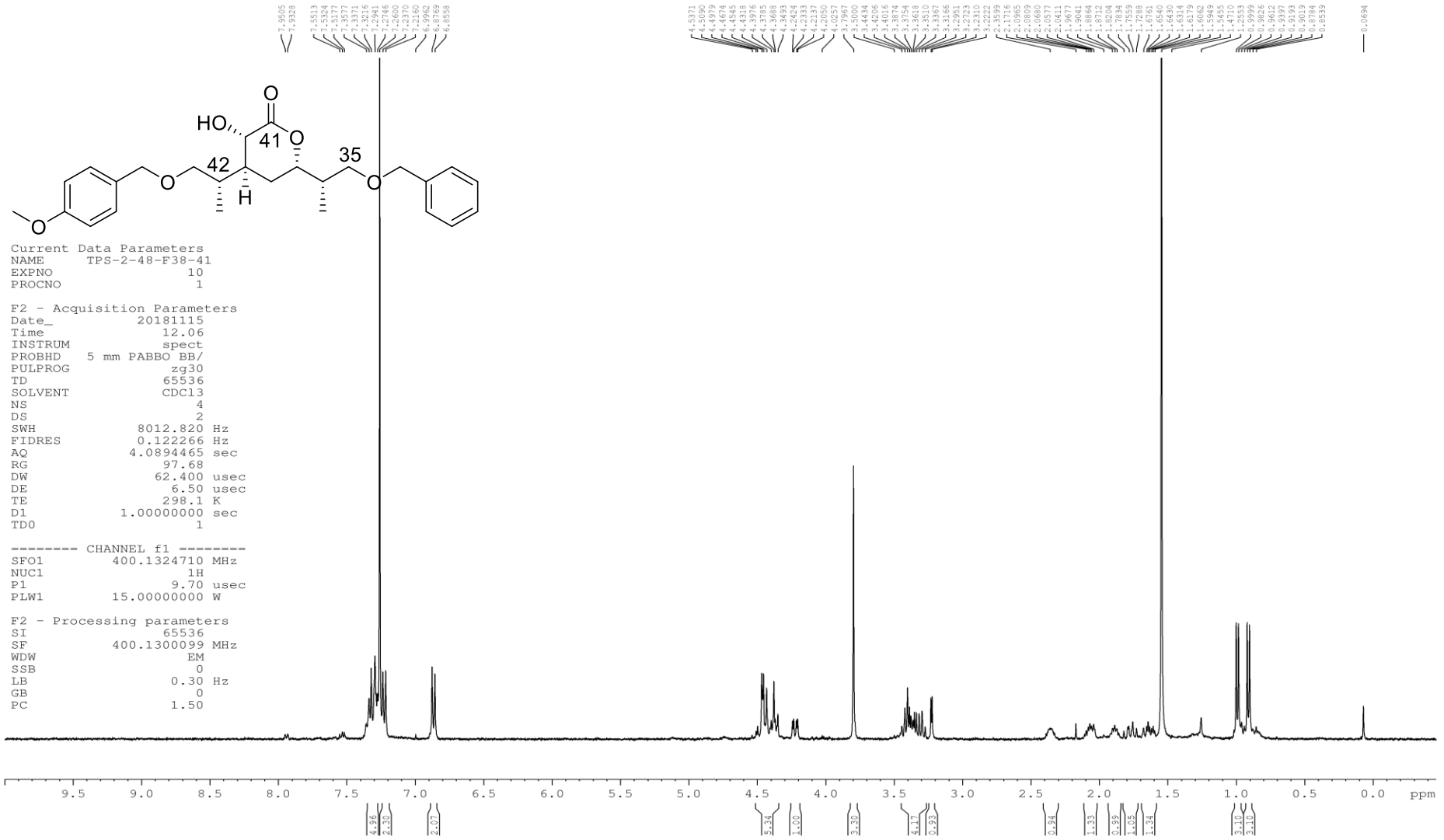

Spectrum 15. α-Hydroxy lactone **133**, $CDCl_3$, ^{13}C NMR, 125 MHz

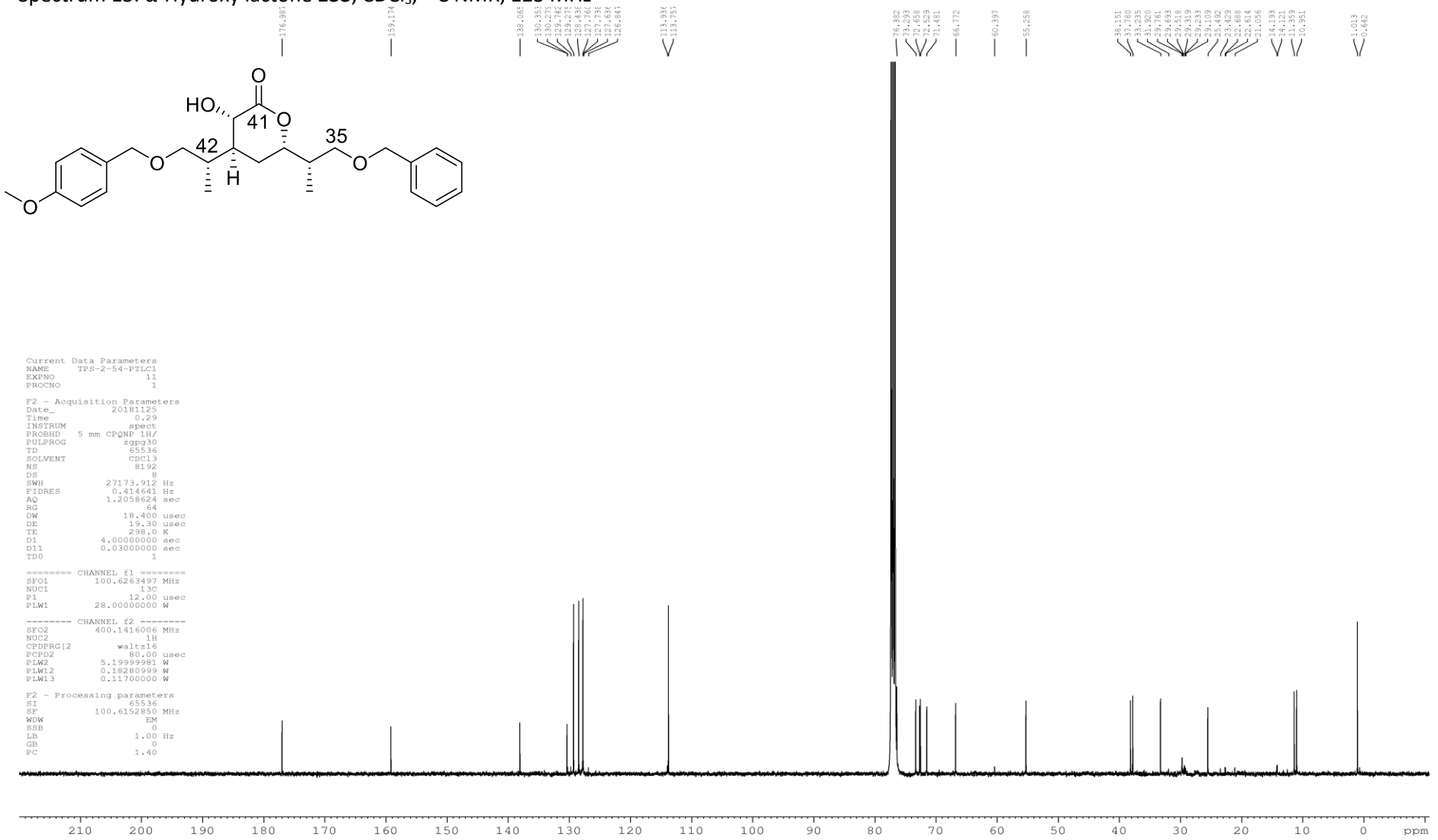

Spectrum 16. TES ether **156**, $CDCl_3$, ^1H NMR, 400 MHz

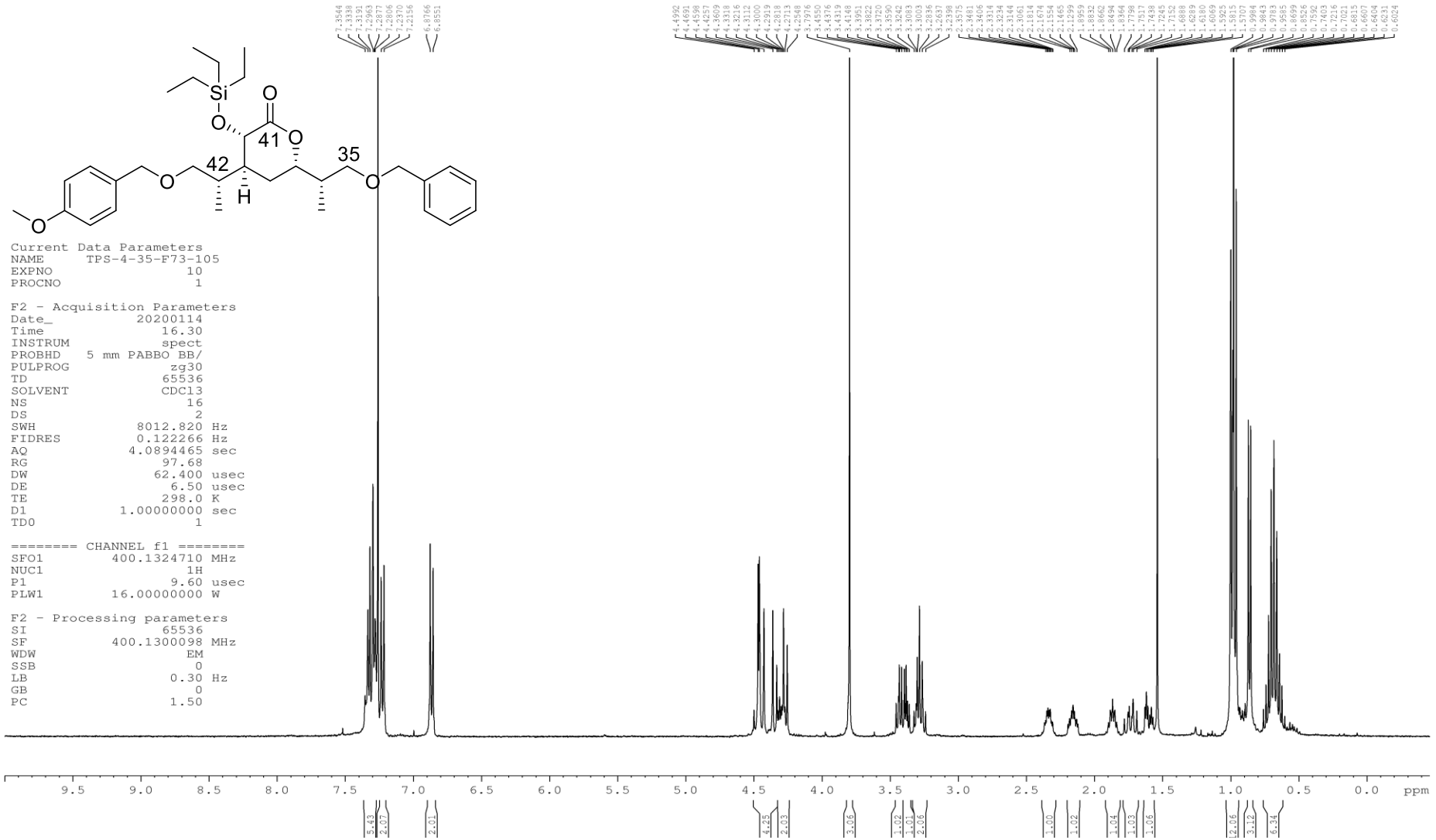

Spectrum 17. TES ether **156**, $CDCl_3$, ^{13}C NMR, 125 MHz

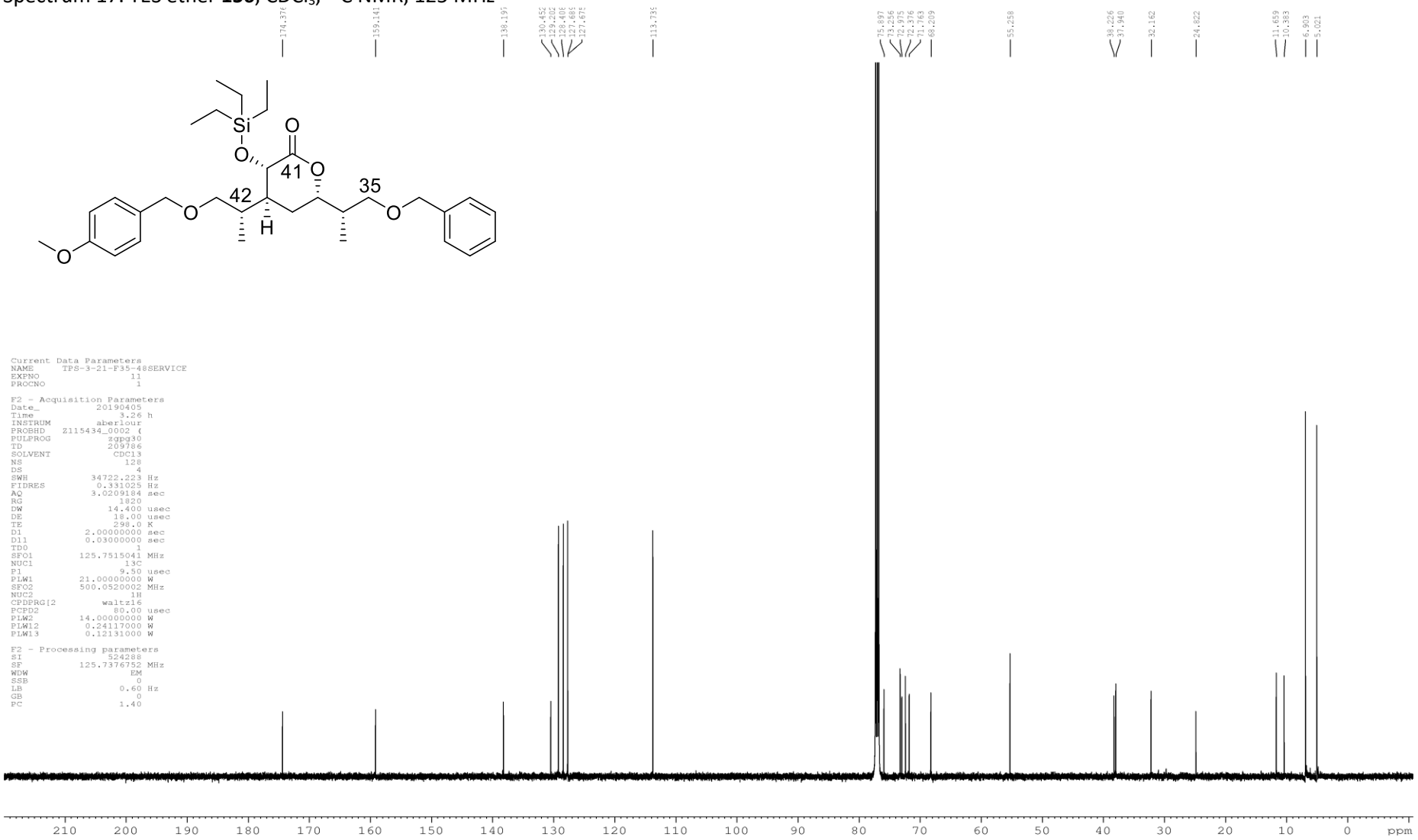

Spectrum 18. Alcohol **157**, $CDCl_3$, ^1H NMR, 400 MHz

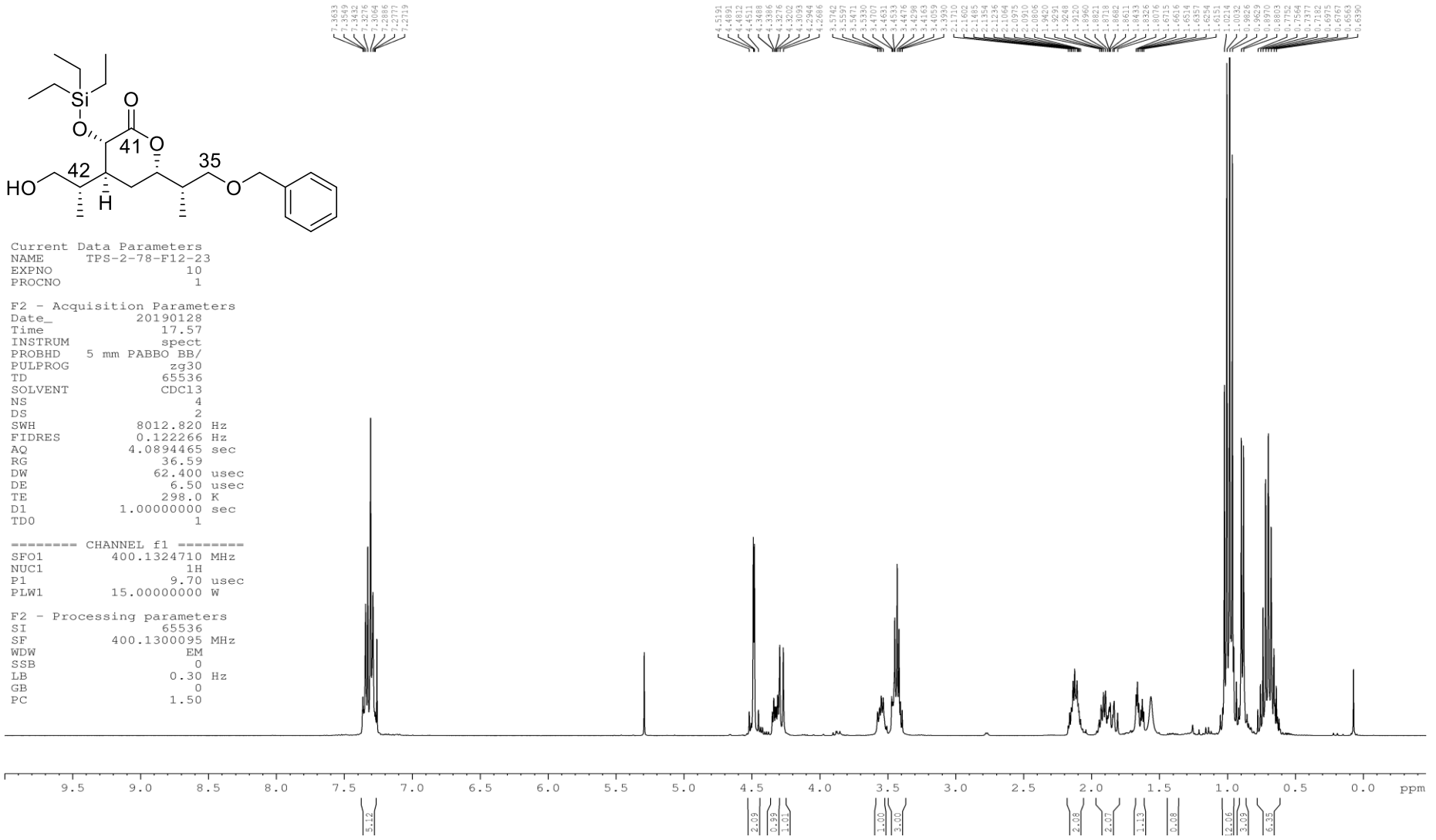

Spectrum 19. Alcohol **157**, $CDCl_3$, ^{13}C NMR, 100 MHz

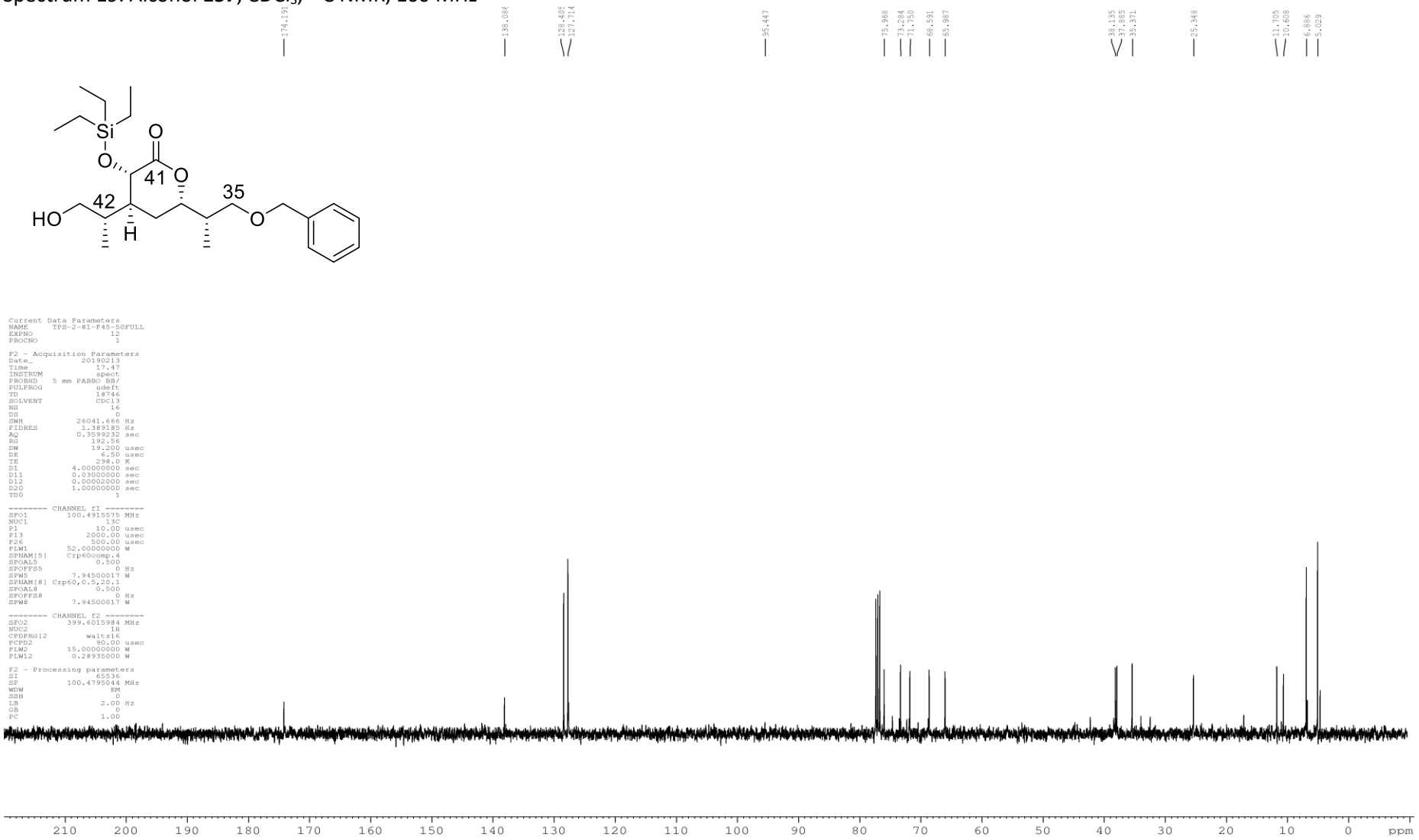

Spectrum 20. Crude Aldehyde **158**, $CDCl_3$, ^1H NMR, 400 MHz

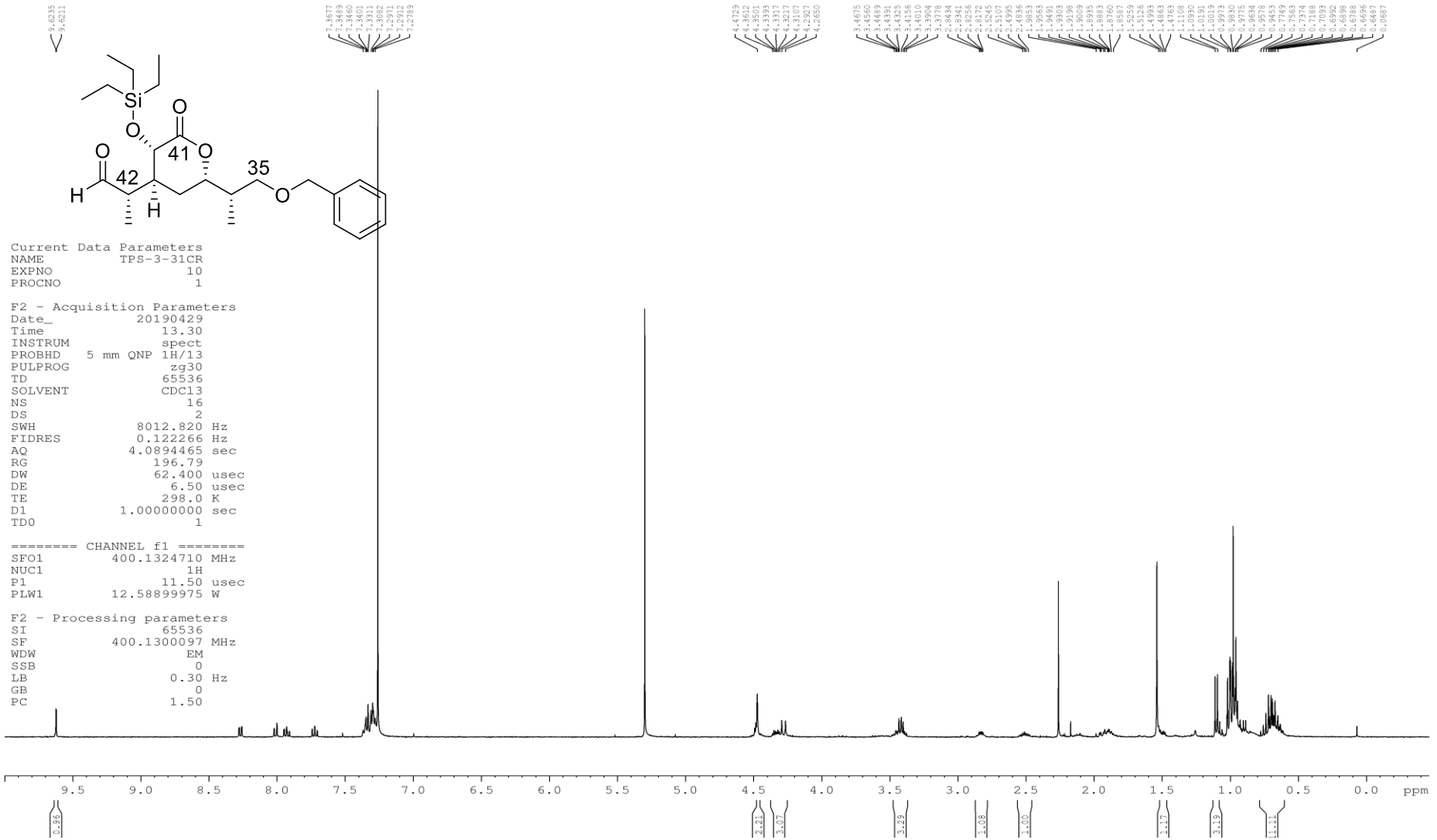

Spectrum 21. Enone (*E*)-**160**, $CDCl_3$, ^1H NMR, 500 MHz

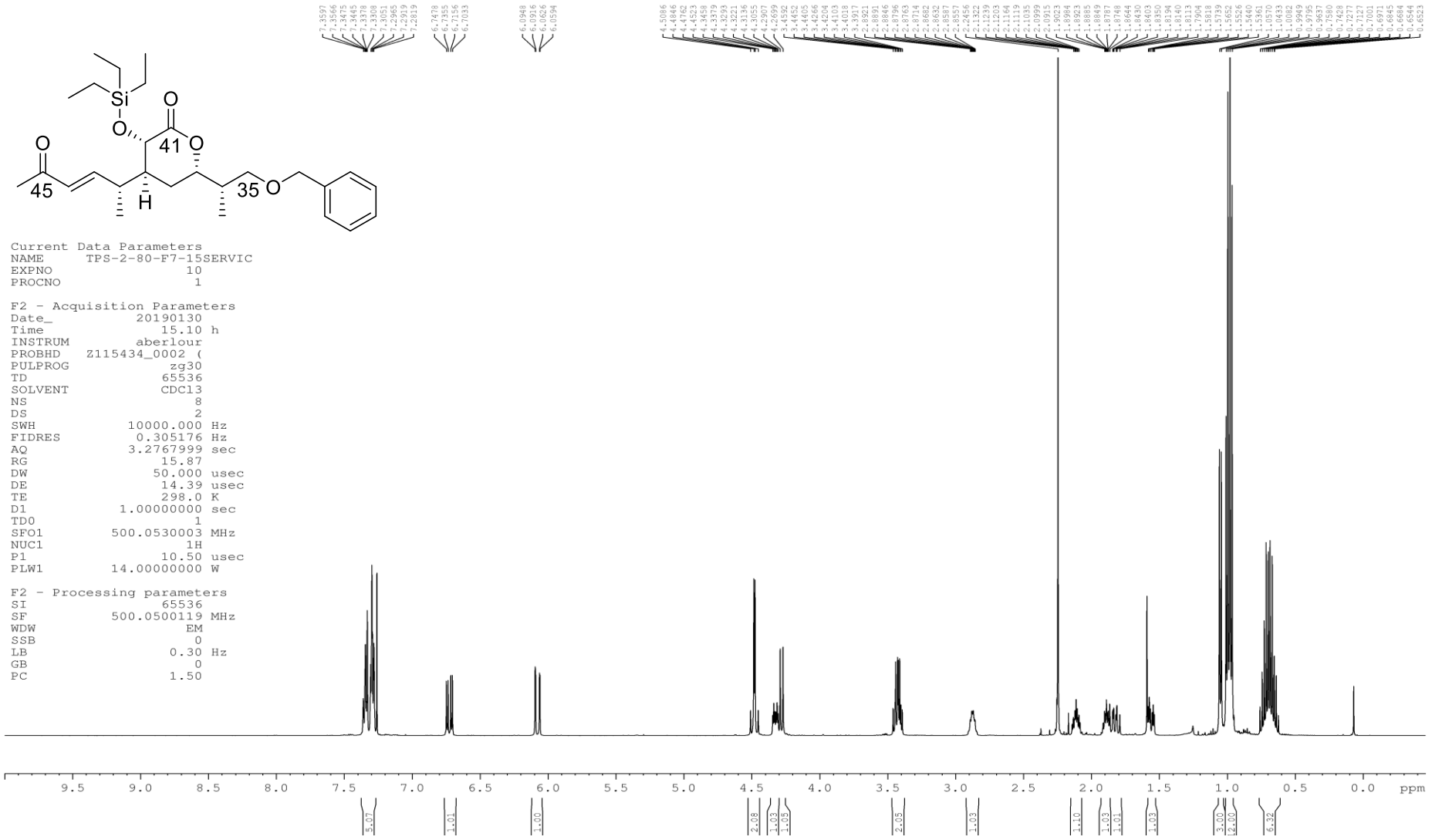

Spectrum 22. Enone (*E*)-**160**, $CDCl_3$, ^{13}C NMR, 125 MHz

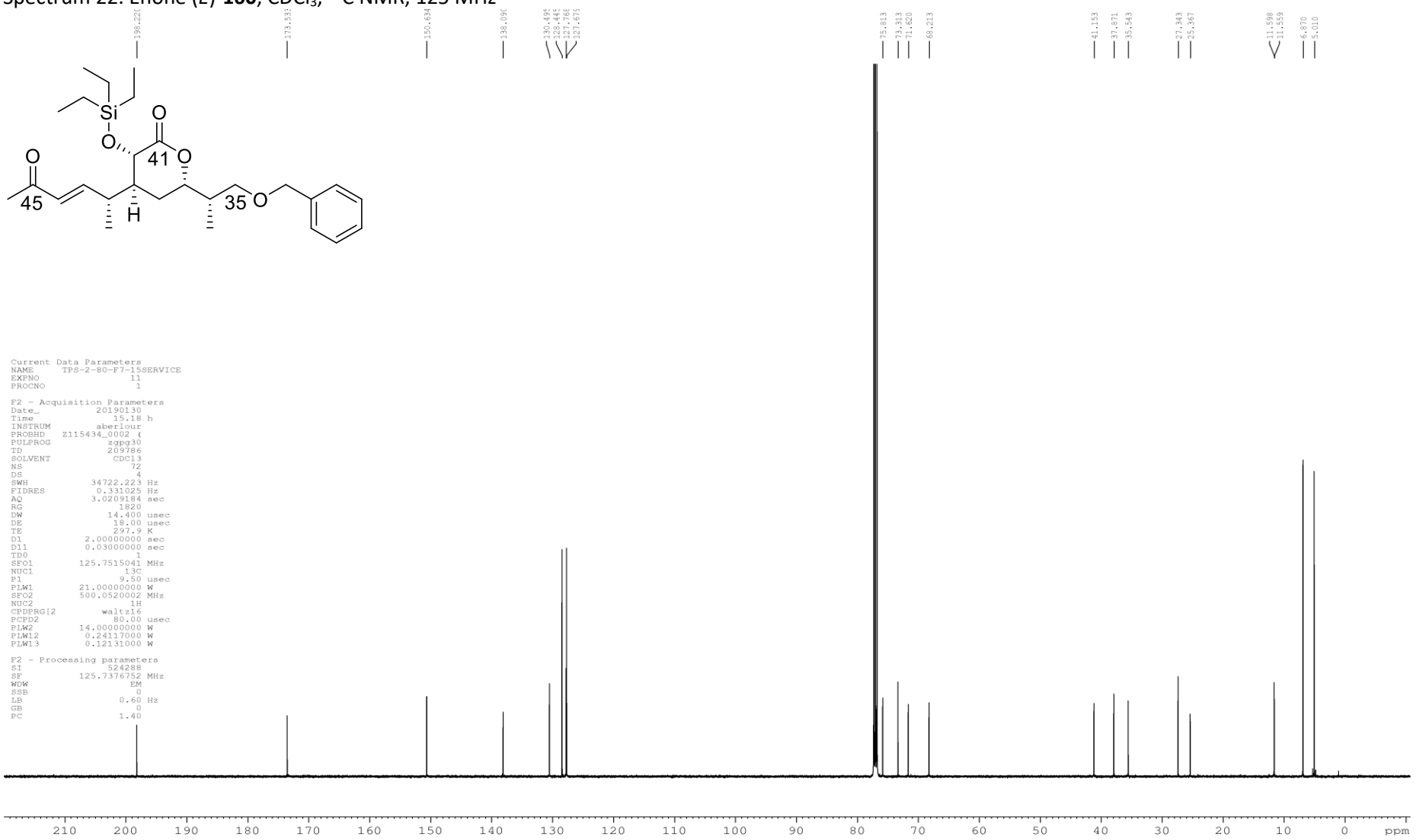

Spectrum 23. Allylic alcohol 42,45-*anti*-**164a**, $CDCl_3$, ^1H NMR, 700 MHz

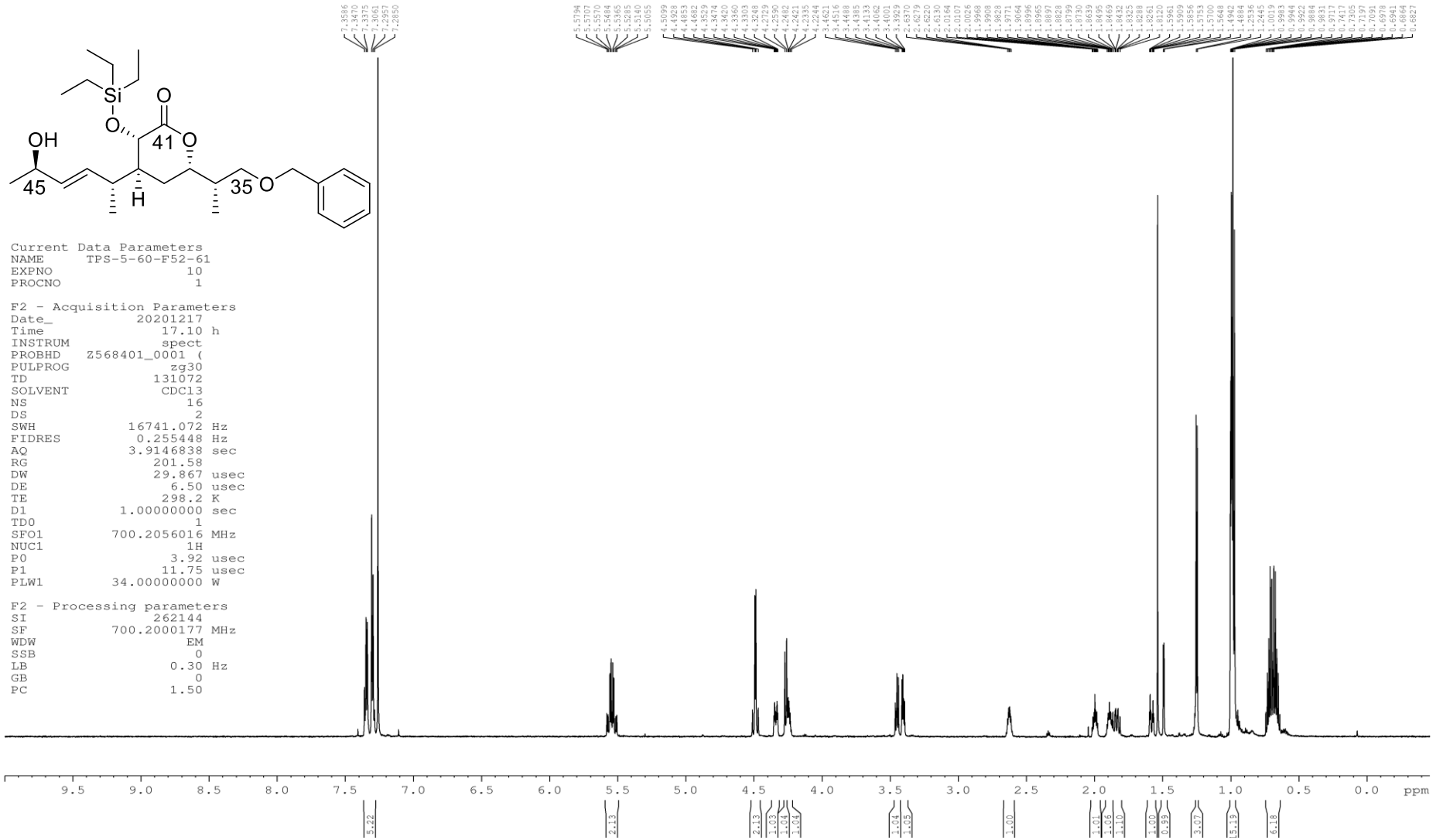

Spectrum 24. Allylic alcohol 42,45-*anti*-**164a**, $CDCl_3$, ^{13}C NMR, 125 MHz

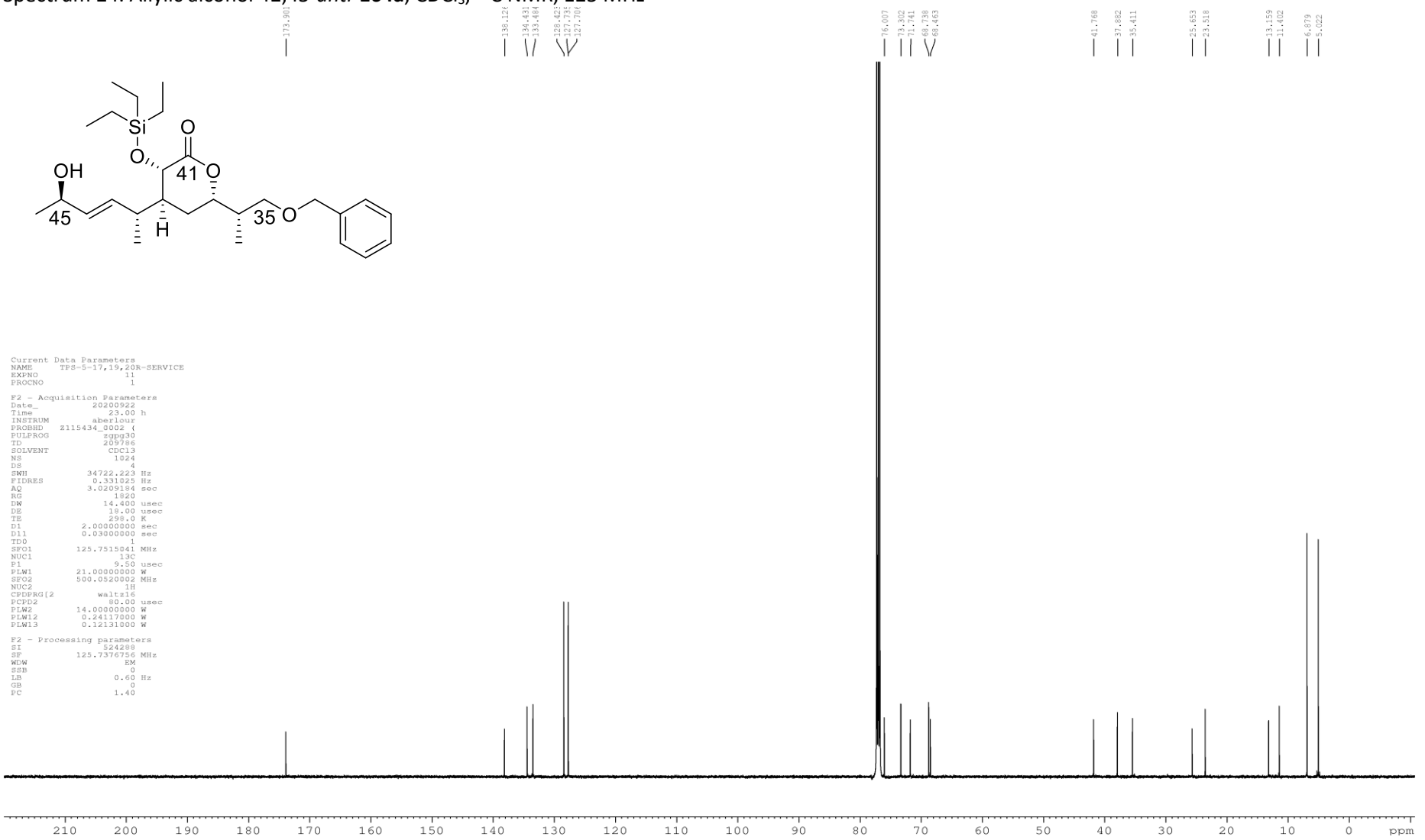

Spectrum 25. Allylic alcohol 42,45-*syn*-**164b**, $CDCl_3$, ^1H NMR, 400 MHz

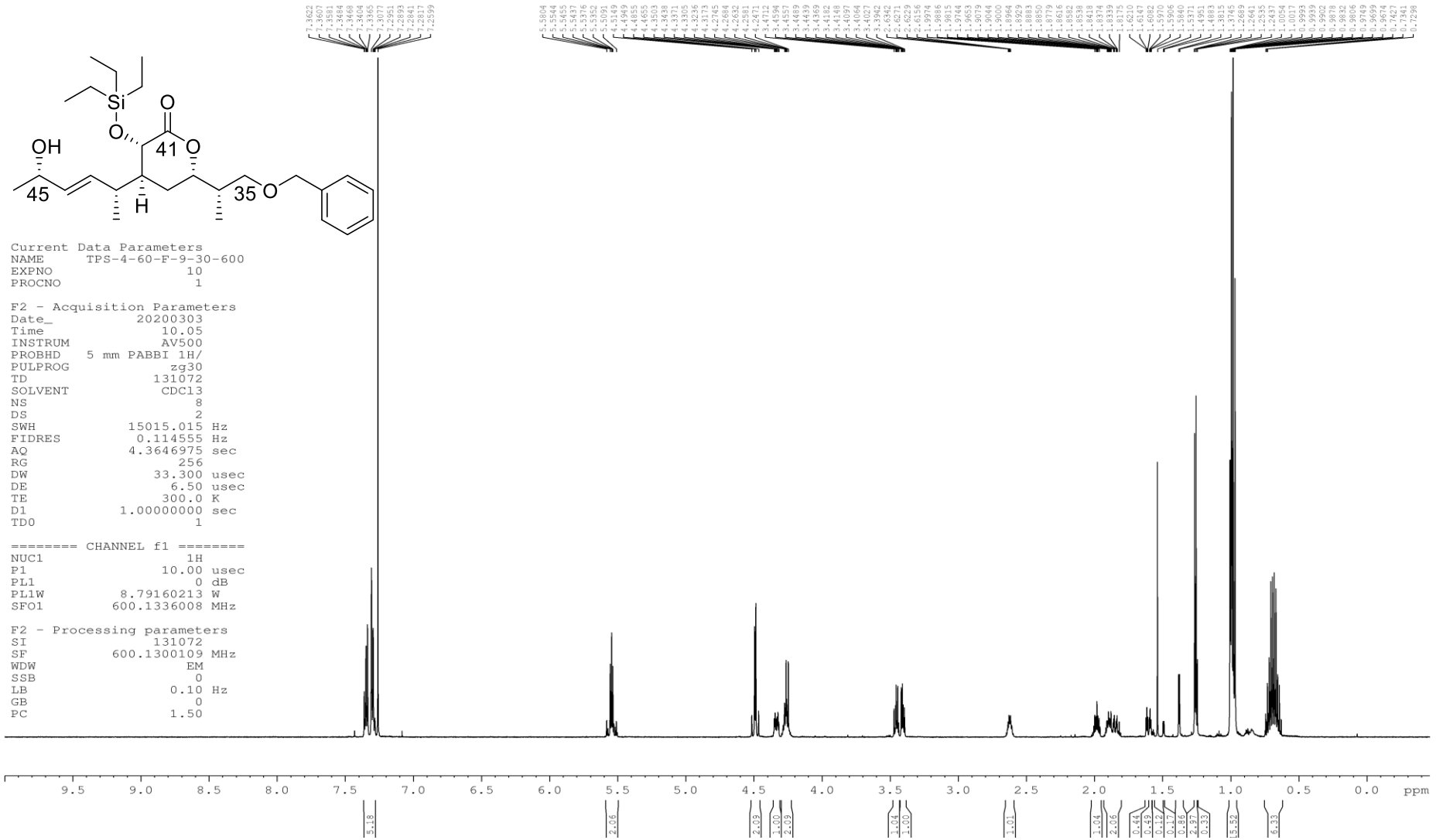

Spectrum 26. Allylic alcohol 42,45-*syn*-**164b**, $CDCl_3$, ^{13}C NMR, 125 MHz

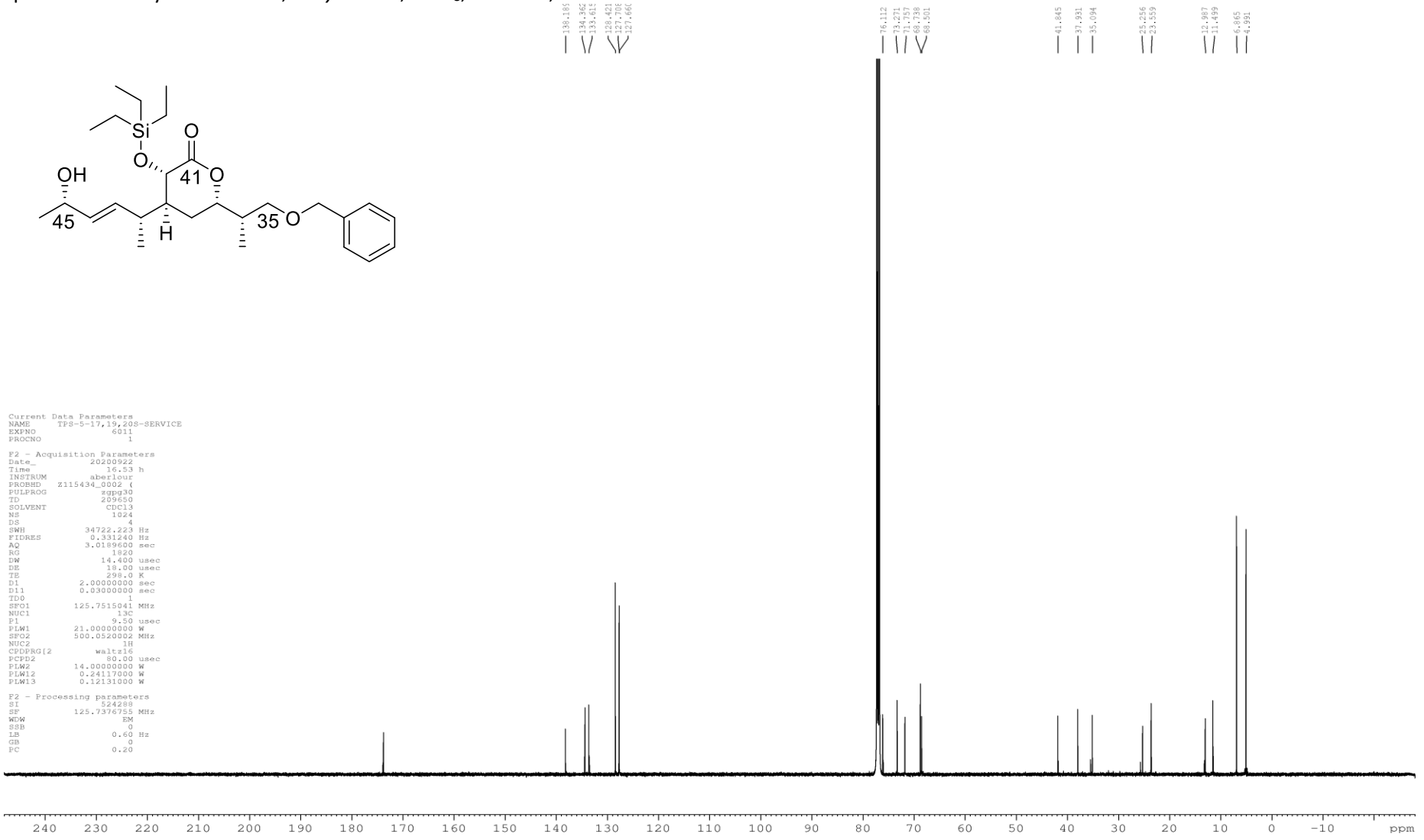

Spectrum 27. TES ether 42,25-*syn*-**167b**, $CDCl_3$, ^1H NMR, 400 MHz

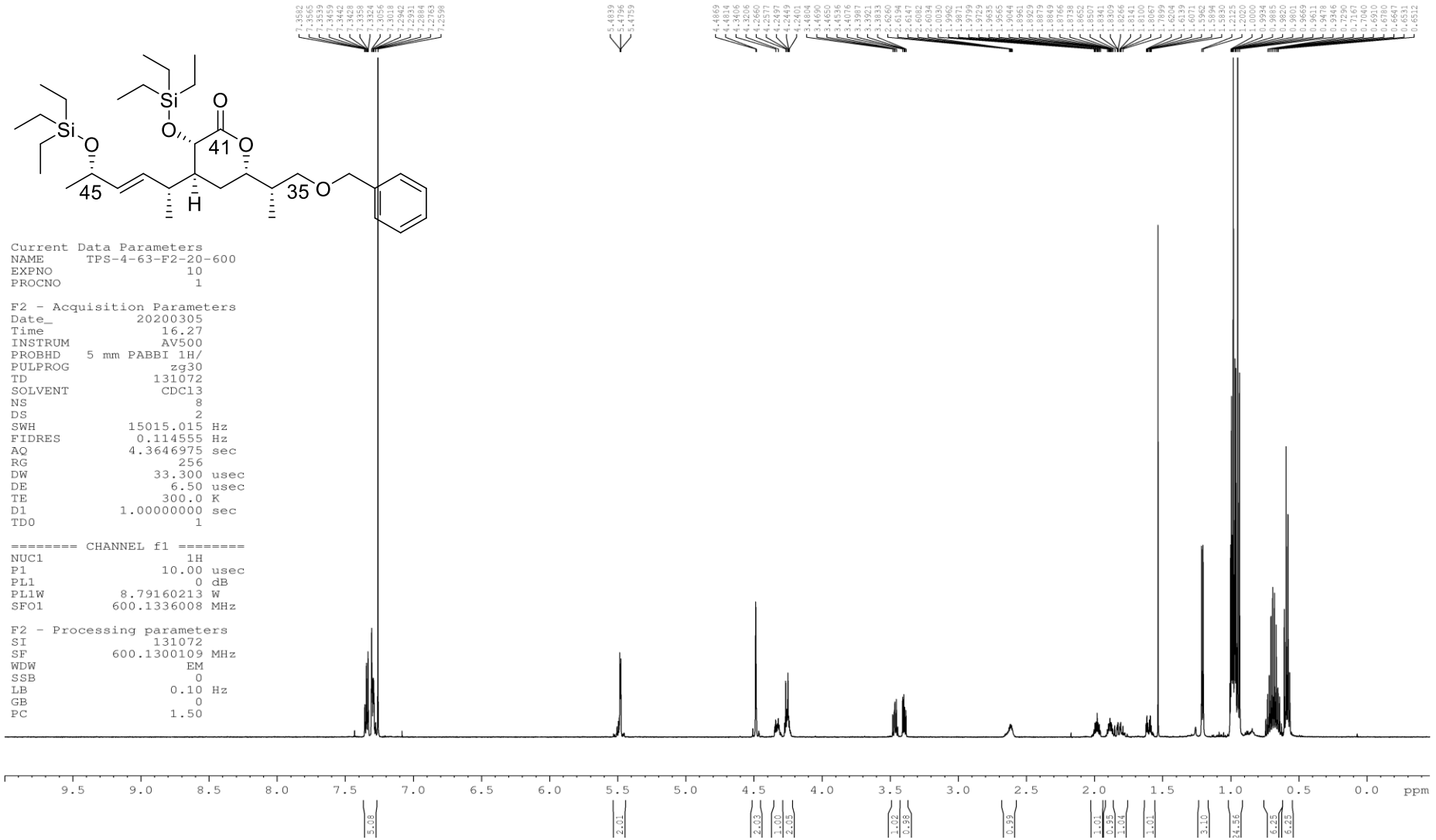

Spectrum 28. TES ether 42,25-*syn*-**167b**, $CDCl_3$, ^{13}C NMR, 125 MHz

Spectrum 29. Primary alcohol 42,25-*syn*-**169b**, $CDCl_3$, ^1H NMR, 500 MHz

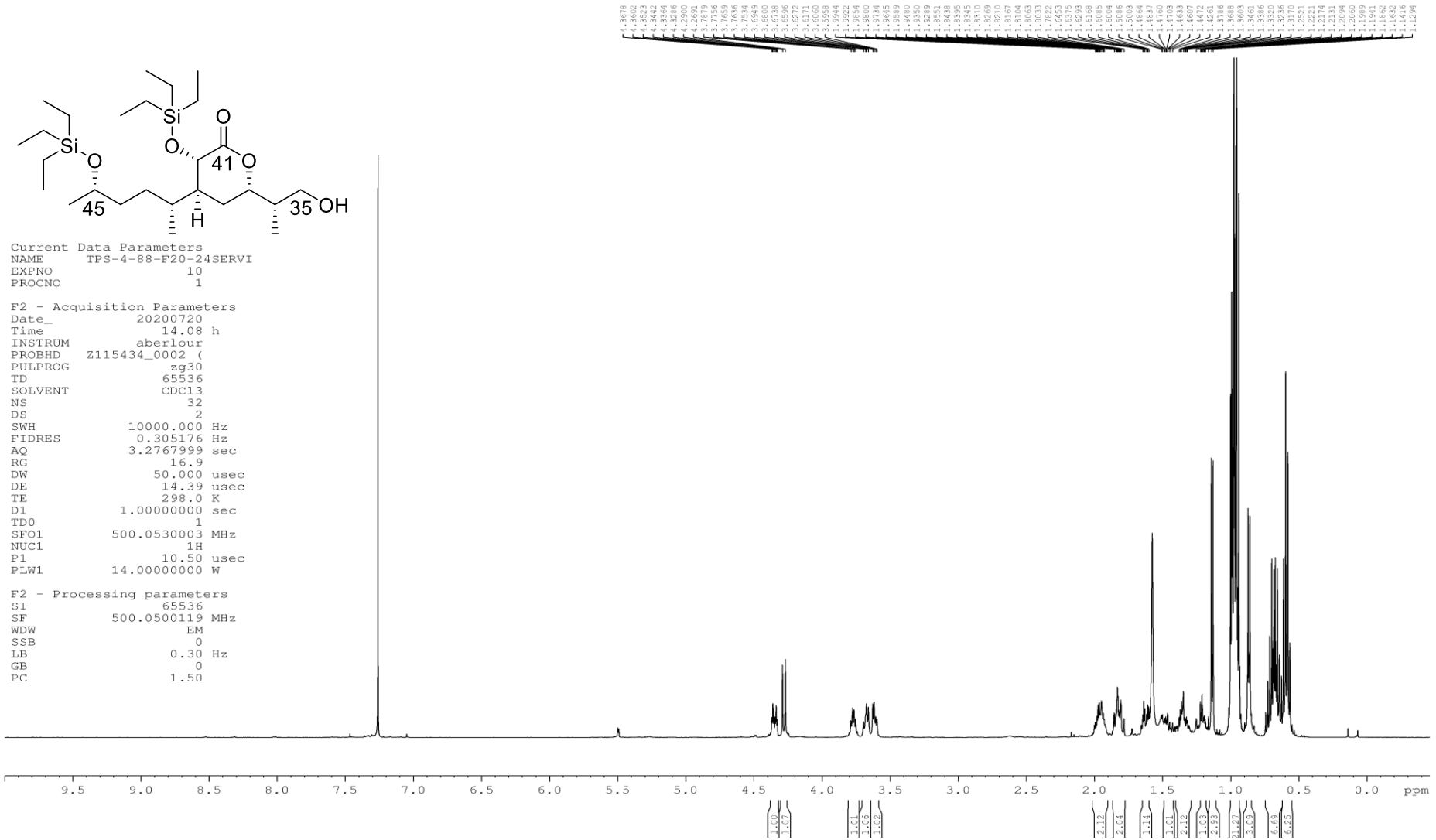

Spectrum 30. Primary alcohol 42,25-*syn*-**169b**, $CDCl_3$, ^{13}C NMR, 125 MHz

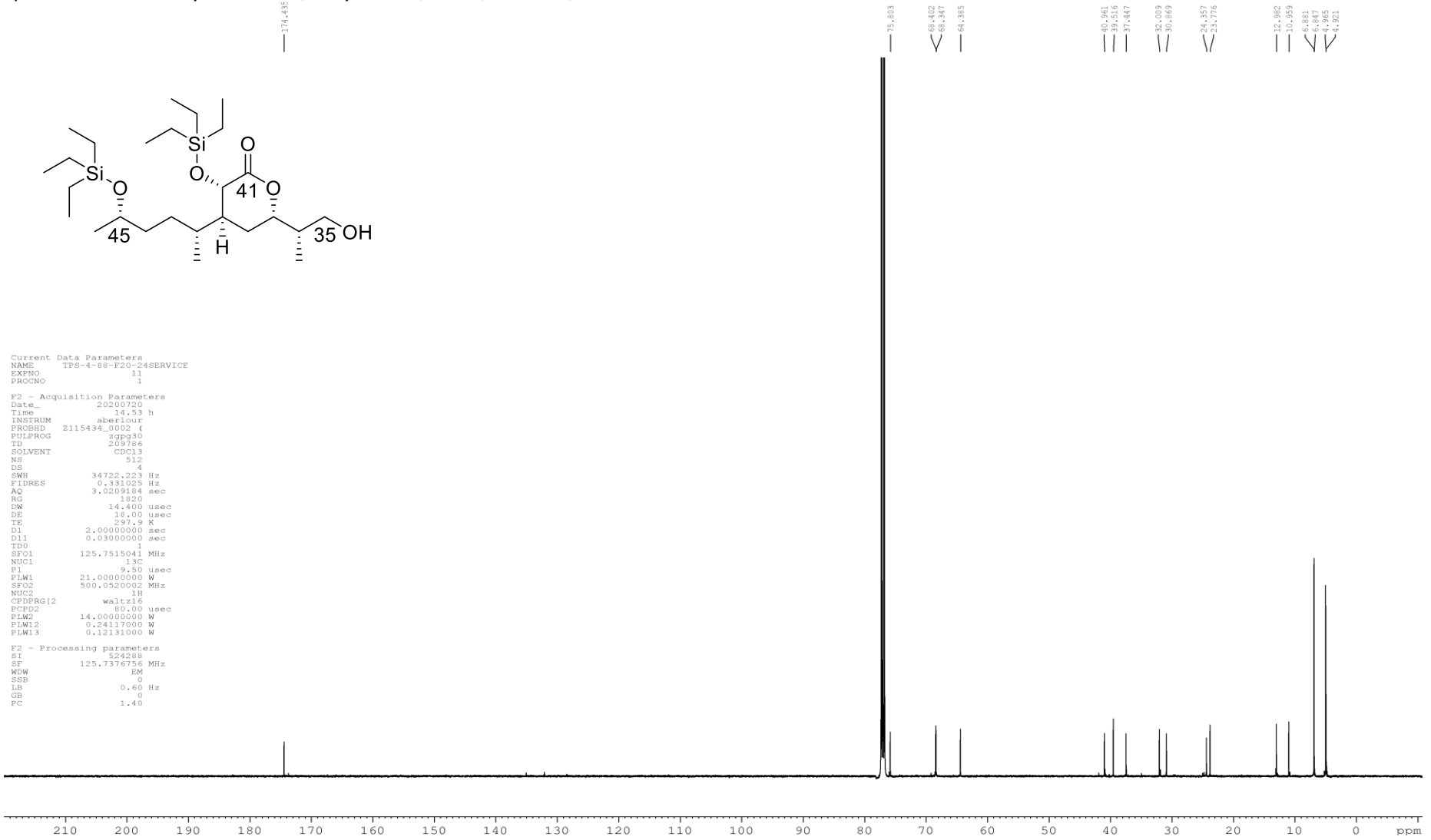

Spectrum 31. Diol 42,25-*syn*-**168b**, $CDCl_3$, ^1H NMR, 500 MHz

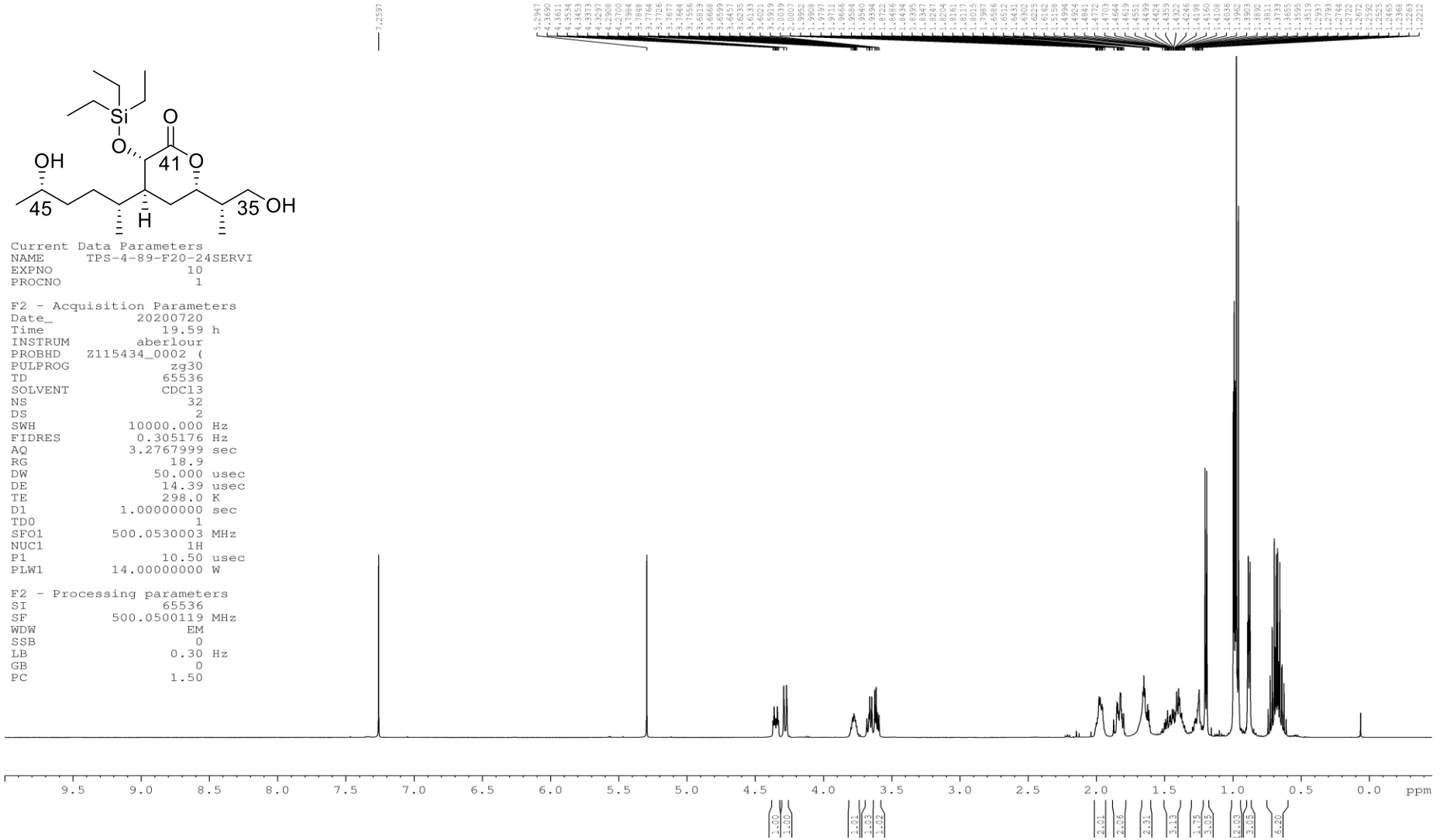

Spectrum 32. Diol 42,25-*syn*-**168b**, $CDCl_3$, ^{13}C NMR, 125 MHz

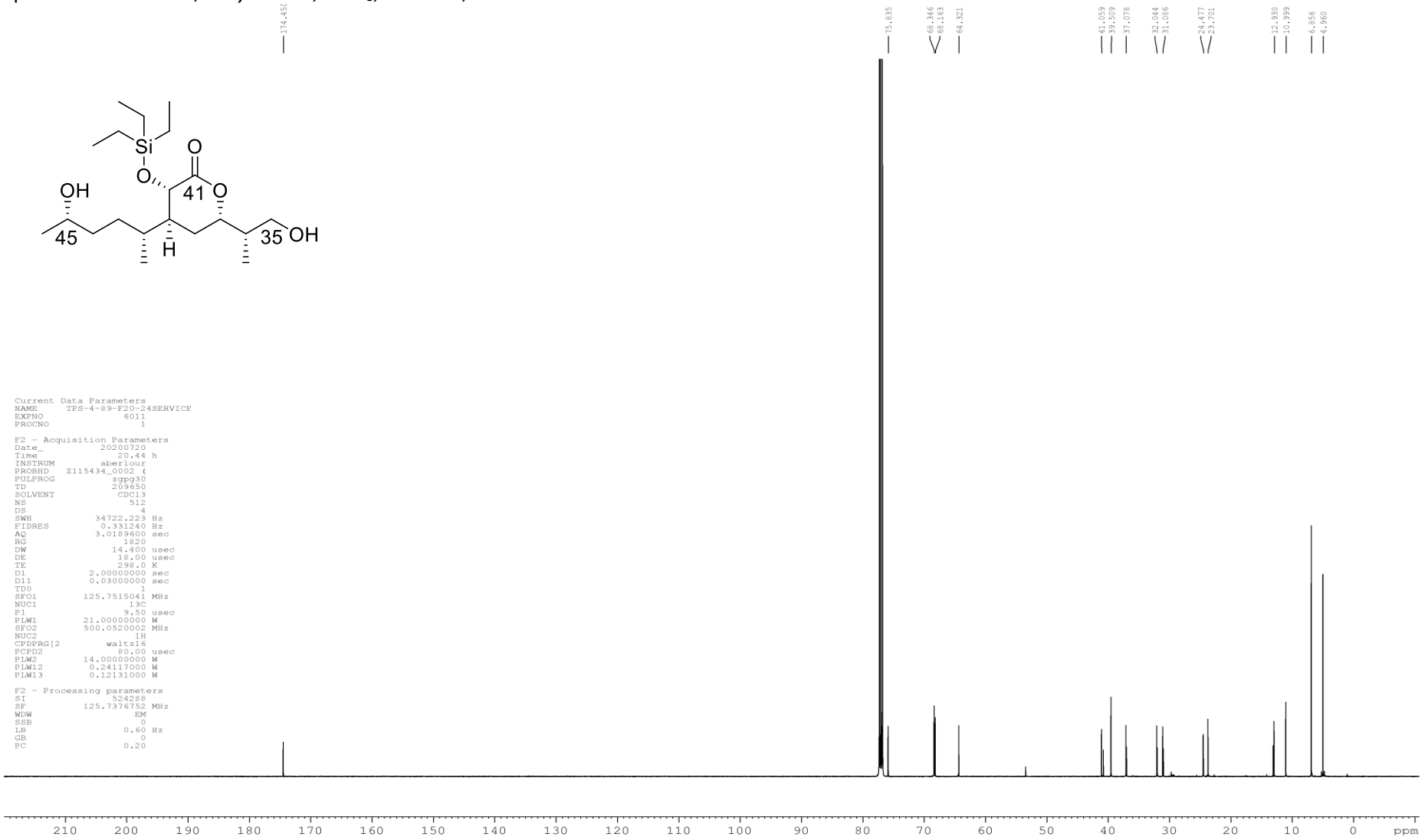

Spectrum 33. Aldehyde 42,25-*syn*-**210b**, $CDCl_3$, ^1H NMR, 400 MHz

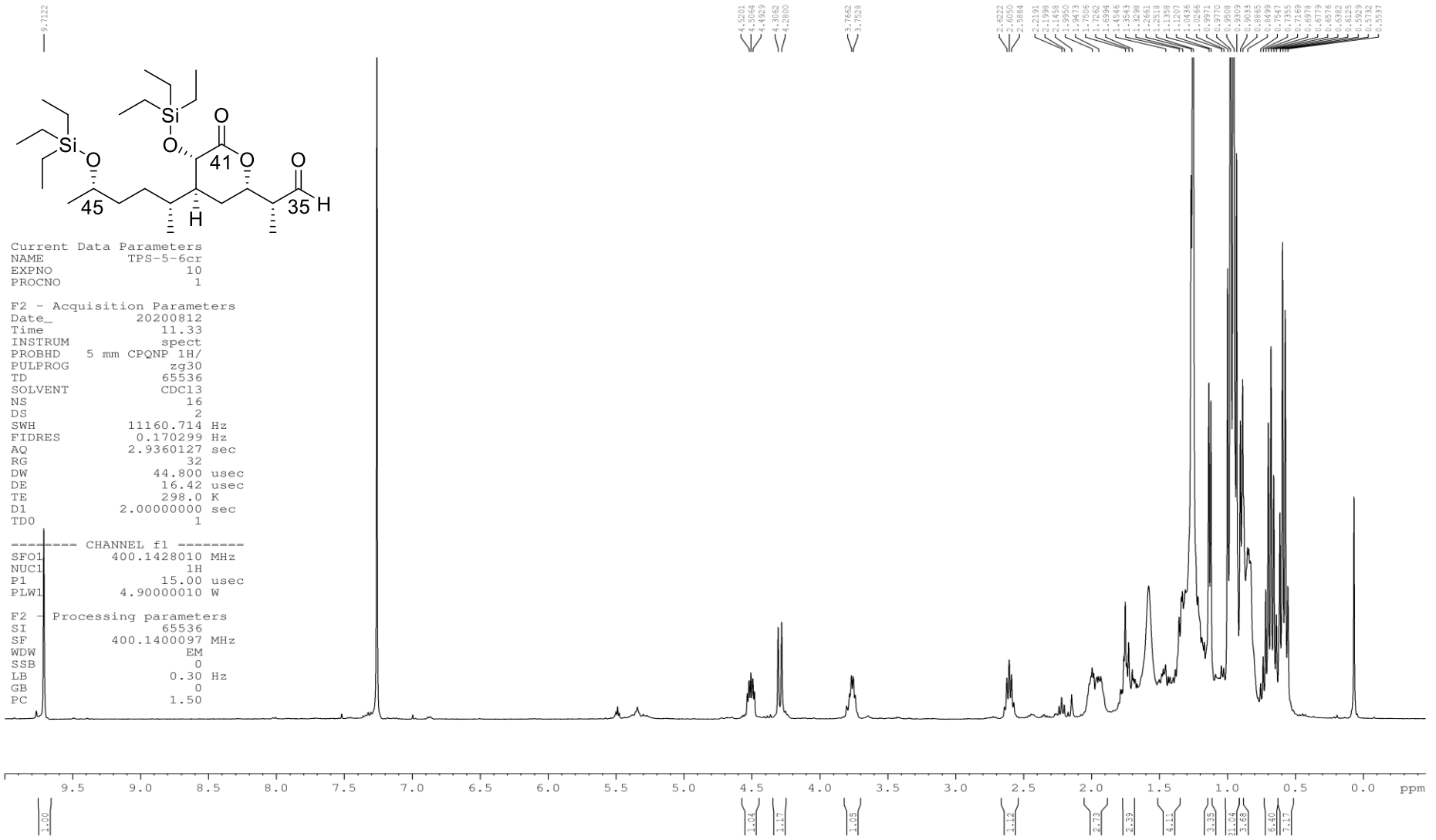

Spectrum 34. Aldehyde 42,25-*syn*-**210b**, $CDCl_3$, ^1H NMR, 400 MHz

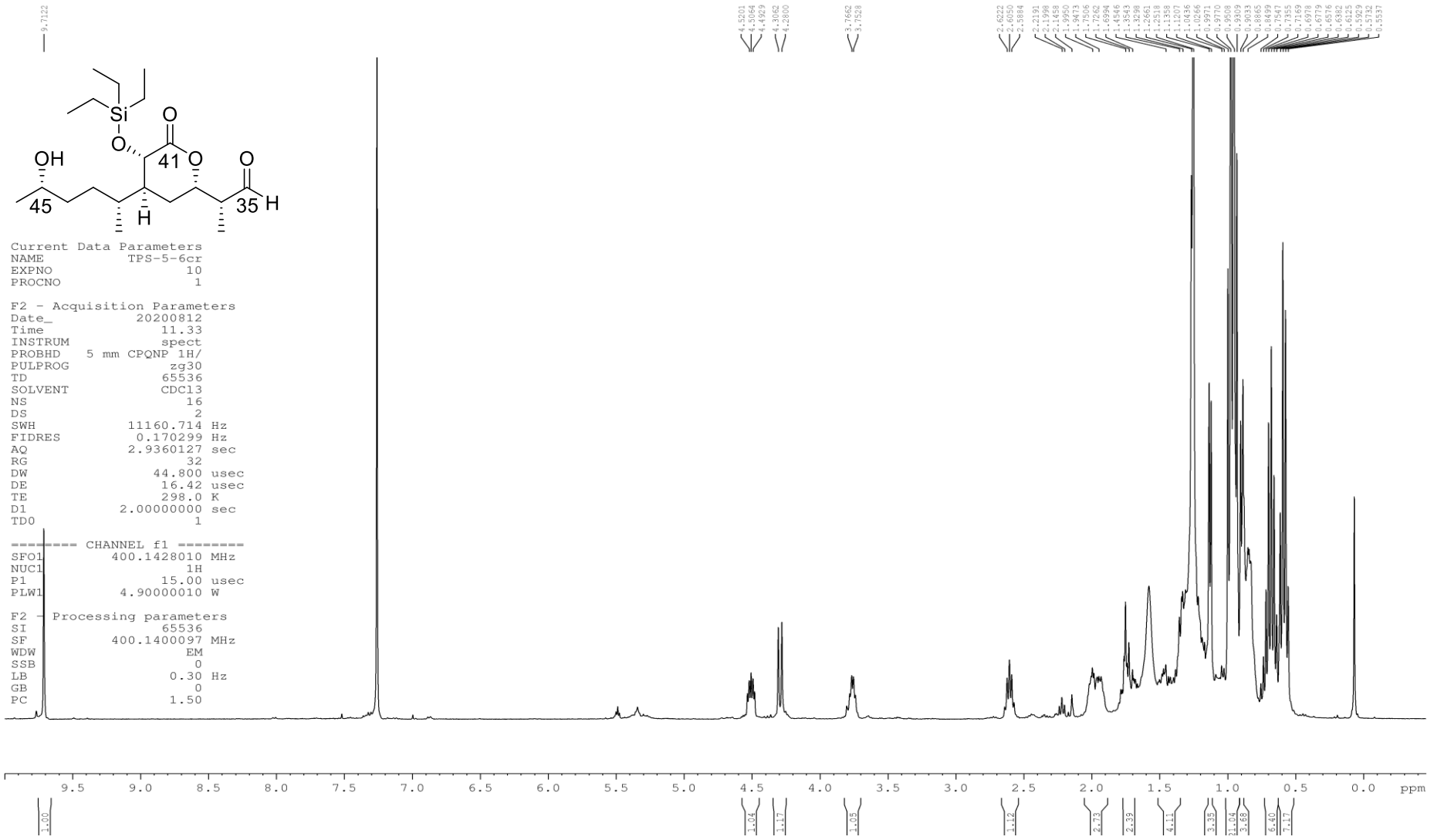

Spectrum 35. Terminal olefin 42,25-*syn*-**170b**, $CDCl_3$, ^1H NMR, 500 MHz

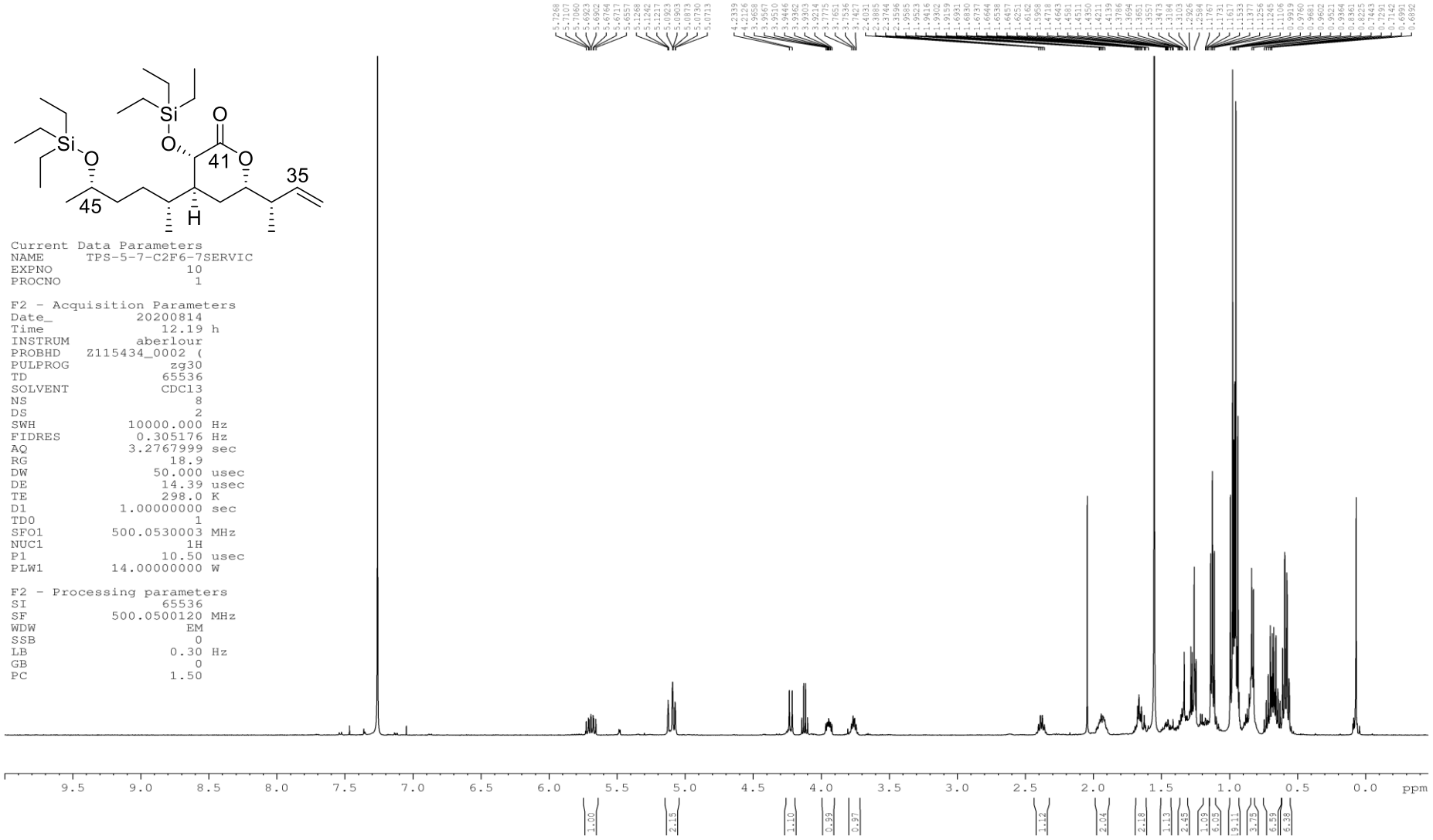

Spectrum 36. Terminal olefin 42,25-*syn*-**170b**, $CDCl_3$, ^{13}C NMR, 125 MHz

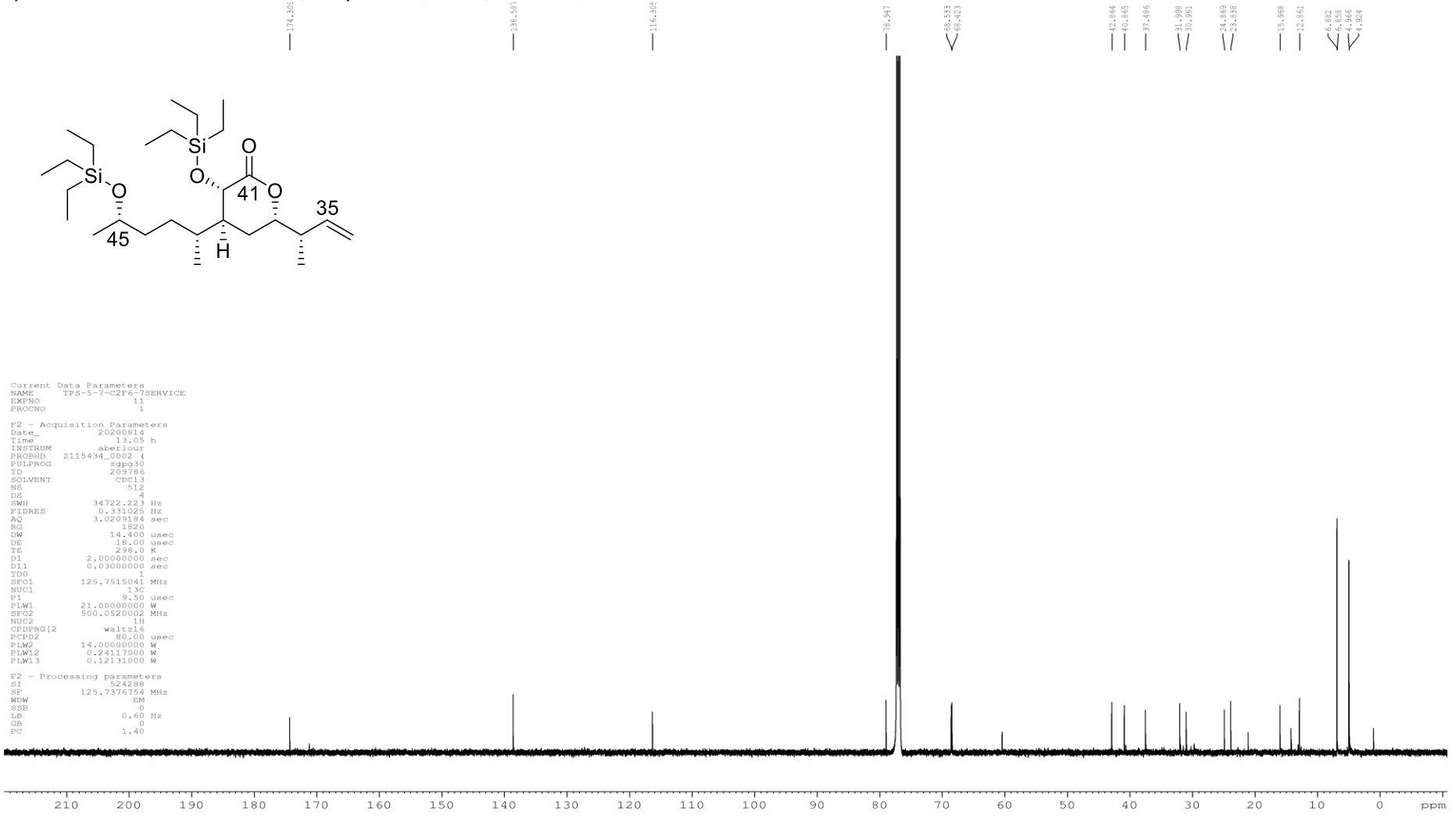

Spectrum 37. Terminal olefin alcohol 42,25-*syn*-**212b**, $CDCl_3$, ^1H NMR, 500 MHz

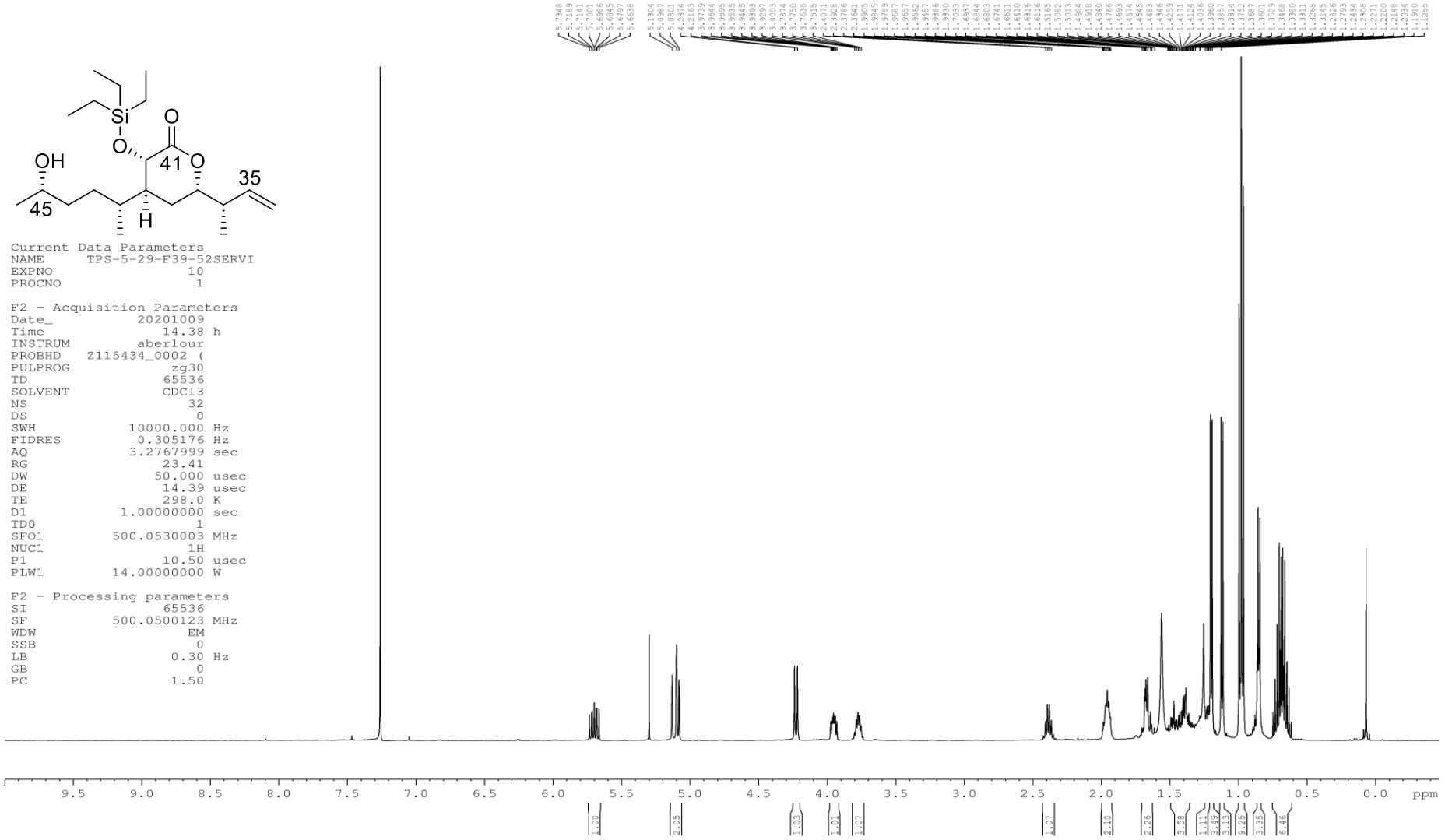

Spectrum 38. Terminal olefin alcohol 42,25-*syn*-**212b**, $CDCl_3$, ^{13}C NMR, 125 MHz

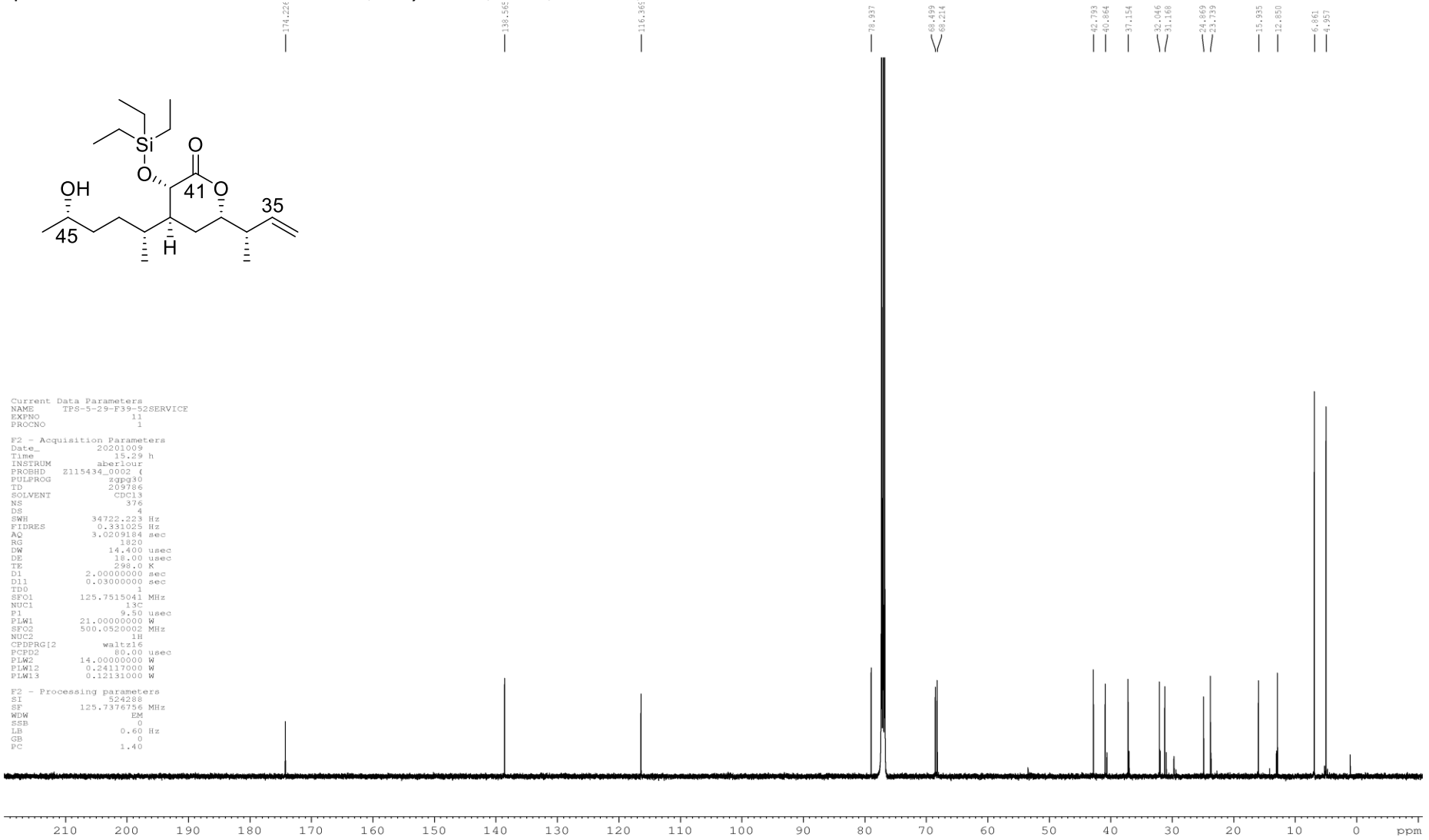

Spectrum 39. Diol terminal olefin 42,25-*syn*-**171b**, CD_3OD, ^1H NMR, 500 MHz

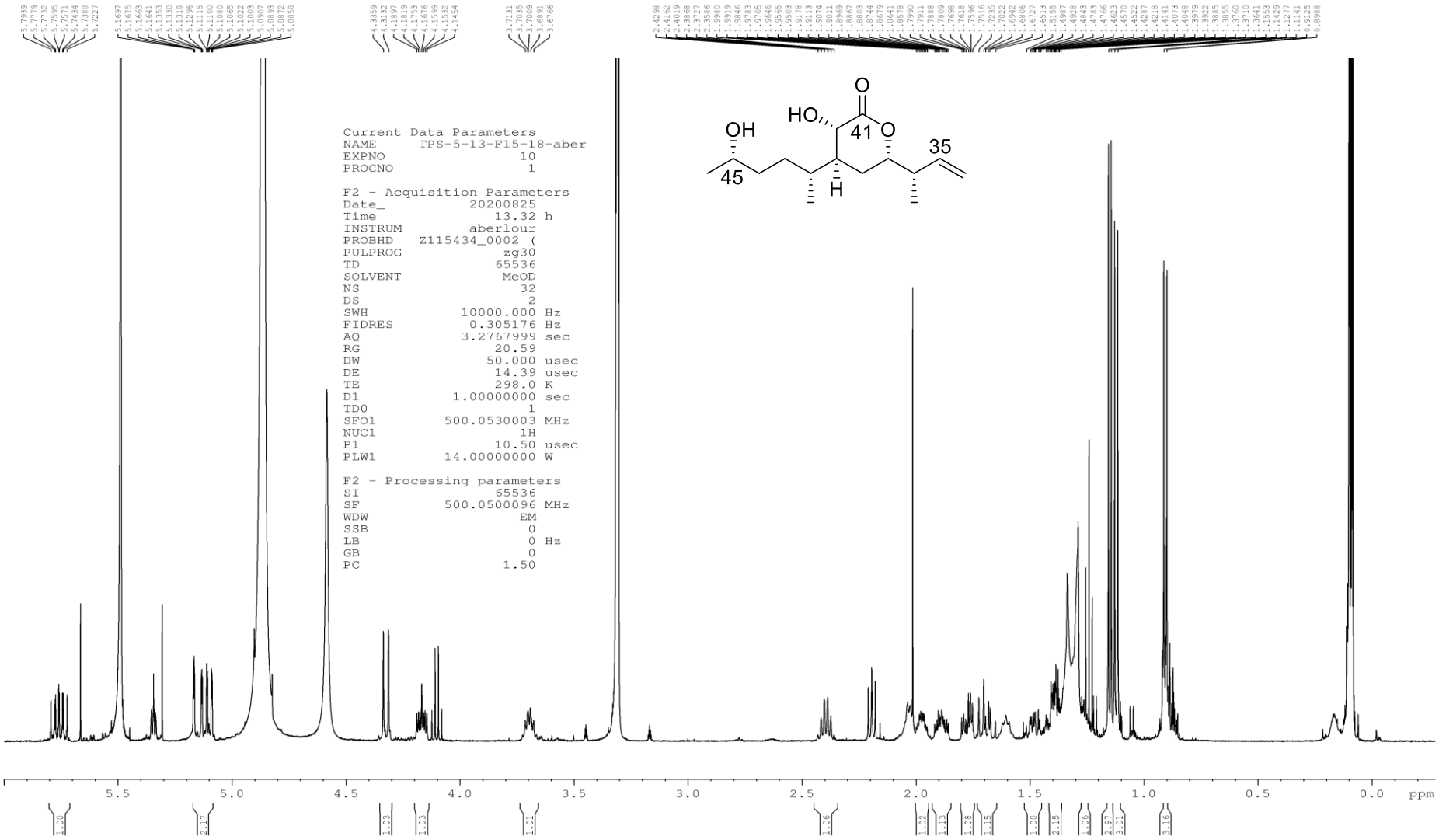

Spectrum 40. Diol terminal olefin 42,25-*syn*-**171b**, CD_3OD, ^{13}C NMR, 125 MHz

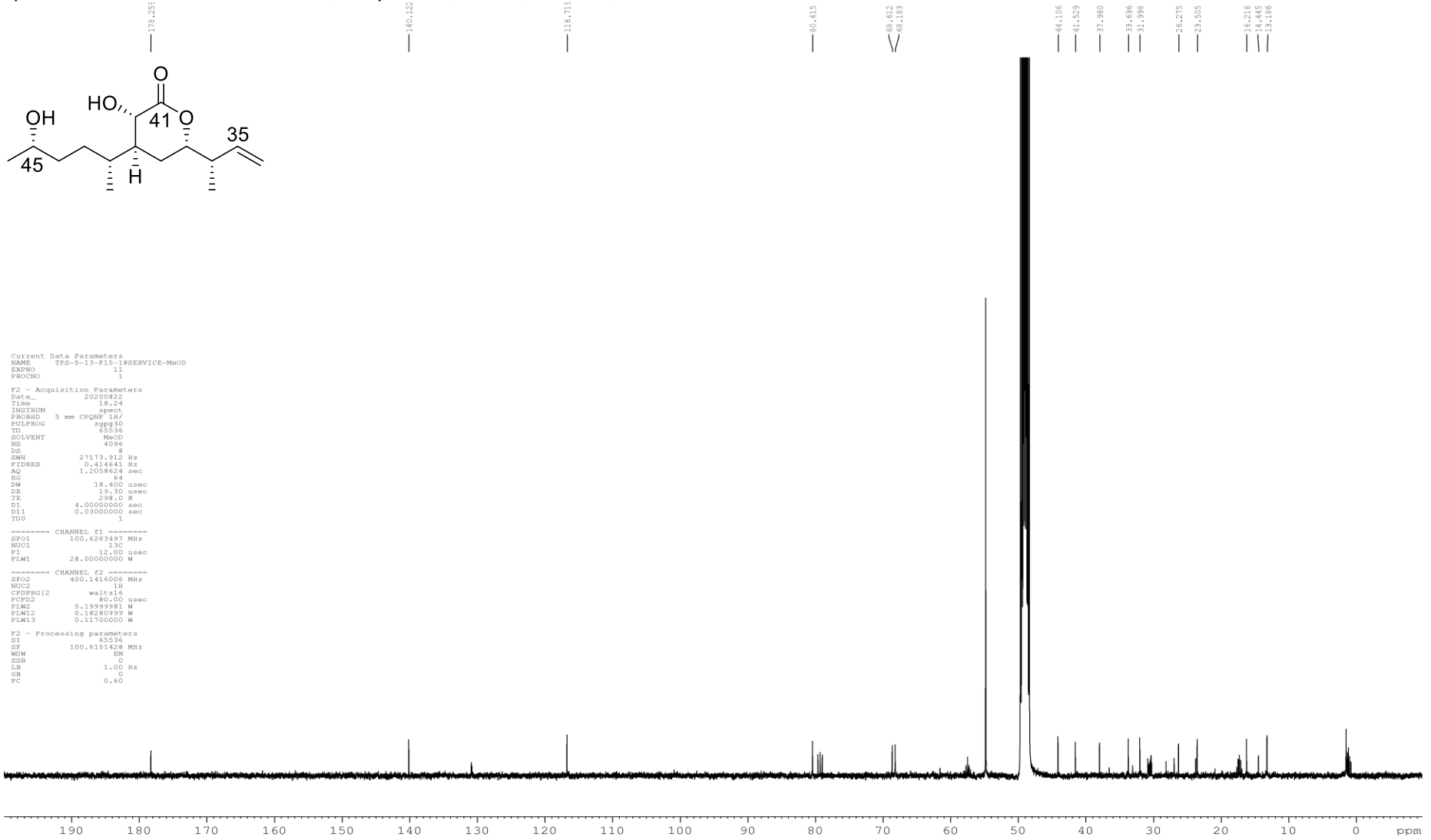

Spectrum 41. TBS ether 42,45-*anti*-**211a**, $CDCl_3$, ^1H NMR, 400 MHz

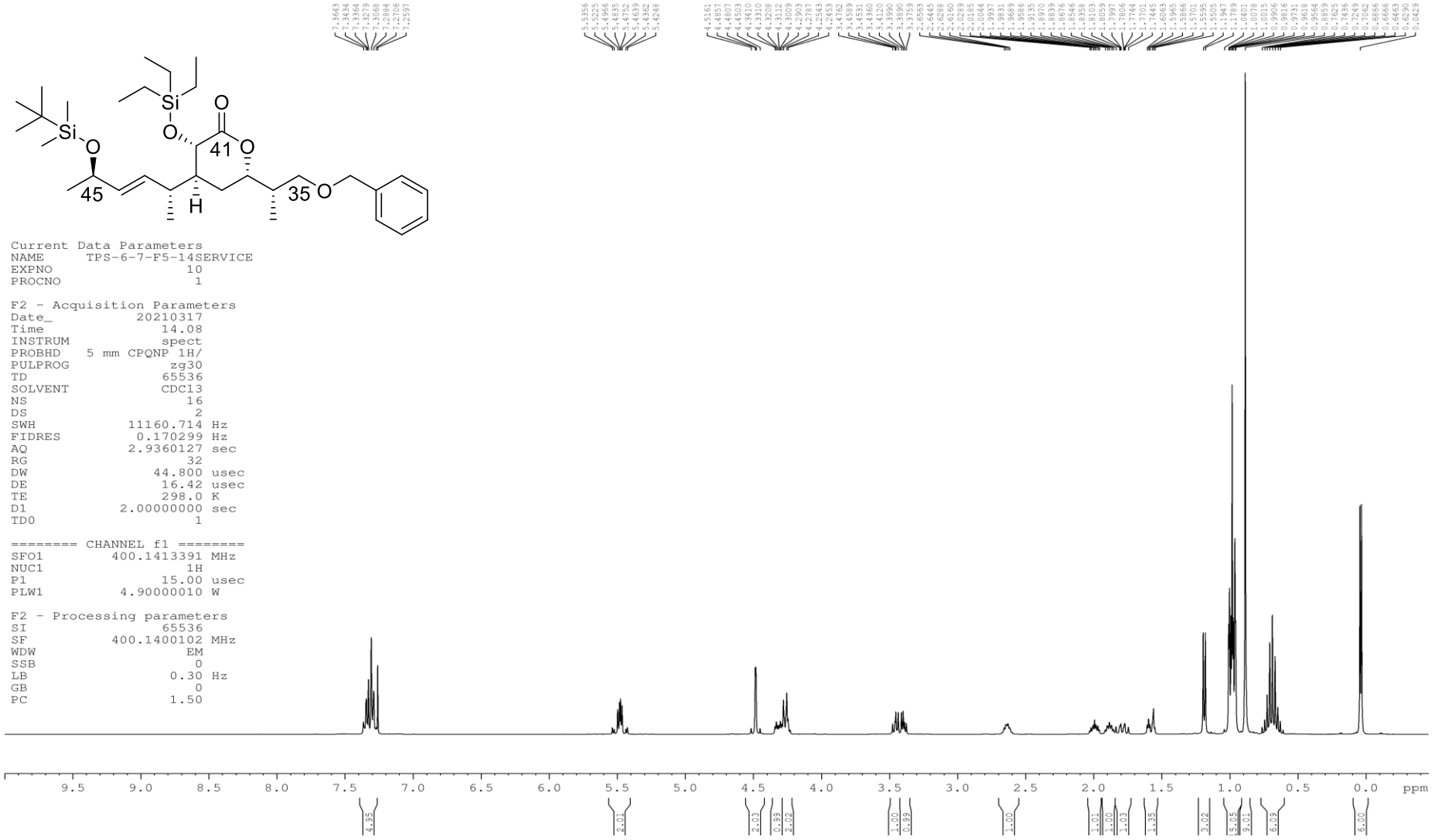

Spectrum 42. TBS ether 42,45-*anti*-**211a**, $CDCl_3$, ^{13}C NMR, 125 MHz

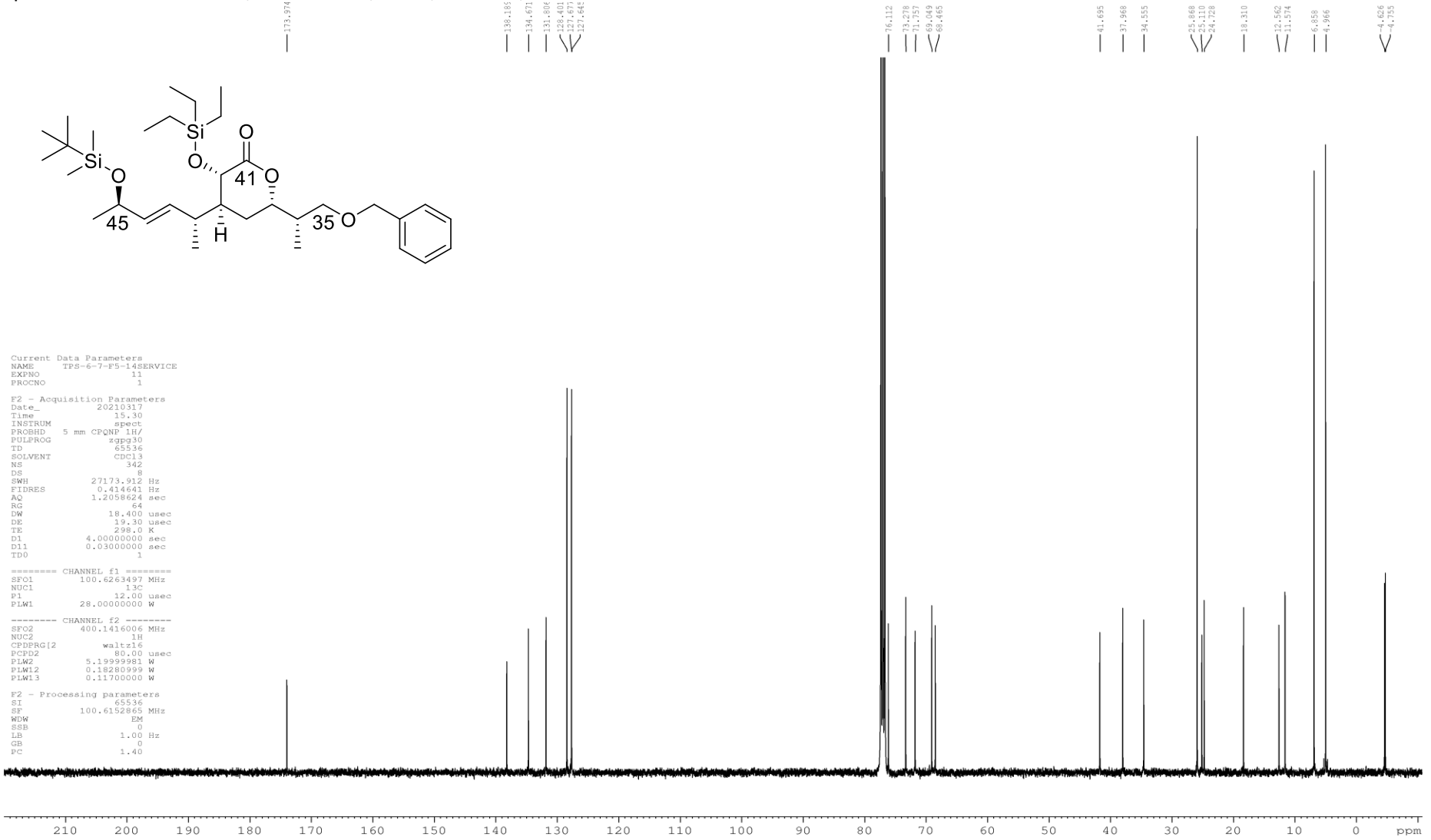

Spectrum 43. Alcohol 42,45-*anti*-**173a**, $CDCl_3$, ^1H NMR, 700 MHz

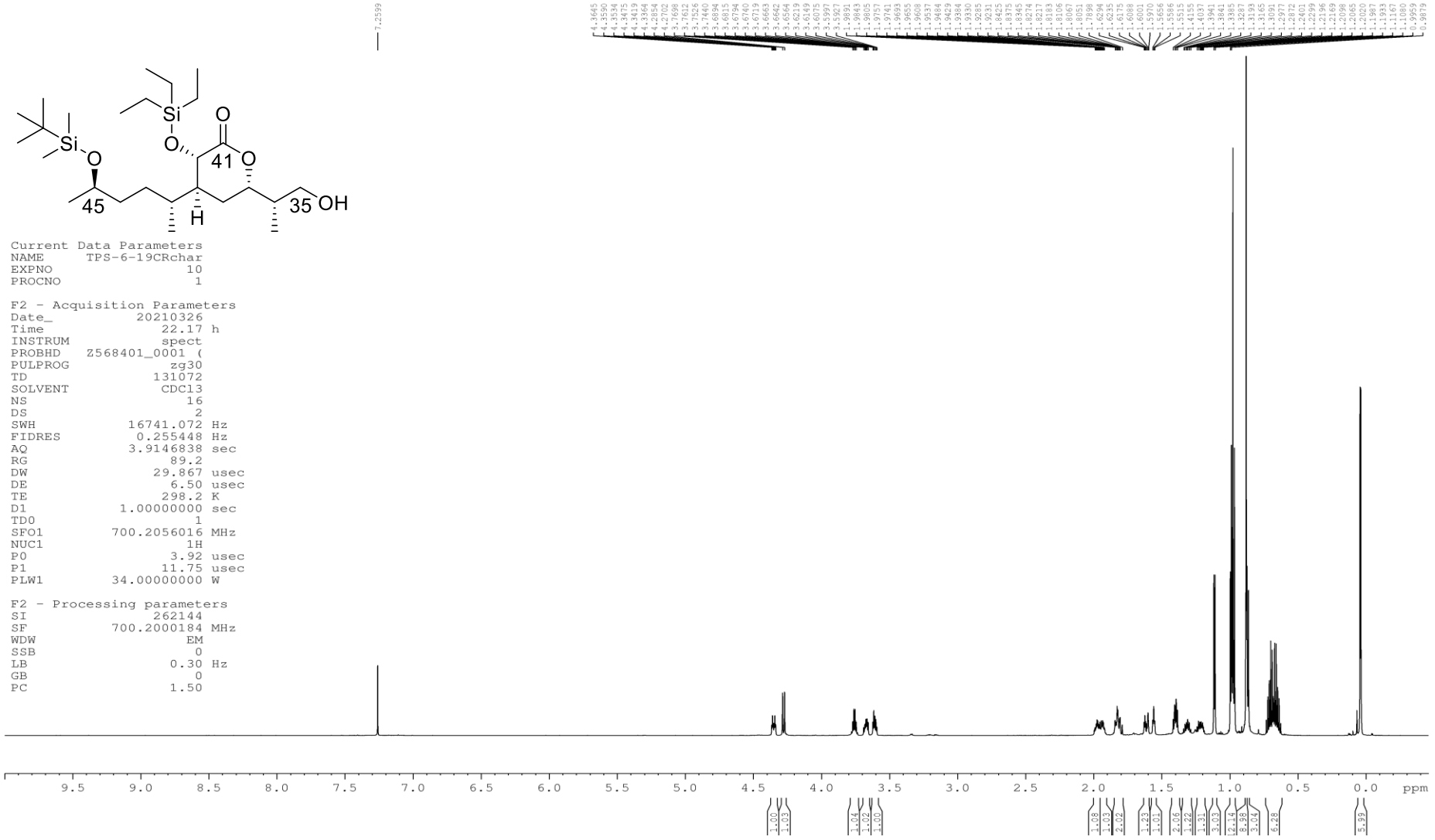

Spectrum 44. Alcohol 42,45-*anti*-**173a**, $CDCl_3$, ^{13}C NMR, 176 MHz

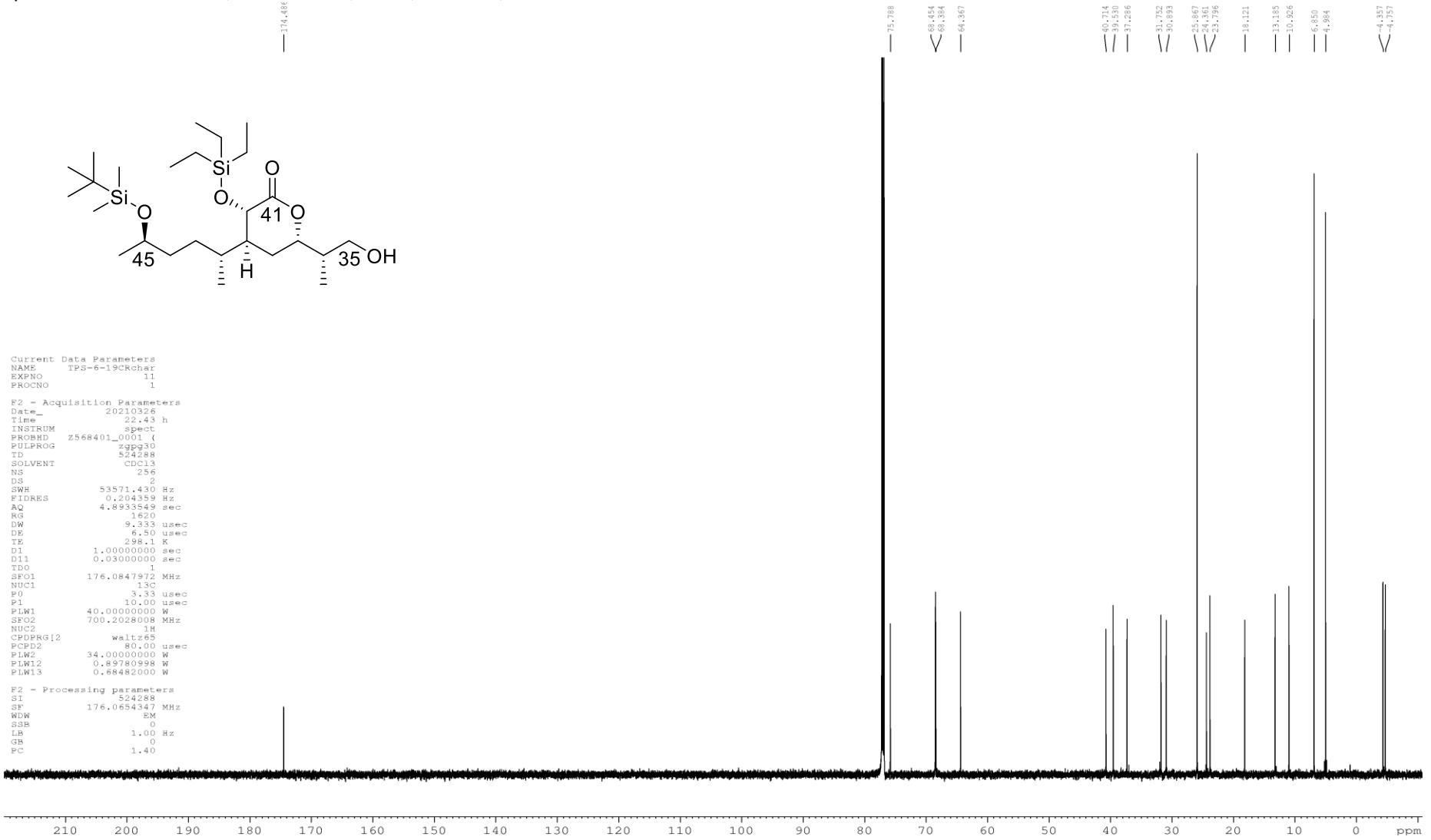

Spectrum 45. Aldehyde 42,45-*anti*-**213a**, $CDCl_3$, ^1H NMR, 400 MHz

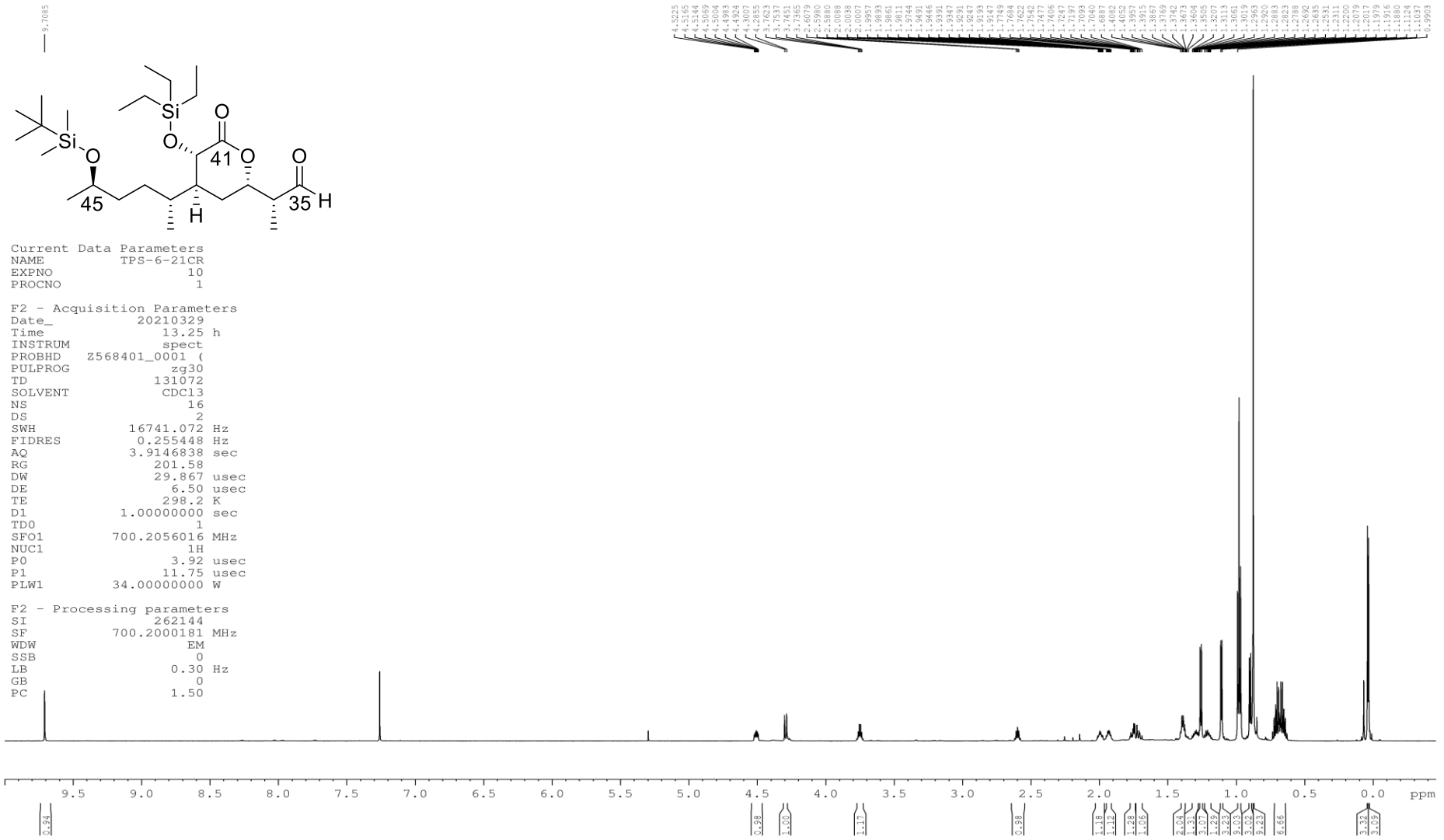

Spectrum 46. Terminal olefin 42,45-*anti*-**2a**, $CDCl_3$, ^1H NMR, 700 MHz

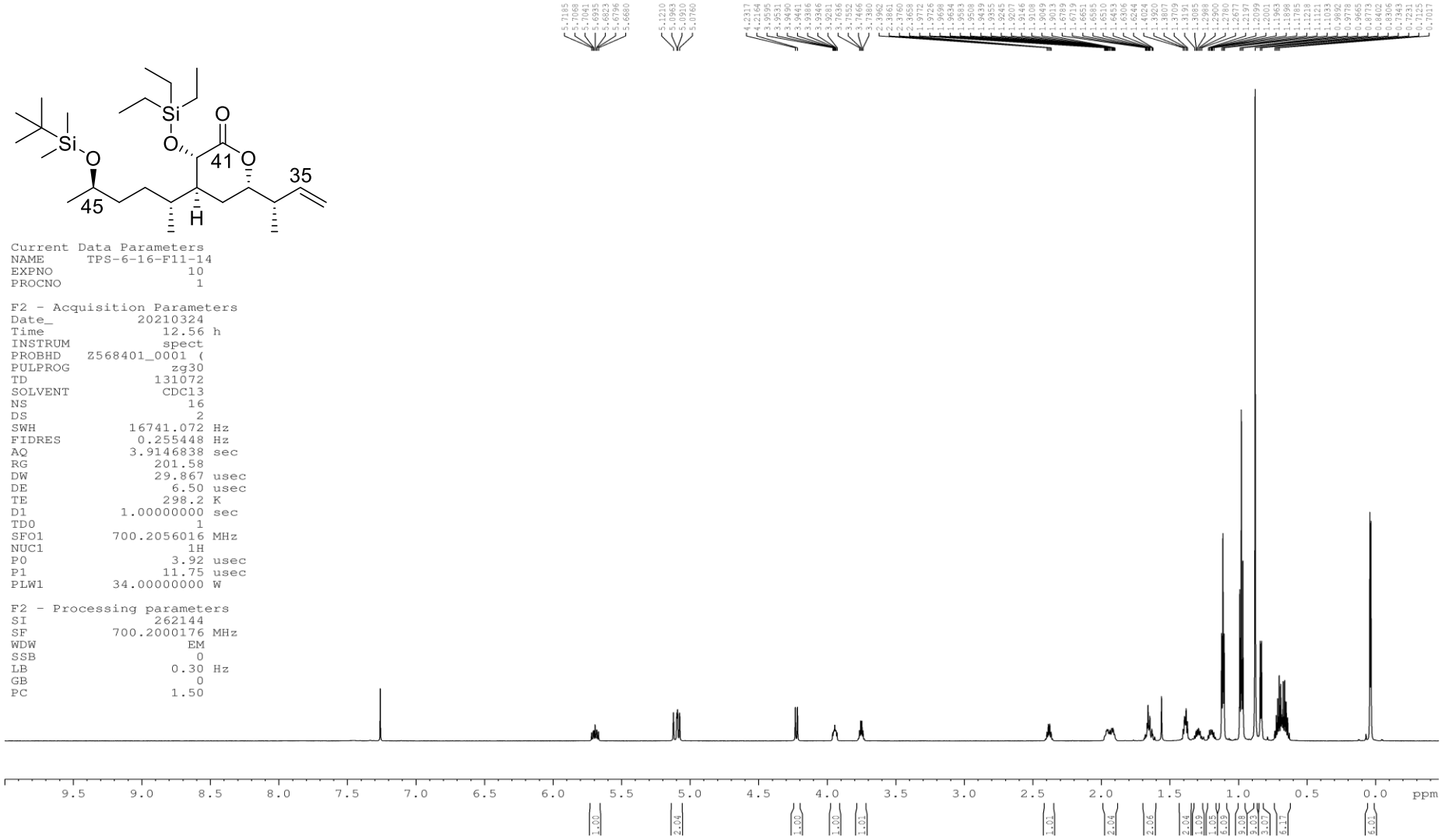

Spectrum 47. 4 Terminal olefin 42,45-*anti*-**2a**, $CDCl_3$, ^{13}C NMR, 125 MHz

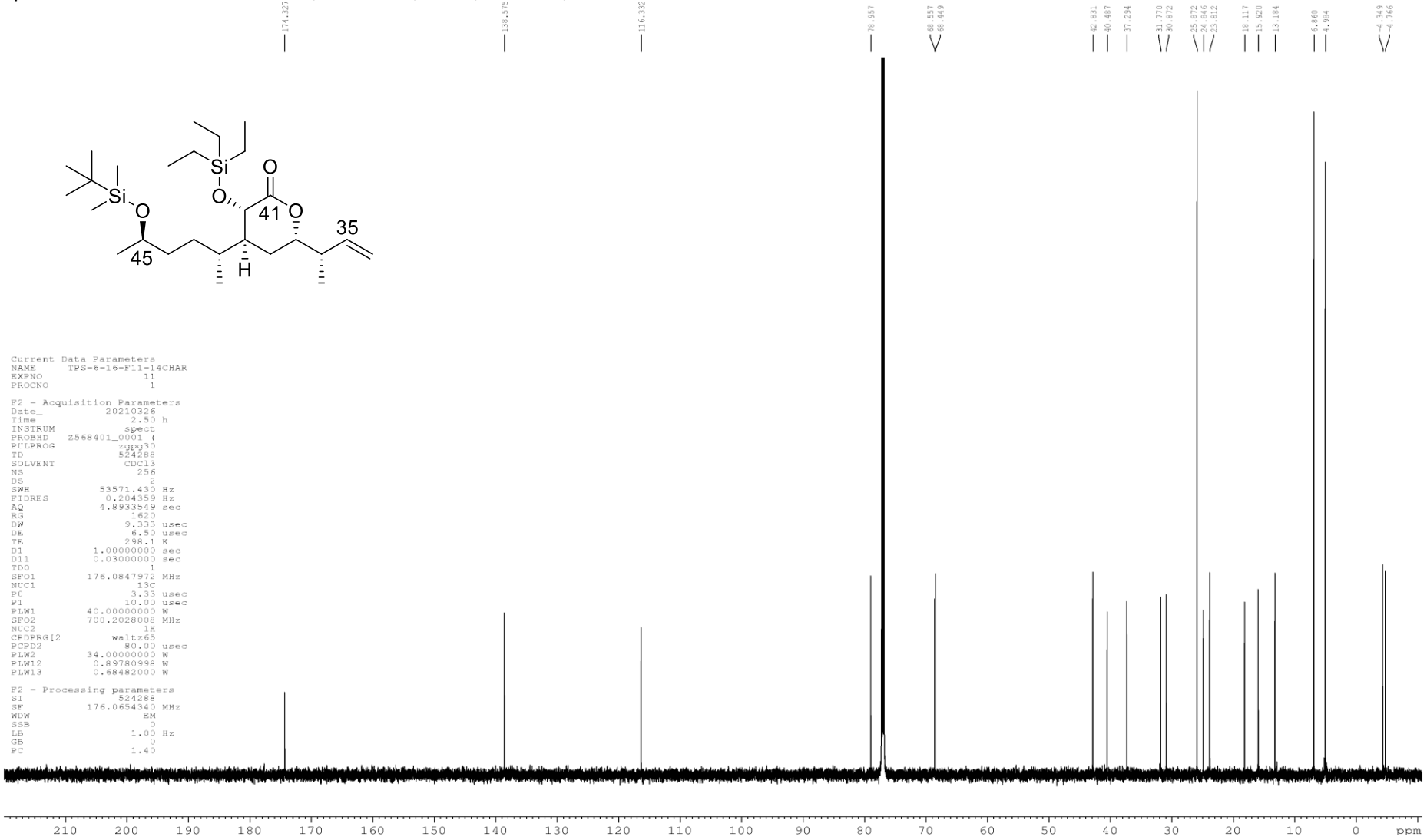

Spectrum 48. Diol 42,45-*anti*-**171a**, $CDCl_3$, ^1H NMR, 500 MHz

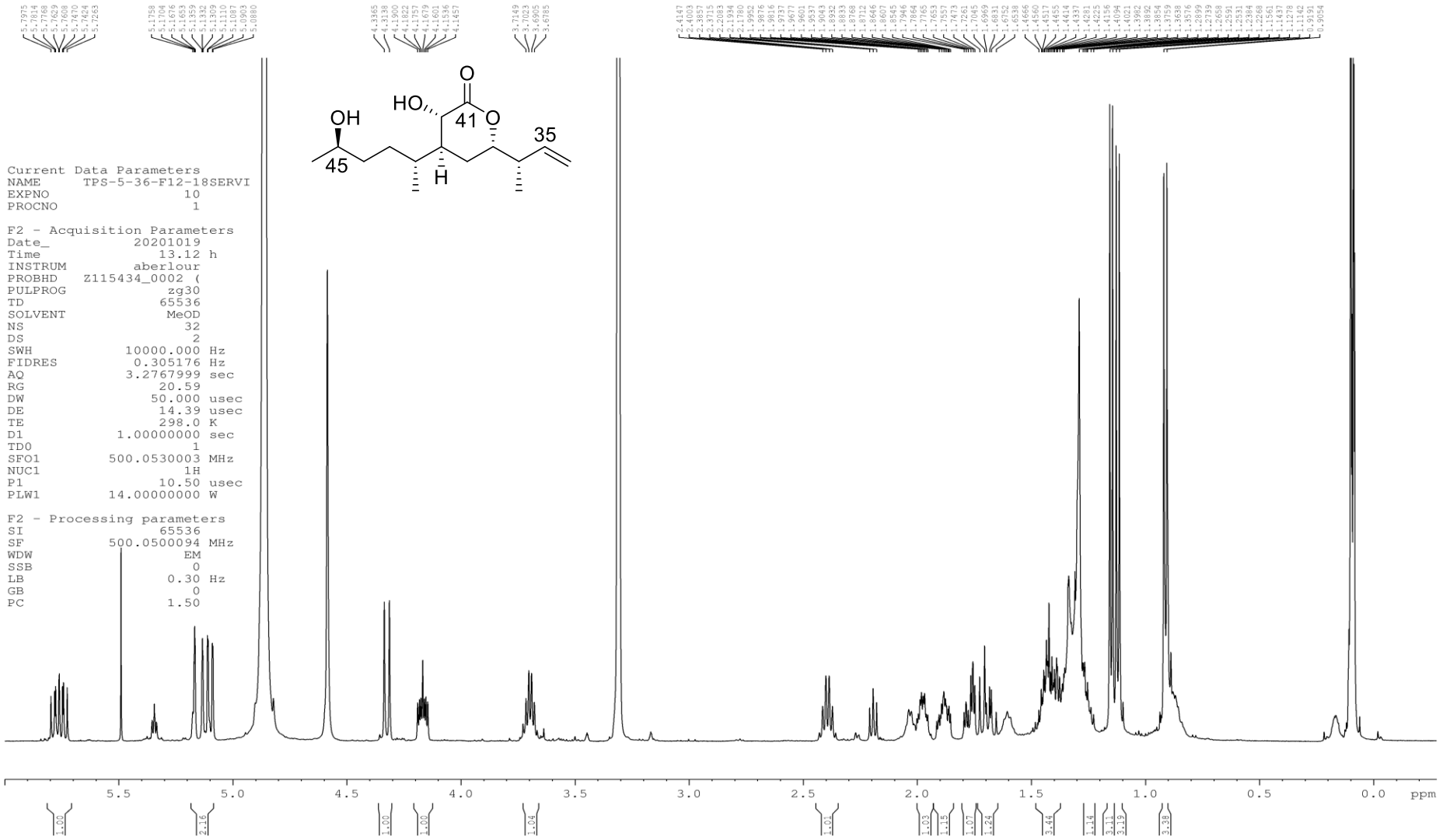

Spectrum 49. Diol 42,45-*anti*-**171a**, $CDCl_3$, ^{13}C NMR, 125 MHz

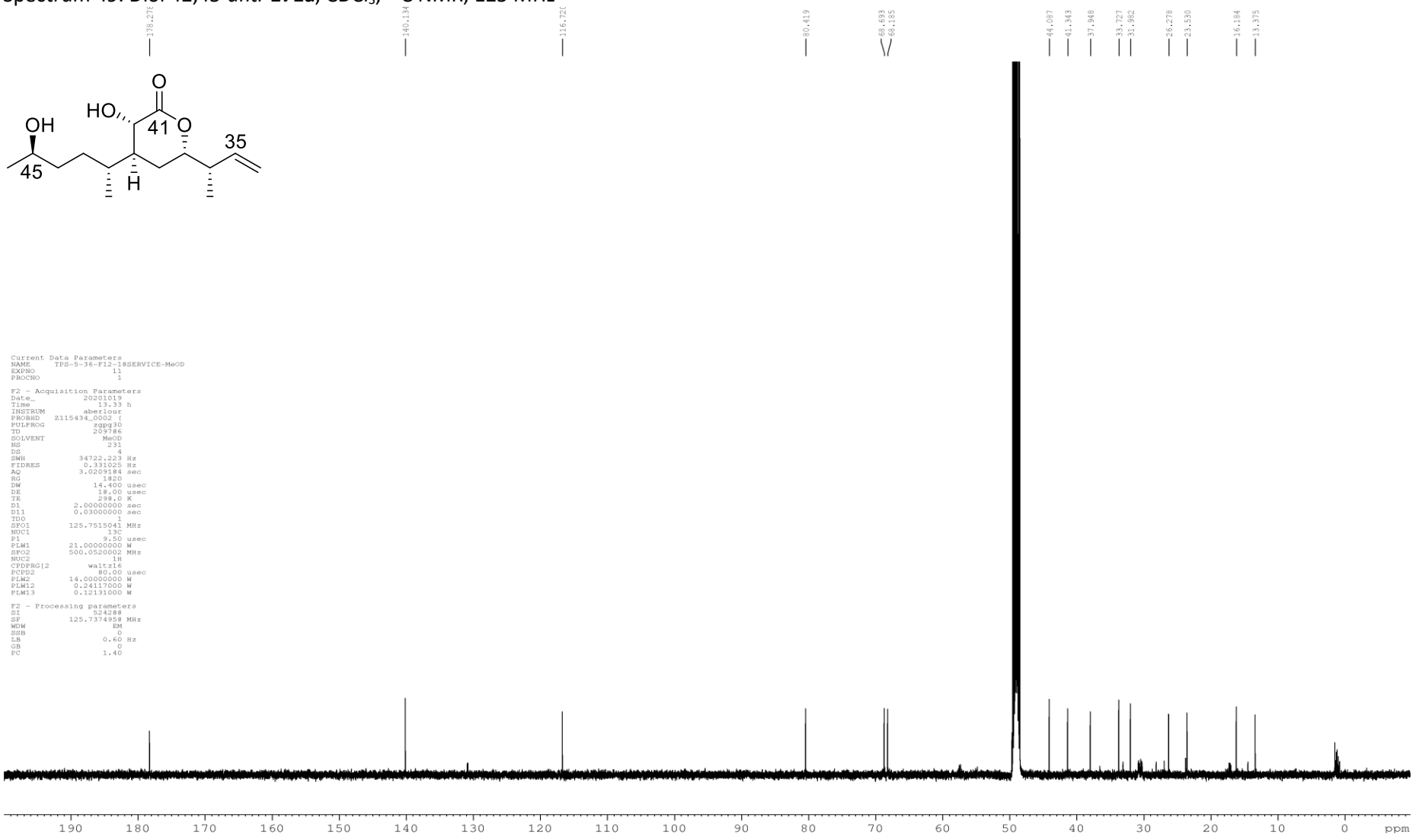


```
Current Data Parameters
NAME      TPS-5-36-F12-18SERVICE-MeOD
EXPNO                 11
PROCNO                 1

F2 - Acquisition Parameters
Date_           20201019
Time              13.33 h
INSTRUM         aberlour
PROBHD    Z115434_0002 (
PULPROG          zgpg30
TD               209786
SOLVENT            MeOD
NS                  231
D2                    4
SWH           34722.223 Hz
FIDRES            0.331025 Hz
AQ              3.0209184 sec
RG                 1820
DW                14.400 usec
DE                18.00 usec
TE                298.0 K
D1             2.00000000 sec
D11            0.03000000 sec
TD0                   1
SFO1          125.7515041 MHz
NUC1                13C
P1                  9.50 usec
PLW1          21.00000000 W
SFO2          500.0520002 MHz
NUC2                1H
CPDPRG[2          waltz16
PCPD2              80.00 usec
PLW2          14.00000000 W
PLW12          0.24117000 W
PLW13          0.12131000 W

F2 - Processing parameters
SI                 524288
SF            125.7374958 MHz
WDW                   EM
SSB                    0
LB                  0.60 Hz
GB                     0
PC                  1.40
```

Spectrum 50. TBS ether 31,32-*syn*-**183a**, $CDCl_3$, ^1H NMR, 700 MHz

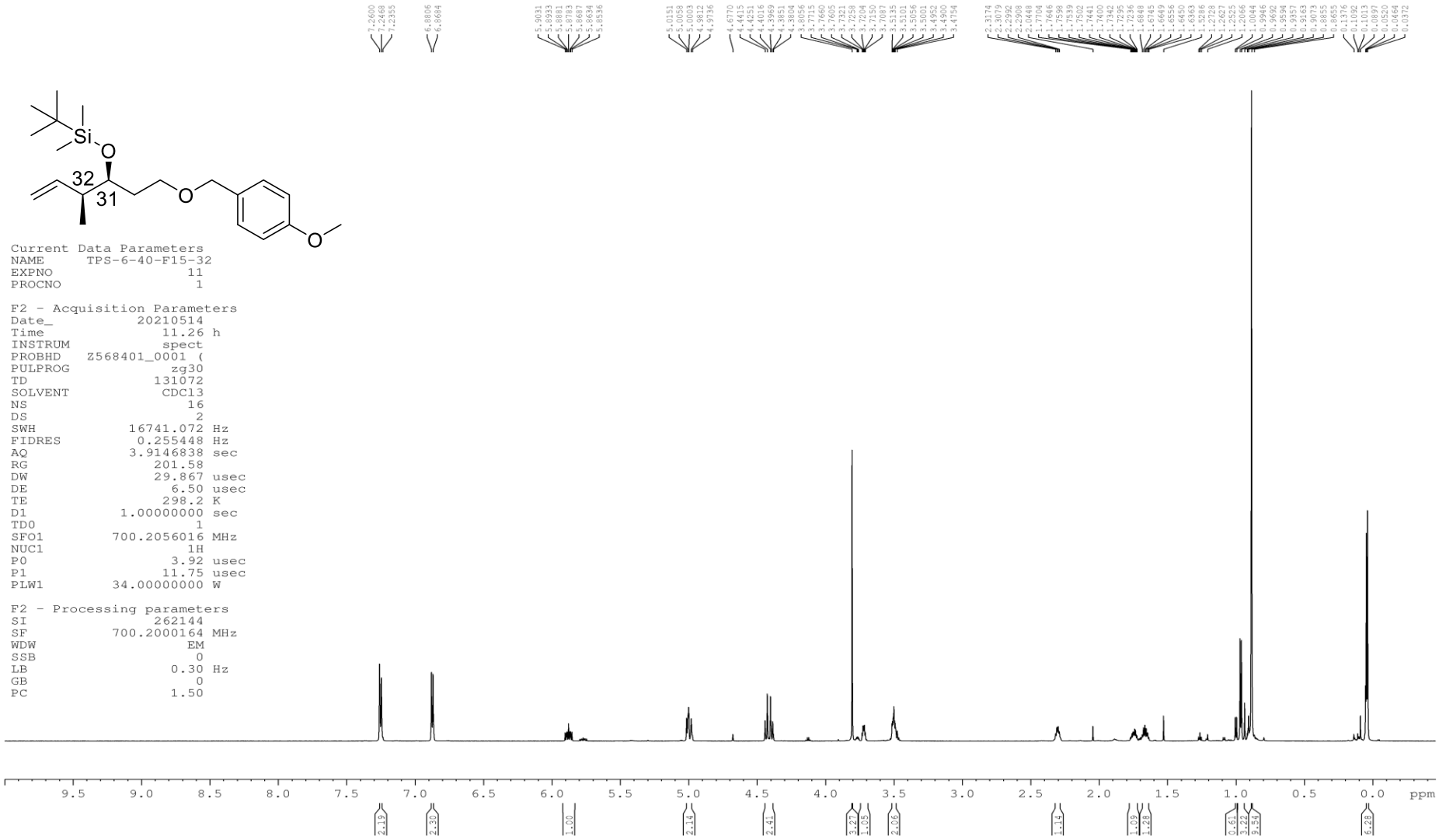

Spectrum 51. TBS ether 31,32-*syn*-**183a**, $CDCl_3$, ^{13}C NMR, 125 MHz

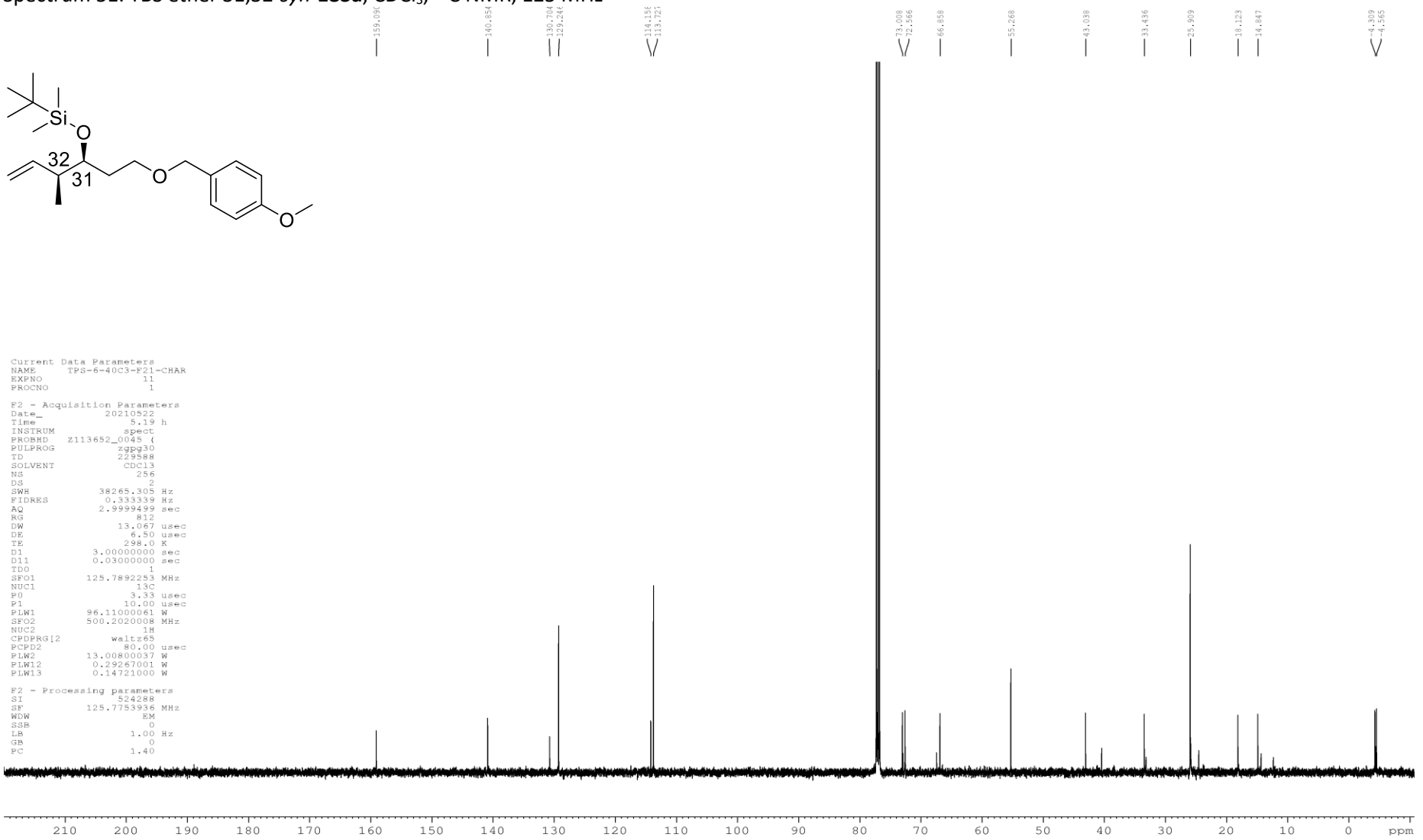

Spectrum 52. Primary alcohol 31,32-*syn*-**184a**, $CDCl_3$, ^1H NMR, 700 MHz

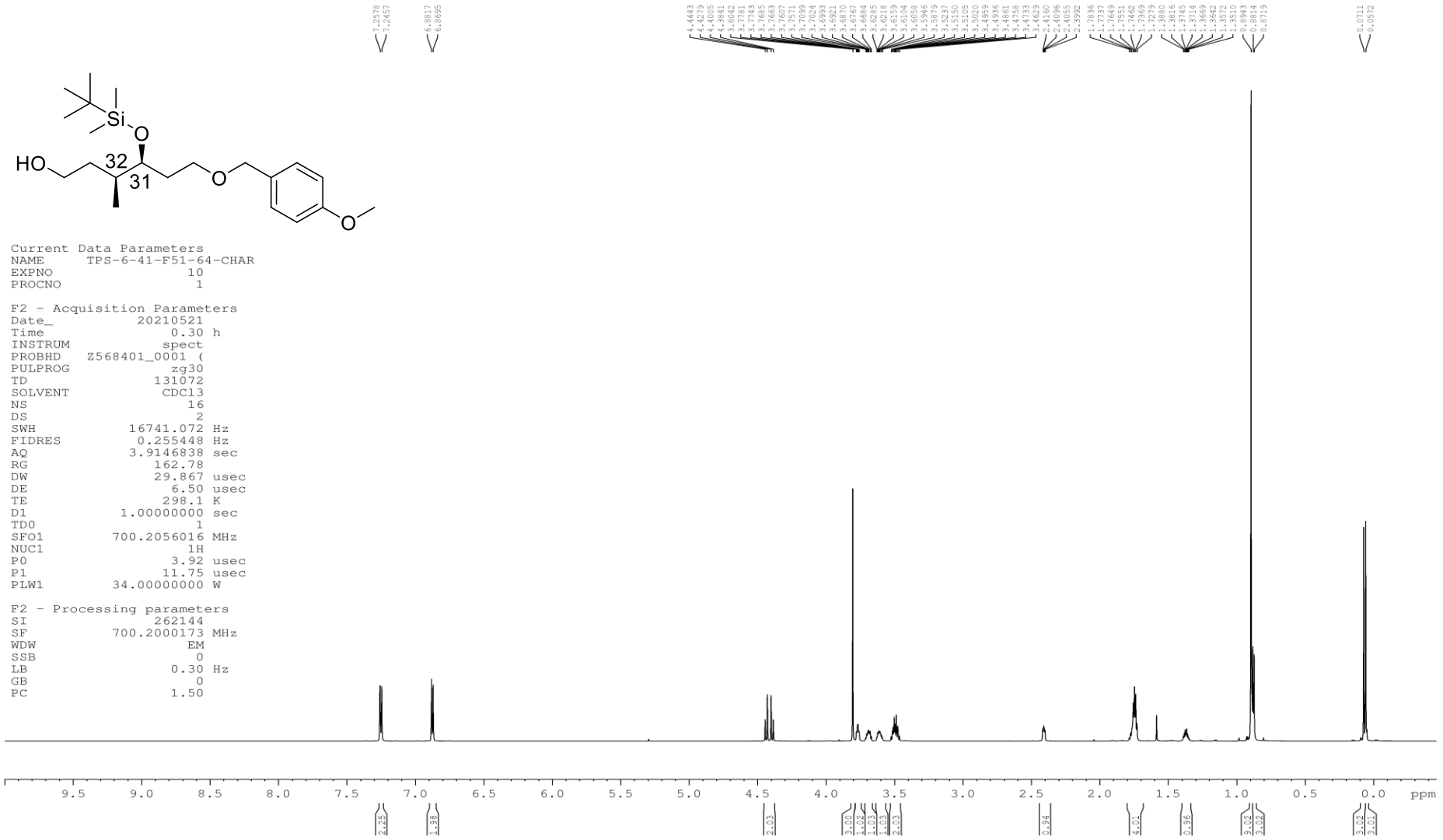

Spectrum 53. Primary alcohol 31,32-*syn*-**184a**, $CDCl_3$, ^{13}C NMR, 176 MHz

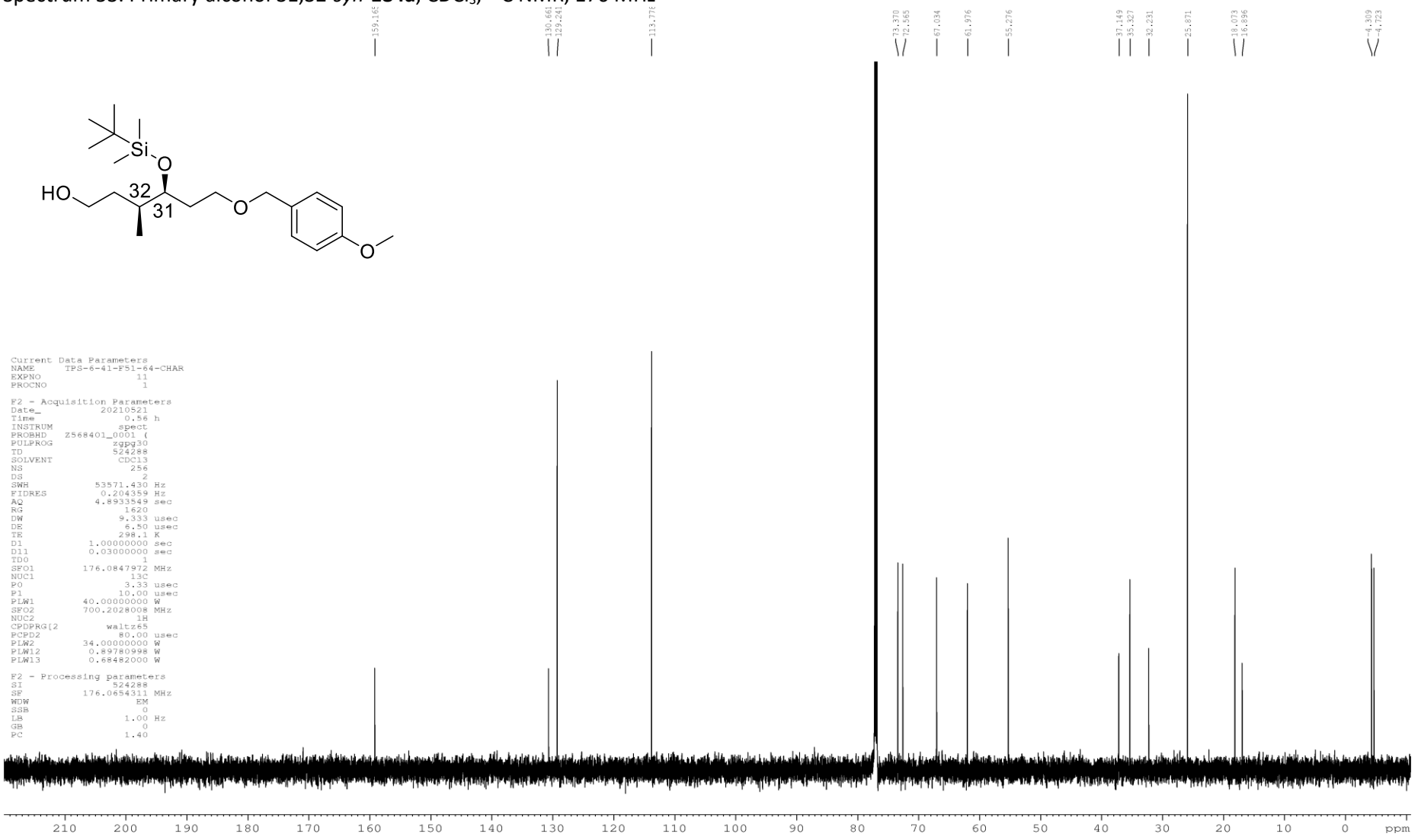

Spectrum 54. Aldehyde 31,32-*syn*-**185a**, $CDCl_3$, ^1H NMR, 700 MHz

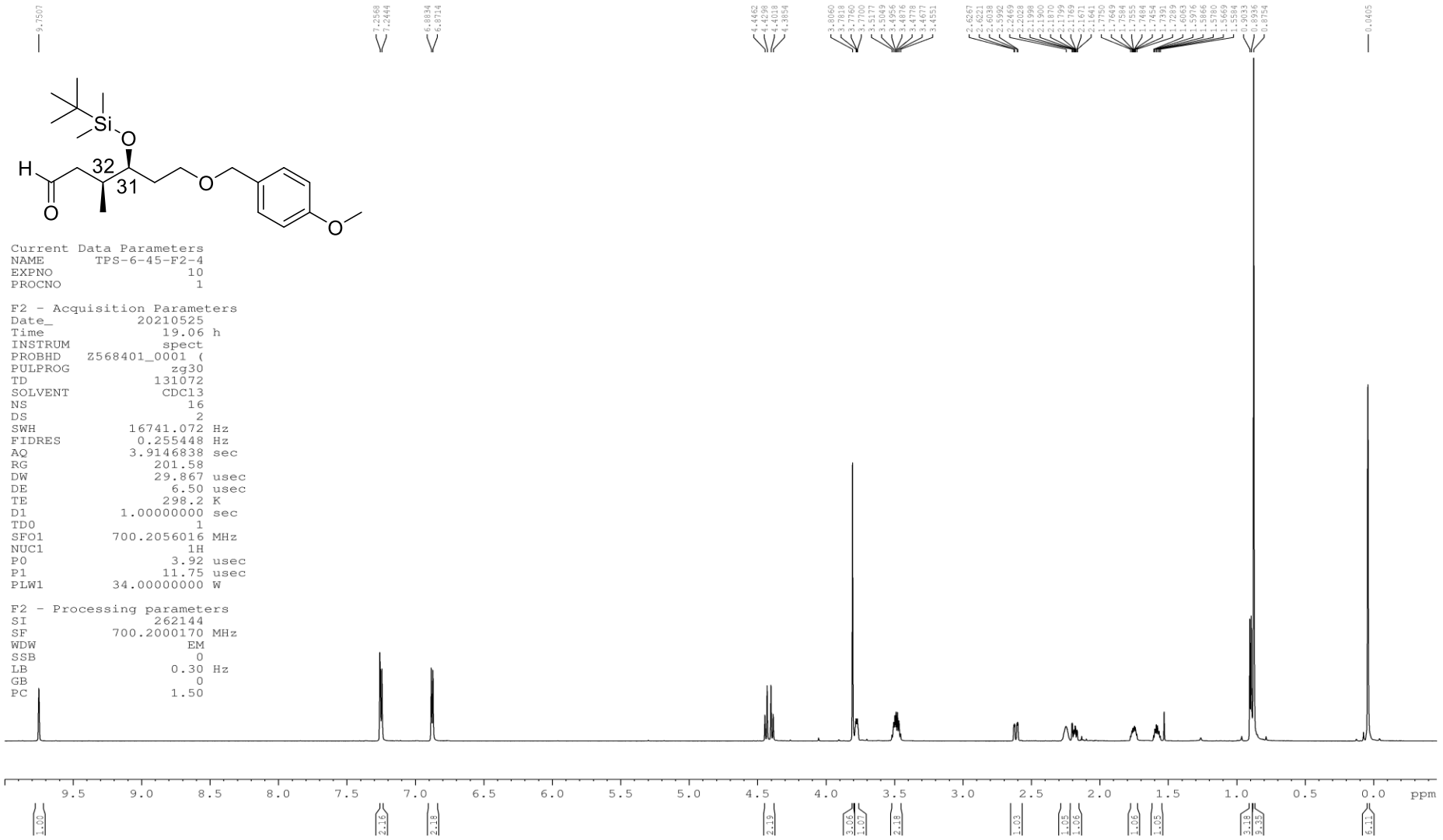

Spectrum 55. Aldehyde 31,32-*syn*-**185a**, $CDCl_3$, ^{13}C NMR, 125 MHz

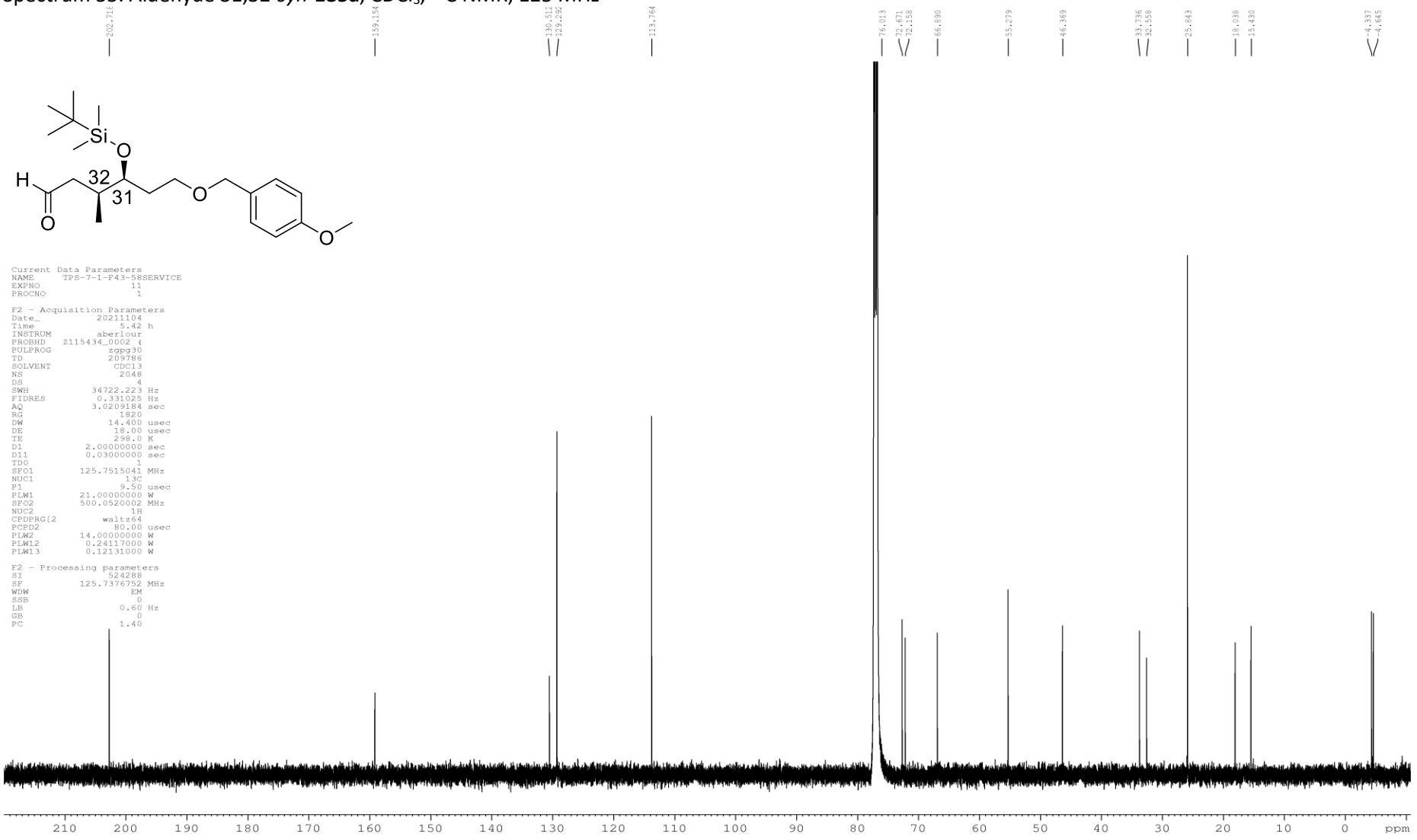

Spectrum 56. Terminal olefin 31,32-*syn*-**3a**, $CDCl_3$, ^1H NMR, 500 MHz

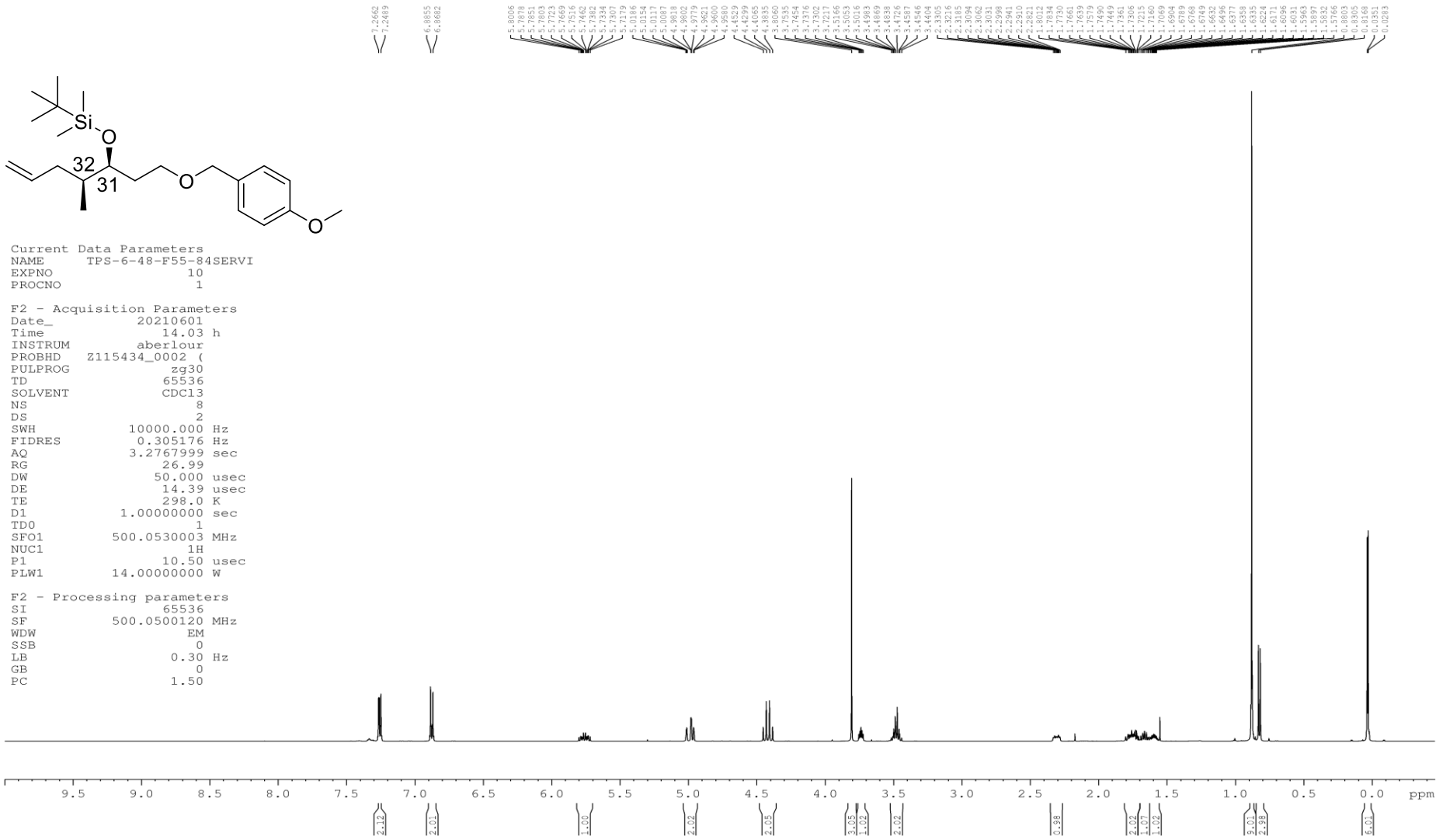

Spectrum 57. Terminal olefin 31,32-*syn*-**3a**, $CDCl_3$, ^{13}C NMR, 125 MHz

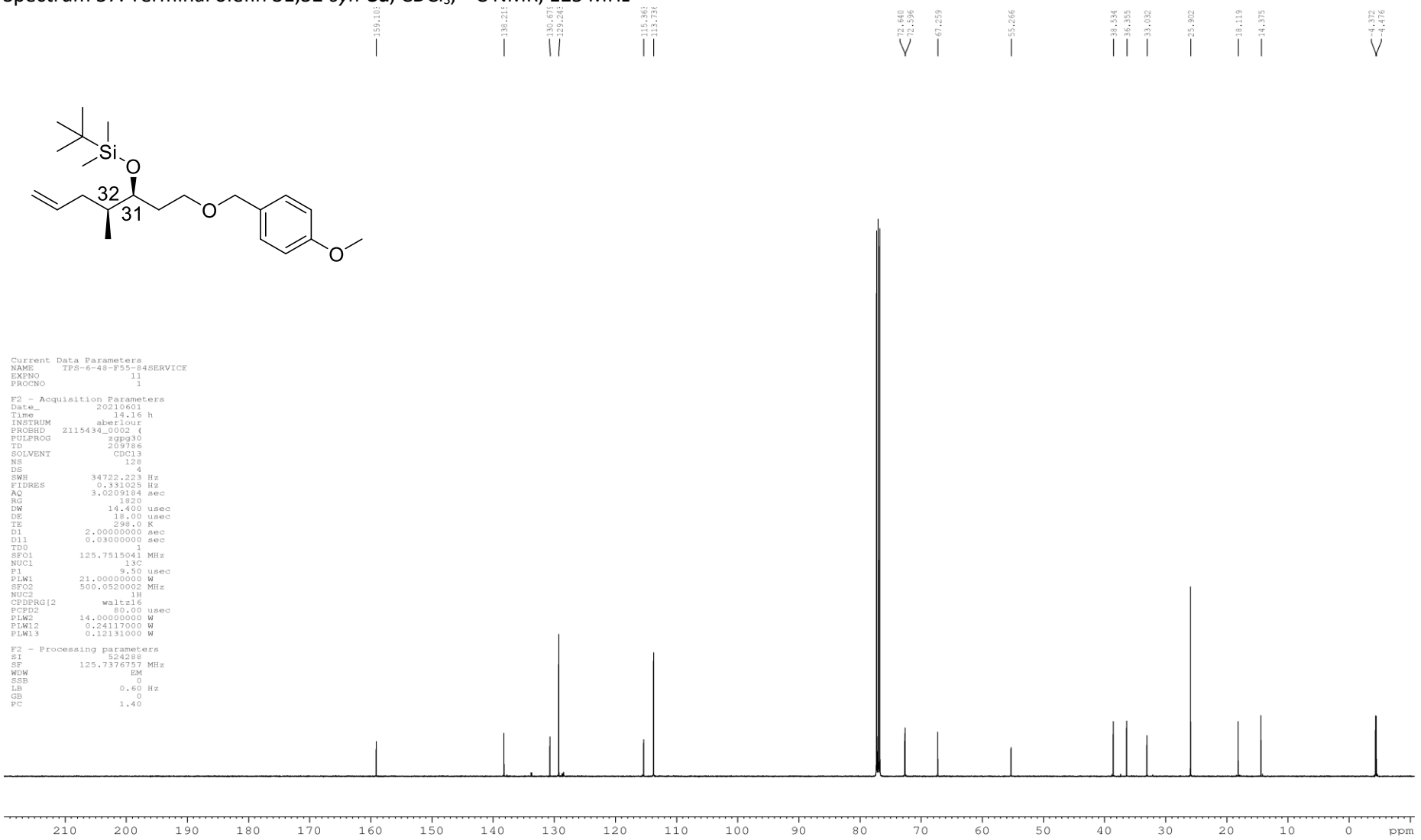

Spectrum 58. Olefin alcohol *syn-anti-anti*-**202a**, $CDCl_3$, ^1H NMR, 500 MHz

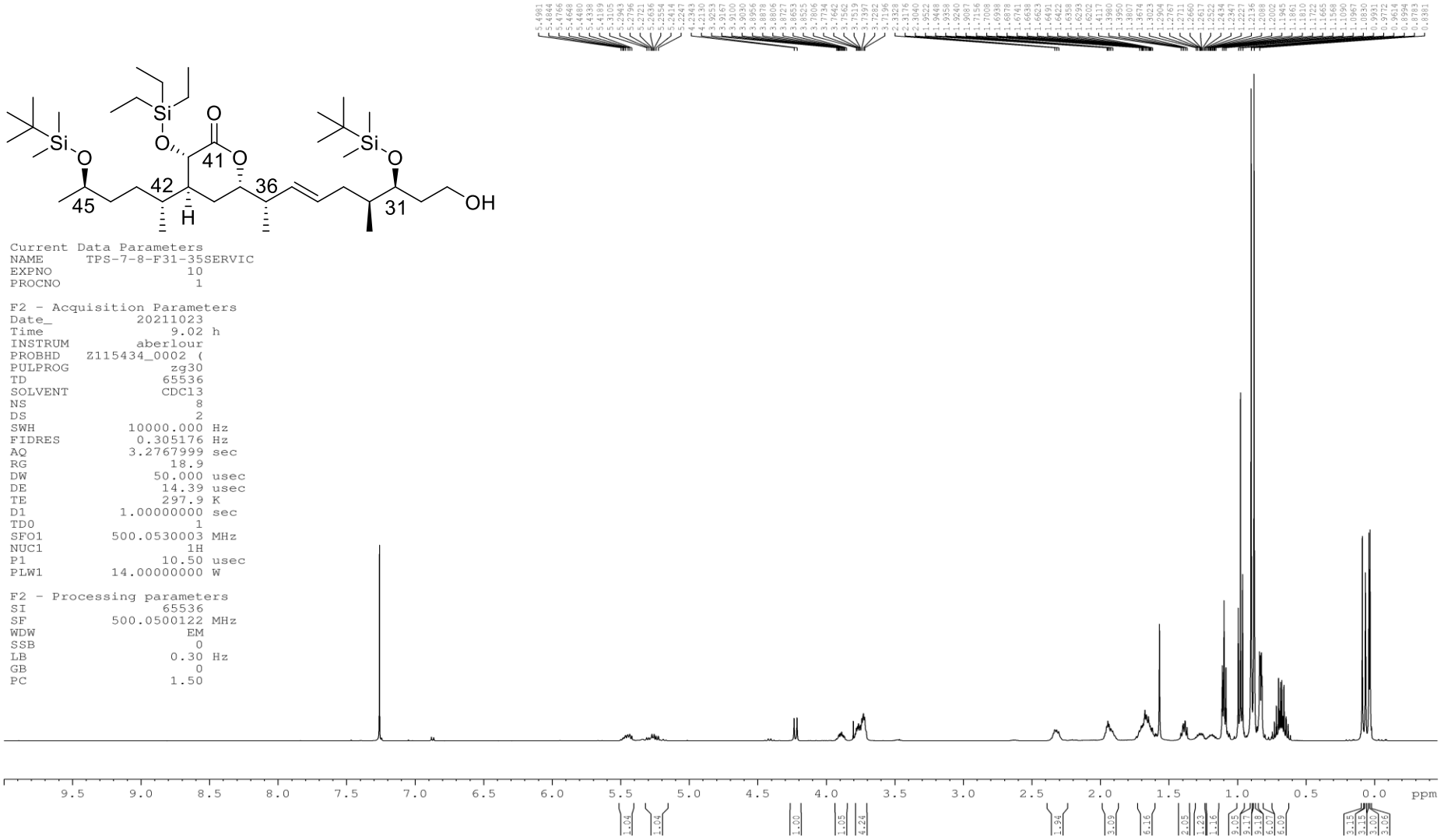

Spectrum 59. Olefin alcohol *syn-anti-anti*-**202a**, $CDCl_3$, ^{13}C NMR, 125 MHz (*not listing minor peaks)

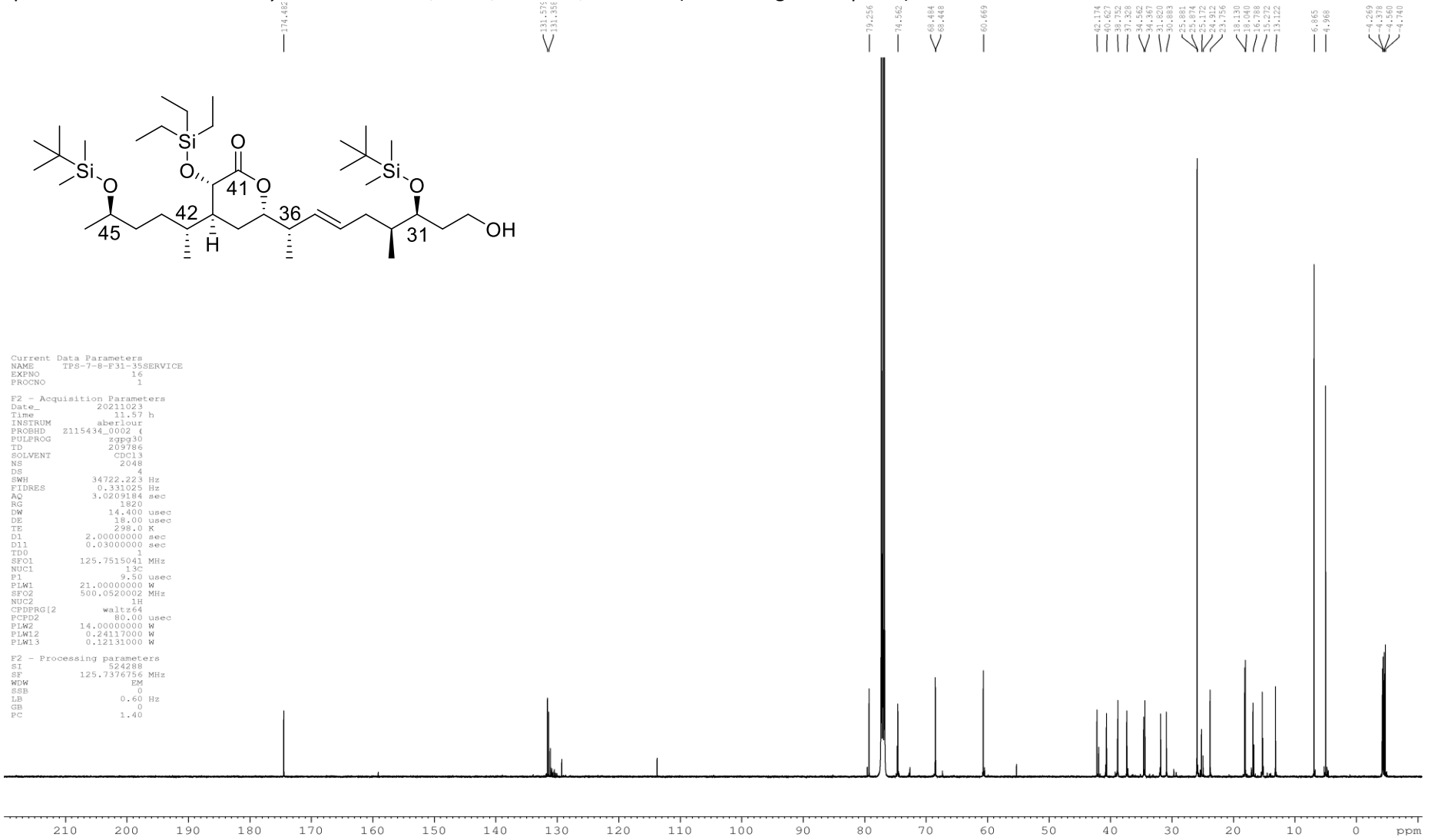

Spectrum 60. Olefin alcohol *syn-syn-anti*-**202b**, $CDCl_3$, ^1H NMR, 500 MHz

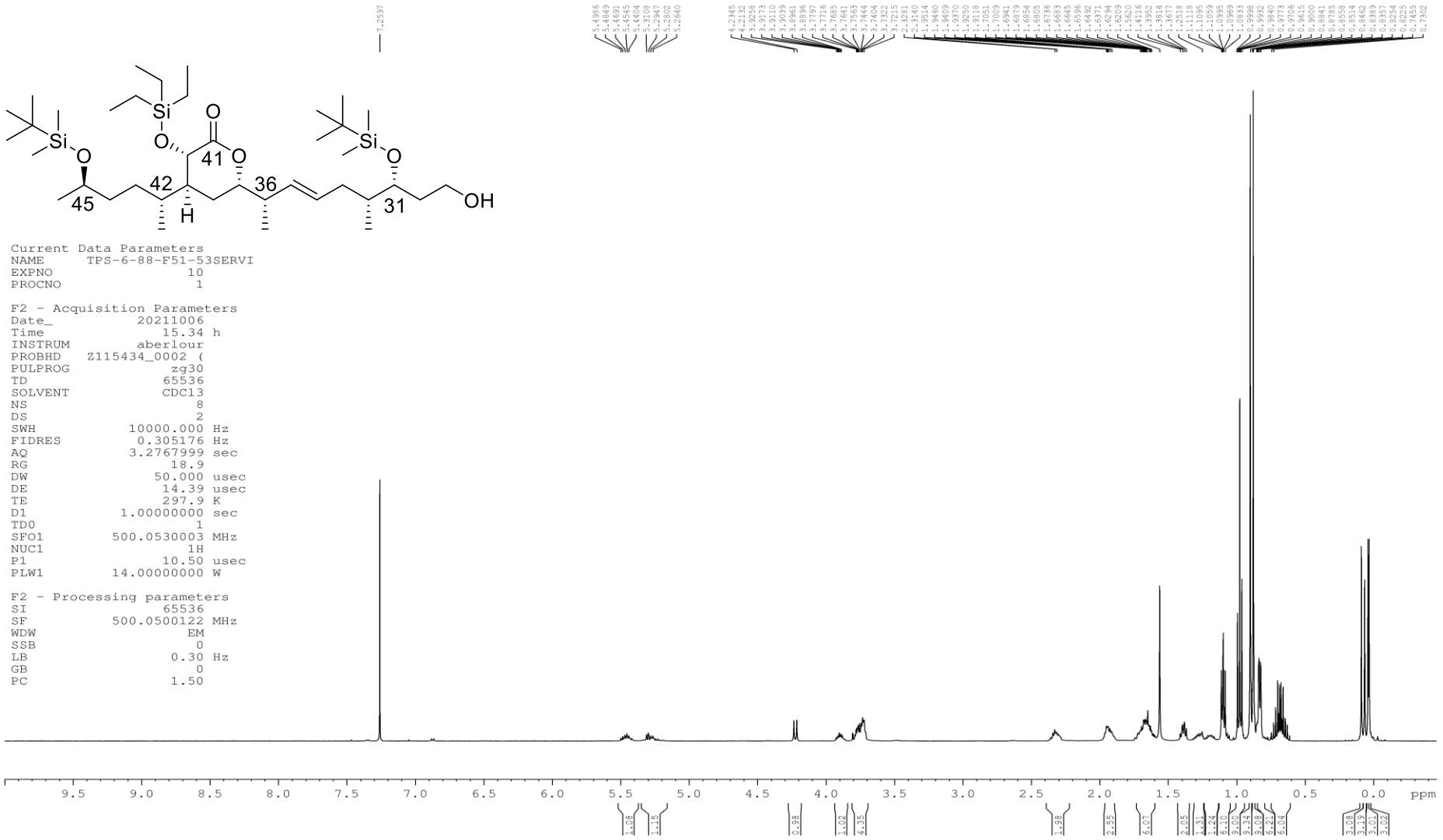

Spectrum 61. Olefin alcohol *syn-syn-anti*-**202b**, $CDCl_3$, ^{13}C NMR, 125 MHz (*not listing minor peaks)

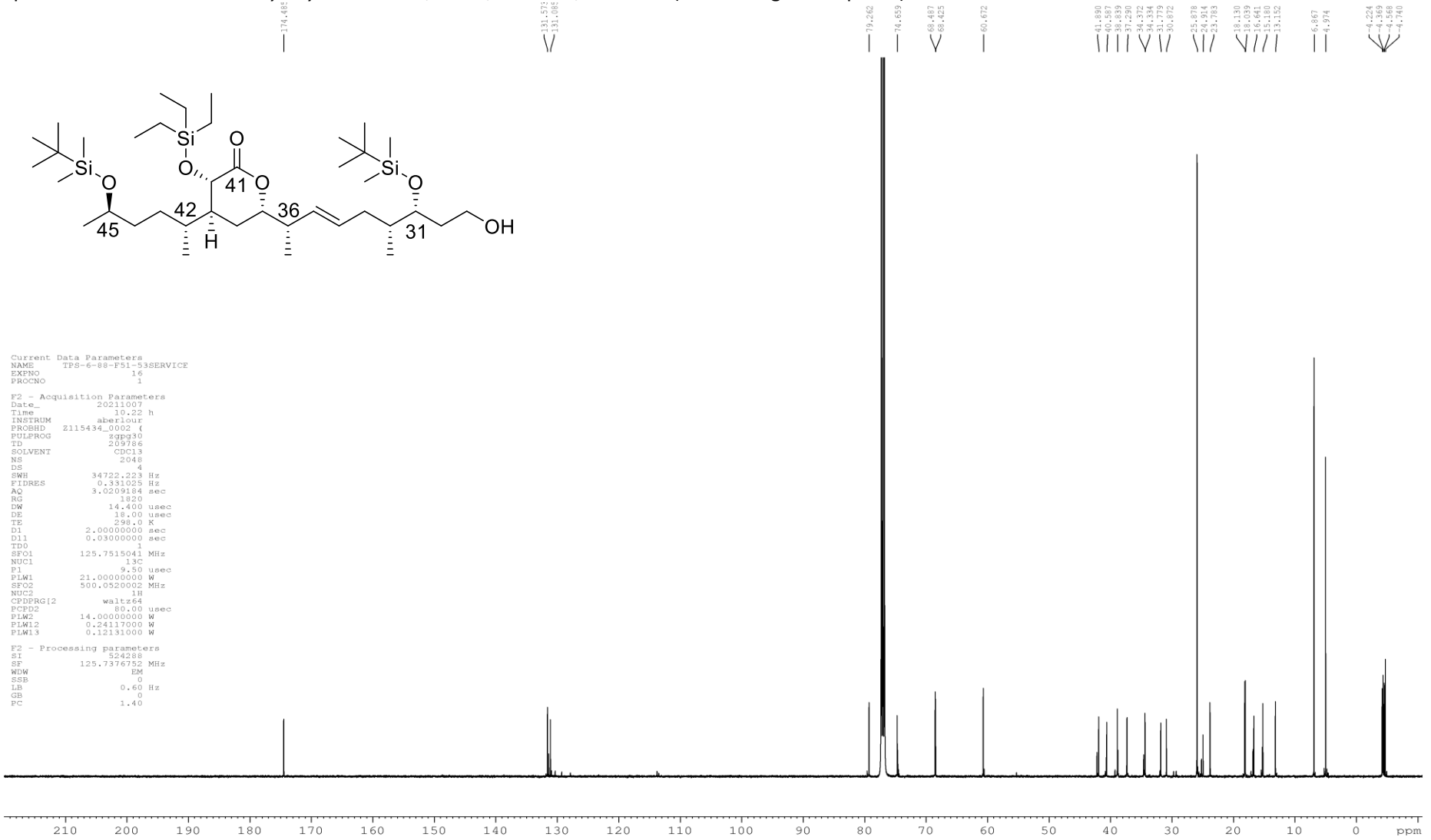

Spectrum 62. Olefin alcohol *syn-syn-syn*-**202c**, $CDCl_3$, ^1H NMR, 500 MHz

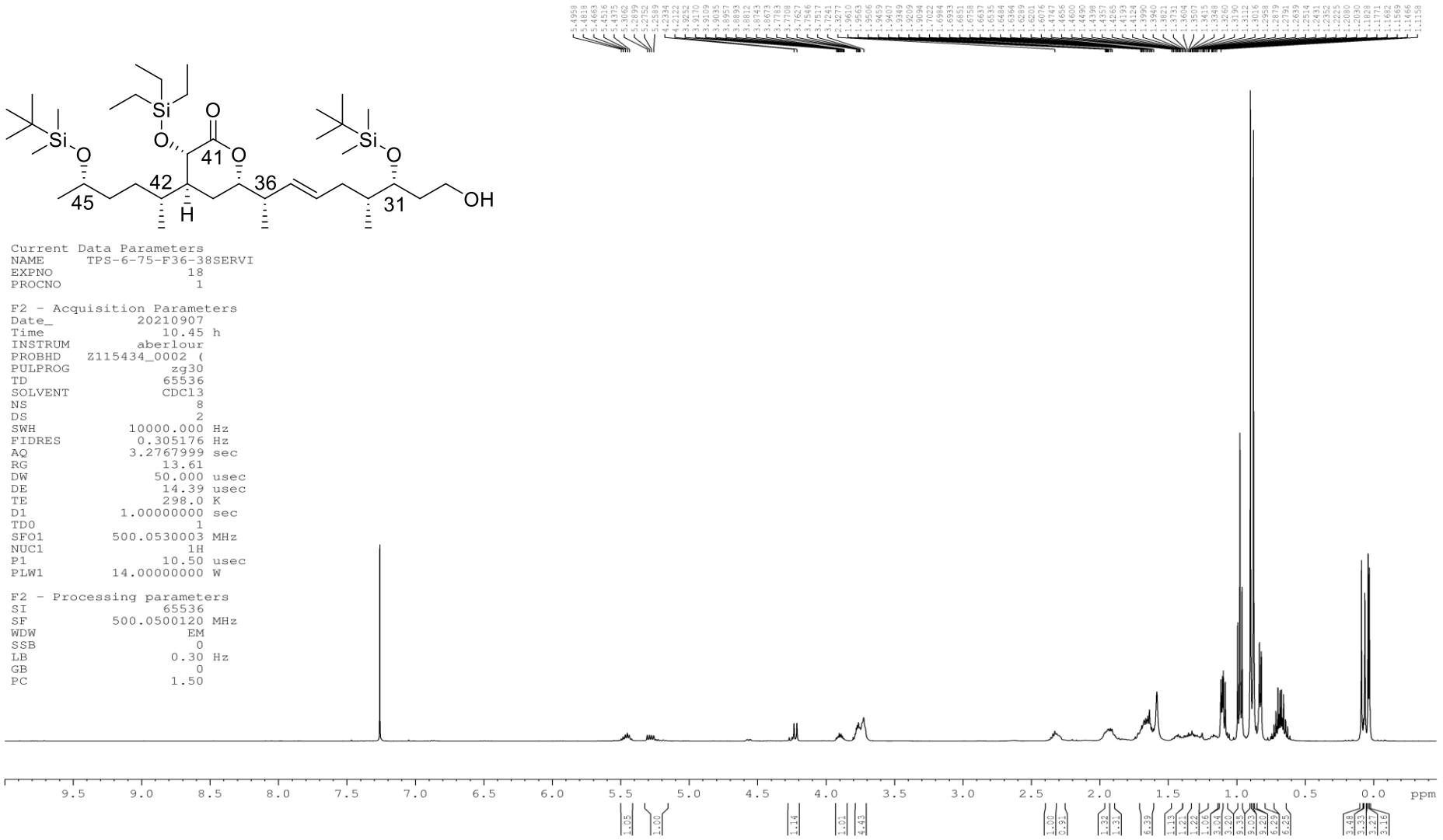

Spectrum 63. Olefin alcohol *syn-syn-syn*-**202c**, $CDCl_3$, ^{13}C NMR, 125 MHz (*not listing minor peaks)

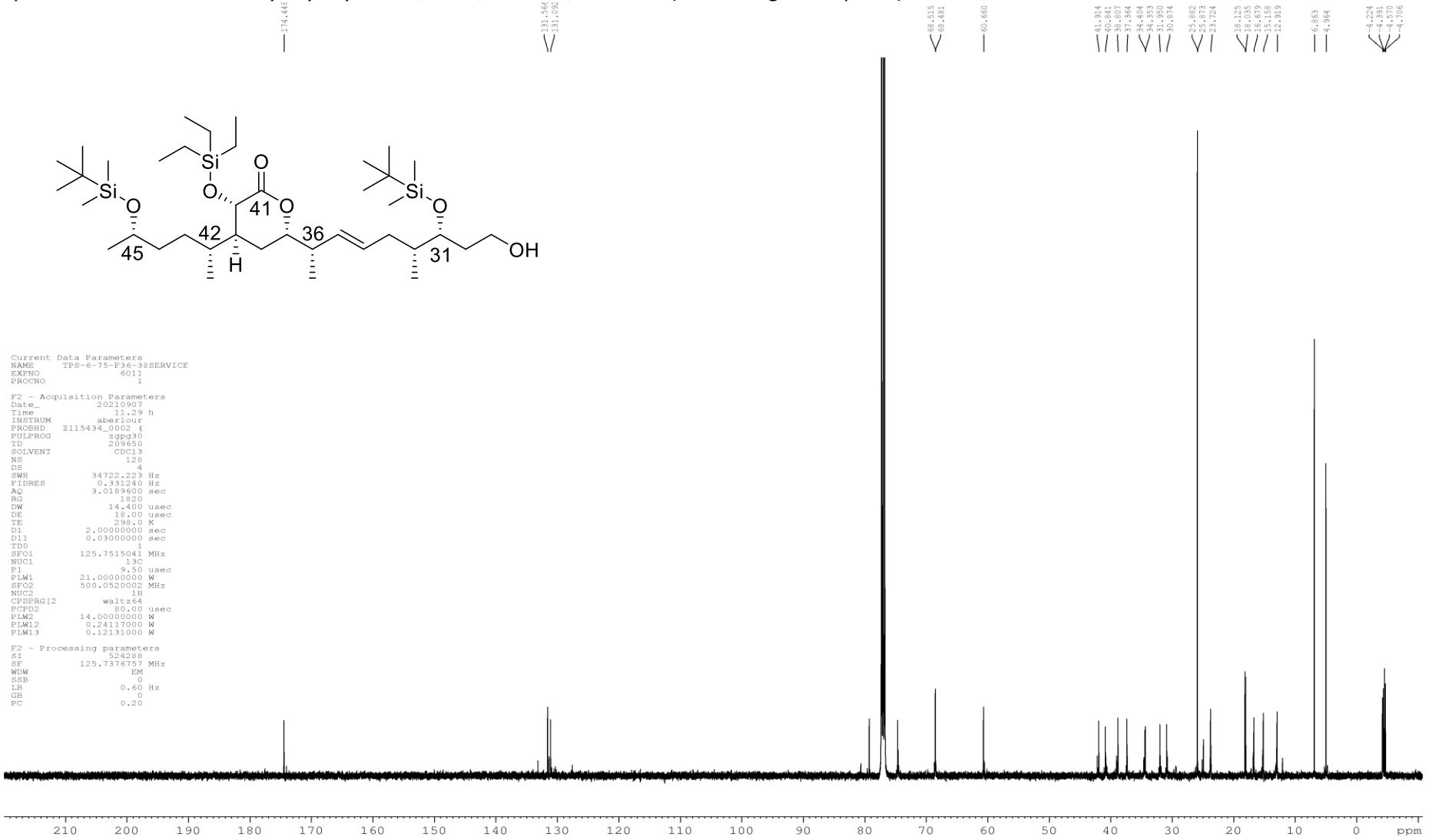

Spectrum 64. Dimer diol **203a**, $CDCl_3$, ^1H NMR, 500 MHz

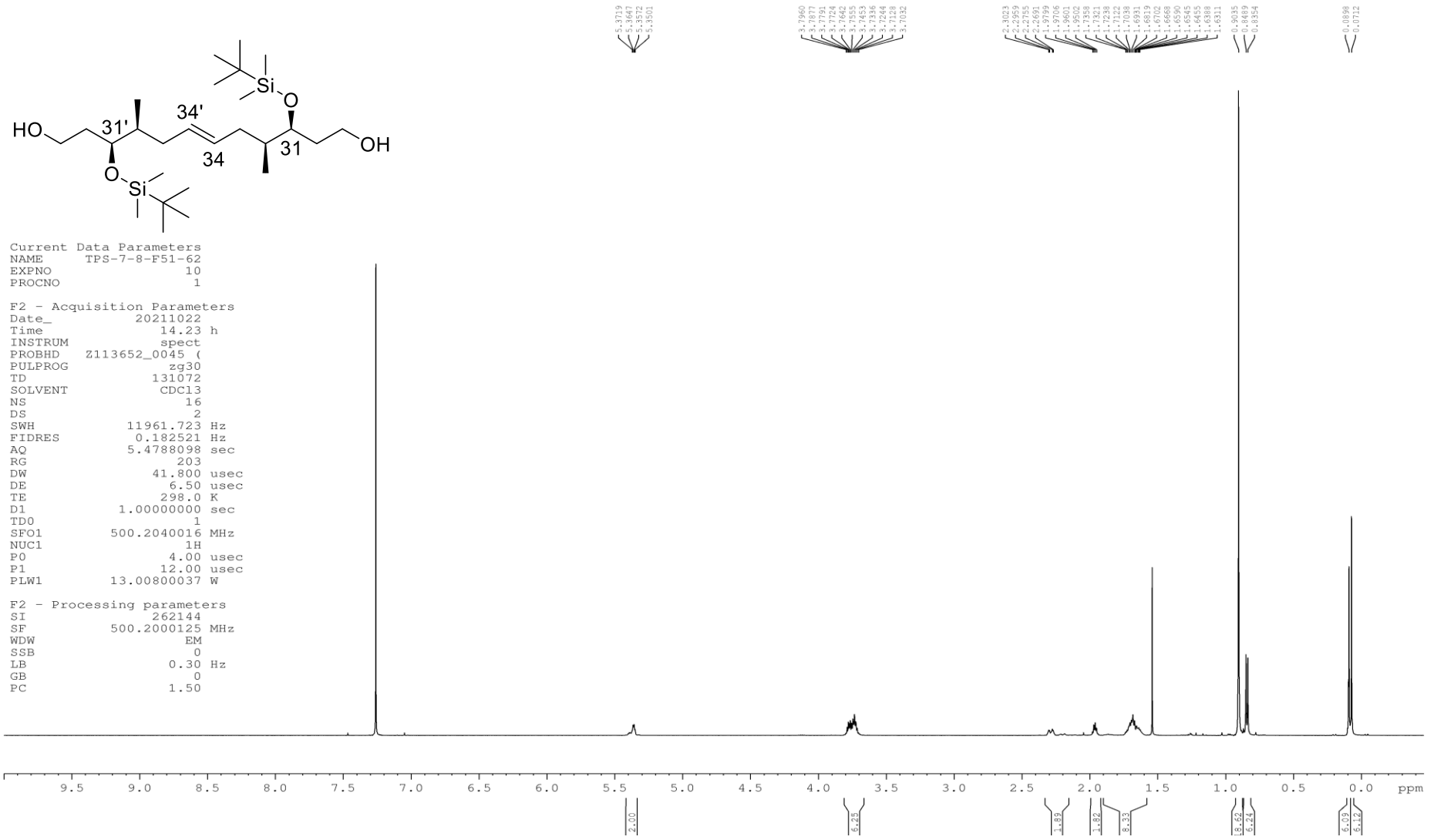

Spectrum 65. Tetraol *syn-anti-anti*-**204a**, $CDCl_3$, ^1H NMR, 500 MHz

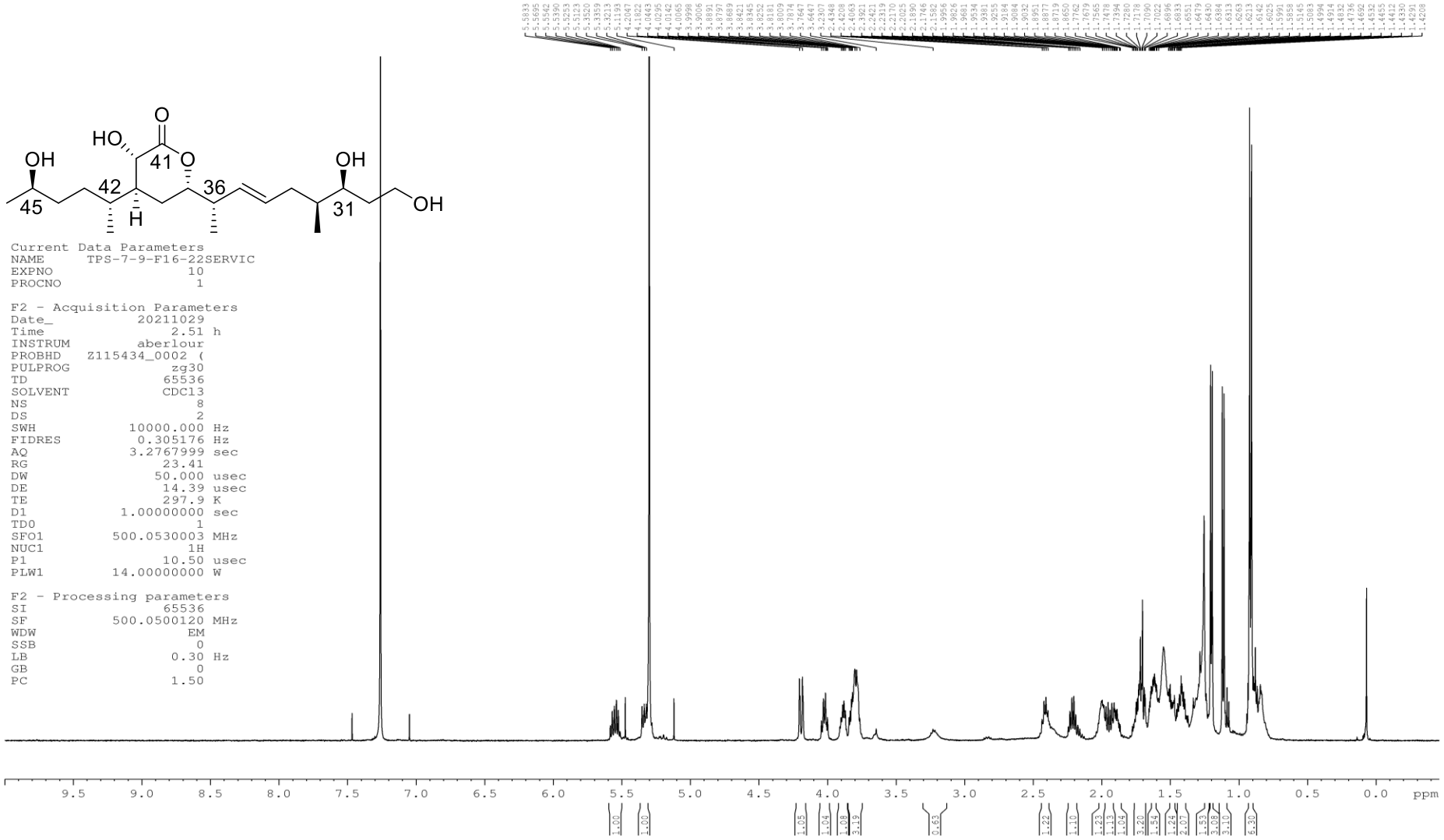

Spectrum 66. Tetraol *syn-anti-anti*-**204a**, $CDCl_3$, ^{13}C NMR, 125 MHz

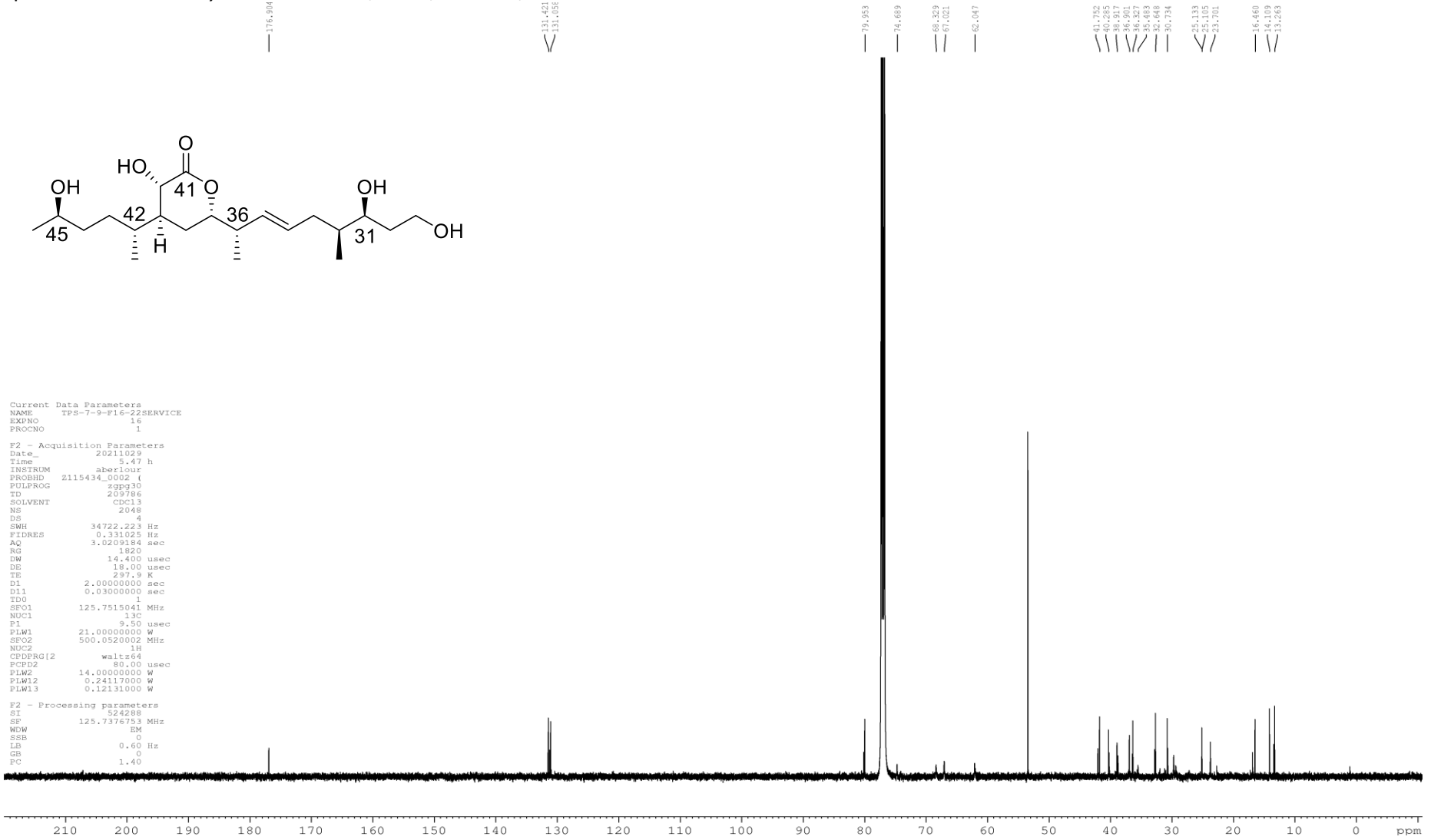

Spectrum 67. Tetraol *syn-syn-anti*-**204b**, $CDCl_3$, ^1H NMR, 500 MHz

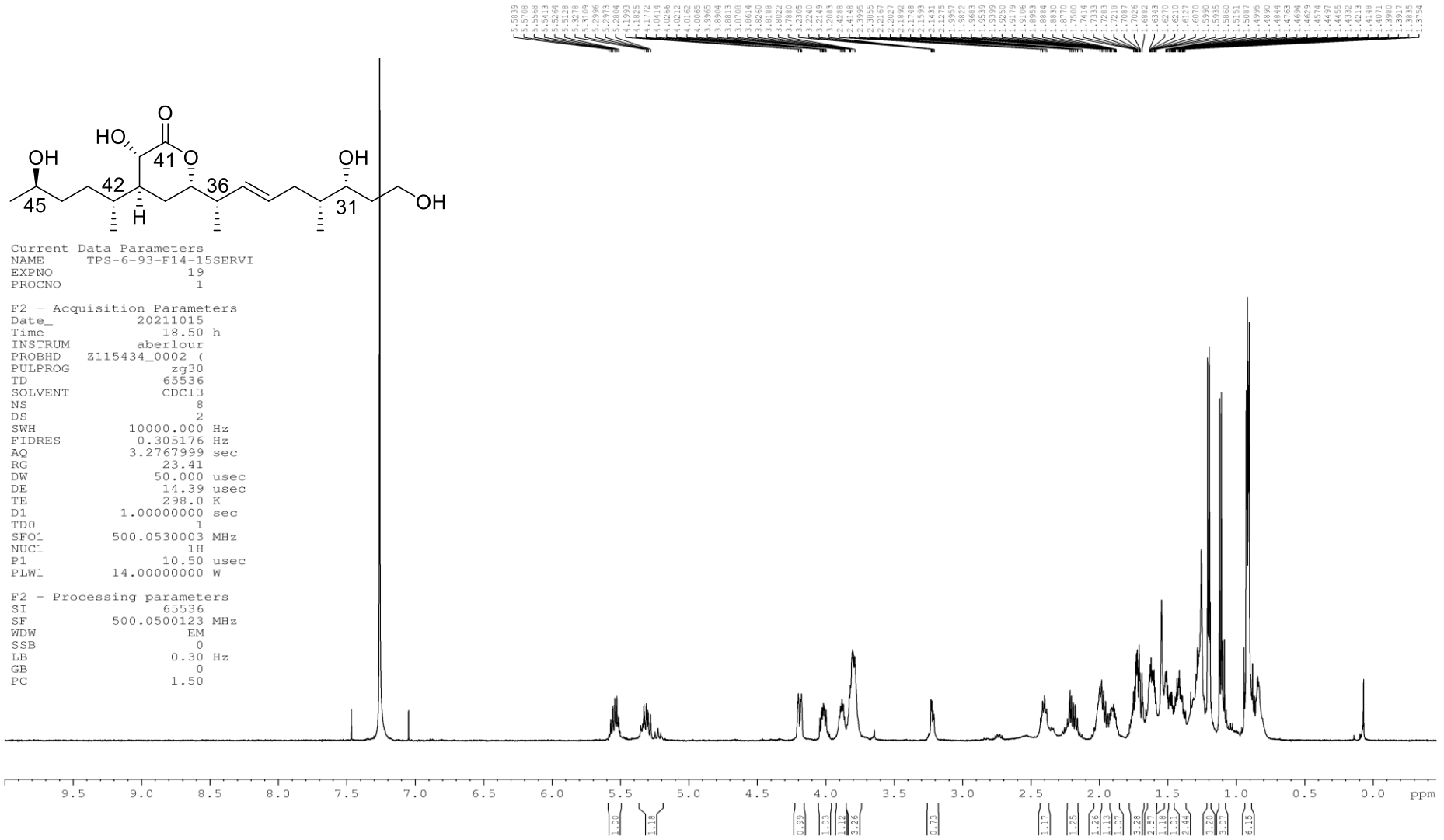

Spectrum 68. Tetraol *syn-syn-anti*-**204b**, $CDCl_3$, ^{13}C NMR, 125 MHz

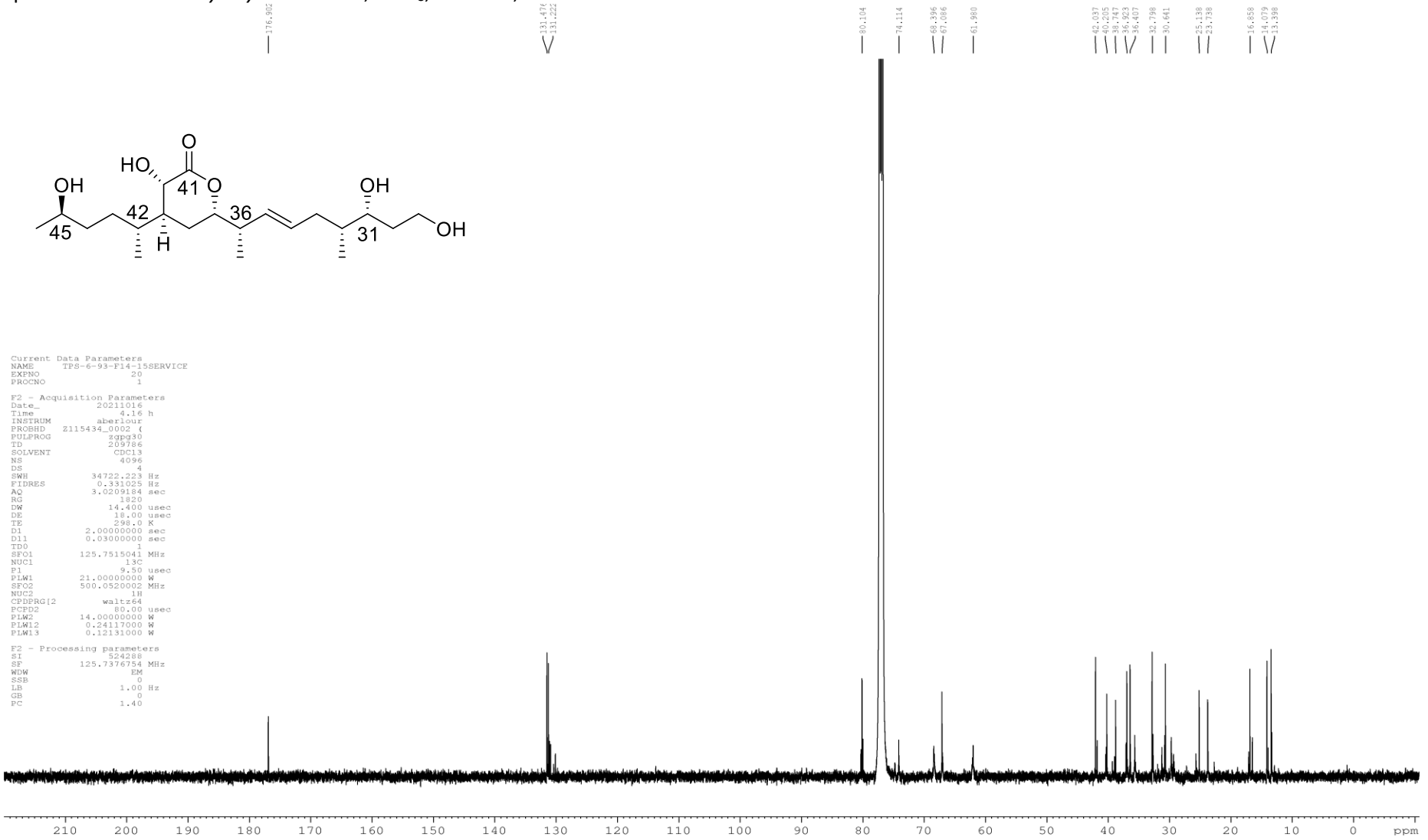

Spectrum 69. Tetraol *syn-syn-syn*-**204c**, $CDCl_3$, ^1H NMR, 500 MHz

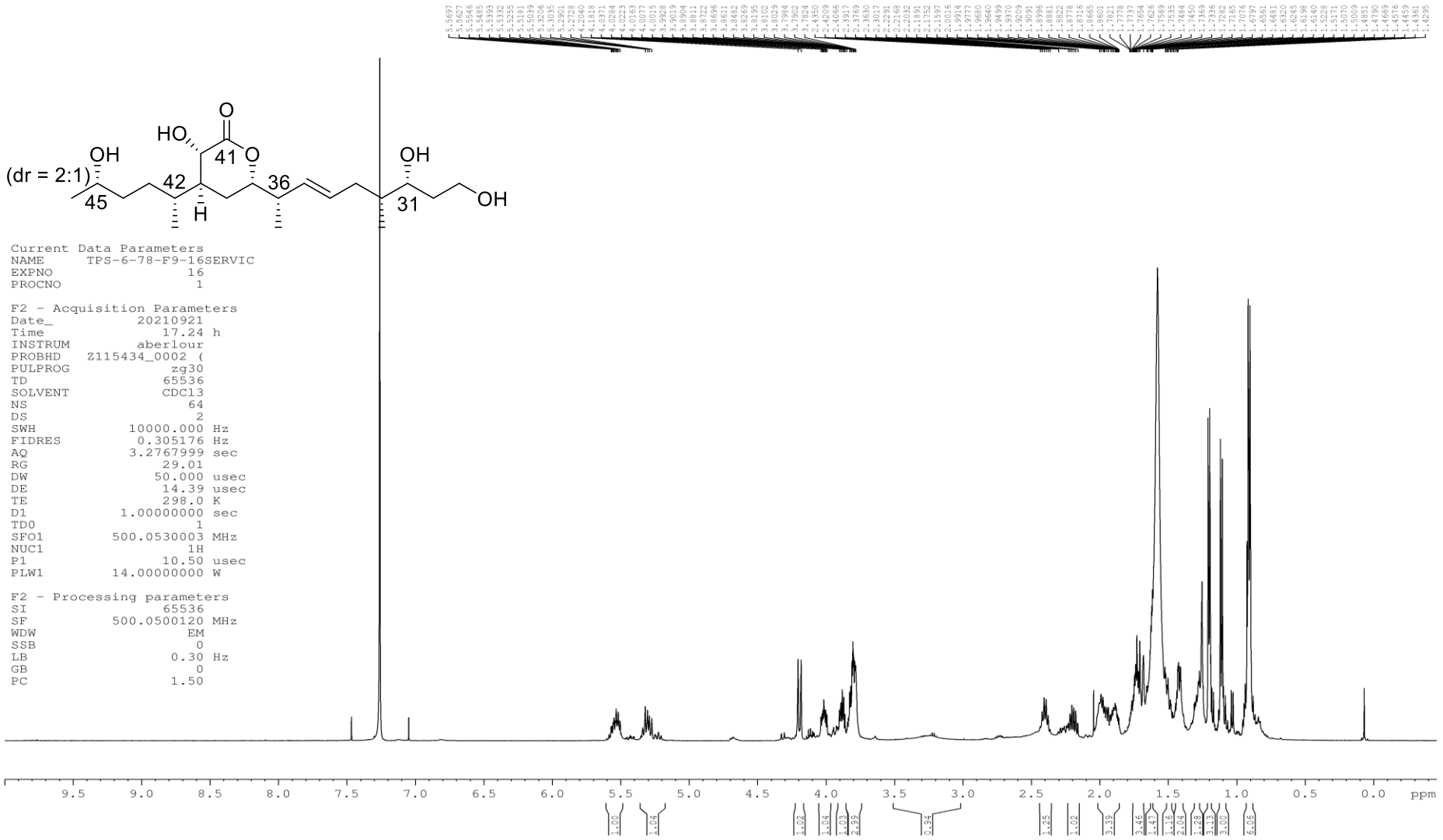

Spectrum 70. Tetraol *syn-syn-syn*-**204c**, $CDCl_3$, ^{13}C NMR, 125 MHz

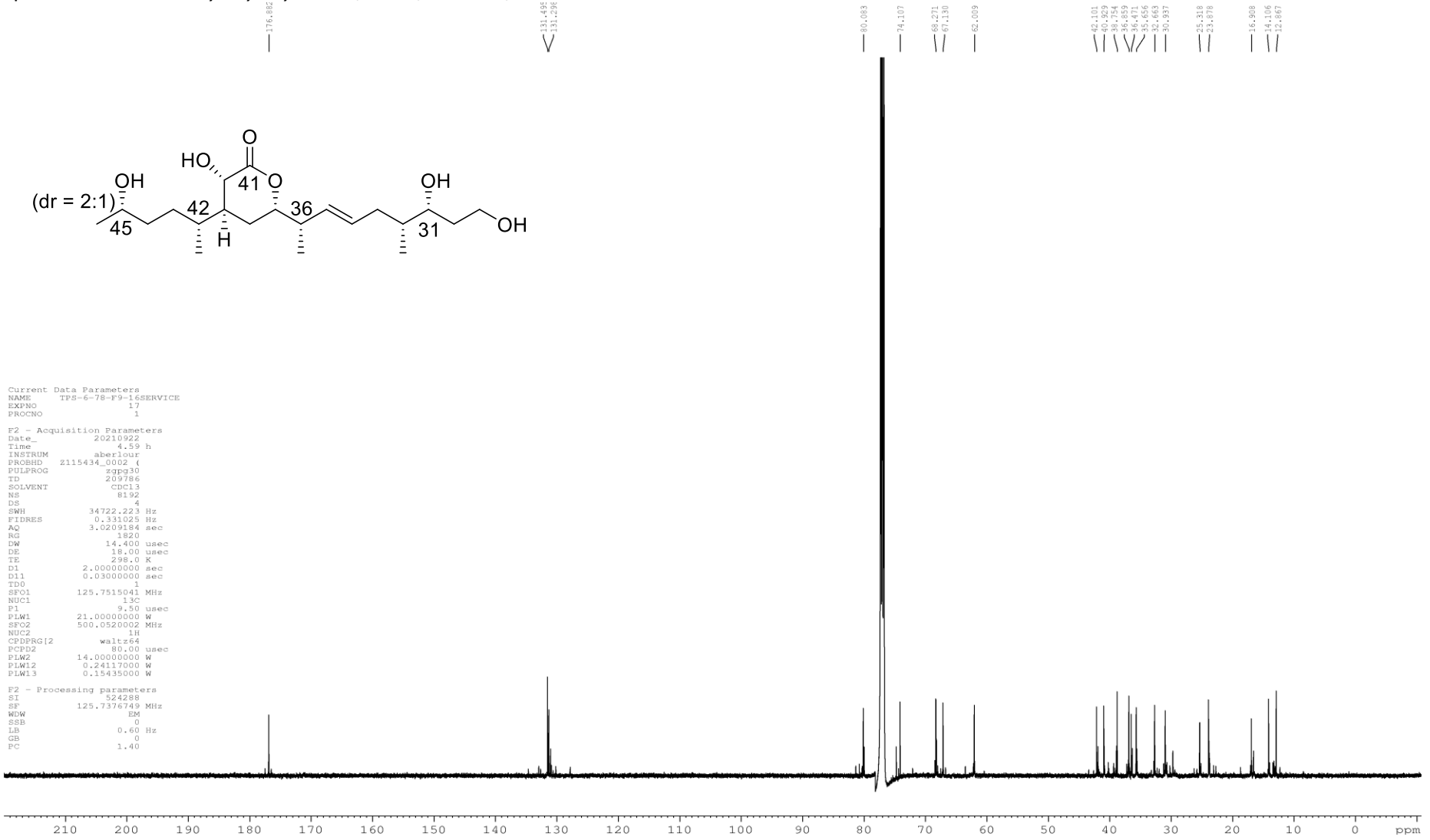

Spectrum 71. Tetraol *syn-anti-anti*-**204a**, CD_3OD, ^1H NMR, 500 MHz

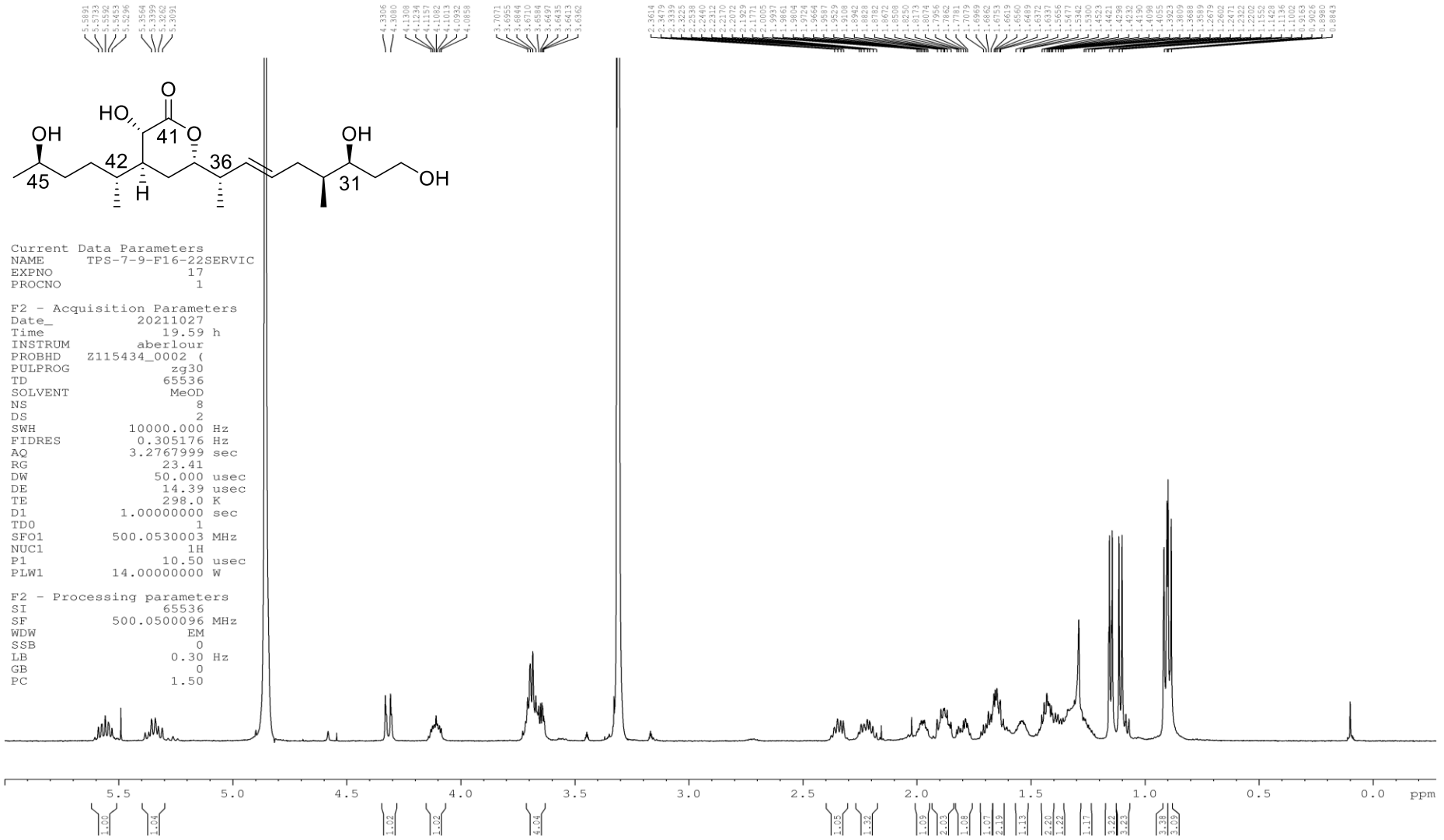

Spectrum 72. Tetraol *syn-anti-anti*-**204a**, CD_3OD, ^{13}C NMR, 125 MHz

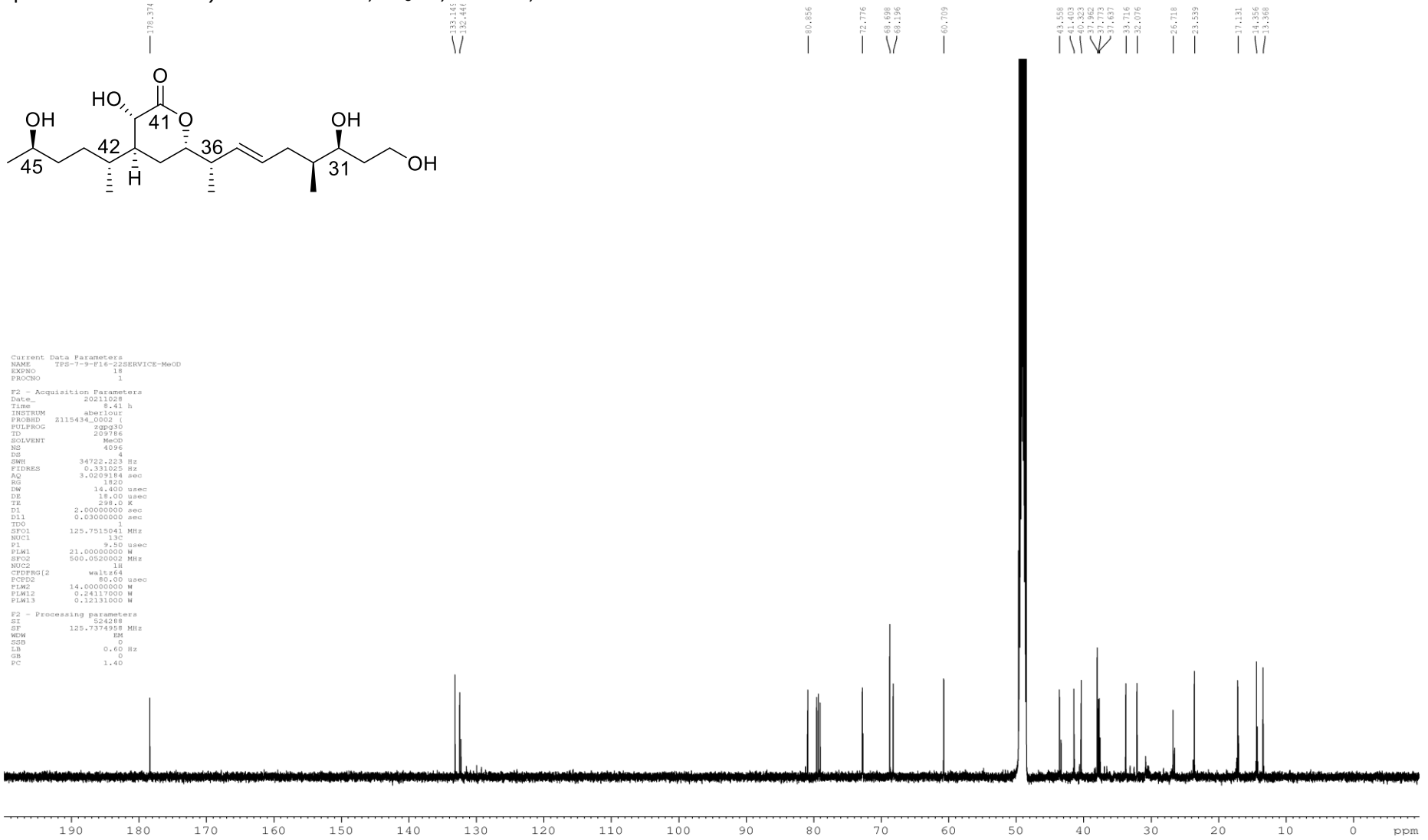

Spectrum 73. Tetraol *syn-syn-anti*-**204b**, CD_3OD, ^1H NMR, ***5***00 MHz

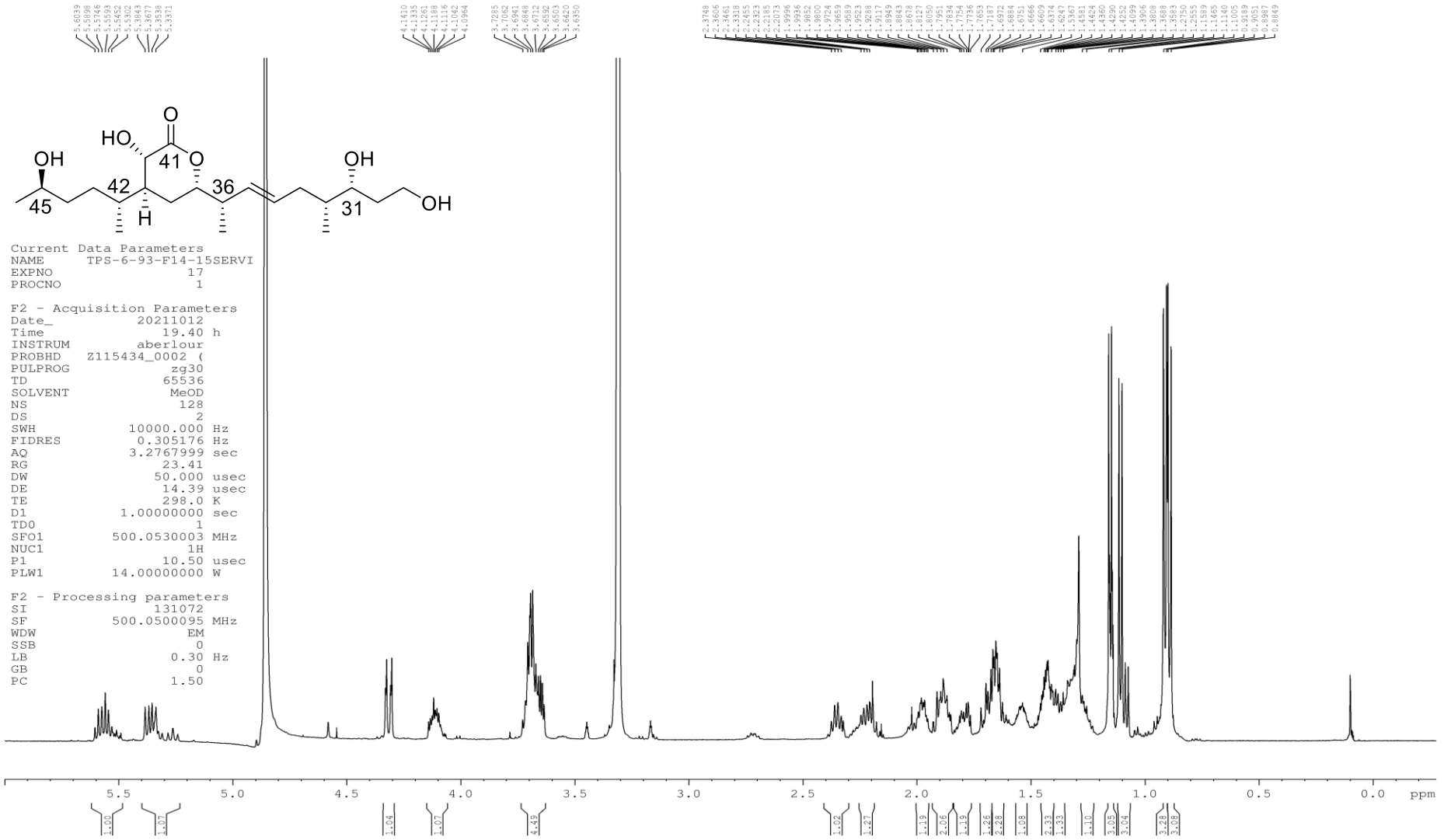

Spectrum 74. Tetraol *syn-syn-anti*-**204b**, CD_3OD, ^{13}C NMR, 125 MHz

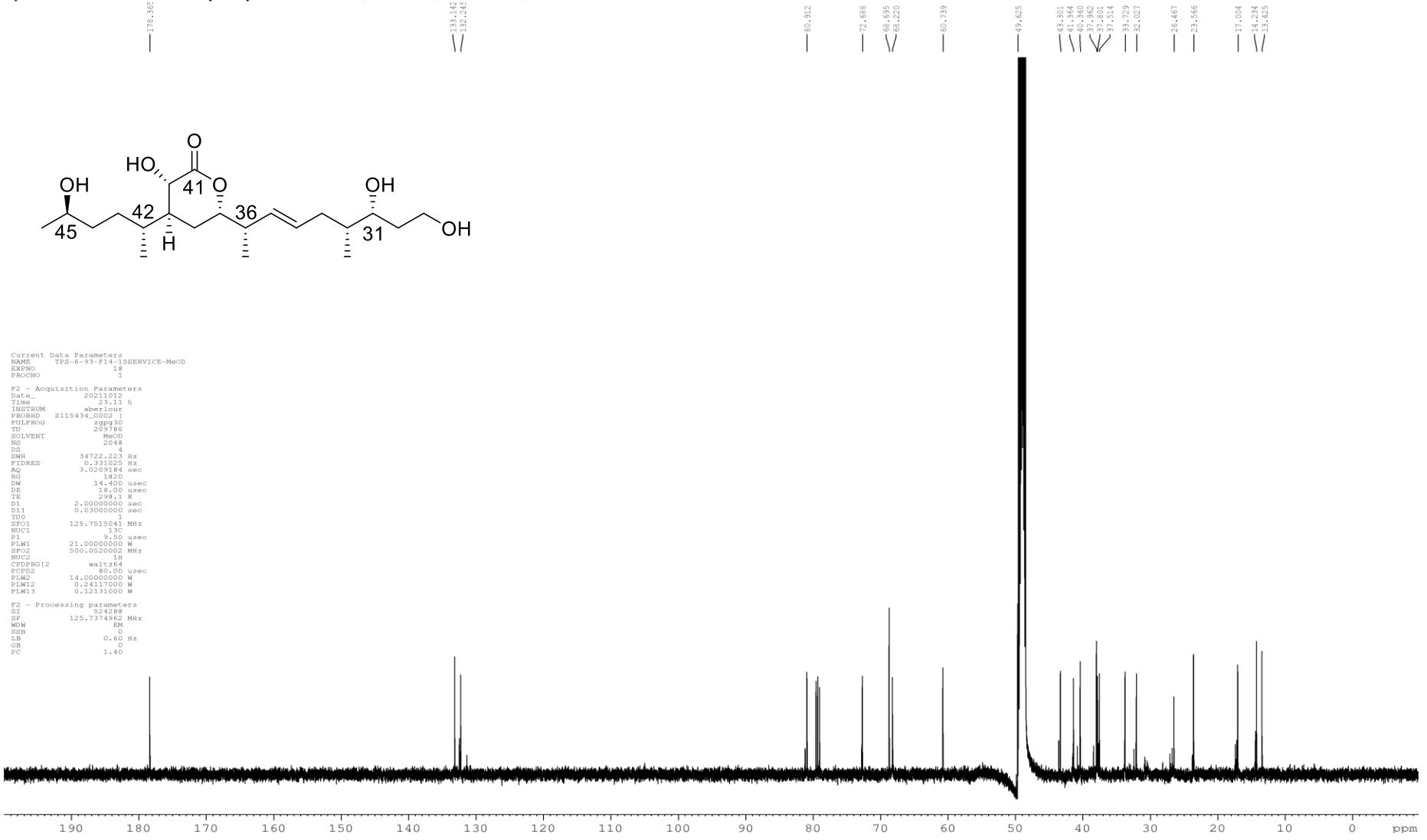

Spectrum 75. Tetraol *syn-syn-syn*-**204c**, CD_3OD, ^1H NMR, ***5***00 MHz

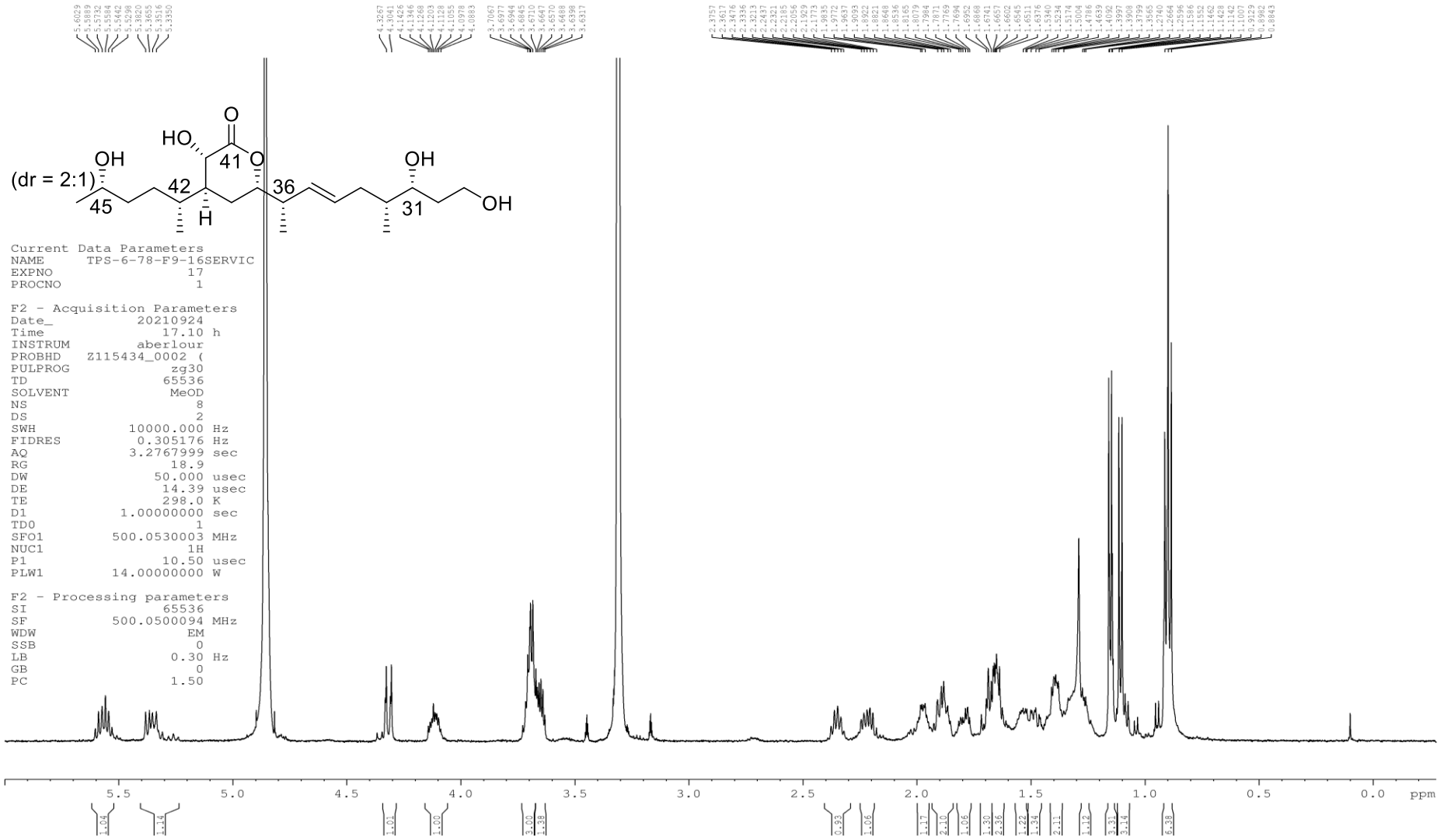

Spectrum 76. Tetraol *syn-syn-syn*-**204c**, CD_3OD, ^{13}C NMR, 125 MHz

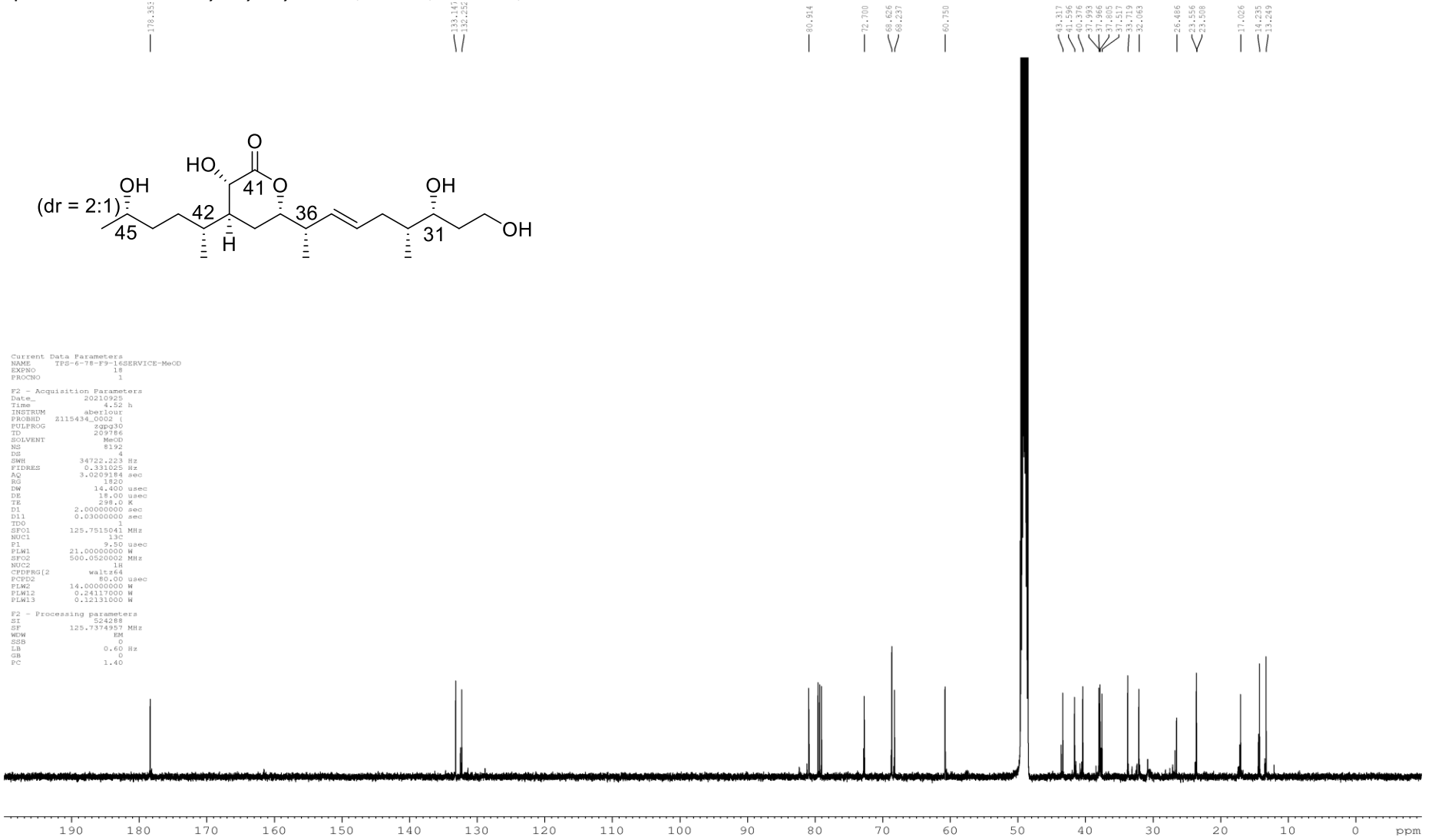

Spectrum 77. Aldehyde *syn-anti-anti*-**131**, $CDCl_3$, ^1H NMR, ***5***00 MHz

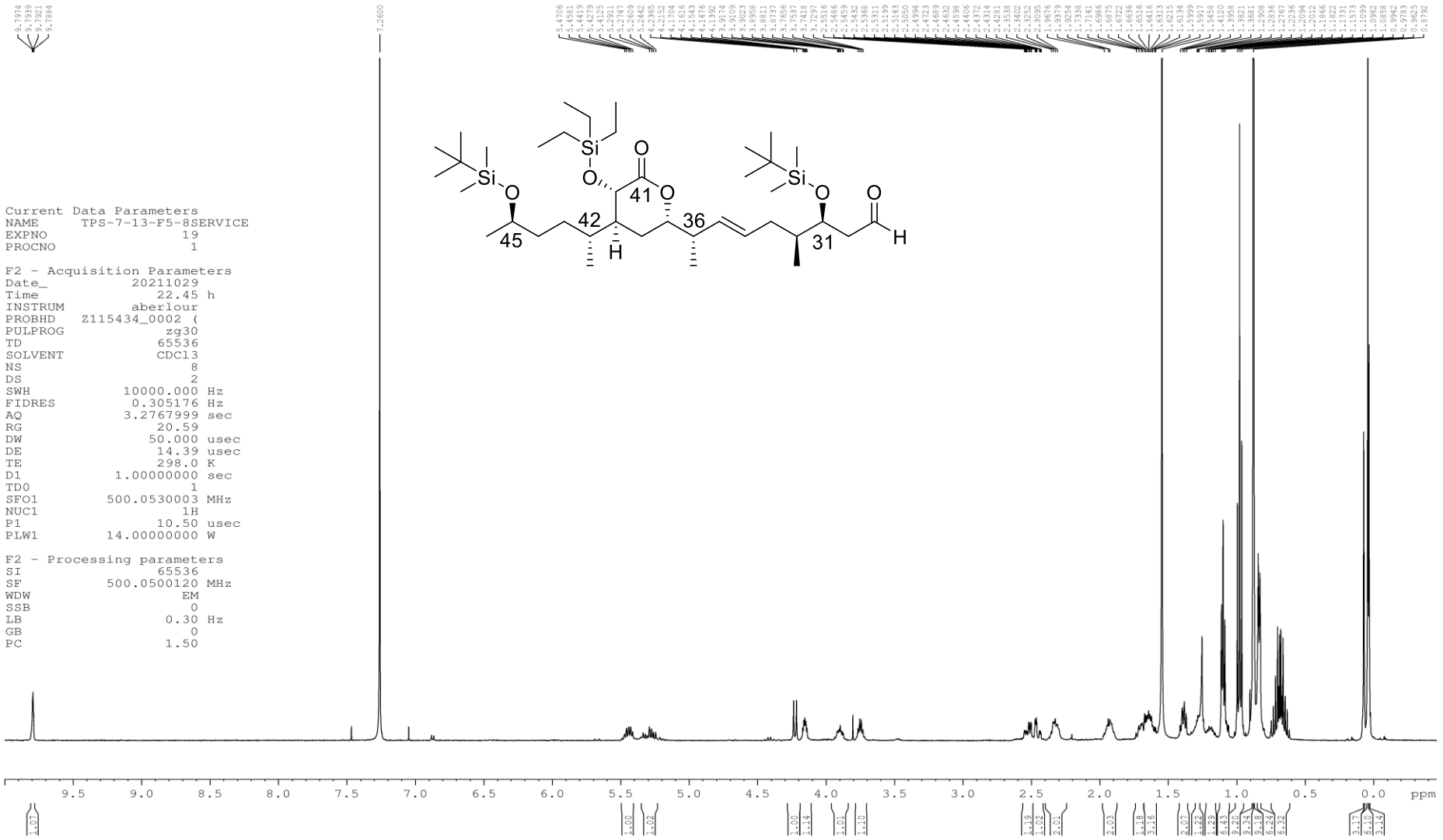

Spectrum 78. Aldehyde *syn-anti-anti*-**131**, $CDCl_3$, ^{13}C NMR, 125 MHz

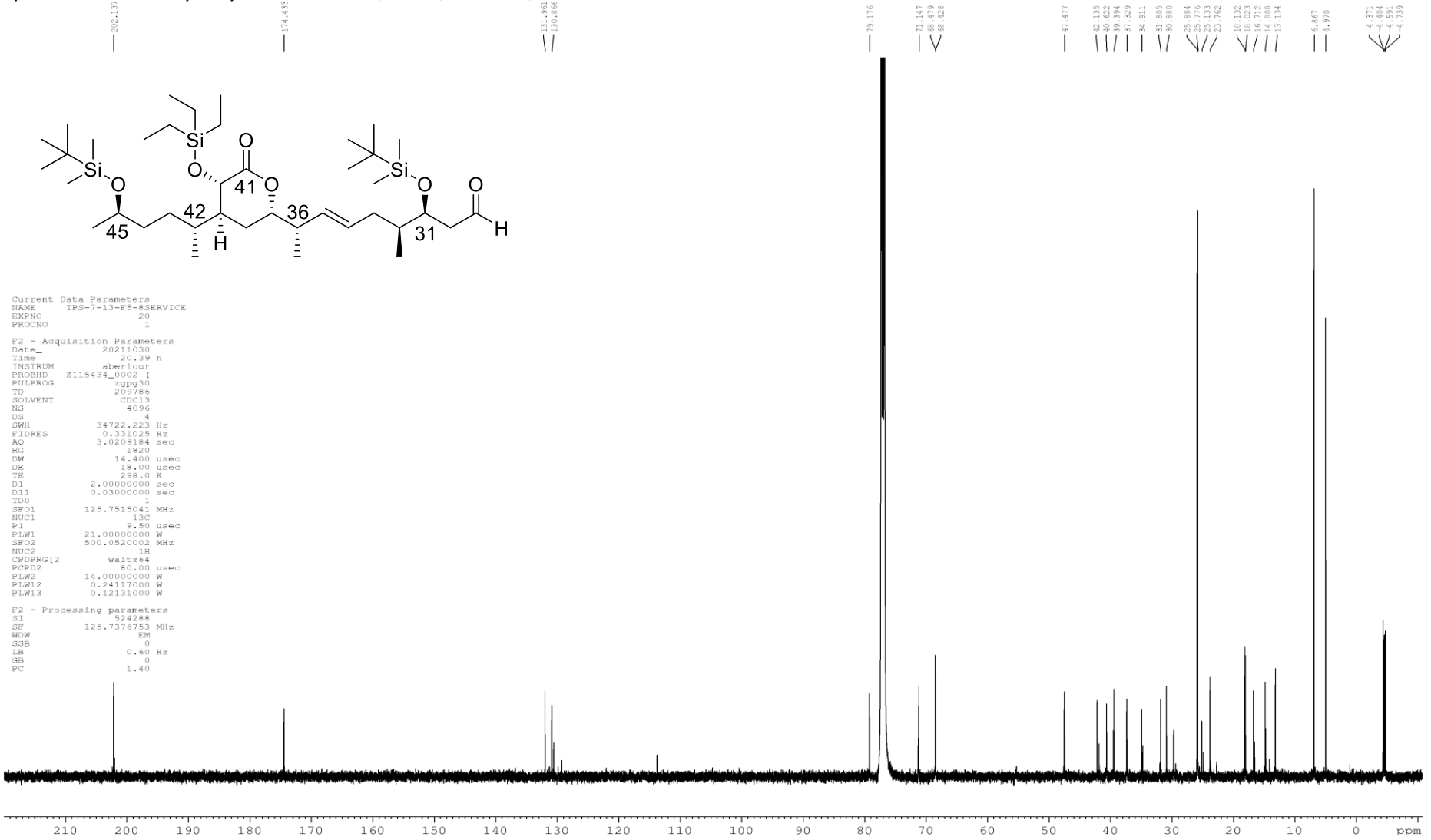

References

(1) Carletti, I.; Debitus, C.; Massiot, G. Molécules Polykétides Comme Agents Anticancéreux. WO2011051380 (A1), 2011.

(2) Masamune, S.; Asrof, A. Sk.; Snitman, D. L.; Garvey, D. S. Highly Stereoselective Aldol Condensation Using an Enantioselective Chiral Enolate. *Angewandte Chemie International Edition in English* **1980**, *19* (7), 557–558. https://doi.org/10.1002/anie.198005571.

(3) van Wyk, B.; Wink, M. *Medicinal Plants of the World*; Briza Publications: Pretoria, South Africa, 2004.

(4) Robinson, M. M.; Zhang, X. *Traditional Medicines: Global Situation, Issues and Challenges*; 2011.

(5) Newman, D. J.; Cragg, G. M. Natural Products as Sources of New Drugs from 1981 to 2014. *Journal of Natural Products* **2016**, *79* (3), 629–661. https://doi.org/10.1021/acs.jnatprod.5b01055.

(6) Newman, D. J.; Cragg, G. M. Natural Products as Sources of New Drugs over the Nearly Four Decades from 01/1981 to 09/2019. *Journal of Natural Products* **2020**, *83* (3), 770–803. https://doi.org/10.1021/acs.jnatprod.9b01285.

(7) Mahdi, J. G. Medicinal Potential of Willow: A Chemical Perspective of Aspirin Discovery. *Journal of Saudi Chemical Society* **2010**, *14* (3), 317–322. https://doi.org/https://doi.org/10.1016/j.jscs.2010.04.010.

(8) Ansari, M. T.; Saify, Z. S.; Sultana, N.; Ahmad, I.; Saeed-Ul-Hassan, S.; Khanum, I. T. and M. Malaria and Artemisinin Derivatives: An Updated Review. *Mini-Reviews in Medicinal Chemistry*. 2013, pp 1879–1902. https://doi.org/http://dx.doi.org/10.2174/13895575113136660097.

(9) Ruiz-Torres, V.; Encinar, A. J.; Herranz-López, M.; Pérez-Sánchez, A.; Galiano, V.; Barrajón-Catalán, E.; Micol, V. An Updated Review on Marine Anticancer Compounds: The Use of Virtual Screening for the Discovery of Small-Molecule Cancer Drugs. *Molecules* . 2017. https://doi.org/10.3390/molecules22071037.

(10) Gomes, G. N.; Dasari, R.; Chandra, S.; Kiss, R.; Kornienko, A. Marine Invertebrate Metabolites with Anticancer Activities: Solutions to the "Supply Problem." *Marine Drugs* . 2016. https://doi.org/10.3390/md14050098.

(11) Sarkar, S.; Pramanik, A.; Mitra, A.; Mukherjee, J. Bioprocessing Data for the Production of Marine Enzymes. *Marine Drugs* . 2010. https://doi.org/10.3390/md8041323.

(12) Williams, D. H.; Stone, M. J.; Hauck, P. R.; Rahman, S. K. Why Are Secondary Metabolites (Natural Products) Biosynthesized? *Journal of Natural Products* **1989**, *52* (6), 1189–1208. https://doi.org/10.1021/np50066a001.

(13) Firn, R. D.; Jones, C. G. Natural Products - a Simple Model to Explain Chemical Diversity. *Natural Product Reports* **2003**, *20* (4), 382–391. https://doi.org/10.1039/B208815K.

(14) Paul, V. J.; Puglisi, M. P. Chemical Mediation of Interactions among Marine Organisms. *Natural Product Reports* **2004**, *21* (1), 189–209. https://doi.org/10.1039/B302334F.

(15) Paul, V. J.; Puglisi, M. P.; Ritson-Williams, R. Marine Chemical Ecology. *Natural Product Reports* **2006**, *23* (2), 153–180. https://doi.org/10.1039/B404735B.

(16) Paul, V. J.; Ritson-Williams, R.; Sharp, K. Marine Chemical Ecology in Benthic Environments. *Natural Product Reports* **2011**, *28* (2), 345–387. https://doi.org/10.1039/C0NP00040J.

(17) Cooper, E. L.; Yao, D. Diving for Drugs: Tunicate Anticancer Compounds. *Drug Discovery Today* **2012**, *17* (11), 636–648. https://doi.org/https://doi.org/10.1016/j.drudis.2012.02.006.

(18) Miller, J. H.; Field, J. J.; Kanakkanthara, A.; Owen, J. G.; Singh, A. J.; Northcote, P. T. Marine Invertebrate Natural Products That Target Microtubules. *Journal of Natural Products* **2018**, *81* (3), 691–702. https://doi.org/10.1021/acs.jnatprod.7b00964.
(19) Hu, Y.; Chen, J.; Hu, G.; Yu, J.; Zhu, X.; Lin, Y.; Chen, S.; Yuan, J. Statistical Research on the Bioactivity of New Marine Natural Products Discovered during the 28 Years from 1985 to 2012. *Marine Drugs* . 2015. https://doi.org/10.3390/md13010202.
(20) Hu, G.-P.; Yuan, J.; Sun, L.; She, Z.-G.; Wu, J.-H.; Lan, X.-J.; Zhu, X.; Lin, Y.-C.; Chen, S.-P. Statistical Research on Marine Natural Products Based on Data Obtained between 1985 and 2008. *Marine Drugs* . 2011. https://doi.org/10.3390/md9040514.
(21) Mayer, M. A.; Rodríguez, D. A.; Taglialatela-Scafati, O.; Fusetani, N. Marine Pharmacology in 2009–2011: Marine Compounds with Antibacterial, Antidiabetic, Antifungal, Anti-Inflammatory, Antiprotozoal, Antituberculosis, and Antiviral Activities; Affecting the Immune and Nervous Systems, and Other Miscellaneous Mechanisms Of . *Marine Drugs* . 2013. https://doi.org/10.3390/md11072510.
(22) Bhatnagar, I.; Kim, S.-K. Marine Antitumor Drugs: Status, Shortfalls and Strategies. *Marine Drugs* . 2010. https://doi.org/10.3390/md8102702.
(23) Hirata, Y.; Uemura, D. Halichondrins - Antitumor Polyether Macrolides from a Marine Sponge. *Pure and Applied Chemistry*. 1986, p 701. https://doi.org/10.1351/pac198658050701.
(24) Leal, M. C.; Madeira, C.; Brandão, C. A.; Puga, J.; Calado, R. Bioprospecting of Marine Invertebrates for New Natural Products — A Chemical and Zoogeographical Perspective. *Molecules* . 2012. https://doi.org/10.3390/molecules17089842.
(25) Aicher, T. D.; Buszek, K. R.; Fang, F. G.; Forsyth, C. J.; Jung, S. H.; Kishi, Y.; Matelich, M. C.; Scola, P. M.; Spero, D. M.; Yoon, S. K. Total Synthesis of Halichondrin B and Norhalichondrin B. *Journal of the American Chemical Society* **1992**, *114* (8), 3162–3164. https://doi.org/10.1021/ja00034a086.
(26) Bai, R. L.; Paull, K. D.; Herald, C. L.; Malspeis, L.; Pettit, G. R.; Hamel, E. Halichondrin B and Homohalichondrin B, Marine Natural Products Binding in the Vinca Domain of Tubulin. Discovery of Tubulin-Based Mechanism of Action by Analysis of Differential Cytotoxicity Data. *Journal of Biological Chemistry* **1991**, *266* (24), 15882–15889.
(27) Kishi, Y.; Fang, F. G.; Forsyth, C. J.; Scola, P. M.; Yoon, S. K. Halichondrins and Related Compounds. 5436238, 1995.
(28) Austad, B. C.; Calkins, T. L.; Chase, C. E.; Fang, F. G.; Horstmann, T. E.; Hu, Y.; Lewis, B. M.; Niu, X.; Noland, T. A.; Orr, J. D.; Schnaderbeck, M. J.; Zhang, H.; Asakawa, N.; Asai, N.; Chiba, H.; Hasebe, T.; Hoshino, Y.; Ishizuka, H.; Kajima, T.; Kayano, A.; Komatsu, Y.; Kubota, M.; Kuroda, H.; Miyazawa, M.; Tagami, K.; Watanabe, T. Commercial Manufacture of Halaven®: Chemoselective Transformations En Route to Structurally Complex Macrocyclic Ketones. *Synlett* **2013**, *24* (3), 333–337. https://doi.org/10.1055/s-0032-1318026.
(29) Yahata, K.; Ye, N.; Ai, Y.; Iso, K.; Kishi, Y. Unified, Efficient, and Scalable Synthesis of Halichondrins: Zirconium/Nickel-Mediated One-Pot Ketone Synthesis as the Final Coupling Reaction. *Angewandte Chemie International Edition* **2017**, *56* (36), 10796–10800. https://doi.org/https://doi.org/10.1002/anie.201705523.
(30) Kawano, S.; Ito, K.; Yahata, K.; Kira, K.; Abe, T.; Akagi, T.; Asano, M.; Iso, K.; Sato, Y.; Matsuura, F.; Ohashi, I.; Matsumoto, Y.; Isomura, M.; Sasaki, T.; Fukuyama, T.; Miyashita, Y.; Kaburagi, Y.; Yokoi, A.; Asano, O.; Owa, T.; Kishi, Y. A Landmark in Drug Discovery Based on Complex Natural Product Synthesis. *Scientific Reports* **2019**, *9* (1), 8656. https://doi.org/10.1038/s41598-019-45001-9.
(31) Martín, M. J.; Coello, L.; Fernández, R.; Reyes, F.; Rodríguez, A.; Murcia, C.; Garranzo, M.; Mateo, C.; Sánchez-Sancho, F.; Bueno, S.; de Eguilior, C.; Francesch, A.; Munt, S.; Cuevas, C. Isolation and First Total Synthesis of PM050489 and PM060184, Two New Marine

Anticancer Compounds. *Journal of the American Chemical Society* **2013**, *135* (27), 10164–10171. https://doi.org/10.1021/ja404578u.

(32) Lopez, M. J. M.; Molinero, L. C.; Benitez, J. F. R.; Vicente, A. R.; Garcia-Ibarrola, M. G.; Perez, C. M.; Solloso, A. F.; Sancho, F. S.; Marchante, M. C. C.; Rodriguez, R. F. Antitumoral Dihydropyran-2- One Compounds. U.S. Patent 8324406B220121204, 2012.

(33) Allred, T. K.; Manoni, F.; Harran, P. G. Exploring the Boundaries of "Practical": De Novo Syntheses of Complex Natural Product-Based Drug Candidates. *Chemical Reviews* **2017**, *117* (18), 11994–12051. https://doi.org/10.1021/acs.chemrev.7b00126.

(34) Prota, A. E.; Bargsten, K.; Diaz, J. F.; Marsh, M.; Cuevas, C.; Liniger, M.; Neuhaus, C.; Andreu, J. M.; Altmann, K.-H.; Steinmetz, M. O. A New Tubulin-Binding Site and Pharmacophore for Microtubule-Destabilizing Anticancer Drugs. *Proceedings of the National Academy of Sciences* **2014**, *111* (38), 13817 LP – 13821.

(35) Martínez-Díez, M.; Guillén-Navarro, M. J.; Pera, B.; Bouchet, B. P.; Martínez-Leal, J. F.; Barasoain, I.; Cuevas, C.; Andreu, J. M.; García-Fernández, L. F.; Díaz, J. F.; Avilés, P.; Galmarini, C. M. PM060184, a New Tubulin Binding Agent with Potent Antitumor Activity Including P-Glycoprotein over-Expressing Tumors. *Biochemical Pharmacology* **2014**, *88* (3), 291–302. https://doi.org/https://doi.org/10.1016/j.bcp.2014.01.026.

(36) Aviles, P.; Guillen, M. J.; Lopez-Casas, P. P.; Sarno, F.; Cataluña, O.; Nuñez, P.; Cuevas, C.; Hidalgo, M. 55 Low, Frequent Doses of PM060184 Induce Remarkable in Vivo Antitumor Activity. *European Journal of Cancer* **2014**, *50*, 23. https://doi.org/https://doi.org/10.1016/S0959-8049(14)70181-9.

(37) Hidalgo, M.; Boni, V.; Tolcher, A.; Smith, L.; Cubillo, A.; Rasco, D.; Calvo, E.; Amaya, A.; Ordoñez, E.; Patnaik, A.; Cerda, S.; Coronado, C.; Fudio, S.; Miguel-Lillo, B.; Prados, R.; Ortega, O.; Soto-Matos, A.; Papadopoulos, K. P. 361 Phase I, Open-Label, Dose-Escalating Clinical and Pharmacokinetic Study of the Novel Antimicrotubulin Agent PM060184 Administered over 10 Minutes on Days 1-3 and 15-17 Every 28 Days to Patients with Advanced Malignant Solid Tumors. *European Journal of Cancer* **2015**, *51*, S74. https://doi.org/https://doi.org/10.1016/S0959-8049(16)30224-6.

(38) Pettit, G. R.; Kamano, Y.; Herald, C. L.; Tuinman, A. A.; Boettner, F. E.; Kizu, H.; Schmidt, J. M.; Baczynskyj, L.; Tomer, K. B.; Bontems, R. J. The Isolation and Structure of a Remarkable Marine Animal Antineoplastic Constituent: Dolastatin 10. *Journal of the American Chemical Society* **1987**, *109* (22), 6883–6885. https://doi.org/10.1021/ja00256a070.

(39) Luesch, H.; Moore, R. E.; Paul, V. J.; Mooberry, S. L.; Corbett, T. H. Isolation of Dolastatin 10 from the Marine Cyanobacterium Symploca Species VP642 and Total Stereochemistry and Biological Evaluation of Its Analogue Symplostatin 1. *Journal of Natural Products* **2001**, *64* (7), 907–910. https://doi.org/10.1021/np010049y.

(40) Niclas, E.; Ana, T.; A., S. L.; Hendrik, L.; J., P. V. Caldora Penicillata Gen. Nov., Comb. Nov. (Cyanobacteria), a Pantropical Marine Species with Biomedical Relevance. *Journal of Phycology* **2015**, *51* (4), 670–681. https://doi.org/10.1111/jpy.12309.

(41) Luesch, H.; Harrigan, G. G.; Horgen, G. G. and F. D. The Cyanobacterial Origin of Potent Anticancer Agents Originally Isolated from Sea Hares. *Current Medicinal Chemistry*. 2002, pp 1791–1806. https://doi.org/http://dx.doi.org/10.2174/0929867023369051.

(42) Pettit, G. R.; Singh, S. B.; Hogan, F.; Lloyd-Williams, P.; Herald, D. L.; Burkett, D. D.; Clewlow, P. J. Antineoplastic Agents. Part 189. The Absolute Configuration and Synthesis of Natural (-)-Dolastatin 10. *Journal of the American Chemical Society* **1989**, *111* (14), 5463–5465. https://doi.org/10.1021/ja00196a061.

(43) Bai, R.; Friedman, S. J.; Pettit, G. R.; Hamel, E. Dolastatin 15, a Potent Antimitotic Depsipeptide Derived from Dolabella Auricularia: Interaction with Tubulin and Effects on Cellular Microtubules. *Biochemical Pharmacology* **1992**, *43* (12), 2637–2645. https://doi.org/https://doi.org/10.1016/0006-2952(92)90153-A.

(44) Younes, A.; Yasothan, U.; Kirkpatrick, P. Brentuximab Vedotin. *Nature Reviews Drug Discovery* **2012**, *11*, 19.
(45) Tsugitaka, N.; Junichi, W.; Kenji, O.; Kazuhiko, Y.; Motohiro, K. Tumor-specific Antivascular Effect of TZT-1027 (Soblidotin) Elucidated by Magnetic Resonance Imaging and Confocal Laser Scanning Microscopy. *Cancer Science* **2007**, *98* (4), 598–604. https://doi.org/10.1111/j.1349-7006.2007.00418.x.
(46) Mita, A. C.; Hammond, L. A.; Bonate, P. L.; Weiss, G.; McCreery, H.; Syed, S.; Garrison, M.; Chu, Q. S. C.; DeBono, J. S.; Jones, C. B.; Weitman, S.; Rowinsky, E. K. Phase I and Pharmacokinetic Study of Tasidotin Hydrochloride (ILX651), a Third-Generation Dolastatin-15 Analogue, Administered Weekly for 3 Weeks Every 28 Days in Patients with Advanced Solid Tumors. *Clinical Cancer Research* **2006**, *12* (17), 5207 LP – 5215.
(47) Canta, A.; Cavaletti, A. C. and G. Tubulin: A Target for Antineoplastic Drugs into the Cancer Cells but Also in the Peripheral Nervous System. *Current Medicinal Chemistry*. 2009, pp 1315–1324. https://doi.org/http://dx.doi.org/10.2174/092986709787846488.
(48) Newman, D.; Cragg, G. Drugs and Drug Candidates from Marine Sources: An Assessment of the Current "State of Play." *Planta Medica* **2016**, *82* (09/10), 775–789. https://doi.org/10.1055/s-0042-101353.
(49) Newman, D. J. The "Utility" of Highly Toxic Marine-Sourced Compounds. *Marine Drugs* **2019**, *17* (6), 324. https://doi.org/10.3390/md17060324.
(50) Altmann, K.-H.; Gertsch, J. Anticancer Drugs from Nature-Natural Products as a Unique Source of New Microtubule-Stabilizing Agents. *Natural Product Reports* **2007**, *24* (2), 327–357. https://doi.org/10.1039/B515619J.
(51) Kaur, R.; Kaur, G.; Gill, R. K.; Soni, R.; Bariwal, J. Recent Developments in Tubulin Polymerization Inhibitors: An Overview. *European Journal of Medicinal Chemistry* **2014**, *87*, 89–124. https://doi.org/https://doi.org/10.1016/j.ejmech.2014.09.051.
(52) Mukhtar, E.; Adhami, V. M.; Mukhtar, H. Targeting Microtubules by Natural Agents for Cancer Therapy. *Molecular Cancer Therapeutics* **2014**, *13* (2), 275 LP – 284.
(53) Bhalla, K. N. Microtubule-Targeted Anticancer Agents and Apoptosis. *Oncogene* **2003**, *22*, 9075.
(54) Fleury, E.; Lannou, M.-I.; Bistri, O.; Sautel, F.; Massiot, G.; Pancrazi, A.; Ardisson, J. Relative Stereochemical Determination and Synthesis of the C1−C17 Fragment of a New Natural Polyketide. *The Journal of Organic Chemistry* **2009**, *74* (18), 7034–7045. https://doi.org/10.1021/jo9012833.
(55) Smith, S. G.; Goodman, J. M. Assigning Stereochemistry to Single Diastereoisomers by GIAO NMR Calculation: The DP4 Probability. *Journal of the American Chemical Society* **2010**, *132* (37), 12946–12959. https://doi.org/10.1021/ja105035r.
(56) Fleury, E.; Sorin, G.; Prost, E.; Pancrazi, A.; Sautel, F.; Massiot, G.; Lannou, M.-I.; Ardisson, J. Relative Stereochemical Determination and Synthesis of the C17–C25 δ-Lactone Fragment of Hemicalide. *The Journal of Organic Chemistry* **2013**, *78* (3), 855–864. https://doi.org/10.1021/jo302440a.
(57) Sorin, G.; Fleury, E.; Tran, C.; Prost, E.; Molinier, N.; Sautel, F.; Massiot, G.; Specklin, S.; Meyer, C.; Cossy, J.; Lannou, M.-I.; Ardisson, J. Synthetic Studies on Hemicalide: Development of a Convergent Approach toward the C1–C25 Fragment. *Organic Letters* **2013**, *15* (18), 4734–4737. https://doi.org/10.1021/ol402077e.
(58) Ewoud, D. G.; Wouter, H.; Simon, S.; Christophe, M.; Janine, C.; Patrick, B. Strength by Joining Methods: Combining Synthesis with NMR, IR, and Vibrational Circular Dichroism Spectroscopy for the Determination of the Relative Configuration in Hemicalide. *Chemistry – A European Journal* **2014**, *20* (52), 17385–17394. https://doi.org/10.1002/chem.201404822.
(59) Specklin, S.; Boissonnat, G.; Lecourt, C.; Sorin, G.; Lannou, M.-I.; Ardisson, J.; Sautel, F.; Massiot, G.; Meyer, C.; Cossy, J. Synthetic Studies toward the C32–C46 Segment of

Hemicalide. Assignment of the Relative Configuration of the C36–C42 Subunit. *Organic Letters* **2015**, *17* (10), 2446–2449. https://doi.org/10.1021/acs.orglett.5b00955.
(60) MacGregor, C. I.; Han, B. Y.; Goodman, J. M.; Paterson, I. Toward the Stereochemical Assignment and Synthesis of Hemicalide: DP4f GIAO-NMR Analysis and Synthesis of a Reassigned C16-C28 Subunit. *Chemical Communications* **2016**, *52* (25), 4632–4635. https://doi.org/10.1039/C6CC01074A.
(61) Lecourt, C.; Boinapally, S.; Dhambri, S.; Boissonnat, G.; Meyer, C.; Cossy, J.; Sautel, F.; Massiot, G.; Ardisson, J.; Sorin, G.; Lannou, M.-I. Elaboration of Sterically Hindered δ-Lactones through Ring-Closing Metathesis: Application to the Synthesis of the C1–C27 Fragment of Hemicalide. *The Journal of Organic Chemistry* **2016**, *81* (24), 12275–12290. https://doi.org/10.1021/acs.joc.6b02208.
(62) Han, B. Y.; Lam, N. Y. S.; MacGregor, C. I.; Goodman, J. M.; Paterson, I. A Synthesis-Enabled Relative Stereochemical Assignment of the C1-C28 Region of Hemicalide. *Chemical Communications* **2018**, *54* (26), 3247–3250. https://doi.org/10.1039/C8CC00933C.
(63) Hoffmann, R. W.; Weidmann, U. Threo/Erythro-Assignment of 1,3-diol Derivatives Based on 13C NMR Spectra. *Chemische Berichte* **1985**, *118* (10), 3980–3992. https://doi.org/10.1002/cber.19851181011.
(64) Evans, D. A.; Clark, J. S.; Metternich, R.; Novack, V. J.; Sheppard, G. S. Diastereoselective Aldol Reactions Using .Beta.-Keto Imide Derived Enolates. A Versatile Approach to the Assemblage of Polypropionate Systems. *Journal of the American Chemical Society* **1990**, *112* (2), 866–868. https://doi.org/10.1021/ja00158a056.
(65) Evans, D. A.; Ng, H. P.; Clark, J. S.; Rieger, D. L. Diastereoselective Anti Aldol Reactions of Chiral Ethyl Ketones. Enantioselective Processes for the Synthesis of Polypropionate Natural Products. *Tetrahedron* **1992**, *48* (11), 2127–2142. https://doi.org/https://doi.org/10.1016/S0040-4020(01)88879-7.
(66) Paterson, I. New Methods and Strategies for the Stereocontrolled Synthesis of Polypropionate-Derived Natural Products. *Pure and Applied Chemistry* **1992**, *64* (12), 1821–1830. https://doi.org/doi:10.1351/pac199264121821.
(67) Paterson, I.; Roger, D. N.; Richard, A. W.; Romea, P.; Anne Lister, M. Studies in Macrolide Synthesis: A Stereocontrolled Synthesis of Oleandolide Employing Reagent-and Substrate-Controlled Aldol Reactions of (S)-1-(Benzyloxy)-2-Methylpentan-3-One. *Journal of the American Chemical Society* **1994**, *116* (25), 11287–11314. https://doi.org/10.1021/ja00104a010.
(68) Lam, N. Y. S.; Stockdale, T. P.; Anketell, M. J.; Paterson, I. Conquering Peaks and Illuminating Depths: Developing Stereocontrolled Organic Reactions to Unlock Nature's Macrolide Treasure Trove. *Chemical Communications* **2021**, *57* (26), 3171–3189. https://doi.org/10.1039/D1CC00442E.
(69) Omura, Kanji.; Sharma, A. K.; Swern, Daniel. Dimethyl Sulfoxide-Trifluoroacetic Anhydride. New Reagent for Oxidation of Alcohols to Carbonyls. *The Journal of Organic Chemistry* **1976**, *41* (6), 957–962. https://doi.org/10.1021/jo00868a012.
(70) Huang, S. L.; Omura, K.; Swern, D. Oxidation of Sterically Hindered Alcohols to Carbonyls with Dimethyl Sulfoxide-Trifluoracetic Anhydride. *The Journal of Organic Chemistry* **1976**, *41* (20), 3329–3331. https://doi.org/10.1021/jo00882a030.
(71) Mancuso, A. J.; Huang, S.-L.; Swern, D. Oxidation of Long-Chain and Related Alcohols to Carbonyls by Dimethyl Sulfoxide "Activated" by Oxalyl Chloride. *The Journal of Organic Chemistry* **1978**, *43* (12), 2480–2482. https://doi.org/10.1021/jo00406a041.
(72) Omura, K.; Swern, D. Oxidation of Alcohols by "Activated" Dimethyl Sulfoxide. a Preparative, Steric and Mechanistic Study. *Tetrahedron* **1978**, *34* (11), 1651–1660. https://doi.org/https://doi.org/10.1016/0040-4020(78)80197-5.

(73) Goodman, J. M.; Paterson, I. Enolisation of Ketones by Dialkylboron Chlorides and Trifiates: A Model for the Effect of Reagent Leaving Group Substrate Structure and Amine Base. *Tetrahedron Letters* **1992**, *33* (47), 7223–7226. https://doi.org/https://doi.org/10.1016/S0040-4039(00)60878-X.

(74) Paterson, I. Polyketide Synthesis Using the Boron-Mediated, Anti-Aldol Reactions of Lactate-Derived Ketones: Total Synthesis of (-)-ACRL Toxin IIIB. *Synthesis* **1998**, 639–652. https://doi.org/10.1055/s-1998-5929.

(75) Paterson, I.; Doughty, V. A. Anti-Aldol Reactions of Lactate-Derived Ketones. Application to the Synthesis of (−)-Tetrahydrolipstatin. *Tetrahedron Letters* **1999**, *40* (2), 393–394. https://doi.org/https://doi.org/10.1016/S0040-4039(98)02321-1.

(76) Paterson, I.; Florence, G. J.; Gerlach, K.; Scott, J. P. Total Synthesis of the Antimicrotubule Agent (+)-Discodermolide Using Boron-Mediated Aldol Reactions of Chiral Ketones. *Angewandte Chemie International Edition* **2000**, *39* (2), 377–380. https://doi.org/https://doi.org/10.1002/(SICI)1521-3773(20000117)39:2<377::AID-ANIE377>3.0.CO;2-E.

(77) Paterson, I.; Wallace, D. J.; Velázquez, S. M. Studies in Polypropionate Synthesis: High π-Face Selectivity in Syn and Anti Aldol Reactions of Chiral Boron Enolates of Lactate-Derived Ketones. *Tetrahedron Letters* **1994**, *35* (48), 9083–9086. https://doi.org/https://doi.org/10.1016/0040-4039(94)88434-X.

(78) Paterson, I.; Chen, D. Y.-K.; Aceña, J. L.; Franklin, A. S. Studies in Marine Polypropionate Synthesis: Total Synthesis of (−)-Baconipyrone C. *Organic Letters* **2000**, *2* (11), 1513–1516. https://doi.org/10.1021/ol000027n.

(79) Evans, D. A. Studies in Asymmetric Synthesis. The Development of Practical Chiral Enolate Synthons. *Aldrichimica Acta* **1982**, *15* (2), 23–32.

(80) Arya, P.; Qin, H. Advances in Asymmetric Enolate Methodology. *Tetrahedron* **2000**, *56* (7), 917–947. https://doi.org/https://doi.org/10.1016/S0040-4020(99)00964-3.

(81) Ian, P.; M., D. S.; C., R. J.; J., N. G.; A., G. E.; Richard, I.; P., P. T.; Pat, L.; Daniela, D.; K., R. J.; E., W. A. Leiodermatolide, a Potent Antimitotic Macrolide from the Marine Sponge Leiodermatium Sp. *Angewandte Chemie International Edition* **2011**, *50* (14), 3219–3223. https://doi.org/10.1002/anie.201007719.

(82) Della-Felice, F.; Pilli, R. A.; Sarotti, A. M. Computer-Guided Total Synthesis of Natural Products. Recent Examples and Future Perspectives . *Journal of the Brazilian Chemical Society* . scielo 2018, pp 1041–1075.

(83) Dess, D. B.; Martin, J. C. Readily Accessible 12-I-5 Oxidant for the Conversion of Primary and Secondary Alcohols to Aldehydes and Ketones. *The Journal of Organic Chemistry* **1983**, *48* (22), 4155–4156. https://doi.org/10.1021/jo00170a070.

(84) Dess, D. B.; Martin, J. C. A Useful 12-I-5 Triacetoxyperiodinane (the Dess-Martin Periodinane) for the Selective Oxidation of Primary or Secondary Alcohols and a Variety of Related 12-I-5 Species. *Journal of the American Chemical Society* **1991**, *113* (19), 7277–7287. https://doi.org/10.1021/ja00019a027.

(85) Baker, R.; Castro, J. L. Total Synthesis of (+)-Macbecin I. *Journal of the Chemical Society, Perkin Transactions 1* **1990**, No. 1, 47–65. https://doi.org/10.1039/P19900000047.

(86) Hoover, J. M.; Stahl, S. S. Highly Practical Copper(I)/TEMPO Catalyst System for Chemoselective Aerobic Oxidation of Primary Alcohols. *Journal of the American Chemical Society* **2011**, *133* (42), 16901–16910. https://doi.org/10.1021/ja206230h.

(87) Hoover, J. M.; Ryland, B. L.; Stahl, S. S. Mechanism of Copper(I)/TEMPO-Catalyzed Aerobic Alcohol Oxidation. *Journal of the American Chemical Society* **2013**, *135* (6), 2357–2367. https://doi.org/10.1021/ja3117203.

(88) Evans, D. A.; Bartroli, J.; Shih, T. L. Enantioselective Aldol Condensations. 2. Erythro-Selective Chiral Aldol Condensations via Boron Enolates. *Journal of the American Chemical Society* **1981**, *103* (8), 2127–2129. https://doi.org/10.1021/ja00398a058.

(89) Nahm, S.; Weinreb, S. M. N-Methoxy-n-Methylamides as Effective Acylating Agents. *Tetrahedron Letters* **1981**, *22* (39), 3815–3818. https://doi.org/https://doi.org/10.1016/S0040-4039(01)91316-4.
(90) Wulff, W. D.; Peterson, G. A.; Bauta, W. E.; Chan, K.-S.; Faron, K. L.; Gilbertson, S. R.; Kaesler, R. W.; Yang, D. C.; Murray, C. K. A Regioselective Entry to Vinyl Lithiums from Unsymmetrical Ketones via Enol Triflates. *The Journal of Organic Chemistry* **1986**, *51* (2), 277–279. https://doi.org/10.1021/jo00352a039.
(91) Narayanan, B. A.; Bunnelle, W. H. The Cerium Mediated Conversion of Esters to Allylsilanes. *Tetrahedron Letters* **1987**, *28* (50), 6261–6264. https://doi.org/https://doi.org/10.1016/S0040-4039(01)91347-4.
(92) Peterson, D. J. Carbonyl Olefination Reaction Using Silyl-Substituted Organometallic Compounds. *The Journal of Organic Chemistry* **1968**, *33* (2), 780–784. https://doi.org/10.1021/jo01266a061.
(93) Dias, L. C.; Giacomini, R. On 1,4-Diastereoselectivity in the Chiral Allylsilane Addition to Chiral α-Substituted Aldehydes. *Tetrahedron Letters* **1998**, *39* (30), 5343–5346. https://doi.org/https://doi.org/10.1016/S0040-4039(98)01066-1.
(94) Giacomini, R.; Dias, L. C. Chiral Allylsilane Additions to Chiral α-Substituted Aldehydes. *Journal of the Brazilian Chemical Society* **1998**, *9* (4), 357–369.
(95) Dias, L. C.; Steil, L. J. Addition of Lactate-Derived Chiral Allyltrichlorostannanes to Chiral Aldehydes. *Tetrahedron Letters* **2004**, *45* (48), 8835–8841. https://doi.org/https://doi.org/10.1016/j.tetlet.2004.09.186.
(96) Neises, B.; Steglich, W. Simple Method for the Esterification of Carboxylic Acids. *Angewandte Chemie International Edition in English* **1978**, *17* (7), 522–524. https://doi.org/https://doi.org/10.1002/anie.197805221.
(97) Nahmany, M.; Melman, A. Studies on the Synthesis of DNA-Damaging Part of Leinamycin: Regioselectivity in Ti(OiPr)4 Mediated Opening of Hydroxy Epoxides with Carboxylic Acids. *Tetrahedron* **2005**, *61* (31), 7481–7488. https://doi.org/https://doi.org/10.1016/j.tet.2005.05.050.
(98) Zambrana, J.; Romea, P.; Urpí, F.; Luján, C. Highly Stereoselective Titanium-Mediated Aldol Reaction from (S)-4-Benzyloxy-3-Methyl-2-Butanone. *The Journal of Organic Chemistry* **2011**, *76* (21), 8575–8587. https://doi.org/10.1021/jo201021z.
(99) Molander, G. A.; Etter, J. B. Lanthanides in Organic Synthesis. 8. 1.3-Asymmetric Induction in Intramolecular Reformatskii-Type Reactions Promoted by Samarium Diiodide. *Journal of the American Chemical Society* **1987**, *109* (21), 6556–6558. https://doi.org/10.1021/ja00255a076.
(100) Lafontaine, J. A.; Provencal, D. P.; Gardelli, C.; Leahy, J. W. Enantioselective Total Synthesis of the Antitumor Macrolide Rhizoxin D. *The Journal of Organic Chemistry* **2003**, *68* (11), 4215–4234. https://doi.org/10.1021/jo034011x.
(101) MacGregor, C. I. Studies towards the Structural Elucidation and Total Synthesis of Hemicalide, University of Cambridge, 2015.
(102) Paterson, I.; Anderson, E. A.; Dalby, S. M.; Lim, J. H.; Maltas, P.; Loiseleur, O.; Genovino, J.; Moessner, C. The Stereocontrolled Total Synthesis of Spirastrellolide A Methyl Ester. Expedient Construction of the Key Fragments. *Organic & Biomolecular Chemistry* **2012**, *10* (30), 5861–5872. https://doi.org/10.1039/C2OB25100K.
(103) Corey, E. J.; Fuchs, P. L. A Synthetic Method for Formyl→ethynyl Conversion (RCHO→RC□CH or RC□CR'). *Tetrahedron Letters* **1972**, *13* (36), 3769–3772. https://doi.org/https://doi.org/10.1016/S0040-4039(01)94157-7.
(104) Smith, A. B.; Lee, D. Total Synthesis of (+)-Tedanolide. *Journal of the American Chemical Society* **2007**, *129* (35), 10957–10962. https://doi.org/10.1021/ja073329u.
(105) Hart, D. W.; Blackburn, T. F.; Schwartz, J. Hydrozirconation. III. Stereospecific and Regioselective Functionalization of Alkylacetylenes via Vinylzirconium(IV) Intermediates.

Journal of the American Chemical Society **1975**, *97* (3), 679–680. https://doi.org/10.1021/ja00836a056.

(106) Paterson, I.; Oballa, R. M. Studies in Marine Macrolide Synthesis: Synthesis of the C1-C15 Subunit of Spongistatin 1 (Altohyrtin A) and 15,16-Anti Aldol Coupling Reactions. *Tetrahedron Letters* **1997**, *38* (47), 8241–8244. https://doi.org/https://doi.org/10.1016/S0040-4039(97)10126-5.

(107) Paterson, I.; Donghi, M.; Gerlach, K. A Combinatorial Approach to Polyketide-Type Libraries by Iterative Asymmetric Aldol Reactions Performed on Solid Support. *Angewandte Chemie International Edition* **2000**, *39* (18), 3315–3319. https://doi.org/10.1002/1521-3773(20000915)39:18<3315::AID-ANIE3315>3.0.CO;2-9.

(108) Paterson, I.; Wallace, D. J.; Gibson, K. R. Studies in Marine Macrolide Synthesis: Synthesis of a C16-C28 Subunit of Spongistatin 1 (Altohyrtin A) Incorporating the CD-Spiroacetal Moiety. *Tetrahedron Letters* **1997**, *38* (51), 8911–8914. https://doi.org/https://doi.org/10.1016/S0040-4039(97)10483-X.

(109) Paterson, I.; Yeung, K.-S.; Smaill, J. B. The Horner-Wadsworth-Emmons Reaction in Natural Products Synthesis: Expedient Construction of Complex (E)-Enones Using Barium Hydroxide. *Synlett* **1993**, *10*, 774–776.

(110) Mahoney, W. S.; Brestensky, D. M.; Stryker, J. M. Selective Hydride-Mediated Conjugate Reduction of .Alpha.,.Beta.-Unsaturated Carbonyl Compounds Using [(Ph3P)CuH]6. *Journal of the American Chemical Society* **1988**, *110* (1), 291–293. https://doi.org/10.1021/ja00209a048.

(111) Erkkilä, A.; Pihko, P. M. Mild Organocatalytic α-Methylenation of Aldehydes. *The Journal of Organic Chemistry* **2006**, *71* (6), 2538–2541. https://doi.org/10.1021/jo052529q.

(112) Trost, B. M.; Herndon, J. W. Inversion of the Electronic Reactivity of Allyl Acetates Using an Aluminum-Tin Reagent. *Journal of the American Chemical Society* **1984**, *106* (22), 6835–6837. https://doi.org/10.1021/ja00334a059.

(113) Smith, A. B.; Sfouggatakis, C.; Risatti, C. A.; Sperry, J. B.; Zhu, W.; Doughty, V. A.; Tomioka, T.; Gotchev, D. B.; Bennett, C. S.; Sakamoto, S.; Atasoylu, O.; Shirakami, S.; Bauer, D.; Takeuchi, M.; Koyanagi, J.; Sakamoto, Y. Spongipyran Synthetic Studies. Evolution of a Scalable Total Synthesis of (+)-Spongistatin 1. *Tetrahedron* **2009**, *65* (33), 6489–6509. https://doi.org/10.1016/J.TET.2009.04.003.

(114) Corey, E. J.; Yu, C. M.; Kim, S. S. A Practical and Efficient Method for Enantioselective Allylation of Aldehydes. *Journal of the American Chemical Society* **1989**, *111* (14), 5495–5496. https://doi.org/10.1021/ja00196a082.

(115) Williams, D. R.; Plummer, S. V; Patnaik, S. Formal Synthesis of Leucascandrolide A. *Angewandte Chemie International Edition* **2003**, *42* (33), 3934–3938. https://doi.org/https://doi.org/10.1002/anie.200351817.

(116) Williams, D. R.; Patnaik, S.; Plummer, S. V. Leucascandrolide A: A Second Generation Formal Synthesis. *Organic Letters* **2003**, *5* (26), 5035–5038. https://doi.org/10.1021/ol036071v.

(117) Miyaura, N.; Yamada, K.; Suginome, H.; Suzuki, A. Novel and Convenient Method for the Stereo- and Regiospecific Synthesis of Conjugated Alkadienes and Alkenynes via the Palladium-Catalyzed Cross-Coupling Reaction of 1-Alkenylboranes with Bromoalkenes and Bromoalkynes. *Journal of the American Chemical Society* **1985**, *107* (4), 972–980. https://doi.org/10.1021/ja00290a037.

(118) Frank, S. A.; Chen, H.; Kunz, R. K.; Schnaderbeck, M. J.; Roush, W. R. Use of Thallium(I) Ethoxide in Suzuki Cross Coupling Reactions. *Organic Letters* **2000**, *2* (17), 2691–2694. https://doi.org/10.1021/ol0062446.

(119) Fürstner, A.; Funel, J.-A.; Tremblay, M.; Bouchez, L. C.; Nevado, C.; Waser, M.; Ackerstaff, J.; Stimson, C. C. A Versatile Protocol for Stille–Migita Cross Coupling Reactions. *Chemical Communications* **2008**, No. 25, 2873–2875. https://doi.org/10.1039/B805299A.

(120) Yoshihisa, K.; Choon-Hong, T.; Yoshito, K. Toward Creation of a Universal NMR Database for Stereochemical Assignment: The Case of 1,3,5-Trisubstituted Acyclic Systems. *Helvetica Chimica Acta* **2000**, *83* (9), 2562–2571. https://doi.org/10.1002/1522-2675(20000906)83:9<2562::AID-HLCA2562>3.0.CO;2-Z.
(121) Hafner, A.; Duthaler, R. O.; Marti, R.; Rihs, G.; Rothe-Streit, P.; Schwarzenbach, F. Enantioselective Syntheses with Titanium Carbohydrate Complexes. Part 7. Enantioselective Allyltitanation of Aldehydes with Cyclopentadienyldialkoxyallyltitanium Complexes. *Journal of the American Chemical Society* **1992**, *114* (7), 2321–2336. https://doi.org/10.1021/ja00033a005.
(122) Cossy, J.; BouzBouz, S.; Pradaux, F.; Willis, C.; Bellosta, V. Chiral Titanium Complexes. Synthesis of Optically Active Unsaturated Alcohols, Diols, Polypropionates and Their Use in the Synthesis of Biologically Active Compounds. *Synlett* **2002**, *10*, 1595−1606.
(123) Sakai, M.; Hayashi, H.; Miyaura, N. Rhodium-Catalyzed Conjugate Addition of Aryl- or 1-Alkenylboronic Acids to Enones. *Organometallics* **1997**, *16* (20), 4229–4231. https://doi.org/10.1021/om9705113.
(124) Takaya, Y.; Ogasawara, M.; Hayashi, T. Rhodium-Catalyzed Asymmetric 1,4-Addition of 2-Alkenyl-1,3,2-Benzodioxaboroles to α,β-Unsaturated Ketones. *Tetrahedron Letters* **1998**, *39* (46), 8479–8482. https://doi.org/https://doi.org/10.1016/S0040-4039(98)01866-8.
(125) Edwards, H. J.; Hargrave, J. D.; Penrose, S. D.; Frost, C. G. Synthetic Applications of Rhodium Catalysed Conjugate Addition. *Chemical Society Reviews* **2010**, *39* (6), 2093–2105. https://doi.org/10.1039/B919762C.
(126) Davis, F. A.; Haque, M. S.; Ulatowski, T. G.; Towson, J. C. Asymmetric Oxidation of Ester and Amide Enolates Using New (Camphorylsulfonyl)Oxaziridines. *The Journal of Organic Chemistry* **1986**, *51* (12), 2402–2404. https://doi.org/10.1021/jo00362a053.
(127) Crabtree, R. H.; Davis, M. W. Directing Effects in Homogeneous Hydrogenation with [Ir(Cod)(PCy3)(Py)]PF6. *The Journal of Organic Chemistry* **1986**, *51* (14), 2655–2661. https://doi.org/10.1021/jo00364a007.
(128) Baudin, J. B.; Hareau, G.; Julia, S. A.; Ruel, O. A Direct Synthesis of Olefins by Reaction of Carbonyl Compounds with Lithio Derivatives of 2-[Alkyl- or (2'-Alkenyl)- or Benzyl-Sulfonyl]-Benzothiazoles. *Tetrahedron Letters* **1991**, *32* (9), 1175–1178. https://doi.org/https://doi.org/10.1016/S0040-4039(00)92037-9.
(129) Blakemore, P. R.; Cole, W. J.; Kocieński, P. J.; Morley, A. A Stereoselective Synthesis of Trans-1,2-Disubstituted Alkenes Based on the Condensation of Aldehydes with Metallated 1-Phenyl-1H-Tetrazol-5-Yl Sulfones. *Synlett* **1998**, 26−28.
(130) Christophe, A. Mechanistic Manifold and New Developments of the Julia–Kocienski Reaction. *European Journal of Organic Chemistry* **2009**, *2009* (12), 1831–1844. https://doi.org/10.1002/ejoc.200801117.
(131) Lecourt, C.; Dhambri, S.; Yamani, K.; Boissonnat, G.; Specklin, S.; Fleury, E.; Hammad, K.; Auclair, E.; Sablé, S.; Grondin, A.; Arimondo, P. B.; Sautel, F.; Massiot, G.; Meyer, C.; Cossy, J.; Sorin, G.; Lannou, M.-I.; Ardisson, J. Assembly of the Entire Carbon Backbone of a Stereoisomer of the Antitumor Marine Natural Product Hemicalide. *Chemistry – A European Journal* **2019**, *25* (11), 2745–2749. https://doi.org/https://doi.org/10.1002/chem.201806327.
(132) Benowitz, A. B.; Fidanze, S.; Small, P. L. C.; Kishi, Y. Stereochemistry of the Core Structure of the Mycolactones. *Journal of the American Chemical Society* **2001**, *123* (21), 5128–5129. https://doi.org/10.1021/ja0105414.
(133) Paterson, I.; Gibson, K. R.; Oballa, R. M. Remote, 1,5-Anti Stereoinduction in the Boron-Mediated Aldol Reactions of β-Oxygenated Methyl Ketones. *Tetrahedron Letters* **1996**, *37* (47), 8585–8588. https://doi.org/https://doi.org/10.1016/0040-4039(96)01962-4.
(134) Paton, R. S.; Goodman, J. M. 1,5-Anti Stereocontrol in the Boron-Mediated Aldol Reactions of β-Alkoxy Methyl Ketones: The Role of the Formyl Hydrogen Bond. *The*

Journal of Organic Chemistry **2008**, *73* (4), 1253–1263. https://doi.org/10.1021/jo701849x.
(135) Narasaka, K.; Pai, H. C. Stereoselective Synthesis of Meso(or Erythro) 1,3-Diols from β-Hydroxyketones. *Chemistry Letters* **1980**, *9* (11), 1415–1418. https://doi.org/10.1246/cl.1980.1415.
(136) Chen, K.-M.; Hardtmann, G. E.; Prasad, K.; Repič, O.; Shapiro, M. J. 1,3-Syn Diastereoselective Reduction of β-Hydroxyketones Utilizing Alkoxydialkylboranes. *Tetrahedron Letters* **1987**, *28* (2), 155–158. https://doi.org/https://doi.org/10.1016/S0040-4039(00)95673-9.
(137) Paterson, I.; Florence, G. J.; Heimann, A. C.; Mackay, A. C. Stereocontrolled Total Synthesis of (−)-Aurisides A and B. *Angewandte Chemie International Edition* **2005**, *44* (7), 1130–1133. https://doi.org/10.1002/anie.200462267.
(138) Paterson, I.; Anne Lister, M. Aldol Condensations of Chiral Ethylketones: Control by Chiral Boron Reagents. *Tetrahedron Letters* **1988**, *29* (5), 585–588. https://doi.org/https://doi.org/10.1016/S0040-4039(00)80157-4.
(139) Sullivan, G. R.; Dale, J. A.; Mosher, H. S. Correlation of Configuration and Fluorine-19 Chemical Shifts of .Alpha.-Methoxy-.Alpha.-Trifluoromethylphenyl Acetate Derivatives. *The Journal of Organic Chemistry* **1973**, *38* (12), 2143–2147. https://doi.org/10.1021/jo00952a006.
(140) Brand, D. J.; Steenkamp, J. A.; Brandt, E. V; Takeuchi, Y. Conformational Studies of (−)-Epicatechin-Mosher Ester. *Tetrahedron Letters* **2007**, *48* (15), 2769–2773. https://doi.org/https://doi.org/10.1016/j.tetlet.2007.02.048.
(141) Dale, J. A.; Mosher, H. S. Nuclear Magnetic Resonance Enantiomer Regents. Configurational Correlations via Nuclear Magnetic Resonance Chemical Shifts of Diastereomeric Mandelate, O-Methylmandelate, and .Alpha.-Methoxy-.Alpha.-Trifluoromethylphenylacetate (MTPA) Esters. *Journal of the American Chemical Society* **1973**, *95* (2), 512–519. https://doi.org/10.1021/ja00783a034.
(142) Hoye, T. R.; Jeffrey, C. S.; Shao, F. Mosher Ester Analysis for the Determination of Absolute Configuration of Stereogenic (Chiral) Carbinol Carbons. *Nature Protocols* **2007**, *2* (10), 2451–2458. https://doi.org/10.1038/nprot.2007.354.
(143) Baker, B. A.; Bošković, Ž. V; Lipshutz, B. H. (BDP)CuH: A "Hot" Stryker's Reagent for Use in Achiral Conjugate Reductions. *Organic Letters* **2008**, *10* (2), 289–292. https://doi.org/10.1021/ol702689v.
(144) Ager, D. J. The Peterson Olefination Reaction. *Synthesis* **1990**, *38*, 1–223.
(145) Fleming, I.; Morgan, I. T.; Sarkar, A. K. The Stereochemistry of the Vinylogous Peterson Elimination. *Journal of the Chemical Society, Chemical Communications* **1990**, No. 22, 1575–1577. https://doi.org/10.1039/C39900001575.
(146) Staden, L. F. van; Gravestock, D.; Ager, D. J. New Developments in the Peterson Olefination Reaction. *Chemical Society Reviews* **2002**, *31* (3), 195–200. https://doi.org/10.1039/A908402I.
(147) Hoveyda, A. H.; Evans, D. A.; Fu, G. C. Substrate-Directable Chemical Reactions. *Chemical Reviews* **1993**, *93* (4), 1307–1370. https://doi.org/10.1021/cr00020a002.
(148) Chittiboyina, A. G.; Peddikotla, P.; Avery, M. A.; Khan, I. A. Directed Hydrogenation of Acyclic Homoallylic Alcohols: Enantioselective Syntheses of (+)- and (−)-Laurenditerpenol. *The Journal of Organic Chemistry* **2013**, *78* (18), 9223–9232. https://doi.org/10.1021/jo401461x.
(149) Zhu, Y.; Burgess, K. Filling Gaps in Asymmetric Hydrogenation Methods for Acyclic Stereocontrol: Application to Chirons for Polyketide-Derived Natural Products. *Accounts of Chemical Research* **2012**, *45* (10), 1623–1636. https://doi.org/10.1021/ar200145q.

(150) Roman, D.; Sauer, M.; Beemelmanns, C. Applications of the Horner–Wadsworth–Emmons Olefination in Modern Natural Product Synthesis. *Synthesis* **2021**, *53* (16), 2713–2739. https://doi.org/10.1055/a-1493-6331.
(151) Ando, K. A Mechanistic Study of the Horner−Wadsworth−Emmons Reaction: Computational Investigation on the Reaction Pass and the Stereochemistry in the Reaction of Lithium Enolate Derived from Trimethyl Phosphonoacetate with Acetaldehyde. *The Journal of Organic Chemistry* **1999**, *64* (18), 6815–6821. https://doi.org/10.1021/jo9909150.
(152) Corey, E. J.; Bakshi, R. K.; Shibata, S. Highly Enantioselective Borane Reduction of Ketones Catalyzed by Chiral Oxazaborolidines. Mechanism and Synthetic Implications. *Journal of the American Chemical Society* **1987**, *109* (18), 5551–5553. https://doi.org/10.1021/ja00252a056.
(153) Han, B. Y. Studies Towards the Total Synthesis of Hemicalide, University of Cambridge, 2018.
(154) Lam, N. Y. S. The Synthesis-Enabled Stereochemical Elucidation of the Marine Natural Products Hemicalide and Phormidolide A, University of Cambridge, 2019.
(155) Tanno, N.; Terashima, S. Asymmetric Synthesis of Optically Active Anthracyclinone Intermediate and 4-Demethoxyanthracyclinones by the Use of a Novel Chiral Reducing Agent. *Chemical and Pharmaceutical Bulletin* **1983**, *31* (3), 821–836. https://doi.org/10.1248/cpb.31.821.
(156) Tanno, N.; Terashima, S. Asymmetric Reduction of Various Types of Ketones with Lithium Aluminum Hydride Partially Decomposed with (-)-N-Methylephedrine and N-Ethylaniline. *Chemical and Pharmaceutical Bulletin* **1983**, *31* (3), 837–851. https://doi.org/10.1248/cpb.31.837.
(157) Maltas, P. The Total Synthesis of (+)-Spirastrellolide A Methyl Ester, University of Cambridge, 2011.
(158) Billica, H. R.; Adkins, H. Catalyst, Raney Nickel, W-6. *Organic Syntheses* **1949**, *29*, 24–27. https://doi.org/10.15227/orgsyn.029.0024.
(159) Maryanoff, B. E.; Reitz, A. B. The Wittig Olefination Reaction and Modifications Involving Phosphoryl-Stabilized Carbanions. Stereochemistry, Mechanism, and Selected Synthetic Aspects. *Chemical Reviews* **1989**, *89* (4), 863–927. https://doi.org/10.1021/cr00094a007.
(160) de Nooy, A. E. J.; Besemer, A. C.; van Bekkum, H. On the Use of Stable Organic Nitroxyl Radicals for the Oxidation of Primary and Secondary Alcohols. *1996 10*, 1153–1176. https://doi.org/10.1055/s-1996-4369.
(161) Brown, H. C.; Jadhav, P. K. Asymmetric Carbon-Carbon Bond Formation via .Beta.-Allyldiisopinocampheylborane. Simple Synthesis of Secondary Homoallylic Alcohols with Excellent Enantiomeric Purities. *Journal of the American Chemical Society* **1983**, *105* (7), 2092–2093. https://doi.org/10.1021/ja00345a085.
(162) Brown, H. C.; Bhat, K. S. Chiral Synthesis via Organoboranes. 7. Diastereoselective and Enantioselective Synthesis of Erythro- and Threo-.Beta.-Methylhomoallyl Alcohols via Enantiomeric (Z)- and (E)-Crotylboranes. *Journal of the American Chemical Society* **1986**, *108* (19), 5919–5923. https://doi.org/10.1021/ja00279a042.
(163) Brown, H. C.; Bhat, K. S. Enantiomeric Z- and E-Crotyldiisopinocampheylboranes. Synthesis in High Optical Purity of All Four Possible Stereoisomers of .Beta.-Methylhomoallyl Alcohols. *Journal of the American Chemical Society* **1986**, *108* (2), 293–294. https://doi.org/10.1021/ja00262a017.
(164) Boiarska, Z.; Braga, T.; Silvani, A.; Passarella, D. Brown Allylation: Application to the Synthesis of Natural Products. *European Journal of Organic Chemistry* **2021**, *2021* (22), 3214–3222. https://doi.org/https://doi.org/10.1002/ejoc.202100258.
(165) Paterson, I.; Collett, L. A. Remote 1,5-Stereoinduction in Boron Aldol Reactions of Methyl Ketones: Application to the Convergent Assembly of the 1,3-Polyol Sequence of (+)-

Roxaticin. *Tetrahedron Letters* **2001**, *42* (6), 1187–1191. https://doi.org/https://doi.org/10.1016/S0040-4039(00)02205-X.
(166) Evans, D. A.; Cee, V. J.; Siska, S. J. Asymmetric Induction in Methyl Ketone Aldol Additions to α-Alkoxy and α,β-Bisalkoxy Aldehydes: A Model for Acyclic Stereocontrol. *Journal of the American Chemical Society* **2006**, *128* (29), 9433–9441. https://doi.org/10.1021/ja061010o.
(167) Racherla, U. S.; Brown, H. C. Chiral Synthesis via Organoboranes. 27. Remarkably Rapid and Exceptionally Enantioselective (Approaching 100% Ee) Allylboration of Representative Aldehydes at -100.Degree. under New, Salt-Free Conditions. *The Journal of Organic Chemistry* **1991**, *56* (1), 401–404. https://doi.org/10.1021/jo00001a072.
(168) Brown, H. C.; Rao, B. C. S. A NEW TECHNIQUE FOR THE CONVERSION OF OLEFINS INTO ORGANOBORANES AND RELATED ALCOHOLS. *Journal of the American Chemical Society* **1956**, *78* (21), 5694–5695. https://doi.org/10.1021/ja01602a063.
(169) Takai, K.; Nitta, K.; Utimoto, K. Simple and Selective Method for Aldehydes (RCHO) .Fwdarw. (E)-Haloalkenes (RCH:CHX) Conversion by Means of a Haloform-Chromous Chloride System. *Journal of the American Chemical Society* **1986**, *108* (23), 7408–7410. https://doi.org/10.1021/ja00283a046.
(170) Anketell, M. J.; Sharrock, T. M.; Paterson, I. A Unified Total Synthesis of the Actinoallolides, a Family of Potent Anti-Trypanosomal Macrolides. *Angewandte Chemie International Edition* **2020**, *59* (4), 1572–1576. https://doi.org/https://doi.org/10.1002/anie.201914042.
(171) Nelson, D. J.; Manzini, S.; Urbina-Blanco, C. A.; Nolan, S. P. Key Processes in Ruthenium-Catalysed Olefin Metathesis. *Chemical Communications* **2014**, *50* (72), 10355–10375. https://doi.org/10.1039/C4CC02515F.
(172) Ashworth, I. W.; Hillier, I. H.; Nelson, D. J.; Percy, J. M.; Vincent, M. A. What Is the Initiation Step of the Grubbs-Hoveyda Olefin Metathesis Catalyst? *Chemical Communications* **2011**, *47* (19), 5428–5430. https://doi.org/10.1039/C1CC11230A.
(173) Thiel, V.; Hendann, M.; Wannowius, K.-J.; Plenio, H. On the Mechanism of the Initiation Reaction in Grubbs–Hoveyda Complexes. *Journal of the American Chemical Society* **2012**, *134* (2), 1104–1114. https://doi.org/10.1021/ja208967h.
(174) Nuñez-Zarur, F.; Solans-Monfort, X.; Rodríguez-Santiago, L.; Sodupe, M. Differences in the Activation Processes of Phosphine-Containing and Grubbs–Hoveyda-Type Alkene Metathesis Catalysts. *Organometallics* **2012**, *31* (11), 4203–4215. https://doi.org/10.1021/om300150d.
(175) Jean-Louis Hérisson, P.; Chauvin, Y. Catalyse de Transformation Des Oléfines Par Les Complexes Du Tungstène. II. Télomérisation Des Oléfines Cycliques En Présence d'oléfines Acycliques. *Die Makromolekulare Chemie* **1971**, *141* (1), 161–176. https://doi.org/https://doi.org/10.1002/macp.1971.021410112.
(176) Chatterjee, A. K.; Choi, T.-L.; Sanders, D. P.; Grubbs, R. H. A General Model for Selectivity in Olefin Cross Metathesis. *Journal of the American Chemical Society* **2003**, *125* (37), 11360–11370. https://doi.org/10.1021/ja0214882.
(177) Ritter, T.; Hejl, A.; Wenzel, A. G.; Funk, T. W.; Grubbs, R. H. A Standard System of Characterization for Olefin Metathesis Catalysts. *Organometallics* **2006**, *25* (24), 5740–5745. https://doi.org/10.1021/om060520o.
(178) Monfette, S.; Fogg, D. E. Equilibrium Ring-Closing Metathesis. *Chemical Reviews* **2009**, *109* (8), 3783–3816. https://doi.org/10.1021/cr800541y.
(179) Rhoades, D.; Rheingold, A. L.; O'Malley, B. W.; Wang, J. Expedient Total Syntheses of Pladienolide-Derived Spliceosome Modulators. *Journal of the American Chemical Society* **2021**, *143* (13), 4915–4920. https://doi.org/10.1021/jacs.1c01135.
(180) Pipaliya, B. V; Trofimova, D. N.; Grange, R. L.; Aeluri, M.; Deng, X.; Shah, K.; Craig, A. W.; Allingham, J. S.; Evans, P. A. Truncated Actin-Targeting Macrolide Derivative Blocks

Cancer Cell Motility and Invasion of Extracellular Matrix. *Journal of the American Chemical Society* **2021**, *143* (18), 6847–6854. https://doi.org/10.1021/jacs.0c12404.
(181) Hong, S. H.; Sanders, D. P.; Lee, C. W.; Grubbs, R. H. Prevention of Undesirable Isomerization during Olefin Metathesis. *Journal of the American Chemical Society* **2005**, *127* (49), 17160–17161. https://doi.org/10.1021/ja052939w.
(182) Heathcock, C. H.; McLaughlin, M.; Medina, J.; Hubbs, J. L.; Wallace, G. A.; Scott, R.; Claffey, M. M.; Hayes, C. J.; Ott, G. R. Multigram Synthesis of the C29−C51 Subunit and Completion of the Total Synthesis of Altohyrtin C (Spongistatin 2). *Journal of the American Chemical Society* **2003**, *125* (42), 12844–12849. https://doi.org/10.1021/ja030317+.
(183) Evans, D. A.; Trotter, B. W.; Coleman, P. J.; Côté, B.; Dias, L. C.; Rajapakse, H. A.; Tyler, A. N. Enantioselective Total Synthesis of Altohyrtin C (Spongistatin 2). *Tetrahedron* **1999**, *55* (29), 8671–8726. https://doi.org/https://doi.org/10.1016/S0040-4020(99)00438-X.
(184) Newton, R. F.; Reynolds, D. P.; Finch, M. A. W.; Kelly, D. R.; Roberts, S. M. An Excellent Reagent for the Removal of the T-Butyldimethylsilyl Protecting Group. *Tetrahedron Letters* **1979**, *20* (41), 3981–3982. https://doi.org/https://doi.org/10.1016/S0040-4039(01)86482-0.
(185) White, J. D.; Kawasaki, M. Total Synthesis of (+)-Latrunculin A. *Journal of the American Chemical Society* **1990**, *112* (12), 4991–4993. https://doi.org/10.1021/ja00168a071.
(186) Smith, A. B.; Friestad, G. K.; Barbosa, J.; Bertounesque, E.; Hull, K. G.; Iwashima, M.; Qiu, Y.; Salvatore, B. A.; Spoors, P. G.; Duan, J. J.-W. Total Synthesis of (+)-Calyculin A and (−)-Calyculin B: Asymmetric Synthesis of the C(9−25) Spiroketal Dipropionate Subunit. *Journal of the American Chemical Society* **1999**, *121* (45), 10468–10477. https://doi.org/10.1021/ja992134m.
(187) Kumagai, D.; Miyazaki, M.; Nishimura, S.-I. Cyclic Di-t-Butylsilylenediyl Ether Group as a Convenient Protective Group for the Glycoconjugate Synthesis. *Tetrahedron Letters* **2001**, *42* (10), 1953–1956. https://doi.org/https://doi.org/10.1016/S0040-4039(01)00044-2.
(188) Wu, J.; Lorenzo, P.; Zhong, S.; Ali, M.; Butts, C. P.; Myers, E. L.; Aggarwal, V. K. Synergy of Synthesis, Computation and NMR Reveals Correct Baulamycin Structures. *Nature* **2017**, *547* (7664), 436–440. https://doi.org/10.1038/nature23265.
(189) Verendel, J. J.; Pàmies, O.; Diéguez, M.; Andersson, P. G. Asymmetric Hydrogenation of Olefins Using Chiral Crabtree-Type Catalysts: Scope and Limitations. *Chemical Reviews* **2014**, *114* (4), 2130–2169. https://doi.org/10.1021/cr400037u.
(190) Patil, V. J. A Simple Access to Trichloroacetimidates. *Tetrahedron Letters* **1996**, *37* (9), 1481–1484. https://doi.org/10.1016/0040-4039(96)00044-5.
(191) Moeder, C. W.; Sowa, J. R. Kinetic Analysis of the Asymmetric Amplification Exhibited by B-Chlorodiisopinocampheylborane. *Journal of Physical Organic Chemistry* **2004**, *17* (4), 317–324. https://doi.org/10.1002/POC.730.
(192) Zampella, A.; Sorgente, M.; D'Auria, M. V. Synthetic Studies on Callipeltin A: Stereoselective Synthesis of (2R,3R,4S)-3-Hydroxy-2,4,6-Trimethylheptanoic Acid. *Tetrahedron: Asymmetry* **2002**, *13* (7), 681–685. https://doi.org/10.1016/S0957-4166(02)00178-7.
(193) Harried, S. S.; Lee, C. P.; Yang, G.; Lee, T. I. H.; Myles, D. C. Total Synthesis of the Potent Microtubule-Stabilizing Agent (+)-Discodermolide. *The Journal of Organic Chemistry* **2003**, *68* (17), 6646–6660. https://doi.org/10.1021/jo034521r.
(194) Davis, F. A.; Lamendola, J.; Nadir, U.; Kluger, E. W.; Sedergran, T. C.; Panunto, T. W.; Billmers, R.; Jenkins, R.; Turchi, I. J. Chemistry of Oxaziridines. 1. Synthesis and Structure of 2-Arenesulfonyl-3-Aryloxaziridines. A New Class of Oxaziridines. *Journal of the American Chemical Society* **1980**, *102* (6), 2000–2005. https://doi.org/10.1021/ja00526a040.

(195) Gao, D.; Li, B.; O'Doherty, G. A. Synthesis of Dehydro-Dephospho-Fostriecin and Formal Total Synthesis of Fostriecin. *Organic Letters* **2019**, *21* (20), 8334–8338. https://doi.org/10.1021/acs.orglett.9b03120.
(196) Meilert, K.; Brimble, M. A. Synthesis of the Bis-Spiroacetal Moiety of Spirolides B and D. *Organic Letters* **2005**, *7* (16), 3497–3500. https://doi.org/10.1021/ol051260u.